
The Effect of Dietary Fatty Acid Composition on Skeletal Muscle and Hepatic Fatty Acid and Glucose Metabolism in Male and Female Mice

Lisa Kate Philp

B.Sc. (Biomedical Science), B.Sc. (Hons)
Discipline of Medicine, School of Medicine
University of Adelaide, South Australia



A thesis submitted in fulfilment of the requirements
for the degree of Doctor of Philosophy

May 2011

TABLE OF CONTENTS

TABLE OF CONTENTS	ii
LIST OF FIGURES AND TABLES.....	xiv
COMMON ABBREVIATIONS	xxvi
THESIS ABSTRACT	xxxiii
DECLARATION.....	xxxv
RELATED PUBLICATIONS.....	xxxvi
ACKNOWLEDGEMENTS	xxxix

<i>Chapter 1 – Literature Review</i>	1
1.1 – OBESITY - AN OVERVIEW	2
<i>1.1.1 – The Obesity Epidemic - Of Growing Concern</i>	2
<i>1.1.2 – Obesity - Influencing Factors and Sites of Metabolic Dysfunction</i>	3
1.2 – KEY PERIPHERAL TISSUES INVOLVED IN ENERGY	
HOMEOSTASIS	3
<i>1.2.1 – Adipose Tissue - A Role in Energy Balance</i>	4
<i>1.2.2 – Skeletal Muscle - A Role in Energy Balance</i>	4
<i>1.2.2.1 – Skeletal Muscle Fibre Type Influences Muscle Metabolism</i>	4
<i>1.2.3 – Liver - A Role in Energy Balance</i>	6
<i>1.2.4 – Obesity Leads to Altered Lipid and Glucose Metabolism in Key Tissues of Energy Homeostasis</i>	7
1.3 – FATTY ACID METABOLISM – CELLULAR FATTY ACID UPTAKE	7
<i>1.3.1 – Fatty acid translocase (FAT/CD36)</i>	10
<i>1.3.2 – Plasma membrane fatty acid binding protein (FABPpm)</i>	11
<i>1.3.3 – Fatty acid transport proteins (FATPs)</i>	12
<i>1.3.3.1 – FATP1 (SLC27A1)</i>	13
<i>1.3.3.2 – FATP2 (SLC27A2)</i>	13

1.3.3.3 – <i>FATP4 (SLC27A4)</i>	14
1.3.3.4 – <i>FATP5 (SLC27A5)</i>	15
1.3.4 – <i>Fatty Acid Metabolism is Altered in Obesity – Implicating Fatty Acid Transporters</i>	16
1.4 – FATTY ACID METABOLISM – FATTY ACID SYNTHESIS, TRIGLYCERIDE SYNTHESIS, STORAGE AND DEGRADATION	18
1.4.1 – <i>Fatty Acid Synthesis</i>	18
1.4.1.1 – <i>Sterol regulatory element binding transcription factor 1 (SREBF1)</i>	19
1.4.1.2 – <i>Acetyl-CoA Carboxylase (ACC)</i>	24
1.4.1.3 – <i>Fatty Acid Synthase (FAS)</i>	25
1.4.1.4 – <i>Stearoyl-Coenzyme A desaturase 1 (SCD1)</i>	26
1.4.2 – <i>Triglyceride Synthesis, Storage and Degradation</i>	26
1.4.2.1 – <i>Diacylglycerol Acyltransferase (DGAT)</i>	27
1.4.2.2 – <i>Hormone Sensitive Lipase (HSL)</i>	32
1.4.3 – <i>Fatty Acid Metabolism is Altered in Obesity – Implicating Fatty Acid Synthesis and Storage</i>	33
1.5 – FATTY ACID METABOLISM – FATTY ACID UTILISATION	35
1.5.1 – <i>Carnitine Palmitoyl Transferase 1 (CPT1)</i>	38
1.5.2 – <i>AMP-Activated Protein Kinase (AMPK)</i>	40
1.5.3 – <i>Peroxisome proliferator activator receptor (PPAR)</i>	45
1.5.4 – <i>Fatty Acid Metabolism is Altered in Obesity – Implicating Impaired Fatty Acid Oxidation</i>	49
1.6 – FATTY ACID AND GLUCOSE METABOLISM – CONTROLLING THE NUTRIENT SHIFT	51
1.7 – GLUCOSE METABOLISM – ACTIVATION OF GLUCOSE	54
1.7.1 – <i>Hexokinase 2 (HK2)</i>	54
1.7.2 – <i>Glucokinase (GCK)</i>	56
1.8 – GLUCOSE METABOLISM – GLYCOLYSIS	59
1.8.1 – <i>Phosphofructokinase (PFK)</i>	59

1.8.1.1 – Muscle Type Phosphofructokinase (PFK-M).....	60
1.8.1.2 – Liver Type Phosphofructokinase (PFK-L).....	60
1.9 – GLUCOSE METABOLISM – GLYCOGENESIS	63
1.9.1 – Glycogen Synthase (GYS)	63
1.10 – GLUCOSE METABOLISM – GLUCONEOGENESIS	66
1.10.1 – Phosphoenolpyruvate carboxykinase (PEPCK)	66
1.11 – GLUCOSE METABOLISM – INSULIN SIGNALLING.....	69
1.11.1 – Phosphoinositol 3-Kinase (PI3K)	69
1.12 – ALTERED GLUCOSE METABOLISM AND INSULIN SIGNALLING WITH HIGH FAT FEEDING	70
1.13 – HIGH FAT INTAKE – IMPLICATING THE IMPORTANCE OF FAT TYPE	70
1.13.1 – <i>The Characteristics of Dietary Fatty Acid Types and their Influence on Metabolic Dysfunction</i>	71
1.13.1.1 – Chain Length.....	71
1.13.1.2 – Saturation.....	72
1.13.2 – <i>The Importance of Fat Type in a High Fat Diet Setting</i>	73
1.13.3 – <i>Saturated Fatty Acids and Polyunsaturated Fatty Acids: Fatty Acid Type and their Effect on Body Weight and Whole-Body Metabolism</i>	75
1.13.4 – <i>n-3 PUFA Enrichment of a HFD Reduces Liver Triglyceride Accumulation by Reducing Lipid Storage and Promoting Fatty Acid Oxidation</i>	77
1.13.5 – <i>n-3 PUFA Enrichment of a HFD Reduces Intramuscular Triglyceride Accumulation</i>	78
1.13.6 – <i>n-3 PUFA Enrichment of a HFD Improves Whole-Body Insulin Sensitivity</i>	79
1.14 – HIGH FAT INTAKE – IMPLICATING THE IMPORTANCE OF GENDER	80

1.15 – AIMS	83
<i>1.15.1 – Chapter 2 – The Effect of Dietary Fatty Acid Composition and Gender on Body Composition in Mice: Model Characterisation.....</i>	83
<i>1.15.2 – Chapter 3 – The Effect of Dietary Fatty Acid Composition on Muscle Fibre Type Composition and Stored Nutrient Content of Skeletal Muscle.....</i>	84
<i>1.15.3 – Chapter 4 – The Effect of Dietary Fatty Acid Composition, Muscle Fibre Type and Gender on Skeletal Muscle Fatty Acid Metabolism in Mice</i>	84
<i>1.15.4 – Chapter 5 – The Effect of Dietary Fatty Acid Composition and Gender on Hepatic Fatty Acid Metabolism in Mice</i>	86
<i>1.15.5 – Chapter 6 – The Effect of Dietary Fatty Acid Composition and Gender on Glucose Metabolism in the Skeletal Muscle and Liver of Mice</i>	87
<i>Chapter 2 - The Effect of Dietary Fatty Acid Composition and Gender on Body Composition in Mice: Model Characterisation</i>	89
2.1 – INTRODUCTION.....	90
2.2 – MATERIALS AND METHODOLOGY.....	95
<i>2.2.1 - Animals and Nutrition Regime</i>	95
<i>2.2.1.1 – Cohort 1 Mice – Measurements Collected During Nutrition Regime.....</i>	98
<i>2.2.1.2 – Cohort 2 Mice – Measurements Collected During Nutrition Regime.....</i>	99
<i>2.2.2 - Tissue Collection from Mice in Cohort 1.....</i>	100
<i>2.2.3 - Analysis of Plasma Samples</i>	105
<i>2.2.3.1 – Plasma Glucose</i>	105
<i>2.2.3.2 – Plasma Insulin</i>	105
<i>2.2.3.3 – Plasma Triglyceride.....</i>	106
<i>2.2.4 - Histological Evaluation of Liver Morphology and Fat Content.....</i>	107
<i>2.2.4.1 – Haematoxylin and Eosin Staining.....</i>	107

2.2.4.2 – Oil Red O Staining	108
2.2.4.3 – Histological Quantification of Liver Fat Content.....	109
2.2.5 - Enzymatic Analysis of Liver Glycogen Content	109
2.2.6 - Statistical Analyses	111
2.3 – RESULTS	113
2.3.1 - Energy Intake, Food Intake, Body Weight, Feed Efficiency, Physical Appearance and Physical Activity	113
2.3.1.1 – Energy Intake	113
2.3.1.2 – Food Intake	115
2.3.1.3 – Body Weight	115
2.3.1.4 – Feed Efficiency.....	116
2.3.1.5 – Physical Appearance of Mice	116
2.3.1.6 – Physical Activity (Cohort 2).....	116
2.3.2 - Adipose Tissue Depot Weights	123
2.3.2.1 – Total Adiposity	123
2.3.2.2 – Absolute Adipose Tissue Weight	123
2.3.2.3 – Relative Adipose Tissue Weight	124
2.3.3 - Plasma Concentration of Glucose, Insulin and Triglyceride	129
2.3.4 - Type of Dietary Fat Consumed Influences Liver Appearance and Liver Weight.....	131
2.3.5 - Type of Dietary Fat Consumed Influences Liver Histology and Liver Fat Accumulation	135
2.3.6 - Type of Dietary Fat Consumed Influences Liver Glucose Metabolism	138
2.4 – DISCUSSION	140
2.4.1 - Effect of Dietary Fatty Acid Composition on Body Weight and Relative Adipose Tissue Weight	140
2.4.2 - Effect of Dietary Fatty Acid Composition on Liver Fat and Glycogen Content	143
2.4.3 - Effect of Dietary Fatty Acid Composition on Dyslipidemia and Insulin Sensitivity.....	145

<i>2.4.4 - Effect of Gender on the HFD-Induced Phenotype</i>	148
<i>2.4.5 - Amount and Type of n-3 Polyunsaturated Fatty Acids Chosen</i>	149
<i>2.4.6 - Limitations</i>	151
<i>2.4.7 - Summary</i>	152

Chapter 3 - The Effect of Dietary Fatty Acid Content on Muscle Fibre

Type, Composition and Stored Nutrient Content of Skeletal

Muscle **153**

3.1 – INTRODUCTION..... **154**

3.2 – MATERIALS AND METHODOLOGY..... **158**

3.2.1 - Animals and Nutrition Regime **158**

3.2.1.1 – Cohort 1 Mice **158**

3.2.1.2 – Cohort 2 Mice **158**

3.2.2 - Tissue Collection..... **159**

3.2.2.1 – Cohort 1 Mice **159**

3.2.2.2 – Cohort 2 Mice **159**

3.2.3 - Histological Evaluation of Skeletal Muscle Morphology and Fat Content **161**

3.2.3.1 – Haematoxylin and Eosin Staining..... **161**

3.2.3.2 – Oil Red O Staining **161**

3.2.4 - Histological Evaluation of Skeletal Muscle Glycogen Content **162**

3.2.4.1 – Periodic Acid-Schiff Staining..... **162**

3.2.4.2 – Histological Quantification of Skeletal Muscle Glycogen Content **164**

3.2.5 - Histological Evaluation of Muscle Fibre Type..... **165**

3.2.5.1 – Staining Skeletal Muscle for Myofibrillar Myosin Adenosine Triphosphatase..... **165**

3.2.5.2 – Staining Skeletal Muscle for Succinic Dehydrogenase **166**

3.2.5.3 – Staining Skeletal Muscle for NADH Tetrazolium

<i>Reductase</i>	167
3.2.5.4 – <i>Histological Quantification of Muscle Fibre Type and Muscle Oxidative Capacity</i>	168
3.2.5.5 – <i>Myofibrillar ATPase</i>	169
3.2.5.6 – <i>Succinic Dehydrogenase and NADH Tetrazolium Reductase</i>	170
3.2.6 – <i>Statistical Analyses</i>	173
3.3 – RESULTS	175
3.3.1 – <i>Muscle Weight</i>	175
3.3.1.1 – <i>Absolute Muscle Weight</i>	175
3.3.1.2 – <i>Relative Muscle Weight</i>	175
3.3.2 – <i>Skeletal Muscle Morphology and Fat Content</i>	178
3.3.3 – <i>Skeletal Muscle Glycogen Content</i>	184
3.3.4 – <i>Characterisation of Muscle Fibre Type in the Extensor Digitorum Longus and Soleus Skeletal Muscles</i>	191
3.3.4.1 – <i>Muscle Fibre Type Composition of the Extensor Digitorum Longus Muscle</i>	191
3.3.4.2 – <i>Muscle Fibre Type Composition of the Soleus Muscle</i>	191
3.3.4.3 – <i>Muscle Cell Cross-sectional Area and Percentage Area Occupied by each Muscle Fibre Type in the Extensor Digitorum Longus Muscle</i>	192
3.3.4.4 – <i>Muscle Cell Cross-sectional Area and Percentage Area Occupied by each Muscle Fibre Type in the Soleus Muscle</i> ..	193
3.3.4.5 – <i>Relationships between Percentage Area Occupied and Cell Size of Muscle Fibre Types in the Extensor Digitorum Longus and Soleus Muscles</i>	194
3.3.5 – <i>Characterisation of Muscle Oxidative Capacity with Respect to Fibre Type in the Extensor Digitorum Longus and Soleus Skeletal Muscles</i>	201
3.3.5.1 – <i>Oxidative Capacity in the Extensor Digitorum Longus Muscle</i>	201

3.3.5.2 – <i>Oxidative Capacity in the Soleus Muscle</i>	202
3.3.5.3– <i>Relationships between the Oxidative Capacity of Muscle Fibre Types in the Extensor Digitorum Longus and Soleus Muscles</i>	203
3.3.6 – <i>Myosin ATPase Staining of the Tibialis, Plantaris and Gastrocnemius Skeletal Muscles</i>	210
3.3.7 – <i>Muscle Oxidative Capacity of the Tibialis, Plantaris and Gastrocnemius Skeletal Muscles</i>	215
3.4 – DISCUSSION	218
3.4.1 – <i>Effect of Dietary Fatty Acid Content on Muscle Fibre Type Composition</i>	218
3.4.2 – <i>Effect of Dietary Fatty Acid Composition on Stored Nutrient Content</i>	220
3.4.3 – <i>Effect of Dietary Fatty Acid Composition on Oxidative Capacity</i>	223
3.4.4 – <i>The Mechanisms behind the Differential Nutrient Storage and Oxidative Capacity in Response to Altered Dietary Fatty Acid Composition</i>	225
3.4.5 – <i>Limitations</i>	226
3.4.6 – <i>Summary</i>	226

Chapter 4 - The Effect of Dietary Fatty Acid Composition, Muscle Fibre Type and Gender on Skeletal Muscle Fatty Acid Metabolism in Mice..... 228

4.1 – INTRODUCTION	229
4.2 – MATERIALS AND METHODOLOGY	234
4.2.1 – <i>Animals, Nutrition Regime and Tissue Collection</i>	234
4.2.2 – <i>Extraction of RNA from Skeletal Muscle Samples</i>	234
4.2.3 – <i>Multiplex Primer Design</i>	236
4.2.4 – <i>Optimisation of Skeletal Muscle Multiplex</i>	237
4.2.5 – <i>Reverse Transcription of RNA Samples to Generate cDNA</i>	242
4.2.6 – <i>Polymerase Chain Reaction (PCR)</i>	242

4.2.7 – <i>Separation of PCR Products by the GenomeLab GeXP Genetic Analysis System</i>	245
4.2.8 – <i>Statistical Analyses</i>	246
4.3 – RESULTS	247
4.3.1 – <i>Fatty Acid Transport (FAT/CD36, FABPpm, FATP1 and FATP4)</i> . 247	
4.3.2 – <i>Lipogenesis, Triglyceride Synthesis and Triglyceride Storage (SREBF1, INSIG1, DGAT1, SCD1 and HSL)</i>	253
4.3.3 – <i>Fatty Acid Utilisation (PDK4, AMPKα1, AMPKα2, ACC-β, CPT1b, UCP2, UCP3, SIRT1, PGC1α, PPARα, PPARδ/β)</i>	262
4.4 – DISCUSSION	280
4.4.1 – <i>Skeletal Muscle Pattern of Gene Expression Reflects Muscle Fibre Type Properties</i>	280
4.4.2 – <i>Effect of Dietary Fatty Acid Composition on Skeletal Muscle Fatty Acid Uptake</i>	281
4.4.3 – <i>Effect of Dietary Fatty Acid Composition on Skeletal Muscle Fatty Acid Storage and Lipogenesis</i>	286
4.4.4 – <i>Effect of Dietary Fatty Acid Composition on Skeletal Muscle Fatty Acid Utilisation</i>	292
4.4.5 – <i>Mechanism behind Increased Oxidative Capacity Observed in HF-n-3 Skeletal Muscle despite Unchanged Muscle Fibre Type</i>	301
4.4.6 – <i>Effect of Gender on Skeletal Muscle Fatty Acid Metabolism</i>	303
4.4.7 – <i>Limitations</i>	304
4.4.8 – <i>Summary</i>	305
Chapter 5 - The Effect of Dietary Fatty Acid Composition and Gender on Hepatic Fatty Acid Metabolism in Mice	307
5.1 – INTRODUCTION	308
5.2 – MATERIALS AND METHODOLOGY	312
5.2.1 – <i>Animals, Nutrition Regime and Tissue Collection</i>	312
5.2.2 – <i>Extraction of RNA from Liver Samples</i>	312

5.2.3 – <i>Multiplex Primer Design</i>	313
5.2.4 – <i>Optimisation of Liver Multiplex</i>	314
5.2.5 – <i>Reverse Transcription of RNA and Subsequent PCR</i>	315
5.2.6 – <i>Separation of PCR Products by the GenomeLab GeXP Genetic Analysis System</i>	318
5.2.7 – <i>Statistical Analyses</i>	318
5.3 – RESULTS	320
5.3.1 - <i>Fatty Acid Transport (FAT/CD36, FABPpm, FATP2 and FATP5)</i> .	320
5.3.2 - <i>Lipogenesis, Triglyceride Synthesis and Storage (SREBF1, INSIG1, FAS, ACC-α, DGAT2, SCD1 and HSL)</i>	325
5.3.3 - <i>Fatty Acid Utilisation (PDK4, AMPKα1, AMPKα2, ACC-β, CPT1a, UCP2, SIRT1, PGC1α, PPARα, PPARδ/β, PPARγ)</i>	332
5.4 – DISCUSSION	342
5.4.1 – <i>Effect of Dietary Fatty Acid Composition on Hepatic Fatty Acid Uptake</i>	342
5.4.2 – <i>Effect of Dietary Fatty Acid Composition on Hepatic Lipogenesis and Triglyceride Storage</i>	348
5.4.3 – <i>Effect of Dietary Fatty Acid Composition on Hepatic Fatty Acid Utilisation</i>	355
5.4.4 – <i>Effect of Gender on Hepatic Fatty Acid Metabolism</i>	366
5.4.5 – <i>Limitations</i>	368
5.4.6 – <i>Summary</i>	368
<i>Chapter 6 - The Effect of Dietary Fatty Acid Composition and Gender on Glucose Metabolism in the Skeletal Muscle and Liver of Mice</i>	371
6.1 – INTRODUCTION.....	372
6.2 – MATERIALS AND METHODOLOGY.....	375
6.2.1 – <i>Animals, Nutrition Regime and Tissue Collection</i>	375

6.2.2 – mRNA Content Analyses using the GenomeLab GeXP Genetic	
Analysis System	375
6.2.3 – Statistical Analyses	376
6.2.3.1 – Skeletal Muscle mRNA Contents of Key Glucose Metabolism	
Genes.....	376
6.2.3.2 – Liver mRNA Contents of Key Glucose Metabolism Genes ...	377
6.3 – RESULTS	378
6.3.1 – Glucose Phosphorylation - Committing to Glucose Metabolism	378
6.3.1.1 – Skeletal Muscle Hexokinase 2.....	378
6.3.1.2 – Liver Glucokinase	379
6.3.2 – Glycolysis	383
6.3.2.1 – Skeletal Muscle Phosphofructokinase.....	383
6.3.2.2 – Liver Phosphofructokinase	383
6.3.3 – Glycogenesis	386
6.3.3.1 – Skeletal Muscle Glycogen Synthase.....	386
6.3.3.2 – Liver Glycogen Synthase.....	386
6.3.4 – Hepatic Gluconeogenesis.....	389
6.3.5 – Influencing Insulin Signalling	391
6.3.5.1 – Skeletal Muscle Phosphatidylinositol 3-kinase.....	391
6.3.5.2 – Skeletal Muscle Suppressor of Cytokine Signalling.....	391
6.3.5.3 – Hepatic Suppressor of Cytokine Signalling	392
6.4 – DISCUSSION	398
6.4.1 – Effect of Dietary Fatty Acid Composition on Skeletal Muscle Glucose	
Metabolism	398
6.4.1.1 – Glucose Phosphorylation – Committing to Glucose Metabolism	
.....	398
6.4.1.2 – Glycolysis	401
6.4.1.3 – Glycogenesis	403
6.4.1.4 – Influencing Insulin Signalling.....	404

6.4.2 – Effect of Dietary Fatty Acid Composition on Hepatic Glucose Metabolism	407
6.4.2.1 – Glucose Phosphorylation – Committing to Glucose Metabolism	407
6.4.2.2 – Glycolysis	409
6.4.2.3 – Glycogenesis	410
6.4.2.4 – Gluconeogenesis	411
6.4.2.5 – Insulin Signalling	412
6.4.3 – Effect of Muscle Fibre Type on Glucose Metabolism	414
6.4.4 – Effect of Gender on Glucose Metabolism	415
6.4.5 – Limitations	416
6.4.6 – Summary	417
Chapter 7 – Summary of Findings, Implications and Future Studies ...	420
7.1 – SUMMARY OF FINDINGS AND IMPLICATIONS	421
7.1.1 – Effect of Diet	421
7.1.2 – Effect of Gender	424
7.1.3 – Effect of Muscle Fibre Type	426
7.1.4 – Implications	427
7.2 – FUTURE STUDIES	428
7.2.1 – Measuring Thermogenesis	428
7.2.2 – Quantifying Muscle Fibre Type with Respect to Gender	429
7.2.3 – Assaying Diacylglycerol (DAG) and Ceramide	429
7.2.4 – Quantifying Protein Abundance or Activity of Key Metabolic Genes or Whole Processes of Metabolic Pathways	430
7.2.5 – Focusing on the Effect of Gender – Gonadectomy Studies	430
7.2.6 – Focusing on the Effect of n-3 PUFAs – Which Fatty Acid is having the Greatest Effect?	431
BIBLIOGRAPHY	432

LIST OF FIGURES AND TABLES

Figure 1.1. Schematic diagram of long chain fatty acid transport.....	9
Figure 1.2. Model depicting the maturation process of SREBF1 protein.....	22
Figure 1.3. Genes and pathways regulated by SREBFs	23
Figure 1.4. Pathways of triglyceride synthesis (glycerolipid synthesis: glycerol phosphate and monoacylglycerol pathways) and degradation.....	28
Figure 1.5. Pathway of fatty acid transport into the mitochondrion for subsequent oxidation.....	37
Figure 1.6. AMPK activation relieves the inhibition of carnitine palmitoyl transferase by malonyl-CoA by phosphorylating and deactivating acetyl-CoA carboxylase whilst phosphorylating and activating malonyl-CoA decarboxylase, leading to reduced malonyl-CoA levels and ultimately to increased fatty acid oxidation.....	42
Figure 1.7. Pathways influenced by AMPK activation in specific tissues.....	43
Table 1.1. Targets of AMPK in the liver and skeletal muscle and their metabolic effects	44
Figure 1.8. Model for transcriptional activation of PPARs as depicted by Desvergne and Wahli (Desvergne and Wahli, 1999).....	47
Figure 1.9. Pathways mediated by peroxisome proliferator activator receptor α (PPAR α) in the liver as reviewed by Mandard and colleagues (Mandard <i>et al.</i> , 2004).....	48
Figure 1.10. PDK4: the mechanism by which high fatty acid availability produces a nutrient shift to favour fatty acid metabolism	53
Figure 1.11. The complete glycolytic pathway	62
Figure 1.12. The glycogen synthesis pathways	65
Figure 1.13. The gluconeogenesis pathway from pyruvate to glucose	68
Table 2.1. Comparison of fatty acid composition of the two high fat diets, high saturated fat diet and high fat n-3 PUFA enriched diet.....	97

Figure 2.1. Procedure of skeletal muscle surgery for the collection of hindlimb skeletal muscles from male and female mice fed control, high saturated fat or high fat n-3 PUFA enriched diet	103
Figure 2.2. Diagram depicting lower hindlimb skeletal muscles collected during skeletal muscle surgery in mice	104
Figure 2.3 [A-B]. Total cumulative energy intake [A] and cumulative energy intake of macronutrients [B] in male and female mice fed control, high saturated fat or high fat n-3 PUFA enriched diets	118
Figure 2.4 [A-B]. Food intake during the experimental dietary period in male [A] and female [B] mice fed control, high saturated fat or high fat n-3 PUFA enriched diets for 14 weeks.....	119
Figure 2.5 [A-B]. Body weight from arrival, during the experimental dietary period, to the final day, of male [A] and female [B] mice fed control, high saturated fat or high fat n-3 PUFA enriched diets for 14 weeks	120
Figure 2.6 [A-D]. Final body weight [A], feed efficiency [B] and representative external [C] and internal [D] images of male and female mice fed control, high saturated fat or high fat n-3 PUFA enriched diets.....	121
Figure 2.7 [A-B]. Mean weekly physical activity [A] and cumulative physical activity [B] during the experimental dietary period of male and female mice fed control, high saturated fat or high fat n-3 PUFA enriched diets.....	122
Table 2.2. The absolute and relative weights of adipose tissue depots in mice fed a control, high saturated fat or high fat n-3 PUFA enriched diet	127
Figure 2.8. The relationships between feed efficiency and relative adipose tissue weight in mice fed a high saturated fat or high fat n-3 PUFA enriched diet	128
Figure 2.9 [A-C]. Plasma concentration of glucose [A], insulin [B] and triglyceride [C] in male and female mice fed control, high saturated fat or high fat n-3 PUFA enriched diets	130
Figure 2.10 [A-D]. Representative whole [A] and close-up [B] images depicting altered liver appearance and graphs illustrating the absolute [C] and relative [D] weight of the liver in mice fed a control, high saturated fat or high fat n-3 PUFA enriched diet	133

Figure 2.11. The relationships between relative liver weight and liver fat content, body weight and liver glycogen content	134
Figure 2.12 [A-D]. H&E [A] and Oil Red O [B] staining of liver sections and histological quantification of liver fat content as area stained positively for fat [C] and fat droplet area [D] of mice fed a control, high saturated fat or high fat n-3 PUFA enriched diet.....	137
Figure 2.13 [A-B]. Liver glycogen [A] and glucose [B] content of male and female mice fed a control, high saturated fat or high fat n-3 PUFA enriched diet	139
Figure 3.1 [A-F]. Muscle groups, including the tibialis and extensor digitorum longus muscles [A-B] and gastrocnemius, plantaris and soleus muscles [C-D] and quadriceps muscles [E-F], collected during muscle surgery in cohort 2 mice	160
Table 3.1. Scheme used to classify muscle fibre type from scores given to muscle fibres stained for myofibrillar ATPase after acid or alkaline preincubation.....	172
Table 3.2. Absolute and relative weights of the extensor digitorum longus and soleus muscles of male and female mice fed a control, high saturated fat or high fat n-3 PUFA enriched diet	177
Figure 3.2 [A-B]. Haematoxylin and eosin [A] and Oil Red O [B] staining of extensor digitorum longus and soleus muscle sections of mice fed a control, high saturated fat or high fat n-3 PUFA enriched diet	179
Figure 3.3. Haematoxylin and eosin staining of tibialis, plantaris and gastrocnemius muscle sections of mice fed a control, high saturated fat or high fat n-3 PUFA enriched diet	180
Figure 3.4. Haematoxylin and eosin staining of quadriceps muscle sections of mice fed a control, high saturated fat or high fat n-3 PUFA enriched diet	181
Figure 3.5. Oil Red O staining of tibialis, plantaris and gastrocnemius muscle sections of mice fed a control, high saturated fat or high fat n-3 PUFA enriched diet	182
Figure 3.6. Oil Red O staining of quadriceps muscle sections of mice fed a control, high saturated fat or high fat n-3 PUFA enriched diet.....	183

Figure 3.7 [A-B]. Periodic Acid-Schiff staining without [A] or with [B] diastase pre-treatment of extensor digitorum longus and soleus muscle sections of mice fed a control, high saturated fat or high fat n-3 PUFA enriched diet	186
Figure 3.8 [A-C]. Histological quantification of glycogen in extensor digitorum longus and soleus muscle sections of mice fed a control, high saturated fat or high fat n-3 PUFA enriched diet, assessed as mean pixel density [A] and the composition of fibres classified with having light, medium or dark Periodic Acid-Schiff staining intensity in extensor digitorum longus [B] and soleus [C] muscles.....	187
Figure 3.9. Periodic Acid-Schiff staining for glycogen content of tibialis, plantaris and gastrocnemius muscle sections of mice fed a control, high saturated fat or high fat n-3 PUFA enriched diet	189
Figure 3.10. Periodic Acid-Schiff staining for glycogen content of quadriceps muscle sections of mice fed a control, high saturated fat or high fat n-3 PUFA enriched diet.....	190
Figure 3.11. Serial sections of the extensor digitorum longus muscle stained for myosin ATPase after preincubation at pH 4.1, pH 4.3 and pH 10.4 in mice fed a control, high saturated fat or high fat n-3 PUFA enriched diet	195
Figure 3.12. Serial sections of the soleus muscle stained for myosin ATPase after preincubation at pH 4.1, pH 4.3 and pH 10.4 in mice fed a control, high saturated fat or high fat n-3 PUFA enriched diet.....	196
Figure 3.13 [A-B]. Muscle fibre type composition (%) of the extensor digitorum longus [A] and soleus [B] muscles of mice fed a control, high saturated fat or high fat n-3 PUFA enriched diet, evaluated histologically by myosin ATPase staining	197
Table 3.3. The mean area of muscle cells and the percentage of total area occupied by each muscle fibre type in the extensor digitorum longus and soleus muscles of mice fed a control, high saturated fat or high fat n-3 PUFA enriched diet	198
Figure 3.14. Relationships between the percentage area occupied and the mean cell cross-sectional area of muscle fibre types in the extensor digitorum longus muscle.....	199

Figure 3.15. Relationships between the percentage area occupied and mean cell area of muscle fibre types in the soleus muscle diet.....	200
Figure 3.16. Serial sections of the extensor digitorum longus muscle stained for SDH and NADH-TR in mice fed a control, high saturated fat or high fat n-3 PUFA enriched diet	205
Figure 3.17. Serial sections of the soleus muscle stained for SDH and NADH-TR in mice fed a control, high saturated fat or high fat n-3 PUFA enriched diet	206
Figure 3.18 [A-B]. Histological quantification of muscle oxidative capacity in extensor digitorum longus [A] and soleus [B] muscle sections of mice fed a control, high saturated fat or high fat n-3 PUFA enriched diet; muscle fibres were stained for SDH and assessed for mean pixel density	207
Figure 3.19 [A-B]. Histological quantification of muscle oxidative capacity in extensor digitorum longus [A] and soleus [B] muscle sections of mice fed a control, high saturated fat or high fat n-3 PUFA enriched diet; muscle fibres were stained for NADH-TR and assessed for mean pixel density	208
Table 3.4. Relationships between the oxidative capacities of muscle fibre types in the extensor digitorum longus and soleus muscles.....	209
Figure 3.20. Serial sections of the tibialis muscle stained for myosin ATPase after preincubation at pH 4.1, pH 4.3 and pH 10.4 in mice fed a control, high saturated fat or high fat n-3 PUFA enriched diet.....	211
Figure 3.21. Serial sections of the plantaris muscle stained for myosin ATPase after preincubation at pH 4.1, pH 4.3 and pH 10.4 in mice fed a control, high saturated fat or high fat n-3 PUFA enriched diet	212
Figure 3.22. Serial sections of the gastrocnemius lateralis muscle stained for myosin ATPase after preincubation at pH 4.1, pH 4.3 and pH 10.4 in mice fed a control, high saturated fat or high fat n-3 PUFA enriched diet	213
Figure 3.23. Serial sections of the gastrocnemius medialis muscle stained for myosin ATPase after preincubation at pH 4.1, pH 4.3 and pH 10.4 in mice fed a control, high saturated fat or high fat n-3 PUFA enriched diet	214

Figure 3.24. Representative images of the tibialis, plantaris and gastrocnemius muscles stained for SDH in mice fed a control, high saturated fat or high fat n-3 PUFA enriched diet.....	216
Figure 3.25. Representative images of the tibialis, plantaris and gastrocnemius muscles stained for NADH-TR in mice fed a control, high saturated fat or high fat n-3 PUFA enriched diet	217
Table 4.1. The sequence, assigned product size and optimised concentration (in reverse multiplex mix) of primers used to determine the mRNA content of key genes of interest in skeletal muscle samples	238
Figure 4.1 [A-D]. Resultant peaks of separated PCR products detected using the GenomeLab GeXP Genetic Analysis System during singlet primer testing. Singlet primer testing was successful if product was separated as a single well-defined peak at the assigned size [A, B], and unsuccessful if product was separated and unassigned peaks were generated [C, D]	240
Figure 4.2. Resultant peaks of separated PCR products detected using the GenomeLab GeXP Genetic Analysis System during multiplex primer testing	241
Figure 4.3. Description of multiplex reverse transcription and PCR reactions using the GenomeLab GeXP Genetic Analysis System	244
Figure 4.4. FAT/CD36 mRNA content in the white extensor digitorum longus and red soleus muscles of male and female mice fed control, high saturated fat or high fat n-3 PUFA enriched diets.....	249
Figure 4.5. FABPpm mRNA content in the white extensor digitorum longus and red soleus muscles of male and female mice fed control, high saturated fat or high fat n-3 PUFA enriched diets.....	250
Figure 4.6. FATP1 mRNA content in the white extensor digitorum longus and red soleus muscles of male and female mice fed control, high saturated fat or high fat n-3 PUFA enriched diets	251
Figure 4.7. FATP4 mRNA content in the white extensor digitorum longus and red soleus muscles of male and female mice fed control, high saturated fat or high fat n-3 PUFA enriched diets	252
Figure 4.8. SREBF1 mRNA content in the white extensor digitorum longus and red soleus muscles of male and female mice fed control, high saturated fat or high fat n-3 PUFA enriched diets.....	256

Figure 4.9. INSIG1 mRNA content in the white extensor digitorum longus and red soleus muscles of male and female mice fed control, high saturated fat or high fat n-3 PUFA enriched diets.....	257
Figure 4.10. DGAT1 mRNA content in the white extensor digitorum longus and red soleus muscles of male and female mice fed control, high saturated fat or high fat n-3 PUFA enriched diets.....	258
Figure 4.11. SCD1 mRNA content in the white extensor digitorum longus and red soleus muscles of male and female mice fed control, high saturated fat or high fat n-3 PUFA enriched diets	259
Figure 4.12. HSL mRNA content in the white extensor digitorum longus and red soleus muscles of male and female mice fed control, high saturated fat or high fat n-3 PUFA enriched diets	260
Figure 4.13. Correlations of plasma glucose concentrations with skeletal muscle DGAT1 mRNA content in mice exposed to a high saturated fat diet	261
Figure 4.14. PDK4 mRNA content in the white extensor digitorum longus and red soleus muscles of male and female mice fed control, high saturated fat or high fat n-3 PUFA enriched diets	267
Figure 4.15. AMPKα1 mRNA content in the white extensor digitorum longus and red soleus muscles of male and female mice fed control, high saturated fat or high fat n-3 PUFA enriched diets.....	268
Figure 4.16. AMPKα2 mRNA content in the white extensor digitorum longus and red soleus muscles of male and female mice fed control, high saturated fat or high fat n-3 PUFA enriched diets.....	269
Figure 4.17. ACC-β mRNA content in the white extensor digitorum longus and red soleus muscles of male and female mice fed control, high saturated fat or high fat n-3 PUFA enriched diets.....	270
Figure 4.18. CPT1b mRNA content in the white extensor digitorum longus and red soleus muscles of male and female mice fed control, high saturated fat or high fat n-3 PUFA enriched diets.....	271
Figure 4.19. UCP2 mRNA content in the white extensor digitorum longus and red soleus muscles of male and female mice fed control, high saturated fat or high fat n-3 PUFA enriched diets	272

Figure 4.20. UCP3 mRNA content in the white extensor digitorum longus and red soleus muscles of male and female mice fed control, high saturated fat or high fat n-3 PUFA enriched diets	273
Figure 4.21. SIRT1 mRNA content in the white extensor digitorum longus and red soleus muscles of male and female mice fed control, high saturated fat or high fat n-3 PUFA enriched diets.....	274
Figure 4.22. PGC1α mRNA content in the white extensor digitorum longus and red soleus muscles of male and female mice fed control, high saturated fat or high fat n-3 PUFA enriched diets.....	275
Figure 4.23. PPARα mRNA content in the white extensor digitorum longus and red soleus muscles of male and female mice fed control, high saturated fat or high fat n-3 PUFA enriched diets.....	276
Figure 4.24. PPARδ/β mRNA content in the white extensor digitorum longus and red soleus muscles of male and female mice fed control, high saturated fat or high fat n-3 PUFA enriched diets.....	277
Figure 4.25. Relationships between liver fat content and the mRNA content of muscle oxidative genes in the soleus muscle of mice exposed to high fat overfeeding.....	278
Figure 4.26. Correlations of plasma triglyceride and glucose concentrations with skeletal muscle PPARα mRNA content in mice exposed to high fat overfeeding.....	279
Figure 4.27. Schematic diagram depicting the differential effects that consuming a high saturated fat diet or n-3 PUFA enriched high fat diet exert on fatty acid transport into skeletal muscle	285
Figure 4.28. Schematic diagram depicting the differential effects that consuming a high saturated fat diet or n-3 PUFA enriched high fat diet exert on fatty acid storage and lipogenesis in skeletal muscle	291
Figure 4.29. Schematic diagram depicting the mechanism by which high fat feeding induces a switch in fuel metabolism in skeletal muscle to reflect the increased availability of fatty acids	294
Figure 4.30. Schematic diagram depicting the mechanism behind the differential responses observed in pathways of skeletal muscle fatty acid utilisation with high saturated fat and high fat n-3 PUFA enriched diet feeding.....	300

Figure 4.31. Schematic diagram depicting the mechanism behind the differential responses observed in pathways of skeletal muscle fatty acid uptake, storage and utilisation with high saturated fat and high fat n-3 PUFA enriched diet feeding.....	306
Table 5.1. The sequence, assigned product size and optimised concentration (in reverse multiplex mix) of primers used to determine the mRNA content of key genes of interest in liver samples	316
Figure 5.1 [A-B]. FAT/CD36 [A] and FABPpm [B] mRNA content in the liver of male and female mice fed control, high saturated fat or high fat n-3 PUFA enriched diets	322
Figure 5.2 [A-B]. FATP2 [A] and FATP5 [B] mRNA content in the liver of male and female mice fed control, high saturated fat or high fat n-3 PUFA enriched diets.....	323
Figure 5.3. The relationships between liver fat content and the hepatic mRNA content of fatty acid transporters FAT/CD36 and FATP2	324
Figure 5.4 [A-B]. SREBF1 [A] and INSIG1 [B] mRNA content in the liver of male and female mice fed control, high saturated fat or high fat n-3 PUFA enriched diets.....	327
Figure 5.5 [A-B]. FAS [A] and ACC-α [B] mRNA content in the liver of male and female mice fed control, high saturated fat or high fat n-3 PUFA enriched diets.....	328
Figure 5.6 [A-B]. DGAT2 [A] and SCD1 [B] mRNA content in the liver of male and female mice fed control, high saturated fat or high fat n-3 PUFA enriched diets.....	329
Figure 5.7. HSL mRNA content in the liver of male and female mice fed control, high saturated fat or high fat n-3 PUFA enriched diets.....	330
Figure 5.8. The relationship between plasma triglyceride concentrations and the hepatic mRNA content of DGAT2.....	331
Figure 5.9. PDK4 mRNA content in the liver of male and female mice fed control, high saturated fat or high fat n-3 PUFA enriched diets.....	335
Figure 5.10 [A-B]. AMPKα1 [A] and AMPKα2 [B] mRNA content in the liver of male and female mice fed control, high saturated fat or high fat n-3 PUFA enriched diets	336

Figure 5.11 [A-B]. ACC-β [A] and CPT1a [B] mRNA content in the liver of male and female mice fed control, high saturated fat or high fat n-3 PUFA enriched diets.....	337
Figure 5.12 [A-B]. UCP2 [A] and SIRT1 [B] mRNA content in the liver of male and female mice fed control, high saturated fat or high fat n-3 PUFA enriched diets.....	338
Figure 5.13 [A-B]. PGC1α [A] and PPARα [B] mRNA content in the liver of male and female mice fed control, high saturated fat or high fat n-3 PUFA enriched diets.....	339
Figure 5.14 [A-B]. PPARδ/β [A] and PPARγ [B] mRNA content in the liver of male and female mice fed control, high saturated fat or high fat n-3 PUFA enriched diets	340
Figure 5.15. The relationships between plasma glucose concentrations and the hepatic mRNA content of PDK4 in high saturated fat-fed mice and between body weight and the hepatic mRNA content of UCP2 in mice fed a high fat n-3 PUFA enriched diet	341
Figure 5.16. Schematic diagram depicting the differential effects that consuming a high saturated fat diet or n-3 PUFA enriched HFD exert on fatty acid transport into the hepatocyte.....	347
Figure 5.17. Schematic diagram depicting the differential effects that consuming a high saturated fat diet or n-3 PUFA enriched high fat diet exert on fatty acid storage and lipogenesis in the liver.....	354
Figure 5.18. Schematic diagram depicting the mechanism by which feeding a high fat diet enriched with n-3 PUFAs may induce a switch in fuel metabolism in the liver to reflect the increased availability of fatty acids and by which exposure to saturated fats fails to increase pyruvate dehydrogenase kinase activity	364
Figure 5.19. Schematic diagram depicting the mechanism behind the differential responses observed in pathways of hepatic fatty acid utilisation with high saturated fat and high fat n-3 PUFA enriched diet feeding	365
Figure 5.20. Schematic diagram depicting the mechanism behind the differential responses observed in pathways of hepatic fatty acid uptake, storage and utilisation with high saturated fat and high fat n-3 PUFA enriched diet feeding.....	370

Figure 6.1. HK2 mRNA content in the white extensor digitorum longus and red soleus muscles of male and female mice fed control, high saturated fat or high fat n-3 PUFA enriched diets	380
Figure 6.2. Correlations between HK2 mRNA content in the EDL muscle with the amount of liver glycogen and fat in mice exposed to a high saturated fat diet	381
Figure 6.3. GCK mRNA content in the liver of male and female mice fed control, high saturated fat or high fat n-3 PUFA enriched diets	382
Figure 6.4. PFK-M mRNA content in the white extensor digitorum longus and red soleus muscles of male and female mice fed control, high saturated fat or high fat n-3 PUFA enriched diets.....	384
Figure 6.5. PFK-L mRNA content in the liver of male and female mice fed control, high saturated fat or high fat n-3 PUFA enriched diets.....	385
Figure 6.6. GYS1 mRNA content in the white extensor digitorum longus and red soleus muscles of male and female mice fed control, high saturated fat or high fat n-3 PUFA enriched diets	387
Figure 6.7. GYS2 mRNA content in the liver of male and female mice fed control, high saturated fat or high fat n-3 PUFA enriched diets	388
Figure 6.8. PEPCK mRNA content in the liver of male and female mice fed control, high saturated fat or high fat n-3 PUFA enriched diets.....	390
Figure 6.9. PI3Kr1 mRNA content in the white extensor digitorum longus and red soleus muscles of male and female mice fed control, high saturated fat or high fat n-3 PUFA enriched diets	393
Figure 6.10. Relationship between the plasma glucose concentration and mRNA content of PI3Kr1 in the soleus muscle of mice exposed to a high saturated fat diet	394
Figure 6.11. SOCS3 mRNA content in the white extensor digitorum longus and red soleus muscles of male and female mice fed control, high saturated fat or high fat n-3 PUFA enriched diets.....	395
Figure 6.12. SOCS3 mRNA content in the liver of male and female mice fed control, high saturated fat or high fat n-3 PUFA enriched diets.....	396

Figure 6.13. Correlation between hepatic SOCS3 mRNA content and the plasma concentration of glucose in mice exposed to a high saturated fat diet	397
Figure 6.14. Schematic diagram depicting the mechanism behind the differential responses observed in pathways of skeletal muscle glucose metabolism with high saturated fat and high fat n-3 PUFA enriched diet feeding	418
Figure 6.15. Schematic diagram depicting the mechanism behind the differential responses observed in pathways of hepatic glucose metabolism with high saturated fat and high fat n-3 PUFA enriched diet feeding	419

COMMON ABBREVIATIONS

A

A	adenine
ACC- α	acetyl-Coenzyme A carboxylase- α
ACC- β	acetyl-Coenzyme A carboxylase- β
<i>Ad libitum</i>	to any desired extent
AICAR	5-aminoimidazole-4-carboxamide-riboside
ALA	α -linoleic acid
AMP	adenosine monophosphate
AMPK α 1	AMP-activated protein kinase catalytic subunit α 1
AMPK α 2	AMP-activated protein kinase catalytic subunit α 2
ANOVA	analysis of variance
ATGL	adipose triglyceride lipase
ATP	adenosine triphosphate
ATPase	adenosine triphosphatase
AU	arbitrary units

B

BMI	body mass index
bp	base pairs

C

C	control diet (standard laboratory diet)
C	cytosine
cDNA	complimentary deoxyribonucleic acid
cm	centimetres
CPT1a	carnitine palmitoyl transferase 1a
CPT1b	carnitine palmitoyl transferase 1b
CoA	coenzyme A

D

DAG	diacylglycerol
DGAT	diacylglycerol acyltransferase
DHA	docosahexaenoic acid
DIO	diet-induced obesity
DNA	deoxyribonucleic acid
DPA	docosapentaenoic acid

E

EDL	extensor digitorum longus muscle
EDTA	ethylenediaminetetraacetic acid
ELISA	enzyme linked immunosorbent assay
EPA	eicosapentaenoic acid

F

F	female
FA	fatty acid
FABPpm	fatty acid binding protein
FADH ₂	flavin adenine dinucleotide (reduced form)
FAS	fatty acid synthase
FAT/CD36	fatty acid translocase
FATP1	fatty acid transport protein 1
FATP2	fatty acid transport protein 2
FATP4	fatty acid transport protein 4
FATP5	fatty acid transport protein 5
FG	fast-twitch glycolytic
FOG	fast-twitch oxidative-glycolytic
FSANZ	Food Standards Australia New Zealand

G

g	grams
G	guanine
GAST LAT	gastrocnemius lateralis
GAST MED	gastrocnemius medialis
GCK	glucokinase
GLUT	glucose transporter
GYS1	glycogen synthase 1
GYS2	glycogen synthase 2

H

H&E	haematoxylin and eosin
HFD	high fat diet
HF-n-3	high fat n-3 polyunsaturated fatty acid enriched diet
HF-S	high saturated fat diet
HK2	hexokinase 2
HSL	hormone sensitive lipase
Hz	hertz

I

IMM	inner mitochondrial membrane
INSIG1	insulin induced gene 1
<i>In situ</i>	in the place where it occurs
IRS	insulin receptor substrate

J

JAK/STAT	Janus kinase/signal transducer and activation of transcription
----------	--

K

kg kilograms

L

L litre

LACS long chain acyl-CoA synthetase

M

M moles per litre

M male

mg milligrams

MJ megajoules

mL millilitres

mm millimetres

mM millimoles per litre

mmol/L millimoles per litre

mol/L moles per litre

mRNA messenger ribonucleic acid

MUFA monounsaturated fatty acid

N

NADH nicotinamide adenine dinucleotide (reduced form)

NADH-TR NADH tetrazolium reductase

NADP, NADPH nicotinamide adenine dinucleotide phosphate

NAFLD non-alcoholic fatty liver disease

ng nanograms

NHMRC National Health and Medical Research Council

nm nanometres

nM nanomoles per litre

O

OD	optical density
OMM	outer mitochondrial membrane

P

PAS	periodic acid-Schiff
PCR	polymerase chain reaction
PDK4	pyruvate dehydrogenase kinase 4
PDPK1	3-phosphoinositide-dependent protein kinase 1
PEPCK	phosphoenolpyruvate carboxykinase
PFK-L	phosphofructokinase - liver isoform
PFK-M	phosphofructokinase - muscle isoform
PGC1 α	peroxisome proliferative activated receptor γ coactivator 1 α
PI3K α 1	phosphatidylinositol 3-kinase, regulatory subunit, polypeptide 1
PIP2	phosphoinositol-4,5-bisphosphate
PIP3	phosphoinositol-3,4,5-triphosphate
PKB	protein kinase B
PKC	protein kinase C
PLAN	plantaris muscle
pmol/L	picomoles per litre
POLR2c	RNA Polymerase 2c
PPAR α	peroxisome proliferator activator receptor α
PPAR δ/β	peroxisome proliferator activator receptor δ/β
PPAR γ	peroxisome proliferator activator receptor γ
PPRE	peroxisome proliferator activator receptor response element
PUFA	polyunsaturated fatty acid

Q, R

r	pearson correlation coefficient
RECT FEM	rectus femoris muscle
RNA	ribonucleic acid
RPLP0	large ribosomal protein P0
rpm	revolutions per minute
rfu	relative fluorescence units

S

S1P	site-1 protease
S2P	site-2 protease
SCAP	SREBP cleavage-activating protein
SCD1	stearoyl-Coenzyme A desaturase 1
SDH	succinic dehydrogenase
SEM	standard error of the mean
SFA	saturated fatty acid
SIRT1	sirtuin 1
SLC27	solute carrier family 27
SO	slow-twitch oxidative
SOCS3	suppressor of cytokine signalling 3
SOL	soleus muscle
SPSS	statistical package for social scientists
SREBF1	sterol regulatory element binding transcription factor 1

T

T	tyrosine
TBP	TATA-binding protein
TG	triglyceride
TGH	triglyceride hydrolase
TIB	tibialis muscle
TMB	tetramethylbenzidine

U

UCP2	uncoupling protein 2
UCP3	uncoupling protein 3
U/mL	units per millilitre

V, W, X, Y

VAST INT	vastus lateralis intermedius
VAST LAT	vastus lateralis muscle
VAST MED	vastus medialis muscle
ver.	version

Z

ZDF	obese insulin resistant Zucker rat
-----	------------------------------------

Symbols

°C	degrees Celcius
µg	micrograms
µl	microlitres
µm	micrometres
≤	less than or equal to
>	greater than or equal to
~	approximately

ABSTRACT

Australian adults consume ~6% above the recommended intake of saturated fat and less than half the recommended daily amount of n-3 polyunsaturated fatty acids (PUFA). There is some evidence that the type and proportion of dietary fat consumed may influence the development of the obese phenotype and associated metabolic complications.

Epidemiological studies indicate that a saturated fat-rich diet (HF-S) is deleterious, whilst consuming n-3 PUFAs is beneficial to metabolic health. Saturated fats have a greater propensity to enter storage in adipose tissue and ectopic stores, as opposed to being oxidised. This is deleterious as ectopic fat deposition in skeletal muscle and liver are strongly associated with insulin resistance. In contrast, diets rich in n-3 PUFA limit adipose tissue hypertrophy, reduce ectopic fat and prevent high fat diet (HFD)-induced insulin resistance in rats. However, the mechanism by which n-3 PUFA enrichment of a HF-S diet (HF-n-3) prevents ectopic fat deposition in muscle and liver is unclear; though pathways of fatty acid uptake, storage and oxidation may be implicated. Furthermore, in skeletal muscle a functional shift in fibre type may be implicated, as increased muscle n-3 PUFA content is associated with an increased proportion of oxidative fibres. The studies in this thesis therefore aimed to determine: (I) the effect of HFD fatty acid composition on metabolic profile, adipose tissue distribution, and muscle fibre type composition of male and female mice; (II) if HF-n-3 feeding influenced the mRNA content of 27 key genes that regulate the uptake (FAT/CD36, FABPpm, FATP), synthesis and storage (SREBF, INSIG, SCD, ACC, DGAT, HSL) and utilisation (PDK, PPAR, PGC1, AMPK, ACC, CPT1, UCP) of fatty acids and

metabolism of glucose (HK, PFK, GYS) in the glycolytic extensor digitorum longus muscle, oxidative soleus muscle and liver of male and female mice. To assess these aims mice were fed either a control diet (16% energy from fat) or one of two HFDs (60% energy from fat), a HF-S or HF-n-3 (7.5% saturated fat replaced with n-3 PUFA) diet. I investigated the hypothesis that HF-n-3 feeding prevents ectopic fat deposition through enhanced uptake and utilisation, and reduced storage, of fatty acids.

Despite similarly increased body weight with both HFDs, mesenteric fat mass decreased and brown fat increased with HF-n-3 feeding compared to HF-S feeding. HF-S feeding increased muscle and liver fat content; this was ameliorated by HF-n-3. As hypothesised, HF-n-3 feeding may ameliorate intramyocellular and intrahepatic fat accumulation through an altered pattern of fatty acid metabolism gene expression in those tissues, specifically through the concurrent activation of pathways regulating fatty acid transport and utilisation, whilst limiting pathways that promote fatty acid storage and lipogenesis. Muscle fibre type composition was unchanged with diet, although HF-n-3 feeding increased muscle oxidative capacity. HF-S mice exhibited increased plasma insulin and glucose metabolism was influenced by HF-n-3 feeding in a tissue-specific manner. These studies highlight the importance of gender and in skeletal muscle, muscle fibre type, to the overall characteristics, profile of gene expression and ultimate function of the skeletal muscle and liver.

DECLARATION

This work contains no material which has been accepted for the award of any other degree or diploma in any university or other tertiary institution to Lisa Kate Philp, and to the best of my knowledge and belief, contains no material previously published or written by another person, except where due reference has been made in the text.

I give consent to this copy of my thesis, when deposited in the University Library, being made available for loan and photocopying, subject to the provisions of the Copyright Act 1968.

The author acknowledges that copyright of published works contained within this thesis (as listed below*) resides with the copyright holder(s) of those works.

I also give permission for the digital version of my thesis to be made available on the web, via the University's digital research repository, the Library catalogue and also through web search engines, unless permission has been granted by the University to restrict access for a period of time.

Signed:

Date:

.....

.....

Lisa Kate Philp

RELATED PUBLICATIONS

Journal Publications

Philp LK, Janovska A, Heilbronn LK, Hatzinikolas G, Mayrhofer G, Wittert GA. (2011) High saturated fat diet enrichment with n-3 PUFA ameliorates intramyocellular fat accretion through pathways that induce fat oxidation and limit fat storage. In preparation.

Philp LK, Janovska A, Heilbronn LK, Hatzinikolas G, Mayrhofer G, Wittert GA. (2011) Omega-3 fatty acid enrichment prevents high saturated fat induced fatty liver in mice by limiting pathways of lipogenesis and storage. In preparation.

Philp LK, Janovska A, Heilbronn LK, Hatzinikolas G, Mayrhofer G, Wittert GA. (2011) Effect of dietary fatty acid content on muscle fibre type composition in predominantly fast-twitch and slow-twitch skeletal muscles. In preparation.

Published Abstracts

Philp LK, Janovska A, Heilbronn L, Mayrhofer G, Wittert GA. (2011) n-3 PUFA Enrichment of a High Saturated Fat Diet Enhances Muscle Oxidative Capacity without Affecting Muscle Fibre Type. *Obesity Research and Clinical Practice* 5 (Suppl 1) S32. Impact Factor: 0.375.

Philp LK, Janovska A, Hatzinikolas G, Heilbronn L, Mayrhofer G, Wittert GA. (2010) n-3 Enrichment of a High Saturated Fat Diet Ameliorates Hepatic Fat Accretion Through Pathways that Limit Fat Storage and Lipogenesis. *Obesity Research and Clinical Practice* 4 (Suppl 1) S5. Impact Factor: 0.375.

Philp LK, Janovska A, Mayrhofer G, Wittert GA. (2010) Omega-3 Enrichment of a High Saturated Fat Diet Ameliorates Intramyocellular Fat Accumulation Through Pathways that Increase Fatty Acid Oxidation and Limit Fat Storage. *Obesity Reviews* 11 (Suppl 1) 160. Impact Factor: 5.086.

Conference Proceedings

Philp LK, Janovska A, Heilbronn L, Mayrhofer G, Wittert GA. (2011) n-3 PUFA Enrichment of a High Saturated Fat Diet Enhances Muscle Oxidative Capacity without Affecting Muscle Fibre Type.

Australian and New Zealand Obesity Society 19th Annual Meeting, Adelaide, South Australia, Australia.

Oral Presentation (National Conference).

Philp LK, Janovska A, Heilbronn L, Mayrhofer G, Wittert GA. (2011) n-3 PUFA Enrichment of a High Saturated Fat Diet Enhances Muscle Oxidative Capacity without Affecting Muscle Fibre Type.

Faculty of Health Sciences, University of Adelaide, 5th Annual Postgraduate Research Expo, Adelaide, South Australia, Australia.

Poster Presentation (Local Conference).

Philp LK, Janovska A, Hatzinikolas G, Heilbronn L, Mayrhofer G, Wittert GA. (2010) n-3 Enrichment of a High Saturated Fat Diet Ameliorates Hepatic Fat Accretion Through Pathways that Limit Fat Storage and Lipogenesis.

Australian and New Zealand Obesity Society 18th Annual Meeting, Sydney, New South Wales, Australia.

Poster Presentation (National Conference).

Philp LK, Janovska A, Hatzinikolas G, Heilbronn L, Mayrhofer G, Wittert GA. (2010) n-3 Enrichment of a High Saturated Fat Diet Ameliorates Hepatic Fat Accretion Through Pathways that Limit Fat Storage and Lipogenesis.

Faculty of Health Sciences, University of Adelaide, 4th Annual Postgraduate Research Expo, Adelaide, South Australia, Australia.

Poster Presentation (Local Conference).

Philp LK, Janovska A, Mayrhofer G, Wittert GA. (2010) Omega-3 Enrichment of a High Saturated Fat Diet Ameliorates Intramyocellular Fat Accumulation Through Pathways that Increase Fatty Acid Oxidation and Limit Fat Storage.

XI International Congress on Obesity, ICO 2010, Stockholm, Sweden.

Poster Presentation (International Conference).

Philp LK, Janovska A, Mayrhofer G, Wittert GA. (2010) Omega-3 Enrichment of a High Saturated Fat Diet Ameliorates Intramyocellular Fat Accumulation Through Pathways that Increase Fatty Acid Oxidation and Limit Fat Storage.

Australian Society for Medical Research, ASMR Medical Research Week Scientific Meeting 2010, Adelaide, South Australia, Australia.

Oral Presentation (Local Conference).

Philp LK, Janovska A, Hatzinikolas G, Mayrhofer G, Wittert GA. (2009) The Effect of a High Saturated Fat and High Fat N-3 Enriched Diets on Fatty Acid Metabolism in Mice.

Australian and New Zealand Obesity Society 17th Annual Meeting, Melbourne, Victoria, Australia.

Oral Presentation (National Conference).

Philp LK, Janovska A, Hatzinikolas G, Mayrhofer G, Wittert GA. (2009) The Effect of High Saturated and High n-3 Polyunsaturated Fat Diets on Obesity in Mice. World Congress on Oils and Fats and 28th ISF Congress, Sydney, New South Wales, Australia.

Oral Presentation (International Conference).

Philp LK, Janovska A, Hatzinikolas G, Mayrhofer G, Wittert GA. (2009) The Effect of High Saturated and High n-3 Polyunsaturated Fat Diets on Obesity in Mice. Faculty of Health Sciences, University of Adelaide, 3rd Annual Postgraduate Research Expo, Adelaide, South Australia, Australia.

Poster Presentation (Local Conference).

Philp LK, Janovska A, Hatzinikolas G, Mayrhofer G, Wittert GA. (2009) The Effect of High Saturated and High n-3 Polyunsaturated Fat Diets on Obesity in Mice. Australian Society for Medical Research, ASMR Medical Research Week Scientific Meeting 2009, Adelaide, South Australia, Australia.

Poster Presentation (Local Conference).

Philp LK, Janovska A, Hatzinikolas G, Mayrhofer G, Wittert GA. (2008) The Effect of a High Saturated and High Polyunsaturated Fat Diets on Obesity in Mice. The 4th Australian Health and Medical Research Congress – Australian and New Zealand Obesity Society, Brisbane, Queensland, Australia.

Oral Presentation (National Conference).

Philp LK, Janovska A, Hatzinikolas G, Mayrhofer G, Wittert GA. (2008) The Effect of a High Saturated and High Polyunsaturated Fat Enriched Diets on Obesity in Mice. Faculty of Health Sciences, University of Adelaide, 2nd Annual Postgraduate Research Expo, Adelaide, South Australia, Australia.

Poster Presentation (Local Conference).

ACKNOWLEDGEMENTS

Firstly, I wish to express sincere appreciation to my supervisors, Professor Gary Wittert, Associate Professor Graham Mayrhofer, Dr Alena Janovska and Associate Professor Leonie Heilbronn. To Gary, thank you for being there when I needed guidance and encouragement but also for allowing me the room to grow, because of which, I believe I have become a more independent scientist. My sincere thanks Gary; it has been a rewarding experience. To Graham, Alena and Leonie, thank you for your support, guidance and knowledge. Also, thanks to Alena for your expert assistance with animal surgery.

Many thanks to the Wittert lab team, Yan Lam, Paul Cavuoto and George Hatzinikolas. It was great sharing my time in the lab with you and I thank you for your assistance and support.

Thanks to the many people with whom I have shared an office during my PhD, Paul Cavuoto, Diana Gentilcore, Radhika Seimon, Amy Ryan, Lora Vanis, Kylie Lange, Ixchel Brennan, Kate Feltrin and Kamilia Tai. It has been interesting seeing the office dynamic change with all the comings and goings over the years. You have all definitely made PhD life more interesting.

Thanks to the many helpful people in the research community who have taken time out of their day to teach me methodology or to help me with equipment. In particular, thanks to Mark Salkeld (Circadian Physiology Laboratory, Research Centre for Reproductive Health, Adelaide) for all your help with the GeXP; to Silke Kantimm (Dame Roma Mitchell Cancer Research Laboratories, IMVS/Hanson Institute,

Adelaide) for teaching me Oil Red O and H&E staining; to Candita Sullivan and Mark Mano (CSIRO Human Nutrition, Adelaide) for their help with the COBAS machine; to Cathy Cash (Neuropathology Laboratory, Hanson Institute, Adelaide) for teaching me the fine art of skeletal muscle sectioning and PAS staining; and to the staff at the Detmold facility (Hanson Institute, Adelaide), particularly to Alan and Katherine, for their assistance with the NanoZoomer.

I would like to acknowledge Nu-mega Ingredients Pty Ltd, Nathan, Queensland, Australia, for generously donating the HiDHA[®] 25N tuna oil and to Australian Biostain Pty Ltd, Traralgon, Victoria, Australia, for kindly supplying the Lillie-Mayer Haematoxylin.

Above all, I would like to thank my support group of family and friends. Thank you for always being there for me, your unwavering devotion is truly appreciated. Without your love and encouragement I may never have finished this PhD, thank you for sharing this journey with me, for supporting me through the lows, and for celebrating with me during the highs. A special thanks to my mum, for always believing in me, for always encouraging me to follow my dreams and for always recognising my potential; you have and always will be my rock.

CHAPTER 1

Literature Review

1.1 – OBESITY – AN OVERVIEW

1.1.1 – The Obesity Epidemic - Of Growing Concern

Worldwide, obesity is reaching epidemic proportions (Greenberg and Obin, 2006). Globally there are estimated to be approximately 1.6 billion overweight adults (with body mass index (BMI) $>25 \text{ kg/m}^2$) and approximately 400 million of these people are obese (BMI $>30 \text{ kg/m}^2$; World Health Organisation (WHO) estimates (WHO, 2010)). Alarming, this estimated prevalence is predicted to grow to a massive 2.3 billion overweight and 700 million obese adults globally by 2015 (WHO, 2010). Australian adults are no exception, reportedly 60% of adults are overweight or obese (Thorburn, 2005), however more recent predictions have exceeded these reported values, with an estimated prevalence of 75.7% of male and 66.5% of female adult Australians exhibiting a BMI over 25 kg/m^2 (Ono *et al.*, 2010). The rising prevalence of obesity is not only a problem confined to the adult population, the incidence of obesity in young people is also escalating, with 20-25% of Australian children and adolescents overweight or obese (Batch and Baur, 2005). The obesity epidemic is of great concern as obese people often develop insulin resistance (Guilherme *et al.*, 2008), hypertension (Lopaschuk *et al.*, 2007; Dickerson and Carek, 2000), hypercholesterolemia and hypertriglyceridemia (Mooradian *et al.*, 2008; Greenberg and Obin, 2006; Mokdad *et al.*, 2003) and are at greater risk of developing type 2 diabetes mellitus (Guilherme *et al.*, 2008; Dickerson and Carek, 2000), metabolic syndrome (Liberopoulos *et al.*, 2005) and cardiovascular disease (Lopaschuk *et al.*, 2007).

1.1.2 – Obesity –Influencing Factors and Sites of Metabolic Dysfunction

At a molecular level, the obese phenotype results from the interaction of environmental factors (Greenberg and Obin, 2006; Astrup *et al.*, 2004) and genetic variation (Greenberg and Obin, 2006). Environmental variables, among many others, include increased consumption of energy-dense foods (Drewnowski, 2007), high fat intake (Drewnowski, 2007; Bray and Popkin, 1998), larger portion sizes (Drewnowski, 2007) and reduced physical activity (Greenberg and Obin, 2006; Astrup *et al.*, 2004). Altered gene expression (up- or down-regulation) and genetic variation (polymorphisms) have also been linked to obesity (Greenberg and Obin, 2006; Astrup *et al.*, 2004).

Not only is obesity influenced by multiple factors, but its development can result from metabolic dysfunction at multiple sites, both central and peripheral, which mediate many different pathways regulating energy intake, energy expenditure and intermediary metabolism. In the periphery, key organs involved in controlling energy homeostasis are the adipose tissue, skeletal muscle and liver.

1.2 – KEY PERIPHERAL TISSUES INVOLVED IN ENERGY HOMEOSTASIS

Maintaining a balance between energy supply and demand is a fundamental process in all living organisms. In today's Western society the failure to regulate energy metabolism and maintain the appropriate balance between energy supply and demand is evident in the increasing prevalence of metabolic disorders, including overweight, obesity and type 2 diabetes (Carling, 2005). As mentioned above, in the periphery, key sites of metabolic dysfunction are the adipose tissue, skeletal muscle and liver.

1.2.1 – Adipose Tissue - A Role in Energy Balance

Adipose tissue is the main location of fat storage and is not just a neutral store for fat, but also acts to secrete adipokines, for example, leptin and adiponectin, which act both peripherally and centrally, to regulate energy balance (Greenberg and Obin, 2006).

1.2.2 – Skeletal Muscle - A Role in Energy Balance

The regulation of energy balance is a fundamental process. Particularly in skeletal muscle, maintaining a balance between energy supply and demand is essential for normal function (Carling, 2005). Skeletal muscle makes up to approximately 40% of body weight and is of varying metabolic rate, with lower energy consumption at rest and times of great energy demand, e.g. muscle contraction (Bonen *et al.*, 2002), hence the skeletal muscle is a major tissue involved in maintaining energy homeostasis. Glucose and fatty acids are the predominant metabolites used by skeletal muscle in energy production (Carling, 2005; Winder and Hardie, 1999). At rest and during exercise, skeletal muscle is the main site of fatty acid oxidation (Jeukendrup, 2002); therefore, the skeletal muscle also plays a key role in maintaining lipid homeostasis (Bonen *et al.*, 2002). Furthermore, skeletal muscle is the chief site of glucose disposal (Liang and Ward, 2006). However, muscle fibre type plays a major role in determining the metabolic characteristics of the whole muscle.

1.2.2.1 – Skeletal Muscle Fibre Type Influences Muscle Metabolism

Furthermore, skeletal muscle is composed of subpopulations of fibres with distinct contractile and metabolic properties (Hickey *et al.*, 1995). Muscle fibres with a high

mitochondrial content, hence high oxidative capacity are termed red, slow-twitch oxidative (SO) or type I fibres. Those muscle fibres with high glycolytic enzyme content are termed white, fast-twitch glycolytic (FG) or type IIB fibres. A further subgroup with both high mitochondrial content and abundant glycolytic enzymes are fast-twitch oxidative-glycolytic (FOG) or type IIA fibres (Hickey *et al.*, 1995; Hintz *et al.*, 1980).

The composition of muscle fibres within the skeletal muscle has been shown to determine the dynamic characteristics of the whole-muscle. For example, fibre type influences muscle fatty acid concentration (including triglycerides, diacylglycerol (DAG) and free fatty acids). A study conducted by laboratory colleagues (Janovská *et al.*, 2010) demonstrated that the white FG-FOG extensor digitorum longus (EDL) muscle exhibits a different profile of phospholipid fatty acid content compared to the red SO soleus muscles in rats. Specifically, the EDL muscle contained greater C22:6 n-3 and C16:0 phospholipid fatty acids in preference to C18:0 when compared to the soleus muscle, whilst the soleus muscle exhibited greater preference for the C18 phospholipid fatty acids, in particular C18:0, C18:1 n-9 and C18:2 n-6 (Janovská *et al.*, 2010). Furthermore, muscle fibre composition has a degree of plasticity (Liu *et al.*, 2005). Hickey *et al.* (Hickey *et al.*, 1995) found fibre type in rectus abdominus muscle (mixed fibre type) to change with obesity. This study showed BMI to be inversely correlated to the percentage of type I fibres ($r = -0.50$, $P < 0.01$) (Hickey *et al.*, 1995). Further investigation illustrated that obese individuals had less type I fibres, and more type IIB fibres (vs. lean controls). Furthermore, the profile of fatty acids present in skeletal muscle is influenced by diet, as high fat overfeeding resulted in lower

membrane unsaturation in the soleus compared to the EDL muscle in rats and this is important to consider as greater membrane fatty acid saturation has been associated with insulin resistance (Janovská *et al.*, 2010).

1.2.3 – Liver - A Role in Energy Balance

The liver is the chief site for storage and release of carbohydrates and therefore plays a key role in maintaining whole-body glucose homeostasis (Long and Zierath, 2006). Furthermore, the liver is a key organ involved in fatty acid synthesis (Viollet *et al.*, 2006) and plays a role in various aspects of fatty acid metabolism (Canbay *et al.*, 2007). The liver contributes to the regulation of whole-body energy homeostasis, given its key roles in carbohydrate and fatty acid metabolism. Following a meal, glucose is driven toward hepatic glycogen storage, with excess carbohydrates being converted to triglycerides, in total promoting energy storage. During fasting, the liver undergoes metabolic processes promoting glucose output and lipolysis, maintaining energy balance (Viollet *et al.*, 2006). Energy balance is therefore required for normal whole-body function, and when this equilibrium between intake and expenditure becomes skewed, the result is metabolic dysfunction.

The liver is a key site of fatty acid processing, it receives dietary fatty acids and free fatty acids derived from adipose tissue lipolysis through the portal circulation and is the chief site of *de novo* lipogenesis, the synthesis of fatty acid from acetyl-Coenzyme A (CoA), a by-product of glucose metabolism (Postic and Girard, 2008; Reddy and Sambasiva Rao, 2006). The liver is also capable of some fatty acid disposal, through

oxidation and exporting processed fatty acids to peripheral tissues (Postic and Girard, 2008; Reddy and Sambasiva Rao, 2006). Given these roles, a normal healthy functioning liver is paramount in maintaining whole-body lipid homeostasis.

1.2.4 – Obesity Leads to Altered Lipid and Glucose Metabolism in Key Tissues of Energy Homeostasis

Obesity has been associated with dysfunctional lipid metabolism, including increased fatty acid uptake, reduced fatty acid oxidation and increased fatty acid esterification (Han *et al.*, 2007; Smith *et al.*, 2007; Chabowski *et al.*, 2006; Bruce *et al.*, 2005; Chen *et al.*, 2005; Thyfault *et al.*, 2004; Steinberg *et al.*, 2004; Luiken *et al.*, 2001; Berk *et al.*, 1997). The resultant intramuscular and intrahepatic triglyceride accumulation have been shown to be associated with reduced insulin sensitivity (Qureshi *et al.*, 2010; Marchesini *et al.*, 2003; Chitturi *et al.*, 2002; Manco *et al.*, 2000).

1.3 – FATTY ACID METABOLISM – CELLULAR FATTY ACID UPTAKE

In order for fatty acids to enter storage or be used as fuel they must be taken up into the cell through the plasma membrane, a step that constitutes one of the many rate-limiting steps of fatty acid metabolism. In the past, there have been divided opinions surrounding how fatty acids are transported into the cell, with some believing fatty acids enter only by passive diffusion and others considering a protein-mediated system to be an alternative method of fatty acid transport (Glatz *et al.*, 2010; Bonen *et al.*, 2004a). Although fatty acid influx into the cell may occur by passive diffusion, there is now strong evidence that fatty acids are taken up by the action of fatty acid transport

proteins (Bonen *et al.*, 2004a; Bonen *et al.*, 2003; Glatz *et al.*, 2002). Fatty acid translocase (FAT/CD36), plasma membrane fatty acid binding protein (FABPpm) and fatty acid transport proteins (FATP) have been identified as key players implicated in protein-mediated fatty acid transport in the skeletal muscle and liver (**Figure 1.1**).

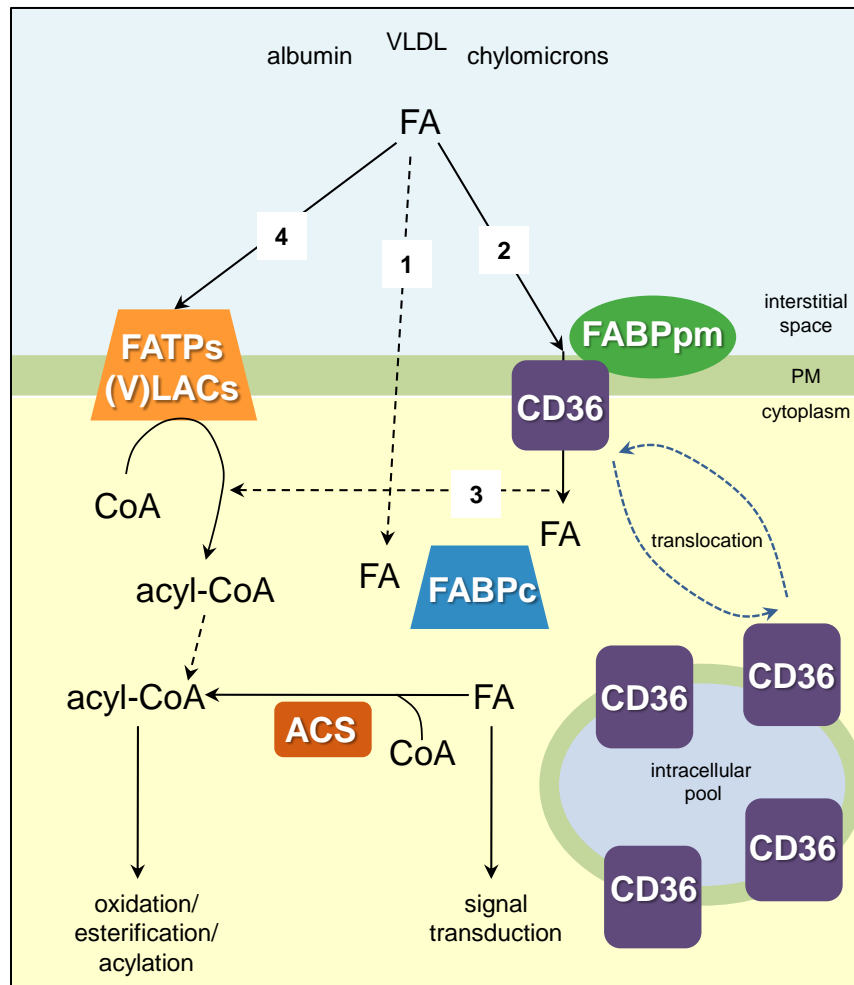


Figure 1.1. Schematic diagram of long chain fatty acid transport.

Numbers 1-4 depict proposed routes of long chain fatty acid uptake. Pathway 1 involves passive diffusion. Pathway 2 depicts the interaction of FAT/CD36 and FABPpm in protein-mediated fatty acid transport. Pathways 3 and 4 illustrate the proposed uptake of fatty acid through the interaction of FATP and FAT/CD36 (3) or directly through FATP across the plasma membrane (4). Once in the cytoplasm, long chain fatty acids are bound to FABPc or may be activated to form fatty acyl-CoA esters at the AMP binding site of FATP. Fatty acids may then enter metabolism or other pathways. Furthermore, there is evidence that fatty acid transporters are located in intracellular stores and translocate when stimulated, as depicted for FAT/CD36 (Koonen *et al.*, 2005).

CD36, fatty acid translocase (FAT/CD36); FATP, fatty acid transport protein; FABPpm, plasma membrane fatty acid binding protein; FABPc, cytoplasmic fatty acid binding protein; CoA, Coenzyme A; FA, fatty acid; (V)LACs (very) long chain acyl-CoA synthetase; ACS, acyl-CoA synthetase; PM, plasma membrane; VLDL, very low density lipoprotein.

1.3.1 – Fatty acid translocase (FAT/CD36)

FAT/CD36 is the best characterised protein involved in protein-mediated fatty acid transport and has been shown to play a role in the high-affinity uptake of long chain fatty acids (Goudriaan *et al.*, 2003; Ibrahimi *et al.*, 1996). FAT/CD36 is widely expressed, having been identified in the liver, adipose tissue, skeletal muscle, brain, heart, breast, intestine, skin, kidney and haematopoietic cells (Glatz *et al.*, 2010; Febbraio *et al.*, 2001). In skeletal muscle, the expression of FAT/CD36 is fibre type-dependent, being more highly expressed in red SO muscle as compared to white FG/FOG muscle (Chabowski *et al.*, 2006; Campbell *et al.*, 2001). In the liver FAT/CD36 expression is gender-dimorphic, with markedly greater expression in females as compared to males (Kano and Doi, 2006; Stahlberg *et al.*, 2004; Zhang *et al.*, 2003). Furthermore, FAT/CD36 is present in an intracellular pool and upon stimulation, by factors such as insulin and contraction, FAT/CD36 is recruited from this pool and translocates to the plasma membrane, allowing fatty acid uptake into the cell (Jain *et al.*, 2009; Bonen *et al.*, 2002). Transfecting FAT/CD36 into fibroblasts, which naturally do not express FAT/CD36 and normally exhibit low long chain fatty acid uptake, has been shown to markedly increase long chain fatty acid uptake (Ibrahimi *et al.*, 1996). Furthermore, overexpression of FAT/CD36 in skeletal muscle cells has been shown to significantly increase the rate of fatty acid uptake (Nickerson *et al.*, 2009). Whilst a null mutation in skeletal muscle FAT/CD36 has been shown to reduce fatty acid uptake into the muscle under basal conditions, and produce a blunted increase in uptake in response to insulin stimulation which is attributed in part through a compensatory increase in FATPs (Bonen *et al.*, 2007). Recent studies have shown

FAT/CD36 to also be present in mitochondria (Holloway *et al.*, 2006; Schenk and Horowitz, 2006). Mitochondrial FAT/CD36 coimmunoprecipitates with carnitine palmitoyl transferase I (CPT1), which acts to shuttle fatty acids into mitochondria (Schenk and Horowitz, 2006) and therefore in cooperation with CPT1, FAT/CD36 has been implicated in mitochondrial fatty acid uptake and in contributing to the regulation of mitochondrial fatty acid oxidation.

1.3.2 – Plasma membrane fatty acid binding protein (FABPpm)

FABPpm was first isolated in the rat liver in 1985 by Stremmel and colleagues (Stremmel *et al.*, 1985). FABPpm has been demonstrated to be located peripherally on the plasma membrane (Kiens, 2006) and is expressed in the skeletal muscle, liver, heart, intestine, adipose tissue and placenta (Glatz *et al.*, 2010; Han *et al.*, 2007; Chabowski *et al.*, 2004; Roepstorff *et al.*, 2004; Luiken *et al.*, 2001; Stump *et al.*, 1993). Similar to FAT/CD36, FABPpm exists in an intracellular pool from which it translocates, when stimulated, to the plasma membrane where it is colocalised with FAT/CD36 (Pelsers *et al.*, 2007; Bonen *et al.*, 2002). FABPpm has also been implicated in long chain fatty acid uptake, since FABPpm cDNA transfected into the soleus muscle concomitantly increases the abundance of sarcolemmal FABPpm and fatty acid uptake (Bonen *et al.*, 2003). Overexpression of FABPpm in giant sarcolemmal vesicles derived from skeletal muscle similarly increased the rate of fatty acid uptake (Nickerson *et al.*, 2009). In contrast, antibodies against the FABPpm protein inhibit long chain fatty acid uptake in hepatocytes (Stremmel *et al.*, 1986) and giant sarcolemmal vesicles derived from skeletal muscle (Turcotte *et al.*, 2000).

Furthermore, a null mutation of FABPpm in mice, partially inhibits skeletal muscle fatty acid uptake in the both the basal state and during contraction, as compared to wild-type mice (Binas *et al.*, 2003). In addition to its role in long chain fatty acid uptake, studies have demonstrated that FABPpm is identical to the mitochondrial enzyme, aspartate aminotransferase (Bonen *et al.*, 2003; Stump *et al.*, 1993).

1.3.3 – Fatty acid transport proteins (FATPs)

The first murine fatty acid transport protein (FATP1) was identified in 1994 by Schaffer and Lodish (Schaffer and Lodish, 1994) and to date, 6 highly homologous FATPs belonging to solute carrier family 27 (SLC27), have been identified (Stahl, 2004). Several studies have implicated FATPs in the cellular transport of long chain fatty acids (DiRusso *et al.*, 2005; Stahl, 2004; Hirsch *et al.*, 1998). FATPs have been identified in both the skeletal muscle and liver, in which the level of expression in rank order is FATP1>FATP4>FATP3 and FATP5>FATP2>FATP3>FATP4, respectively (Wu *et al.*, 2006). A common feature of all FATP genes is the AMP binding sequence at the beginning, followed by the FATP signature sequence (Stahl, 2004). Without this AMP binding motif, transport activity is inhibited (Stahl, 2004). Whilst several studies have added to the body of knowledge describing the functional characteristics of FATP proteins, further research is required to fully elucidate the role of each FATP in their respective tissues of expression. Of particular interest in the skeletal muscle are fatty acid transporters FATPs 1 and 4 (Jain *et al.*, 2009; Nickerson *et al.*, 2009), and in the liver, FATPs 2 and 5 (Falcon *et al.*, 2010; Doege *et al.*, 2006).

1.3.3.1 – FATP1 (*SLC27A1*)

FATP1 is most highly expressed in the heart, skeletal muscle and fat (Schaffer and Lodish, 1994) and is also present in the brain, kidney, skin, testes and lung (Glatz *et al.*, 2010; Hirsch *et al.*, 1998). Expression of FATP1 in skeletal muscle is fibre type-dependent, being more highly expressed in red SO muscle as compared to white FG muscle (Marotta *et al.*, 2004). Overexpression of FATP1 in skeletal muscle myotubes enhances the uptake of saturated fat, palmitate, and monounsaturated fatty acid, oleate, leading to an increased incorporation of fatty acids into triglyceride and phospholipid (García-Martínez *et al.*, 2005). Deletion of FATP1 (FATP1^{-/-} mice) does not, under basal conditions, alter the rate of fatty acid uptake into soleus muscle strips, but under insulin-stimulated conditions, the rate of fatty acid uptake into the soleus was blunted in FATP1^{-/-} compared to wild-type mice. Therefore FATP1 has been implicated in the insulin-stimulated uptake of long chain fatty acids (Wu *et al.*, 2006). Furthermore, under conditions of insulin stimulation and contraction, FATP1 protein translocates from the intracellular store to the plasma membrane (Jain *et al.*, 2009). FATP1 also exhibits long chain and very long chain acyl-CoA synthetase activity and is therefore believed to play a role in the activation of long chain and very long chain fatty acids by catalysing the covalent linking of a CoA molecule (Hall *et al.*, 2003; Coe *et al.*, 1999).

1.3.3.2 – FATP2 (*SLC27A2*)

FATP2 has been identified to be exclusively expressed in the liver, cortex of the kidney (Hirsch *et al.*, 1998) and small intestine (Glatz *et al.*, 2010; Hirai *et al.*, 2007). Whilst

FATP2 is mainly localised at the plasma membrane in hepatocytes, approximately 10% of total FATP2 protein is found in the peroxisome (Falcon *et al.*, 2010). In addition to its role as a fatty acid transporter (Hirsch *et al.*, 1998), FATP2 also exhibits long chain and very long chain acyl-CoA synthetase (LACS/VLACS) activity (Falcon *et al.*, 2010; Berger *et al.*, 1998; Hirsch *et al.*, 1998) and is therefore involved in activating long and very long chain fatty acids by attaching a CoA molecule (Falcon *et al.*, 2010; Doege *et al.*, 2006; Steinberg *et al.*, 1999). Knock-down of hepatic FATP2, resulting in an almost complete loss of FATP2 protein, has been shown to elicit a 40% reduction in fatty acid uptake *in vivo* and in high fat-fed rodents FATP2 knock-down leads to reduced hepatic triglyceride content (Falcon *et al.*, 2010).

1.3.3.3 – FATP4 (SLC27A4)

FATP4 is widely expressed and has been localised in the intestine, adipose tissue, skeletal muscle, heart, lung, brain, kidney, skin and liver (Glatz *et al.*, 2010; Wu *et al.*, 2006; Gimeno *et al.*, 2003; Hirsch *et al.*, 1998). One study has demonstrated that targeted deletion of FATP4 (FATP4^{-/-} mice) results in early embryonic fatality and FATP4 is therefore required to meet fat absorption requirements during embryonic development (Gimeno *et al.*, 2003). Other studies have similarly shown that targeted deletion of FATP4 results in neonatal mortality shortly after birth, which may, in part, be attributed to abnormal epidermal barrier function and transcutaneous water loss (Moulson *et al.*, 2003; Herrmann *et al.*, 2003). FATP4 overexpression increases the rate of palmitate transport in giant sarcolemmal vesicles derived from skeletal muscle (Nickerson *et al.*, 2009). Like FATP1, FATP4 has been shown to translocate from

intracellular stores to the plasma membrane under conditions of insulin stimulation and contraction (Jain *et al.*, 2009; Nickerson *et al.*, 2009). FATP4 also exhibits acyl-CoA synthetase activity, preferentially activating very long chain fatty acids by attaching a CoA molecule (Herrmann *et al.*, 2001).

1.3.3.4 – FATP5 (SLC27A5)

FATP5 is expressed solely in the liver (Glatz *et al.*, 2010; Doege *et al.*, 2006; Hirsch *et al.*, 1998) and is localised at the plasma membrane of hepatocytes (Doege *et al.*, 2006). In addition to playing a role in fatty acid uptake (Hirsch *et al.*, 1998), FATP5 exhibits long chain and very long chain acyl-CoA synthetase activity and is therefore involved in activating long and very long chain fatty acids by attaching a CoA molecule (Doege *et al.*, 2006; Steinberg *et al.*, 1999). Furthermore, FATP5 exhibits choloyl-CoA synthetase activity (Steinberg *et al.*, 2000), and therefore is implicated in the reactivation of bile acids to their CoA derivatives (Doege *et al.*, 2006). Targeted deletion of FATP5 (FATP5^{-/-}) in mice results in a 40-50% reduction in long chain fatty acid uptake by hepatocytes, whilst FATP5 overexpression increases the uptake of monounsaturated fatty acid, oleate, by hepatocytes (Doege *et al.*, 2006). FATP5 knockout mice exhibit a ~60% reduction in total liver triglyceride content and display impaired clearance of circulating free fatty acid and triglyceride in the post-absorptive state (Doege *et al.*, 2006).

1.3.4 – Fatty Acid Metabolism is Altered in Obesity – Implicating Fatty Acid Transporters

Research in rodent models has implicated increased fatty acid transport in the increase in fat accumulation observed in the obese skeletal muscle and liver (Doege *et al.*, 2008; Koonen *et al.*, 2007; Smith *et al.*, 2007; Chabowski *et al.*, 2006; Marotta *et al.*, 2004; McAinch *et al.*, 2003; Luiken *et al.*, 2001; Berk *et al.*, 1997). Studies in obese, insulin resistant Zucker (ZDF) rats, have implicated enhanced skeletal muscle fatty acid uptake in obesity (Chabowski *et al.*, 2006; Luiken *et al.*, 2001; Berk *et al.*, 1997). Luiken and colleagues (Luiken *et al.*, 2001) found that saturated fatty acid (palmitate) uptake was significantly increased (1.8-fold) in the hind-limb muscles (mixed fibre type) of obese ZDF rats, compared to lean littermates. Similarly, Chabowski and associates (Chabowski *et al.*, 2006) demonstrated that palmitate transport was significantly increased in giant vesicles prepared from red, but not white, skeletal muscle in obese ZDF rats, compared to lean controls. In humans, Steinberg and colleagues (Steinberg *et al.*, 2004) reported that the total uptake of palmitate was increased in rectus abdominus muscle (mixed fibre type, SO and FOG fibre predominant (Hickey *et al.*, 1995)) of obese females as compared to lean females. Given that skeletal muscle fatty acid uptake is enhanced in obese individuals (Han *et al.*, 2007; Chabowski *et al.*, 2006; Steinberg *et al.*, 2004; Luiken *et al.*, 2001; Berk *et al.*, 1997), several studies have examined the mechanism involved, focusing on fatty acid transporters. There is some evidence that the increased in fatty acid uptake in obese skeletal muscle is associated with an increase in the expression of fatty acid transporters (Smith *et al.*, 2007; Marotta *et al.*, 2004; McAinch *et al.*, 2003). In particular, Marotta and colleagues

(Marotta *et al.*, 2004) demonstrated that male Wistar rats fed a high saturated fat (HF-S) diet (lard) gained twice as much weight in 4 weeks as their high carbohydrate diet-fed counterparts and this was associated with a significant increase in FATP1 protein abundance in the SO soleus muscle of the HF-S group (Marotta *et al.*, 2004). Furthermore, McAinch and associates (McAinch *et al.*, 2003) demonstrated that an 8 week-long HF-S diet induced the mRNA expression of FAT/CD36 in the FG-FOG EDL muscle of female Sprague-Dawley rats (McAinch *et al.*, 2003). Whilst Smith and colleagues (Smith *et al.*, 2007) similarly showed that 8 weeks high fat diet (HFD) consumption in female obese ZDF rats increased the protein abundance of FAT/CD36 in the whole muscle and at the sarcolemma in the SO red gastrocnemius muscle. Therefore, these studies provide evidence of altered fatty acid uptake in the skeletal muscle as a consequence of diet-induced obesity and indicate that fatty acid transport proteins may contribute to an increased flux of fatty acid entering the skeletal muscle.

Furthermore, increased fatty acid uptake via transporter proteins is believed to contribute to fatty liver development (Bradbury, 2006). Intrahepatic storage of triglyceride has long been thought deleterious and is strongly associated with impaired insulin sensitivity (Qureshi *et al.*, 2010; Marchesini *et al.*, 2003; Chitturi *et al.*, 2002). An altered capacity for fatty acid transport via fatty acid transporter proteins has been shown to influence the flux of fatty acids into liver cell, which consequently effects the amount of fat channelled into pathways of esterification, ultimately contributing to or protecting from the development of fatty liver (Falcon *et al.*, 2010; Doege *et al.*, 2008; Bradbury, 2006). Koonen and colleagues (Koonen *et al.*, 2007) demonstrated that HF-S diet consumption in mice induces a parallel increase in fatty acid transporter,

FAT/CD36, and liver triglyceride content (Koonen *et al.*, 2007). In contrast, research by Doege and associates (Doege *et al.*, 2008) demonstrated that silencing hepatic fatty acid transport protein, FATP5, reversed HF-S-induced fatty liver in mice. Therefore the role of fatty acid transporters in contributing to the metabolic dysfunction observed in the skeletal muscle and livers of obese individuals is an important consideration.

1.4 – FATTY ACID METABOLISM – FATTY ACID SYNTHESIS, TRIGLYCERIDE SYNTHESIS, STORAGE AND DEGRADATION

1.4.1 – Fatty Acid Synthesis

Once transported into the cell, fatty acids may be used as fuel or may be metabolised in desaturation and elongation reactions to produce longer or more unsaturated fatty acids (Vessby *et al.*, 2002). In an environment of energy excess, glucose may also be converted to fatty acids through the conversion of substrates of the citric acid cycle (Browning and Horton, 2004) in a process known as lipogenesis. Furthermore, fatty acids may undergo esterification to generate triglycerides, the storage form of fatty acids, or may be incorporated into various lipids including phospholipids, which maintain cellular structural integrity. Moreover, fatty acids may accumulate in the cell as various lipid metabolites, including DAG and ceramide.

In the case of energy excess, glucose may be converted to pyruvate which enters the citric acid cycle in the mitochondrion. The citric acid cycle generates citrate which is shuttled to the cytoplasm and converted to acetyl-CoA. Acetyl-CoA carboxylase α (ACC- α) catalyses the reaction of acetyl-CoA to malonyl-CoA, which in turn is used as

a substrate to form palmitic acid by fatty acid synthase (FAS). Palmitic acid may then be desaturated by stearoyl-CoA desaturase (SCD) to form palmitoleic acid, which may be used to synthesise triglyceride, the storage form of fatty acids (Browning and Horton, 2004).

1.4.1.1 – Sterol regulatory element binding transcription factor 1 (SREBF1)

Lipogenesis is chiefly regulated by the SREBFs, also known as sterol regulatory element binding proteins (SREBP), which directly activate the expression of over 30 genes influencing the synthesis and uptake of fatty acids, cholesterol, triglycerides and phospholipids (Horton *et al.*, 2002). As reviewed by Horton and colleagues (Horton *et al.*, 2002), two SREBF genes exist, SREBF1, which generates both SREBF1a and SREBF1c transcripts through the use of alternative transcription start sites, and SREBF2. Of the two SREBF1 isoforms, SREBF1c is more abundant, constituting 90% of SREBF1 transcripts in the mouse liver (Nakatani *et al.*, 2003; Shimomura *et al.*, 1997), and acts to mediate the expression of predominantly fatty acid synthesis genes. In contrast, SREBF1a and SREBF2 mediate cholesterol synthesis (Horton *et al.*, 2002). Studies exploring the effect of SREBF1 knockout have revealed the aforementioned functional roles (Liang *et al.*, 2002; Shimano *et al.*, 1997). These studies demonstrated that SREBF1 is important for embryonic development as mice homozygous for a disruption in the SREBF1 (SREBF1^{-/-}) gene mostly (50-85%) die *in utero* between days 11.5 – 14.5 (Shimano *et al.*, 1997). Of the few mice that survive SREBF1 disruption, they appear physiologically normal at birth and during adulthood; their survival appears to be reliant on an adaptive upregulation of SREBF2 mRNA and mature nuclear

SREBP2 protein in the liver, resulting in an increase in cholesterol, but not fatty acid, synthesis (Shimano *et al.*, 1997). In contrast, mice deficient in only the SREBF1c isoform do not exhibit embryonic mortality and appear normal at birth and during their life span, suggesting SREBF1a plays a more major role in embryonic development (Liang *et al.*, 2002). Though SREBF1c deficient mice exhibit reduced basal mRNA expression of enzymes controlling fatty acid and triglyceride synthesis in the liver under fasting conditions (Liang *et al.*, 2002; Shimano *et al.*, 1997).

The maturation of SREBF precursor protein is essential as it is the mature nuclear SREBF1 that acts as a transcription factor (Horton *et al.*, 2002; Brown and Goldstein, 1999). The SREBF precursor protein is comprised of 3 domains: a NH₂ terminal domain including a bHLH-Zip motif for DNA binding; 2 hydrophobic transmembrane-spanning regions between which is a short loop of ~30 amino acids that projects into the lumen of the endoplasmic reticulum; and a COOH terminal domain which is involved in regulatory functions (Horton *et al.*, 2002; Brown and Goldstein, 1999). The maturation of the SREBF precursor protein is regulated by escort protein SREBP cleavage-activating protein (SCAP) and proteases, site-1 protease (S1P) and site-2 protease (S2P) and is summarised in **Figure 1.2**. Insulin induced gene 1 (INSIG1) regulates SREBF1 by limiting its induction at both the mRNA and protein levels in times of lipid excess (Qin *et al.*, 2008; Engelking *et al.*, 2004; Takaishi *et al.*, 2004), resulting in the suppression of lipogenesis (Qin *et al.*, 2008). In the liver, peroxisome proliferator activator receptor (PPAR) δ/β has been shown to be responsible for the induction of INSIG1, and ultimately the suppression of SREBF1 (Qin *et al.*, 2008).

Several genes that mediate the synthesis of fatty acids are transcriptionally regulated by SREBF1 (**Figure 1.3**), and as described in **Figure 1.2**, this occurs through the binding of mature SREBF1 at the sterol response element in the promoter region of the target gene (Horton *et al.*, 2002; Brown and Goldstein, 1999). SREBF1 target genes involved in fatty acid synthesis include ACC, FAS and SCD1 (Gutiérrez-Juárez *et al.*, 2006; Abu-Elheiga *et al.*, 2003; Shimano, 2001; Latasa *et al.*, 2000).

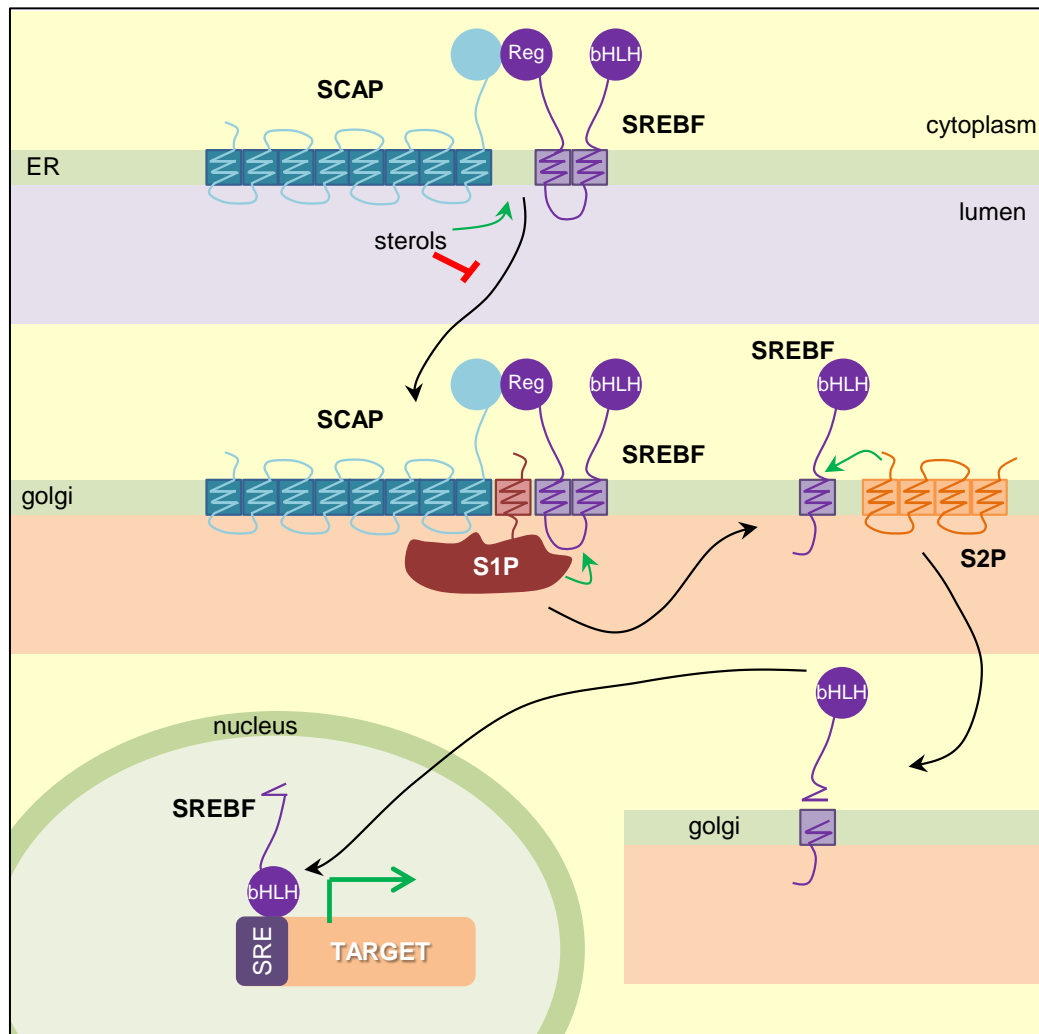


Figure 1.2. Model depicting the maturation process of SREBF1 protein.

In the endoplasmic reticulum, SCAP senses sterols through its sterol-sensing domain. When sterol is plentiful, the SCAP/SREBF complex changes conformation so they are no longer incorporated into vesicles for export from the ER. When the cell is sterol-deplete, SCAP escorts SREBF from the ER to the golgi. In the golgi body, site-1 protease cleaves SREBF in half through its protease action at SREBF's luminal loop. The bHLH-Zip motif is then released from the membrane through site-2 protease activity. The cleaved bHLH-Zip motif translocates to the nucleus where it activates transcription by binding to sterol response elements in the promoter region of SREBF target genes (Horton *et al.*, 2002; Brown and Goldstein, 1999).

ER, endoplasmic reticulum; SREBF, sterol regulatory element binding transcription factors; SCAP, SREBP cleavage-activating protein; Reg, regulatory COOH domain of SREBF; bHLH, bHLH-Zip NH₂ domain of SREBF; S1P, site-1 protease; S2P, site-2 protease; SRE, sterol response elements; TARGET, SREBF target genes.

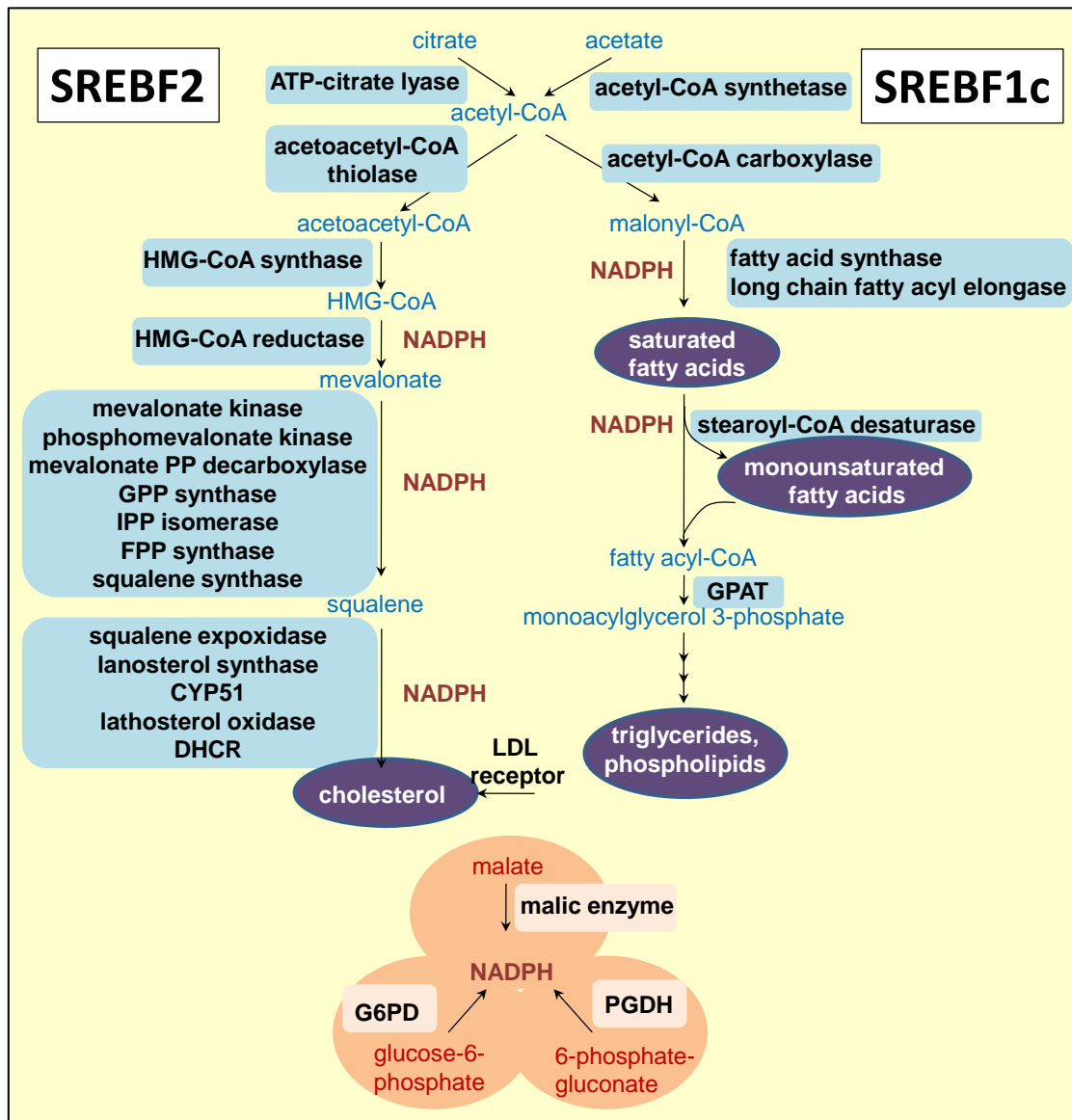


Figure 1.3. Genes and pathways regulated by SREBFs.

This diagram depicts the major metabolic intermediates in the pathways for synthesis of cholesterol, fatty acids and triglycerides as described by Horton and colleagues (Horton *et al.*, 2002). SREBF2 preferentially activates genes involved in cholesterol metabolism, whereas SREBF1c preferentially activates pathways of fatty acid and triglyceride metabolism.

DHCR, 7-dehydrocholesterol reductase; FPP, farnesyl diphosphate; GPP, geranylgeranyl pyrophosphate synthase; CYP51, lanosterol 14 α -demethylase; G6PD, glucose-6-phosphate dehydrogenase; PGDH, 6-phosphogluconate dehydrogenase; GPAT, glycerol 3-phosphate acyltransferase.

1.4.1.2 – Acetyl-CoA Carboxylase (ACC)

ACC is the enzyme responsible for the conversion of acetyl-CoA to malonyl-CoA, an intermediate substrate that plays a key role in regulating fatty acid metabolism (Wakil and Abu-Elheiga, 2009). Two isoforms of ACC exist, ACC- α (ACC1) and ACC- β (ACC2) (Wakil and Abu-Elheiga, 2009) and both exhibit high sequence homology except for an additional 114 amino acid-long sequence present at the N-terminus of ACC- β (Abu-Elheiga *et al.*, 2003). In lipogenic tissues such as the liver, ACC- α catalyses the carboxylation of acetyl-CoA to malonyl-CoA and the malonyl-CoA generated serves as the source of carbon (C₂) units for fatty acid synthesis (Abu-Elheiga *et al.*, 2000; Abu-Elheiga *et al.*, 1997; Trumble *et al.*, 1995; Wakil, 1989). A second isoform, ACC- β is the major isoform in skeletal muscle and is also expressed to a lesser extent in the liver. Compared to the ACC- α isoform, the ACC- β isoform is more highly expressed in the skeletal muscle and liver (Castle *et al.*, 2009). The first 20 amino acids of the extra peptide featured in the ACC- β isoform are highly hydrophobic and are therefore responsible for guiding ACC- β to the mitochondrial membrane where it catalyses the formation of malonyl-CoA, unlike the ACC- α isoform which remains in the cytosol (Abu-Elheiga *et al.*, 2003). Although due to its locality, the malonyl-CoA from this reaction acts as a signalling molecule to regulate fatty acid oxidation through CPT1 (Abu-Elheiga *et al.*, 2003; Abu-Elheiga *et al.*, 2000; Abu-Elheiga *et al.*, 1997; McGarry and Brown, 1997; Trumble *et al.*, 1995).

The respective roles of ACC- α and - β are highlighted in studies using knockout mice (Choi *et al.*, 2007; Harada *et al.*, 2007; Mao *et al.*, 2006). Deletion of the ACC- α gene

(ACC- $\alpha^{-/-}$) leads to embryonic lethality at day 7.5 (Harada *et al.*, 2007). In contrast, liver-specific ACC- α knockout mice breed normally, but exhibit reduced *de novo* lipogenesis in primary hepatocytes without altered fatty acid oxidation (Mao *et al.*, 2006). These data highlight that the malonyl-CoA produced by ACC- α is a regulator of *de novo* fatty acid synthesis, but not fatty acid oxidation (Mao *et al.*, 2006). On the other hand, mice deficient in the ACC- β isoform (ACC- $\beta^{-/-}$) exhibit increased fat oxidation and are protected from fat-induced peripheral and hepatic insulin resistance (Choi *et al.*, 2007).

1.4.1.3 – Fatty Acid Synthase (FAS)

FAS catalyses the conversion of substrates acetyl-CoA, which acts as a primer; malonyl-CoA, a 2 carbon donor, and NADPH, a reducing equivalent; to generate a long chain fatty acid, predominantly palmitate (Menendez *et al.*, 2009; Latasa *et al.*, 2000). FAS is expressed at highest levels in the liver and lung, but is also present in the skeletal muscle, intra-abdominal adipose tissue, heart, brain, kidney and pancreas (Semenkovich *et al.*, 1995). Research in FAS null mice has demonstrated that mice with a homozygous FAS null mutation (FAS $^{-/-}$) experience early embryonic lethality, dying before embryonic day 3.5 (Chirala *et al.*, 2003). Furthermore, those mice with a heterozygous mutation in FAS gene (FAS $^{+/-}$) die at various stages of their embryonic development with a 60-90% less FAS $^{+/-}$ mice born than expected from Mendelian inheritance (Chirala *et al.*, 2003), highlighting the importance of *de novo* fatty acid synthesis in embryogenesis. Meanwhile, liver-specific FAS knockout mice develop fatty liver as a result of reduced β -oxidation as indicated by increased hepatic malonyl-

CoA content and reduced plasma ketone bodies (Chakravarthy *et al.*, 2005).

1.4.1.4 – Stearoyl-Coenzyme A desaturase 1 (SCD1)

SCD1, also known as a delta-9 desaturase, catalyses the synthesis of monounsaturated fatty acyl-CoA from saturated fatty acyl-CoA molecules (Gutiérrez-Juárez *et al.*, 2006). Palmitoyl- (16:0) and stearoyl- (18:0) CoA are the preferred substrates for SCD1, leading to the formation of palmitoleoyl- (16:1 n-7) and oleoyl- (18:1 n-9) CoA, respectively (Stefan *et al.*, 2008). Fatty acyl-CoAs generated by SCD1 are common components of membrane phospholipids, triglycerides, cholesterol esters and wax esters (Lee *et al.*, 2004; Ntambi *et al.*, 2002). Mice deficient in SCD1 exhibit reduced adiposity and energy expenditure as a consequence of reduced expression of genes mediating lipid synthesis and enhanced expression of fatty acid oxidation genes (Dobrzyn *et al.*, 2005; Dobrzyn *et al.*, 2004; Ntambi *et al.*, 2002).

1.4.2 – Triglyceride Synthesis, Storage and Degradation

As mentioned previously, fatty acids may undergo esterification to generate triglycerides, the major storage form of fatty acids. The accumulation of intra-organ triglyceride serves as a neutral store and is believed to be a marker for other potentially detrimental bioactive lipid metabolites, such as DAG and ceramide. DAG can accumulate either through conversion of fatty acids in the glycerolipid synthesis pathway, which controls the formation of triglyceride and DAG or through the degradation of triglyceride. Acyl-CoA:diacylglycerol acyltransferase (DGAT) is the enzyme responsible for catalysing the final step in the biosynthesis of triglyceride,

whilst hormone sensitive lipase (HSL) catalyses the hydrolysis of triglycerides, DAG and monoacylglycerides.

1.4.2.1 – Diacylglycerol Acyltransferase (DGAT)

DGAT is a key enzyme involved in the biosynthesis of triglyceride and acts to catalyse the final step of the glycerol phosphate pathway. Two DGAT genes have been identified and although they share no sequence homology and belong to differing gene families (Cases *et al.*, 2001), both enzymes act to covalently link DAG and fatty acyl-CoA to form triglyceride (**Figure 1.4**). DGAT1 and DGAT2 are widely expressed, with greatest expression in tissues associated with triglyceride metabolism (Cases *et al.*, 2001; Cases *et al.*, 1998). There is however some variance in the level of expression of DGAT enzymes in tissues, with DGAT1 expressed more highly in adipose tissue, small intestine and skeletal muscle (Cases *et al.*, 1998), and DGAT2 having greatest expression in liver and adipose tissue (Cases *et al.*, 2001). The role both enzymes play has been further elucidated in gene-targeted knockout studies.

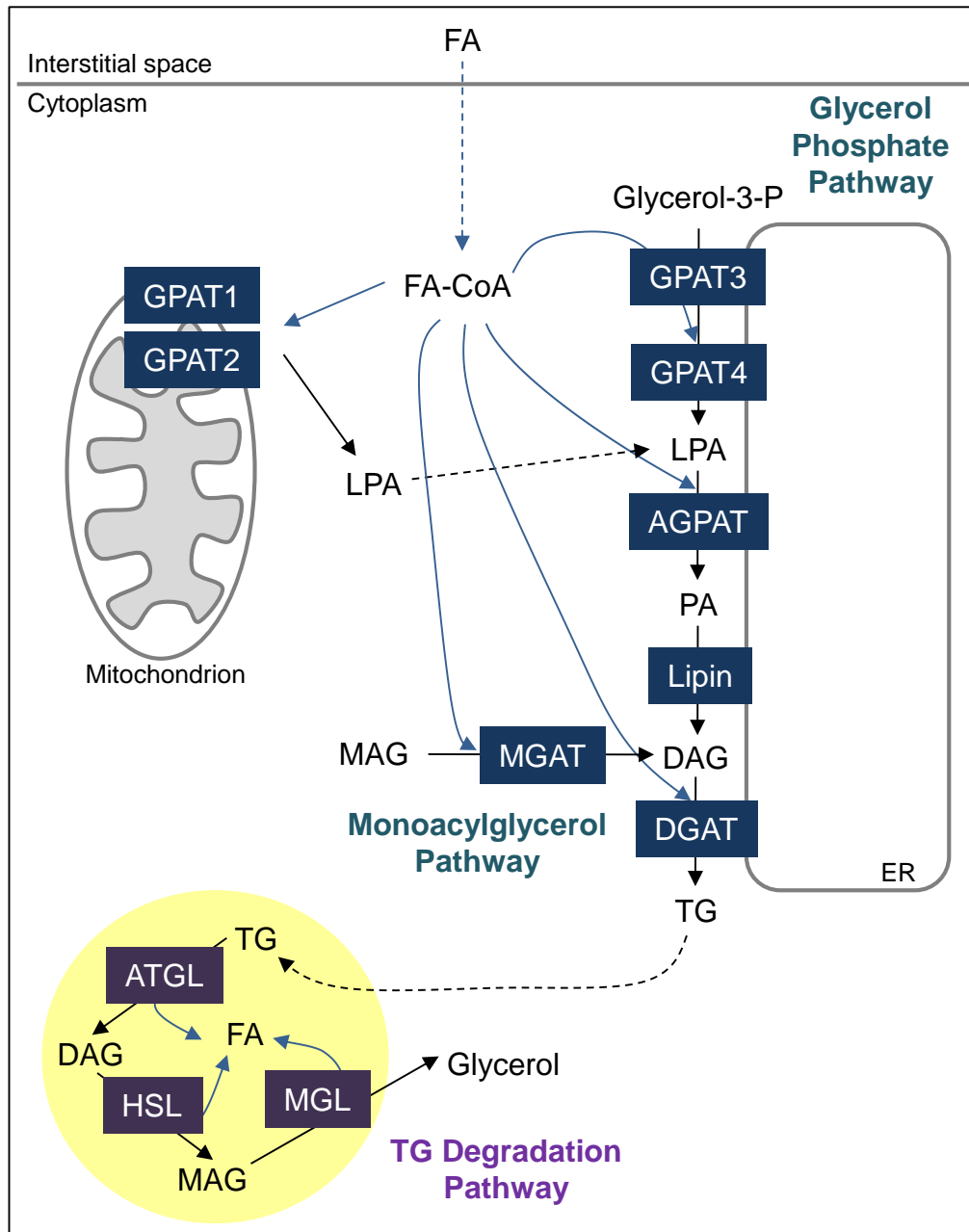


Figure 1.4. Pathways of triglyceride synthesis (glycerolipid synthesis: glycerol phosphate and monoacylglycerol pathways) and degradation.

FA, fatty acid; FA-CoA, fatty acyl-CoA; Glycerol-3-P, glycerol-3-phosphate; LPA, lysophosphatidic acid; PA, phosphatidic acid; DAG, diacylglycerol; TG, triglyceride; MAG, monoacylglycerol; GPAT, glycerol-3-phosphate acyltransferases; AGPAT, acylglycerol-phosphate-acyltransferase; DGAT, acyl-CoA:diacylglycerol acyltransferase; ER, endoplasmic reticulum; ATGL, adipose triglyceride lipase; HSL, hormone sensitive lipase; MGL, monoacylglycerol lipase; MGAT, acyl-CoA:monoacylglycerol acyltransferase.

Although both DGAT1 and DGAT2 knockout mice exhibit reduced tissue triglyceride contents, the deficiency of DGAT isoforms results in distinct phenotypes. Mice deficient in DGAT1 (DGAT1-knockout, DGAT^{-/-}) are viable, exhibit reduced adiposity and are resistant to diet-induced obesity (Smith *et al.*, 2000). Diet-induced obesity resistance is a consequence of increased energy expenditure, 2-fold greater locomotor activity (Smith *et al.*, 2000) and constitutively active thermogenesis, resulting in energy dissipated as heat into the environment (Chen *et al.*, 2003b). DGAT1 deficient mice also exhibit increased insulin sensitivity, with greater insulin-stimulated glucose uptake and increased insulin-stimulated activity of phosphatidylinositol 3-kinase (PI3K), protein kinase B (PKB) and protein kinase C (PKC)- λ in skeletal muscle when compared to mice expressing DGAT1 (DGAT^{+/+} mice) (Chen *et al.*, 2004). This improved insulin sensitivity is proposed to be a consequence of altered endocrine function of white adipose tissue lacking DGAT1 (Chen *et al.*, 2003a).

Alternatively, mice deficient in DGAT2 (DGAT2^{-/-}) are born small, due to intrauterine growth retardation, and die within hours of birth (Stone *et al.*, 2004). DGAT2^{-/-} mice exhibit severe triglyceride deficiency, with 93% reduced carcass triglyceride content, and lack vital substrates for oxidative metabolism (Stone *et al.*, 2004). DGAT2^{-/-} mice are deficient in essential fatty acids, resulting in abnormal skin lipid content and impaired epidermal barrier function, causing severe dehydration (Stone *et al.*, 2004). Furthermore, mice with mixed genetic background, DGAT2^{-/+}, are not protected from the development of diet-induced obesity, suggesting a 50% reduction in DGAT2 expression is not sufficient to limit triglyceride synthesis (Chen and Farese, 2005).

From these knockout studies we can see DGAT1, whilst involved in triglyceride synthesis, plays a key role in modulating signals of energy homeostasis, and DGAT2 plays a comparatively greater role in triglyceride synthesis.

Studies investigating the overexpression of DGAT1, particularly in skeletal muscle, have also shown the importance of this gene in modulating triglyceride synthesis and insulin sensitivity. Overexpression of DGAT1 *in vivo* in rodent skeletal muscle and *in vitro* in C2C12 myocytes by multiple techniques, including DNA electroporation, muscle creatine kinase (MCK) promoter or recombinant adenoviruses, resulted in the similar outcome of increased DGAT1 activity concurrent with increased intramuscular triglyceride content (Liu *et al.*, 2007; Roorda *et al.*, 2005) and reduced DAG content (Liu *et al.*, 2007). Mice with transgenic overexpression of DGAT1 in skeletal muscle (MCK-DGAT1) exhibited a 37% increase in intramuscular triglyceride, and reduction in DAG (-23%) and ceramide (-35%) in the soleus muscle (compared to wild-type mice) when exposed to a standard chow diet, and this increased intramuscular triglyceride was pronounced (+120%) when fed a 8 week HFD (Liu *et al.*, 2007). MCK-DGAT mice, despite displaying increased intramuscular triglyceride, exhibit normal fasting plasma glucose and insulin concentrations and normal glucose tolerance when fed a standard chow diet. When exposed to a HFD, MCK-DGAT1 mice maintain normal glucose and insulin tolerance, unlike their HFD-fed wild-type counterparts which display signs of glucose intolerance and insulin resistance (Liu *et al.*, 2007). Whilst DGAT1^{-/-} and DGAT1 overexpression studies have both provided evidence of increased insulin sensitivity, under conditions of lipid overload, there are vast differences in insulin sensitivity. Insulin-stimulated glucose uptake when exposed to

lipid overload is abolished in DGAT1-knockout (DGAT^{-/-}) mice (60% → 0%), reduced 5-fold in wild-type mice (123 → 26%) and reduced to a lesser extent (3-fold) in MCK-DGAT1 mice (130% → 61%) (Liu *et al.*, 2007). This is concurrent with intramuscular triglyceride reduced by 46% in DGAT1^{-/-} and increased by 58% in MCK-DGAT1 mice and muscle DAG and ceramide content increased by 33% and 26% in DGAT1^{-/-} and reduced by 20% and 39% in MCK-DGAT1 mice (respectively) (Liu *et al.*, 2007). Mice overexpressing DGAT1 have also been shown to possess increased fatty acid capacity in conjunction with higher mitochondrial efficiency (Liu *et al.*, 2009). These data suggest that when exposed to a high fat environment, DGAT deficiency results in harmful build up of DAG and ceramide in skeletal muscle, resulting in poor insulin responsiveness, whilst DGAT overexpression, reduces DAG and ceramide levels, resulting in a protective effect from high fat-induced insulin resistance (Liu *et al.*, 2007).

Despite overexpression of DGAT1 in skeletal muscle (by MCK-DGAT1) providing protection against HFD-induced insulin resistance, MCK-DGAT1 mice lacked insulin-mediated suppression of hepatic glucose output when exposed to a HFD, suggesting DGAT overexpression provided no protection from HFD-induced hepatic insulin resistance (Liu *et al.*, 2009). This suggests that DGAT1 overexpression provides increased tolerance to lipotoxicity in skeletal muscle but does not completely protect against whole-body insulin resistance.

1.4.2.2 – Hormone Sensitive Lipase (HSL)

In contrast, HSL is a broad substrate specificity enzyme capable of hydrolysing triglycerides, DAG and monoacylglycerides, as well as cholesteryl, retinyl and lipoidal esters (Watt, 2009). *In vitro* studies have demonstrated that HSL exhibits 11-fold greater hydrolase activity against DAG than triglyceride (Watt and Steinberg, 2008; Fredrikson *et al.*, 1981). Furthermore, HSL has been shown to exhibit preference for activity against fatty acids in the *n*-1 or *n*-3 position (Watt and Steinberg, 2008; Fredrikson and Belfrage, 1983). HSL null mice appear physically normal, but exhibit lower fat mass compared to wild-type controls (Wang *et al.*, 2001). When challenged with a HFD, HSL null mice are protected from the development of diet-induced obesity, despite an increase in food intake, and this may be the result of their increased core body temperature (Watt, 2009; Harada *et al.*, 2003). However, *in vitro* studies have revealed that although HSL was ablated in adipocytes, some triglyceride lipase activity remained (40-50%), suggesting other triglyceride lipases play a role in lipolysis (Watt, 2009; Haemmerle *et al.*, 2002; Wang *et al.*, 2001). Furthermore, triglyceride lipases may influence the amount of triglyceride accumulated within the liver by catalysing the breakdown of triglycerides to free fatty acids. This is directed to pathways of re-esterification in which re-formed triglyceride is packaged into very low density lipoprotein precursor molecules for secretion or to pathways of oxidation for disposal (Turpin *et al.*, 2010; Nagle *et al.*, 2009; Gibbons *et al.*, 2004). Although it has been suggested that the re-esterification is the primary fate of fatty acids entering liver cells in the fed-state (McGarry and Foster, 1980), fatty acid oxidation also contributes to the disposal of excess fatty acid within the liver (Lavoie and Gauthier, 2006).

1.4.3 – Fatty Acid Metabolism is Altered in Obesity – Implicating Fatty Acid Synthesis and Storage

Obesity results from an imbalance between energy supply and expenditure. When energy homeostasis is not maintained, majority of surplus calories consumed are converted to triglyceride and stored in adipose tissue. Excess triglyceride is also channelled into ectopic fat stores, depots not primarily designed for fat storage, such as skeletal muscle and liver. In the obese adult, a significant 2-fold increase in intramuscular triglyceride content is observed, when compared to lean controls (Bonen *et al.*, 2004b). Similarly, Smith *et al.* (Smith *et al.*, 2007) showed that exogenous triglyceride esterification was significantly increased in the SO soleus muscle of obese ZDF rats, compared to lean controls. Correspondingly, Steinberg *et al.* (Steinberg *et al.*, 2004) reported increased rectus abdominus muscle triglyceride esterification in obese (+119%) compared to lean subjects. Furthermore, an increase in skeletal muscle triglyceride content has been shown to negatively correlate with whole-body insulin sensitivity ($r^2=0.56$, $P<0.0001$) (Manco *et al.*, 2000). However, observations in athletes have provided evidence against triglyceride accumulation playing a causal role in reduced insulin sensitivity. Known as “the Athlete’s Paradox”, trained athletes exhibit increased intramuscular triglyceride content with exercise, concurrent with increased insulin sensitivity (Goodpaster *et al.*, 2001). This finding suggests that muscle triglyceride content may instead serve as a neutral store and as a marker for other potentially detrimental lipid metabolites, leading to studies investigating the effect of accumulation of bioactive lipid metabolites, such as DAG and ceramide, on insulin sensitivity.

In skeletal muscle, DAG can accumulate either through conversion of fatty acids in the glycerolipid synthesis pathway, which controls the formation of triglyceride and DAG or through the degradation of triglyceride (**Figure 1.4**). In obese insulin resistant rodents, DAG levels increase by 136% in the hind-limb muscle (Turinsky *et al.*, 1990), whilst rats subjected to intravenous lipid infusion exhibit a transient ~3-4-fold increase in intramuscular DAG content (Yu *et al.*, 2002) and rats provided a 8-week HF-S diet also display a significant elevation in muscle DAG content (Lee *et al.*, 2006a), when compared to their respective controls. Accumulated skeletal muscle DAG is believed to potentially activate PKC- θ resulting in increased phosphorylation of the Ser³⁰⁷ residue of insulin receptor substrate-1 (IRS-1), which in turn leads to reduced phosphorylation of IRS-1 tyrosine and decreased activation of IRS-1-associated PI3K, finally resulting in lower insulin-stimulated glucose transport activity and reduced insulin sensitivity (Yu *et al.*, 2002; Griffin *et al.*, 1999). Therefore the conversion of DAG to neutral lipid storage form, triglyceride, may confer advantages in insulin signalling, resulting in many studies focusing on the enzyme responsible for this conversion, DGAT. Furthermore, given that lipolysis has been reported to decrease in skeletal muscle upon consumption of a HFD (Kim *et al.*, 2003), concurrent with a reduction in the mRNA content of muscle lipolytic enzyme, HSL (Guillerm-Regost *et al.*, 2006), increased triglyceride accumulation in skeletal muscle may be an adaptive response to prevent the accumulation of detrimental lipid metabolites, such as DAG.

Furthermore, aberrant fatty acid synthesis has been implicated in the development of fatty liver, insulin resistance and obesity (Horton *et al.*, 2002). Horton and associates (Horton *et al.*, 2002) summarised that the fatty liver of insulin resistant individuals

involves upregulation of hepatic SREBF1c as a result of high insulin levels. Studies in obese insulin resistant (*ob/ob*) mice have demonstrated that despite these mice exhibiting peripheral insulin resistance, insulin continues to activate the transcription and maturation of hepatic SREBF. This may contribute to fatty liver (Horton *et al.*, 2002), as increased levels of mature SREBF1c upregulate lipogenic gene expression in the liver, increasing fatty acid synthesis and accelerating triglyceride accretion (Horton *et al.*, 2002). Similarly, skeletal muscle also exhibits SREBF1 activity, at a level comparable to that observed in the liver and SREBF1 plays a role in mediating the glucose- and insulin-induced upregulation of lipogenic genes in skeletal muscle also (Dulloo *et al.*, 2004). Therefore, *de novo* lipogenesis, although only occurring at low levels in skeletal muscle (Dulloo *et al.*, 2004), may also contribute to increased triglyceride accumulation observed in obese skeletal muscle (Kim *et al.*, 2000b; Mullen *et al.*, 2007; Simoncıkova *et al.*, 2002).

1.5 – FATTY ACID METABOLISM – FATTY ACID UTILISATION

Once within the cell, fatty acids may undergo β -oxidation in the mitochondria or peroxisomes. In the mitochondria, short, medium and long chain fatty acids are oxidised resulting in the generation of ATP (Reddy and Hashimoto, 2001). Majority of dietary fatty acids consumed are long chain and therefore the bulk of fatty acid oxidation occurs in the mitochondrion (Hu *et al.*, 2005). Fatty acid oxidation is therefore regulated by mitochondrial activity and number. The peroxisomes preferentially oxidise long and very long chain fatty acids that are unable to be catabolised in the mitochondria, generally those fatty acids which are greater than 20

carbons in length (Hu *et al.*, 2005). However, peroxisomal β -oxidation is incomplete as peroxisomes lack the enzymes of the citric acid cycle, and consequently hydrogen peroxide is produced (Hu *et al.*, 2005; Reddy and Hashimoto, 2001).

To be used as fuel within the mitochondria, fatty acids must first undergo an activation reaction. On the outer mitochondrial membrane, fatty acyl-CoA synthase catalyses the reaction between a fatty acid, CoA and ATP molecule, resulting in the generation of fatty acyl-CoA (Kiens, 2006; Elliott and Elliott, 2001). This fatty acyl-CoA enters the mitochondrion by a specialized transport mechanism, involving CPT1 and CPT2 (Jeukendrup, 2002; Elliott and Elliott, 2001) (**Figure 1.5**). Inside the mitochondrion, fatty acids undergo β -oxidation, which involves several rounds of shortening the fatty acyl-CoA molecule by two carbon atoms, liberating acetyl-CoA, FADH_2 and NADH. Acetyl-CoA subsequently feeds into the citric acid cycle and is oxidised. NADH and FADH_2 supply the electron transport chain, leading to the generation of ATP (Elliott and Elliott, 2001).

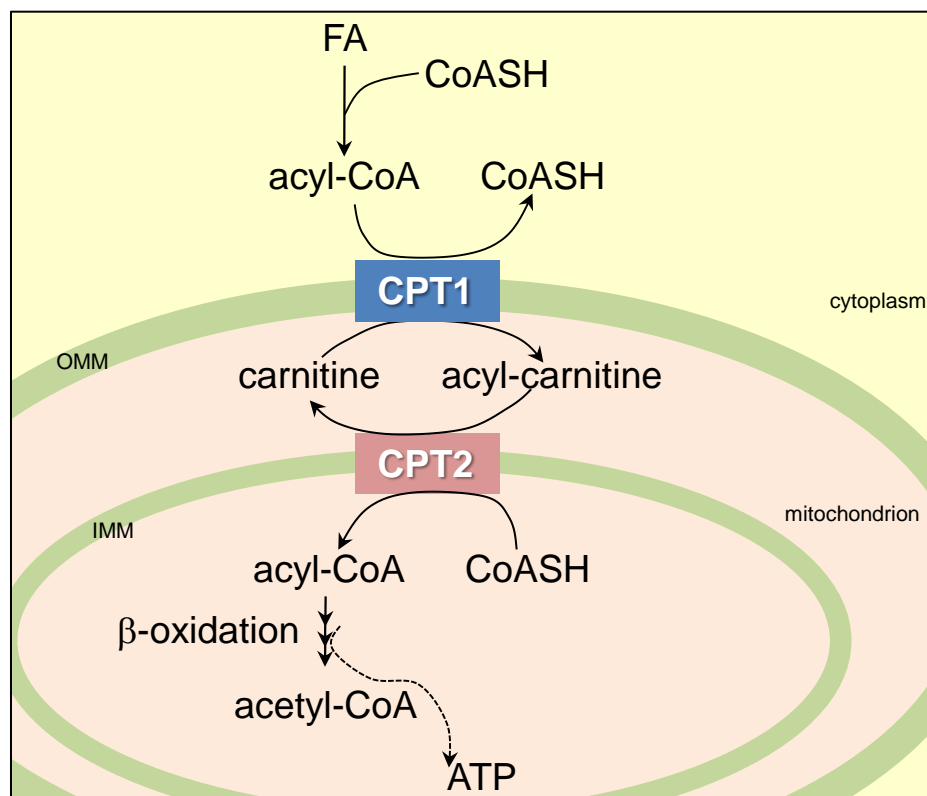


Figure 1.5. Pathway of fatty acid transport into the mitochondrion for subsequent oxidation.

FA, fatty acid; CoA, Coenzyme A; CPT, carnitine palmitoyl transferase; ATP, adenosine triphosphate; IMM, inner mitochondrial membrane; OMM, outer mitochondrial membrane; CoASH, Coenzyme A (not attached to an acyl group).

1.5.1 – Carnitine Palmitoyl Transferase 1 (CPT1)

CPT1 is an enzyme located at the outer mitochondrial membrane and catalyses the transfer of an acyl-CoA molecule from an activated fatty acyl-CoA to carnitine, forming acyl-carnitine. Acyl-carnitine then reacts with CPT2 located on the inner mitochondrial membrane, which results in the reformation of the fatty acyl-CoA molecule, allowing entry into the mitochondria (Doh *et al.*, 2005; Jeukendrup, 2002; Elliott and Elliott, 2001). CPT1 is therefore believed to constitute the rate-limiting step of mitochondrial fatty acid uptake and hence oxidation (Jeukendrup, 2002; McGarry and Brown, 1997).

Three CPT1 isoforms have been identified, CPT1a, identified as the liver isoform (L-CPT1), CPT1b, termed the skeletal muscle isoform (M-CPT1) (Brown *et al.*, 1997; McGarry and Brown, 1997) and the novel brain-specific CPT1c isoform (Gao *et al.*, 2009). CPT1a is expressed in the liver, kidney, lung, spleen, intestine, pancreas, white adipose tissue, ovary, fibroblasts and brain, whilst CPT1b is expressed in the skeletal muscle, heart, brown and white adipose tissues, testes, lung, kidney and ovary (Brown *et al.*, 1997; McGarry and Brown, 1997).

In humans, CPT1 deficiency was recognised to manifest in two different clinical disorders, one with “muscular” symptoms and the other with “liver” symptoms (Demaugre *et al.*, 1988), leading to the identification of CPT1 isoforms. CPT1 “liver” deficiency, associated with the CPT1a isoform, is symptomatically expressed in fasting hypoglycaemia with inappropriately low ketogenesis, whilst CPT1 “muscle” deficiency, involved CPT1b, is scarcely reported, but presents as episodic muscle

necrosis with paroxysmal myoglobinuria (Demaugre *et al.*, 1988). Studies in mice have demonstrated that separate knockout models of the CPT1a (CPT1a^{-/-}) (Nyman *et al.*, 2005) and CPT1b (CPT1b^{-/-}) (Ji *et al.*, 2008) isoforms both result in early embryonic mortality. Male, but not female, heterozygous CPT1a mice (CPT1a^{+/-}) exhibit reduced CPT1 activity (55%) and in males this is accompanied by reduced glucose and elevated free fatty acids in serum following a 24 hour fast (Nyman *et al.*, 2005). Despite CPT1 deficiency, CPT1b^{+/-} mice challenged with cold conditions following a 24 hour fast (an indicator used to assess fatty acid oxidative capacity) were cold tolerant suggesting fatty acid oxidation is maintained (Nyman *et al.*, 2005). Heterozygous CPT1b mice (CPT1b^{+/-}) appear normal in phenotype, despite exhibiting reduced CPT1b activity (~55-60%) and mRNA (~50%) in muscle (Ji *et al.*, 2008). However, their deficient capacity for fatty acid oxidation is highlighted during a 6 hour cold challenge, with 3.75-fold higher occurrence of fatal hypothermia (Ji *et al.*, 2008).

Malonyl-CoA has long been acknowledged to be a potent inhibitor of CPT1 (Bird and Saggerson, 1984) and studies have also demonstrated that the muscle CPT1b isoform is more sensitive to inhibition by malonyl-CoA than the liver CPT1a isoform (Alam and Saggerson, 1998; Lloyd *et al.*, 1986). The formation of malonyl-CoA is catalysed by enzyme, ACC (Abu-Elheiga *et al.*, 1997; Trumble *et al.*, 1995) as mentioned previously (**Chapter 1 Section 4.1.2**). The malonyl-CoA generated from the reaction catalysed by the second isoform of ACC, ACC-β, acts as a signalling molecule to regulate fatty acid oxidation through CPT1 (Abu-Elheiga *et al.*, 2000; Abu-Elheiga *et al.*, 1997; McGarry and Brown, 1997; Trumble *et al.*, 1995) (**Figure 1.6**). Furthermore, the regulation of fatty acid oxidation is controlled by AMP-activated protein kinase (AMPK) which

plays a role in the de-activation of ACC- β and the activation of the enzyme responsible for malonyl-CoA degradation, malonyl-CoA decarboxylase (**Figure 1.6**). Therefore activation of AMPK inhibits the pathway of malonyl-CoA synthesis and enhances malonyl-CoA degradation, reducing the inhibition of CPTI, allowing an increased rate of β -oxidation (Winder, 2001).

1.5.2 – AMP-Activated Protein Kinase (AMPK)

AMPK is a metabolic master switch which is involved in maintaining energy balance at the cellular level. AMPK exists as a heterotrimeric complex containing one catalytic subunit (α) and two regulatory subunits (β , γ) and is activated upon phosphorylation at the Thr172 residue or allosterically by AMP (Lage *et al.*, 2008; Winder and Hardie, 1999) when levels of the ratio of AMP to ATP is high (Lage *et al.*, 2008). Each subunit exists in two or three isoforms (α 1, α 2, β 1, β 2, γ 1, γ 2, γ 3). In the skeletal muscle and liver the catalytic α 1 and α 2 subunits are present (Winder, 2001), with the α 2 isoform more abundant in skeletal muscle (Philp *et al.*, 2008) and approximately equal amounts of α 1 and α 2 containing AMPK complexes in the liver (Viollet *et al.*, 2006). Furthermore, in the skeletal muscle the regulatory β subunits are fibre type-dependent, with both β 1 and β 2 subunits expressed in type II muscle fibres and only the β 1 isoform present in type I muscle fibres (Winder, 2001). In the liver, β 1 containing complexes contribute approximately 95% of total AMPK activity, compared to just 5% of activity provided by β 2 containing complexes (Viollet *et al.*, 2006). Furthermore, the abundance of the γ regulatory subunit is controversial in skeletal muscle, with immunoprecipitation studies demonstrating the γ 1 isoform is most abundant in skeletal

muscle, and Northern blot analyses finding the $\gamma 3$ isoform to be more highly expressed (Winder, 2001). However, the $\gamma 1$ isoform is ubiquitously expressed and the $\gamma 2$ and $\gamma 3$ subunits are preferentially expressed in skeletal muscle (Osler and Zierath, 2008). In contrast the liver exhibits 90% of $\gamma 1$ containing complexes, 10% of $\gamma 2$ containing complexes and only minor $\gamma 3$ containing complexes (Viollet *et al.*, 2006).

Activation of AMPK (Winder and Hardie, 1999) results in increased activation of energy producing pathways and inhibition of energy utilising pathways (Winder, 2001; Winder and Hardie, 1999). Such pathways that are promoted by AMPK activation are glucose uptake, glycolysis, fatty acid oxidation and mitochondrial biogenesis, whilst AMPK activation inhibits pathways of protein, glycogen and fatty acid synthesis and gluconeogenesis (Lage *et al.*, 2008; Hardie *et al.*, 2006; Winder, 2001; Winder and Hardie, 1999) (**Figure 1.7**). As reviewed by Lage and colleagues (Lage *et al.*, 2008), the activation and inhibition of the aforementioned pathways occurs through AMPK influencing the activity and or expression of key metabolic enzymes (**Table 1.1**).

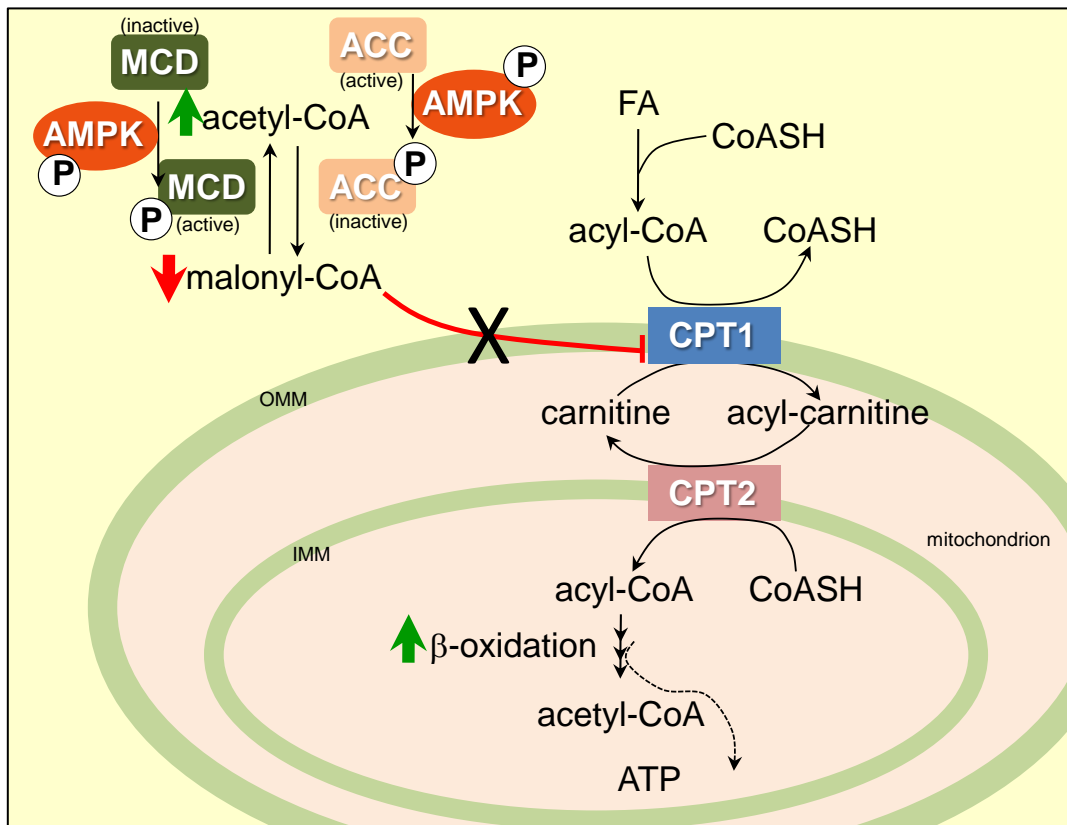


Figure 1.6. AMPK activation relieves the inhibition of carnitine palmitoyl transferase by malonyl-CoA by phosphorylating and deactivating acetyl-CoA carboxylase whilst phosphorylating and activating malonyl-CoA decarboxylase, leading to reduced malonyl-CoA levels and ultimately to increased fatty acid oxidation. (Winder, 2001).

FA, fatty acid; CoA, Coenzyme A; CPT, carnitine palmitoyl transferase; ATP, adenosine triphosphate; IMM, inner mitochondrial membrane; OMM, outer mitochondrial membrane; CoASH, Coenzyme A (not attached to an acyl group); MCD, malonyl-CoA decarboxylase; ACC, acetyl-CoA carboxylase, AMPK, AMP-activated protein kinase; P, phospho.

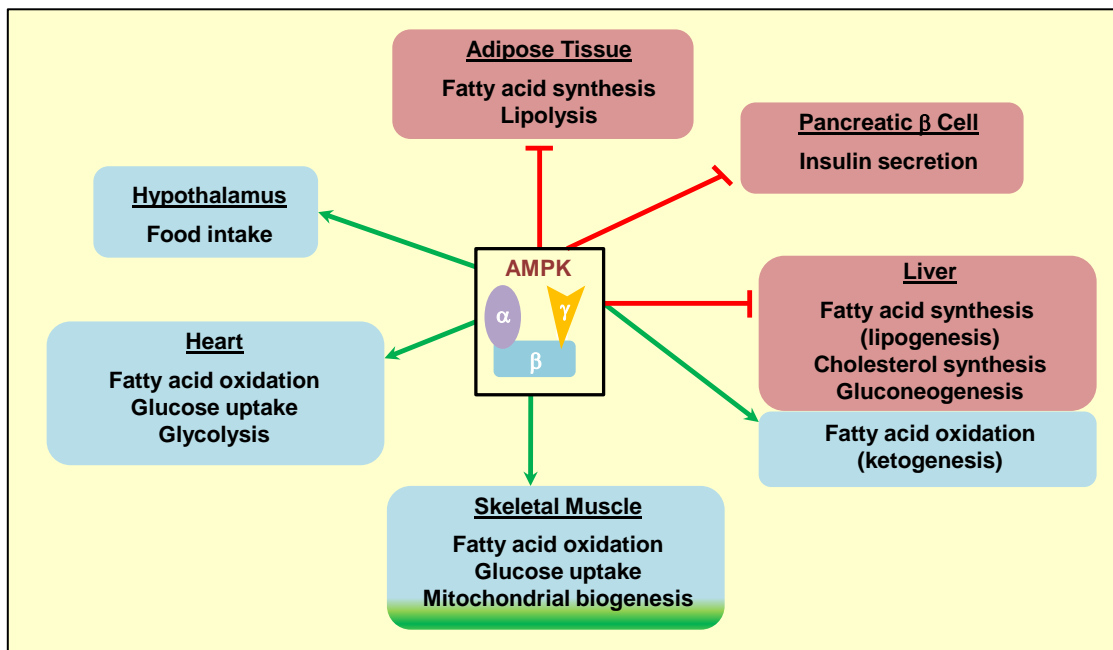


Figure 1.7. Pathways influenced by AMPK activation in specific tissues. (Lage *et al.*, 2008; Winder, 2001; Winder and Hardie, 1999).

Tissue/ Organ	Pathway	Target Enzyme	Immediate Effect	Metabolic Effect
Liver	Lipid metabolism	Acetyl-CoA carboxylase- α	↓ Enzyme activity	↓ Fatty acid synthesis
		Malonyl-CoA decarboxylase	↑ Enzyme activity	↓ Fatty acid synthesis
		Fatty acid synthase	↓ Transcription	↓ Fatty acid synthesis
		Acetyl-CoA carboxylase- β	↓ Enzyme activity	↑ Fatty acid oxidation
		Glycerol-3-phosphate acyltransferase	↓ Enzyme activity	↑ Triglyceride synthesis
		3-hydroxy-3-methylglutaryl-Coenzyme A reductase	↓ Enzyme activity	↑ Cholesterol synthesis
	Glucose metabolism	Phosphoenolpyruvate carboxykinase	↓ Expression	↓ Gluconeogenesis
		Glucose-6-phosphatase	↓ Expression	↓ Gluconeogenesis
Muscle	Lipid metabolism	Acetyl-CoA carboxylase- β	↓ Enzyme activity	↑ Fatty acid oxidation
		Malonyl-CoA decarboxylase	↑ Enzyme activity	↑ Fatty acid oxidation
	Glucose metabolism	Glucose transporter 4	↑ Translocation to cell membrane and ↑ Expression	↑ Glucose uptake
		Hexokinase	↑ Enzyme activity	↑ Glycolytic flux
		Glycogen synthase	↓ Enzyme activity	↓ Glycogen synthesis
	Mitochondrial biogenesis	Nuclear respiratory factor 1	↑ Expression	↑ Mitochondrial biogenesis
		Peroxisomal proliferator activated receptor γ coactivator 1	↑ Expression	↑ Mitochondrial biogenesis
		Uncoupling protein 3	↑ Expression	↑ Mitochondrial proton leak
	Protein Synthesis	Mammalian target of rapamycin	↓ Enzyme activity	↓ Protein synthesis
		Tuberous sclerosis complex 2	↑ Enzyme activity	↓ Protein synthesis
		Eukaryotic elongation factor 2 kinase	↑ Enzyme activity	↓ Protein synthesis
	↓ - inhibition; ↑ - stimulation. (Lage <i>et al.</i> , 2008; Viollet <i>et al.</i> , 2006)			

1.5.3 – Peroxisome proliferator activator receptor (PPAR)

Whilst AMPK is capable of controlling several pathways involved in intermediary metabolism, the peroxisome proliferator activator receptor family (PPAR) also play key roles in mediating several pathways of fatty acid metabolism, including pathways of cellular fatty acid uptake, intracellular binding and activation, storage and oxidation (Desvergne and Wahli, 1999). In the PPAR family there are three ligand-activated transcription factors, PPAR α , PPAR δ/β and PPAR γ , that regulate the transcription of key target genes. **Figure 1.8** depicts the model for transcription activation of key target genes by PPAR. PPAR α is involved in fatty acid catabolism and is therefore mainly expressed in organs where this process is vital, such as the liver, skeletal muscle, kidney and heart (Seedorf and Aberle, 2007; Mandard *et al.*, 2004; Bocher *et al.*, 2002). PPAR α , particularly when co-activated with its coactivator, peroxisome proliferative activated receptor γ coactivator 1 α (PGC1 α), has been shown to enhance fatty acid oxidation (Liang and Ward, 2006) and there is some evidence that this occurs through activation of AMPK in skeletal muscle (Lee *et al.*, 2006b). As reviewed by Mandard and colleagues (Mandard *et al.*, 2004), PPAR α also plays a key role in activating many pathways involved in hepatic lipid metabolism (**Figure 1.9**). Furthermore, PPAR α is the target of the fibrate drugs, well known to combat hyperlipidemia (Desvergne and Wahli, 1999).

Despite being ubiquitously expressed, PPAR δ/β is the least understood PPAR isoform (Bocher *et al.*, 2002). However, more recent studies have demonstrated a role for PPAR δ/β in regulating SREBF1 activity through INSIG1 in the liver, making it a

potential target in ameliorating fatty liver (Qin *et al.*, 2008). In contrast, PPAR γ is preferentially expressed in adipose tissue where in the adipocyte PPAR γ regulates cellular differentiation and lipid storage (Bocher *et al.*, 2002). PPAR γ does, however, demonstrate some lower level expression in the skeletal muscle, liver, heart and spleen (Vidal-Puig *et al.*, 1996). Furthermore, PPAR γ is the target of the thiazolidinedione drugs, known for their insulin sensitising characteristics (Desvergne and Wahli, 1999).

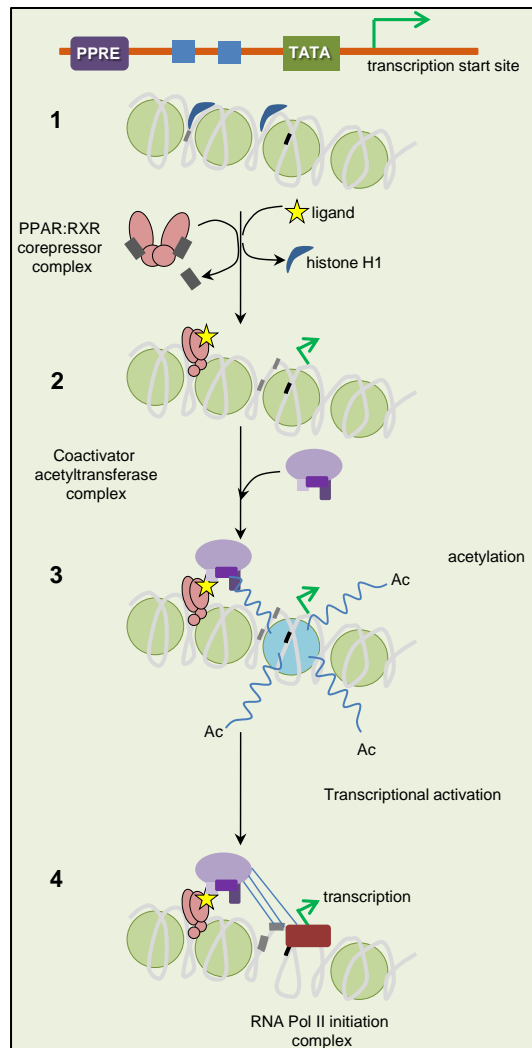


Figure 1.8. Model for transcriptional activation of PPARs as depicted by Desvergne and Wahli (Desvergne and Wahli, 1999).

1. Diagram of a PPAR-responsive promoter in linear form, comprised of a PPAR response element (PPRE), 2 binding sites for transcription (blue boxes), the TATA box and transcription start site. Below is demonstrated the same region, but organised in repressive chromatin structure. The PPAR:RXR co-repressor complex (not bound to DNA) is activated by a ligand, leading to the dissociation of the co-repressors from the activated PPAR:RXR complex. 2. Activated PPAR:RXR complex binds to the PPRE, leading to a change in chromatin structure and histone H1 release. The PPAR:RXR binding to the PPRE targets a coactivator acetyltransferase complex to the promoter. 3. The promoter chromatin at the transcription initiation site is modified by this complex, acetylating histone tails (Ac), leading to a structure capable of transcription. Acetylation of histones is selectively enriched at the transcription initiation region, involving one or two nucleosomes. 4. Additional transcription factors and the RNA Pol II initiation complex are recruited to the promoter and transcription is initiated (Desvergne and Wahli, 1999).

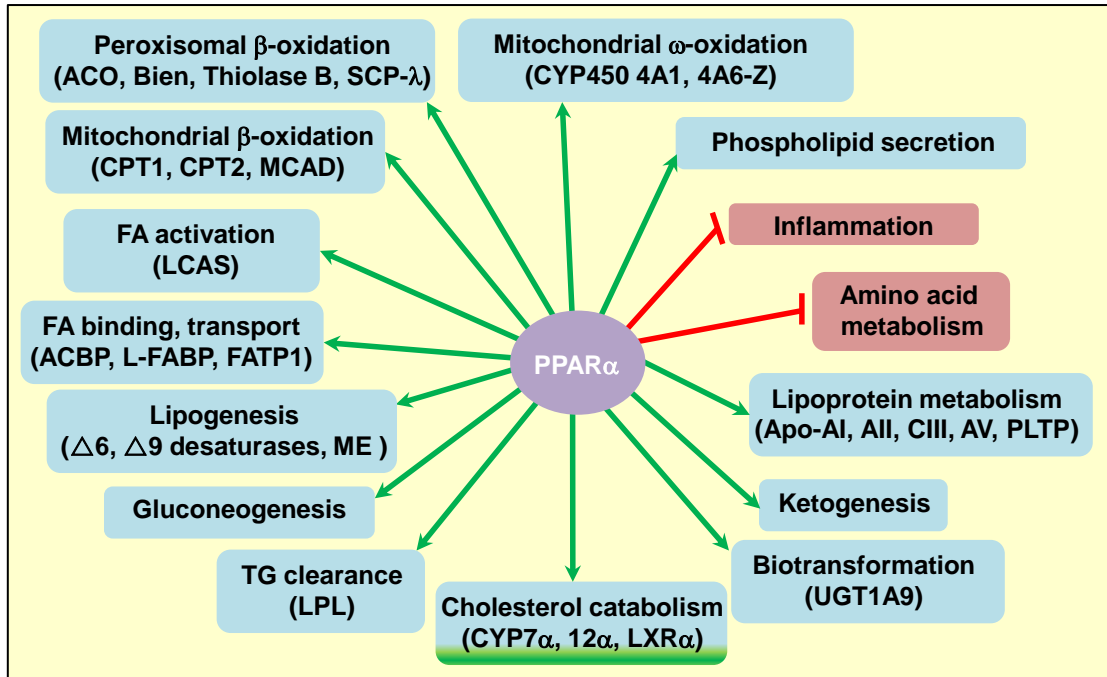


Figure 1.9. Pathways mediated by peroxisome proliferator activator receptor α (PPAR α) in the liver as reviewed by Mandard and colleagues (Mandard *et al.*, 2004).

FA, fatty acid; TG, triglyceride; LPL, lipoprotein lipase; ME, malic enzyme; ACBP, acyl-CoA binding protein; L-FABP, cytosolic fatty acid binding protein; FATP, fatty acid transport protein; LCAS, long chain acyl-CoA synthetase; CPT, carnitine palmitoyl transferase; MCAD, medium chain acyl-CoA dehydrogenase; ACO, acyl-CoA oxidase; Bien, bifunctional enzyme; SCP, sterol carrier protein; CYP, cytochrome; PLTP, phospholipid transfer protein; Apo, apolipoprotein; UGT, UDP-glucuronosyl. Green arrow signifies activation, red line signifies inhibition. Known target genes of PPAR α are shown in brackets.

1.5.4 - Fatty Acid Metabolism is Altered in Obesity – Implicating Impaired Fatty Acid Oxidation

The role of fatty acid oxidation in obesity has been extensively examined. Smith and associates (Smith *et al.*, 2007) showed that oxidation of exogenous fatty acid was significantly reduced in the soleus muscle of obese ZDF rats fed a HFD, compared to lean controls. Similarly, Han *et al.* (Han *et al.*, 2007) found that under basal conditions, palmitate oxidation was significantly decreased (-28%) in the hind-limb muscle of obese ZDF rats as compared to lean rats. However, in humans there are conflicting reports as to whether fatty acid oxidation is impaired in obese individuals (Bruce *et al.*, 2005; Chen *et al.*, 2005; Steinberg *et al.*, 2004; Thyfault *et al.*, 2004). Myotubes, cultured from the human rectus abdominus muscle, showed no change in palmitate oxidation between obese, obese diabetic and lean subjects (Chen *et al.*, 2005). Correspondingly, Bruce and colleagues (Bruce *et al.*, 2005) found skeletal muscle fatty acid oxidation to be comparable between obese (average BMI=33.3 kg/m²) and lean women (average BMI=24.1 kg/m²). Furthermore, Steinberg *et al.* (Steinberg *et al.*, 2004) found no difference in basal palmitate oxidation when comparing obese and lean subjects. However, the ratio of total palmitate esterification (into phospholipid + DAG + triglyceride lipid pools) to palmitate oxidation was significantly higher in the obese as compared to the lean women, suggesting that fatty acids are being preferentially directed into esterification, rather than oxidation. In extremely obese women (average BMI=40.8 kg/m²) the percentage of free fatty acid uptake which was oxidised, was significantly reduced, compared to that of normal weight subjects (average BMI=22.6 kg/m²) (Thyfault *et al.*, 2004). Discrepant results regarding the fate of fatty acid

oxidation in obese humans (Thyfault *et al.*, 2004; Bruce *et al.*, 2005) may be explained by differences in the phenotype, amount and distribution of fat and similar variation in the lean controls.

Furthermore, studies have identified changes in the oxidative capacity of individual skeletal muscle fibres. When exposed to altered conditions, such as obesity, the skeletal muscle exhibits a significant degree of plasticity and is capable of altering its metabolic properties in response to altered functional demands (Pette and Staron, 2000). An increased BMI is negatively correlated with the proportion of type I fibres (Hickey *et al.*, 1995) and positively associated with the proportion of type IIB fibres (Tanner *et al.*, 2002) in skeletal muscle, indicating a functional switch to a more glycolytic muscle. Furthermore, it has been demonstrated that obese (Tanner *et al.*, 2002; Hickey *et al.*, 1995) and type 2 diabetic (Oberbach *et al.*, 2006; Hickey *et al.*, 1995) individuals exhibit a reduction in the proportion of type I fibres and increased proportion of type IIB fibres in skeletal muscle. These studies provide further evidence of a reduced capacity for oxidation in skeletal muscle in obese individuals. Furthermore, oxidative capacity is dependent on mitochondrial number and activity. Recent research has provided some evidence that intermyofibrillar mitochondrial content is reduced in obese insulin resistant subjects, which may in turn influence muscle oxidative capacity as reduced mitochondrial content is correlated with lower lipid oxidation (Chomentowski *et al.*, 2011).

1.6 – FATTY ACID AND GLUCOSE METABOLISM – CONTROLLING THE NUTRIENT SHIFT

Pyruvate dehydrogenase is the enzyme responsible for the irreversible oxidative decarboxylation of pyruvate to generate acetyl-CoA. This reaction essentially links glycolysis to oxidative metabolism as the product acetyl-CoA links into the citric acid cycle, promoting glucose utilisation (Houten *et al.*, 2009; Holness *et al.*, 2000; Fryer *et al.*, 1995). Metabolic flexibility is the term used to describe the ability of the cell to appropriately switch fuel oxidation dependent on the availability of substrates and in response to insulin. The Randle cycle describes the mechanism by which transition between oxidative fuels occurs, as fatty acid storage and oxidation are dynamically regulated throughout the day in response to changing nutrient availability and insulin. Pyruvate dehydrogenase kinase (PDK) is the major regulatory enzyme responsible for the shift in nutrient utilisation from glucose to fatty acids in response to increased fatty acid supply (Huang *et al.*, 2002). PDK acts to inhibit pyruvate dehydrogenase via its phosphorylation and deactivation, preventing the formation of acetyl-CoA and its entry into the citric acid cycle (Bowker-Kinley *et al.*, 1998) (**Figure 1.10**). Four PDK isoenzymes exist and are distributed in a tissue-specific pattern (Bowker-Kinley *et al.*, 1998). The PDK2 and PDK4 isoenzymes are widely expressed, with PDK2 highly expressed in the skeletal muscle, liver, heart, brain, kidney and testes (Bowker-Kinley *et al.*, 1998). The PDK4 isoenzyme is most highly expressed in skeletal muscle, with lower expression in the liver, kidney, lung and heart (Bowker-Kinley *et al.*, 1998). In contrast, PDK1 is found almost exclusively in the heart and PDK3 is most highly expressed in the testes (Bowker-Kinley *et al.*, 1998). Not only are the PDK isoenzymes

different in their tissue distribution, but they also show different kinetic parameters and regulation. PDK2 exhibits low specific activity and strongly reacts to NADH and acetyl-CoA levels, whilst PDK4 exhibits high specific activity and is less sensitive to inhibition by a synthetic pyruvate analogue, but also shows less response to NADH and acetyl-CoA (Bowker-Kinley *et al.*, 1998). Leading to the suggestion by Bowker-Kinley and colleagues (Bowker-Kinley *et al.*, 1998) that PDK2 is involved in short-term metabolic control of pyruvate dehydrogenase, in contrast to PDK4 which has been suggested to be more involved in adaptive responses of pyruvate dehydrogenase. Furthermore, PDK4 is highly responsive to increased fatty acid concentrations, with a 7.5-9-fold increase in PDK4 mRNA in response to incubation with fatty acids, palmitate and oleate, in 7800 C1 cells (Huang *et al.*, 2002). This is echoed in mice, with a 10-fold increase in PDK4 protein abundance following 18 weeks HFD (Jeoung and Harris, 2008).

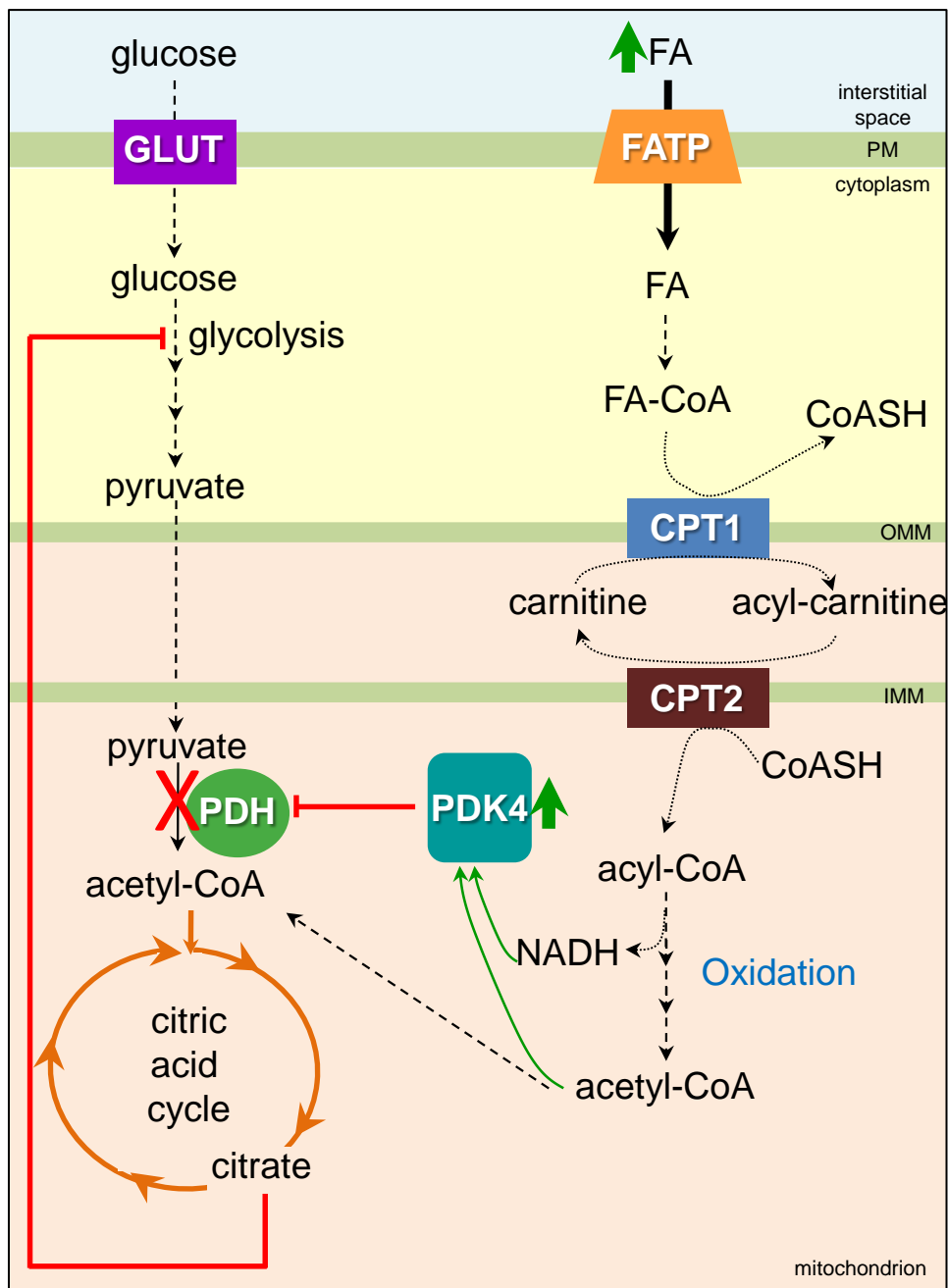


Figure 1.10. PDK4: the mechanism by which high fatty acid availability produces a nutrient shift to favour fatty acid metabolism.

FA, fatty acid; FA-CoA, fatty acyl-Coenzyme A; CoASH, Coenzyme A (not attached to an acyl group); CPT, carnitine palmitoyl transferase; NADH, nicotinamide adenine dinucleotide; PDK4, pyruvate dehydrogenase kinase 4; PDH, pyruvate dehydrogenase; GLUT, glucose transporter; FATP, fatty acid transporter; IMM, inner mitochondrial membrane; OMM, outer mitochondrial membrane. Thick green arrow, increased; thin green arrow, activates, red line, inhibits.

1.7 – GLUCOSE METABOLISM – ACTIVATION OF GLUCOSE

When glucose is taken up into the cell, it is rapidly phosphorylated to glucose-6-phosphate in an irreversible reaction catalysed by hexokinase (HK) in the skeletal muscle or by glucokinase (GCK) in the liver (Elliott and Elliott, 2001). The glucose-6-phosphate produced in this first committing step is the substrate for subsequent non-oxidative glucose metabolism, glycogen synthesis, or oxidative glycolysis (Pehleman *et al.*, 2005).

1.7.1 – Hexokinase 2 (HK2)

Of three HK isoforms, HK2 is the predominant isoform expressed in insulin sensitive tissues (Chang *et al.*, 1996), such as skeletal muscle (Printz *et al.*, 1993; Katzen, 1967). In an early study, Lawrence and Trayer (Lawrence and Trayer, 1985) reported that the HK2 enzyme is more abundant in red than white muscle and HK activity is greater type I and IIA muscle fibres than IIB fibres. HK2 exhibits high affinity for glucose and is inhibited by a feed-back control loop when the cellular concentration of glucose-6-phosphate increases (Ardehali *et al.*, 1999; Heikkinen *et al.*, 1999). In addition to its role in phosphorylating glucose, HK2 can bind to the mitochondria, where it is believed to interact with voltage-dependent anion channels through a PKC- ϵ -dependent pathway, leading to reduced intracellular levels of reactive oxygen species and ultimately protects the cell from apoptosis (Sun *et al.*, 2008).

In the skeletal muscle, HK2 expression and activity can be upregulated during times of energy demand, such as exercise, to ensure glucose supply to muscle cells is adequate

(Fu *et al.*, 2009; Kim *et al.*, 2000a; Koval *et al.*, 1998; Ivy *et al.*, 1986). Furthermore, research in mice has shown that HK2 overexpression consequently increases basal and insulin-stimulated glucose uptake in skeletal muscle (Chang *et al.*, 1996). An acute single bout of moderate-intensity exercise increases HK2 mRNA expression and activity in human skeletal muscle (Fu *et al.*, 2009; Koval *et al.*, 1998). Exercise training also elicits a similar response, as rats subjected to 3 hours of swimming exercise for 3 hour bouts over a 3 week period exhibited increased HK2 activity in skeletal muscle (Kim *et al.*, 2000a). The exercise-induced increase in skeletal muscle HK2 is believed to involve the activation of AMPK α 2, as nuclear AMPK α 2 protein abundance is enhanced by exercise (McGee *et al.*, 2003) and exposure to AMPK activator, AICAR, for 5 days stimulates HK2 activity (Holmes *et al.*, 1999).

In skeletal muscle, HK2 expression is also regulated by circulating hormones (Fu *et al.*, 2009; Ducluzeau *et al.*, 2001; Kruszynska *et al.*, 1998; Printz *et al.*, 1993). In human skeletal muscle HK2 is influenced by gonadal hormone levels, as women in the midfollicular phase of the menstrual cycle exhibit greater HK2 mRNA content than men (Fu *et al.*, 2009). HK2 also is controlled by insulin. In skeletal muscle, insulin stimulates the expression and activity of HK2 (Ducluzeau *et al.*, 2001; Kruszynska *et al.*, 1998; Printz *et al.*, 1993). In type 2 diabetics, HK2 is significantly reduced in skeletal muscle at both the levels of mRNA expression (Ducluzeau *et al.*, 2001) and activity (Kruszynska *et al.*, 1998). In individuals with normal insulin sensitivity, exposure to a 3 hour insulin infusion induces the expression of HK2 mRNA in skeletal muscle, but this response is defective in type 2 diabetic patients (Ducluzeau *et al.*, 2001). Type 2 diabetic patients exposed to a hyperinsulinemic clamp also failed to

exhibit an insulin-stimulated increase in HK2 activity in skeletal muscle (Kruszynska *et al.*, 1998).

In contrast to type 2 diabetics with severe insulin resistance, non-diabetic obese subjects with normal or slightly impaired insulin sensitivity exhibited similar basal and insulin-stimulated HK2 expression and activity in skeletal muscle to lean healthy individuals (Ducluzeau *et al.*, 2001; Kruszynska *et al.*, 1998). These studies therefore implicate HK2 deficiency in the development of severe insulin resistance; however a rodent model of HK2 gene deletion has not confirmed this hypothesis. Mice deficient in HK2 (HK2^{-/-}) have been shown to die within a week of fertilization, suggesting HK2 is essential for early embryogenesis (Heikkinen *et al.*, 1999). Unexpectedly heterozygous HK2 deficient (HK2^{+/-}) mice, in which 50% of HK2 activity is preserved, show no signs of glucose intolerance or impaired insulin sensitivity following standard chow or HFD feeding (Heikkinen *et al.*, 1999).

1.7.2 – Glucokinase (GCK)

GCK is the major enzyme involved in glucose phosphorylation in the liver, the first committing reaction in hepatic glucose metabolism that determines the rate of glucose oxidation (glycolysis) and glycogen storage (glycogenesis) (Gorman *et al.*, 2008). Although HK1-3 are expressed at very low levels in hepatocytes (Reyes and Cárdenas, 1984), GCK (HK4) is considered as an additional isoenzyme of hexokinase enzymes 1-3, despite its smaller molecular weight and exhibiting unique kinetic properties (Agius, 2008; Seoane *et al.*, 1999). Two isoforms of GCK exist, a liver-specific isoform expressed purely in hepatocytes and an islet isoform that is predominantly expressed in

pancreatic β -cells, the pituitary, hypothalamus and entero-endocrine K and L cells (Gorman *et al.*, 2008; Jetton *et al.*, 1994; Iynedjian *et al.*, 1989). In contrast to HK2, GCK exhibits lower affinity for glucose and is not subject to feed-back inhibition by physiological levels of glucose-6-phosphate (Ardehali *et al.*, 1999; Heikkinen *et al.*, 1999). When cellular glucose levels are low, such as during fasting, inactive GCK is sequestered in the nucleus bound to a specific regulatory protein, glucokinase regulatory protein, which reduces glucose phosphorylation to 15% of total GCK activity (Agius, 2008; Agius, 1998). However, in the postprandial state, in response to glucose, inactive GCK reserves are rapidly mobilised and GCK translocates to the cytoplasm where it acts to phosphorylate glucose (Agius, 2008; Agius, 1998).

Research in transgenic mice overexpressing GCK has provided evidence that GCK is the rate-limiting enzyme controlling hepatic glucose metabolism and also plays a role in mediating whole-body glucose homeostasis (Wu *et al.*, 2005; Ferre *et al.*, 1996). Rodents overexpressing GCK exhibit increased hepatic glucose disposal through pathways of oxidative (glycolysis) (Wu *et al.*, 2005; Ferre *et al.*, 1996) and non-oxidative (glycogen) glucose metabolism (Ferre *et al.*, 1996) and consequently exhibit marked reductions in plasma glucose and insulin (Wu *et al.*, 2005; O'Doherty *et al.*, 1999; Ferre *et al.*, 1996). Similarly overexpression of liver-type GCK in primary rat hepatocytes has been reported to elicit a 2.9-fold increase in glucose oxidation (Takeuchi *et al.*, 1996) and promote the activation of glycogen synthase (Seoane *et al.*, 1996). However, some studies have demonstrated that GCK overexpression leads to hyperlipidemia (O'Doherty *et al.*, 1999), especially in models of long-term overexpression (Ferre *et al.*, 2003) and this subsequently impairs insulin action

(Ferre *et al.*, 2003). The hyperlipidemia observed is believed to be a consequence of greater malonyl-CoA produced as a by-product of enhanced glucose metabolism; malonyl-CoA acts to suppress hepatic fatty acid oxidation and a corresponding increase in liver fat accumulation is observed, whilst hepatic fat secretion is also believed to increase (Wu *et al.*, 2005; Ferre *et al.*, 2003; O'Doherty *et al.*, 1999).

Whilst longer-term studies demonstrate that GCK overexpression can lead to reduced insulin sensitivity (Ferre *et al.*, 2003), reduced GCK activation is also believed to be implicated in abnormal hepatic glucose homeostasis and impaired insulin secretion in type 2 diabetes (Gorman *et al.*, 2008). Transgenic mice with global and islet isoform-specific GCK deletion ($gk^{\text{del/wt}}$) exhibit ~40% reduction in both liver and islet GCK mRNA and liver GCK activity and this is associated with early-onset mild diabetes (Gorman *et al.*, 2008). Isolated hepatocytes from obese ZDF rats exhibit reduced GCK activity compared to those from lean Zucker rats (Seoane *et al.*, 1999). High fat feeding streptozotocin-treated rats similarly elicited a marked suppression on hepatic GCK activity, compared to lean streptozotocin-treated rats (Chisholm and O'Dea, 1987). Given the defective activity of GCK in diabetes, activation of GCK has been considered as potential pharmaceutical therapeutic against diabetes, but given the consequences of long-term GCK activation reported by Ferre and colleagues (Ferre *et al.*, 2003), they suggested that the consequences of long-term activation should be considered.

1.8 – GLUCOSE METABOLISM – GLYCOLYSIS

Following the irreversible phosphorylation of glucose, it is channelled into pathways of oxidative (glycolysis) or non-oxidative (glycogenesis) glucose metabolism. The glucose-6-phosphate that is channelled into the glycolytic pathway is converted to fructose-6-phosphate (Elliott and Elliott, 2001). Fructose-6-phosphate is the substrate of the subsequent reaction, along with ATP, that is catalysed by 6-phosphofructo-1-kinase (phosphofructokinase, PFK) and yields fructose-1:6-bisphosphate (Elliott and Elliott, 2001). Given the irreversible nature of this reaction (Elliott and Elliott, 2001), PFK is a key rate-limiting enzyme controlling glycolysis (Ristow *et al.*, 1997; Dunaway *et al.*, 1988) (see **Figure 1.11**).

1.8.1 – Phosphofructokinase (PFK)

Three major isoforms of PFK exist in mammalian tissues and each isoform is encoded by a distinct gene (Getty-Kaushik *et al.*, 2010; Nakajima *et al.*, 2002; Dunaway and Kasten, 1987). Skeletal muscle exhibits a high level of total PFK activity and specifically expresses the PFK-M isoform (Dunaway *et al.*, 1988; Dunaway and Kasten, 1987). The liver displays much lower total PFK activity, and of the PFK isoforms expressed in the liver, PFK-L is the most predominant (~80%), with modest expression of PFK-M (~20%) and scarce expression of PFK-C (~0-4%) (Dunaway and Kasten, 1987), sometimes known as PFK-P or -F (Getty-Kaushik *et al.*, 2010; Nakajima *et al.*, 2002).

1.8.1.1 – Muscle Type Phosphofructokinase (PFK-M)

Whilst the majority of PFK-expressing tissues exhibit all three PFK isoforms, the skeletal muscle is unique in possessing only the PFK-M isoform; however multiple transcripts of the PFK-M isoform exist (Richard *et al.*, 2007). The PFK-M gene possesses both a proximal and a distal promoter which are capable of producing multiple transcripts; the proximal promoter functions predominantly in skeletal muscle and the distal promoter plays a ubiquitous role (Richard *et al.*, 2007). In humans, a deficiency in the PFK-M enzyme is an autosomal recessive condition commonly known as Tarui's disease (glycogen storage disease type VII) (Nakajima *et al.*, 2002; Ristow *et al.*, 1997) which occurs in 1 in every 100,000 people (homozygous form) (Ristow *et al.*, 1997). These individuals commonly present with exercise-induced muscle pain at an early age, which progressively leads to the development of mature-onset severe physical disability (Nakajima *et al.*, 2002) and insulin resistance (Ristow *et al.*, 1997). In mice, PFK-M deficiency (PFK-M^{-/-}) significantly reduces lifespan, with 60% of PFK-M^{-/-} mice dying around the time of weaning and any survivors dying within 3-6 months of life (García *et al.*, 2009). PFK-M null mice exhibit glycogenosis manifested in increased glycogen content, due to the lack of glycolysis, in cardiac muscle this leads to cardiac hypertrophy and given the lack of the PFK-M isoform in erythrocytes, hemolysis is also observed (García *et al.*, 2009).

1.8.1.2 – Liver Type Phosphofructokinase (PFK-L)

The liver exhibits fairly low levels of PFK activity, of which the PFK-L isoform predominates (Dunaway and Kasten, 1987). The PFK-L isoform is also expressed in

the brain, heart, testes, thyroid, spleen, intestine, kidney, adipose tissue, placenta and lungs (Dunaway *et al.*, 1988; Dunaway and Kasten, 1987). In the liver, the mRNA and protein expression of the PFK-L isoform is influenced by both hormonal and nutritional changes, being suppressed by fasting and induced upon refeeding, and is also suppressed in diabetic individuals (Gehrich *et al.*, 1988). The reduced abundance of PFK-L protein in diabetic and starved rats may be due to accelerated degradation of PFK-L protein, and the increased expression upon refeeding due to increased synthesis and reduced degradation of the PFK-L protein (Hotta *et al.*, 1991).

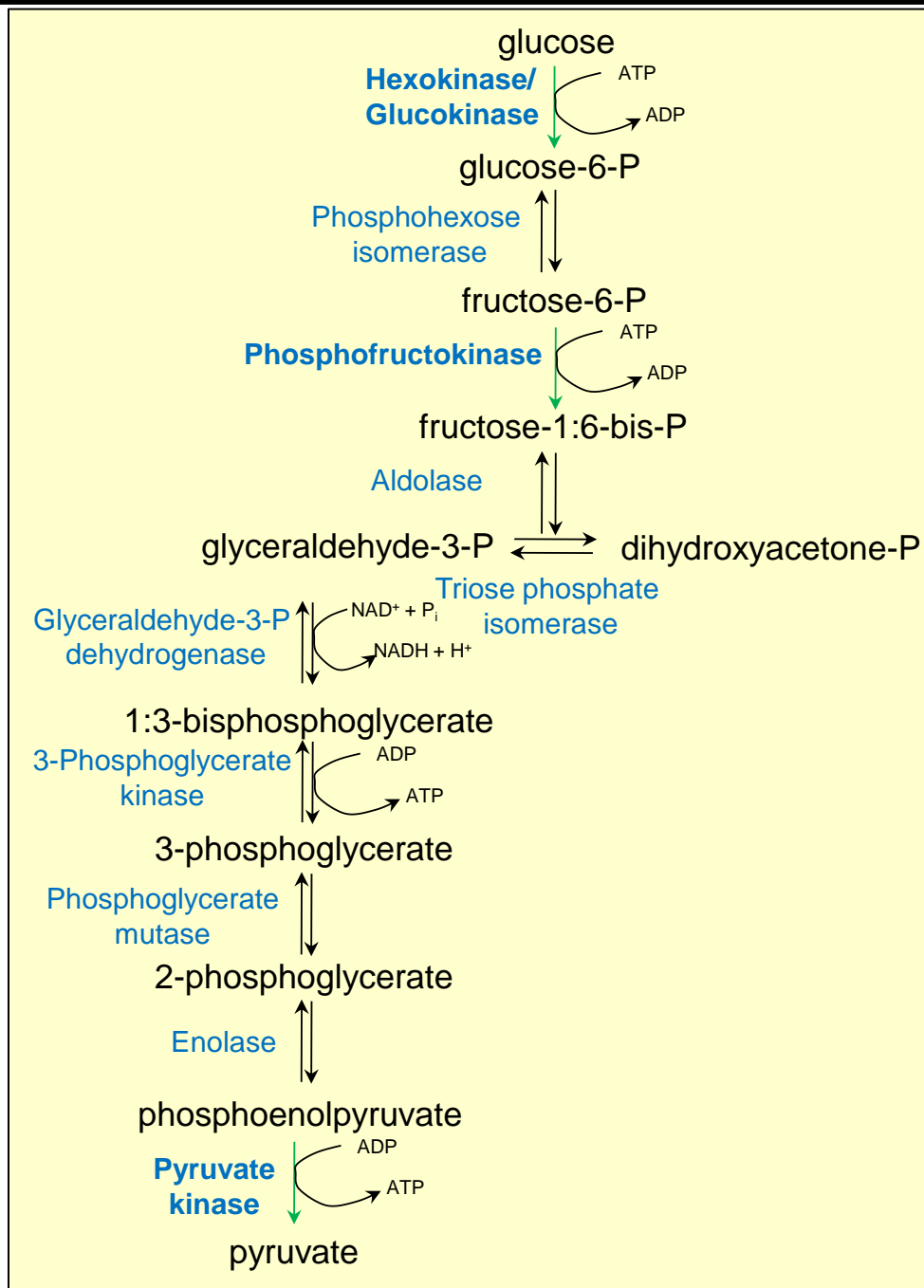


Figure 1.11. The complete glycolytic pathway.

Glycolysis constitutes the primary step in the oxidation of glucose to generate energy. The pathway involves several reactions which convert activated glucose (glucose-6-phosphate) to 2 pyruvate molecules. These pyruvate molecules are then, during aerobic conditions, transported to the mitochondria where they are converted to acetyl-CoA. Ultimately acetyl-CoA enters the citric acid cycle, where it is oxidised to release energy. Irreversible reactions are represented using green arrows and bold font. (Elliott and Elliott, 2001).

1.9 – GLUCOSE METABOLISM – GLYCOGENESIS

Glucose is stored in a limited reserve in the form of glycogen, a long branched polymer chain. By using these glycogen stores, the liver plays a key role in maintaining blood glucose levels. During times of low energy availability, the liver is able to break down glycogen, releasing glucose into the circulation for uptake by glucose-dependent tissues, such as the brain, although in humans these stores are finite and hepatic glycogen stores are exhausted following 24 hours starvation (Elliott and Elliott, 2001). In contrast, the skeletal muscle stores much less glycogen, approximately 13% of the reserve stored in the liver (Alonso *et al.*, 1995).

1.9.1 – Glycogen Synthase (GYS)

Glycogen synthase (GYS) is the enzyme responsible for the addition of a glucose residue from UDP-glucose to an amylose chain leading to the enlargement of the pre-existing glycogen molecule, a reaction that constitutes one of the key rate-limiting reactions in glycogen synthesis (Elliott and Elliott, 2001; Ivy and Kuo, 1998; Villar-Palasi and Guinovart, 1997) (**Figure 1.12**). Glycogen synthase exists in either the inactive D-form or active I-form and the interconversion between these forms is via phosphorylation or de-phosphorylation reactions at 3 of glycogen synthases' 9 phosphorylation sites (Ivy and Kuo, 1998). The muscle isoform of GYS (GYS1) is 32-34 amino acids longer than that observed in the liver (GYS2), whilst the two enzymes share only 69% amino acid homology (Villar-Palasi and Guinovart, 1997). Furthermore, the liver enzyme lacks the 2a and 2b phosphorylation sites which are phosphorylated on the skeletal muscle isoform by cyclic AMP-dependent protein

kinase, however, this kinase phosphorylates serines in a peptide with strong homology to the sites of 3a, 3b and 3c of muscle GYS, phosphorylated by muscle GYS kinase-3 (Villar-Palasi and Guinovart, 1997). Similar to the muscle isoform, the liver isoform of GYS undergoes phosphorylation at a threonine residue, most likely by enzyme casein kinase II (Villar-Palasi and Guinovart, 1997). Activation of GYS occurs through dephosphorylation which is catalysed in skeletal muscle by protein phosphatase 1 and to a lesser extent by protein phosphatase 2A, and in the liver by protein phosphatase 2A and to a lesser extent by phosphatase 1 (Villar-Palasi and Guinovart, 1997). Furthermore, phosphatase 2c is also able to dephosphorylate both GYS1 and GYS2, but exhibits lower activity in the muscle (15%) and liver (6%) (Villar-Palasi and Guinovart, 1997). *In vitro* studies have demonstrated that glucose-6-phosphate is able to bind GYS, leading to allosteric activation of GYS and therefore GYS is more susceptible to dephosphorylation and activation by phosphatases (Villar-Palasi and Guinovart, 1997). In contrast, glycogen breakdown occurs through the action of enzyme glycogen phosphorylase (glycogen chain +Pi \rightarrow glucose-1-phosphate + glycogen chain (glucose units)_{n-1}) (Elliott and Elliott, 2001).

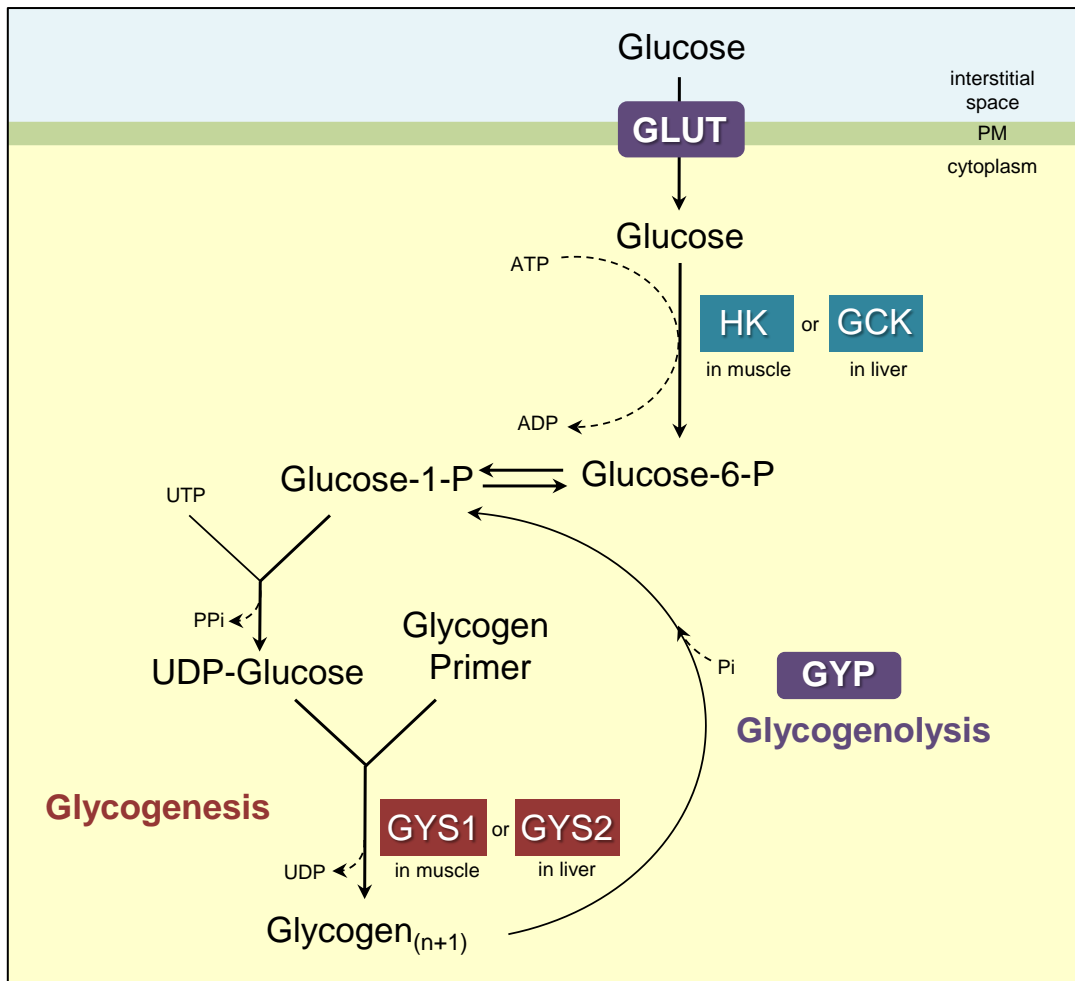


Figure 1.12. The glycogen synthesis pathway.

GYS, glycogen synthase; GYP, glycogen phosphorylase; GLUT, glucose transporter; HK, hexokinase; GCK, glucokinase. (Elliott and Elliott, 2001).

1.10 – GLUCOSE METABOLISM – GLUCONEOGENESIS

Gluconeogenesis is the *de novo* synthesis of glucose from substrates such as gluconeogenic amino acids, glycerol and lactate. This process occurs mainly in the liver and to a lesser extent in the kidneys (Elliott and Elliott, 2001) and is important during times of starvation, during which it provides the organism with a source of glucose (Barthel and Schmoll, 2003; Elliott and Elliott, 2001). Mitochondrial fuel oxidation supplies the energy required for gluconeogenesis from precursors that pass through pyruvate (Bizeau *et al.*, 2001). The initiating step of gluconeogenesis is catalysed by mitochondrial enzyme, pyruvate carboxylase, which converts pyruvate to oxaloacetate (Barthel and Schmoll, 2003; Bizeau *et al.*, 2001; Elliott and Elliott, 2001).

Figure 1.13 demonstrates the pathway of gluconeogenesis (Elliott and Elliott, 2001). A key rate limiting step of gluconeogenesis is the reaction catalysed by phosphoenolpyruvate carboxykinase (PEPCK), in which oxaloacetate is then converted to phosphoenolpyruvate (Barthel and Schmoll, 2003; Bizeau *et al.*, 2001; Elliott and Elliott, 2001).

1.10.1 – Phosphoenolpyruvate carboxykinase (PEPCK)

The decarboxylation and phosphorylation of oxaloacetate to phosphoenolpyruvate, catalysed by PEPCK, constitutes the earliest rate-limiting step of gluconeogenesis (Samuel *et al.*, 2009). Transcription of PEPCK is closely regulated by several transcription factors, including HNF3, FKHR1 and C/EBP, and other proteins, such as SIRT1, PGC1 α and TRB3 (Samuel *et al.*, 2009). Furthermore activation of AMPK in primary cell cultured hepatocytes has been demonstrated to reduce PEPCK expression

(Foretz *et al.*, 2005). Whilst under fasting conditions, glucagon acts through CAMP-responsive factor, CREB, (CREB binding protein) to enhance the transcription of gluconeogenic genes (Viollet *et al.*, 2006). As a result coactivators TORC2 and CBP are recruited, leading to the transcription of PGC1 α . Subsequently PEPCK is transcribed in association with transcription factor HNF4 α and fork head family activator, FoxO1, leading to gluconeogenesis (Viollet *et al.*, 2006). High fat feeding increases gluconeogenic flux in male Sprague-Dawley rats, as a result of increased pyruvate flux through PEPCK (Bizeau *et al.*, 2001). Hepatic PEPCK expression is also increased in diabetic ZDF and GK rats, and *db/db* mice (Samuel *et al.*, 2009). Although in humans with type 2 diabetes, PEPCK mRNA expression is unchanged, despite marked increases in fasting plasma glucose (Samuel *et al.*, 2009).

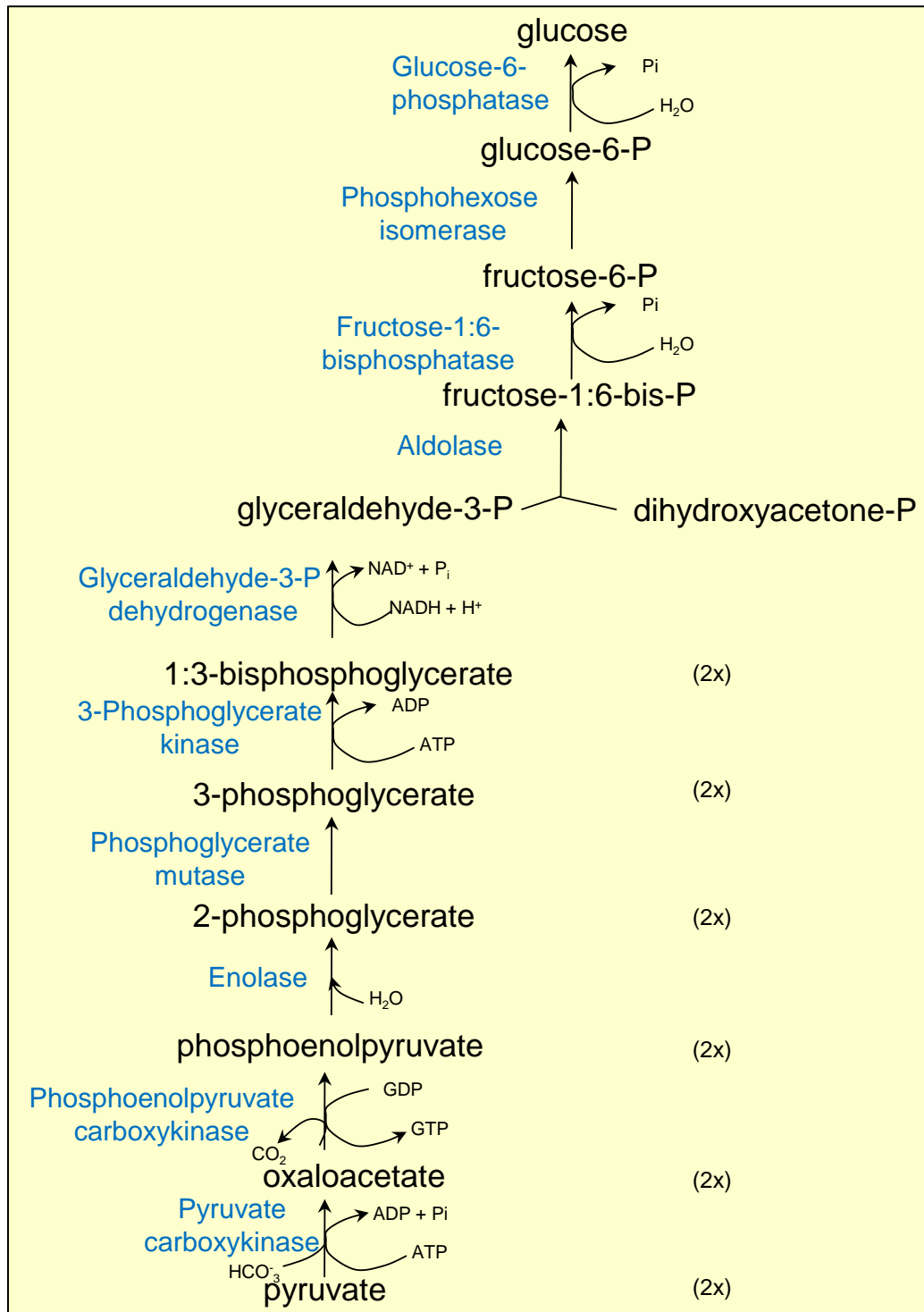


Figure 1.13. The gluconeogenesis pathway from pyruvate to glucose.

P, phosphate. (Elliott and Elliott, 2001).

1.11 – GLUCOSE METABOLISM – INSULIN SIGNALLING

As reviewed by Khan and Pessin (Khan and Pessin, 2002) and Watson and Pessin (Watson and Pessin, 2001), insulin-induced glucose uptake occurs in a series of steps. Initially, at the plasma membrane, insulin binds to its receptor, leading to its autophosphorylation and activation. This then aids binding and ensuing tyrosine phosphorylation of the insulin receptor substrate (IRS) family of proteins. IRS engages and subsequently activates PI3K, producing phosphoinositol-3,4,5-triphosphate (PIP3) and subsequently activates 3-phosphoinositide-dependent protein kinase 1 (PDK1). In turn PDK1 phosphorylates and activates PKC and PKB, which stimulate exocytosis of glucose transporter 4 (GLUT4) vesicles. Finally at the plasma membrane, the translocation and fusion of the GLUT4 storage vesicles initiates glucose uptake into the cell.

1.11.1 – Phosphoinositol 3-Kinase (PI3K)

As described briefly above, PI3Ks act to phosphorylate the 3'-OH position on the inositol ring of phosphatidylinositol-4,5-bisphosphate (PIP2) to generate PIP3, a lipid second messenger (Luo *et al.*, 2006). Class I_A PI3K exists as a heterodimer comprised of the p110 catalytic subunit and p85 regulatory subunit, essential for the stability of p110 subunit (Luo *et al.*, 2006). A single gene, PI3K α , encodes the main p85 isoforms, p85 α , p55 α and p50 α , through alternative transcription initiation sites (Luo *et al.*, 2006). Research by Luo and colleagues (Luo *et al.*, 2006), in which they generated mice deficient in both the p85 α /p55 α /p50 α and p85 β regulatory subunits of PI3K in skeletal muscle, demonstrates that knockout of the p85 subunit critically impairs PI3K

signalling, leading to loss of muscle mass and fibre size. Furthermore as a consequence of p85 deletion, these mice exhibit skeletal muscle insulin resistance and whole-body glucose intolerance (Luo *et al.*, 2006). Furthermore, p85 knockout animals display greater body fat mass and exhibit elevated serum free fatty acid and triglyceride concentrations, suggesting that loss of PI3K p85 is a critical mediator of PI3K signalling in regulating muscle metabolism (Luo *et al.*, 2006).

1.12 ALTERED GLUCOSE METABOLISM AND INSULIN SIGNALLING WITH HIGH FAT FEEDING

Intramuscular and intrahepatic triglyceride accretion are associated with reduced insulin sensitivity (Qureshi *et al.*, 2010; Marchesini *et al.*, 2003; Chitturi *et al.*, 2002; Manco *et al.*, 2000). As reviewed by Taouis and colleagues (Taouis *et al.*, 2002), high fat feeding leads to reduced levels of the insulin receptor, less phosphorylation of IRS proteins and subsequently diminished activation of PI3K. Furthermore, the activity, translocation and expression of GLUT4 is altered, which in total suggests that high fat feeding leads to the impairment of the early stages of insulin signalling (Taouis *et al.*, 2002).

1.13 – HIGH FAT INTAKE – IMPLICATING THE IMPORTANCE OF FAT TYPE

Although genetics clearly contribute to the development of the obese phenotype, Swinburn and colleagues (Swinburn *et al.*, 2009) recently demonstrated that energy overconsumption alone is able to sufficiently account for the increased weight gain

associated with increased obesity incidence in the US. Consuming a diet rich in fat has long been considered obesogenic and this may be in part due to fat having over twice the energy density of carbohydrate and protein (Thomas *et al.*, 2007; Drewnowski, 2004). Ecological studies that combined data from a sample population with BMI ≥ 25 from 20 countries (Bray and Popkin, 1998; Drewnowski, 2007) demonstrated that as the proportion of dietary energy from fat is increased, the prevalence of overweight increased ($P < 0.001$, $R^2 = 0.78$) (Bray and Popkin, 1998; Drewnowski, 2007). Recent studies, however, have shown that the type of dietary fat consumed may either influence the likelihood of developing obesity and its co-morbidities.

1.13.1 – The Characteristics of Dietary Fatty Acid Types and their Influence on Metabolic Dysfunction

Fatty acids are comprised of hydrocarbon chains of varying length, linked by chemical bonds and capped with a carboxyl group and a methyl group at the extremities. Fatty acids are classified according to chain length and saturation, both of which influence the metabolic fate of the fatty acid.

1.13.1.1 - Chain Length

Fatty acids are classified by their chain length; short chain fatty acids exhibit ≤ 8 carbon atoms, medium chain fatty acids are typically 8-12 carbon atoms long, long chain fatty acids exhibit ≥ 12 carbon atoms (Papamandjaris *et al.*, 1998; Nettleton, 1995) and very long chain fatty acids are $> 20-22$ carbon atoms in length (Leonard *et al.*, 2004; Poulos, 1995). Fatty acid chain length has been shown to influence metabolism during the

early stages of digestion and absorption, with short and medium chain fatty acids (≤ 11 carbon atoms) being absorbed directly from the gut to the portal vein, and in contrast, long chain fatty acids undergo re-esterification, chylomicron packaging and enter the circulation via the lymph system (Little *et al.*, 2007; Papamandjaris *et al.*, 1998). During the later stages of metabolism, fatty acyl-CoA molecules (fatty acids which have been converted to allow entry to the mitochondria) may undergo several rounds of cleavage in a process known as β -oxidation, resulting in energy generation. Chain length also influences metabolism at this advanced time point, as cleaving enzymes are structurally and mechanically different, accommodating substrates of specific chain length (Kim and Battaile, 2002). The time frame in which fats of different chain length are oxidised also differs, during a set period of time shorter chain fatty acids have a higher percentage oxidation, than longer chain fatty acids oxidised in the same time frame (DeLany *et al.*, 2000).

1.13.1.2 - Saturation

The nature of the chemical bonds and amount of hydrogen atoms featured in fatty acids, prompts their saturation classification (Nettleton and Katz, 2005). Fatty acids carrying the maximum amount of hydrogen atoms (H^+), and hence having single (CH_2-CH_2) bonds, are described as saturated fatty acids. When a pair of hydrogen atoms are removed and replaced with a double bond ($C=C$), the fatty acid becomes unsaturated. Varying levels of saturation exist, ranging from saturated, no double bonds; monounsaturated, containing one double bond; to polyunsaturated, containing multiple (≥ 2) double bonds. The position of the double bond/s are often conserved, and are

labelled according to their position in the chain (n), examples include n-3, n-6, n-9 (Chong *et al.*, 2006; Nettleton and Katz, 2005). Fatty acid saturation has been shown to influence lipid metabolism, an example of which is seen in fatty acid fate, with saturated fats being less likely to undergo oxidation, accumulating as DAG and ceramides, whilst monounsaturated or polyunsaturated fatty acids accumulate as intra-tissue triglycerides or free fatty acids (Lee *et al.*, 2006a). Like chain length, saturation also influences the rate of fatty acid oxidation, with the number of double bonds exhibiting a positive relationship with percentage of fatty acid oxidised over a set time frame (DeLany *et al.*, 2000) .

Therefore not only does the quantity of fat consumed affect energy metabolism, but the fatty acid qualities may possibly increase the likelihood of weight gain and disordered metabolism (Moussavi *et al.*, 2008).

1.13.2 – The Importance of Fat Type in a High Fat Diet Setting

In Australia, the average adult consumes approximately 6% above the recommended intake of saturated fat and less than half of the recommended daily amount of long chain n-3 polyunsaturated fatty acids (PUFA) (Food Standards Australia New Zealand, 2009). This is important as there is some evidence that the type and proportion of dietary fat consumed may influence the development of the obese phenotype (Buettner *et al.*, 2006; Ikemoto *et al.*, 1996). Diets rich in saturated fat, often from animal or dairy sources (Tomé *et al.*, 2004), have been implicated in the development of obesity (Ikemoto *et al.*, 1996; Buettner *et al.*, 2006; Rustan *et al.*, 1993; Marotta *et al.*, 2004; Wang *et al.*, 2002) due to their greater propensity to enter storage in adipose tissue as

opposed to being oxidised (Pan *et al.*, 1994; Piers *et al.*, 2003). Diets rich in saturated fat also result in ectopic fat deposition, with increased triglyceride concentration in skeletal muscle (Kim *et al.*, 2000b; Mullen *et al.*, 2007; Simončíkova *et al.*, 2002) and liver (Buettner *et al.*, 2006; Ukropec *et al.*, 2003).

In contrast, it has been shown that consumption of n-3 PUFA, also known as Omega-3 fatty acids, have positive health benefits (Flachs *et al.*, 2006; Ruzickova *et al.*, 2004). A rich source of n-3 PUFAs are marine oils from fish, shellfish and sea mammals, containing fatty acids such as eicosapentaenoic acid (EPA, 20:5n-3) and docosahexaenoic acid (DHA, 22:6n-3) (Flachs *et al.*, 2006; Lombardo and Chicco, 2006; Ruzickova *et al.*, 2004). n-3 PUFAs have been shown to help with regulating lipid levels and have anti-inflammatory (Biscione *et al.*, 2007; Lombardo and Chicco, 2006), anti-atherosclerotic (Biscione *et al.*, 2007), anti-thrombolytic, anti-arrhythmic and vasodilatory properties (Lombardo and Chicco, 2006). It is also believed that n-3 PUFAs could play a vital role in the prevention and management of insulin resistance and type 2 diabetes mellitus (Lombardo and Chicco, 2006; Nettleton and Katz, 2005), heart disease (Biscione *et al.*, 2007; Lombardo and Chicco, 2006), hypertension (Lombardo and Chicco, 2006), dyslipidemia and obesity (Biscione *et al.*, 2007; Lombardo and Chicco, 2006). Diets rich in n-3 PUFA also limit adipose tissue hypertrophy in the perirenal and epididymal depots of rats (Parrish *et al.*, 1990; Belzung *et al.*, 1993; Rokling-Andersen *et al.*, 2009), reduce ectopic fat deposition in skeletal muscle (Rossmesl *et al.*, 2009) and liver (Ruzickova *et al.*, 2004; Buettner *et al.*, 2006) and prevent HFD-induced insulin resistance in rats (Storlien *et al.*, 1987).

1.13.3 – Saturated Fatty Acids and Polyunsaturated Fatty Acids: Fatty Acid Type and their Effect on Body Weight and Whole-Body Metabolism

Diets rich in saturated fat induce weight gain in rodents (Buettner *et al.*, 2006; Marotta *et al.*, 2004; Wang *et al.*, 2002; Ikemoto *et al.*, 1996; Rustan *et al.*, 1993). A growing body of evidence suggests that the consumption of a HFD enriched with n-3 PUFAs can ameliorate the weight gain and/or increased fat mass associated with high fat overfeeding. Numerous studies have investigated the replacement of all or part of fatty acids in a HFD with n-3 PUFAs, resulting in discordant results, possibly the result of differing dietary time frames, dietary fatty acid combinations and species tested.

Research conducted by Rustan and colleagues (Rustan *et al.*, 1993) showed that n-3 PUFA enrichment (6.5% FAs) of a HFD comprised of saturated fat-rich lard (40% energy from fat) for ~7 weeks did not significantly alter body weight in male Wistar rats, when compared to rats receiving a low n-3 HFD (lard). During the dietary period, lard-fed rats exhibited similar food intake and energy expenditure to their n-3 enriched counterparts (Rustan *et al.*, 1993). Similar responses to the high fat lard diet and high fat n-3 PUFA enriched diet may be explained by the dietary time frame. Incorporation of n-3 PUFAs into red blood cells or metabolic tissues requires at least 4 months to reach steady state (Arterburn *et al.*, 2006; Krebs *et al.*, 2006) and therefore the short time course of this study may not have allowed adequate time for n-3 PUFAs to exert their full metabolic effects. Despite the lack of physical differences in this study, rats exhibited differential metabolic effects upon feeding HFDs with/without n-3 PUFA enrichment (Rustan *et al.*, 1993). Rats exposed to the n-3 PUFA enriched HFD showed an increased respiratory quotient, which was accounted for by increased carbohydrate

oxidation (Rustan *et al.*, 1993). Significantly higher plasma glucose concentrations and significantly reduced plasma lipid (triglycerides, phospholipids, unesterified fatty acids) and glycerol contents in rats fed the n-3 PUFA enriched HFD are indicative of altered whole-body metabolism (Rustan *et al.*, 1993). Disparate structuring of substrate utilisation could in time change body composition in these animals, potentially producing weight loss in mice receiving an n-3 enriched HFD, compared to those consuming a saturated fat-rich HFD.

Many studies have shown that n-3 PUFA enrichment of a HFD reduces body weight gain and fat deposition (Buettner *et al.*, 2006; Wang *et al.*, 2002; Ikemoto *et al.*, 1996). A study conducted by Buettner and associates (Buettner *et al.*, 2006) demonstrated that male Wistar rats fed a HFD (42% E from fat) composed of n-3 PUFA-rich cod liver oil weighed significantly less following a 12 week diet, than rats consuming isocaloric saturated fat-rich HFDs comprised of lard or coconut fat (Buettner *et al.*, 2006). In this study, however, reduced cumulative energy intake may explain reduced body weight in fish oil-fed rats, when compared to lard-fed rats (Buettner *et al.*, 2006). Although in the coconut fat-fed and fish oil-fed groups energy intake was not significantly different and therefore cannot explain the reduced weight gain upon n-3 PUFA enrichment (Buettner *et al.*, 2006). A longer-term study (19 weeks) conducted by Ikemoto and colleagues (Ikemoto *et al.*, 1996) also showed that feeding female C57BL/6J mice a HFD (60.2% energy from fat) of n-3 PUFA-rich fish oil halved body weight gain and reduced fat accumulation in the white adipose tissue depot, when compared to mice fed isocaloric HFDs of saturated fat-rich palm oil or lard. Again, this reduction in weight upon n-3 PUFA consumption was not explained by energy intake as fish oil-fed mice

had a tendency for higher energy intake than saturated fat-fed mice (Ikemoto *et al.*, 1996). What is more striking is that high fat fish oil fed-rodents had significantly lower body weight and fat deposition than rodents fed a low fat diet (~11% energy from fat), concurrent with unchanged or increased cumulative energy intake in the fish oil group (Ikemoto *et al.*, 1996). Such research provides compelling evidence to suggest that n-3 PUFA enrichment of a HFD can ameliorate the changes in body composition of a saturated fat-rich HFD. As a result, a body of evidence is growing, investigating the mechanistic reasons for improved metabolic function upon n-3 enrichment of a HFD in tissues of high metabolic demand, such as the skeletal muscle and liver.

1.13.4 – n-3 PUFA Enrichment of a HFD Reduces Liver Triglyceride Accumulation by Reducing Lipid Storage and Promoting Fatty Acid Oxidation

A high saturated fat intake increases triglyceride content in the liver (Buettner *et al.*, 2006; Ukropec *et al.*, 2003). Buettner and colleagues (Buettner *et al.*, 2006) showed that liver triglyceride content was significantly reduced in rats fed a HFD comprising fish oil, compared to rats consuming saturated fat-rich HFDs of lard or coconut fat, and that this reduction in the fish oil group resulted in a similar triglyceride level to high carbohydrate diet-fed animals. With further investigation into key hepatic genes involved in fatty acid metabolism by gene array studies, it was found that saturated fats and n-3 PUFAs had differential effects on lipid metabolism in the liver (Buettner *et al.*, 2006). Genes involved in lipid synthesis, such as SCD and FAS were upregulated in saturated fat-fed rats, but were upregulated to a lesser extent or unchanged in n-3 PUFA-fed animals (Buettner *et al.*, 2006). Genes implicated in fatty acid oxidation,

such as CPT and enoyl-CoA hydratase, were downregulated in lard- or coconut fat-fed rats, but were unchanged or upregulated in n-3 PUFA-fed animals (Buettner *et al.*, 2006). Furthermore, key regulator of fatty acid oxidation, PPAR α was upregulated only in fish oil-fed rats, compared to rats fed lard and coconut fat (Buettner *et al.*, 2006). In summary, saturated fat-rich HFDs promote lipid deposition and suppress fatty acid oxidation in the liver, whilst n-3 PUFA-rich HFDs promote fatty acid oxidation, concurrent with reduced lipid storage.

1.13.5 – n-3 PUFA Enrichment of a HFD Reduces Intramuscular Triglyceride Accumulation

A high saturated fat intake increases triglyceride content in skeletal muscle (Mullen *et al.*, 2007; Simončíkova *et al.*, 2002; Kim *et al.*, 2000b). Simončíkova and colleagues (Simončíkova *et al.*, 2002) showed that intramuscular triglyceride content was significantly reduced in rats fed a HFD comprising fish oil (10% weight of saturated fatty acids replaced with n-3 PUFAs), compared to rats consuming saturated fat-rich HFD (70% energy from fat), and that this reduction in the fish oil group resulted in a similar triglyceride level to rats fed standard chow. Interestingly, it has been shown that intramuscular triglyceride content has a negative relationship with whole-body glucose uptake ($R^2=0.56$, $P<0.0001$) (Manco *et al.*, 2000). Storlien and colleagues (Storlien *et al.*, 1991) similarly showed that skeletal muscle insulin sensitivity was inversely correlated with intramuscular triglyceride accumulation in the SO soleus and red quadriceps muscles ($r=0.95$ and 0.86 respectively; $P<0.01$). Furthermore, it is believed that the fatty acid profile within the membrane phospholipids of skeletal muscle

strongly influences insulin's binding and activity (Storlien *et al.*, 1997). Sohal and associates (Sohal *et al.*, 1992) showed that both healthy and diabetic rats fed diets high in n-3 PUFAs (20% fat) had significantly increased insulin-stimulated glucose transport into the EDL muscle compared to their counterparts receiving a low n-3 PUFA diet. Similarly, Borkman and associates (Borkman *et al.*, 1993) showed that the percentage of C20-22 PUFAs (including EPA and DHA) present in the vastus lateralis muscle of humans positively correlated with insulin sensitivity ($r=0.76$, $P=0.002$).

1.13.6 – n-3 PUFA Enrichment of a HFD Improves Whole-Body Insulin Sensitivity

Consuming a diet high in saturated fat for as little as 4 weeks has been shown to evoke peripheral insulin resistance in rodents (Holness *et al.*, 2004). Holness and colleagues (Holness *et al.*, 2004) demonstrated that female Wistar rats experience insulin hypersecretion, accompanied by a significantly increased acute glucose response when maintained on a 4 week HF-S diet (22% lipid) followed by a challenge with an intravenous glucose bolus, compared to high carbohydrate diet-fed mice (3% lipid). Enrichment of this HFD (7% of fatty acids replaced) with n-3 PUFAs for just 24 hours completely reversed the increased insulin response to a level comparable to rats receiving a high carbohydrate diet, as n-3 PUFAs directly altered the response of pancreatic β -cells (Holness *et al.*, 2004). Interestingly, glucose disposal rates measured similarly in rats fed HF-S and low fat diets, whereas rats fed the 24 hour n-3 PUFA enriched diet exhibited significantly lower rates of glucose disappearance than both the HFD and high carbohydrate diet groups (Holness *et al.*, 2004). Therefore acute n-3 PUFA enrichment selectively reversed high-saturated fat feeding-induced insulin

hypersecretion, but did not improve peripheral insulin resistance (Holness *et al.*, 2004). A longer-term study, also conducted by Holness and associates (Holness *et al.*, 2003), demonstrated that substituting 7% of dietary fatty acids for n-3 PUFAs in a HFD for 4 weeks prevented the effect of HF-S feeding to induce insulin resistance when challenged with glucose *in vivo*, in regards to peripheral glucose disposal and insulin hypersecretion. However, these effects were associated with insulin resistance with respect to suppression of endogenous glucose production and impaired glucose tolerance *in vivo* (Holness *et al.*, 2003). Reduced hyperinsulinemia, despite glucose intolerance, indicates that n-3 PUFAs directly impair the cellular response to saturated fat in a way that insulin secretion cannot be increased (Holness *et al.*, 2003). Chronic dietary fish oil enrichment (23.3% lipid) in obese, insulin resistant *ob/ob* mice (Steerenberg *et al.*, 2002), significantly increased plasma insulin levels at 3 months, and remained elevated for a further 3 months, when compared to high saturated fat-fed mice (25 % lipid). Glucose tolerance tests at 3, 6, 8 and 10 month time points revealed a tendency for more effective peripheral glucose uptake in the fish oil-fed mice compared to those receiving the HF-S diet (Steerenberg *et al.*, 2002). These studies therefore suggest that n-3 PUFA enrichment of a HFD can in the short- and long-term, partially or fully, reduce HF-S-induced insulin resistance, respectively.

1.14 – HIGH FAT INTAKE – IMPLICATING THE IMPORTANCE OF GENDER

Some recent research has shown that there are gender differences in the development of obesity in humans (Haugaard *et al.*, 2009; Moro *et al.*, 2009) and in response to

obesogenic HFDs in rodents (Català-Niell *et al.*, 2008; Gómez-Pérez *et al.*, 2008; Priego *et al.*, 2008). In humans, obese females exhibit greater intramuscular triglyceride accumulation than obese males (when matched for body mass index) (Haugaard *et al.*, 2009; Moro *et al.*, 2009). In rodents, females more aptly handle the fuel excess of a HFD with elevated adipose tissue storage and enhanced fatty acid oxidation capacity in muscle, whilst males exhibit less efficient adipose tissue storage, with enhanced hepatic fatty acid oxidation rate and greater hepatic triglyceride storage, which may relate to reduced insulin sensitivity (Priego *et al.*, 2008).

Gender-specific differences in the development of obesity can, in part, be explained by the influence of gonadal steroids, testosterone and oestrogen, on body composition and energy homeostasis (Geer and Shen, 2009; Lovejoy *et al.*, 2009). Post-menopausal women, lacking oestrogen production, exhibit a higher waist circumference (Perrone *et al.*, 1999) and reduced insulin sensitivity (Geer and Shen, 2009) than those treated with hormone replacement therapy, suggesting oestrogen may limit visceral fat storage and play a role in insulin sensitivity. Consistently, testosterone is believed to positively regulate the deposition of fat in the central adipose tissue depot, as men tend to have greater central adiposity and obese post-menopausal women treated with testosterone exhibit greater visceral fat distribution (Geer and Shen, 2009; Lovejoy *et al.*, 1996). At the molecular level, there is also evidence that gender and gender-specific hormone secretion may effect the expression of some key genes that influence energy homeostasis. In humans, Moro and colleagues (Moro *et al.*, 2009) demonstrated that the activity of triglyceride hydrolase was significantly higher in female individuals, compared to males. Whilst in rodents, a study conducted by Stahlberg and colleagues

(Stahlberg *et al.*, 2004) analysed the effect of gender on the expression of 1800 liver genes, and found 246 of these genes to be significantly different between genders. The most notable of these was fatty acid transporter, FAT/CD36, which was confirmed to have 18-fold higher levels of mRNA and greater protein abundance in the liver of female rodents, when compared to males (Stahlberg *et al.*, 2004). Although oestrogen treatment did not influence FAT/CD36 mRNA expression in castrated female rodents, continuous infusion of growth hormone (like in females) into male rodents, which normally display an episodic pattern of growth hormone secretion, produced a small but significant increase in FAT/CD36 mRNA (Stahlberg *et al.*, 2004). Therefore the aforementioned studies highlight the importance of gender and the effect of gender-specific hormone secretion on the key metabolic pathways influencing energy balance. Hence the differing vulnerability of males and females to an identical obesogenic HFD may therefore require important consideration when contemplating perspective treatments or interventions. Given that the vast majority of studies investigating the partial replacement of saturated fat with n-3 PUFAs were conducted in male rodents, and it is unknown whether there is a gender dimorphic response to this altered dietary fatty acid composition, it is therefore an important point to consider.

1.15 – AIMS

1.15.1 – Chapter 2 – The Effect of Dietary Fatty Acid Composition and Gender on Body Composition in Mice: Model Characterisation

The research in Chapter 2 aimed to determine:

- I. the effect of replacing 7.5% of saturated fat in a high saturated fat diet with n-3 PUFAs (derived from fish oil) on body composition, body fat distribution and insulin sensitivity
- II. the mechanism by which n-3 PUFA enrichment of a high saturated fat diet improves body fat distribution and insulin sensitivity
- III. the influences of gender on body composition, body fat distribution and insulin sensitivity, with respect to dietary fatty acid composition

In relation to aim (I) I hypothesised that replacement of 7.5% of saturated fat with n-3 PUFAs would exert beneficial effects by: (a) promoting the redistribution of adipose tissue from visceral stores to the subcutaneous depot, (b) reducing ectopic fat accumulation in the liver and (c) improving insulin sensitivity.

In relation to aim (II) I hypothesised that the mechanism by which the hypothesised effects of n-3 PUFA enrichment improve insulin sensitivity are through the reduced deposition of fat in the visceral depot and ectopic stores, such as the liver.

And finally, in relation to aim (III) I hypothesised that the male mice would exhibit greater visceral adiposity, increased hepatic fat accumulation and lower insulin sensitivity, in response to high fat overfeeding.

1.15.2 – Chapter 3 – The Effect of Dietary Fatty Acid Composition on Muscle Fibre Type Composition and Stored Nutrient Content of Skeletal Muscle

The research in Chapter 3 aimed to determine:

- I. the effect of replacing 7.5% of saturated fat in a high saturated fat diet with n-3 PUFAs (derived from fish oil) on the biochemical characteristics and muscle fibre type distribution of skeletal muscles with predominantly fast-twitch (EDL) and slow-twitch (soleus) characteristics

In relation to aim (I), I hypothesised that consuming a HF-S diet would promote intramyocellular fat accumulation and induce a muscle fibre type switch, increasing the proportion of FOG-FG fibres. Furthermore, I hypothesised that replacement of 7.5% of saturated fat with n-3 PUFAs would prevent this muscle fat accumulation and the fibre type switch favouring glycolytic metabolism, and may potentially even increase the proportion of SO fibres.

1.15.3 – Chapter 4 – The Effect of Dietary Fatty Acid Composition, Muscle Fibre Type and Gender on Skeletal Muscle Fatty Acid Metabolism in Mice

The research in Chapter 4 aimed to determine:

- I. the mechanism by which replacing 7.5% of saturated fat with n-3 PUFAs (derived from fish oil) in a high saturated fat diet reduced intramyocellular fat accretion in mice. In doing so, I aimed to determine the effect of dietary fatty acid composition on fatty acid metabolism in the white FG-FOG extensor digitorum longus muscle (EDL) and red SO soleus muscle

by specifically examining the mRNA content of key genes involved in:

- i) fatty acid uptake
 - ii) lipogenesis and triglyceride storage
 - iii) fatty acid utilisation
- II. the effect of muscle fibre type on the mRNA content of key genes involved in skeletal muscle fatty acid metabolism in mice; i.e., white FG-FOG EDL as compared to red SO soleus muscle
- III. the influence of gender on the mRNA content of key genes involved in skeletal muscle fatty acid metabolism in mice

In relation to aim (I) I hypothesised that replacement of 7.5% of saturated fat with n-3 PUFAs prevents the ectopic deposition of fat in skeletal muscle by:

- i) promoting the mRNA expression of genes influencing the uptake of fatty acids into skeletal muscle
- ii) preventing the mRNA expression of genes controlling lipogenesis and
- iii) upregulating the mRNA expression of genes that would lead to enhanced oxidation.

In relation to aim (II) I hypothesised that the mRNA content of genes influencing fatty acid metabolism would be greater in the SO soleus muscle, a muscle that predominantly utilises fatty acids as substrate, as compared to the FG-FOG EDL muscle, which primarily uses glucose as substrate.

And finally, in relation to aim (III) I hypothesised that the female mice would exhibit greater mRNA content of genes influencing fatty acid uptake and storage, as compared to male mice.

1.15.4 – Chapter 5 – The Effect of Dietary Fatty Acid Composition and Gender on Hepatic Fatty Acid Metabolism in Mice

The research in Chapter 5 aimed to determine:

- I. the effect of replacing 7.5% of saturated fat with n-3 PUFAs (derived from fish oil) in a high saturated fat diet on the hepatic mRNA content of key genes involved in:
 - i) fatty acid uptake
 - ii) lipogenesis and triglyceride storage
 - iii) fatty acid utilisation
- II. the influence of gender on the mRNA content of key genes involved in hepatic fatty acid metabolism in mice

In relation to aim (I) I hypothesised that replacement of 7.5% of saturated fat with n-3 PUFAs prevents the ectopic deposition of fat in the liver by:

- i) promoting the mRNA expression of genes influencing the uptake of fatty acids into the liver
- ii) preventing the mRNA expression of genes controlling lipogenesis and
- iii) upregulating the mRNA expression of genes that would lead to enhanced oxidation.

And finally, in relation to aim (II) I hypothesised that given previous studies have shown that males exhibit greater liver fat accretion (Priego *et al.*, 2008), male mice would exhibit greater mRNA content of genes influencing fatty acid uptake and storage, as compared to female mice.

1.15.5 – Chapter 6 – The Effect of Dietary Fatty Acid Composition and Gender on Glucose Metabolism in the Skeletal Muscle and Liver of Mice

The research in Chapter 6 aimed to determine:

- I. the effect of replacing 7.5% of saturated fat in a high saturated fat diet with n-3 PUFAs (derived from fish oil) on glucose metabolism in the skeletal muscle and liver
- II. the influences of muscle fibre type on glucose metabolism in the skeletal muscle
- III. the influences of gender on glucose metabolism in the skeletal muscle and liver

In relation to aim (I) I hypothesised that replacement of 7.5% of saturated fat with n-3 PUFAs would exert beneficial effects on insulin sensitivity by maintaining the phosphorylation and subsequent disposal of glucose in skeletal muscle and liver (assessed by mRNA expression analyses).

In relation to aim (II) I hypothesised that the expression of genes influencing glycolysis would be greater in the fast-twitch glycolytic (FG)-fast-twitch oxidative-glycolytic (FOG) extensor digitorum longus (EDL) muscle, and those influencing insulin sensitivity would be greater in the slow-twitch oxidative (SO) soleus muscle.

And finally, in relation to aim (III) I hypothesised that the male mice would exhibit a greater impairment in skeletal muscle and liver glucose metabolism with HF-S feeding than female mice.

CHAPTER 2

*The Effect of Dietary Fatty Acid Composition
and Gender on Body Composition in Mice:
Model Characterisation*

2.1 – INTRODUCTION

Ecologic (between-population) studies have shown that an increase in the proportion of energy intake from fat is associated with an elevated prevalence of overweight (Drewnowski, 2007; Bray and Popkin, 1998). In Western society, the high saturated fat content of the “Western style” diet has been implicated in the development of obesity (Buettner *et al.*, 2006; Marotta *et al.*, 2004; Wang *et al.*, 2002; Ikemoto *et al.*, 1996; Rustan *et al.*, 1993). The mechanism by which saturated fat increases body weight gain (Buettner *et al.*, 2006; Ikemoto *et al.*, 1996) and adipose tissue mass (Wang *et al.*, 2002; Ikemoto *et al.*, 1996) is believed to involve saturated fats’ greater propensity to enter storage in adipose tissue, as opposed to being oxidised (Piers *et al.*, 2003; Pan *et al.*, 1994). Population studies have demonstrated that excess visceral fat in particular, as estimated by waist circumference, is associated with increased saturated fat intake in men (Krachler *et al.*, 2009). Rodent studies have consistently shown that consumption of a diet rich in saturated fat (HF-S) elicits a marked enlargement in the detrimental visceral adipose tissue store (de Meijer *et al.*, 2010; Hageman *et al.*, 2010; Belzung *et al.*, 1993). In HF-S-fed rodents, excess triglycerides are also channelled into ectopic fat stores such as the liver (Buettner *et al.*, 2006; Ukropec *et al.*, 2003) and skeletal muscle (Mullen *et al.*, 2007; Simončíkova *et al.*, 2002; Kim *et al.*, 2000) which are not primarily designed for fat storage. Increased visceral adiposity (Kim *et al.*, 2000) and ectopic fat deposition (Lara-Castro and Garvey, 2008; Manco *et al.*, 2000) have detrimental consequences for whole-body metabolism, having been implicated in the development of impaired insulin sensitivity in HF-S-fed rodents (Buettner *et al.*, 2006; Holness *et al.*, 2004; Steerenberg *et al.*, 2002).

In contrast, epidemiological research has shown that greater consumption of fish, and therefore an increased intake of n-3 polyunsaturated fatty acids (PUFA), is associated with lower rates of obesity (Yamori, 2004). In comparison to saturated fats, n-3 PUFAs are less effective at promoting fat deposition in adipose tissue and are believed to stimulate lipid oxidation (Piers *et al.*, 2003; Ukropec *et al.*, 2003; Raclot *et al.*, 1997; Shillabeer and Lau, 1994). In rodents, enrichment of a high fat diet with n-3 PUFAs (HF-n-3) has been shown in some studies to reduce body weight gain (Buettner *et al.*, 2006; Wang *et al.*, 2002; Ikemoto *et al.*, 1996). Diets rich in n-3 PUFAs also limit adipose tissue storage in the epididymal and perirenal depots (Rokling-Andersen *et al.*, 2009; Belzung *et al.*, 1993; Parrish *et al.*, 1990) and reduce ectopic fat deposition in the liver (Buettner *et al.*, 2006; Ruzickova *et al.*, 2004) and skeletal muscle (Rossmeisl *et al.*, 2009). Moreover fish oil, a rich source of n-3 PUFAs, has been shown to be effective in preventing high fat diet (HFD)-induced insulin resistance in rats when supplemented into a HFD (Storlien *et al.*, 1987).

Consuming a HF-S diet providing 60% of energy as fat is well-established to promote rapid obesity development in rodents. Exposure to this diet has been shown to, in female C57BL/6J mice, induce a 39% increase in body mass after 12 weeks (Johnston *et al.*, 2007) and in male C57BL/6 mice, produce a 19 gram body weight gain after 9 weeks (de Meijer *et al.*, 2010). Whilst much research has investigated the effect of n-3 PUFA enrichment of a HFD on body weight, fat mass and insulin sensitivity, majority of studies used diets with varying energy intake from fat, differing proportions of n-3 PUFA incorporated into the total fat intake of the HFD and varying compositions of

n-3 PUFA subtypes (docosahexaenoic acid (DHA), eicosapentaenoic acid (EPA) or α -linoleic acid (ALA)).

Studies have also utilised n-3 PUFAs from a range of sources, such as n-3 PUFAs derived from fish and plant extracts, which are known to produce different metabolic effects (Ruzickova *et al.*, 2004; Ikemoto *et al.*, 1996). Furthermore, the amount of n-3 PUFAs consumed may influence the effect observed, as long-term administration of a very high dose of fish oil has been proposed to, in addition to beneficial outcomes, generate harmful side-effects that may be a consequence of toxicity (Rabbani *et al.*, 2001). However, replacement of approximately 6-7% of dietary fat with fish oil-derived n-3 PUFAs, which extrapolates to a high intake of n-3 PUFAs in humans, has been shown to exert beneficial effects on insulin action and sensitivity (Holness *et al.*, 2004; Storlien *et al.*, 1987), dyslipidemia and substrate utilisation (Rustan *et al.*, 1993). The proportion of n-3 PUFAs required in the total dietary fat intake to elicit beneficial effects and the mechanisms by which n-3 PUFAs exert these effects are not clear. In Australia, the average adult consumes approximately 6% above the recommended intake of saturated fat (FSANZ, 2009a; FSANZ, 2009b) and less than half of the recommended daily amount of long chain n-3 PUFAs (NHMRC, 2006; Howe *et al.*, 2006a; Howe *et al.*, 2006b; Meyer *et al.*, 2003) and this may therefore have relevant health implications.

An issue often ignored is whether the response to high fat feeding is gender-specific; the vast majority of studies investigating the effect of n-3 PUFA enrichment of a HFD on obesity development, body fat mass and fatty acid metabolism have been conducted

in males. Gonadal steroids, testosterone and oestrogen, are well-established gender-specific effectors of body composition (Geer and Shen, 2009). Post-menopausal women, lacking oestrogen production, exhibit a higher waist circumference (Perrone *et al.*, 1999) and reduced insulin sensitivity (Geer and Shen, 2009) than those treated with hormone replacement therapy, suggesting oestrogen may limit visceral fat storage and play a role in insulin sensitivity. Consistently, testosterone is believed to positively regulate the deposition of fat in the central adipose tissue depot, as men tend to have greater central adiposity and obese post-menopausal women treated with testosterone exhibit greater visceral fat distribution (Geer and Shen, 2009; Lovejoy *et al.*, 1996). Some research has shown that there are gender differences in the development of obesity (Haugaard *et al.*, 2009; Moro *et al.*, 2009) and in response to obesogenic HFDs (Català-Niell *et al.*, 2008; Gómez-Pérez *et al.*, 2008; Priego *et al.*, 2008). In humans, obese females exhibit greater intramuscular triglyceride accumulation than obese males (when matched for body mass index) (Haugaard *et al.*, 2009; Moro *et al.*, 2009). In rodents, research has suggested females more aptly handle the fuel excess of a HFD by channelling excess fatty acid into adipose tissue storage, unlike HFD-fed males that have less efficient fat storage in adipose tissue and greater fat storage ectopically in the liver (Priego *et al.*, 2008). Furthermore, female rats are also less likely to exhibit an impaired insulin sensitivity profile in response to high fat feeding, as compared to males (Gómez-Pérez *et al.*, 2008). The differing vulnerability of males and females to an identical obesogenic HFD may therefore require important consideration when contemplating perspective treatments or interventions.

In the current study, I therefore aimed to determine:

- I. the effect of replacing 7.5% of saturated fat in a high saturated fat diet with n-3 PUFAs (derived from fish oil) on body composition, body fat distribution and insulin sensitivity
- II. the mechanism by which n-3 PUFA enrichment of a high saturated fat diet improves body fat distribution and insulin sensitivity
- III. the influences of gender on body composition, body fat distribution and insulin sensitivity, with respect to dietary fatty acid composition

In relation to aim (I) I hypothesised that replacement of 7.5% of saturated fat with n-3 PUFAs would exert beneficial effects by: (a) promoting the redistribution of adipose tissue from visceral stores to the subcutaneous depot, (b) reducing ectopic fat accumulation in the liver and (c) improving insulin sensitivity.

In relation to aim (II) I hypothesised that the mechanism by which the hypothesised effects of n-3 PUFA enrichment improve insulin sensitivity are through the reduced deposition of fat in the visceral depot and ectopic stores, such as the liver.

And finally, in relation to aim (III) I hypothesised that the male mice would exhibit greater visceral adiposity, increased hepatic fat accumulation and lower insulin sensitivity, in response to high fat overfeeding.

2.2 – MATERIALS AND METHODOLOGY

2.2.1 - *Animals and Nutrition Regime*

Specific pathogen-free male and female C57BL/6J mice, aged 6 weeks, were purchased from Laboratory Animal Services, University of Adelaide (Adelaide, South Australia, Australia). Mice were housed on pelleted paper bedding in individual cages in a conventional animal holding room with fixed photoperiod (12 hour/12 hour light/dark cycle) and temperature (24.5°C). All procedures were approved by the University of Adelaide Animal Ethics Committee and the Institute of Medical and Veterinary Science Animal Ethics Committee. On arrival, mice underwent an acclimatisation period of 2 weeks, during which they were provided a standard chow diet (AIN-93G, Specialty Feeds Pty Ltd, Glen Forrest, Western Australia, Australia) and water *ad libitum*. Following the acclimatisation period, mice were randomly assigned to one of three diets, fed either a standard chow (control (C) (AIN-93G, Specialty Feeds Pty Ltd, Glen Forrest, Western Australia, Australia), 16.1 MJ/kg, 15.91% energy from fat, 25.08% energy from protein, 58.48% energy from carbohydrate), high saturated fat (HF-S (SF07-066, Specialty Feeds Pty Ltd, Glen Forrest, Western Australia, Australia), 21.8 MJ/kg, 59.60% energy from fat, 18.53% energy from protein, 21.20% energy from carbohydrate) or high fat n-3 PUFA enriched (HF-n-3 (SF07-067, Specialty Feeds Pty Ltd, Glen Forrest, Western Australia, Australia), 21.8 MJ/kg, 59.60% energy from fat, 18.53% energy from protein, 21.27% energy from carbohydrate) diet (n-3 PUFAs kindly donated by Nu-mega Ingredients Pty Ltd, Nathan, Queensland, Australia (HiDHA[®] 25N tuna oil (26% DHA, 6% EPA, 35% total n-3 PUFA content)).

Both HFDs were stored at -20°C, whilst the HF-n-3 diet was also stored in aliquots under nitrogen gas to avoid oxidation. The fatty acid compositions of both HFDs are presented in **Table 2.1**. Two cohorts of mice received the aforementioned diets, one of which (cohort 1) was used to characterise body composition, while the other (cohort 2) was used to characterise physical activity and muscle fibre type (**Chapter 3**).

Table 2.1. Comparison of fatty acid composition of the two high fat diets, high saturated fat diet and high fat n-3 PUFA enriched diet.

	Fatty Acid Composition (% as fed)	
	High Saturated Fat (HF-S) SF07-066	High Fat n-3 PUFA Enriched (HF-n-3) SF07-067
Total SFA	23.0	9.00
Total MUFA	11.3	15.3
Total PUFA	1.20	9.70
Total n-6 PUFA	1.10	2.10
Total n-3 PUFA	0.10	7.50
Less than C12	1.00	0.10
14:0, SFA (Myristic Acid)	0.38	0.82
15:0, SFA (Pentadecyclic Acid)	-	0.22
16:0, SFA (Palmitic Acid)	8.90	5.90
17:0, SFA (Margaric Acid)	-	0.22
18:0, SFA (Stearic Acid)	12.2	1.60
20:0, SFA (Arachidic Acid)	0.40	0.16
22:0, SFA (Behenic Acid)	0.04	0.02
24:0, SFA (Tetracosanoic Acid)	-	0.04
16:1, n-7 MUFA (Palmitoleic Acid)	0.10	1.20
17:1, n-7 MUFA (Heptadecenoic Acid)	-	0.16
18:1, n-9 MUFA (Oleic Acid)	11.2	13.0
20:1, n-9 MUFA (Gadoleic Acid)	0.02	0.21
22:1, n-9 MUFA (Erucic Acid)	-	0.20
18:2, n-6 PUFA (Linoleic Acid)	1.10	1.36
20:4, n-6 PUFA (Arachadonic Acid)	Trace	0.35
22:5, n-6 PUFA (Clupanodonic Acid)	-	0.31
18:3, n-3 PUFA (α -Linolenic Acid)	0.09	0.17
18:4, n-3 PUFA (Stearidonic Acid)	-	0.28
20:5, n-3 PUFA (Eicosapentaenoic Acid)	Not detected	1.20
22:5, n-3 PUFA (Docosapentaenoic Acid)	-	0.26
22:6, n-3 PUFA (Docosahexaenoic Acid)	Not detected	5.40

SFA, saturated fatty acid; MUFA, monounsaturated fatty acid; PUFA, polyunsaturated fatty acid.

2.2.1.1 – Cohort 1 Mice – Measurements Collected During Nutrition Regime

Mice were maintained on their respective diets for a period of 14 weeks (\pm 4 days) during which food and water were provided daily *ad libitum*. Body weight (g) was measured thrice weekly and at the time points of arrival and surgery (n = C(male)=10, C(female)=12, HF-S(male)=11, HF-S(female)=11, HF-n-3(male)=9, HF-n-3(female)=11). Body weight upon arrival (see **Chapter 2, Section 3.1.3, Figure 2.5**) and during the acclimatisation period (data not shown) was similar in all dietary groups (start weight: F(2, 118.9)=1.9, $P=0.15$; pairwise comparisons: $P=0.16$ (C vs HF-S), $P=1.00$ (C vs HF-n-3), $P=0.99$ (HF-S vs HF-n-3); acclimatisation weight: F(2, 118.9)=1.8, $P=0.17$; pairwise comparisons: $P=0.24$ (C vs HF-S), $P=0.42$ (C vs HF-n-3), $P=1.00$ (HF-S vs HF-n-3)). Food intake (g) was measured daily and calculated as the difference between food provided and food remaining (including crumbs collected from bedding). Daily energy intake (MJ) was calculated as the product of daily food intake (converted to kg) and the digestible energy (MJ/kg) of the diet consumed. Energy intake is reported as the cumulative energy intake (MJ), the sum of daily energy intakes over the experimental dietary period. Cumulative energy intake (MJ) of the macronutrients fat, protein and carbohydrate, were calculated according to their respective percentages present in the diet. Feed efficiency (g/MJ), body weight gain per unit energy consumed, was calculated for the experimental dietary period.

2.2.1.2 – Cohort 2 Mice – Measurements Collected During Nutrition Regime

Mice were maintained on their respective diets for 11 weeks (± 7 days) during which food and water were provided daily *ad libitum* (n = C(male)=3, C(female)=3, HF-S(male)=3, HF-S(female)=3, HF-n-3(male)=3, HF-n-3(female)=2).

Physical activity was measured during the experimental dietary period, using a similar protocol to those described previously (Loizzo *et al.*, 2006; Dauncey, 1986; Heal, 1975). During the acclimatisation period, a series of motion detectors were introduced to the animal holding room, providing time for mice to habituate to the changed environment. Motion detectors were installed above individual cages and barriers were fixed between cages to ensure only the cage of interest was monitored by a single detector. During the experimental dietary period, physical activity was measured continuously from 11:30 am on day one until 10:00 am on the consecutive day and no access to the animal holding room was permitted during this period. The modified motion detector system relayed the frequency of movement (counts) to a data logger, which recorded the frequency of physical activity in 2 minute periods and this information was then transferred to a computer each day. On average, the physical activity of each mouse was measured 4 times per week, and the total physical activity for each day measured during that week was averaged to provide mean weekly physical activity (counts). Physical activity is also reported as the cumulative physical activity (counts), the sum of mean weekly physical activities over the experimental dietary period.

2.2.2 - Tissue Collection from Mice in Cohort 1

Following the experimental dietary period and whilst in the fed-state, mice underwent non-recovery surgery for the excision of skeletal muscle. Surgeries were scheduled and performed to minimise temporal variation. Anaesthesia was induced using a mixture of oxygen (0.5 L/minute), nitrous oxide (0.5 L/minute) and 2% isoflurane (Forthane[®], Abbott Australasia Pty Ltd, Kurnell, New South Wales, Australia). After loss of the hindlimb reflex, anaesthesia was maintained using 1.5% isoflurane, 0.4 L/minute oxygen and 0.4 L/minute nitrous oxide. **Figure 2.1** represents a detailed flow chart of tasks performed for skeletal muscle surgery. Lower hindlimb muscles were exposed and trimmed of superficial muscle and fat. Subsequently the branch of the femoral artery supplying the gastrocnemius and soleus skeletal muscles was occluded, and the whole soleus and whole plantaris muscles were each dissected. The superficial sural artery and small saphenous vein were then occluded and the gastrocnemius muscle was dissected into lateral and medial parts, allowing removal of the gastrocnemius lateralis and medialis muscles separately. The popliteal artery and vein were then occluded and the whole tibialis and whole extensor digitorum longus (EDL) muscles were each dissected. The lower hindlimb muscles dissected during surgery are illustrated in **Figure 2.2**.

Fur and skin were then removed from the thigh to hip and muscles were trimmed of superficial muscle and fat. The descending branch of the lateral circumflex artery was then occluded and the whole quadriceps (vastus lateralis, vastus medialis, vastus intermedius and rectus femoris) muscles were dissected undivided. Firstly, all relevant muscles were collected from the left leg, and subsequently surgery was performed to

collect right leg muscles. As collected, skeletal muscles were rapidly snap frozen in liquid nitrogen and then stored under liquid nitrogen vapour phase storage until subsequent analyses. In the case of the EDL and soleus muscles, this included analysis of weight and mRNA content (left leg muscles).

Following skeletal muscle surgery, a cardiac puncture was performed and blood was collected in Microvette[®] CB300 tubes treated with EDTA dipotassium salt (Sarstedt, Nümbrecht, Germany, Europe). Plasma was prepared by centrifugation at 3,200 rpm for 15 minutes at 4°C and stored in aliquots at -80°C until subsequent analysis for the concentration of glucose, insulin and triglycerides.

Post-mortem, livers were rapidly dissected, weighed and sectioned. The right lobe of the liver was snap frozen in liquid nitrogen and subsequently stored under liquid nitrogen vapour phase storage until subsequent analysis of mRNA content. The left lobe of the liver was sectioned into slices which were embedded in Tissue-Tek[®] OCT (Sakura Finetek Co Ltd, Tokyo, Japan, Asia) and gently frozen in a bath of liquid nitrogen pre-cooled isopentane before storage under liquid nitrogen vapour phase storage for subsequent histological evaluation of morphology and fat content. The remainder of the left lobe and the whole caudate and median lobes were snap frozen in liquid nitrogen and stored at -80°C for subsequent analyses of glycogen and glucose content. Post-mortem, adipose tissue from the pooled posterior and anterior subcutaneous (dorso-lumbar, inguinal, gluteal, white interscapular, subscapular, axillo-toracic and superficial cervical depots), mesenteric, pooled perirenal and retroperitoneal, pooled brown deep cervical and interscapular and perigonadal

(periovariac, females; epididymal, males) depots were dissected, snap frozen in liquid nitrogen and stored under liquid nitrogen vapour phase storage for subsequent evaluation of weight.

The absolute weights of the EDL muscle, soleus muscle, liver and each of the adipose tissue depots were determined. Subsequently, the relative weights of the EDL muscle, soleus muscle, liver and each of the adipose tissue depots were calculated per gram of body weight (weight of tissue/g body weight).

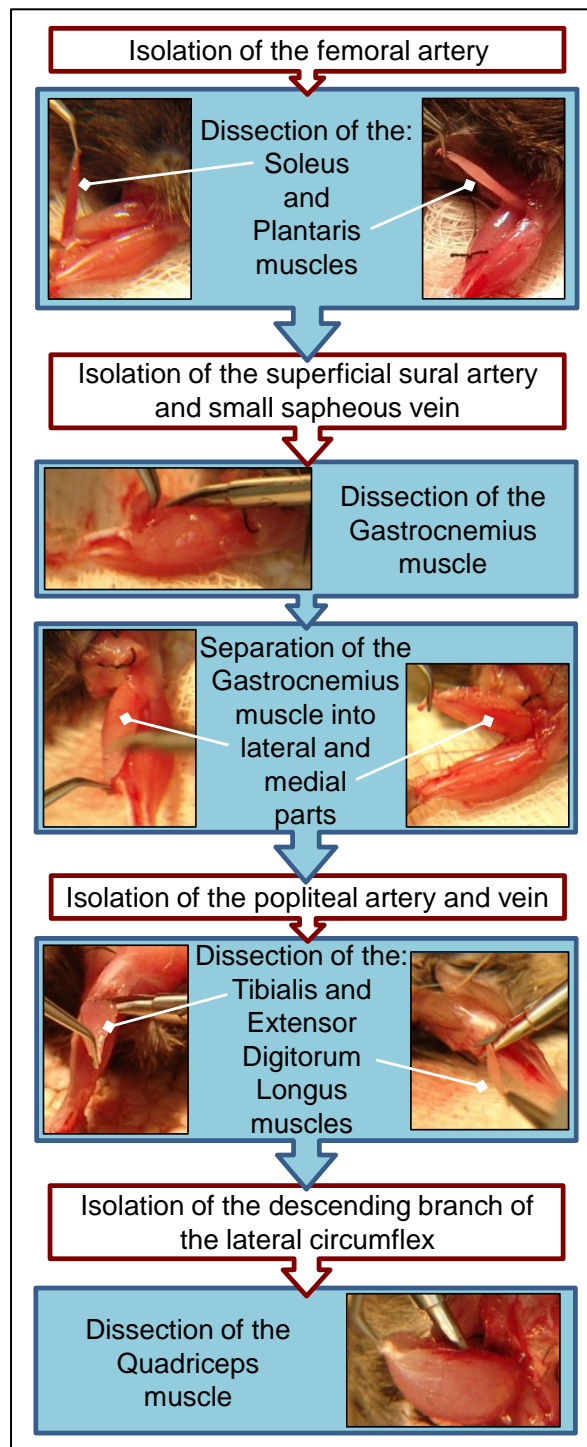


Figure 2.1. Procedure of skeletal muscle surgery for the collection of hindlimb skeletal muscles from male and female mice fed control, high saturated fat or high fat n-3 PUFA enriched diet.

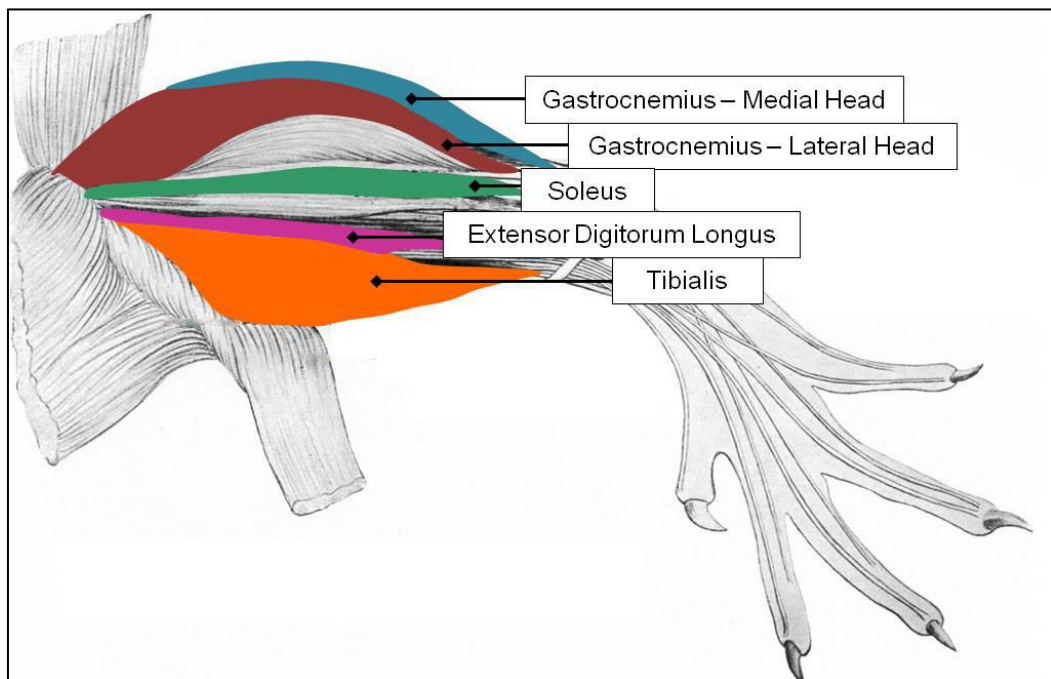


Figure 2.2. Diagram depicting lower hindlimb skeletal muscles collected during skeletal muscle surgery in mice.

Figure adapted from (Greene, 1955).

2.2.3 - Analysis of Plasma Samples

Plasma collected from mice in cohort 1 was assayed for glucose, insulin and triglycerides.

2.2.3.1 - Plasma Glucose

Glucose concentrations (mmol/L) in 50 μ l aliquots of plasma were measured by a glucose oxidation method, using the Gluco-quant Glucose/HK kit (Roche Diagnostics Pty Ltd, Mannheim, Germany, Europe) on the Cobas Bio automated analysis system (Roche Diagnostics Australia Pty Ltd, Castle Hill, New South Wales, Australia). In principle, the phosphorylation of plasma glucose to glucose-6-phosphate by ATP was catalysed by hexokinase. In the presence of NADP, glucose-6-phosphate dehydrogenase then catalysed the oxidation of glucose-6-phosphate to gluconate-6-phosphate, forming NADPH. The rate of NADPH formation from the oxidation reaction was directly proportional to the glucose concentration, measured spectrophotometrically at 340 nm. Each plasma aliquot was run in duplicate reactions and results are presented as the mean.

2.2.3.2 - Plasma Insulin

Plasma insulin concentrations (pmol/L) were measured using 5 μ l aliquots of plasma on the DRG[®] Ultrasensitive Mouse Insulin ELISA (DRG Instruments GmbH, Marburg, Germany), a solid phase two-site enzyme immunoassay. Based on the direct sandwich technique, plasma insulin molecules are bound by an anti-mouse insulin monoclonal

antibody used to coat the microtitre plate wells, and detected by a horseradish peroxidase-conjugated anti-insulin antibody directed against an independent epitope.

The insulin-bound conjugate was detected by reaction with 3,3', 5,5'-tetramethylbenzidine (TMB). The reaction was stopped following 30 minutes incubation with TMB, by using 0.5M sulphuric acid, and the colourmetric endpoint was measured spectrophotometrically at 450 nm.

2.2.3.3 - Plasma Triglyceride

Triglyceride concentrations (mmol/L) were measured in a 50 µl aliquot of plasma by enzymatic analysis using the Cobas Bio automated analysis system (Roche Diagnostics Australia Pty Ltd, Castle Hill, New South Wales, Australia) and Triglyceride GPO-PAP kit (Roche Diagnostics Pty Ltd, Mannheim, Germany, Europe). Lipoprotein lipase was used to catalyse the rapid and complete hydrolysis of triglycerides to glycerol (Wahlefeld, 1974). Glycerol was then oxidised to dihydroxyacetone phosphate and hydrogen peroxide. Under the catalytic action of peroxidase, oxygen generated from hydrogen peroxide reacted with the 4-aminophenazone and 4-chlorophenol to form a red dyestuff. The formation of the red dyestuff was directly proportional to the triglyceride concentration and was measured spectrophotometrically at 505 nm. Each plasma aliquot was run in duplicate reactions and results are presented as the mean.

2.2.4 - Histological Evaluation of Liver Morphology and Fat Content

2.2.4.1 - Haematoxylin and Eosin Staining

OCT-embedded frozen liver samples (from cohort 1) were cut to 4 µm thick cross-sections at -20°C using a cryostat and stained with haematoxylin and eosin to evaluate morphology at the cellular level. Sections were briefly fixed in 10% neutral buffered formalin (1 minute) and subsequently washed with tap water. Nuclei were stained blue using Lillie-Mayer Haematoxylin (kindly donated by Australian Biostain Pty Ltd, Traralgon, Victoria, Australia) for 3.5 minutes and subsequently washed with tap water. Haematoxylin undergoes *in situ* oxidation, forming an oxidation product that acts like an indicator, being blue and less soluble in aqueous alkaline conditions and red and more soluble in alcoholic acidic conditions (Lillie, 1965). To remove excess stain and non-specific background colouration, sections were differentiated with 0.3% acid alcohol (30 seconds) and rinsed with tap water, resulting in cell nuclei stained blue. Cytoplasm was stained pink using Accustain[®] Eosin Y solution (alcoholic with phloxine; Sigma-Aldrich Inc, St Louis, Missouri, USA) for 1.5 minutes and excess stain was removed under running tap water. Sections were then dehydrated with 100% ethanol, cleared using xylene and mounted with DPX Mounting Media (Gurr, BDH Ltd, Poole, United Kingdom, Europe).

Sections were scanned using the NanoZoomer Digital Pathology image scanner in conjunction with NDP Scan 2.0 software (Hamamatsu Photonics K. K., Hamamatsu City, Japan, Asia) and viewed using NDP.view software (ver. 1.1.6, Hamamatsu Photonics

K. K., Hamamatsu City, Japan, Asia), the resultant images exhibited staining of nuclei in blue and acidophilic cytoplasm in pink.

2.2.4.2 - Oil Red O Staining

OCT-embedded frozen liver samples (from cohort 1) were cut to 10 μm thick cross-sections at -20°C using a cryostat and stained with Oil Red O to evaluate fat content. Oil Red O is an inert oil-soluble bis-azo dye (Nunnari *et al.*, 1989), used to stain neutral lipids by virtue of its greater solubility in the lipid being stained than in the vehicular solvent used in staining. Sections were briefly fixed in 10% neutral buffered formalin and then washed with tap water. Following brief washing with 60% 2-propanol (Sigma-Aldrich Inc, St Louis, Missouri, USA), sections were stained for 15 minutes with freshly prepared 7.34 mM Oil Red O (Sigma-Aldrich Inc, St Louis, Missouri, USA) solution made with 60% 2-propanol. Sections were then rinsed with 60% 2-propanol, washed with tap water and counterstained for light colouration of nuclei using 10% Lillie-Mayer Haematoxylin (kindly donated by Australian Biostain Pty Ltd, Traralgon, Victoria, Australia). Sections were mounted using aqueous mountant (Biomedata™ Gel/Mount, Biomedata Corp, Foster City, California, USA) and the coverslip edges were sealed with a clear varnish.

Sections were scanned in three 0.2 μm layers using the NanoZoomer Digital Pathology image scanner in conjunction with NDP Scan 2.0 software (Hamamatsu Photonics K. K., Hamamatsu City, Japan, Asia). Scanned images were visualised using NDP.view 1.1.6 software (Hamamatsu Photonics K. K., Hamamatsu City, Japan, Asia), the resultant images exhibiting red staining of fat and pale blue staining of nuclei.

2.2.4.3 - Histological Quantification of Liver Fat Content

The images obtained from Oil Red O stained sections were viewed using NDP.view 1.1.6 software, and three areas of 500 μm^2 were randomly selected per liver. Within each area, the areas stained positively for fat (fat droplets) were measured by tracing the perimeters of the fat droplets, using the NDP.view freehand tool. Bias was negated by slide blinding; each slide was randomly assigned a number, evaluated whilst blinded to dietary group and gender, and following quantification of all slides were subsequently unblinded to evaluate group statistics. The percentage area stained positively for fat provided an estimate of total liver fat content. This was calculated (mean of triplicate scores) as the total area stained positively for fat relative to the total area evaluated (Karunaratne *et al.*, 2005; McManus *et al.*, 1995). The mean fat droplet area (μm^2) was calculated from the areas of the individual fat droplets traced in the triplicate areas (McManus *et al.*, 1995). Whilst the technique of using Oil Red O staining to determine lipid content of tissues is subjective and a simple lipid extraction may have provided more quantitative results, Oil Red O staining and quantification were performed to minimise the use of liver tissue, leaving liver for more important assays such as Western blot analysis of key proteins of interest.

2.2.5 - Enzymatic Analysis of Liver Glycogen Content

Liver glycogen content ($\mu\text{g}/\text{mg}$ wet weight) was measured by quantitative hydrolysis of glycogen by glucoamylase (Keppler and Decker, 1984) and measurement of the resultant glucose produced by a glucose oxidation method, using the Gluco-quant Glucose/HK kit (Roche Diagnostics Pty Ltd, Mannheim, Germany, Europe) on the

Cobas Bio automated analysis system (Roche Diagnostics Australia Pty Ltd, Castle Hill, New South Wales, Australia). Samples of liver (approximately 100 mg) from cohort 1 mice were homogenised in ice-cold 0.6 M perchloric acid (1 part liver to 5 parts acid) using 5 mm stainless steel beads (Qiagen GmbH, Hilden, Germany, Europe) in a Qiagen TissueLyser (Qiagen GmbH, Hilden, Germany, Europe) set at 30 Hz for 1 minute. Two 200 µl aliquots of liver homogenate were removed for analysis, one for measurement of liver glycogen determination (treated with glucoamylase) and the other for measurement of free glucose (not treated with glucoamylase). To the aliquot reserved for glycogen determination, 100 µl of 1M potassium hydrogen carbonate solution and 2 mL of glucoamylase solution (10 U/mL glucoamylase (Invitrogen Australia Pty Ltd, Mount Waverley, Victoria, Australia), 0.2 M acetate buffer (pH 4.8; 0.5% acetic acid, 0.12 M sodium acetate)) were added. Capped sample tubes were incubated at 40°C for 2 hours with gentle agitation. The reaction was stopped by addition of 1 mL of 0.6 M perchloric acid and the samples were vortexed and centrifuged at 4°C for 10 minutes at 10,000 rpm. The resultant supernatant was collected and a 50 µl aliquot was used to measure glucose content. The aliquot of homogenate reserved for free glucose measurement was centrifuged at 4°C for 15 minutes at 10,000 rpm. The supernatant was collected and to this was added 100 µl of 1 M potassium hydrogen carbonate solution. The sample was then centrifuged at 4°C for 15 minutes at 10,000 rpm, the supernatant was collected and a 50 µl aliquot was used to measure glucose content. In both assays, the glucose concentrations in duplicate 50 µl aliquots of the final supernatant were measured using the Gluco-quant Glucose/HK kit on the Cobas Bio automated analysis system as described in **Chapter 2**

Section 2.3.1. Duplicate aliquots were run for glucose determination and results are presented as the mean of duplicate reactions.

The glucose concentrations in the final supernatant from the glycogen hydrolysis reaction and the sample for free glucose estimation were each adjusted for the respective dilution factors in each assay. The resultant glucose concentration from the glycogen hydrolysis reaction was then corrected for the concentration of free glucose present in the liver before glycogen hydrolysis (glucose concentration of glycogen hydrolysis aliquot minus glucose concentration of free glucose aliquot). The weight (μg) of glycogen in the sample was determined using the molecular weight of the glucosyl moiety in glycogen and glycogen content was then calculated as the amount of glycogen present (μg) relative to the wet weight of the liver sample used (mg) (Keppler and Decker, 1984). Similarly, the liver free glucose content ($\mu\text{g}/\text{mg}$) was determined as the amount of free glucose present (μg) relative to the wet weight of the liver sample (mg).

2.2.6 – Statistical Analyses

All data are presented as mean \pm standard error of the mean (SEM). The effects of diet (C, HF-S, HF-n-3), gender (male, female) and time (weeks on respective diet) on body weight were assessed using a linear mixed model. The effects of diet (C, HF-S, HF-n-3), gender (male, female) and time (weeks on respective diet) on food intake were assessed using a linear mixed model. The effects of diet (C, HF-S, HF-n-3), gender (male, female) and time (weeks on respective diet) on physical activity were also

assessed using a linear mixed model. Two-way Analysis of Variance (ANOVA), with pairwise comparisons (Bonferroni post-hoc analysis), was used to determine the effect of diet (C, HF-S, HFn-3), gender (male, female) and their interaction on final body weight; cumulative energy intake; cumulative energy intake of macronutrients; feed efficiency; absolute and relative weights of the subcutaneous, mesenteric, perirenal-retroperitoneal and brown adipose tissue depots; plasma glucose, insulin and triglyceride concentrations; absolute and relative weights of the liver; liver fat content, area stained positively for fat (%) and mean fat droplet area; and liver glycogen and free glucose content. One-way ANOVA was used to determine the effect of diet (C, HF-S, HF-n-3) (Bonferroni post-hoc analysis) on the absolute and relative weights of the epididymal (males) and periovariac (females) adipose tissue depots. Simple linear regression analyses were used to determine the relationship of relative adipose tissue weight with feed efficiency; relative liver weight with measures of liver fat accumulation, body weight and liver glycogen content; and plasma insulin concentrations with measures of liver fat accumulation. Pearson correlation coefficients (r) were used to evaluate linear relationships. The differences in the slope of relationships were determined by analysis of covariance.

All statistics were performed using the Statistical Package for Social Scientists (SPSS) (ver. 17.0.0, SPSS Inc, Chicago, Illinois, USA). A probability of less than 5% ($P < 0.05$) was considered statistically significant. Analyses are reported as percentage change; statistical effect: $F(\text{degrees of freedom: between subjects effect, degrees of freedom: within subjects effect}) = F$ value, P value of effect; and subsequent P values of post-hoc or pairwise analyses.

2.3 – RESULTS

2.3.1 - Energy Intake, Food Intake, Body Weight, Feed Efficiency, Physical Appearance and Physical Activity

2.3.1.1 - Energy Intake

Total cumulative energy intake was calculated for the duration of the experimental dietary period. Total cumulative energy intake (**Figure 2.3A**) was greater in male HF-S and HF-n-3 mice as compared to male controls (+25%, +16%, respectively; diet*gender interaction: $F(2, 58)=4.2$, $P=0.02$; pairwise comparisons: $P\leq 0.001$, $P\leq 0.005$, respectively). Similarly, total cumulative energy intake was significantly increased in female HF-S and HF-n-3 mice as compared to female controls (+39%, +16%, respectively; diet*gender interaction: $F(2, 58)=4.2$, $P=0.02$; pairwise comparisons: $P\leq 0.001$). There were no significant differences in total cumulative energy intake between the HF-S and HF-n-3 groups in either male or female mice (pairwise comparisons: $P=0.24$, $P=1.0$, respectively). Total cumulative energy intake was greater in male control mice as compared to female control mice (+11%; diet*gender interaction: $F(2, 58)=4.2$, $P=0.02$; pairwise comparison: $P\leq 0.05$).

Cumulative energy intake of key macronutrients, including fat, carbohydrate and protein were each calculated (**Figure 2.3B**) from total cumulative energy intake during the experimental dietary period to confirm that macronutrient intake did indeed match the designed intake. Conforming to diet design, cumulative energy intake from fat was greater in HF-S and HF-n-3 mice as compared to control mice (+4.0-fold, +3.8-fold,

respectively; effect of diet: $F(2, 58)=792.0$, $P\leq 0.001$; post-hoc tests: $P\leq 0.001$). There were no significant differences in cumulative energy intake from fat between the HF-S and HF-n-3 groups (post-hoc test: $P=0.55$). There was no effect of gender on the cumulative energy intake from fat ($F(1, 58)=1.3$, $P=0.26$).

Cumulative energy intake from carbohydrate was lower in male HF-S and HF-n-3 mice as compared to male controls (-54.7%, -57.6%, respectively; diet*gender interaction: $F(2, 58)=6.1$, $P=0.004$; pairwise comparisons: $P\leq 0.001$). Similarly, cumulative energy intake from carbohydrate was reduced in female HF-S and HF-n-3 mice as compared to female controls (-49.5%, -49.4%, respectively; diet*gender interaction: $F(2, 58)=6.1$, $P=0.004$; pairwise comparisons: $P\leq 0.001$). The cumulative energy intake from carbohydrate was influenced by gender; in control mice, males exhibited greater cumulative energy intake from carbohydrate as compared to female mice (+10.6%; diet*gender interaction: $F(2, 58)=6.1$, $P=0.004$; pairwise comparisons: $P\leq 0.001$).

Cumulative energy intake from protein was similar in all dietary groups, with the exception that male HF-n-3 mice exhibited lower cumulative energy intake from protein as compared to male control mice (-14.0%; diet*gender interaction: $F(2, 58)=4.9$, $P=0.011$; pairwise comparison: $P\leq 0.005$). The cumulative energy intake from protein was also influenced by gender; in control mice, males exhibited greater cumulative energy intake from protein as compared to female mice (+10.6%; diet*gender interaction: $F(2, 58)=4.9$, $P=0.011$; pairwise comparison: $P\leq 0.02$) and in HF-n-3 mice, females tended to exhibit greater cumulative energy intake from protein as compared to male mice (+8.1%; pairwise comparison: $P=0.078$).

2.3.1.2 – Food Intake

Food intake was not significantly different between dietary groups during the experimental dietary period (diet*time: $F(26, 710.9)=1.1, P=0.34$) (**Figure 2.4**). Food intake was not significantly different between genders during the experimental dietary period (gender*time: $F(13, 710.9)=0.7, P=0.78$) (**Figure 2.4**).

2.3.1.3 – Body Weight

Following 1 week of experimental diet, HF-S mice weighed more than control mice (+8%; diet*time interaction: $F(2, 118.9)=7.0, P\leq 0.001$; pairwise comparison: $P\leq 0.001$) and this increased weight persisted to the final day (diet*time interaction: $F(2, 118.9)=45.2, P\leq 0.001$; pairwise comparison: $P\leq 0.001$) (**Figure 2.5**). Following 2 weeks of experimental diet, HF-n-3 mice weighed more than control mice (+5%; diet*time interaction: $F(2, 118.9)=8.6, P\leq 0.001$; pairwise comparison: $P\leq 0.05$) and this increased weight persisted to the final day (diet*time interaction: $F(2, 118.9)=45.2, P\leq 0.001$; pairwise comparison: $P\leq 0.001$) (**Figure 2.5**). There were no significant differences in the body weight of HF-S and HF-n-3 mice at any time point. At all time points male mice weighed more than female mice (gender*time interaction: $P\leq 0.001$).

At the final time point, prior to collection of tissues and blood, body weight was greater in HF-S and HF-n-3 mice, as compared to controls (+16%, +19%, respectively; effect of diet: $F(2, 58)=26.0, P\leq 0.001$; post-hoc tests: $P\leq 0.001$) (**Figure 2.6A**). HF-S and HF-n-3 mice exhibited similar final body weights (post-hoc test: $P=0.56$). Male mice were heavier than female mice (+21%; effect of gender: $F(1, 58)=84.1, P\leq 0.001$).

2.3.1.4 – Feed Efficiency

Feed efficiency was greater in HF-n-3 mice as compared to control and HF-S mice (+56%, +26%, respectively; effect of diet: $F(2, 58)=12.5$, $P\leq 0.001$; post-hoc tests: $P\leq 0.001$, $P\leq 0.02$, respectively) (**Figure 2.6B**). There was a trend towards increased feed efficiency in the HF-S group as compared to controls but this did not reach significance (+23%; post-hoc test: $P=0.10$). There was no effect of gender on feed efficiency ($F(1, 58)=1.7$, $P=0.19$).

2.3.1.5 – Physical Appearance of Mice

Representative images of mice fed their respective experimental diets for 14 weeks show that those fed a HF-S or HF-n-3 diet appeared physically fatter than those consuming a control diet (**Figure 2.6C**). The representative internal images of mice fed their respective experimental diets for 14 weeks show that those in the HFD groups appear to have more intra-abdominal fat. However, there was a striking difference in liver colour and size between groups, with those fed a HF-n-3 diet having larger livers with darker colouration (**Figure 2.6D**).

2.3.1.6 – Physical Activity (Cohort 2)

Mean weekly physical activity was not significantly different between dietary groups during the experimental dietary period (diet*time: $F(18, 74.0)=0.9$, $P=0.57$) (**Figure 2.7A**). Mean weekly physical activity was also not significantly different between genders during the experimental dietary period (gender*time: $F(9, 70.8)=0.4$, $P=0.94$) (**Figure 2.7A**). There was, however, a diet*gender interaction on mean weekly physical

activity during the experimental dietary period; HF-S female mice exhibited greater physical activity as compared to their control and HF-n-3 counterparts (+118%, +182%, respectively: $F(2, 25.9)=21.6$, $P\leq 0.001$; pairwise comparisons: $P\leq 0.001$) (**Figure 2.7A**).

There was a diet*gender*time interaction on cumulative physical activity during the experimental dietary period (diet*gender*time: $F(18, 73.6)=4.8$, $P\leq 0.001$; pairwise comparisons: $P\leq 0.001$) (**Figure 2.7B**). Following 5 weeks of experimental diet, female HF-S mice exhibited greater cumulative physical activity than female HF-n-3 mice (+146%; pairwise comparison: $P\leq 0.05$). This increased physical activity persisted to the final week of measurement (+180%; pairwise comparison: $P\leq 0.001$). Following 6 weeks of experimental diet, female HF-S mice exhibited greater cumulative physical activity than female control mice (+92%; pairwise comparison: $P\leq 0.01$). This increased physical activity also persisted to the final week of measurement (+114%; pairwise comparison: $P\leq 0.001$). There were no significant differences in the cumulative physical activity of control and HF-n-3 females at any time point. Furthermore, following 4 weeks of experimental diet, female HF-S mice exhibited greater cumulative physical activity than male HF-S mice (+3.70-fold; pairwise comparison: $P\leq 0.05$). This increased physical activity also persisted to the final week of measurement (+4.1-fold; pairwise comparison: $P\leq 0.001$). There were no significant differences in the cumulative physical activity of control, HF-S and HF-n-3 males at any time point.

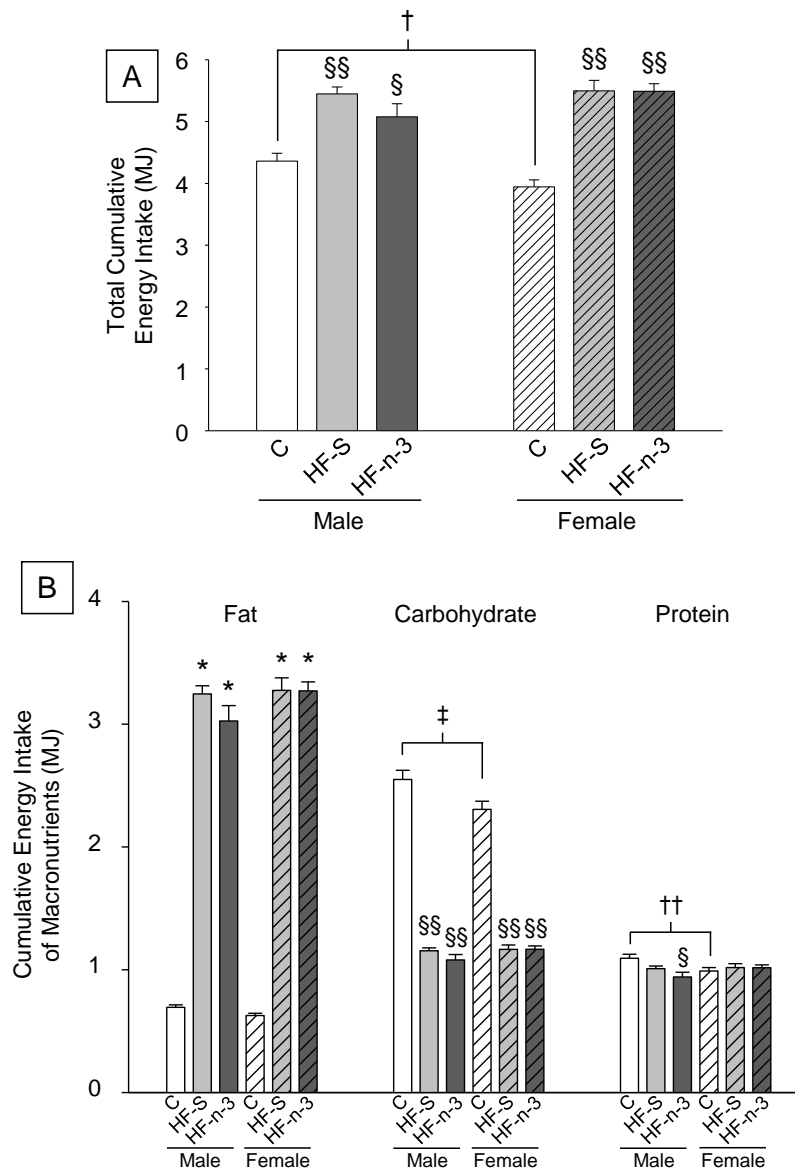


Figure 2.3 [A-B]. Total cumulative energy intake [A] and cumulative energy intake of macronutrients [B] in male and female mice fed control, high saturated fat or high fat n-3 PUFA enriched diets.

Data are expressed as mean (bars) ± SEM (error bars). Bar type represents gender: male (M), solid bars; female (F), lined bars, and bar colour represents dietary group: white, control (C); pale grey, high saturated fat (HF-S); dark grey, high fat n-3 PUFA enriched (HF-n-3).

n: C(M/F) = 10/12, HF-S(M/F) = 11/11, HF-n-3(M/F) = 9/11.

Statistics: Effect of diet: * $P \leq 0.001$, compared to C. Diet*gender interaction: § $P \leq 0.005$, §§ $P \leq 0.001$, compared to C (of same gender); † $P \leq 0.05$, †† $P \leq 0.02$, ‡ $P \leq 0.001$, M compared to F (of same dietary group).

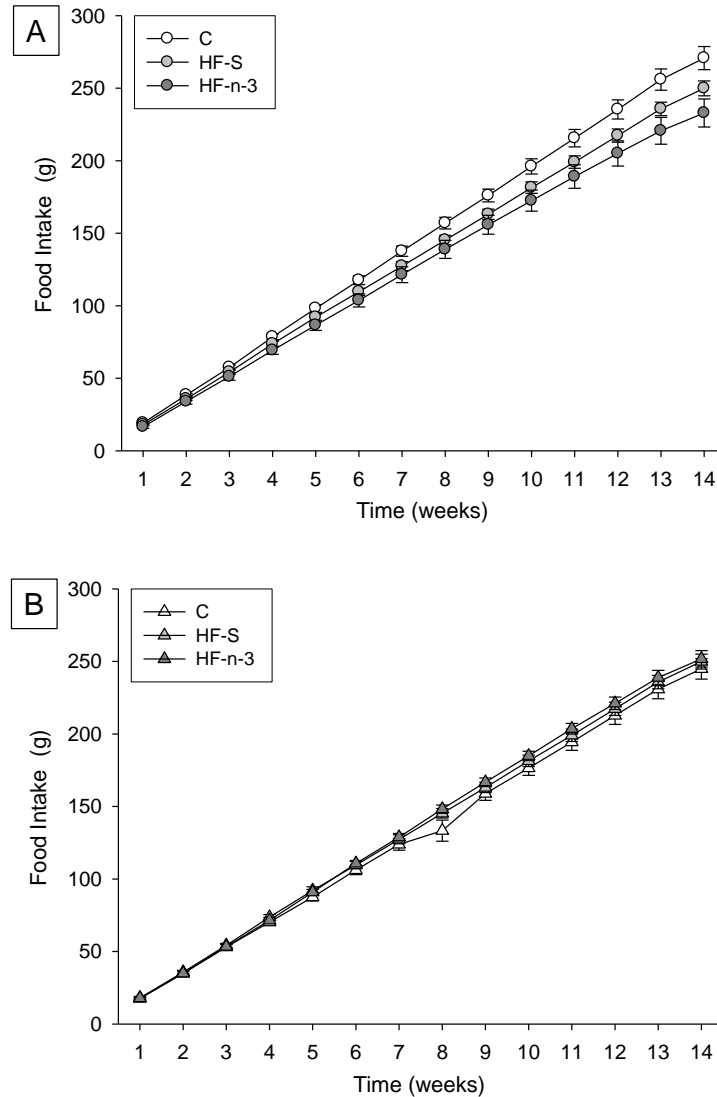


Figure 2.4 [A-B]. Food intake during the experimental dietary period in male [A] and female [B] mice fed control, high saturated fat or high fat n-3 PUFA enriched diets for 14 weeks.

Data expressed as mean (circles, males (M); triangles, females (F)) \pm SEM (error bars). Values are reported in g. Control diet, C; high saturated fat diet, HF-S; high fat n-3 PUFA enriched diet, HF-n-3.

n: C(M/F) = 10/12, HF-S(M/F) = 11/11, HF-n-3(M/F) = 9/11.

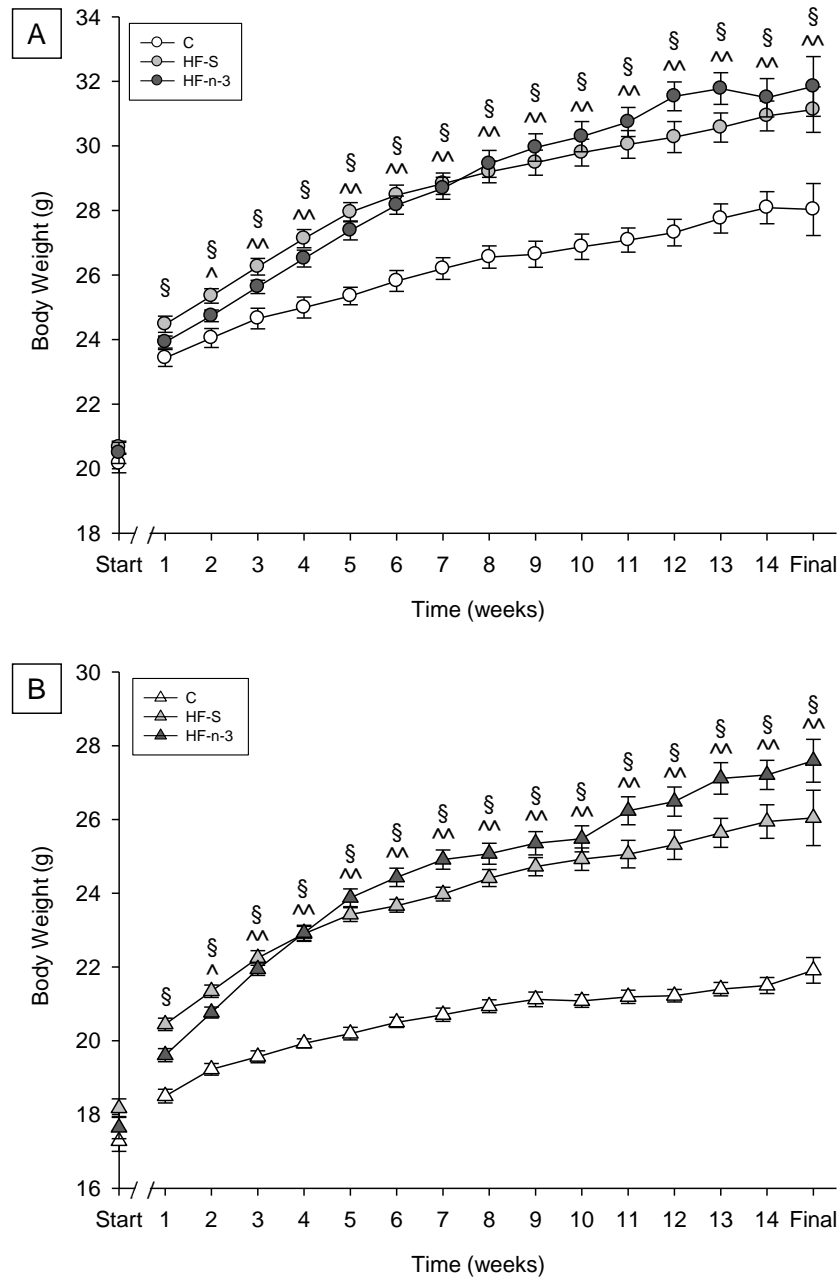


Figure 2.5 [A-B]. Body weight from arrival, during the experimental dietary period, to the final day, of male [A] and female [B] mice fed control, high saturated fat or high fat n-3 PUFA enriched diets for 14 weeks.

Data expressed as mean (circles, males (M); triangles, females (F)) ± SEM (error bars). Values are reported in g. Control diet, C; high saturated fat diet, HF-S; high fat n-3 PUFA enriched diet, HF-n-3.

n: C(M/F) = 10/12, HF-S(M/F) = 11/11, HF-n-3(M/F) = 9/11.

Statistics: Diet*time interaction: § $P \leq 0.001$, C compared to HF-S; ^ $P \leq 0.05$, ^^ $P \leq 0.001$, C compared to HF-n-3.

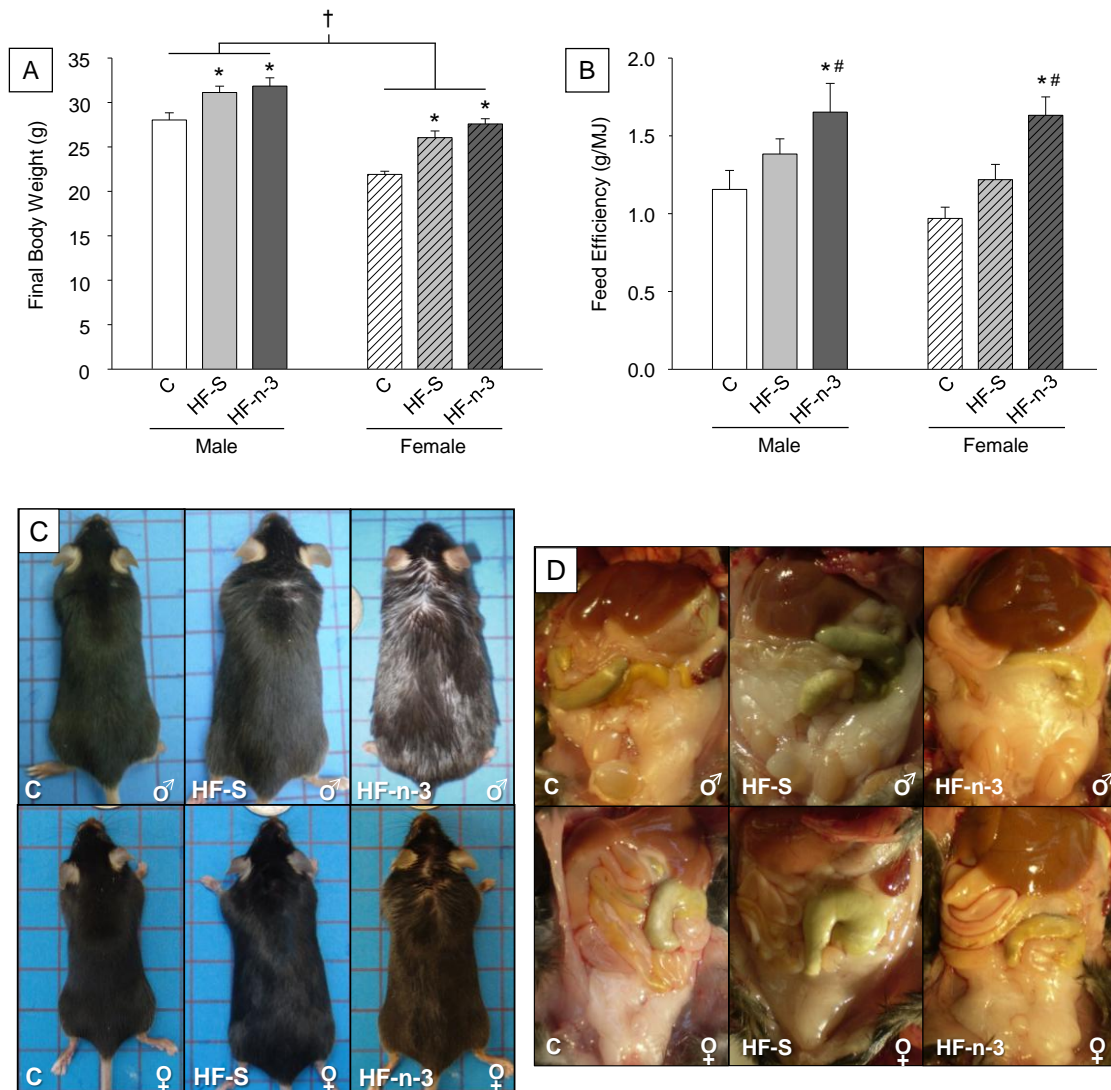


Figure 2.6 [A-D]. Final body weight [A], feed efficiency [B] and representative external [C] and internal [D] images of male and female mice fed control, high saturated fat or high fat n-3 PUFA enriched diets.

[A-D]: Control diet, C; high saturated fat diet, HF-S; high fat n-3 PUFA enriched diet, HF-n-3.

[A, B]: Data are expressed as mean (bars) \pm SEM (error bars). Values are reported in [A]: g, [B]: g/MJ. Bar type represents gender: male (M), solid bars; female (F), lined bars, and bar colour represents dietary group: white, control; pale grey, HF-S; dark grey, HF-n-3. n: C(M/F) = 10/12, HF-S(M/F) = 11/11, HF-n-3(M/F) = 9/11.

[C]: grid scale represents 1.5 cm²; [C, D]: ♂ = M, ♀ = F.

Statistics: Effect of diet: * $P \leq 0.001$, compared to C; # $P \leq 0.02$, compared to HF-S. Effect of gender: † $P \leq 0.001$, M compared to F.

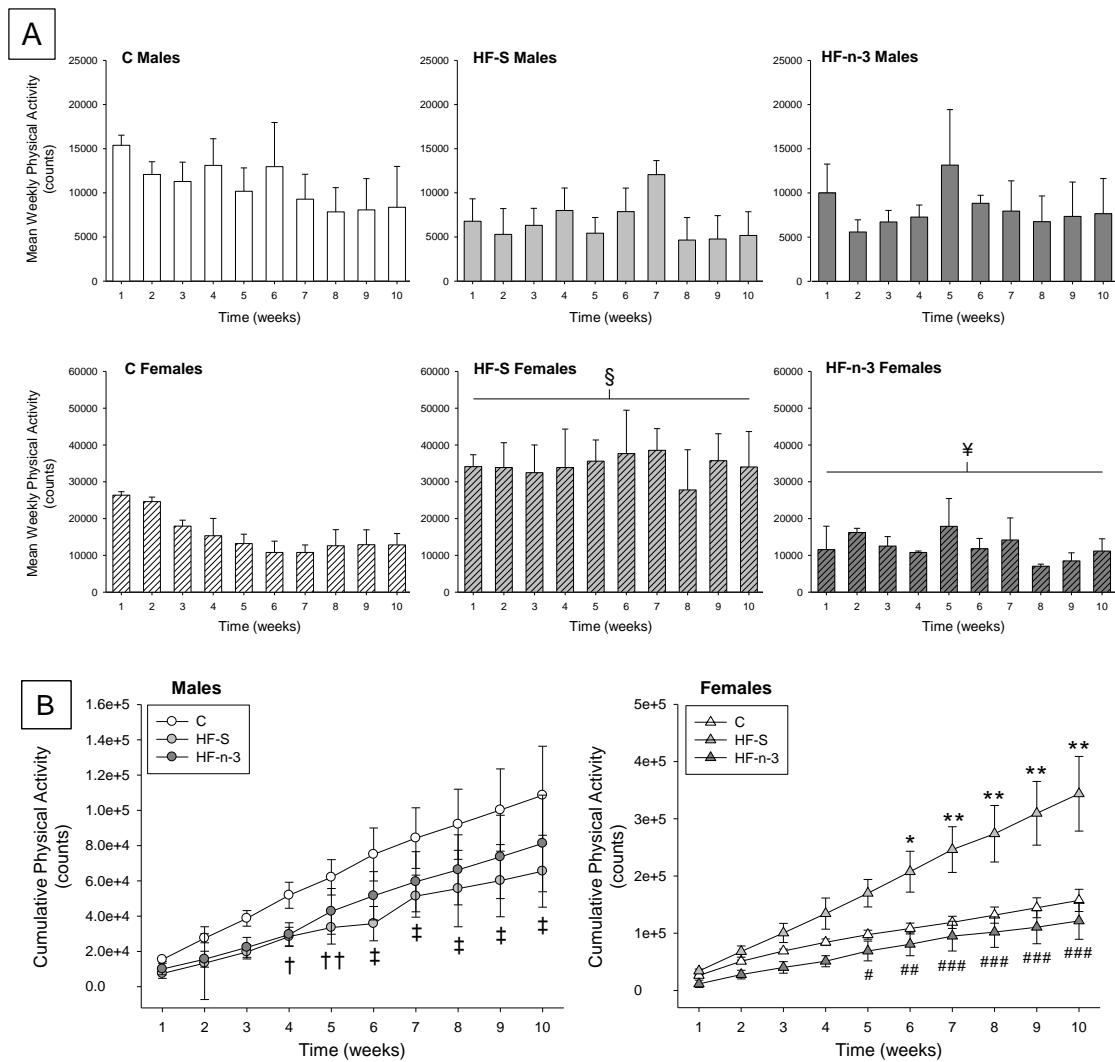


Figure 2.7 [A-B]. Mean weekly physical activity [A] and cumulative physical activity [B] during the experimental dietary period of male and female mice fed control, high saturated fat or high fat n-3 PUFA enriched diets.

Control diet, C; high saturated fat diet, HF-S; high fat n-3 PUFA enriched diet, HF-n-3.

[A]: Data are expressed as mean (bars) \pm SEM (error bars). Bar type represents gender: male (M), solid bars; female (F), lined bars, and bar colour represents dietary group: white, control; pale grey, HF-S; dark grey, HF-n-3.

[B]: Data expressed as mean (circles, males (M); triangles, females (F)) \pm SEM (error bars). Data point type represents dietary group: white, C; pale grey, HF-S; dark grey, HF-n-3. n: C(M/F) = 3/3, HF-S(M/F) = 3/3, HF-n-3(M/F) = 3/2.

Statistics: [A]: Diet*gender*time interaction: * $P \leq 0.01$, ** $P \leq 0.001$, HF-S F compared to C F; # $P \leq 0.05$, ### $P \leq 0.01$, #### $P \leq 0.001$, HF-S F compared to HF-n-3 F; † $P \leq 0.05$, †† $P \leq 0.005$, ‡ $P \leq 0.001$, HF-S M compared to HF-S F. [B]: Diet*gender*time interaction: § $P \leq 0.001$, HF-S F compared to C F; ¥ $P \leq 0.001$, HF-n-3 F compared to HF-S F.

2.3.2 – Adipose Tissue Depot Weights

2.3.2.1 – Total Adiposity

The combined absolute weight of the adipose tissue depots collected was determined as a measure of total adiposity (**Table 2.2**). Total adiposity was increased in HF-S and HF-n-3 mice as compared to controls (+40%, +50%, respectively; effect of diet: $F(2, 57)=5.4$, $P=0.007$; post-hoc tests: $P\leq 0.05$, $P\leq 0.01$, respectively), but was similar between both high fat groups (post-hoc test: $P=1.0$). Although there was no significant effect of gender on the total adiposity, there was a tendency for total adiposity to be greater in male as compared to female mice (+22%, $F(1, 57)=3.6$, $P=0.064$).

2.3.2.2 – Absolute Adipose Tissue Weight

The absolute weight of the subcutaneous adipose tissue was greater in HF-S and HF-n-3 mice as compared to controls (+47%, +58%, respectively; effect of diet: $F(2, 57)=5.0$, $P=0.010$; post-hoc tests: $P\leq 0.05$, $P\leq 0.01$, respectively) (**Table 2.2**). There was no effect of gender on the absolute weight of the subcutaneous adipose tissue depot ($F(1, 57)=0.7$, $P=0.39$). The absolute weight of the visceral mesenteric adipose tissue was greater in HF-S mice as compared to controls (+24%; effect of diet: $F(2, 58)=3.5$, $P=0.036$; post-hoc test: $P\leq 0.05$) (**Table 2.2**). There was a trend towards greater absolute weight of the visceral mesenteric adipose tissue weight in male mice as compared to female mice ($F(1, 58)=3.1$, $P=0.084$). The absolute weight of the pooled perirenal and retroperitoneal adipose tissue depot was greater in HF-n-3 mice as compared to controls (+83%; effect of diet: $F(2, 58)=7.2$, $P=0.002$; post-hoc test: $P\leq 0.001$) and was also greater in male mice as compared to female mice (+48%; effect

of gender: $F(1, 58)=9.6$, $P=0.003$) (**Table 2.2**). The absolute weight of the brown adipose tissue was greater in HF-n-3 mice as compared to control and HF-S mice (+41%, +45%, respectively; effect of diet: $F(2, 58)=12.9$, $P\leq 0.001$; post-hoc tests: $P\leq 0.001$) (**Table 2.2**). The absolute weight of the brown adipose tissue was also greater in male mice as compared to female mice (+20%; effect of gender: $F(1, 58)=7.3$, $P=0.009$). There was no effect of diet on the absolute weight of the male perigonadal adipose tissue depot, epididymal adipose tissue ($F(2, 27)=1.2$, $P=0.32$) (**Table 2.2**). The absolute weight of the female perigonadal adipose tissue depot (**Table 2.2**), periovaric adipose tissue, was greater in HF-n-3 females as compared to control females (+117%; effect of diet: $F(2, 31)=6.0$, $P=0.006$; post-hoc test: $P\leq 0.005$).

2.3.2.3 – Relative Adipose Tissue Weight

Relative weight (mg adipose tissue per g body weight) of the subcutaneous adipose tissue depot was not influenced by diet ($F(2, 57)=2.6$, $P=0.08$) or gender ($F(1, 57)=0.7$, $P=0.42$) (**Table 2.2**). There was however a trend towards increased relative weight of subcutaneous adipose tissue in HF-n-3 mice as compared to control mice (+30%; $P=0.10$). The relative weight of the visceral mesenteric adipose tissue depot (**Table 2.2**) was lower in HF-n-3 mice as compared to HF-S mice (-18%; effect of diet: $F(2, 58)=3.6$, $P=0.035$; post-hoc test: $P\leq 0.05$). There was no effect of gender on the relative weight of the visceral mesenteric adipose tissue depot ($F(1, 58)=1.5$, $P=0.22$). The relative weight of the pooled perirenal and retroperitoneal adipose tissue depot (**Table 2.2**) was greater in HF-n-3 mice as compared to control mice (+52%; effect of diet: $F(2, 58)=5.5$, $P=0.006$; post-hoc test: $P\leq 0.005$) and was also greater in male mice as

compared to female mice (+23%; effect of gender: $F(1, 58)=4.2, P=0.044$). The relative weight of the brown adipose tissue (**Table 2.2**) was greater in HF-n-3 mice as compared to HF-S mice (+41%; effect of diet: $F(2, 58)=9.5, P\leq 0.001$; post-hoc test: $P\leq 0.05$). There was no effect of gender on the relative weight of brown adipose tissue ($F(1, 58)=0.0, P=0.99$). There was no effect of diet on relative weight of the male perigonadal adipose tissue depot, epididymal adipose tissue ($F(2, 27)=0.5, P=0.62$) (**Table 2.2**). The relative weight of the female perigonadal adipose tissue depot (**Table 2.2**), periovaric adipose tissue, was greater in HF-n-3 females as compared to control females (+66%; effect of diet: $F(2, 31)=4.0, P=0.028$; post-hoc test: $P\leq 0.05$).

In both the HF-S and HF-n-3 groups, there was a positive relationship between feed efficiency and the relative weight of the subcutaneous adipose tissue depot (HF-S, $r = +0.69, F(1, 19)=16.9, P=0.001$; HF-n-3, $r = +0.92, F(1, 18)=103.1, P\leq 0.001$) (**Figure 2.7**), however in HF-n-3 mice the slope of the relationship was greater (slope: HF-n-3, 22.1 vs HF-S, 13.3; $F(1, 37)=5.3, P=0.027$). In both HF-S and HF-n-3 mice there was a positive relationship between feed efficiency and the relative weight of the pooled perirenal-retroperitoneal adipose tissue depot (HF-S, $r = +0.82, F(1, 20)=42.5, P\leq 0.001$; HF-n-3, $r = +0.92, F(1, 18)=97.0, P\leq 0.001$) (**Figure 2.7**), and the slopes of the relationships were similar (slope: HF-S, 75.4 vs HF-n-3, 92.0; $F(1, 38)=1.2, P=0.27$). Similarly, in both HF-S and HF-n-3 mice there was a positive relationship between feed efficiency and the relative weight of the gonadal tissue depots (epididymal, HF-S, $r = +0.83, F(1, 9)=19.2, P=0.002$; HF-n-3, $r = +0.94, F(1, 7)=50.7, P\leq 0.001$; periovaric, HF-S, $r = +0.74, F(1, 9)=11.0, P=0.009$; HF-n-3, $r = +0.80, F(1,$

9)=15.9, $P=0.003$) (**Figure 2.8**), and the slopes of the relationships were similar (epididymal slope: HF-S, 34.1 vs HF-n-3, 43.2; $F(1, 16)=0.8$, $P=0.37$; periovariac slope: HF-S, 32.2 vs HF-n-3, 32.2; $F(1, 18)=0.0$, $P=1.0$).

Table 2.2. The absolute and relative weights of adipose tissue depots in mice fed a control, high saturated fat or high fat n-3 PUFA enriched diet.

<i>Absolute Weight of Adipose Tissue (g)</i>						
	Male			Female		
	C	HF-S	HF-n-3	C	HF-S	HF-n-3
Total Adiposity	2.48 ± 0.20	3.00 ± 0.33*	3.19 ± 0.52**	1.64 ± 0.09	2.64 ± 0.35*	2.92 ± 0.33**
Subcutaneous	0.99 ± 0.09	1.29 ± 0.18*	1.36 ± 0.24**	0.74 ± 0.05	1.21 ± 0.18*	1.34 ± 0.19**
Mesenteric	0.56 ± 0.04	0.59 ± 0.03*	0.50 ± 0.05	0.39 ± 0.01	0.57 ± 0.07*	0.51 ± 0.03
Perirenal- Retroperitoneal [†]	0.23 ± 0.03	0.30 ± 0.04	0.38 ± 0.07***	0.13 ± 0.01	0.21 ± 0.04	0.28 ± 0.03***
Brown [‡]	0.13 ± 0.01	0.12 ± 0.01	0.17 ± 0.02***##	0.10 ± 0.01	0.10 ± 0.01	0.15 ± 0.01***##
Perigonadal	0.56 ± 0.05	0.71 ± 0.09	0.78 ± 0.15	0.29 ± 0.03	0.50 ± 0.07	0.63 ± 0.10**
<i>Relative Weight of Adipose Tissue (mg Adipose Tissue/g Body Weight)</i>						
	Male			Female		
	C	HF-S	HF-n-3	C	HF-S	HF-n-3
Subcutaneous	35.0 ± 2.4	40.5 ± 4.8	41.5 ± 6.3	34.0 ± 2.1	44.9 ± 5.4	47.3 ± 6.0
Mesenteric	20.0 ± 1.0	18.7 ± 0.6	15.6 ± 1.1 [#]	17.9 ± 0.6	21.7 ± 2.2	18.4 ± 0.8 [#]
Perirenal- Retroperitoneal [†]	8.2 ± 0.7	9.3 ± 1.1	11.5 ± 2.0**	5.9 ± 0.4	7.8 ± 1.0	9.9 ± 1.0**
Brown	4.7 ± 0.4	3.8 ± 0.3	5.2 ± 0.5 [#]	4.4 ± 0.4	3.8 ± 0.2	5.5 ± 0.4 [#]
Perigonadal	20.0 ± 1.3	22.3 ± 2.4	23.8 ± 4.0	13.4 ± 1.4	18.6 ± 2.3	22.4 ± 2.9*

Data presented as mean ± SEM. Control diet, C; high saturated fat diet, HF-S; high fat n-3 PUFA enriched diet, HF-n-3; male mice, M; female mice, F.
n: C(M/F) all depots = 10/11, HF-S (M/F) subcutaneous = 11/10, all other depots = 11/11, HF-n-3(M/F) all depots = 9/11.
Statistics: Effect of diet: * $P \leq 0.05$, ** $P \leq 0.01$, *** $P \leq 0.001$, compared to C; # $P \leq 0.05$, ## $P \leq 0.001$, compared to HF-S. Effect of gender: [†] $P \leq 0.05$, [‡] $P \leq 0.01$, M compared to F.

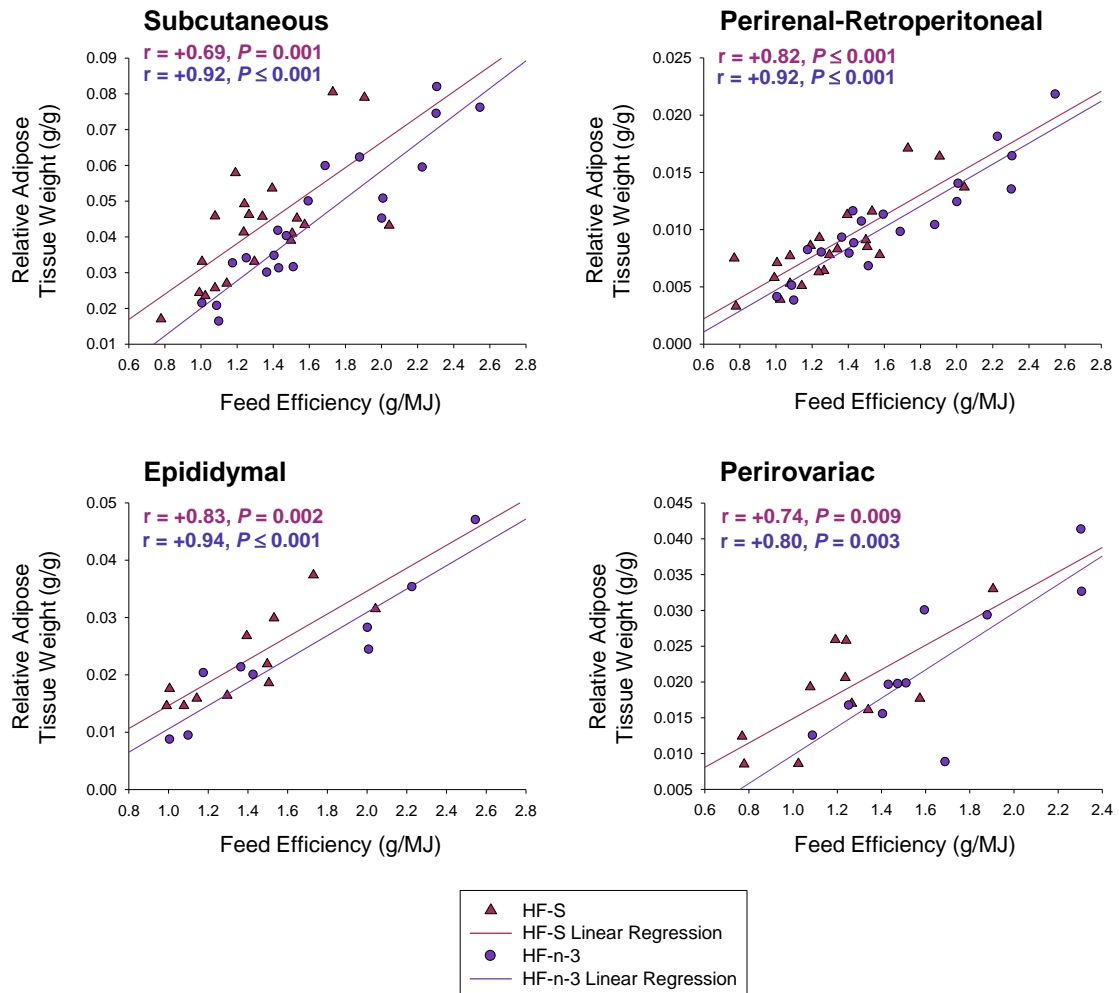


Figure 2.8. The relationships between feed efficiency and relative adipose tissue weight in mice fed a high saturated fat or high fat n-3 PUFA enriched diet.

Symbol type represents dietary group: see legend. High saturated fat diet, HF-S; high fat n-3 PUFA enriched diet, HF-n-3.

Subcutaneous, perirenal-retroperitoneal, n: HF-S = 22, HF-n-3 = 20.

Epididymal, n: HF-S = 11, HF-n-3 = 9. Periovariac, n: HF-S = 11, HF-n-3 = 11.

There was a significant positive relationship between the feed efficiency and relative weight of the subcutaneous and perirenal-retroperitoneal adipose tissue depots in HF-S and HF-n-3 mice (male and females combined). There was also a significant positive relationship between the feed efficiency and relative weight of the epididymal and periovariac adipose tissue depots in HF-S and HF-n-3 mice.

2.3.3 – Plasma Concentration of Glucose, Insulin and Triglyceride

The plasma concentration of glucose (**Figure 2.9A**) was not significantly influenced by diet ($F(2, 56)=1.5, P=0.23$). However, male mice exhibited greater plasma glucose concentration as compared to female mice (+15%; $F(1, 56)=4.4, P=0.040$). Plasma insulin concentrations (**Figure 2.9B**) tended to be higher in HF-S mice as compared to C and HF-n-3 mice, however the differences did not reach statistical significance (+64%, +71%, respectively; $F(2, 55)=3.3, P=0.043$; post-hoc tests: $P=0.11, P=0.085$, respectively). There was no effect of gender ($F(1, 55)=0.2, P=0.64$) on the plasma concentration of insulin. Plasma triglycerides (**Figure 2.9C**) were lower in HF-n-3 mice as compared to C and HF-S mice (-43%, -30%, respectively; effect of diet: $F(2, 56)=6.3, P=0.003$; post-hoc tests: $P\leq 0.005, P\leq 0.05$, respectively). There was no effect of gender on plasma triglyceride concentration ($F(1, 56)=0.2, P=0.65$).

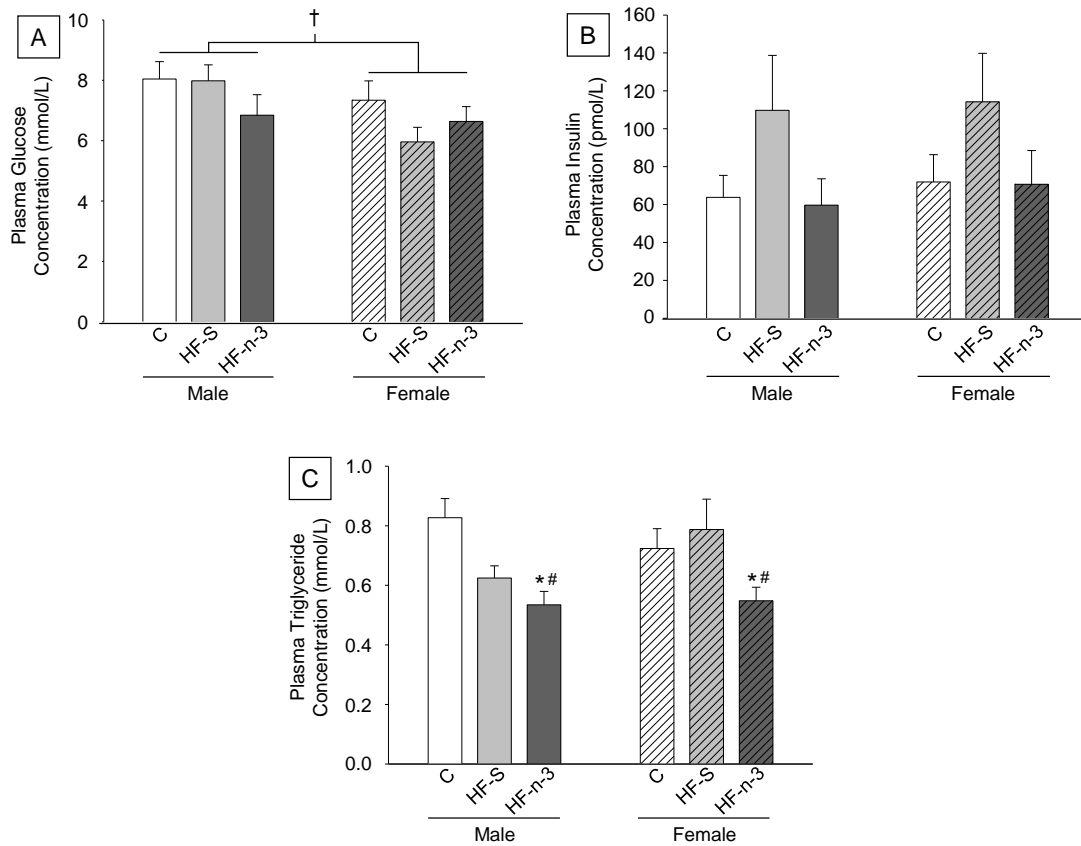


Figure 2.9 [A-C]. Plasma concentration of glucose [A], insulin [B] and triglyceride [C] in male and female mice fed control, high saturated fat or high fat n-3 PUFA enriched diets.

Data are expressed as mean (bars) \pm SEM (error bars).

Values are reported in [A, C]: mmol/L, [B]: pmol/L. Bar type represents gender: male (M), solid bars; female (F), lined bars, and bar colour represents dietary group: white, control (C); pale grey, high saturated fat (HF-S); dark grey, high fat n-3 PUFA enriched (HF-n-3).

n: C(M/F) = 10/11, HF-S(M/F) = 11/11, HF-n-3(M/F) = 9/11.

Statistics: Effect of diet: * $P \leq 0.005$, compared to C; # $P \leq 0.05$, compared to HF-S.

Effect of gender: † $P \leq 0.05$, M compared to F.

2.3.4 – Type of Dietary Fat Consumed Influences Liver Appearance and Liver Weight

A marked difference was observed in the colour of livers between dietary groups at post-mortem. Mice consuming the HF-S diet exhibited pale livers, when visually compared to the livers of C and HF-n-3 mice, whilst the livers of mice consuming the HF-n-3 diet were darker than those of either C and HF-S mice (**Figure 2.10A**), irrespective of gender. In close-up images, HF-n-3 livers exhibit a “dotty” appearance, which is not visible in control or HF-S livers (**Figure 2.10B**).

The absolute weight of the liver (**Figure 2.10C**) was increased in HF-n-3 mice when compared to control and HF-S mice (+69%, +35%, respectively; effect of diet: $F(2, 56)=133.5$, $P\leq 0.001$; post-hoc tests: $P\leq 0.001$). The absolute weight of the liver was also increased in HF-S mice when compared to controls (+25%; effect of diet: $F(2, 56)=133.5$, $P\leq 0.001$; post-hoc test: $P\leq 0.001$). Male mice exhibited greater absolute liver weight as compared to female mice (+9%, effect of gender: $F(1, 56)=11.4$, $P=0.001$).

The relative weight of the liver (g/g body weight) (**Figure 2.10D**) was increased in HF-n-3 mice when compared to C and HF-S mice (+41%, +33%, respectively; effect of diet: $F(2, 56)=108.2$, $P\leq 0.001$; post-hoc tests: $P\leq 0.001$). There was also a trend towards greater relative liver weight in HF-S mice as compared to control mice, but this was not significant (+7%; $P=0.08$). Female mice exhibited greater relative liver weight as compared to male mice (+10%, effect of gender: $F(1, 56)=17.1$, $P\leq 0.001$).

Relative liver weight positively correlated with liver fat content (fat droplet area) in HF-S, but not C or HF-n-3, mice (HF-S, $r = +0.62$, $F(1, 17)=10.4$, $P=0.005$; C, $r = +0.10$, $F(1, 18)=0.2$, $P=0.67$; HF-n-3, $r = +0.12$, $F(1, 17)=0.2$, $P=0.64$) (**Figure 2.11**). In the HF-n-3 group only, there was a negative correlation between relative liver weight and final body weight (HF-n-3, $r = -0.79$, $F(1, 18)=30.6$, $P\leq 0.001$; C, $r = +0.24$, $F(1, 20)=1.3$, $P=0.28$; HF-S, $r = +0.16$, $F(1, 18)=0.16$, $P=0.49$) (**Figure 2.11**). In all dietary groups, relative liver weight correlated positively with liver glycogen content (C, $r = +0.66$, $F(1, 20)=15.5$, $P\leq 0.001$; HF-S, $r = +0.72$, $F(1, 18)=19.4$, $P\leq 0.001$; HF-n-3, $r = +0.55$, $F(1, 16)=7.0$, $P=0.018$) (**Figure 2.11**). The slopes of the relationships between liver glycogen and relative liver weight tended to be greater in control and HF-S mice, although this did not reach statistical significance (slope: C, 1530.4; HF-S, 1056.4; HF-n-3, 563.1; $F(2, 54)=2.7$, $P=0.077$).

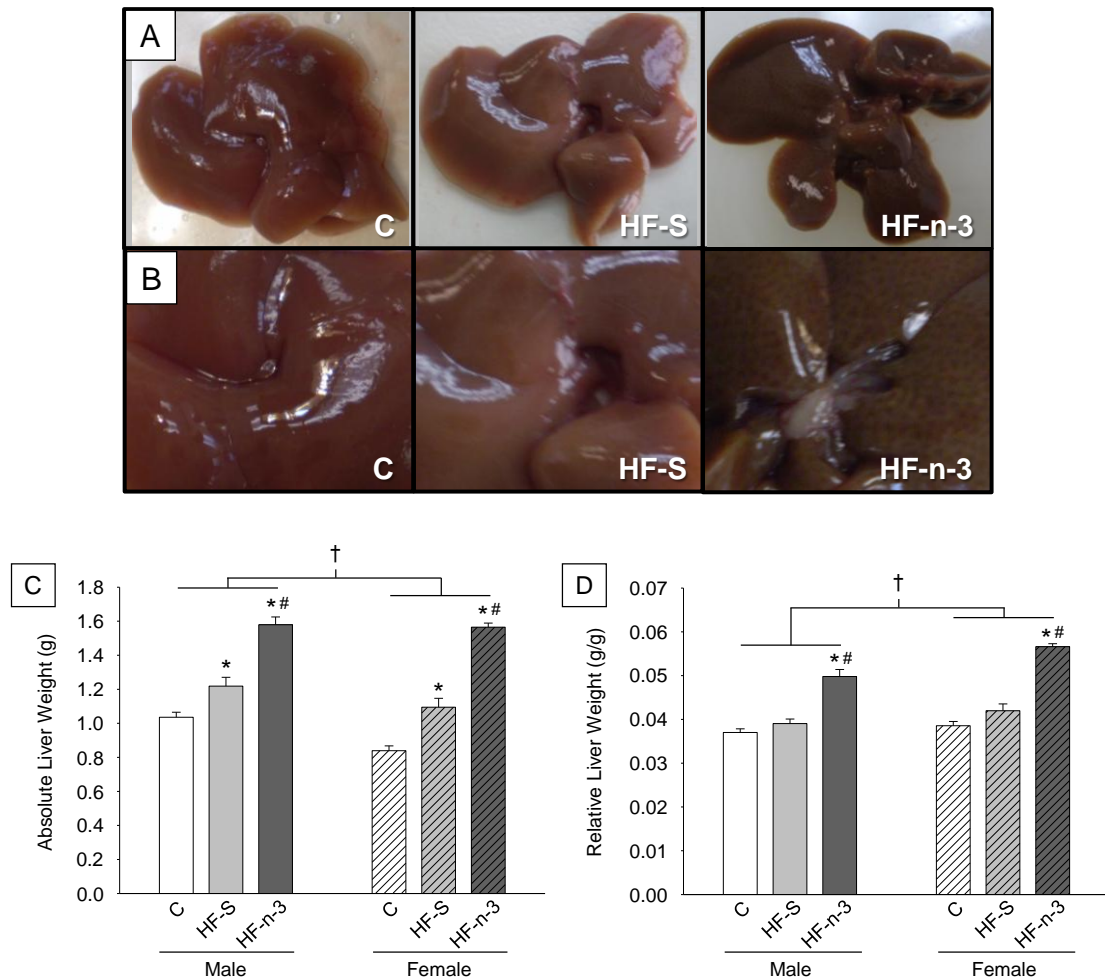


Figure 2.10 [A-D]. Representative whole [A] and close-up [B] images depicting altered liver appearance and graphs illustrating the absolute [C] and relative [D] weight of the liver in mice fed a control, high saturated fat or high fat n-3 PUFA enriched diet.

Data are expressed as mean (bars) \pm SEM (error bars). Values are presented in [C]: g, [D]: g/g body weight. Bar type represents gender: male (M), solid bars; female (F), lined bars, and bar colour represents dietary group: white, control (C); pale grey, high saturated fat (HF-S); dark grey, high fat n-3 PUFA enriched (HF-n-3).

n: C(M/F) = 10/11, HF-S(M/F) = 11/9, HF-n-3(M/F) = 9/11.

Statistics: Effect of diet: * $P \leq 0.001$, compared to C; # $P \leq 0.001$, compared to HF-S. Effect of gender: † $P \leq 0.001$, M compared to F.

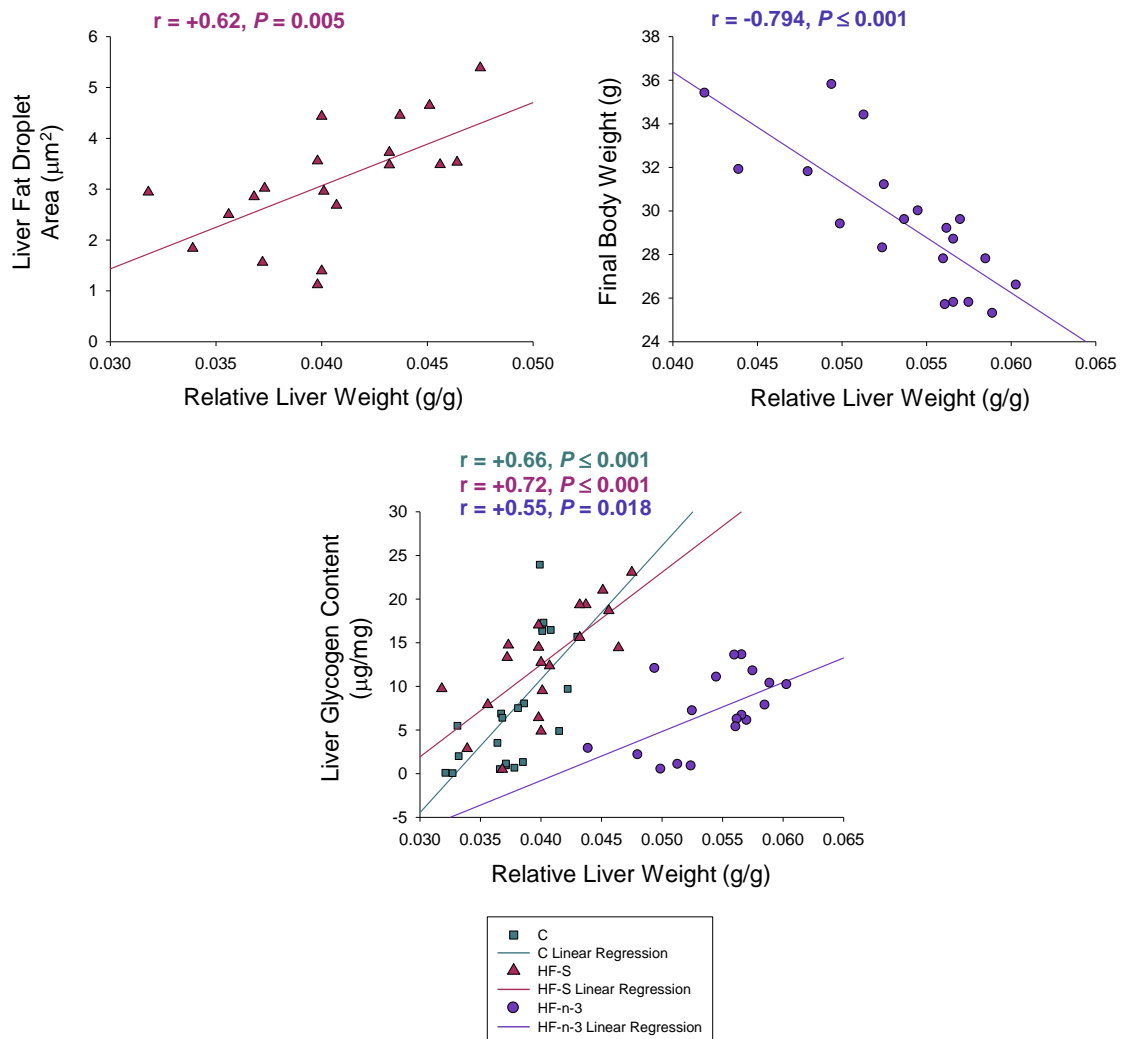


Figure 2.11. The relationships between relative liver weight and liver fat content, body weight and liver glycogen content.

Symbol type represents dietary group: see legend. C, control diet; HF-S, high saturated fat diet; HF-n-3, high fat n-3 PUFA enriched diet.

Liver fat content, n: HF-S = 19. Body weight, n: HF-n-3 = 20. Liver glycogen content n: C = 21, HF-S = 20, HF-n-3 = 18.

There was a significant positive relationship between relative liver weight and liver fat droplet area in HF-S mice only (males and females combined). There was a significant negative relationship between relative liver weight and body weight in HF-n-3 mice only (males and females combined). There was a significant positive relationship between relative liver weight and liver glycogen content in C, HF-S and HF-n-3 mice (males and females combined).

2.3.5 – Type of Dietary Fat Consumed Influences Liver Histology and Liver Fat Accumulation

Histological evaluation, using haematoxylin and eosin staining, demonstrated many large clear vacuoles in the livers of HF-S mice, suggestive of fatty liver (**Figure 2.12A**). Livers of control and HF-n-3 mice appeared normal, containing fewer clear vacuoles. Liver fat content, assessed by Oil Red O staining, was visibly increased in HF-S mice, as compared to control and HF-n-3 mice (**Figure 2.12B**) and this was confirmed upon quantification (**Figure 2.12C-D**). Percentage area stained positively for fat (**Figure 2.12C**) was greater in HF-S livers as compared to control and HF-n-3 livers (+40%, +50%, respectively; effect of diet: $F(2, 54)=16.7$, $P\leq 0.001$; post-hoc tests: $P\leq 0.001$). The mean fat droplet area (**Figure 2.12D**) was also increased in HF-S livers as compared to control and HF-n-3 livers (+134%, +95%, respectively; effect of diet: $F(2, 54)=27.5$, $P\leq 0.001$; post-hoc tests: $P\leq 0.001$). The percentage area stained positively for fat and mean fat droplet area were similar in control and HF-n-3 livers (post-hoc tests: $P=0.60$, $P=1.0$, respectively). There was also an effect of gender on measures of liver fat accretion; the percentage area stained positively for fat and the mean area of fat droplets were greater in the livers of female mice as compared to male mice (+16%; effect of gender: $F(1, 54)=5.7$, $P=0.021$; and, +25%, effect of gender: $F(1, 54)=5.2$, $P=0.009$; respectively).

There was a positive relationship between measure of liver fat content, fat droplet area, and plasma insulin concentrations ($r = +0.29$, $F(1, 55)=5.1$, $P=0.028$, all groups), whilst

the percentage area stained positively for fat tended to correlate with plasma insulin concentrations ($r = +0.21$, $F(1, 55)=2.7$, $P=0.11$, all groups) (data not shown).

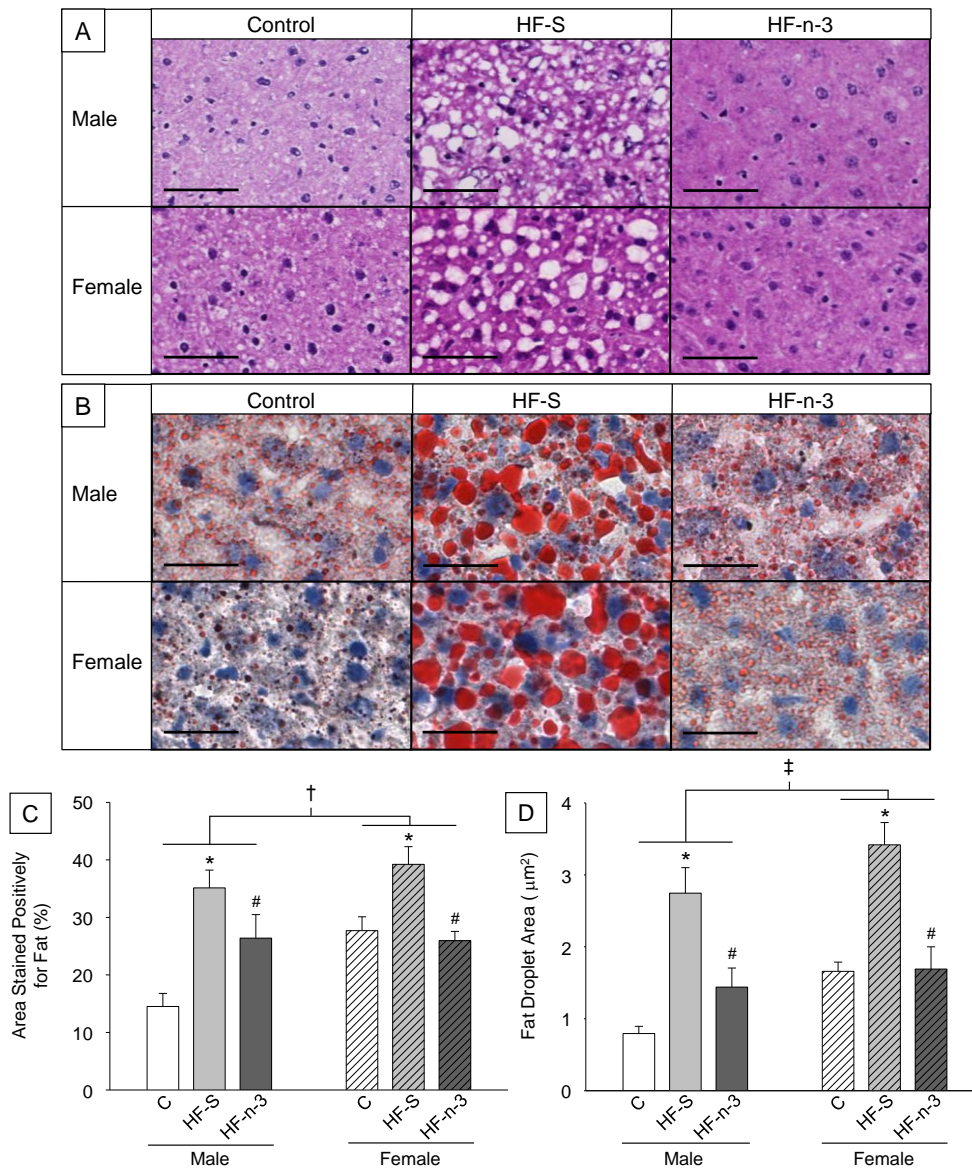


Figure 2.12 [A-D]. H&E [A] and Oil Red O [B] staining of liver sections and histological quantification of liver fat content as area stained positively for fat [C] and fat droplet area [D] of mice fed a control, high saturated fat or high fat n-3 PUFA enriched diet.

Scale bar represents, [A]: 50 µm, [B]: 25 µm. [C, D] Data are expressed as mean (bars) ± SEM (error bars). Values are presented in [C]: %, [D]: µm². Bar type represents gender: male (M), solid bars; female (F), lined bars, and bar colour represents dietary group: white, control (C); pale grey, high saturated fat (HF-S); dark grey, high fat n-3 PUFA enriched (HF-n-3).

n: C(M/F) = 8/12, HF-S(M/F) = 11/10, HF-n-3(M/F) = 9/10.

Statistics: Effect of diet: * $P \leq 0.001$, compared to C; # $P \leq 0.001$, compared to HF-S. Effect of gender: † $P \leq 0.05$ ‡ $P \leq 0.01$, M compared to F.

2.3.6 – Type of Dietary Fat Consumed Influences Liver Glucose Metabolism

Liver glycogen content (**Figure 2.13A**) was greater in HF-S mice as compared to control and HF-n-3 livers (+79%, +87%, respectively; effect of diet: $F(2, 56)=7.7$, $P=0.001$; post-hoc tests: $P\leq 0.005$). Liver glycogen content was not significantly different in control and HF-n-3 mice ($P=1.0$). Liver glycogen content was influenced by gender; female mice exhibited greater liver glycogen content as compared to male mice (+35%; effect of gender: $F(1, 56)=4.4$, $P=0.040$).

Liver glucose content (**Figure 2.13B**) was lower in HF-n-3 mice as compared to HF-S mice (-40%; effect of diet: $F(2, 58)=4.5$, $P=0.016$; post-hoc test: $P\leq 0.020$). Although not significantly different, there was a strong trend towards reduced liver glucose content in HF-n-3 mice as compared to control mice (-33%; post-hoc test: $P=0.064$). Liver glucose content was not significantly different between control and HF-S mice (post-hoc test: $P=1.0$). There was no effect of gender on liver glucose content ($F(1, 58)=1.5$, $P=0.23$).

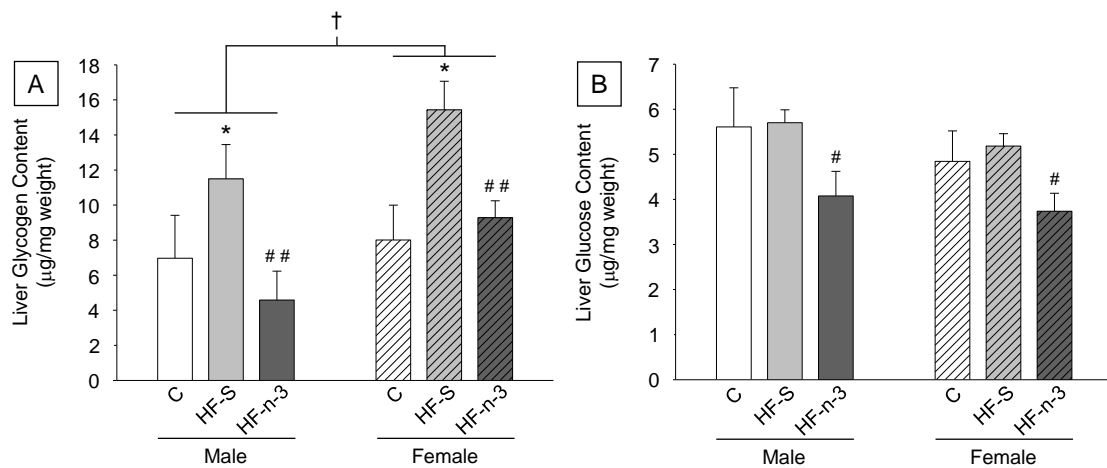


Figure 2.13 [A-B]. Liver glycogen [A] and glucose [B] content of male and female mice fed a control, high saturated fat or high fat n-3 PUFA enriched diet.

Data are expressed as mean (bars) \pm SEM (error bars). Values are presented in $\mu\text{g}/\text{mg}$ liver weight. Bar type represents gender: male (M), solid bars; female (F), lined bars, and bar colour represents dietary group: white, control; pale grey, high saturated fat (HF-S); dark grey, high fat n-3 PUFA enriched (HF-n-3).

[A] n: C(M/F) = 10/12, HF-S(M/F) = 11/10, HF-n-3(M/F) = 8/10. [B] n: C(M/F) = 10/12, HF-S(M/F) = 11/11, HF-n-3(M/F) = 9/11.

Statistics: Effect of diet: * $P < 0.005$, compared to C; # $P < 0.02$, ## $P < 0.005$, compared to HF-S. Effect of gender: † $P < 0.05$, M compared to F.

2.4 – DISCUSSION

This study demonstrates that although body weight and total fat mass increased similarly with both HFDs, there were significant effects of substituting saturated fat with n-3 PUFAs on the distribution of adipose tissue, ectopic fat storage and insulin sensitivity. Specifically n-3 PUFA enrichment of a HF-S diet reduced visceral adiposity, increased brown fat mass, prevented ectopic fat deposition and ameliorated insulin resistance.

2.4.1 – Effect of Dietary Fatty Acid Composition on Body Weight and Relative Adipose Tissue Weight

The observation that body weight was similar in both HFD groups is in contrast to other studies showing a reduced body weight gain with n-3 PUFA enrichment of a HFD (Wang *et al.*, 2002; Ikemoto *et al.*, 1996). There are however, other studies that also show no difference in body weight with HF-n-3 feeding (Dorfmeister *et al.*, 2006; Rustan *et al.*, 1993). Despite similar body weight and total absolute fat mass, adipose tissue distribution was altered upon n-3 PUFA enrichment of a HFD. Visceral adiposity was reduced in HF-n-3 mice, as previously reported (Rokling-Andersen *et al.*, 2009). In contrast, in this study, no HF-n-3-induced reduction in the mass of the epididymal and perirenal adipose tissue depots was observed as previously described (Rokling-Andersen *et al.*, 2009; Belzung *et al.*, 1993; Parrish *et al.*, 1990). In the present study, an increase in subcutaneous adipose tissue mass in mice fed a HF-n-3 diet as has been previously reported, was also not observed (Rokling-Andersen *et al.*, 2009), but the greater slope of the relationship between feed efficiency and subcutaneous

fat mass in HF-n-3 mice suggests that subcutaneous adipose tissue mass makes a larger contribution to the increased body weight gain in HF-n-3 mice.

The current study also demonstrated that the major brown adipose tissue store, interscapular fat, and minor brown adipose tissue depots (also containing white adipocytes), the perirenal and retroperitoneal depots and periovariac depot (Cinti, 2005), were increased with HF-n-3 feeding. This observation has not, as far as I can determine, been previously reported. The enlargement of the brown adipose tissue depot may indicate an increased capacity for thermogenesis in HF-n-3 mice, and consequently despite the apparent increase in feed efficiency, may have mitigated excess weight gain. Consistent with this notion, consumption of a corn oil diet, rich in PUFAs, preferentially stimulates thermogenesis in brown fat when compared to a HF-S feeding (Mercer and Trayhurn, 1987). Increased thermogenic capacity, and hence energy expenditure, may over time mediate a reduction in body weight gain, which may explain the discrepancies in body weight observed in HF-n-3 feeding studies (Dorfmeister *et al.*, 2006; Wang *et al.*, 2002; Ikemoto *et al.*, 1996; Rustan *et al.*, 1993). However, physical activity also influences body weight gain. Brownlow and colleagues (Brownlow *et al.*, 1996) reported that C57BL/6J mice fed a HFD exhibit increased physical activity, which was believed to be an adaptive response to low metabolic rate or low diet-induced thermogenesis. Furthermore, Chalon and colleagues (Chalon *et al.*, 1998) showed that consumption of a HF-S diet enriched with fish oil-derived n-3 PUFAs reduced physical activity by 25% in rats. The current study also showed that physical activity was increased by HF-S feeding, but reduced by n-3 PUFA enrichment of a HFD in female mice. Therefore, greater physical activity in

HF-S mice may act to compensate for the increased energy intake of a HFD, whilst in HF-n-3 mice, lower physical activity may be a compensatory response for the HF-n-3-induced increase in thermogenesis, with the aim of maintaining energy balance, and this may therefore explain the similar body weight gain in HF-n-3 mice to their HF-S-fed counterparts.

The mechanism behind the HF-n-3-induced redistribution of fat from visceral to subcutaneous depots may involve the differential regulation of genes influencing triglyceride storage in the two fat depots. Although adipose tissue gene expression was not assessed in the current study, there is some evidence that the type of dietary fatty acids consumed may influence the expression of genes regulating triglyceride lipolysis and synthesis in the subcutaneous and visceral fat depots. Hormone sensitive lipase (HSL), an enzyme involved in triglyceride lipolysis, exhibits suppressed mRNA expression in the subcutaneous adipose tissue depot, but is markedly upregulated in mesenteric adipose tissue upon n-3 PUFA enrichment of a lard diet (Rokling-Andersen *et al.*, 2009). These data suggest that in response to HF-n-3 feeding less triglyceride is broken down to free fatty acid in the subcutaneous depot, whilst increased triglyceride hydrolysis in the visceral depot may account for the lower visceral fat mass.

Differential triglyceride synthesis and hence storage in the two adipose tissue depots with HF-n-3 feeding may also account for changes in adipose tissue distribution. Diacylglycerol acyltransferase (DGAT), catalyses the last step of triglyceride synthesis (Hou *et al.*, 2009; Chen *et al.*, 2002) and when overexpressed in white adipose tissue induces adipocyte hypertrophy and increased fat mass (Chen *et al.*, 2002). DGAT is

differentially regulated in the visceral and subcutaneous adipose tissue stores, being positively associated with an increased rate of free fatty acid storage in visceral, but not subcutaneous fat (Hou *et al.*, 2009). Therefore altered DGAT activity may also contribute to the changes in adipose tissue distribution observed with HF-n-3 feeding.

Whilst it is possible to speculate that HSL and DGAT may be involved, further research is required to elucidate the mechanism behind the adipose tissue redistribution upon HF-n-3 feeding. Although the mechanism requires further investigation, the significance of this adipose tissue redistribution is clear, reduced visceral fat preferentially redirected to subcutaneous depots would confer advantages in insulin signalling, as visceral adiposity correlates strongly with insulin resistance (Bonora, 2000; Kim *et al.*, 2000) and a more peripheral distribution of fat is believed to preserve insulin sensitivity (Bonora, 2000).

2.4.2 – Effect of Dietary Fatty Acid Composition on Liver Fat and Glycogen Content

The liver plays a central role in maintaining energy balance, actively participating in fat metabolism and mediating whole-body glucose homeostasis. Consumption of a diet rich in n-3 PUFAs has been previously described to induce hepatomegaly (Buettner *et al.*, 2006; Nakatani *et al.*, 2003; De Craemer *et al.*, 1994) and the current study demonstrated a consistent increase in liver weight relative to body weight in HF-n-3, but not HF-S, mice. It has been suggested that the HFD-induced increase in liver weight may be accounted for by increased liver fat accumulation. Similarly, the present study demonstrated that there was a positive relationship between relative liver weight and liver fat content in HF-S mice; however, this relationship did not prevail in

HF-n-3 mice, suggesting another factor may influence the enlarged livers of HF-n-3 mice. Glycogen is a large polymer chain comprised of several glucose residues and acts as the storage form for glucose (Elliott and Elliott, 2001). In the postprandial state, the liver takes up approximately 30% of ingested glucose (Kelley *et al.*, 1988; Ferrannini *et al.*, 1985), with much of this converted to glycogen (Moore *et al.*, 1991). When stores are fully saturated, glycogen accounts for approximately 5% of liver mass (Postic and Girard, 2008) and as glycogen is associated with large amounts of water (Kreitzman *et al.*, 1992), greater hepatic glycogen content may contribute in part to increased liver weight. Accordingly, this study showed that increasing relative liver weight was associated with greater liver glycogen, a relationship that held in all dietary groups. However, it was also demonstrated that hepatic glycogen content was reduced by HF-n-3 feeding; consistent with previous research in which hepatic glycogen content was lowered upon supplementation of standard rat chow with fish oil (Gaíva *et al.*, 2003) and n-3 PUFA enrichment of a HF-S diet (Holness *et al.*, 2003; Rustan *et al.*, 1993).

Therefore, a different factor must play a role in the HF-n-3-induced increase in liver weight and although hepatomegaly has been associated with n-3 PUFA consumption (Buettner *et al.*, 2006; Nakatani *et al.*, 2003; De Craemer *et al.*, 1994), no study has confirmed the cause. HF-n-3 livers are histologically normal (Buettner *et al.*, 2006; Nakatani *et al.*, 2003). Some studies have suggested, without evidence, that liver cell hypertrophy (Otto *et al.*, 1991) or hyperplasia (Buettner *et al.*, 2006) may contribute to the increased liver weight during HF-n-3 feeding; however, the current study did not detect such a phenomenon. Moreover, some research speculates that peroxisomal

proliferation may be a factor of increased liver weight (Nakatani *et al.*, 2003; De Craemer *et al.*, 1994).

In the current study HF-n-3 livers also exhibited an increase in brown pigmentation, the cause of which is unknown; accordingly further research is required to elucidate the factors inducing liver modifications with HF-n-3 feeding. Therefore, in future investigations, beyond the studies of this thesis, the effect of consuming a HF-n-3 diet on peroxisomal metabolism may be investigated, given that the livers of HF-n-3 mice were larger, which may suggest peroxisomal proliferation, and leaner which may indicate enhanced fatty acid oxidation either in the mitochondria or peroxisomes.

2.4.3 – Effect of Dietary Fatty Acid Composition on Dyslipidemia and Insulin Sensitivity

HF-S feeding is believed to alter the relative contribution of the metabolic pathways regulating whole-body fatty acid metabolism, resulting in dyslipidemia. In the current study it was demonstrated that HF-S diet consumption promoted dyslipidemia, as indicated by the increased hepatic triglyceride accumulation upon HF-S feeding, and this is in agreement with several previous studies in which HF-S feeding induced ectopic fat deposition in peripheral tissues such as the liver (de Meijer *et al.*, 2010; Buettner *et al.*, 2006; Ukropec *et al.*, 2003). In contrast to HF-S feeding, n-3 PUFA enrichment of a HFD prevented HF-S-induced dyslipidemia; this was evident in reduced plasma triglyceride concentrations and the amelioration of hepatic fat accumulation. Reduced liver triglyceride content with HF-n-3 feeding may be a consequence of n-3 PUFAs promoting the suppression of pathways mediating hepatic

triglyceride storage (Pérez-Echarri *et al.*, 2009) and the activation of fatty acid oxidation in the liver (Buettner *et al.*, 2006; Ukropec *et al.*, 2003). Increased intrahepatic triglyceride accumulation is strongly associated with diminished insulin sensitivity (Qureshi *et al.*, 2010; Marchesini *et al.*, 2003; Chitturi *et al.*, 2002). Therefore a reduction in hepatic triglyceride content may be advantageous in the maintenance of insulin sensitivity described in studies upon n-3 PUFA dietary enrichment (Storlien *et al.*, 1987).

Consumption of a HF-S diet has been well-established to promote insulin resistance in both rodents (Buettner *et al.*, 2006; Holness *et al.*, 2004) and humans (Lovejoy *et al.*, 1998; Mayer-Davis *et al.*, 1997). In the current study, insulin sensitivity was not measured using the gold-standard hyperinsulinaemic euglycaemic clamp technique (DeFronzo *et al.*, 1979). This study did, however, measure the plasma glucose and insulin concentrations in the fed-state. It was demonstrated that plasma insulin tended to be greater in HF-S mice, despite unchanged plasma glucose concentration and this is in agreement with research by Holness and colleagues (Holness *et al.*, 2004; Holness *et al.*, 2003) in which HF-S feeding resulted in insulin hypersecretion. These data suggest that HF-S feeding may induce peripheral insulin resistance and in a compensatory response, insulin secretion is increased, in an effort to maintain glucose tolerance. Furthermore, in the present study, it was shown that consuming a HF-n-3 diet prevented the tendency for a HF-S-induced elevation in plasma insulin concentrations. This too is in accordance with Holness and colleagues' work (Holness *et al.*, 2004; Holness *et al.*, 2003) in which exposure to n-3 PUFAs reversed the hypersecretory insulin response to HF-S diet consumption. However, HF-S plasma insulin levels in

the current study only tended to be different from those of control and HF-n-3 mice. This may be reflective of the large variation in plasma insulin in similarly treated animals and may result from differences in the feeding status of individual mice. Therefore this study may have benefited from either performing a hyperinsulinaemic euglycaemic clamp or measuring plasma insulin levels in the fasted state to provide a more definitive conclusion on the effect of HF-n-3 feeding on insulin sensitivity.

In accordance with research (Qureshi *et al.*, 2010; Marchesini *et al.*, 2003; Chitturi *et al.*, 2002) that demonstrated associations between HF-S-induced liver fat accumulation and reduced insulin sensitivity, the current study too showed that there was a relationship between elevated plasma insulin concentrations and increased hepatic fat accumulation. It is tempting to speculate that reduced hepatic fat accumulation observed in HF-n-3-fed mice in the current study may play a causal role in retaining insulin sensitivity, however there were concomitant reductions in visceral adiposity and plasma triglyceride concentrations also, and therefore it is likely that improved insulin sensitivity observed in HF-n-3-fed mice is the result of multiple changes in lipid metabolism and fat storage. In HFD-fed rodents, the peroxisome proliferator activator receptor α (PPAR α) agonist, WY-14,643, reduces liver fat accumulation (Ye *et al.*, 2001). n-3 PUFAs are natural agonists of PPAR α (Hihi *et al.*, 2002). The responses elicited by n-3 PUFA enrichment of a HFD may therefore be a consequence of PPAR α activation, resulting in the repartitioning of fatty acids away from storage toward oxidation (Davidson, 2006; Dorfmeister *et al.*, 2006; Ukropec *et al.*, 2003; Rustan *et al.*, 1993). Therefore to determine if PPAR α is implicated in the amelioration of dyslipidemia observed with HF-n-3 feeding, the effect of HF-n-3 feeding on PPAR α

expression in the skeletal muscle and liver has been assessed in subsequent **Chapters 4** and **5**.

2.4.4 – Effect of Gender on the HFD-Induced Phenotype

Several studies have described gender differences in the development of the obese phenotype and in response to high fat overfeeding (Haugaard *et al.*, 2009; Moro *et al.*, 2009; Català-Niell *et al.*, 2008; Gómez-Pérez *et al.*, 2008; Priego *et al.*, 2008). Although females have been shown to have a greater propensity for adipose tissue storage with high fat feeding (Priego *et al.*, 2008), in the current study, total adiposity tended to be greater in males than females. The current study has also demonstrated that three of the four uni-sex adipose tissue depots were of similar relative weight in male and female mice, and the fat store that showed a significant gender difference, the perirenal-retroperitoneal depot, was greater in males. In the present study, male mice exhibited greater plasma glucose concentrations in comparison to females, and as female mice are less likely to exhibit an impaired insulin sensitivity profile in response to increased fatty acid supply (Gómez-Pérez *et al.*, 2008; Hevener *et al.*, 2002), increased plasma glucose levels may predispose males to the development of HFD-induced impaired insulin sensitivity. Lower plasma glucose levels may also be a consequence of a greater capacity for glucose uptake in the peripheral tissues, and the increase in hepatic storage of glycogen observed in female mice is consistent with this notion. Furthermore, these observations are in keeping with female gonadal hormone, oestrogen's ability to promote insulin sensitivity (Geer and Shen, 2009). In the current study it was also demonstrated that female mice exhibited greater hepatic storage of fat,

and this is in contrast to research by Priego and associates (Priego *et al.*, 2008) in which male mice retained greater liver fat content upon HFD feeding. The current study did not however observe an interaction of gender and diet. Gonadal steroids mediate the expression of hepatic fatty acid transporter, fatty acid translocase (FAT/CD36). FAT/CD36 is more abundant in female rats and humans (Stahlberg *et al.*, 2004), and ovariectomy elicits a marked reduction on hepatic FAT/CD36 expression (Kano and Doi, 2006). Therefore increased liver fat in female mice may be consequential of a greater affinity of fatty acids for hepatic fatty acid transport system (Sorrentino *et al.*, 1992).

2.4.5 – Amount and Type of n-3 Fatty Acids Chosen

Whilst much research has investigated the effect of n-3 PUFA enrichment of a HFD on body weight, fat mass and insulin sensitivity, majority of studies used diets with varying energy intake from fat, differing proportions of n-3 PUFA incorporated into the total fat intake of the HFD, varying compositions of n-3 PUFA subtypes (DHA, EPA or ALA) and differing sources of n-3 PUFAs. The current study demonstrated that replacing 7.5% of saturated fat for n-3 PUFAs in a high fat diet setting reduced visceral adiposity, increased brown fat mass, prevented ectopic fat deposition in the liver and may have ameliorated insulin resistance. This is consistent with previous studies in which replacement of approximately 6-7% of dietary fat with fish oil-derived n-3 PUFAs, exerted beneficial effects on insulin action and sensitivity (Holness *et al.*, 2004; Storlien *et al.*, 1987), dyslipidemia and substrate utilisation (Rustan *et al.*, 1993). Replacement of approximately 6-7% of dietary fat with fish oil-derived n-3 PUFAs,

extrapolates to a high intake of n-3 PUFAs in humans. This dose was chosen to minimise the harmful side-effects that may be a consequence of toxicity associated with long-term administration of a very high dose of fish oil (Rabbani *et al.*, 2001), whilst promoting the aforementioned beneficial effects.

Furthermore, studies have utilised n-3 PUFAs from a range of sources, such as n-3 PUFAs derived from fish and plant extracts, which are known to produce different metabolic effects (Ruzickova *et al.*, 2004; Ikemoto *et al.*, 1996). Ruzickova and colleagues (Ruzickova *et al.*, 2004; Ikemoto *et al.*, 1996) demonstrated epididymal fat was reduced only when 15% of dietary fat was replaced with lipids of marine origin, not plant origin, and the EPA/DHA n-3 PUFA content increased from 1% to 12% (w/w) of dietary lipids, which extrapolates to an intake of 11g of EPA/DHA per day in humans. Similarly, Ikemoto and colleagues (Ruzickova *et al.*, 2004; Ikemoto *et al.*, 1996) demonstrated that EPA- and DHA-rich tuna oil (7% EPA, 23% DHA) was more effective at preventing body weight gain and increased white adipose tissue accumulation than ALA-rich perilla oil. Therefore an EPA- and DHA- rich fish oil similar to that used by Ikemoto and colleagues (Ruzickova *et al.*, 2004; Ikemoto *et al.*, 1996) was chosen for the current experiment (Nu-mega Ingredients Pty Ltd, Nathan, Queensland, Australia (HiDHA[®] 25N tuna oil (26% DHA, 6% EPA, 35% total n-3 PUFA content)).

2.4.6 – Limitations

A potential confounder exists in the current study; the assessment of body temperature may have provided additional information when considering the mechanisms behind the different phenotypes observed with HF-S and HF-n-3 feeding. As described previously, an enlargement of the brown adipose tissue depot, an important site of energy expenditure in rodents (Vidal-Puig *et al.*, 1997), may indicate an increased capacity for thermogenesis. Furthermore, PUFAs have been shown to stimulate thermogenesis in brown fat (Mercer and Trayhurn, 1987). Therefore increased thermogenic capacity, and hence energy expenditure, may over time mediate a reduction in body weight gain, which may explain the discrepancies in body weight observed in HF-n-3 feeding studies (Dorfmeister *et al.*, 2006; Wang *et al.*, 2002; Ikemoto *et al.*, 1996; Rustan *et al.*, 1993). Heat is dissipated in the thermogenic process; therefore measuring body temperature may provide information on the whole-body level of thermogenesis.

Furthermore, whilst an increase in brown fat was identified, brown adipose tissue was dissected according to visual identification. Given that adipose tissue may be a combination of brown and white adipose tissue at the cellular level, more detailed morphological analysis is required to confirm the presence of brown fat and differentiate it from white adipocytes.

2.4.6 – Summary

Whilst high fat overfeeding, irrespective of the fatty acid composition of the HFD consumed, is obesogenic in nature, this study highlights that phenotypic differences are observed when saturated fat is partially replaced by n-3 PUFAs. Specifically, n-3 PUFA enrichment of a HF-S diet reduced visceral adiposity, increased brown fat mass, prevented ectopic fat deposition in the liver and may have ameliorated insulin resistance (although not measured by the gold-standard hyperinsulinaemic euglycaemic clamp technique), when compared to a HF-S diet alone. These metabolic responses to HF-n-3 feeding are similar to those seen upon treatment with PPAR α agonists. It is therefore possible to speculate that the phenotypic changes observed with HF-n-3 feeding may be a consequence of n-3 PUFAs, a natural PPAR α ligand, promoting the activation of PPAR α in peripheral tissues, resulting in enhanced fatty acid oxidation and reduced triglyceride storage.

CHAPTER 3

*The Effect of Dietary Fatty Acid Content on
Muscle Fibre Type, Composition and Stored
Nutrient Content of Skeletal Muscle*

3.1 – INTRODUCTION

The regulation of energy balance is a fundamental process and particularly in the skeletal muscle, maintaining a balance between energy supply and demand is essential for normal function (Carling, 2005). Skeletal muscle plays a major role in maintaining whole-body energy homeostasis; it accounts for approximately 40-50% of body weight (Bonen *et al.*, 2002), is the chief site of glucose disposal (Liang and Ward, 2006) and is the main site of fatty acid oxidation at rest and during exercise (Bonen *et al.*, 2002; Jeukendrup, 2002). Peripheral insulin sensitivity is largely influenced by the amount of insulin-stimulated glucose uptake in skeletal muscle. When the supply of fatty acids surpasses the metabolic demands of skeletal muscle, excess fat may enter intramyocellular storage (Mullen *et al.*, 2007; Simončíkova *et al.*, 2002; Kim *et al.*, 2000). It has long been thought that increased storage of fatty acid derivatives in skeletal muscle is deleterious and that this is associated with reduced whole-body glucose uptake and diminished insulin sensitivity (Liu *et al.*, 2007; Manco *et al.*, 2000).

Skeletal muscle is composed of subpopulations of muscle fibres with distinct contractile and metabolic properties (Hickey *et al.*, 1995). Skeletal muscle fibres can be separated into three major categories (type I, IIB and IIA fibres), according to their functional and biochemical nature. Muscle fibres with high mitochondrial content have high oxidative capacity, are termed red, slow-twitch oxidative (SO, type I) fibres (Hickey *et al.*, 1995; Hintz *et al.*, 1980) and rely predominantly on lipids as fuel (Samec *et al.*, 2002). Muscle fibres with high glycogenolytic enzyme content are termed white, fatigable fast-twitch glycolytic (FG, type IIB) fibres and these rely

primarily on glucose for energy production (Samec *et al.*, 2002; Hickey *et al.*, 1995; Hintz *et al.*, 1980). A further fast-twitch fibre type, exhibiting both high mitochondrial content and abundant in glycogenolytic enzymes, are classified as fatigue-resistant fast-twitch oxidative-glycolytic (FOG, type IIA) fibres (Hickey *et al.*, 1995; Hintz *et al.*, 1980). They depend on a mixture of fuel sources, in which glucose makes a significant contribution (Samec *et al.*, 2002). A further type of fast-twitch fibre has since been identified, termed type IID/X. Despite being difficult to distinguish from type IIB fibres (Hamalainen and Pette, 1993; Termin *et al.*, 1989a; Bär and Pette, 1988), they exhibit distinct metabolic properties with intermediate fatigability and greater activity of enzymes mediating oxidative metabolism (Hamalainen and Pette, 1993). Furthermore, a population of fibres forms a continuum between the extremes of slow-twitch type I fibres and fast-twitch type IIA fibres; fibres known as type IC exhibit properties between type I and IIC fibres, whilst type IIC fibres display properties between type IC and IIA fibres (Staron *et al.*, 1999; Termin *et al.*, 1989a).

The composition of muscle fibres within skeletal muscle determines the dynamic characteristics of the muscle as a whole. Muscles abundant in SO fibres predominantly store triglycerides, whilst muscles comprised mainly of FG and FOG fibres exhibit lower triglyceride concentrations (Hwang *et al.*, 2001) and preferentially store glycogen (Zierath and Hawley, 2004). Moreover, the proportion of type I fibres present in skeletal muscle is positively correlated with increased insulin sensitivity, while conversely, the proportion of type IIB muscle fibres possessed is inversely related to insulin sensitivity (Hickey *et al.*, 1995; Mårin *et al.*, 1994; Lillioja *et al.*, 1987). The extensor digitorum longus (EDL) muscle, a skeletal muscle in the hindlimb,

exhibits fast-twitch characteristics and is found to contain type IIA, IIB and IID/X fibres and few type I fibres (Staron *et al.*, 1999; Delp and Duan, 1996). In contrast, the soleus muscle, also a hindlimb skeletal muscle, exhibits slow-twitch characteristics, and contains mainly type I fibres, with some type IIA, IC and IIC fibres (Delp and Duan, 1996; Staron *et al.*, 1999; Termin *et al.*, 1989a).

Although the metabolic capacity of skeletal muscle is dependent on its muscle fibre type composition (Adachi *et al.*, 2007; Nakatani *et al.*, 1999), the composition of skeletal muscle is dynamic. When exposed to altered conditions, the skeletal muscle exhibits a significant degree of plasticity and is capable of altering its metabolic properties in response to altered functional demands (Pette and Staron, 2000). Greater body mass index (BMI) is associated with a reduction in the proportion of type I fibres ($r = -0.50$, $P < 0.01$) (Hickey *et al.*, 1995) and a greater proportion of type IIB fibres present in skeletal muscle ($r = 0.49$, $P < 0.001$) (Tanner *et al.*, 2002), resulting in a functional switch to a more glycolytic muscle. Furthermore, it has been demonstrated that obese (Tanner *et al.*, 2002; Hickey *et al.*, 1995) and type 2 diabetic (Oberbach *et al.*, 2006; Hickey *et al.*, 1995) individuals exhibit a reduction in the proportion of type I fibres and increased proportion of type IIB fibres in skeletal muscle. Moreover, research has shown that the fatty acid composition of the skeletal muscle is related to the proportion of fibre types present; a greater skeletal muscle content of n-3 polyunsaturated fatty acids (PUFA) is associated with an increased proportion of type I fibres ($r = 0.37$, $P < 0.05$) and a diminished proportion of type IIB fibres ($r = -0.33$, $P < 0.05$) (Kriketos *et al.*, 1996). However, the effect of n-3 PUFA enrichment of a high fat diet (HFD) on muscle fibre type composition has not been investigated.

In the current study, I therefore aimed to determine:

- I. the effect of replacing 7.5% of saturated fat in a high saturated fat diet with n-3 PUFAs (derived from fish oil) on the biochemical characteristics and muscle fibre type distribution of skeletal muscles with predominantly fast-twitch (EDL) and slow-twitch (soleus) characteristics.

In relation to aim (I), I hypothesised that consuming a HF-S diet would promote intramyocellular fat accumulation and induce a muscle fibre type switch, increasing the proportion of FOG-FG fibres. Furthermore, I hypothesised that replacement of 7.5% of saturated fat with n-3 PUFAs would prevent this muscle fat accumulation and the fibre type switch favouring glycolytic metabolism, and may potentially even increase the proportion of SO fibres.

3.2 – MATERIALS AND METHODOLOGY

3.2.1 - *Animals and Nutrition Regime*

As described in **Chapter 2 Section 2.1**, male and female C57BL/6J mice, aged 6 weeks, were, following a 2 week acclimatisation period, randomly assigned to one of three diets, fed either a standard chow (C), high saturated fat (HF-S) or high fat n-3 PUFA enriched (HF-n-3) diet. All procedures were approved by the University of Adelaide Animal Ethics Committee and the Institute of Medical and Veterinary Science Animal Ethics Committee. Two cohorts of mice received the aforementioned diets; mice in cohort 1 were used to determine the effect of diet on muscle weight and mice in cohort 2 were used to determine the effect of diet on the fibre type and metabolic characteristics of skeletal muscle.

3.2.1.1 – *Cohort 1 Mice*

As described in **Chapter 2 Section 2.1.1**, mice were maintained on their respective diets for 14 weeks (± 4 days), during which food and water were provided daily *ad libitum*.

3.2.1.2 – *Cohort 2 Mice*

As described in **Chapter 2 Section 2.1.2**, mice were maintained on their respective diets for 11 weeks (± 7 days), during which food and water were provided daily *ad libitum*.

3.2.2 - Tissue Collection

3.2.2.1 – Cohort 1 Mice

The procedure for collecting skeletal muscles was as described in **Chapter 2 Section 2.2**. The weights of the EDL and soleus muscles were measured and subsequently, the relative weights of the EDL and soleus muscles were calculated per gram of body weight (mg muscle/ g body weight).

3.2.2.2 – Cohort 2 Mice

The procedure for collecting skeletal muscles was as described in **Chapter 2 Section 2.2**. However, in the current study, the whole soleus, whole plantaris and whole gastrocnemius (lateralis and medialis) muscles were dissected as a group. Furthermore, the whole tibialis and whole EDL skeletal muscles were dissected as a group. The whole quadriceps (vastus lateralis, vastus medialis, vastus intermedius and rectus femoris) skeletal muscles were also dissected undivided. In contrast to the snap freezing of muscles described in the surgical procedure (see **Chapter 2 Section 2.2**) for cohort 1 mice, skeletal muscles of cohort 2 mice were embedded at resting tension in Tissue-Tek[®] OCT (Sakura Finetek Co Ltd, Tokyo, Japan, Asia) and frozen gently. Muscle groups embedded in OCT, the EDL and tibialis muscles; the gastrocnemius, plantaris and soleus muscles; and the quadriceps muscles (as visualised in **Figure 3.1**), were then stored under liquid nitrogen vapour phase storage until subsequent histological analyses.

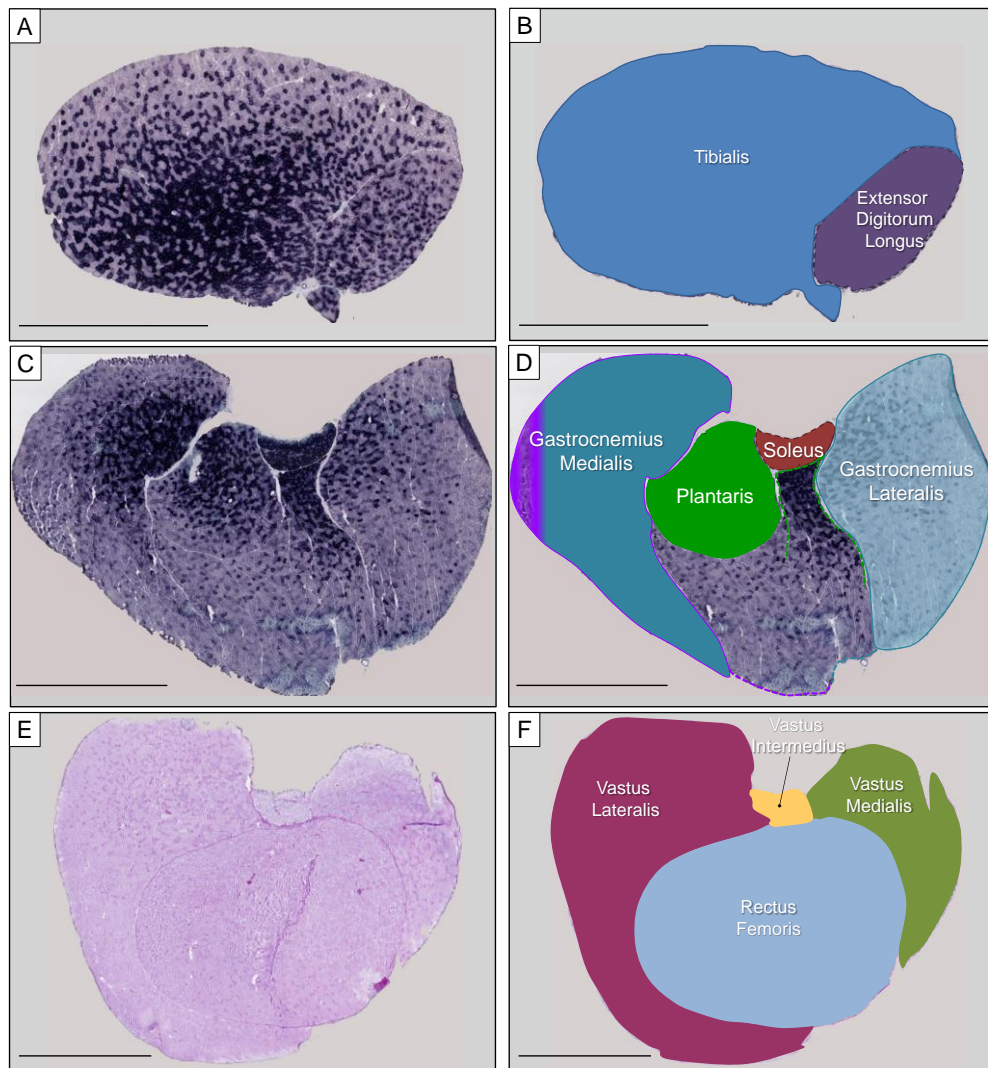


Figure 3.1 [A-F]. Muscle groups, including the tibialis and extensor digitorum longus muscles [A-B] and gastrocnemius, plantaris and soleus muscles [C-D] and quadriceps muscles [E-F], collected during muscle surgery in cohort 2 mice.

The extensor digitorum longus (EDL) and tibialis muscle group [A], gastrocnemius, plantaris and soleus muscle group [C], and the quadriceps muscle group [E] as seen in muscle cross-sections (stained for succinic dehydrogenase [A, C] and glycogen [E]). Colour-coded illustrations of anatomical regions in muscle cross-sections; the EDL - purple and tibialis - blue [B]; the soleus - red, plantaris - green, gastrocnemius medialis - purple and gastrocnemius lateralis - teal, whilst the area in the dashed green line indicates the plantaris adjacent to the gastrocnemius lateralis and the area in the dashed purple and teal lines indicates the superficial gastrocnemius [D] (Hallauer and Hastings, 2000); and the quadriceps: vastus lateralis - plum, vastus intermedius - yellow, vastus medialis - green, and rectus femoris - blue [F] (Greene, 1955; Li *et al.*, 2005). Scale bars represent 2 mm [A-F].

3.2.3 - Histological Evaluation of Skeletal Muscle Morphology and Fat Content

3.2.3.1 - Haematoxylin and Eosin Staining

OCT-embedded frozen skeletal muscle groups from cohort 2 mice (the EDL and tibialis group; the soleus, gastrocnemius and plantaris group; and the grouped quadriceps muscles) were cut to 4 µm thick cross-sections at -20°C using a cryostat and stained with haematoxylin and eosin to evaluate morphology at the cellular level. The procedure for haematoxylin and eosin staining of skeletal muscle sections was as described in **Chapter 2 Section 2.4.1**.

Sections were scanned using the NanoZoomer Digital Pathology image scanner in conjunction with NDP Scan 2.0 software (Hamamatsu Photonics K. K., Hamamatsu City, Japan, Asia) and viewed using NDP.view software (ver. 1.1.6, Hamamatsu Photonics K. K., Hamamatsu City, Japan, Asia), the resultant images exhibited staining of nuclei in blue and acidophilic cytoplasm in pink.

3.2.3.2 - Oil Red O Staining

OCT-embedded frozen skeletal muscle groups from cohort 2 mice (the EDL and tibialis group; the soleus, gastrocnemius and plantaris group; and the grouped quadriceps muscles) were cut to 10 µm thick cross-sections at -20°C using a cryostat and stained with Oil Red O to evaluate fat content. The procedure for Oil Red O staining of skeletal muscle sections was as described in **Chapter 2 Section 2.4.2**.

Sections were scanned in three 0.2 µm layers using the NanoZoomer Digital Pathology image scanner in conjunction with NDP Scan 2.0 software. Scanned images were

visualised using NDP.view 1.1.6 software, the resultant images exhibited red staining of fat and pale blue staining of nuclei. Whilst the technique of using Oil Red O staining to determine lipid content of tissues is subjective and a simple lipid extraction may have provided more quantitative results, Oil Red O staining and quantification were performed to minimise the use of limited muscle tissue, leaving muscle for more important assays such as Western blot analysis of key proteins of interest.

3.2.4 - Histological Evaluation of Skeletal Muscle Glycogen Content

3.2.4.1 - Periodic Acid-Schiff Staining

OCT-embedded frozen skeletal muscle samples (from cohort 2 mice) were cut to 9 μm thick cross-sections at -20°C using a cryostat and stained with Periodic Acid-Schiff (PAS) stain to evaluate glycogen content in skeletal muscle groups. To prevent loss of glycogen from tissues, sections were coated with chilled 0.25% celloidin in a 50% ethanol 50% ether solution, which was subsequently set with 70% ethanol solution and rinsed with distilled water. Sections were treated for 10 minutes with 1% periodic acid solution, which acts to oxidise 1,2-glycol groups ($2(\text{H-C-OH})$) to a dialdehyde ($2(\text{R-CHO})$). The sections were then rinsed well with distilled water, stained with Schiff's reagent (Australian Biostain Pty Ltd, Traralgon, Victoria, Australia) for 20 minutes and then washed under running tap water for 10 minutes. Treatment of sections with leuco fuchsin (Schiff's reagent) reveals the dialdehyde groups, resulting in precipitation of an insoluble magenta coloured complex (aldehyde fuchsin). Sections were counterstained with 10% Lillie-Mayer Haematoxylin to colour the nuclei lightly and rinsed with tap water. They were then dehydrated with 100% ethanol, cleared using xylene and

mounted using DPX Mounting Media. A duplicate set of sections was used as a negative control. These sections were treated with diastase (α -amylase), which cleaves glycogen to yield water soluble mono-, di- and oligo-saccharides that are washed from the section. The negative control (diastase treated) sections were fixed in absolute ethanol for 10 minutes, rinsed with tap water and incubated in saliva (a source of diastase) for 10 minutes at room temperature. Diastase treated sections were then washed in tap water, rinsed with distilled water and brought together with the test sections for the PAS staining procedure, light counterstaining with 10% Lillie-Mayer Haematoxylin and mounting.

Sections were scanned in three 0.2 μ m layers using the NanoZoomer Digital Pathology image scanner in conjunction with NDP Scan 2.0 software. Scanned images were visualised using NDP.view 1.1.6 software, the resultant PAS stained images exhibited staining of glycogen in magenta and nuclei in pale blue in test sections, whilst there was no magenta staining in the diastase treated negative control images.

Whilst the technique of using PAS staining to determine glycogen content of tissues is subjective and a simple glycogen assay (as used in the liver) may have provided more quantitative results, PAS staining and quantification were performed to minimise the use of limited muscle tissue, leaving muscle for more important assays such as Western blot analysis of key proteins of interest.

3.2.4.2 - *Histological Quantification of Skeletal Muscle Glycogen Content*

Resultant images of the PAS stained skeletal muscle sections were viewed using NDP.view 1.1.6 software, and two images of each EDL muscle and four images of each soleus muscle were randomly selected per mouse. Bias was negated by slide blinding. Each image was randomly assigned a number, evaluated whilst blinded to dietary group and only after quantification of all images were they un-blinded for statistical analysis. Using ImageJ software (ver. 1.42q, National Institute of Health, Bethesda, Maryland, USA), colour images were converted to 8-bit greyscale images and the perimeters of muscle fibres were traced using the ImageJ freehand trace tool.

The pixel density was measured for each muscle fibre within the traced area. Each pixel was quantified as one of 256 grey levels. In the EDL muscle, the mean number of fibres quantified was 113.8 (\pm 4.3) per image and in the soleus muscle, the mean number of fibres quantified was 80.8 (\pm 2.9) per image. The mean pixel density of all pixels within a PAS stained muscle cell, corrected for the mean pixel density of the background (containing no muscle fibres), provided a quantitative measure of PAS staining (Hawes *et al.*, 2007; Stellingwerff *et al.*, 2007). The mean of pixel densities for the fibres quantified in each muscle provided a measure of whole muscle glycogen content. Furthermore, fibres were separated according to pixel density as those with light (0-165), medium (165-180) or dark (180-255) staining intensity. A subsample of PAS stained cells was visually classified as having light, medium and dark staining intensity. The mean pixel densities of these cells were then determined, and these were translated into the pixel density limits for the separation of fibres into groups according

to staining intensity. The percentage of fibres stained with light, medium or dark intensity, relative to the total number of fibres quantified, provided an estimate of the distribution of PAS staining in fibres within each muscle.

3.2.5 - Histological Evaluation of Muscle Fibre Type

3.2.5.1 - Staining Skeletal Muscle for Myofibrillar Myosin Adenosine Triphosphatase

OCT-embedded frozen skeletal muscle groups from cohort 2 mice (the EDL and tibialis group, and the soleus, gastrocnemius and plantaris group) were cut to 9 μm thick serial cross-sections. These were stained for myofibrillar myosin adenosine triphosphatase (ATPase), following alkaline (pH 10.4) and acidic (pH 4.1, pH 4.3) preincubations, to evaluate muscle fibre type (based on methodology by Guth and Samaha (Guth and Samaha, 1970; Guth and Samaha, 1969)). This staining technique allows muscle fibres to be identified as distinct types and subtypes based on differences in the acid and alkali stability of the myofibrillar ATPase reaction (Green *et al.*, 1982a; Guth and Samaha, 1970; Guth and Samaha, 1969). Sections for alkaline preincubation were fixed for 5 minutes at 4°C in 0.19 M sodium cacodylate buffer containing 0.34 M sucrose, 68 mM calcium chloride and 5% formalin solution, adjusted to pH 7.6. Sections for alkaline preincubation were then rinsed with wash solution (99 mM Tris HCl, 18 mM calcium chloride, pH 7.8) for 1 minute. Sections were preincubated for 15 minutes at 4°C in either: 20 mM calcium chloride buffer adjusted to pH 4.1; 20 mM calcium chloride buffer adjusted to pH 4.3; or a Sigma-Aldrich 100 mM alkaline buffer solution (Sigma-Aldrich Inc, St Louis, Missouri, USA) and 18 mM calcium chloride

adjusted to pH 10.4. Slides were then rinsed 3 times with wash solution, 1 minute for each wash. Sections were incubated for 25 minutes at 37°C in adenosine triphosphate (ATP) incubation medium (100 mM Sigma-Aldrich alkaline buffer solution, 50 mM potassium chloride, 2.8 mM ATP, 18 mM calcium chloride adjusted to pH 9.4) and then washed in 1% calcium chloride solution 3 times (30 seconds each). Sections were then incubated in chilled 2% cobalt chloride solution for 3 minutes and rinsed in distilled water 4 times (30 seconds each). They were then incubated in 2% aqueous ammonium sulphide solution and rinsed in distilled water for 1 minute. Sections were dehydrated and cleared using a series of ethanol, xylene and finally ethanol (2 changes each). Sections were rinsed with tap water, mounted with Aquatex mounting medium (Merck Pty Ltd, Kilsyth, Victoria, Australia) and the edges of coverslips were sealed with clear varnish.

Sections were scanned using the NanoZoomer Digital Pathology image scanner in conjunction with NDP Scan 2.0 software. Scanned images were visualised using NDP.view 1.1.6 software, the resultant images exhibited differential staining of fibre types within the muscles, ranging from light grey to dark grey/black in colour, allowing for the quantification of muscle fibre type composition.

3.2.5.2 - *Staining Skeletal Muscle for Succinic Dehydrogenase*

OCT-embedded frozen skeletal muscle groups from cohort 2 mice (the EDL and tibialis group, and the soleus, gastrocnemius and plantaris group) were cut to 9 µm thick serial cross-sections and stained for succinic dehydrogenase (SDH) to evaluate muscle fibre type and oxidative capacity. In the presence of excess sodium succinate,

the mitochondrial enzyme SDH catalyses the reaction that converts succinate to fumarate; this reaction is detected by the reduction of tetrazolium salt with deposition of the blue formazan insoluble reduction product in the vicinity of mitochondria (Pool *et al.*, 1979). Sections were incubated at 37°C for 60 minutes in incubation medium (0.2 M Tris buffer (pH 7.4), 0.2 M sodium succinate, 5 mM Nitro-Blue tetrazolium and 0.9 mM phenazine methosulphate (electron carrier)) and were subsequently washed under running distilled water for approximately 10 minutes. Sections were mounted using Von Apathy's medium and slide edges were sealed.

Sections were scanned using the NanoZoomer Digital Pathology image scanner in conjunction with NDP Scan 2.0 software. Scanned images were visualised using NDP.view 1.1.6 software. In the resultant images, blue staining indicated sites of SDH activity.

3.2.5.3 - Staining Skeletal Muscle for NADH Tetrazolium Reductase

OCT-embedded frozen skeletal muscle groups from cohort 2 mice (the EDL and tibialis group, and the soleus, gastrocnemius and plantaris group) were cut to 9 µm thick serial cross-sections at -20°C using a cryostat and stained for NADH tetrazolium reductase (NADH-TR) to evaluate muscle fibre type and oxidative capacity. NADH-TR is a diaphorase that catalyses transfer of hydrogen to a suitable acceptor. In the histochemical reaction, hydrogen is accepted by a tetrazolium salt, producing insoluble blue-purple formazan deposits on cellular regions with elevated oxidative capacity (Freitas *et al.*, 2002; Troyer *et al.*, 1991). Sections were incubated at 37°C for approximately 40 minutes in incubation medium (69 mM disodium hydrogen

phosphate solution (pH 7.6), 0.9 mM NADH and 0.4 mM Nitro-Blue tetrazolium) and were subsequently washed under running distilled water for approximately 5 minutes. Sections were fixed in 10% buffered formalin for 10 minutes and washed under running distilled water for 5 minutes. Sections were dehydrated with 100% ethanol and cleared using xylene. The sections were then rinsed with distilled water, mounted with Aquatex mounting medium and the slide edges were sealed.

Sections were scanned using the NanoZoomer Digital Pathology image scanner in conjunction with NDP Scan 2.0 software. Scanned images were visualised using NDP.view 1.1.6 software. In the resultant images, areas of NADH-TR activity were stained blue-purple.

3.2.5.4 - Histological Quantification of Muscle Fibre Type and Muscle Oxidative Capacity

EDL and soleus muscle sections stained for myofibrillar ATPase, SDH and NADH-TR were examined to determine muscle fibre type and muscle oxidative capacity. Within serial cross-sections the same muscle fibres were assessed for each stain type, using NDP.view 1.1.6 software. In this way, duplicate images of the EDL and soleus muscle were selected and within each image, 75 muscle fibres were assessed. Bias was negated by slide blinding; each image series was randomly assigned a number and evaluated whilst blinded to dietary group. Only after assessment of all images, were they unblinded to perform group statistics. Results are reported as the mean of duplicate assessments.

3.2.5.5 - *Myofibrillar ATPase*

As described by Green and colleagues (Green *et al.*, 1982a), the activity of myofibrillar ATPase was judged on a subjective basis by one observer and muscle fibres were given a score from 1-5 based on the intensity of staining (1 = light, 2 = light-moderate, 3 = moderate, 4 = moderate-dark, 5 = dark). **Table 3.1** depicts the scheme used to classify muscle fibre type, based on scores given to muscle fibres stained for myofibrillar ATPase after acid or alkaline preincubation.

Staining following alkaline preincubation at pH 10.4 can be used to differentiate slow oxidative (SO) muscle fibres (type I, IC), which exhibit light-moderate staining intensity, from fast oxidative-glycolytic (FOG) and glycolytic (FG) muscle fibres (type IIC, IIA, IID/X, IIB), which exhibit dark staining intensity. The pattern of staining following alkaline preincubation also allows the type I and IC muscle fibres to be distinguished according to their staining intensity of light-moderate and moderate-dark, respectively. Staining following acidic preincubation at pH 4.1 allows differentiation of SO muscle fibres, which exhibit dark staining intensity, from FOG and FG muscle fibres, which exhibit light staining intensity. Furthermore, staining following acidic preincubation at pH 4.3 allows differentiation of the types of FG and FOG muscle fibres present; in the EDL muscle, light-moderate, moderate-dark and dark staining intensity differentiates type IIA, IID/X and IIB fibres, respectively (Staron *et al.*, 1999), while in the soleus muscle, moderate staining as compared to light-moderate staining differentiates type IIC and IIA fibres, respectively (Termin *et al.*, 1989b). The staining intensities of the same muscle fibres in serial sections stained for SDH and NADH-TR

also provides a supplementary point of reference in the identification of muscle fibre type. When stained for SDH and NADH-TR, SO and FOG fibres exhibit strong staining intensity, while FG fibres display quite weak staining intensity (Soukup *et al.*, 1979; Peter *et al.*, 1972).

The muscle fibre type composition (%) of the EDL and soleus muscles was calculated as the proportion of each muscle fibre type present relative to the total number of muscle fibres scored.

3.2.5.6 - Succinic Dehydrogenase and NADH Tetrazolium Reductase

Serial images of EDL and soleus muscle stained for SDH and NADH-TR were assessed using ImageJ software (ver. 1.42q, National Institute of Health, Bethesda, Maryland, USA). Colour images were converted to 8-bit greyscale images and the perimeters of muscle fibres were then traced using the ImageJ freehand trace tool. The pixel density and area of each muscle fibre was measured and each pixel was scored as one of 256 grey levels. As described for PAS staining (**Chapter 3 Section 2.4**) (Hawes *et al.*, 2007; Stellingwerff *et al.*, 2007), the mean pixel density provided a quantitative measure of the intensity of SDH and NADH-TR staining (Tengan *et al.*, 2007; Puustjärvi *et al.*, 1994). The same fibres used to assess the activity of both SDH and NADH-TR were also used to determine muscle fibre type by myofibrillar ATPase staining. This allowed for classification of oxidative activity in each muscle fibre type. Results are presented as the mean pixel density of classified muscle fibres measured in both SDH and NADH-TR stained sections.

The areas of each selected muscle fibre were measured using ImageJ software, providing a measure of the mean cell size for each fibre type within the EDL and soleus muscles. The area of each muscle fibre type was also calculated relative to the total area measured; this provided the relative area occupied by each muscle fibre type within the EDL and soleus muscles. Results are presented as the mean cross-sectional cell area of classified fibres and the percentage area occupied by each muscle fibre type.

Table 3.1. Scheme used to classify muscle fibre type from scores given to muscle fibres stained for myofibrillar ATPase after acid or alkaline preincubation.

	Fibre type	Myofibrillar ATPase staining, following acid (pH 4.1, pH 4.3) and alkaline (pH 10.4) preincubations		
		pH 4.1	pH 4.3	pH 10.4
EDL Muscle	I	Dark	Moderate/Dark	Moderate
	IIA	Light	Light/Light-Moderate	Dark
	IID/X	Light	Moderate/Dark	Dark
	IIB	Light	Dark	Moderate/Dark
SOL Muscle	I	Dark	Dark	Light/Moderate
	IC	Dark	Dark	Moderate/Dark
	IIC	Light/Light-Moderate	Moderate	Dark
	IIA	Light/Light-Moderate	Light/Light-Moderate	Dark

EDL, extensor digitorum longus; SOL, soleus.

3.2.6 – *Statistical Analyses*

All data are presented as mean \pm standard error of the mean (SEM). Two-way Analysis of Variance (ANOVA), with pairwise comparisons (Bonferroni post-hoc analysis), was used to determine the effect of diet (C, HF-S, HF-n-3), gender (male, female), and the interaction of diet and gender, on the relative weight of the EDL and soleus muscles. To enhance statistical power, data from male (n=3 per group) and female (n=2-3 per group) mice from cohort 2 were combined in statistical analyses. Two-way ANOVA was also used to determine the effect of diet (C, HF-S, HF-n-3) and muscle fibre type (EDL, soleus) on whole muscle glycogen content assessed as the mean pixel density of PAS stained muscle fibres. One-way ANOVA, with Bonferroni post-hoc analysis, was used to determine the effect of diet (C, HF-S, HF-n-3) in the EDL muscle on whole muscle glycogen content (assessed as the mean pixel density of PAS stained muscle fibres), glycogen staining intensity of muscle fibres (assessed as the mean pixel density of light, medium and dark PAS stained muscle fibres), muscle fibre type composition, muscle cell cross-sectional area, percentage area occupied by muscle fibres types and muscle oxidative capacity (assessed as the mean pixel density of muscle fibres stained for SDH and NADH-TR).

One-way ANOVA, with Bonferroni post-hoc analysis, was used to determine the effect of diet (C, HF-S, HF-n-3) in the soleus muscle on whole muscle glycogen content (assessed as the mean pixel density of PAS stained muscle fibres), glycogen staining intensity of muscle fibres (assessed as the mean pixel density of light, medium and dark PAS stained muscle fibres), muscle fibre type composition, muscle cell cross-sectional

area, percentage area occupied by muscle fibre types and muscle oxidative capacity (assessed as the mean pixel density of muscle fibres stained for SDH and NADH-TR).

One-way ANOVA, with Bonferroni post-hoc analysis, was used to determine the effect of muscle fibre type (I, IIA, IID/X, IIB) in the EDL muscle on muscle fibre type composition, muscle cell cross-sectional area, percentage area occupied by muscle fibre types and muscle oxidative capacity (assessed as the mean pixel density of muscle fibres stained for SDH and NADH-TR). One-way ANOVA, with Bonferroni post-hoc analysis, was used to determine the effect of muscle fibre type (I, IC, IIC, IIA) in the soleus muscle on muscle fibre type composition, muscle cell cross-sectional area, percentage area occupied by muscle fibre types and muscle oxidative capacity (assessed as the mean pixel density of muscle fibres stained for SDH and NADH-TR).

Simple linear regression analyses were used to determine the relationships between measures of the percentage composition, muscle cell cross-sectional area, percentage area occupied and oxidative capacity of muscle fibre types. Regression analyses were performed separately for the EDL and soleus muscle data and Pearson correlation coefficients (r) were used to evaluate linear relationships.

All statistics were performed using the Statistical Package for Social Scientists (SPSS) (ver. 17.0.0, SPSS Inc, Chicago, Illinois, USA). A probability of less than 5% ($P < 0.05$) was considered statistically significant. Analyses are reported as percentage change; statistical effect: $F(\text{degrees of freedom: between subjects effect, degrees of freedom: within subjects effect}) = F$ value, P value of effect; and subsequent P values of post-hoc or pairwise analyses.

3.3 – RESULTS

3.3.1 – Muscle Weight

3.3.1.1 – Absolute Muscle Weight

There was a diet*gender interaction on the absolute weight of the EDL muscle; in male mice, the absolute weight of the EDL was lower in those fed the HF-n-3 diet as compared to those fed the control diet (-22.0% ; $F(2, 58)=5.0$, $P=0.010$; post-hoc test: $P\leq 0.05$) (**Table 3.2**). In the control and HF-S groups, the absolute weight of the EDL muscle was greater in male as compared to female mice (+40.0%, +23.0%, respectively; post-hoc tests: $P\leq 0.001$ and $P\leq 0.01$, respectively).

There was no significant effect of diet on the absolute weight of the soleus muscle ($F(2, 58)=0.2$, $P=0.80$) (**Table 3.2**). There was, however, a significant gender effect; male mice exhibited greater absolute weight of the soleus muscle as compared to females ($F(1, 58)=13.9$, $P\leq 0.001$).

3.3.1.2 – Relative Muscle Weight

HF-S and HF-n-3 mice exhibited lower EDL muscle relative weight as compared to control mice (-16.7%, -17.5%, respectively; effect of diet: $F(2, 58)=7.6$, $P=0.001$; post-hoc tests: $P\leq 0.01$, $P\leq 0.005$, respectively) (**Table 3.2**). There was no effect of gender on the relative weight of the EDL muscle ($F(1, 58)=0.04$, $P=0.85$).

There was no significant effect of diet ($F(2, 58)=2.5$, $P=0.087$) or gender ($F(1, 58)=0.6$, $P=0.44$) on the relative weight of the soleus muscle (**Table 3.2**). There was, however,

a trend towards a lower relative weight of the soleus muscle in HF-S mice as compared to control mice, but this did not reach significance (-16.6%; post-hoc test: $P=0.10$).

Table 3.2. Absolute and relative weights of the extensor digitorum longus and soleus muscles of male and female mice fed a control, high saturated fat or high fat n-3 PUFA enriched diet.

	<i>Absolute Muscle Weight (mg)</i>					
	Male			Female		
	C	HF-S	HF-n-3	C	HF-S	HF-n-3
EDL	13.2 ± 0.55 ^{††}	12.0 ± 0.66 [†]	10.9 ± 0.10 ⁺	9.46 ± 0.62	9.73 ± 0.46	10.9 ± 0.34
SOL [‡]	9.92 ± 0.60	9.86 ± 0.65	10.80 ± 1.45	8.14 ± 0.65	7.75 ± 0.28	7.82 ± 0.69
	<i>Relative Muscle Weight (mg muscle/ g body weight)</i>					
	Male			Female		
	C	HF-S	HF-n-3	C	HF-S	HF-n-3
EDL	0.47 ± 0.02	0.38 ± 0.03 [*]	0.34 ± 0.03 ^{**}	0.44 ± 0.03	0.37 ± 0.02 [*]	0.40 ± 0.01 ^{**}
SOL	0.35 ± 0.02	0.31 ± 0.02	0.35 ± 0.05	0.37 ± 0.03	0.30 ± 0.01	0.28 ± 0.03

Data presented as mean ± SEM. Absolute weight (mg) and relative weight, mg muscle per g body weight.

EDL, extensor digitorum longus muscle; SOL, soleus muscle; M, male; F, female; C, control diet; HF-S, high saturated fat diet; HF-n-3, high fat n-3 PUFA enriched diet. n: C(M/F) = 10/12, HF-S(M/F) = 11/11, HF-n-3(M/F) = 9/11.

Statistics: Diet*gender interaction: ⁺ $P \leq 0.05$, compared to C (M only); [†] $P \leq 0.01$ M compared to F (C only), ^{††} $P \leq 0.001$, M compared to F (HF-S only). Effect of diet: ^{*} $P \leq 0.01$, ^{**} $P \leq 0.005$, compared to C. Effect of gender: [‡] $P \leq 0.001$ M compared to F.

3.3.2 – Skeletal Muscle Morphology and Fat Content

The morphology of all muscles was similar among dietary groups as assessed by haematoxylin and eosin staining (**Figure 3.2A, Figure 3.3, Figure 3.4**).

Muscle fat content was greater in the soleus muscle of HF-S mice as compared to control and HF-n-3 mice, but was unchanged by diet in the EDL muscle (**Figure 3.2B**).

Increased fat content was also observed in the tibialis, plantaris, gastrocnemius (**Figure 3.5**) and quadriceps (**Figure 3.6**) muscles of HF-S mice as compared to control and HF-n-3 mice. Oil Red O staining of muscle fibres was heterogeneous and the proportion of stained fibres varied between muscles. The highest proportion of stained fibres was observed in the soleus, vastus medialis and vastus intermedius muscles and was the lowest in the EDL muscle.

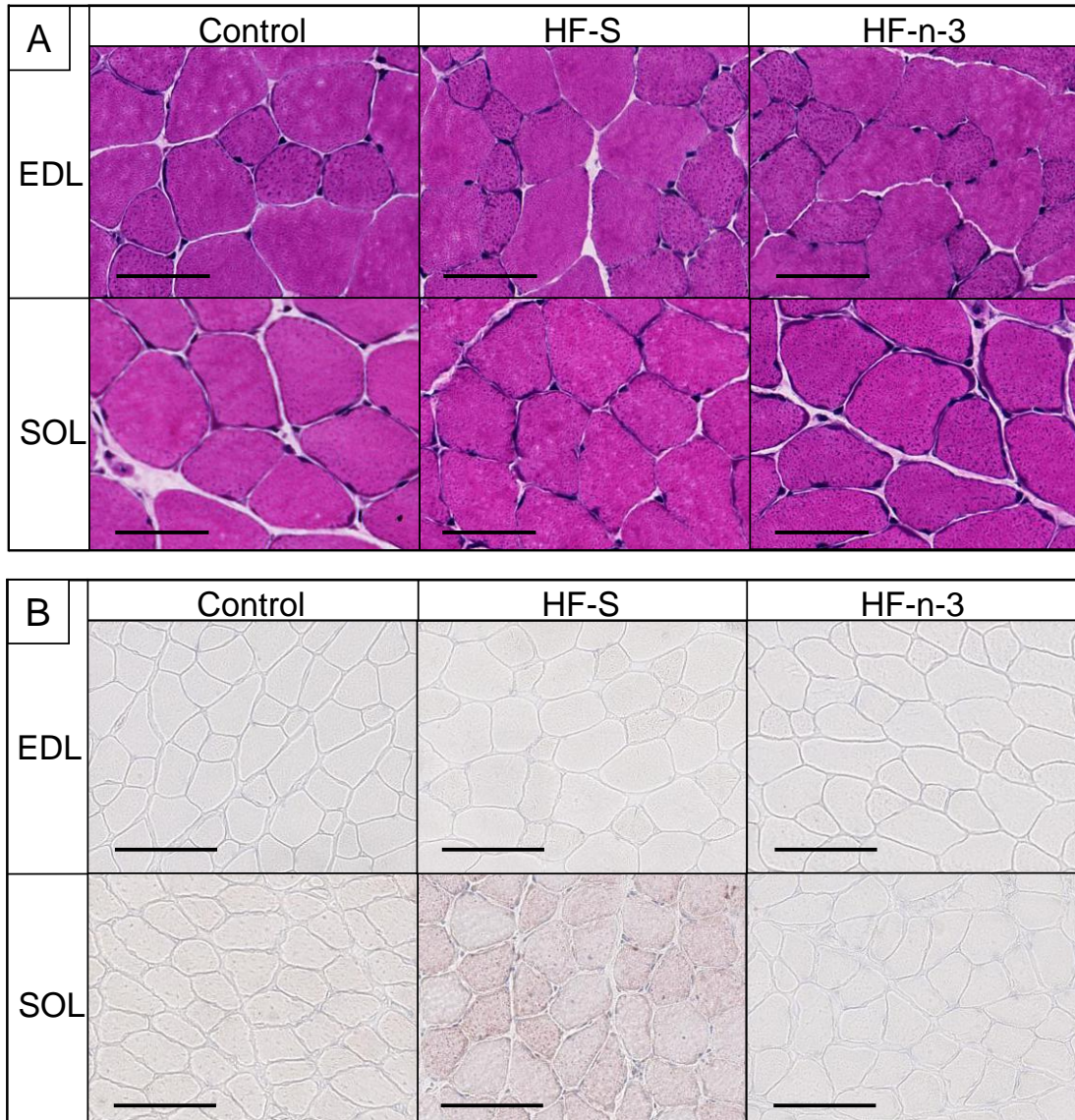


Figure 3.2 [A-B]. Haematoxylin and eosin [A] and Oil Red O [B] staining of extensor digitorum longus and soleus muscle sections of mice fed a control, high saturated fat or high fat n-3 PUFA enriched diet.

Scale bars represent: [A] 50 μm ; [B] 100 μm . EDL, extensor digitorum longus muscle; SOL, soleus muscle; HF-S, high saturated fat diet; HF-n-3, high fat n-3 PUFA enriched diet.

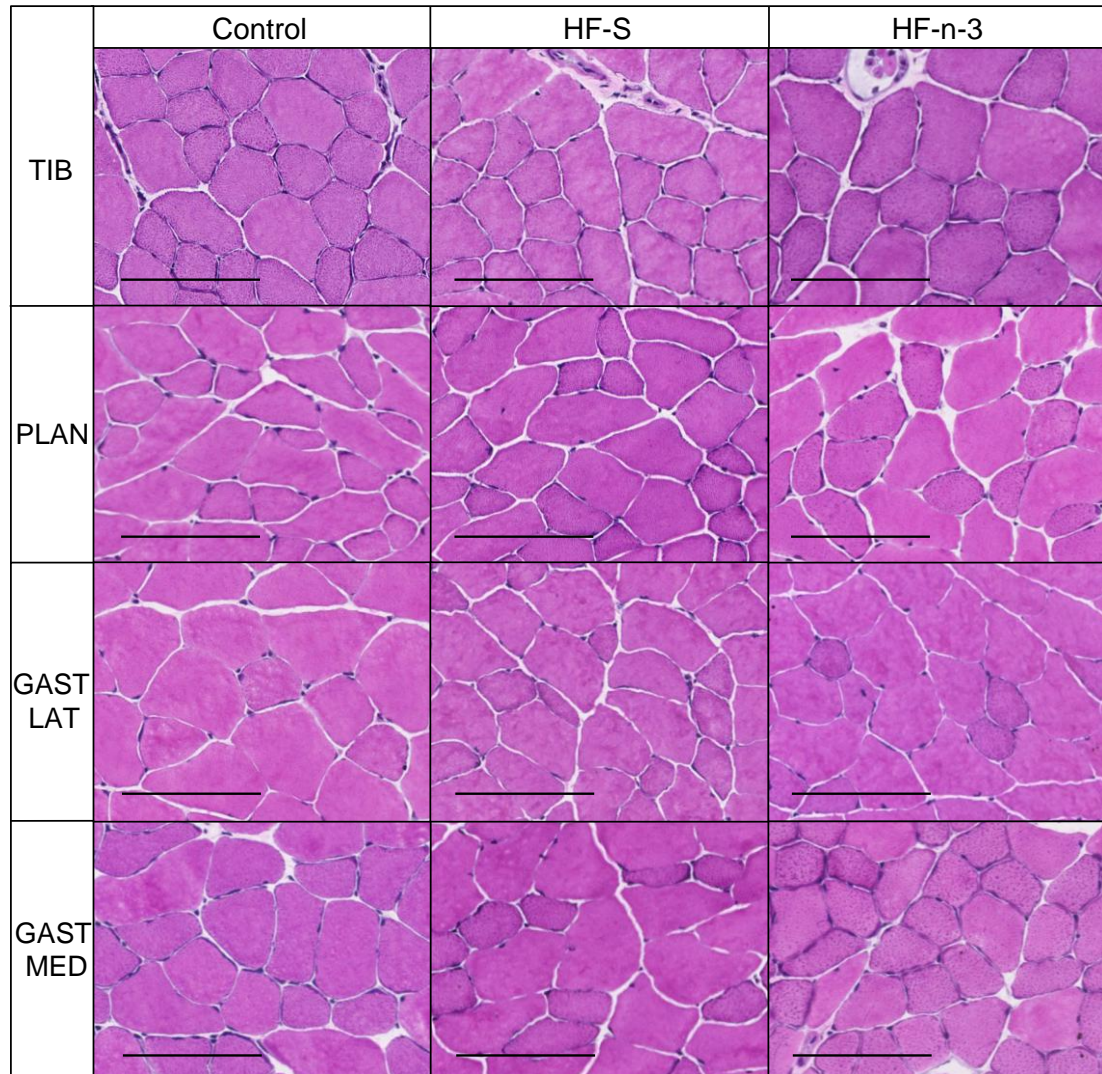


Figure 3.3. Haematoxylin and eosin staining of tibialis, plantaris and gastrocnemius muscle sections of mice fed a control, high saturated fat or high fat n-3 PUFA enriched diet.

Scale bars represent 100 μm . HF-S, high saturated fat diet; HF-n-3, high fat n-3 PUFA enriched diet; TIB, tibialis muscle; PLAN, plantaris muscle; GAST LAT, gastrocnemius lateralis muscle; GAST MED, gastrocnemius medialis muscle.

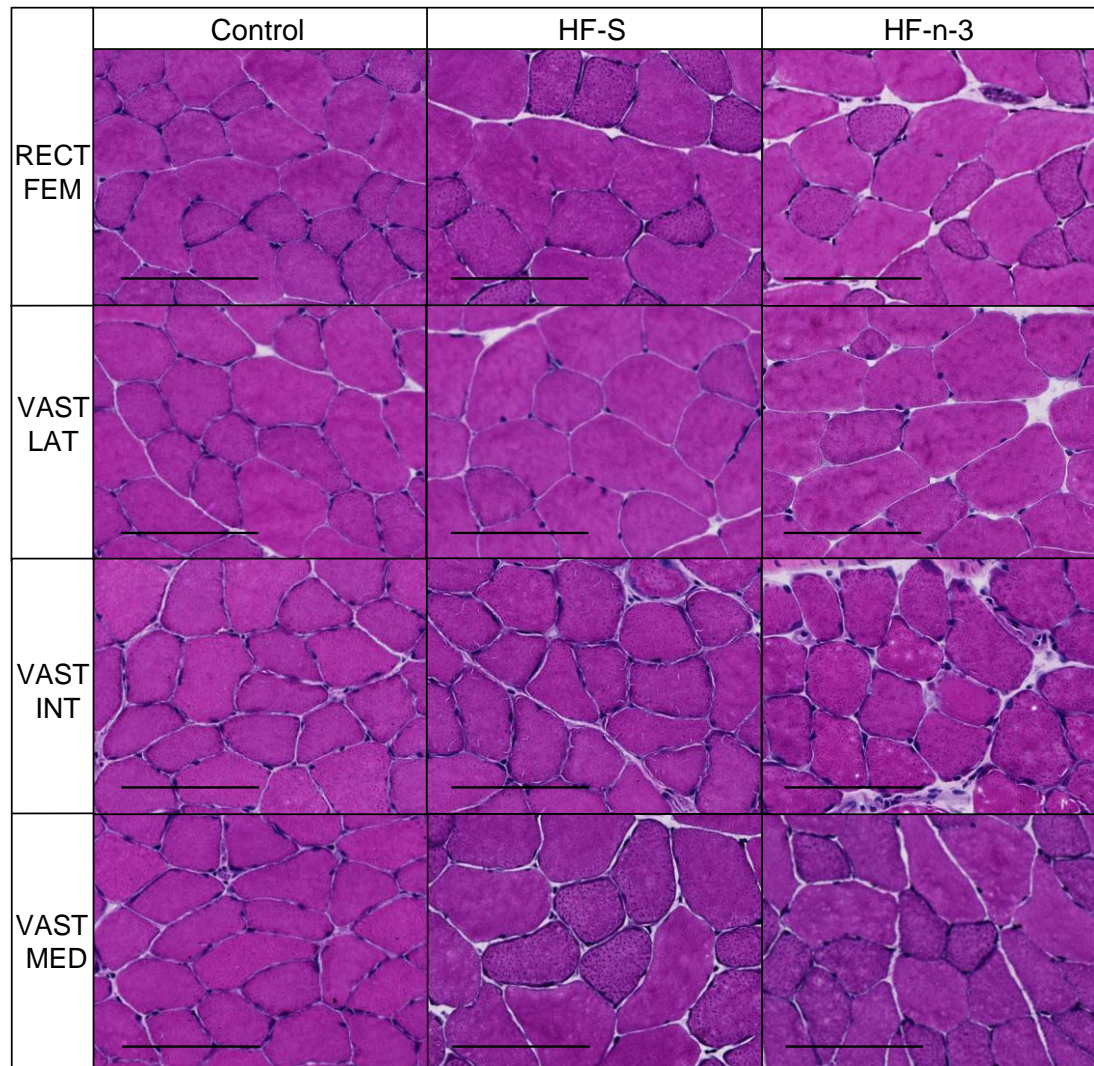


Figure 3.4. Haematoxylin and eosin staining of quadriceps muscle sections of mice fed a control, high saturated fat or high fat n-3 PUFA enriched diet.

Scale bars represent 100 μm . HF-S, high saturated fat diet; HF-n-3, high fat n-3 PUFA enriched diet; RECT FEM, rectus femoris muscle; VAST LAT, vastus lateralis muscle; VAST INT, vastus intermedius muscle; VAST MED, vastus medialis muscle.

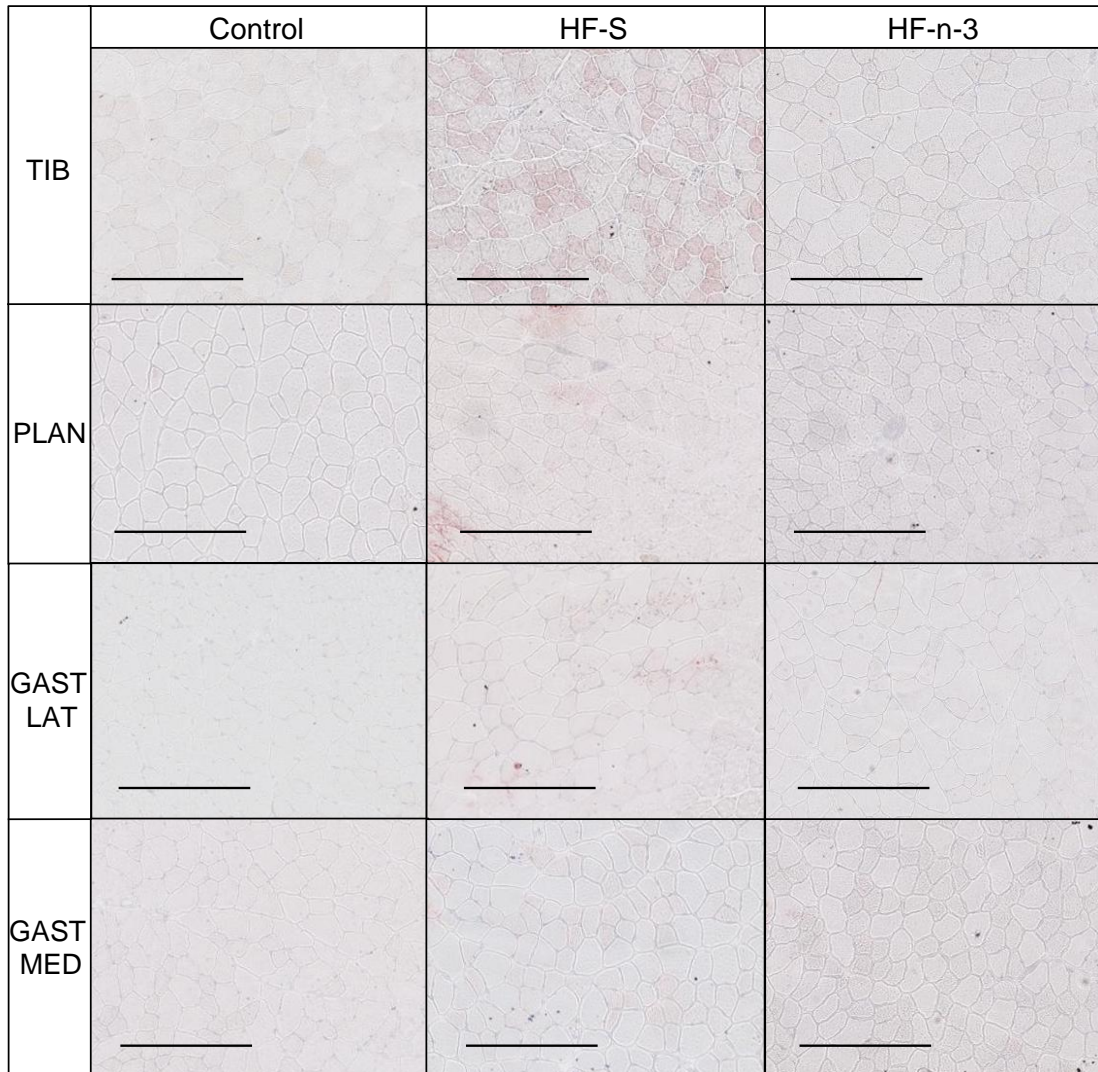


Figure 3.5. Oil Red O staining of tibialis, plantaris and gastrocnemius muscle sections of mice fed a control, high saturated fat or high fat n-3 PUFA enriched diet.

Scale bars represent 0.25 mm. HF-S, high saturated fat diet; HF-n-3, high fat n-3 PUFA enriched diet; TIB, tibialis muscle; PLAN, plantaris muscle; GAST LAT, gastrocnemius lateralis muscle; GAST MED, gastrocnemius medialis muscle.

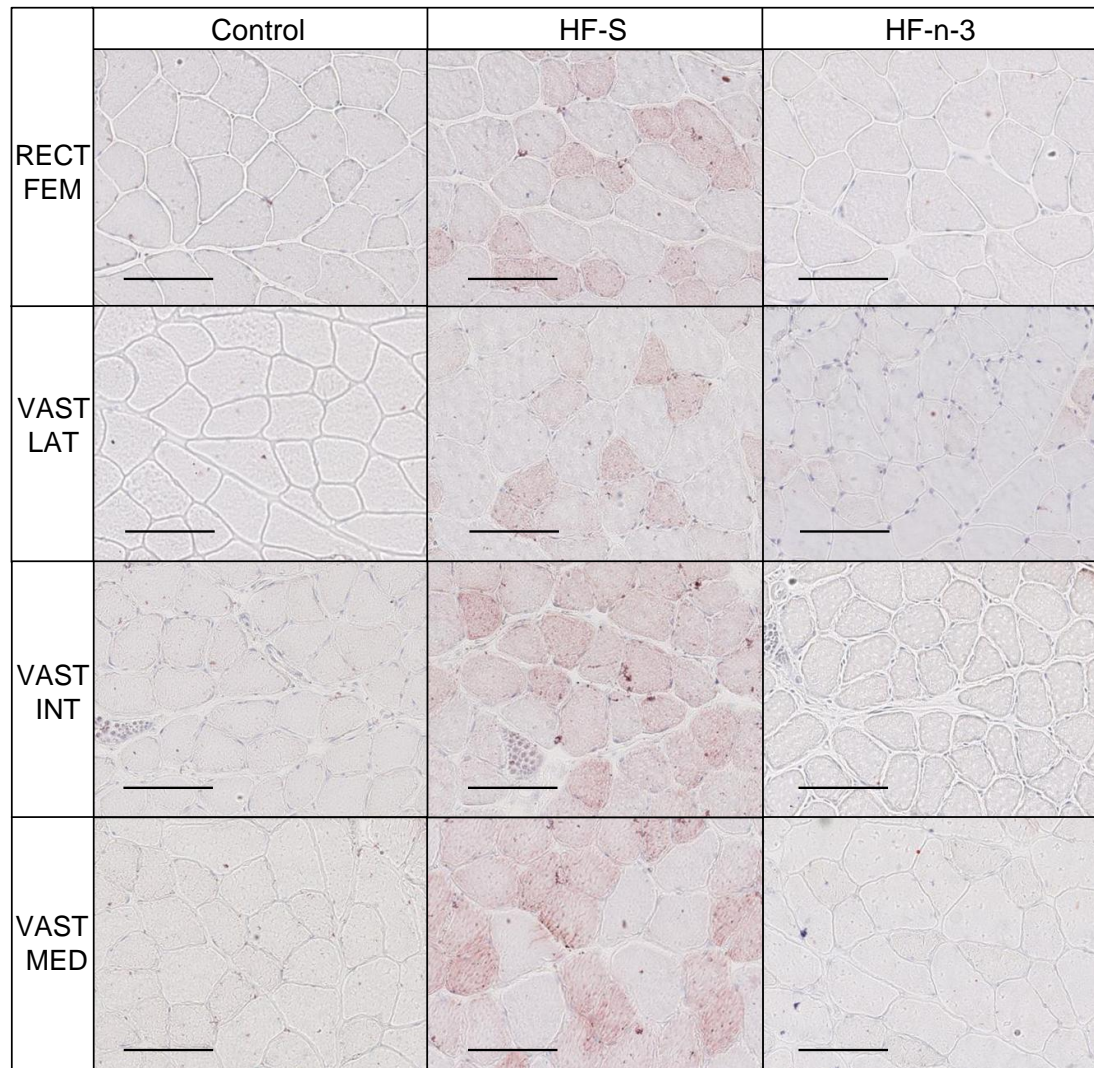


Figure 3.6. Oil Red O staining of quadriceps muscle sections of mice fed a control, high saturated fat or high fat n-3 PUFA enriched diet.

Scale bars represent 100 μm . HF-S, high saturated fat diet; HF-n-3, high fat n-3 PUFA enriched diet; RECT FEM, rectus femoris muscle; VAST LAT, vastus lateralis muscle; VAST INT, vastus intermedius muscle; VAST MED, vastus medialis muscle.

3.3.3 – Skeletal Muscle Glycogen Content

Visual inspection showed clearly that overall, muscle glycogen content, as assessed by Periodic Acid-Schiff (PAS) staining intensity, was altered by diet in the EDL and soleus muscles (**Figure 3.7A**). The specificity of the staining for glycogen was validated by diastase pre-treatment (**Figure 3.7B**). Whole skeletal muscle glycogen content was assessed by quantifying the intensity of PAS staining as the mean pixel density of PAS stained muscle fibres. There was no effect of diet ($F(2, 28)=2.8$, $P=0.076$) on the mean pixel density of the whole population of stained muscle fibres (**Figure 3.8A**). There was also no effect of the individual muscles (and thus muscle fibre type) on the mean pixel density of PAS stained muscle fibres ($F(1, 28)=4.0$, $P=0.056$). However, PAS-stained fibres in the soleus muscle tended to have greater mean pixel density compared with those in the EDL muscle (+13.7%, $P=0.056$). Although there was no diet*muscle interaction on the mean pixel density of PAS stained muscle fibres ($F(2, 28)=1.4$, $P=0.27$), diet appeared to have a greater effect on PAS staining intensity in the soleus muscle. For this reason, the effect of diet on the mean pixel density of PAS stained muscle fibres was analysed separately in both muscle types by One-way ANOVA. There was no effect of diet on the mean pixel density of PAS stained muscle fibres in the EDL ($F(2, 14)=0.3$, $P=0.77$) or soleus muscle ($F(2, 14)=3.6$, $P=0.054$). There was, however, a trend towards reduced mean pixel density of PAS stained muscle fibres in the soleus muscle of HF-n-3 mice as compared control mice (-24.7%; post-hoc test: $P=0.063$).

Whilst the overall mean pixel density of PAS stained muscle fibres provided a snapshot of whole muscle glycogen content, PAS staining intensity differed between muscle fibres.

PAS stained muscle fibres were therefore placed into cohorts according to their mean pixel density, reflecting the intensity of staining (light, medium, or dark). The muscle composition in terms of light, medium or dark stained fibres is shown in **Figures 3.8B** and **3.8C**.

In the EDL muscle, there was an effect of diet ($F(2, 14)=8.2$, $P=0.004$) on the percentage of muscle fibres classified as having medium staining intensity (**Figure 3.8B**); HF-S and HF-n-3 mice exhibited more fibres with medium staining intensity as compared to control mice (+1.8-fold, +1.4-fold, respectively; post-hoc tests: $P\leq 0.005$, $P\leq 0.05$, respectively). There was however no significant effect of diet on the percentage of muscle fibres classified as having light ($F(2, 14)=0.6$, $P=0.54$) and dark ($F(2, 14)=0.3$, $P=0.32$) staining intensity in the EDL muscle.

In the soleus muscle, there was an effect of diet ($F(2, 14)=4.7$, $P=0.027$) on the percentage of muscle fibres classified as having light staining intensity (**Figure 3.8C**); HF-n-3 mice exhibited more fibres with light staining intensity as compared to HF-S mice (+2.3-fold; post-hoc test: $P\leq 0.05$). HF-n-3 mice also tended to have more fibres with light staining intensity as compared to control mice (+2.3-fold; post-hoc test: $P=0.052$). There was no effect of diet on the percentage of muscle fibres classified as having medium ($F(2, 14)=0.9$, $P=0.43$) and dark ($F(2, 14)=3.2$, $P=0.071$) staining intensity in the soleus muscle. There was, however, a trend in HF-n-3 mice towards fewer fibres with dark staining intensity as compared to control mice (-78.7%; post-hoc test: $P=0.080$).

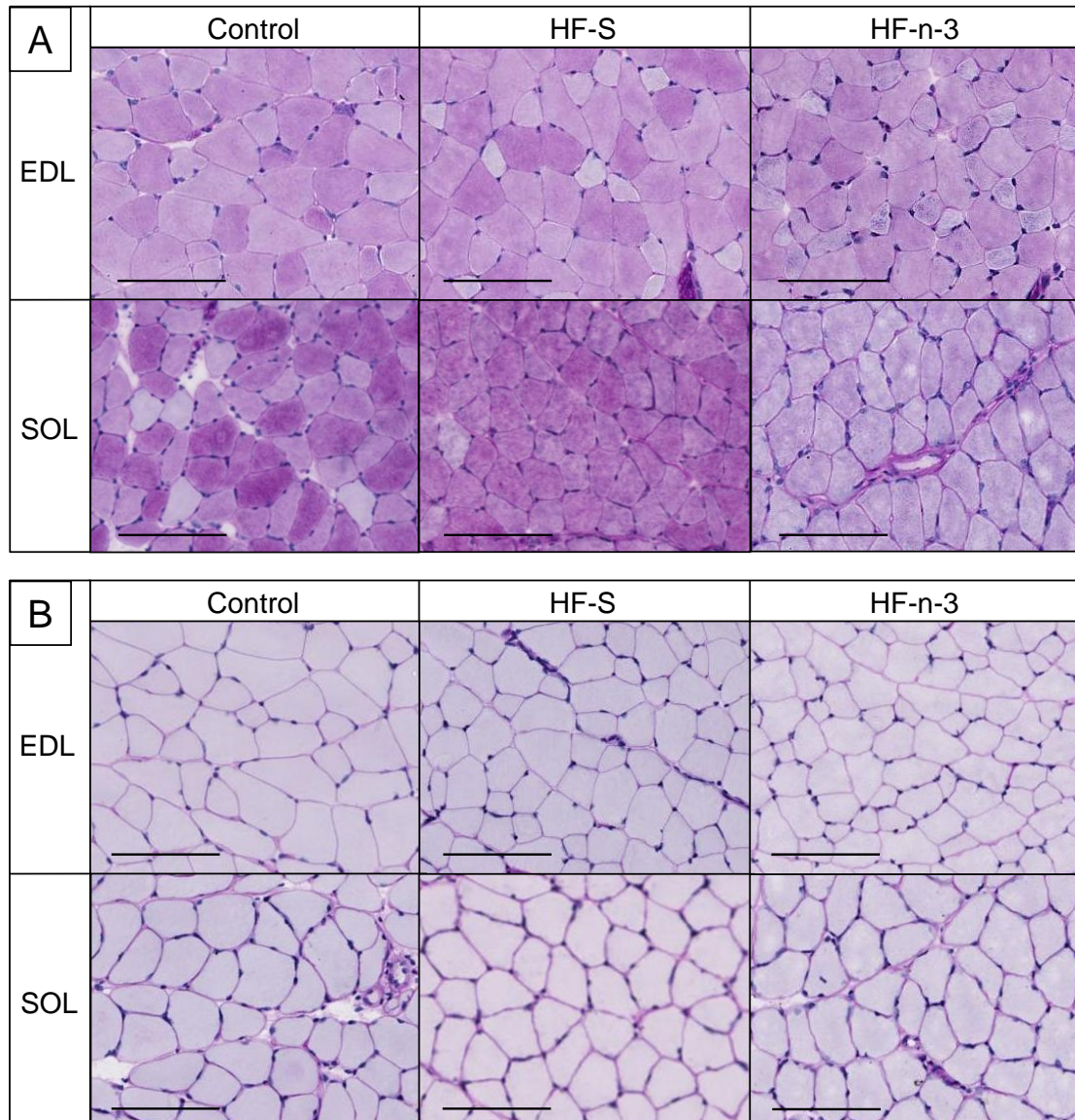


Figure 3.7 [A-B]. Periodic Acid-Schiff staining without [A] or with [B] diastase pre-treatment of extensor digitorum longus and soleus muscle sections of mice fed a control, high saturated fat or high fat n-3 PUFA enriched diet.

Scale bars represent [A-B]: 100 μm . EDL, extensor digitorum longus muscle; SOL, soleus muscle; HF-S, high saturated fat diet; HF-n-3, high fat n-3 PUFA enriched diet.

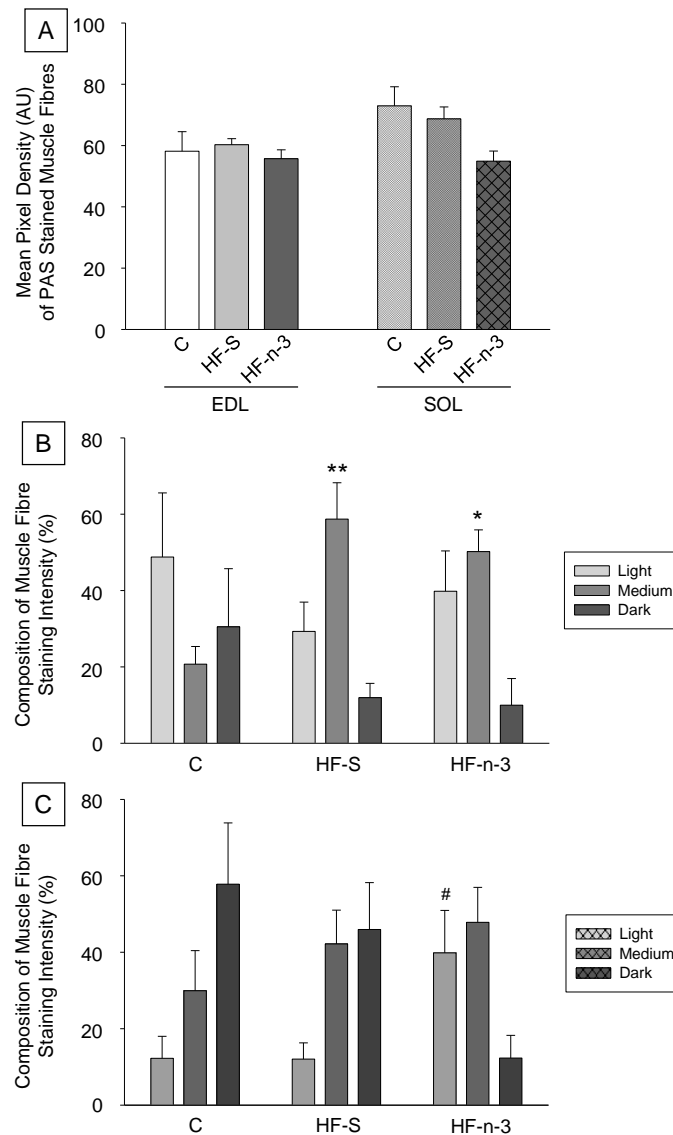


Figure 3.8 [A-C]. Histological quantification of glycogen in extensor digitorum longus and soleus muscle sections of mice fed a control, high saturated fat or high fat n-3 PUFA enriched diet, assessed as mean pixel density [A] and the composition of fibres classified with having light, medium or dark Periodic Acid-Schiff staining intensity in extensor digitorum longus [B] and soleus [C] muscles.

Data are expressed as mean (bars) \pm SEM (error bars). Bar type represents muscle: EDL, solid bars; SOL, checked bars, and [A] bar colour represents dietary group: white, C; pale grey, HF-S; dark grey, HF-n-3, and [B, C] bar colour represents staining intensity: see legend. EDL, extensor digitorum longus muscle; SOL, soleus muscle; C, control diet; HF-S, high saturated fat diet; HF-n-3, high fat n-3 PUFA enriched diet.

n: C(EDL/SOL) = 6/6, HF-S(EDL/SOL) = 6/6, HF-n-3(EDL/SOL) = 5/5.

Statistics: Effect of diet: * $P \leq 0.05$, ** $P \leq 0.005$, compared to C (of medium intensity); # $P \leq 0.05$, compared to HF-S (of light intensity).

Muscle glycogen content, as assessed by PAS staining intensity, was also visibly altered by diet in the tibialis, plantaris and gastrocnemius muscles (**Figure 3.9**) and the quadriceps muscles (**Figure 3.10**). In the tibialis muscle, the intensity of PAS staining was greatest in control mice, whilst HF-S mice exhibited moderate staining intensity and HF-n-3 mice exhibited the least intense staining. A similar pattern of staining intensity was displayed in the plantaris and gastrocnemius lateralis muscles, despite the overall intensity of staining in these muscles being less. In all four of the quadriceps muscles, the intensity of PAS staining was greatest in control mice, whilst HF-S and HF-n-3 mice exhibited less intense staining. The staining in all of these muscles was specific, as it was eliminated by treating a set of duplicate sections with diastase prior to staining with PAS (data not shown).

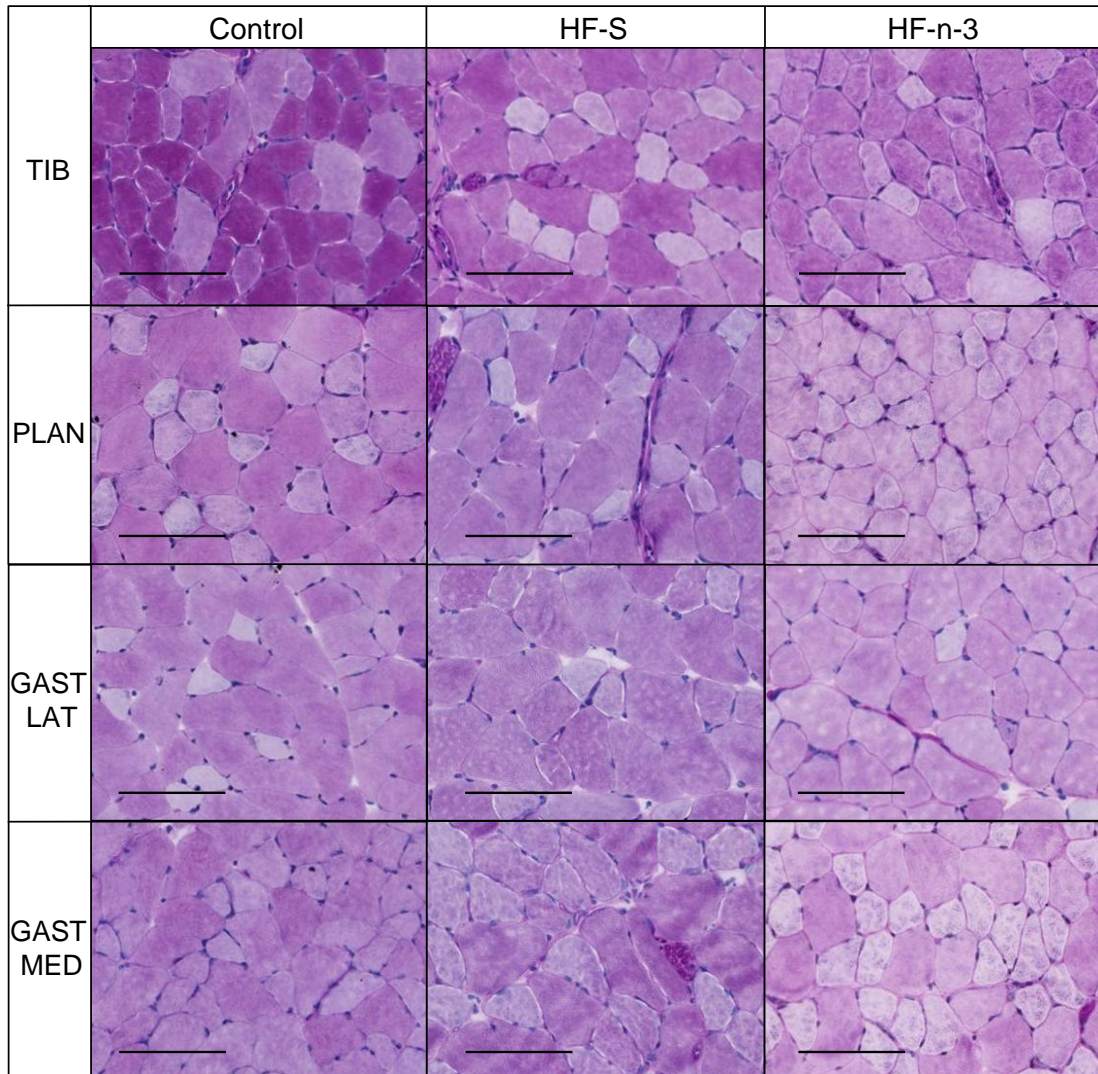


Figure 3.9. Periodic Acid-Schiff staining for glycogen content of tibialis, plantaris and gastrocnemius muscle sections of mice fed a control, high saturated fat or high fat n-3 PUFA enriched diet.

Scale bars represent 100 μm. HF-S, high saturated fat diet; HF-n-3, high fat n-3 PUFA enriched diet; TIB, tibialis muscle; PLAN, plantaris muscle; GAST LAT, gastrocnemius lateralis muscle; GAST MED, gastrocnemius medialis muscle.

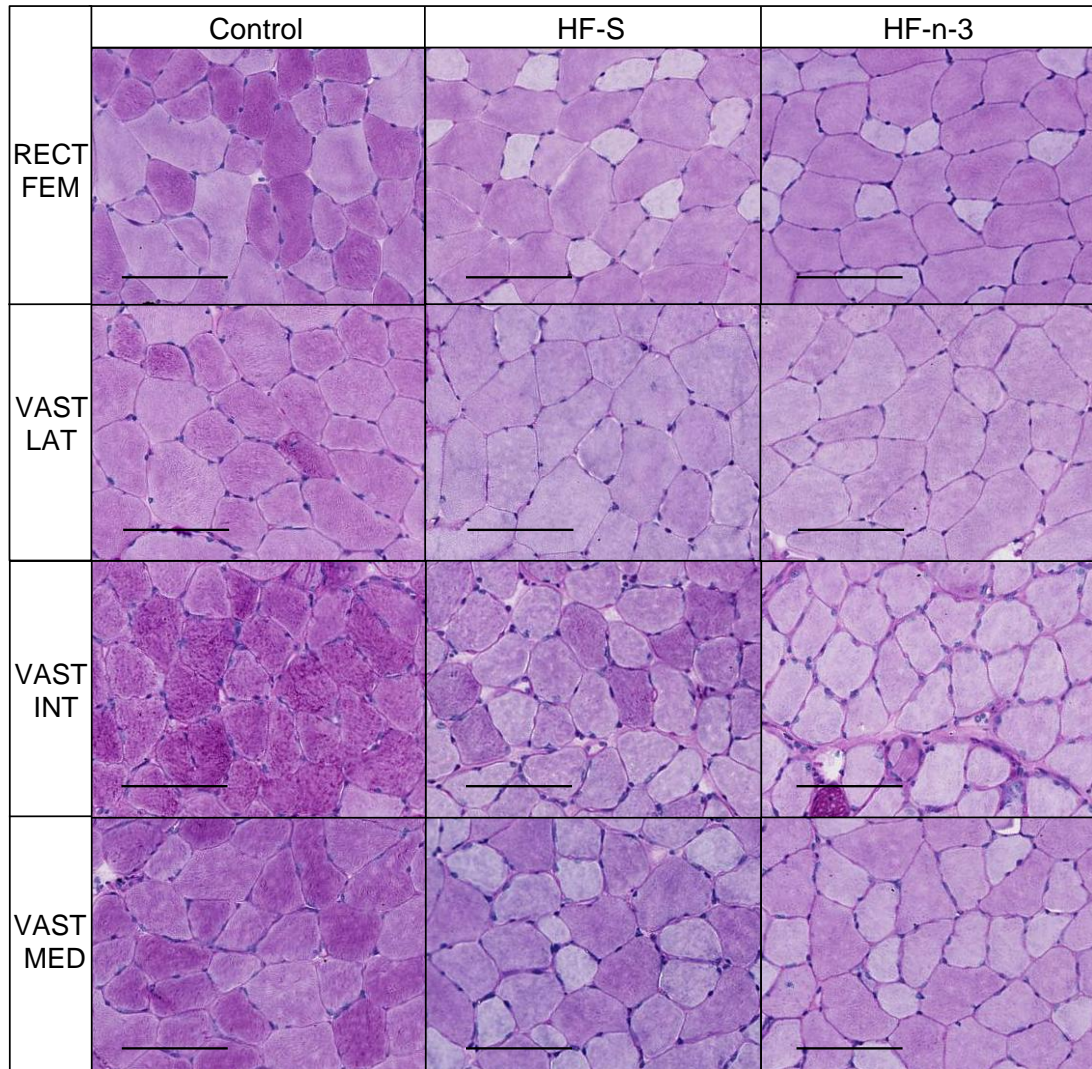


Figure 3.10. Periodic Acid-Schiff staining for glycogen content of quadriceps muscle sections of mice fed a control, high saturated fat or high fat n-3 PUFA enriched diet.

Scale bars represent 100 μm . HF-S, high saturated fat diet; HF-n-3, high fat n-3 PUFA enriched diet; RECT FEM, rectus femoris muscle; VAST LAT, vastus lateralis muscle; VAST INT, vastus intermedius muscle; VAST MED, vastus medialis muscle.

3.3.4 - Characterisation of Muscle Fibre Type in the Extensor Digitorum Longus and Soleus Skeletal Muscles

Myosin ATPase staining of muscle sections, following acid (pH 4.1, pH 4.3) and alkaline (pH 10.4) preincubation, was used to determine the composition of muscle fibre types in the EDL (**Figure 3.11**) and soleus (**Figure 3.12**) muscles. The mean cross-sectional area of muscle cells classified in each muscle fibre type, and the percentage area occupied by each muscle fibre type relative to the total area assessed was also determined in the EDL and soleus muscles. **Figures 3.11** and **3.12** show examples of muscle fibres classified according to the scheme as described previously in **Table 3.1**.

3.3.4.1 – Muscle Fibre Type Composition of the Extensor Digitorum Longus Muscle

In the EDL muscle, the general profile of percentage muscle fibre composition present was IIB>IID/X=IIA>I ($F(3, 64)=668.6, P\leq 0.001$; post-hoc tests: all $P\leq 0.001$, except type IID/X compared to IIA, $P=0.48$).

There was no effect of diet on the percentage of Type I ($F(2, 14)=2.8, P=0.096$), Type IIA ($F(2, 14)=1.2, P=0.32$), Type IID/X ($F(2, 14)=0.3, P=0.77$) and Type IIB ($F(2, 14)=0.5, P=0.59$) muscle fibres in the EDL muscle (**Figure 3.13A**).

3.3.4.2 – Muscle Fibre Type Composition of the Soleus Muscle

In the soleus muscle, the general profile of percentage muscle fibre composition present was IIA=I>IIC=IC ($F(3, 64)=311.0, P\leq 0.001$; post-hoc tests: all $P\leq 0.001$, except type

IIC compared to IC, $P=0.056$ and type I compared to IIA, $P=1.0$).

There was no significant effect of diet on the percentage of Type I ($F(2, 14)=0.2$, $P=0.78$), Type IC ($F(2, 14)=2.2$, $P=0.15$), Type IIC ($F(2, 14)=0.1$, $P=0.88$) and Type IIA ($F(2, 14)=1.1$, $P=0.35$) muscle fibres in the soleus muscle (**Figure 3.13B**).

3.3.4.3 – Muscle Cell Cross-sectional Area and Percentage Area Occupied by each Muscle Fibre Type in the Extensor Digitorum Longus Muscle

In the EDL muscle, muscle fibre type ($F(3, 64)=174.4$, $P\leq 0.001$) influenced the mean cross-sectional area of muscle cells. The muscle fibre types each exhibited significantly different cross-sectional areas (post-hoc tests: $P\leq 0.001$), with the general profile of cell area in the EDL being $IIB>IID>IIA>I$.

There was no effect of diet on the cross-sectional areas of type I ($F(2, 14)=1.2$, $P=0.32$), type IIA ($F(2, 14)=1.3$, $P=0.30$), type IID/X ($F(2, 14)=2.0$, $P=0.17$) and type IIB ($F(2, 14)=0.4$, $P=0.68$) fibres in the EDL muscle (**Table 3.3**).

In the EDL muscle, muscle fibre type ($F(3, 64)=536.0$, $P\leq 0.001$) influenced the percentage area occupied by each fibre type; all fibre types were significantly different in the percentage area occupied (post-hoc tests: $P\leq 0.001$), except when comparing type IIA and IID/X fibres (post-hoc test: $P=0.42$). The general profile of percentage area occupied by each muscle fibre type in the EDL muscle was therefore, $IIB>IID/X=IIA>I$.

There was no effect of diet on the percentage area occupied by each muscle fibre type, type I ($F(2, 14)=1.2, P=0.32$), type IIA ($F(2, 14)=1.7, P=0.22$), type IID/X ($F(2, 14)=3.2, P=0.071$) and type IIB ($F(2, 14)=0.7, P=0.50$) (**Table 3.3**) in the EDL muscle. However, there was a trend towards increased percentage area occupied by type IID/X muscle fibres in the EDL muscle of HF-n-3 mice as compared to control mice (+80.4%; post-hoc test: $P=0.088$).

3.3.4.4 – Muscle Cell Cross-sectional Area and Percentage Area Occupied by Muscle Fibre Type in the Soleus Muscle

In the soleus muscle, the mean cross-sectional area was similar among the muscle fibre types ($F(3, 58)=0.9, P=0.44$), i.e. I=IC=IIC=IIA.

There was no effect of diet on the cross-sectional area of type I ($F(2, 14)=0.9, P=0.42$), type IC ($F(2, 14)=0.8, P=0.47$), type IIC ($F(2, 14)=0.6, P=0.57$) and type IIA ($F(2, 14)=0.7, P=0.52$) fibres in the soleus muscle (**Table 3.3**).

In this muscle also, muscle fibre type ($F(3, 58)=168.5, P\leq 0.001$) influenced the percentage area occupied by each fibre type; all fibre types were significantly different in the percentage area occupied (post-hoc tests: $P\leq 0.005$), except when comparing type IC and IIC fibres (post-hoc test: $P=0.48$). The general profile of percentage area occupied by each muscle fibre type in the soleus muscle was therefore $I>IIA>IIC=IC$.

Diet had no significant effect on the percentage area occupied by each muscle fibre type, type I ($F(2, 14)=0.1, P=0.91$), type IC ($F(2, 14)=0.02, P=0.98$), type IIC ($F(2,$

14)=1.6, $P=0.24$) and type IIA ($F(2, 14)=0.1$, $P=0.91$), in the soleus muscle (**Table 3.3**).

3.3.4.5– Relationships between Percentage Area Occupied and Cell Size of Muscle

Fibre Types in the Extensor Digitorum Longus and Soleus Muscles

In the EDL muscle, the percentage area occupied by type IIB fibres was positively correlated with the mean cell area of type IIB fibres ($r = +0.50$, $P=0.032$, all dietary groups combined; **Figure 3.14**).

In the soleus muscle, the percentage area occupied by type I fibres was inversely related to the mean cell area of type IIA ($r= -0.52$, $P=0.032$, all dietary groups combined; **Figure 3.15**) and type IC fibres ($r= -0.62$, $P=0.044$, all dietary groups combined; **Figure 3.15**). There was also an indication of an inverse relationship between the percentage area occupied by type I fibres and the mean cell area of type IIC ($r= -0.47$, $P=0.056$, all dietary groups combined; data not shown) in the soleus muscle, but this did not reach statistical significance.

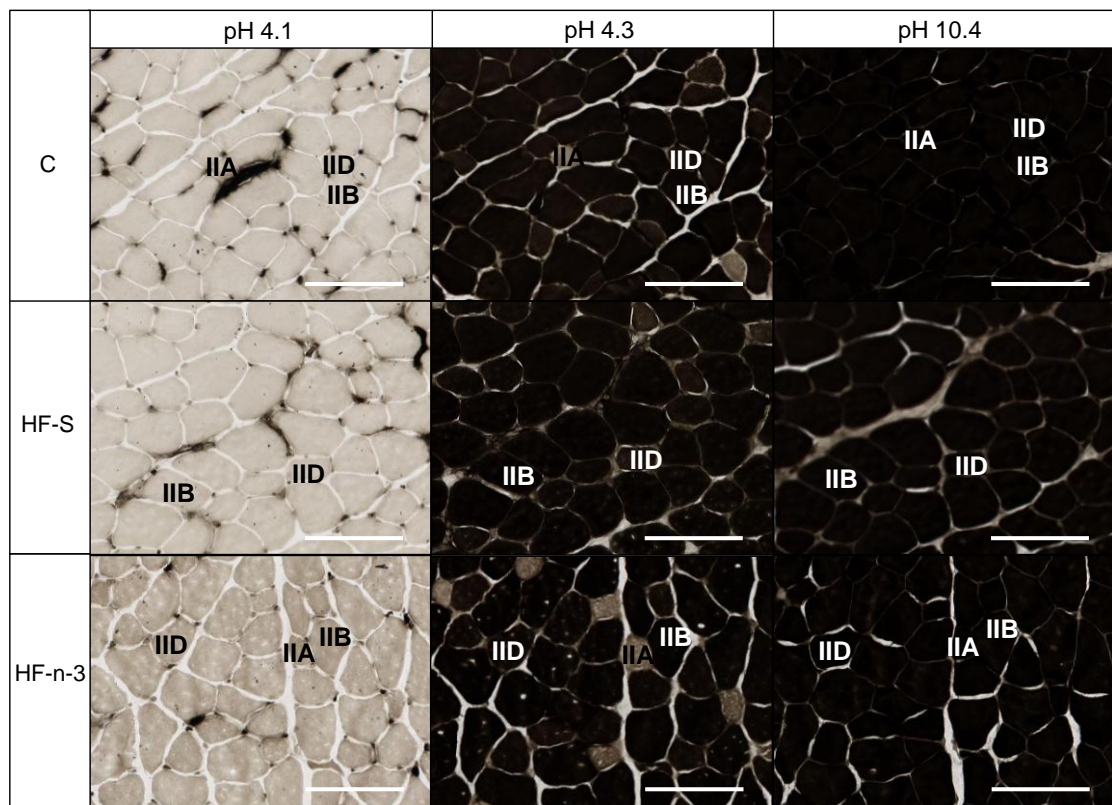


Figure 3.11. Serial sections of the extensor digitorum longus muscle stained for myosin ATPase after preincubation at pH 4.1, pH 4.3 and pH 10.4 in mice fed a control, high saturated fat or high fat n-3 PUFA enriched diet.

Scale bars represent 100 μm . Example muscle fibres indicated IIA, IID (IID/X), IIB. C, control diet; HF-S, high saturated fat diet; HF-n-3, high fat n-3 PUFA enriched diet.

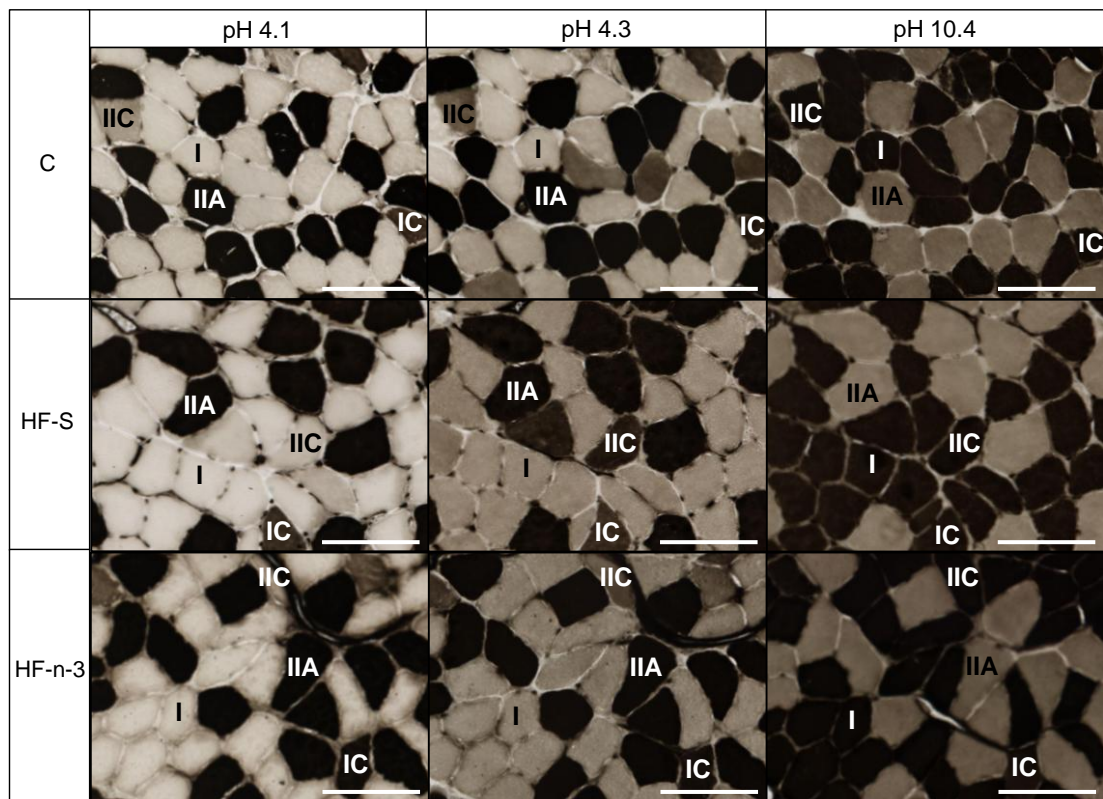


Figure 3.12. Serial sections of the soleus muscle stained for myosin ATPase after preincubation at pH 4.1, pH 4.3 and pH 10.4 in mice fed a control, high saturated fat or high fat n-3 PUFA enriched diet.

Scale bars represent 100 μm . Example muscle fibres indicated I, IC, IIC, IIA. C, control diet; HF-S, high saturated fat diet; HF-n-3, high fat n-3 PUFA enriched diet.

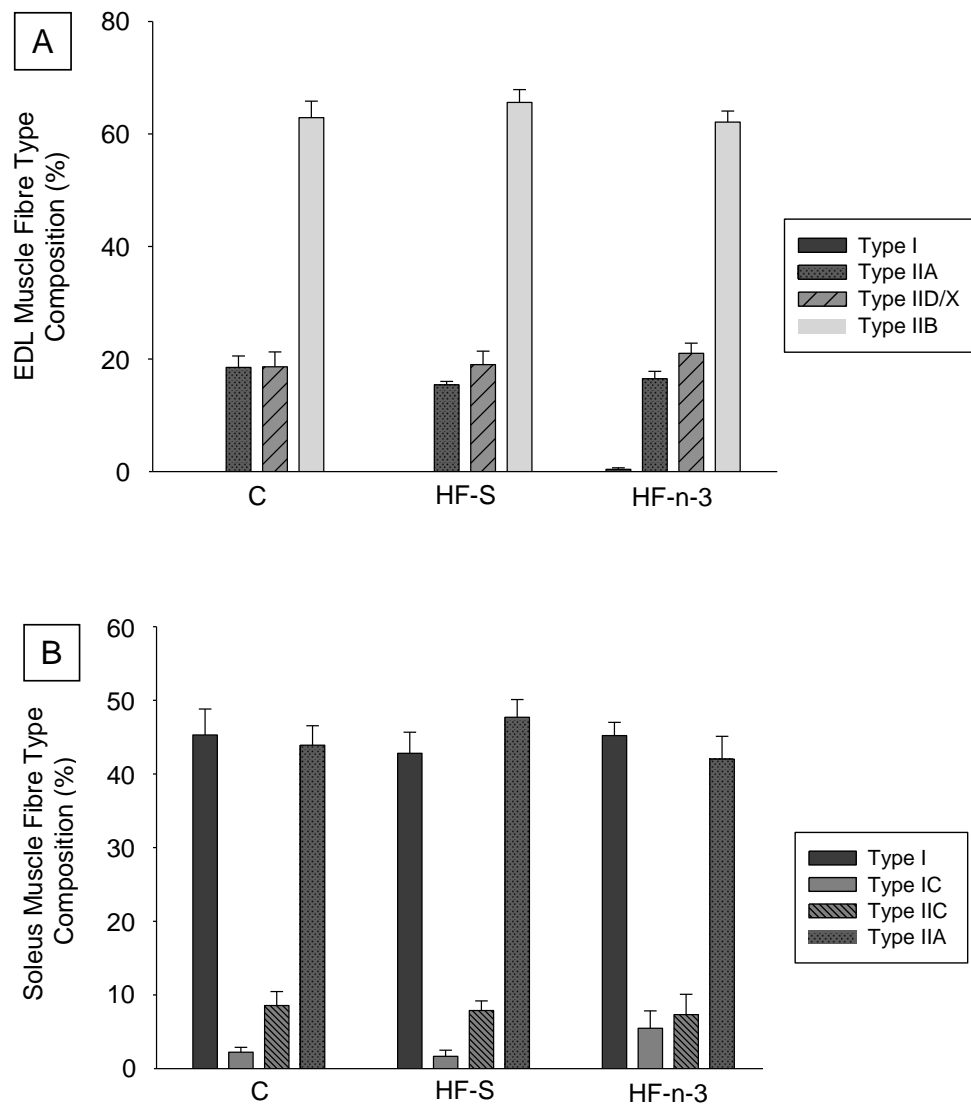


Figure 3.13 [A-B]. Muscle fibre type composition (%) of the extensor digitorum longus [A] and soleus [B] muscles of mice fed a control, high saturated fat or high fat n-3 PUFA enriched diet, evaluated histologically by myosin ATPase staining.

Data are expressed as mean (bars) \pm SEM (error bars). Bar type represented in legend. EDL, extensor digitorum longus muscle; C, control diet; HF-S, high saturated fat diet; HF-n-3, high fat n-3 PUFA enriched diet.

n: C(EDL/SOL) = 6/6, HF-S(EDL/SOL) = 6/6, HF-n-3(EDL/SOL) = 5/5.

Table 3.3. The mean area of muscle cells and the percentage of total area occupied by each muscle fibre type in the extensor digitorum longus and soleus muscles of mice fed a control, high saturated fat or high fat n-3 PUFA enriched diet.

EDL	Mean Cell Cross-sectional Area of each Muscle Fibre Type (μm^2)			
	I	IIA	IID/X	IIB
C	0.0 \pm 0.0	628.5 \pm 33.3	866.5 \pm 49.9	1560.3 \pm 70.7
HF-S	0.0 \pm 0.0	775.9 \pm 97.6	1091.9 \pm 95.2	1696.8 \pm 94.1
HF-n-3	89.2 \pm 89.2	647.8 \pm 66.9	957.8 \pm 96.9	1562.1 \pm 205.4
SOL	Mean Cell Cross-sectional Area of each Muscle Fibre Type (μm^2)			
	I	IC	IIC	IIA
C	1664.4 \pm 126.9	1274.9 \pm 181.4	1271.8 \pm 109.4	1223.7 \pm 102.9
HF-S	1843.2 \pm 134.8	1221.3 \pm 83.0	1465.1 \pm 129.8	1383.2 \pm 83.9
HF-n-3	1578.6 \pm 159.9	1019.7 \pm 144.0	1279.0 \pm 201.5	1312.1 \pm 111.7
EDL	Percentage of Total Area Occupied by each Muscle Fibre Type			
	I	IIA	IID/X	IIB
C	0.00 \pm 0.00	13.02 \pm 1.37	11.25 \pm 2.05	75.73 \pm 2.42
HF-S	0.00 \pm 0.00	10.10 \pm 2.10	13.00 \pm 2.92	76.59 \pm 5.02
HF-n-3	0.18 \pm 0.18	8.77 \pm 1.19	20.28 \pm 2.73	70.41 \pm 3.12
SOL	Percentage of Total Area Occupied by each Muscle Fibre Type			
	I	IC	IIC	IIA
C	48.47 \pm 3.17	3.34 \pm 1.63	10.18 \pm 2.06	39.73 \pm 2.32
HF-S	50.89 \pm 3.84	2.93 \pm 1.37	6.99 \pm 0.86	40.44 \pm 3.31
HF-n-3	49.17 \pm 5.57	3.10 \pm 1.41	6.30 \pm 1.86	42.05 \pm 5.28

Data presented as mean \pm SEM. Classified fibres I, IC, IIC, IIA, IID/X, IIB. EDL, extensor digitorum longus muscle; SOL, soleus muscle; C, control diet; HF-S, high saturated fat diet; HF-n-3, high fat n-3 PUFA enriched diet. n: C(EDL/SOL) = 6/6, HF-S(EDL/SOL) = 6/6, HF-n-3(EDL/SOL) = 5/5.

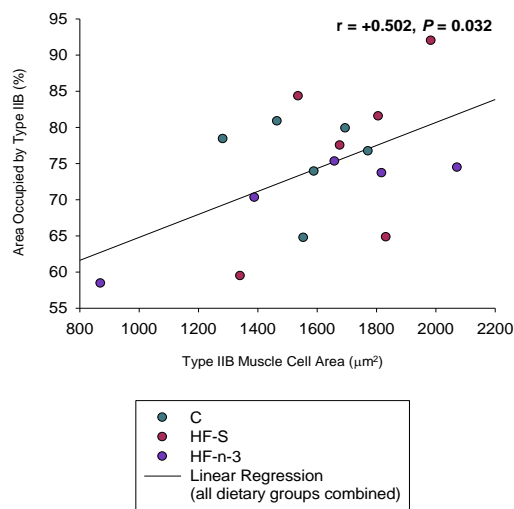


Figure 3.14. Relationships between the percentage area occupied and the mean cell cross-sectional area of muscle fibre types in the extensor digitorum longus muscle.

Symbols represent dietary group: white, control diet; pale grey, high saturated fat diet; dark grey, high fat n-3 PUFA enriched diet. Linear regression analyses were performed by incorporating data from all dietary groups. $n = 17$.

There was a significant positive relationship between percentage area occupied by type IIB fibres and mean muscle cell area of type IIB fibres (control, HF-S and HF-n-3 groups combined).

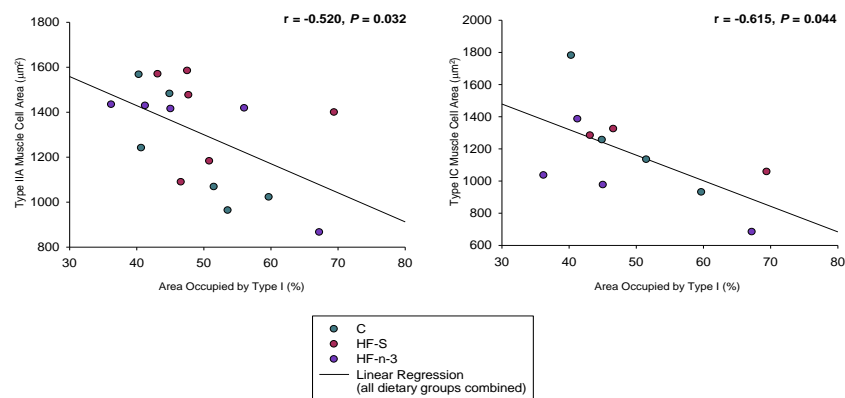


Figure 3.15. Relationships between the percentage area occupied and mean cell area of muscle fibre types in the soleus muscle.

Symbols represent dietary group: white, control diet; pale grey, high saturated fat diet; dark grey, high fat n-3 PUFA enriched diet. Linear regression analyses were performed by incorporating data from all dietary groups. All, $n = 17$; except type IC muscle cell area, $n = 11$.

There was a significant negative correlation between percentage area occupied by type I fibres and the mean muscle cell area of type IIA and IC fibres (dietary groups combined).

3.3.5 - Characterisation of Muscle Oxidative Capacity with Respect to Fibre Type in the Extensor Digitorum Longus and Soleus Skeletal Muscles

The intensity of succinic dehydrogenase (SDH) and NADH tetrazolium reductase (NADH-TR) staining in EDL (**Figure 3.16**) and soleus (**Figure 3.17**) muscle sections was assessed by mean pixel density of muscle fibres and this provided an indication of muscle oxidative capacity.

3.3.5.1 – Oxidative Capacity in the Extensor Digitorum Longus Muscle

In the EDL muscle, the general profile of staining intensity for SDH was IIA=IID/X>IIB (F(2, 48)=27.5, $P\leq 0.001$; post-hoc tests: $P\leq 0.001$). Staining intensities of type IIA and IID/X fibres were similar (post-hoc test: $P=0.92$).

There was no overall effect of diet on the mean pixel density of SDH staining in muscle cells classified as type IIA (F(2, 14)=3.1, $P=0.078$), IID/X (F(2, 14)=3.7, $P=0.052$), or IIB (F(2, 14)=2.5, $P=0.12$) fibres in the EDL muscle. However, type IIA and type IID/X muscle fibres in the EDL of HF-n-3 mice tended to have greater mean pixel density when compared to the same fibre types in control EDL muscles (+22.0%, +21.1%, respectively; post-hoc tests: $P=0.10$, $P=0.062$, respectively) (**Figure 3.18A**).

In the EDL muscle, the general profile of staining intensity for NADH-TR was IIA>IID/X>IIB (F(2, 45)=149.0, $P\leq 0.001$; post-hoc tests: $P\leq 0.001$).

There was no effect of diet on the mean pixel density of NADH-TR staining in muscle cells classified as type IIA (F(2, 13)=3.2, $P=0.076$), IID/X (F(2, 13)=3.0, $P=0.083$), or

IIB ($F(2, 13)=1.3, P=0.31$) in the EDL muscle. However, types IIA and type IID/X tended to have greater mean pixel density in the EDL muscle from HF-n-3 mice as compared to HF-S mice (+9.8%, +9.3%, respectively; post-hoc tests: $P=0.079, P=0.086$, respectively) (**Figure 3.19A**).

3.3.5.2 – Oxidative Capacity in the Soleus Muscle

In the soleus muscle stained for SDH, all muscle fibre types exhibited similar staining intensity ($F(3, 58)=1.1, P=0.35$), i.e. I=IC=IIC=IIA.

In the soleus muscle, there was an effect of diet on the mean pixel density of muscle fibres classified as type I ($F(2, 14)=4.0, P=0.042$) and IIC ($F(2, 14)=5.3, P=0.019$) stained for SDH. Type I muscle fibres tended to have greater mean pixel density in HF-n-3 mice as compared to HF-S mice (+21.0%, post-hoc test: $P=0.053$) and type IIC muscle fibres exhibited greater mean pixel density in HF-n-3 mice as compared to control and HF-S mice (+21.5%, +24.6%, respectively; post-hoc tests: $P\leq 0.05$) (**Figure 3.18B**). There was no effect of diet on the mean pixel density of muscle cells, stained for SDH classified as type IC ($F(2, 8)=3.4, P=0.085$) and IIA ($F(2, 14)=2.9, P=0.089$) fibres in the soleus muscle.

The general profile of staining intensity for NADH-TR in the soleus muscle was IIA=IIC=IC>I. Muscle fibre type ($F(3, 58)=8.2, P\leq 0.001$) influenced the mean pixel density of muscle cells stained for NADH-TR in the soleus muscle, with type I fibres exhibiting significantly different mean pixel densities to type IC, IIC and IIA fibres (post-hoc tests: $P\leq 0.005, P\leq 0.005, P\leq 0.001$, respectively). However type IC, IIA, and IIC muscle fibres exhibited similar staining intensity (post-hoc tests: $P=1.0$).

There was an effect of diet on the mean pixel density of NADH-TR staining in muscle cells classified as type I ($F(2, 14)=4.2, P=0.037$), IC ($F(2, 8)=14.5, P=0.002$) and IIC ($F(2, 14)=4.5, P=0.031$) fibres in the soleus muscle. Type I and IIC muscle fibres exhibited greater mean pixel density in HF-n-3 mice as compared to HF-S mice (+12.6%, +23.4%, respectively post-hoc tests: $P\leq 0.05$) and type IC muscle fibres exhibited greater mean pixel density in HF-n-3 mice as compared to control and HF-S mice (+26.3%, +31.0%, respectively; post-hoc tests: $P\leq 0.005, P\leq 0.02$, respectively) (**Figure 3.19B**). In the soleus muscle, there was no effect of diet on the mean pixel density of muscle cells, stained for NADH-TR classified as type IIA ($F(2, 14)=2.2, P=0.15$) fibres.

3.3.5.3– Relationships between the Oxidative Capacity of Muscle Fibre Types in the Extensor Digitorum Longus and Soleus Muscles

In the EDL muscle, the mean staining intensity for SDH exhibited by type IIA fibres was positively related to mean staining intensity for SDH in type IID/X and IIB fibres (all dietary groups combined) (**Table 3.4**). The mean staining intensity for SDH exhibited by type IID/X fibres was also positively related to mean staining intensity for SDH in type IIB fibres (all dietary groups combined) (**Table 3.4**). This suggests that, in the EDL muscle, the staining intensity for SDH is co-ordinately increased in type IIA, IIB and IID/X fibres.

Similarly, in the soleus muscle, the mean staining intensity for NADH-TR exhibited by type I fibres was positively related to mean staining intensity for NADH-TR in type IC, IIC and IIA fibres (all dietary groups combined) (**Table 3.4**). The mean staining

intensity for NADH-TR exhibited by type IC fibres was also positively correlated with the mean staining intensity for NADH-TR in type IIC and IIA fibres (all dietary groups combined) (**Table 3.4**). Furthermore, the mean staining intensity for NADH-TR exhibited by type IIC fibres was positively related to the mean staining intensity for NADH-TR in type IIA fibres (all dietary groups combined) (**Table 3.4**). Thus, in the soleus muscle, activity of NADH-TR is co-ordinately increased in type I, IC, IIC and IIA fibres.

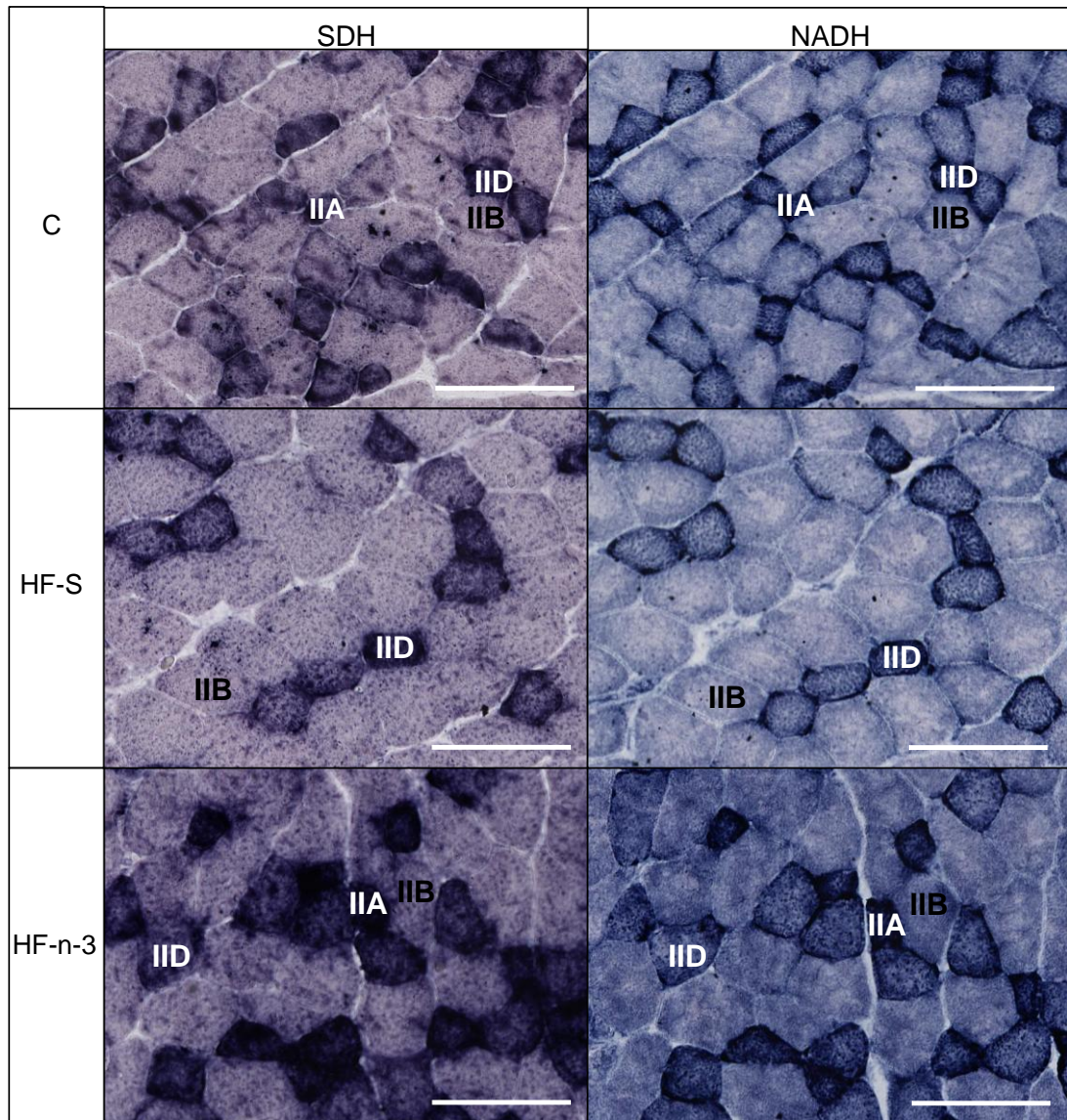


Figure 3.16. Serial sections of the extensor digitorum longus muscle stained for SDH and NADH-TR in mice fed a control, high saturated fat or high fat n-3 PUFA enriched diet.

Scale bars represent 100 μm . C, control diet; HF-S, high saturated fat diet; HF-n-3, high fat n-3 PUFA enriched diet. Example muscle fibres indicated IIA, IID (IID/X), IIB.

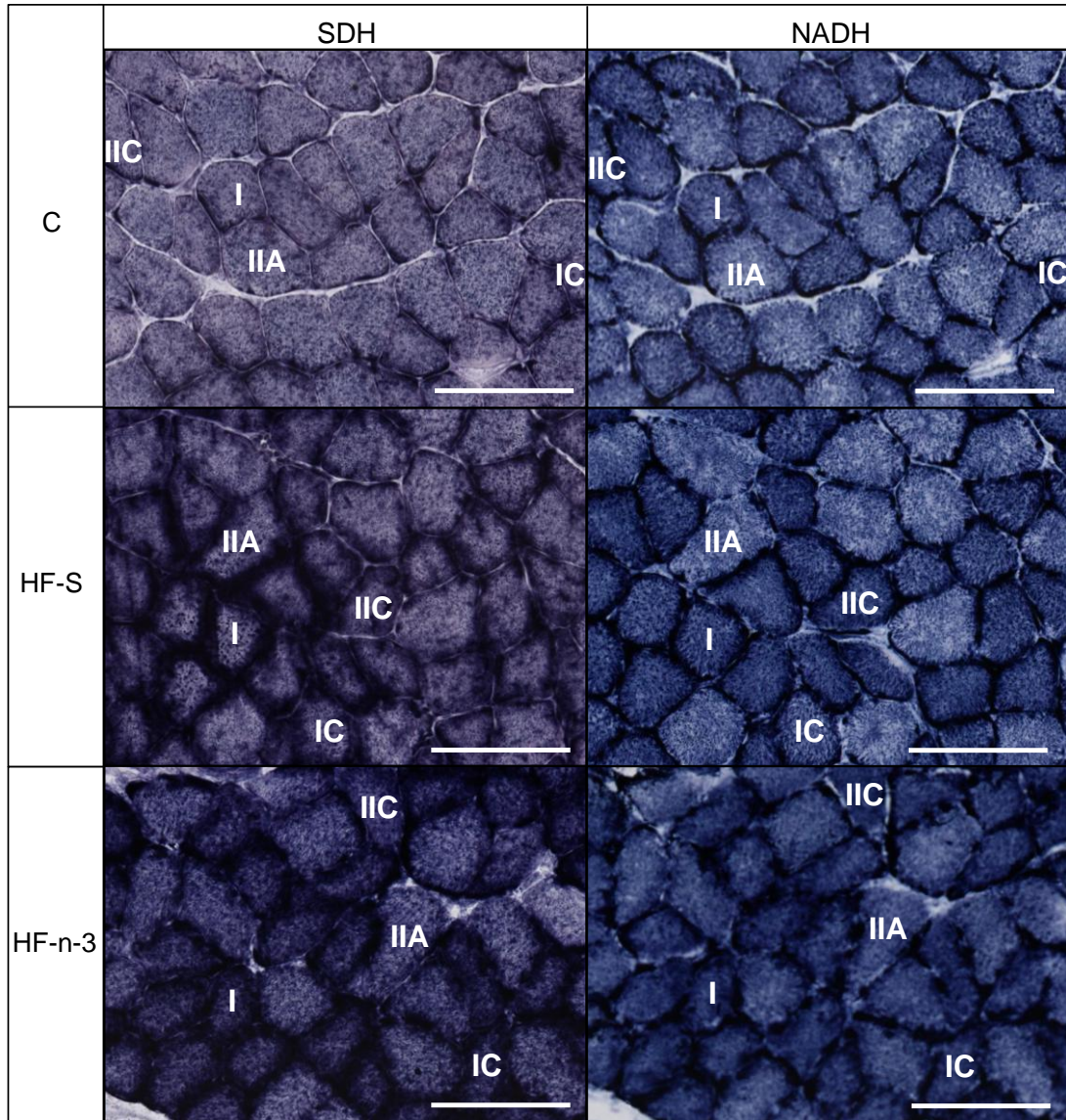


Figure 3.17. Serial sections of the soleus muscle stained for SDH and NADH-TR in mice fed a control, high saturated fat or high fat n-3 PUFA enriched diet.

Scale bars represent 100 μm . C, control diet; HF-S, high saturated fat diet; HF-n-3, high fat n-3 PUFA enriched diet. Example muscle fibres indicated I, IC, IIC, IIA.

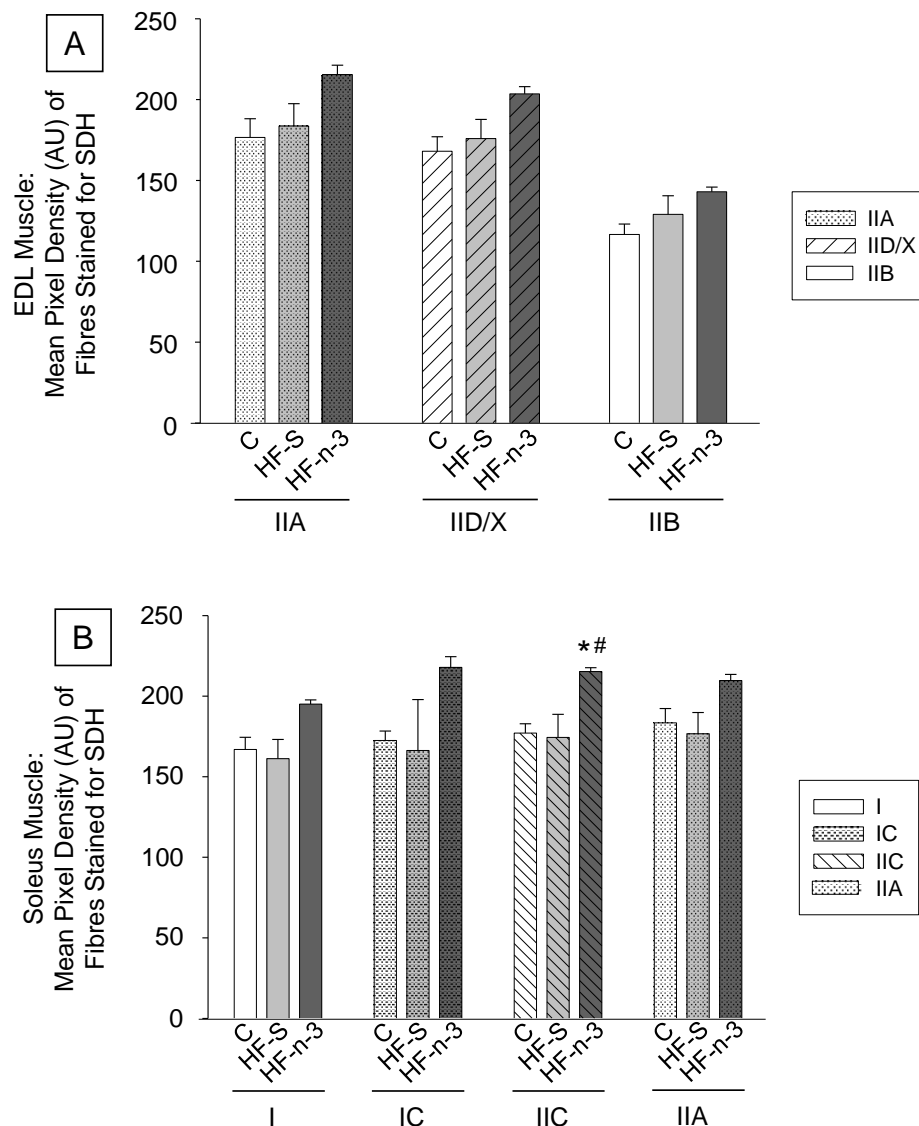


Figure 3.18 [A-B]. Histological quantification of muscle oxidative capacity in extensor digitorum longus [A] and soleus [B] muscle sections of mice fed a control, high saturated fat or high fat n-3 PUFA enriched diet; muscle fibres were stained for SDH and assessed for mean pixel density.

Data are expressed as mean (bars) \pm SEM (error bars). Bar colour represents dietary group white, C; pale grey, HF-S; dark grey, HF-n-3. Bar type represented in legend. EDL, extensor digitorum longus muscle; C, control diet; HF-S, high saturated fat diet; HF-n-3, high fat n-3 PUFA enriched diet.

n: C(EDL/SOL) = 6/6, HF-S(EDL/SOL) = 6/6, HF-n-3(EDL/SOL) = 5/5.

Statistics: Effect of diet: * $P \leq 0.05$, compared to C (of same fibre type); # $P \leq 0.05$, compared to HF-S (of same fibre type).

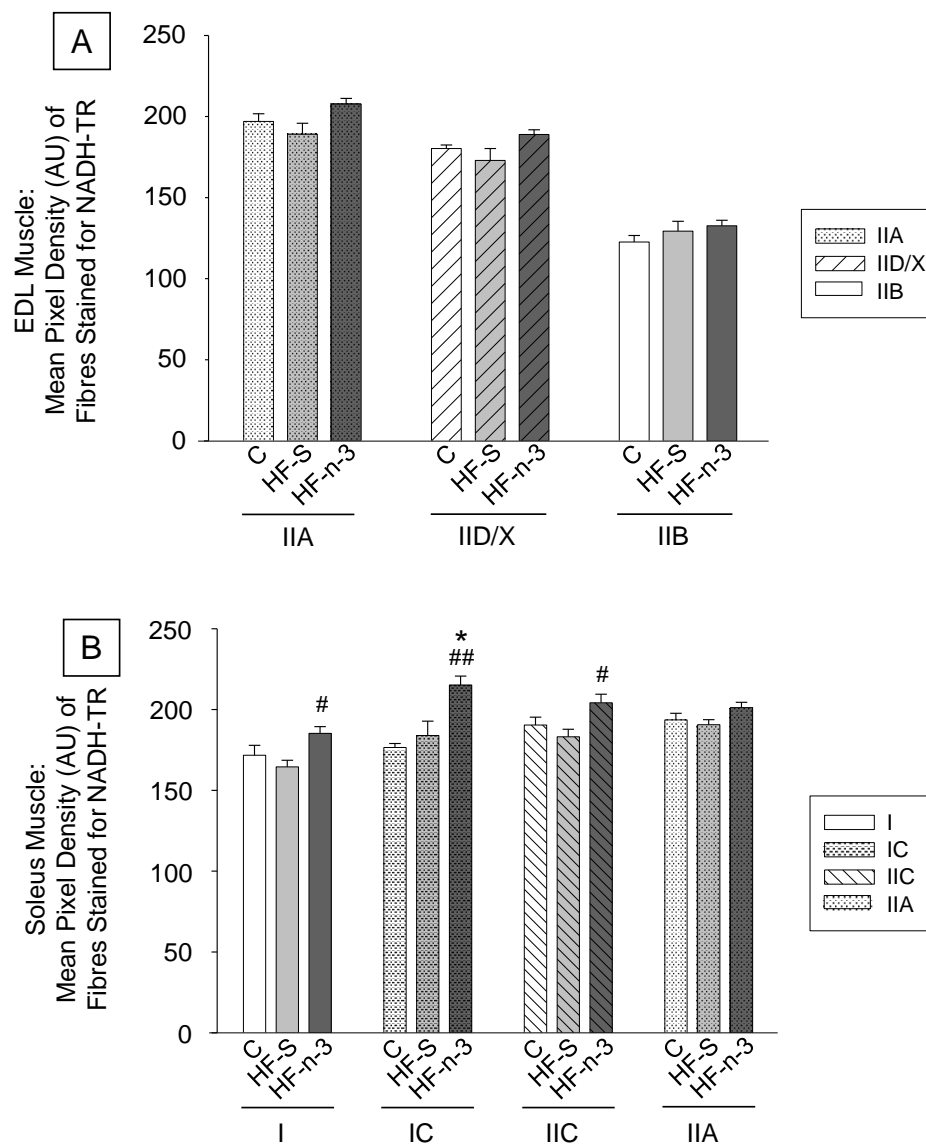


Figure 3.19 [A-B]. Histological quantification of muscle oxidative capacity in extensor digitorum longus [A] and soleus [B] muscle sections of mice fed a control, high saturated fat or high fat n-3 PUFA enriched diet; muscle fibres were stained for NADH-TR and assessed for mean pixel density.

Data are expressed as mean (bars) \pm SEM (error bars). Bar colour represents dietary group white, C; pale grey, HF-S; dark grey, HF-n-3. Bar type represented in legend. EDL, extensor digitorum longus muscle; C, control diet; HF-S, high saturated fat diet; HF-n-3, high fat n-3 PUFA enriched diet.

n: C(EDL/SOL) = 6/6, HF-S(EDL/SOL) = 6/6, HF-n-3(EDL/SOL) = 5/5.

Statistics: Effect of diet: $*P \leq 0.005$, compared to C (of same fibre type); $^{\#}P \leq 0.05$, $^{##}P \leq 0.02$, compared to HF-S (of same fibre type).

Table 3.4. Relationships between the oxidative capacities of muscle fibre types in the extensor digitorum longus and soleus muscles.				
EDL: Mean Pixel Density of Muscle Fibres Stained For SDH				
Type	IIA	IID/X	IIB	
IIA	.	$r = +0.98,$ $P < 0.001$	$r = +0.75,$ $P = 0.001$	
IID/X	$r = +0.98,$ $P < 0.001$.	$r = +0.71,$ $P = 0.01$	
IIB	$r = +0.75,$ $P = 0.001$	$r = +0.71,$ $P = 0.01$.	
SOL: Mean Pixel Density of Muscle Fibres Stained For NADH-TR				
Type	I	IC	IIC	IIA
I	.	$r = +0.82,$ $P = 0.002$	$r = +0.75,$ $P = 0.001$	$r = +0.65,$ $P = 0.005$
IC	$r = +0.82,$ $P = 0.002$.	$r = +0.83,$ $P = 0.002$	$r = +0.82,$ $P = 0.002$
IIC	$r = +0.75,$ $P = 0.001$	$r = +0.83,$ $P = 0.002$.	$r = +0.88,$ $P < 0.001$
IIA	$r = +0.65,$ $P = 0.005$	$r = +0.82,$ $P = 0.002$	$r = +0.88,$ $P < 0.001$.

Linear regression analyses were performed by incorporating data from all dietary groups. $n = 17$, except comparisons using type IC, $n = 11$. EDL, extensor digitorum longus; SOL, soleus.

There was a significant positive correlation between SDH staining intensity of type IIA fibres and SDH staining intensity of type IIB and IID/X fibres in the EDL muscle (control, HF-S and HF-n-3 groups combined). There was also a significant positive relationship between SDH staining intensity of type IIB fibres and SDH staining intensity of type IID/X fibres in the EDL muscle (control, HF-S and HF-n-3 groups combined). There was a significant positive correlation between NADH-TR staining intensity of type I fibres and NADH-TR staining intensity of type IC, IIC and IIA fibres in the soleus muscle (control, HF-S and HF-n-3 groups combined). There was a significant positive relationship between NADH-TR staining intensity of type IC fibres and NADH-TR staining intensity of type IIC and IIA fibres in the soleus muscle (control, HF-S and HF-n-3 groups combined). There was also a significant positive correlation between NADH-TR staining intensity of type IIC fibres and NADH-TR staining intensity of type IIA fibres in the soleus muscle (control, HF-S and HF-n-3 groups combined).

3.3.6 – Myosin ATPase Staining of the Tibialis, Plantaris and Gastrocnemius

Skeletal Muscles

Myosin ATPase staining of muscle sections following acid (pH 4.1, pH 4.3) and alkaline (pH 10.4) preincubation was used to also visualise muscle fibre type in the tibialis, plantaris and gastrocnemius muscles. From visual assessment, the tibialis (**Figure 3.20**), plantaris (**Figure 3.21**), gastrocnemius lateralis (**Figure 3.22**) and gastrocnemius medialis (**Figure 3.23**) muscles did not exhibit any striking changes in muscle fibre type composition. Therefore, no quantification was performed due to time constraints.

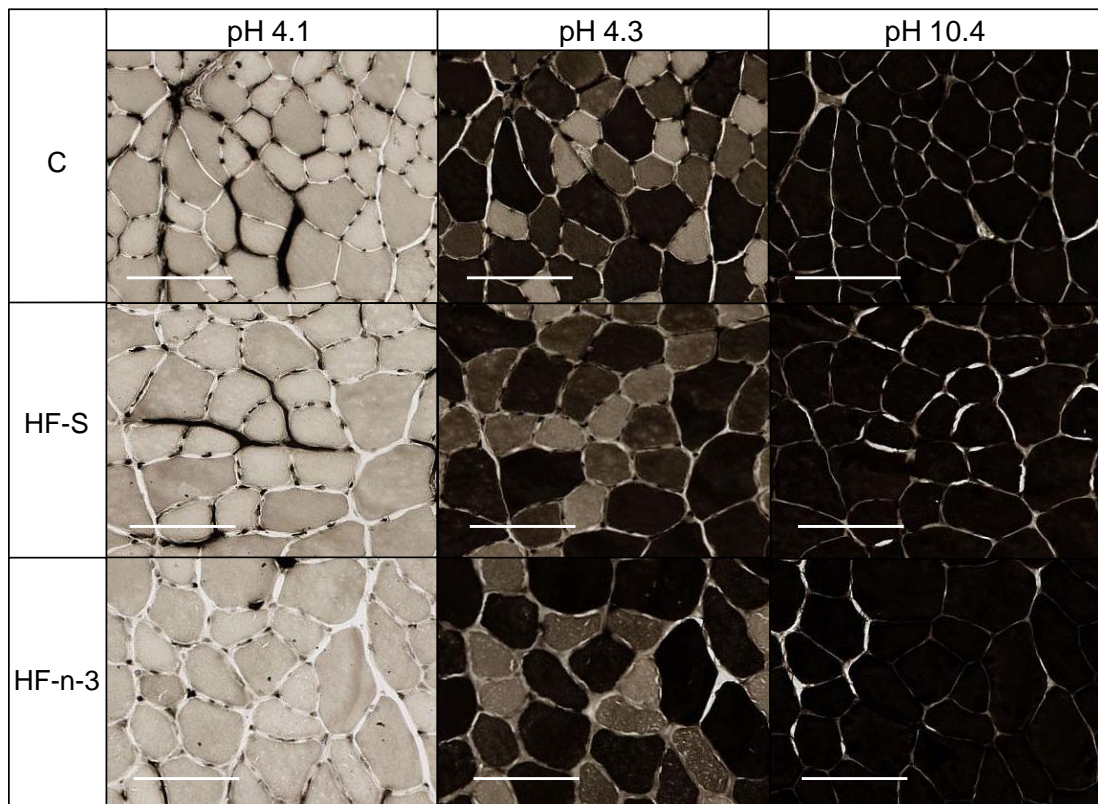


Figure 3.20. Serial sections of the tibialis muscle stained for myosin ATPase after preincubation at pH 4.1, pH 4.3 and pH 10.4 in mice fed a control, high saturated fat or high fat n-3 PUFA enriched diet.

Scale bars represent 100 μm . C, control diet; HF-S, high saturated fat diet; HF-n-3, high fat n-3 PUFA enriched diet.

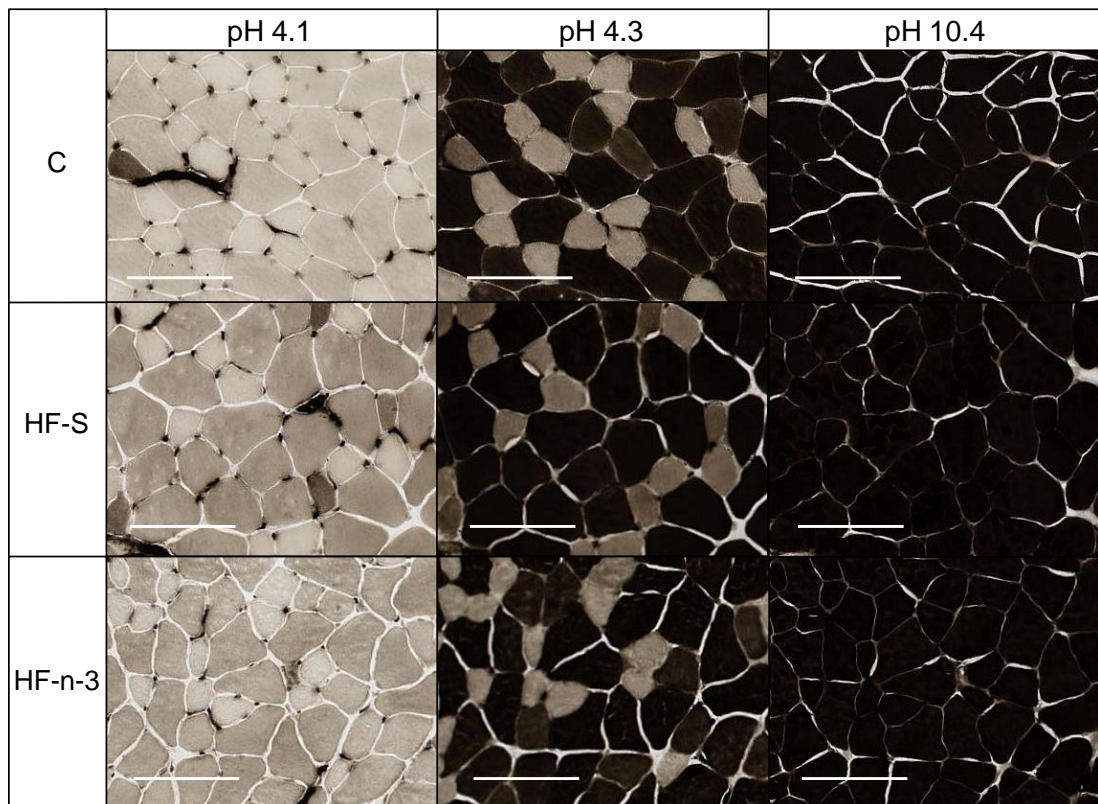


Figure 3.21. Serial sections of the plantaris muscle stained for myosin ATPase after preincubation at pH 4.1, pH 4.3 and pH 10.4 in mice fed a control, high saturated fat or high fat n-3 PUFA enriched diet.

Scale bars represent 100 μm . C, control diet; HF-S, high saturated fat diet; HF-n-3, high fat n-3 PUFA enriched diet.

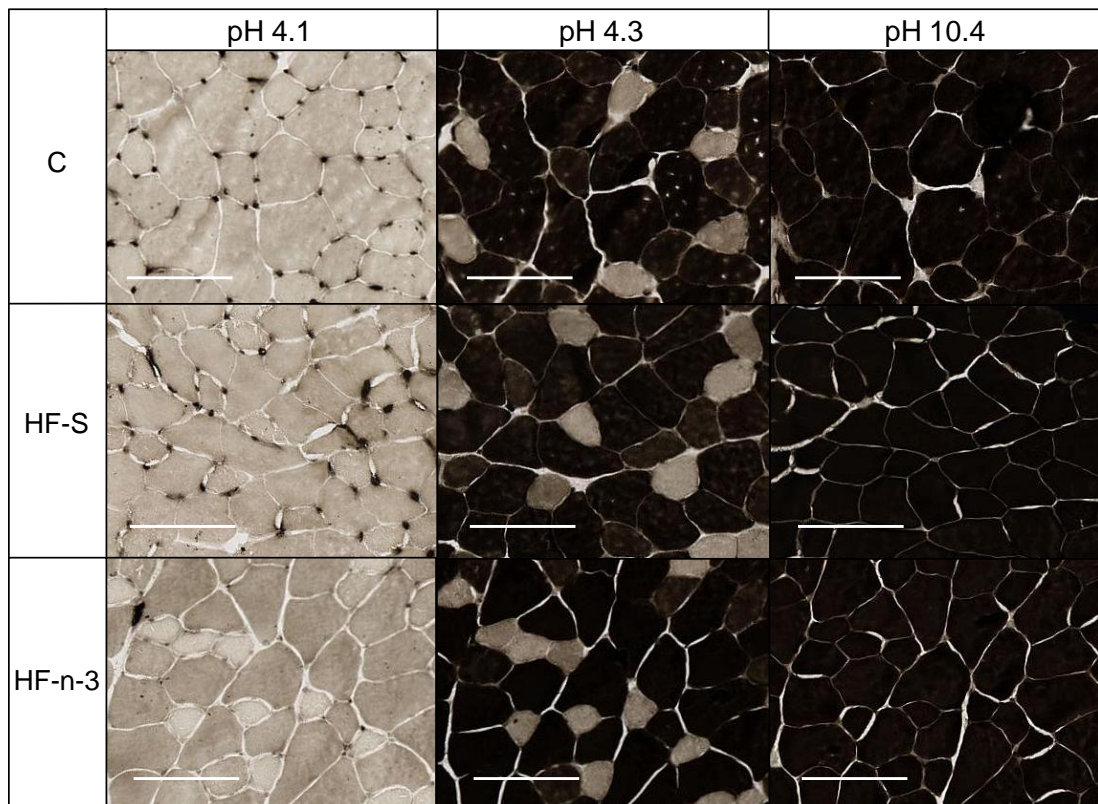


Figure 3.22. Serial sections of the gastrocnemius lateralis muscle stained for myosin ATPase after preincubation at pH 4.1, pH 4.3 and pH 10.4 in mice fed a control, high saturated fat or high fat n-3 PUFA enriched diet.

Scale bars represent 100 μm . C, control diet; HF-S, high saturated fat diet; HF-n-3, high fat n-3 PUFA enriched diet.

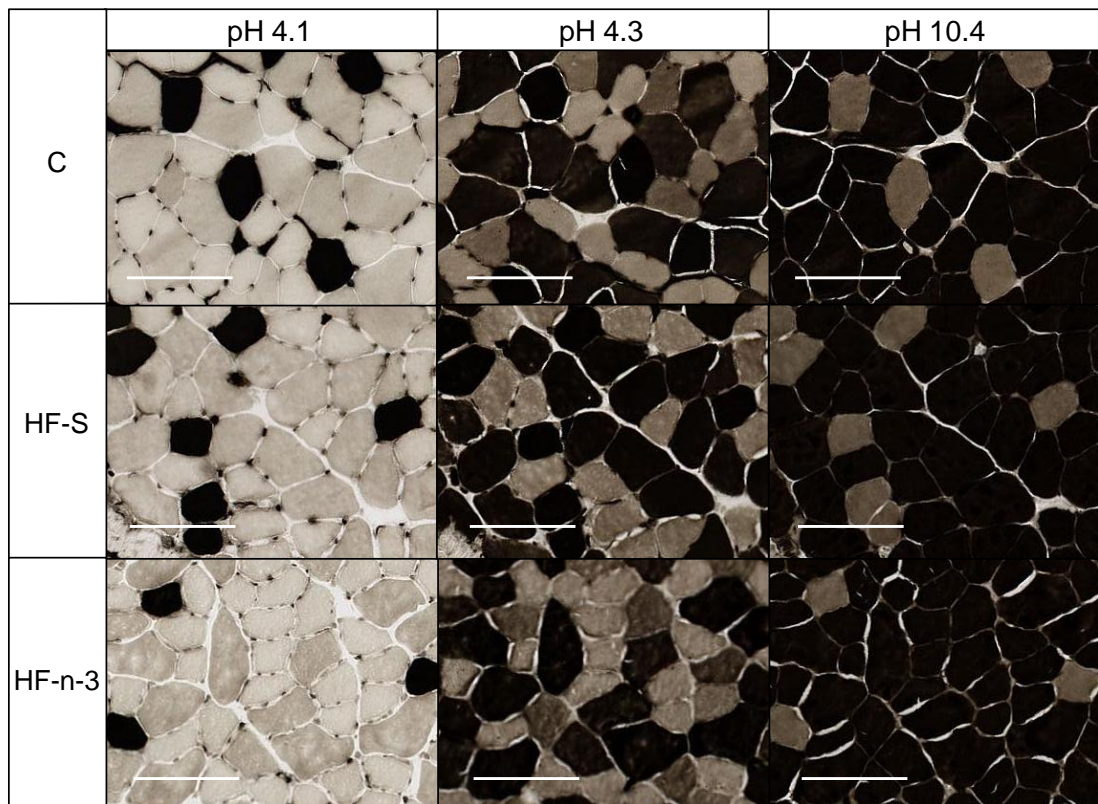


Figure 3.23. Serial sections of the gastrocnemius medialis muscle stained for myosin ATPase after preincubation at pH 4.1, pH 4.3 and pH 10.4 in mice fed a control, high saturated fat or high fat n-3 PUFA enriched diet.

Scale bars represent 100 μm . C, control diet; HF-S, high saturated fat diet; HF-n-3, high fat n-3 PUFA enriched diet.

3.3.7 – Muscle Oxidative Capacity of the Tibialis, Plantaris and Gastrocnemius

Skeletal Muscles

The staining intensity for SDH and NADH-TR in the tibialis, plantaris and gastrocnemius muscles were also assessed visually. From these visual assessments, muscle oxidative capacity appeared to be altered by diet (**Figures 3.24** and **3.25**). In all muscles, the intensities of staining for SDH and NADH-TR were greater in HF-n-3 mice than in control and HF-S mice. However, in the tibialis and gastrocnemius medialis muscles, those from HF-S mice displayed greater staining intensity for SDH than control mice.

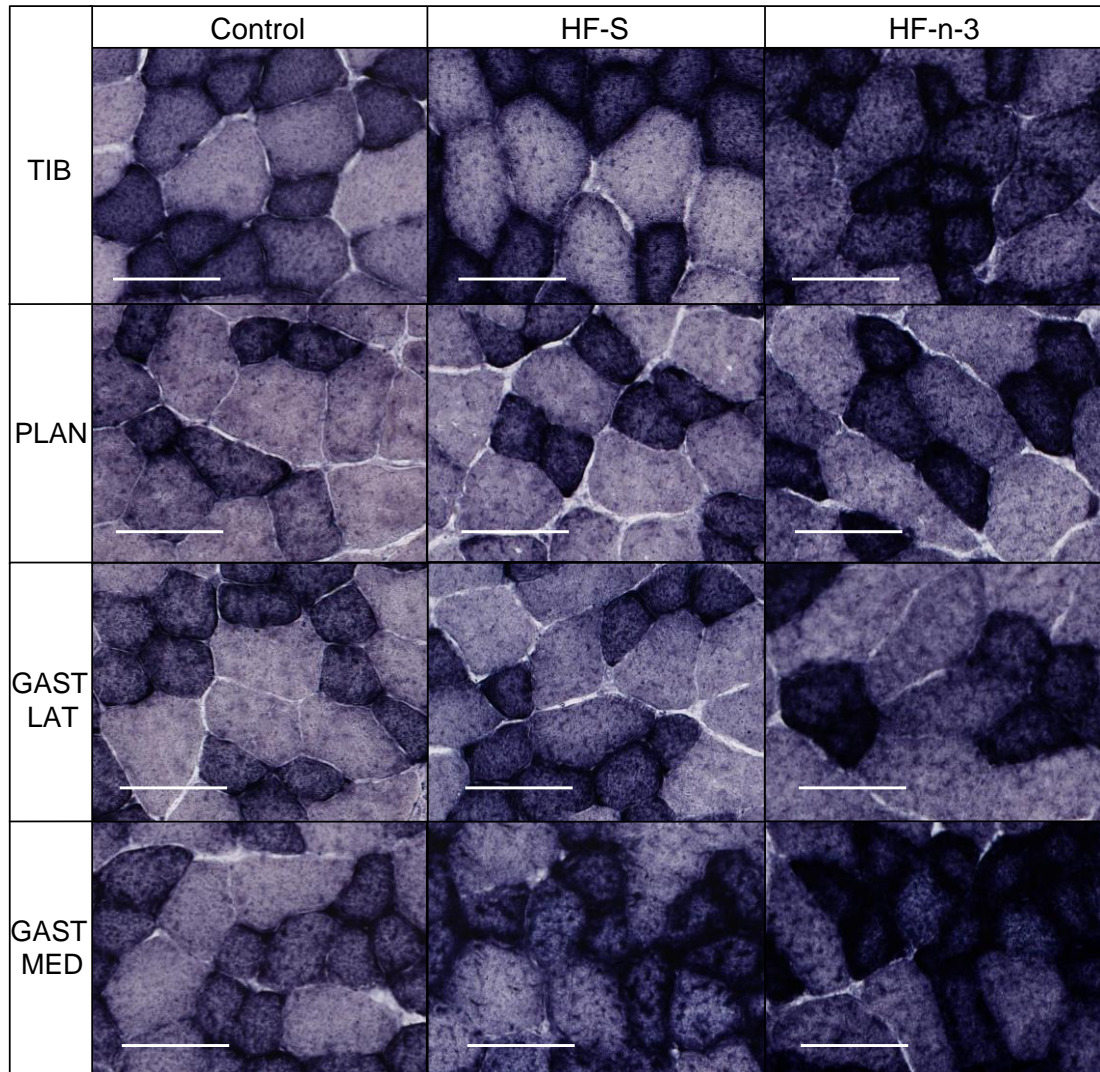


Figure 3.24. Representative images of the tibialis, plantaris and gastrocnemius muscles stained for SDH in mice fed a control, high saturated fat or high fat n-3 PUFA enriched diet.

Scale bars represent 50 μm . HF-S, high saturated fat diet; HF-n-3, high fat n-3 PUFA enriched diet; TIB, tibialis muscle; PLAN, plantaris muscle; GAST LAT, gastrocnemius lateralis muscle; GAST MED, gastrocnemius medialis muscle.

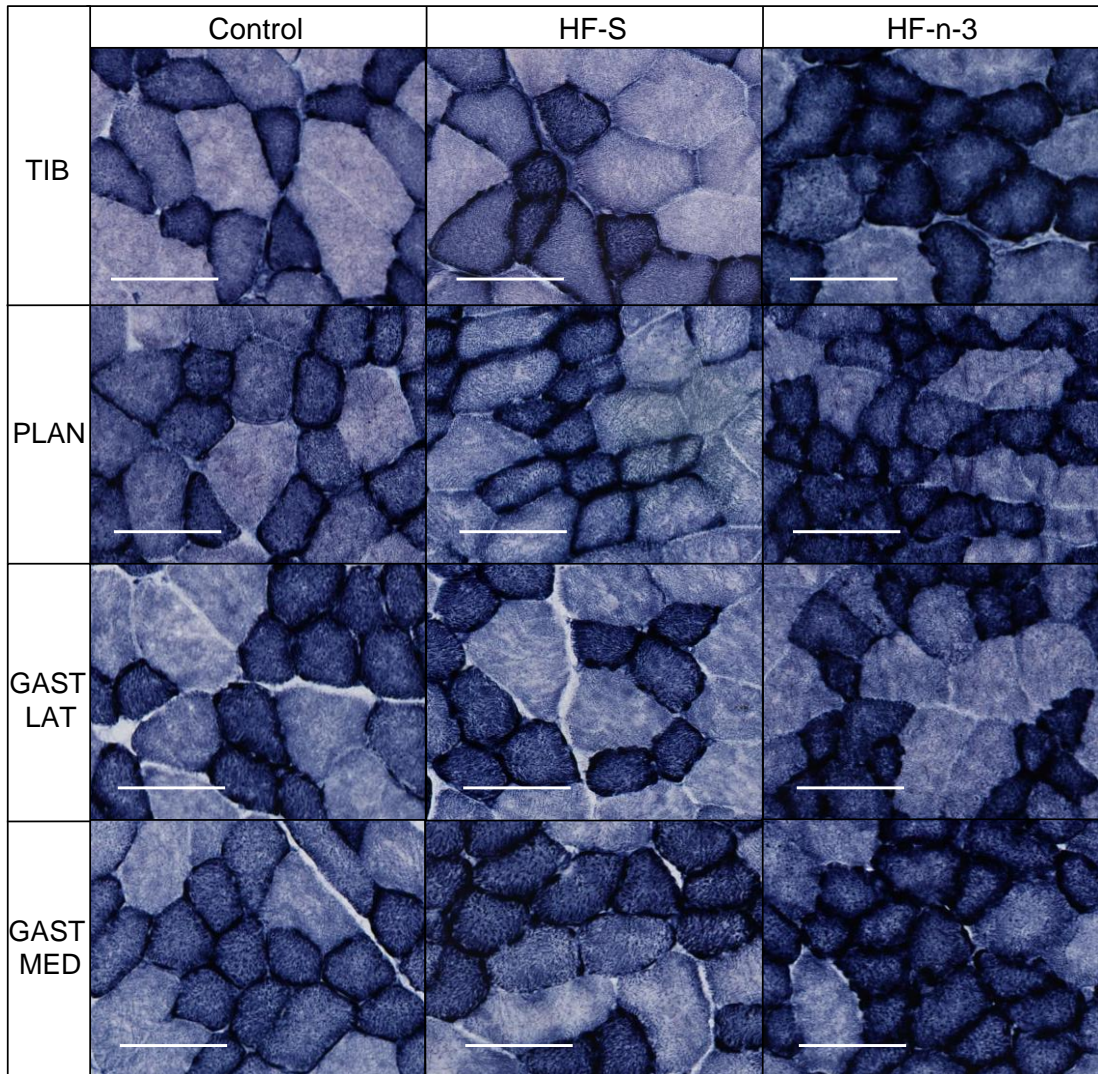


Figure 3.25. Representative images of the tibialis, plantaris and gastrocnemius muscles stained for NADH-TR in mice fed a control, high saturated fat or high fat n-3 PUFA enriched diet.

Scale bars represent 50 μm . HF-S, high saturated fat diet; HF-n-3, high fat n-3 PUFA enriched diet; TIB, tibialis muscle; PLAN, plantaris muscle; GAST LAT, gastrocnemius lateralis muscle; GAST MED, gastrocnemius medialis muscle.

3.4 – DISCUSSION

The present study demonstrates that the EDL muscle is composed predominantly of FG type IIB fibres, and the soleus muscle is composed principally of SO type I and FOG type IIA fibres. These observations are consistent with earlier reports (Handschin *et al.*, 2007; Bobinac *et al.*, 2000; Kraemer *et al.*, 2000; Nakatani *et al.*, 1999; Staron and Pette, 1986). Although a muscle fibre type switch has previously been described in obesity (Oberbach *et al.*, 2006; Hickey *et al.*, 1995), the present study did not detect any effect of diet induced obesity (DIO) on muscle fibre type distribution. The effect of dietary n-3 PUFA consumption on muscle fibre type composition has not been previously investigated and this study is the first to demonstrate that n-3 PUFA enrichment of a HFD has no effect on muscle fibre type distribution. However, the amount of nutrient stored and the activity and expression of enzymes regulating fuel storage in skeletal muscle were influenced by obesity in a fibre type- and fatty acid-dependent manner.

3.4.1 – Effect of Dietary Fatty Acid Content on Muscle Fibre Type Composition

Consistent with previous reports (Handschin *et al.*, 2007; Bobinac *et al.*, 2000; Kraemer *et al.*, 2000; Nakatani *et al.*, 1999; Staron and Pette, 1986), the EDL muscle exhibited predominantly FG type IIB fibres, accompanied by equal proportions of FOG type IIA and IID/X fibres, while the soleus muscle exhibited principally SO type I and FOG type IIA fibres, supplemented with a few type IC and type IIC fibres. Because the muscle fibre type compositions observed in the present study were in accordance with the previously reported mainly FG-FOG characteristics of the EDL muscle and

predominantly SO nature of the soleus muscle, the EDL and soleus muscles were chosen to represent respectively muscles with predominant glycolytic and oxidative nature in the remainder of this thesis.

Exposure to an altered nutrient environment triggers an adaptive response in skeletal muscle, modifying the muscle's propensity for oxidative or glycolytic metabolism (Adachi *et al.*, 2007). Research has shown that in skeletal muscle from obese individuals, muscle fibre type plasticity drives a switch in the functional nature of the muscle, indicating a switch from both oxidative and glycolytic metabolic capacity to possessing predominantly glycolytic characteristics (Oberbach *et al.*, 2006; Hickey *et al.*, 1995). The effect of consuming a HFD rich in saturated fat (HF-S) on muscle fibre type has been described previously (de Wilde *et al.*, 2008), but the effect of n-3 PUFA enrichment of a HFD (HF-n-3) on muscle fibre type composition has not been investigated. In the current study, it was demonstrated that the percentage muscle fibre type composition, mean fibre cross-sectional area and percentage area occupied by each muscle fibre type in the FG-FOG EDL and SO soleus muscles were unchanged by obesity or by the dietary composition of fatty acid consumed. There was an association observed between the percentage area occupied by FG type IIB fibres and the mean cell cross-sectional area of type IIB fibres. Furthermore, the percentage area occupied by SO type I fibres was associated with smaller cross-sectional area of type IIA and IC fibres. Whether these relationships reflect the development of a trend towards a fibre type switch that may have become evident with more prolonged feeding of the HFDs, or may have reached statistical significance with a greater sample size, is unknown and this requires further investigation. Furthermore, research has demonstrated that

different methods of muscle fibre typing can provide slightly different answers (Termin *et al.*, 1989a; Green *et al.*, 1982b). It may therefore be worthwhile quantifying muscle fibre type by separating the myosin heavy chain protein isoforms by gel electrophoresis, to determine if a shift in fibre type was observed using different methodology.

3.4.2 – Effect of Dietary Fatty Acid Composition on Stored Nutrient Content

An increase in skeletal muscle mass has been described as a characteristic of obesity (Kelley and Storlien, 2004; Goodpaster *et al.*, 1997). Similarly, the current study demonstrated that a larger body weight was associated with greater muscle mass (combined EDL and soleus muscle mass) in the control and HF-S groups. Although there was a positive relationship between muscle mass and body weight in HF-S mice, the relative weight of the EDL muscle was reduced in the HF-S group. The association between obesity and increased muscle mass was not apparent in HF-n-3 mice, and the relative weight of FG-FOG EDL muscle was reduced by HF-n-3 feeding. The reason for this change is unknown, but may be related to kinaesthetic changes secondary to obesity. Alternatively, as described previously in **Chapter 2**, the amount of glycogen stored may influence the relative weight of an organ, as demonstrated by the correlation of relative liver weight with liver glycogen content (see **Figure 2.11**). Although the skeletal muscle has a lower storage capacity for glycogen than the liver (Maughan and Williams, 1982; Surovtseva, 1974), up to 90% of the glucose flux into muscle may enter non-oxidative glucose metabolism, being channelled into glycogen stores (Jue *et al.*, 1989). In the development of the obese phenotype, not only does the mass of

skeletal muscle change, but the stored nutrient milieu of muscle is also altered (Kelley and Storlien, 2004; Goodpaster *et al.*, 1997). Previous studies have shown that n-3 PUFA enrichment of a HFD decreases muscle glycogen in rats (Rustan *et al.*, 1993) and treatment of skeletal muscle myotubes with the n-3 PUFA, eicosapentaenoic acid (EPA), reduces basal glycogen synthesis (Aas *et al.*, 2006). It is, therefore, possible that reduced glycogen content may account for the lower EDL muscle weight. However, the total glycogen content of the FG-FOG EDL muscle was not different between dietary groups. However, more cells containing intermediate glycogen content were observed in the EDL muscle of HF-n-3 mice, which in part may be the result of a reduction in fibres exhibiting high glycogen content, but it is not clear whether this is sufficient to account for the altered relative weight of the EDL muscle.

Findings of previous studies (Aas *et al.*, 2006; Rustan *et al.*, 1993) have been extended by the present study which showed that muscle glycogen is influenced by dietary fatty acid content in a muscle fibre type-dependent manner. Although total glycogen content was unchanged in the FG-FOG EDL muscle, glycogen content in the SO soleus muscle was reduced by HF-n-3 feeding compared to control and HF-S feeding. Whilst consumption of a HFD (in which dietary carbohydrate content is reduced to make way for greater fat content) results in less glucose entering metabolism than when consuming a high carbohydrate diet, there was no reduction in glycogen content with HF-S feeding. Therefore the differential response observed when consuming a saturated fat or n-3 PUFA enriched diet suggests glucose metabolism is altered by the fatty acid composition of the diet. Reduced glycogen content may indicate that muscle glucose oxidation is stimulated by HF-n-3 (Rustan *et al.*, 1993). However, the theory

of the glucose-fatty acid or Randle cycle predicts that consumption of a HFD, by increasing the availability of fatty acids, should inhibit the use of glucose as a fuel and promote the metabolism of fatty acids, the current fuel in greatest abundance (Hue and Taegtmeyer, 2009; Randle *et al.*, 1963). Furthermore, increased intramyocellular fat content has been shown to be associated with reduced insulin-stimulated activity of the glycogen storage enzyme, glycogen synthase (Phillips *et al.*, 1996). It was important, therefore, to examine the effect of dietary fatty acid composition on intramyocellular fat accumulation.

Diets rich in saturated fat promote the deposition of fat not only in adipose tissue, but also in ectopic depots. One tissue affected is skeletal muscle, a site not primarily designed for fat storage (Mullen *et al.*, 2007; Simoncıkova *et al.*, 2002; Kim *et al.*, 2000). Enriching a HFD with n-3 PUFAs has been shown to ameliorate the increase in intramyocellular fat accumulation induced by a HF-S diet (Rossmeisl *et al.*, 2009). The current study extends this observation by showing that this effect occurs in a fibre type-dependent manner. The HF-S diet, but not the HF-n-3 diet, promoted the deposition of fat in the SO soleus muscle, whilst neither diet affected fat content in the FG-FOG EDL muscle. Muscles abundant in SO fibres predominantly store triglycerides, whilst muscles composed of FG and FOG fibres exhibit lower triglyceride content (Hwang *et al.*, 2001), and store energy predominantly as glycogen (Zierath and Hawley, 2004). Therefore, detection of changes in muscle fat content within the soleus by staining with Oil Red O probably reflects the capacity of this muscle to store triglycerides. In contrast, more sensitive methods may be needed to detect changes in muscle fat content in the EDL.

An additional observation was that the HF-S diet, but not HF-n-3 diet, promoted intramyocellular fat accumulation in muscles of predominantly mixed fibre type. There was a marked increase in fat content in the chiefly FG-FOG tibialis and vastus medialis muscles, as well as the mainly SO vastus intermedius muscle (Delp and Duan, 1996) in HF-S mice. There was also a moderate increase in fat deposition in the predominantly FG-FOG rectus femoris and vastus lateralis muscles (Delp and Duan, 1996) in the HF-S group, and a small increase in stored fat in the chiefly FG-FOG plantaris and mixed gastrocnemius muscles (Delp and Duan, 1996) of these mice. It was interesting that in these muscles of predominantly mixed fibre type in HF-S mice, the pattern of fat staining resembled a “checkerboard” appearance, with some fibres displaying intense staining and others devoid of colour. This pattern is typical of that observed when staining for other indicators of metabolic activity in muscles comprised of a mixed composition of fibre types (De Paepe *et al.*, 2009). As mixed fibre type muscles exhibited a “checkerboard” pattern of staining and the predominantly FG-FOG EDL muscle of HF-S mice exhibited mostly cells lacking staining for fat, we speculate that in HF-S mice the majority of cells stained positively for fat were oxidative in nature, whilst those devoid of colour were glycolytic fibres, which lack fat storage as a reflection of their typically glucose-dependent energy metabolism.

3.4.3 – Effect of Dietary Fatty Acid Composition on Oxidative Capacity

The current study shows that there is an altered profile of stored nutrient content following high fat overfeeding. This occurred in a dietary fatty acid- and muscle-dependent manner, despite unchanged composition of muscle fibre types. This

suggested that a reduction in the glycogen content in the soleus muscle of HF-n-3 mice may indicate an increase in glucose oxidation, stimulated by HF-n-3 (Rustan *et al.*, 1993). However, this speculation challenges the theory of the Randle cycle (Hue and Taegtmeyer, 2009; Randle *et al.*, 1963) in which glucose oxidation is believed to be inhibited by increased fatty acid availability. However, this system can be bypassed, as it has been shown that activation of AMP-activated protein kinase (AMPK) in skeletal muscle elicits both an increase in fatty acid oxidation (Saha *et al.*, 2000; Winder *et al.*, 1997) whilst at the same time enhancing both glucose uptake (Wojtaszewski *et al.*, 2002; Zheng *et al.*, 2001; Holmes *et al.*, 1999) and glycolytic flux (Holmes *et al.*, 1999), while reducing glycogen storage (Wojtaszewski *et al.*, 2002). This pathway may, therefore, play a role in the concomitant amelioration of muscle fat content and reduction in muscle glycogen storage in the soleus muscle with HF-n-3 feeding.

Staining muscle sections for succinic dehydrogenase (SDH) and NADH tetrazolium reductase (NADH-TR) provides a surrogate measure of oxidative capacity. SDH is an enzyme that plays key roles in both the citric acid cycle and the electron transport chain in mitochondria (Elliott and Elliott, 2001; Scheffler, 1998) and it is, therefore, a mitochondrial marker (den Hoed *et al.*, 2008; Bertoni-Freddari *et al.*, 2001). Because the NADH-TR reaction is reliant on the capacity of the electron transfer chain complex component, the capacity of NADH dehydrogenase to transfer electrons provides a measure of oxidation and energy generation (Troyer *et al.*, 1991). The present study shows that HF-n-3 feeding, but not HF-S, increases the potential oxidative capacity of skeletal muscle.

Theoretically, this increase in potential oxidative capacity could be due to a change in the proportions of the fibre types within the muscle, or to enhancement of the oxidation rate in specific fibre types. The results herein suggest that the change is due to a universal increase in oxidative capacity in all fibre types of the EDL and soleus muscle, leading to the speculation that this occurs as the result of a coordinate increase in the expression and/or activity of enzymes involved in oxidation in all fibre types. In particular, and as discussed in **Chapter 2**, n-3 PUFAs act as natural peroxisome proliferator activator receptor α (PPAR α) agonists (Hihi *et al.*, 2002), which may stimulate pathways of skeletal muscle fatty acid oxidation. It is known that when the coactivator of PPAR α expression, peroxisome proliferative activated receptor γ coactivator 1 α (PGC1 α), is overexpressed it results in a fibre type switch, promoting the development of fibres with greater oxidative capacity (Mortensen *et al.*, 2006; Lin *et al.*, 2002). Therefore the mechanism underlying the increased oxidative capacity following n-3 PUFA enrichment of a HFD requires further investigation.

3.4.4 – The Mechanisms behind the Differential Nutrient Storage and Oxidative Capacity in Response to Altered Dietary Fatty Acid Composition

It is speculated above that altered skeletal muscle oxidative capacity may contribute to the changes in glycogen and fat storage in the muscle. It is also suggested that AMPK may play a role in coordinating the concomitant reduction in glycogen content and the amelioration of intramyocellular fat accretion in the soleus muscle of HF-n-3 mice, as PPAR α has been implicated in the effects of n-3 PUFA consumption on promoting pathways of oxidation. The mechanism behind the differential pattern of nutrient

storage in skeletal muscle in response to changes in dietary fatty acid consumption, with respect to fibre type will be investigated in later chapters. These chapters will focus on the effects of dietary fatty acid content on skeletal muscle fatty acid metabolism (see **Chapter 4**) and glycogen content, by examining the influence of dietary fatty acid composition on skeletal muscle glucose metabolism (see **Chapter 6**).

3.4.5 – Limitations

This study would have benefited from a larger sample size as male (n=3 per group) and female (n=2-3 per group) mice from cohort 2 were combined in analyses to enhance statistical power. Furthermore, studies in untrained male and female humans have suggested that although muscle fibre type composition is not gender-specific, the area occupied by slow-twitch fibres is greater in women, and the area occupied by fast-twitch fibres is greater in men (Staron *et al.*, 2000). Therefore, a greater sample size of male and female mice in future studies would allow exploration and comparison of the effects of diet on muscle fibre type with respect to gender.

3.4.6 – Summary

Previous studies have shown that skeletal muscle oxidative capacity may be increased with n-3 PUFA enrichment of a HFD (Kuda *et al.*, 2009; Pérez-Echarri *et al.*, 2009), providing protection against diet-induced insulin resistance. This study is the first to demonstrate that while the dietary fatty acid content of a HFD influenced the oxidative capacity of skeletal muscle, it did not alter the percentage composition of muscle fibres within the individual muscles. As expected, the HF-S diet induced ectopic fat

deposition in skeletal muscle, particularly in SO muscle fibres. Importantly, this effect was ameliorated by HF-n-3 feeding, suggesting that oxidative capacity increased with HF-n-3 consumption. Subsequent testing supported this suggestion by revealing enhanced staining for enzymes that reflect oxidative capacity in the muscle fibres of HF-n-3 fed mice. Interestingly, muscle glycogen content in the SO soleus muscle was also reduced with HF-n-3 feeding. The concurrent reduction in stored muscle fuels, glycogen and fat, in response to HF-n-3 feeding suggests that this diet results in the concurrent activation of both fatty acid and glucose oxidation. However, further research is required to elucidate the effects of n-3 PUFA enrichment of a HFD on fatty acid and glucose metabolism in muscles with mainly SO or FG-FOG characteristics.

CHAPTER 4

*The Effect of Dietary Fatty Acid Composition,
Muscle Fibre Type and Gender on Skeletal
Muscle Fatty Acid Metabolism in Mice*

4.1 – INTRODUCTION

Diets rich in saturated fat stimulate the ectopic deposition of fat in peripheral tissues such as skeletal muscle (Mullen *et al.*, 2007; Simončíkova *et al.*, 2002; Kim *et al.*, 2000b). Acute exposure to a high saturated fat diet (HF-S) in lean individuals stimulates fatty acid oxidation, and as a consequence excess fatty acids are cleared (Blaak *et al.*, 2006; Cameron-Smith *et al.*, 2003). The clearance of surplus fatty acids occurs in part through the uptake of fatty acids into skeletal muscle and their subsequent disposal by oxidation in healthy normally functioning muscle (Cameron-Smith *et al.*, 2003). In contrast, obese individuals exhibit an impaired response to the increased fatty acid availability of HF-S consumption, with a slower adaptive increase in fatty acid oxidation (Blaak *et al.*, 2006; Schrauwen *et al.*, 1997; Thomas *et al.*, 1992). The inability to appropriately switch to the use of fatty acids in the face of increased fatty acid availability, is a hallmark of metabolic inflexibility (Storlien *et al.*, 2004). Obese individuals have been shown to exhibit impaired whole-body metabolic flexibility (Zurlo *et al.*, 1990). Furthermore, in obese females, the oxidation of palmitate in skeletal muscle is depressed by 50% (Kim *et al.*, 2000a); this may therefore play a causal role in increased intramyocellular fat storage (Mullen *et al.*, 2007; Simončíkova *et al.*, 2002; Kim *et al.*, 2000b) (also see **Chapter 3**).

Whilst some studies have shown that skeletal muscle oxidative capacity is impaired as a consequence of obesity (Han *et al.*, 2007; Holloway *et al.*, 2007b; Thyfault *et al.*, 2004; Kim *et al.*, 2000a), and this may contribute to ectopic fat deposition, several mechanisms may be responsible for intramyocellular triglyceride accumulation. The

dysfunction of two other major pathways regulating skeletal muscle fatty acid metabolism, besides impaired oxidation, have also been implicated; fatty acid uptake and triglyceride lipolysis (Smith *et al.*, 2007; Guillerm-Regost *et al.*, 2006; Marotta *et al.*, 2004; Kim *et al.*, 2003; McAinch *et al.*, 2003; Jeukendrup, 2002). Skeletal muscle fatty acid uptake is enhanced in obese individuals (Han *et al.*, 2007; Chabowski *et al.*, 2006; Steinberg *et al.*, 2004; Luiken *et al.*, 2001; Berk *et al.*, 1997) and a corresponding increase in the expression of fatty acid transporters, fatty acid translocase (FAT/CD36) (Smith *et al.*, 2007; McAinch *et al.*, 2003) and fatty acid transport protein 1 (FATP1) (Marotta *et al.*, 2004) is observed with HF-S feeding. Furthermore, skeletal muscle triglyceride lipolysis is suppressed by HF-S feeding (Kim *et al.*, 2003), concurrent with reduced mRNA content of muscle lipolytic enzyme, hormone sensitive lipase (HSL) (Guillerm-Regost *et al.*, 2006). Therefore the concurrent increased flux of fatty acids entering the muscle, reduced breakdown of triglyceride stores and diminished capacity for fatty acid oxidation may all contribute to the increased intramyocellular fat accumulation observed with HF-S feeding.

In **Chapter 3** the importance of the fatty acid composition of the high fat diet (HFD) in determining its impact on intramyocellular triglyceride storage was highlighted. Whilst HF-S feeding induced a striking increase in intramyocellular fat accumulation, replacement of 7.5% of saturated fat with n-3 polyunsaturated fatty acids (PUFA) in a HF-S diet prevented the increase in muscle triglyceride content (**Chapter 3**). Whilst several studies have examined the reason for intramyocellular fat accumulation as a consequence of diet-induced obesity, the mechanism by which n-3 PUFAs prevent intramuscular fat deposition is not clear. In the liver, n-3 PUFA enrichment of a HFD

reduces storage (Pérez-Echarri *et al.*, 2009) and increases oxidation (Buettner *et al.*, 2006; Ukropec *et al.*, 2003) of fatty acids. Similarly, n-3 PUFAs may inhibit lipogenesis and stimulate fatty acid oxidation in skeletal muscle (Kuda *et al.*, 2009; Pérez-Echarri *et al.*, 2009). However, both of these studies were conducted in skeletal muscle of mixed fibre type. The composition of muscle fibres within skeletal muscle is known to determine the dynamic characteristics of the whole-muscle. Therefore, further research is required to elucidate the effects of n-3 PUFA enrichment of a HFD on skeletal muscle fatty acid metabolism in muscles with mainly slow-twitch oxidative (SO) or fast-twitch glycolytic (FG) and oxidative-glycolytic (FOG) characteristics.

Recent research has also revealed a gender dimorphic response to high fat feeding in rats (Català-Niell *et al.*, 2008; Priego *et al.*, 2008). Priego and colleagues (Priego *et al.*, 2008) showed that female rodents more aptly handle the fuel excess of a HFD, with elevated adipose tissue storage and enhanced capacity for fatty acid oxidation in muscle. In comparison, male rodents exhibit less efficient adipose tissue storage, with enhanced hepatic fatty acid oxidation rate and greater hepatic triglyceride storage, which may relate to reduced insulin sensitivity. The vast majority of studies investigating the partial replacement of saturated fat with n-3 PUFAs were conducted in male rodents, and it is unknown whether there is a gender dimorphic response to altered dietary fatty acid composition.

In the current study, I therefore aimed to determine:

- I. the mechanism by which replacing 7.5% of saturated fat with n-3 PUFAs (derived from fish oil) in a high saturated fat diet reduced intramyocellular fat accretion in mice. In doing so, I aimed to determine the effect of dietary fatty acid composition on fatty acid metabolism in the white FG-FOG extensor digitorum longus muscle (EDL) and red SO soleus muscle by specifically examining the mRNA content of key genes involved in:
 - i) fatty acid uptake
 - ii) lipogenesis and triglyceride storage
 - iii) fatty acid utilisation
- II. the effect of muscle fibre type on the mRNA content of key genes involved in skeletal muscle fatty acid metabolism in mice; i.e., white FG-FOG EDL as compared to red SO soleus muscle
- III. the influence of gender on the mRNA content of key genes involved in skeletal muscle fatty acid metabolism in mice.

In relation to aim (I) I hypothesised that replacement of 7.5% of saturated fat with n-3 PUFAs prevents the ectopic deposition of fat in skeletal muscle (as described in **Chapter 3**) by:

- i) promoting the mRNA expression of genes influencing the uptake of fatty acids into skeletal muscle
- ii) preventing the mRNA expression of genes controlling lipogenesis and
- iii) upregulating the mRNA expression of genes that would lead to enhanced oxidation.

In relation to aim (II) I hypothesised that the mRNA content of genes influencing fatty acid metabolism would be greater in the SO soleus muscle, a muscle that predominantly utilises fatty acids as substrate, as compared to the FG-FOG EDL muscle, which primarily uses glucose as substrate.

And finally, in relation to aim (III) I hypothesised that the female mice, given their increased propensity for liver fat storage (see **Chapter 2**), would exhibit greater mRNA content of genes influencing fatty acid uptake and storage, as compared to male mice.

4.2 – MATERIALS AND METHODOLOGY

4.2.1 – *Animals, Nutrition Regime and Tissue Collection*

As described in **Chapter 2 Section 2.1**, male and female C57BL/6J mice in cohort 1 were provided either a standard chow (control, C), high saturated fat (HF-S) or high fat n-3 PUFA enriched (HF-n-3) diet for 14 weeks (\pm 4 days). All procedures were approved by the University of Adelaide Animal Ethics Committee and the Institute of Medical and Veterinary Science Animal Ethics Committee. As described in **Chapter 2 Section 2.2**, following the experimental dietary period, surgery was performed on mice, whilst in the fed-state, to collect skeletal muscles; muscles were subsequently snap frozen in liquid nitrogen and stored under liquid nitrogen vapour phase storage until later analyses. The whole EDL and soleus muscles of the left leg were used for the extraction of RNA and subsequent mRNA content analyses.

4.2.2 – *Extraction of RNA from Skeletal Muscle Samples*

Total RNA from whole EDL and soleus muscles was isolated using TRIzol[®] reagent (Invitrogen Australia Pty Ltd, Mount Waverley, Victoria, Australia) at a volume of 800 μ l for tissue \leq 10 mg and 1,000 μ l for tissue $>$ 10 mg. Tissue samples were homogenised using 5 mm stainless steel beads (Qiagen GmbH, Hilden, Germany, Europe) and Qiagen TissueLyser (Qiagen GmbH, Hilden, Germany, Europe) set at 30 Hz for 2 minutes. The resultant homogenate was centrifuged at 13,200 rpm for 15 minutes at 4°C to pellet cell debris. The supernatant was collected and chloroform was added at a volume of 300 μ l for tissue \leq 10 mg and 400 μ l for tissue $>$ 10 mg, samples

were inverted several times and placed on ice for 5 minutes. Samples were then centrifuged at 13,000 rpm for 15 minutes at 4°C to separate RNA (upper-phase) from DNA and protein. The upper-phase was collected and 2-propanol was added at a volume of 400 µl for tissue ≤10 mg and 500 µl for tissue >10 mg, which was then incubated at -20°C for 2 hours to precipitate RNA. Samples were then centrifuged at 13,200 rpm for 20 minutes at 4°C to pellet RNA and subsequently, RNA pellets were washed with ethanol. RNA was re-suspended in nuclease free water and incubated at 60°C for 10 minutes. RNA quality and concentration were evaluated by measuring absorbance at 260 nm and 280 nm (NanoDrop 1000 Spectrophotometer (ThermoScientific Inc, Wilmington, Delaware, USA)). The ratio of OD260 to OD280 provided a score of RNA quality and all calculated ratios scored >1.8. RNA concentration was determined using the modified Beer-Lambert equation, where concentration (ng/µl) is equal to the absorbance at 260 nm (AU) multiplied by the extinction coefficient constant of RNA (40 ng-cm/µl) divided by the pathlength (cm). RNA was subsequently treated to eliminate genomic DNA contamination using deoxyribonuclease I (amplification grade; Invitrogen Australia Pty Ltd, Mount Waverley, Victoria, Australia). RNA integrity and deoxyribonuclease I efficiency were confirmed by ethidium bromide agarose gel electrophoresis. RNA was subsequently stored at -80°C, until incorporation into mRNA content analyses on the GenomeLab GeXP Genetic Analysis System (Beckman Coulter Inc, Fullerton, California, USA).

4.2.3 – Multiplex Primer Design

Forward and reverse primers were designed using the accession numbers of genes of interest (*mus musculus* mRNA transcripts). Accession numbers were imported into GenomeLab GeXP eXpress Profiler software (ver.10.0 Beckman Coulter Inc, Fullerton, California, USA). Primers were designed to generate amplified products with similar guanine (G)/cytosine (C) content (50%) and melting temperature (60°C). Primers utilised to amplify genes of interest in skeletal muscle samples were designed to generate an amplified product with a gene fragment length between 137-356 nucleotides and separation size of at least 6 nucleotides between products. Under additional constraints, primers were targeted to amplify a section of the protein coding sequence as determined by Entrez Nucleotide (National Center for Biotechnology Information, Bethesda, Maryland, USA). To ensure amplification of cDNA without unwanted amplification of contaminating DNA, where possible, forward and reverse primers were designed to be positioned in different exons, as determined by Ensembl (European Bioinformatics Institute/Wellcome Trust Sanger Institute, Cambridge, United Kingdom, Europe). Finally primer sequences were submitted to BLAST (Basic Local Alignment Search Tool, National Center for Biotechnology Information, Bethesda, Maryland, USA) to ensure primer sequences aligned specifically with the gene of interest. When aligned, if any mRNA sequence was found to have a high similarity defined by a probability (E value) of ≤ 0.05 , the primer was redesigned. The design software then added a universal primer sequence to both forward and reverse designed primer sequences, generating chimeric primers.

Resultant forward and reverse primers (GeneWorks Pty Ltd, Hindmarsh, South Australia, Australia) utilised to amplify genes of interest in skeletal muscle samples are listed in **Table 4.1**.

4.2.4 – Optimisation of Skeletal Muscle Multiplex

A reference muscle RNA sample was generated by combining equal parts of RNA from all muscle samples. Using the muscle reference RNA, primers designed to amplify muscle genes were tested in singlet reactions to ensure PCR products, when separated using the GenomeLab GeXP Genetic Analysis System, resulted in one well-defined peak at the assigned size (**Figure 4.1**). Primers that failed to generate one well-defined peak at the appropriate product size, such as those with unassigned peaks or those with poorly formed peaks, were redesigned and retested in further singlet reactions (**Figure 4.1**). Subsequently, using the muscle reference RNA, primers designed to amplify muscle genes were tested in multiplex reactions to ensure PCR products, when separated using the GenomeLab GeXP Genetic Analysis System, resulted in well-defined peaks of the sizes assigned. The concentrations of reverse primers, in multiplex, were then optimised (**Figure 4.2**) to ensure adequate detection of assigned product peaks (**Table 4.1**).

Table 4.1. The sequence, assigned product size and optimised concentration (in reverse multiplex mix) of primers used to determine the mRNA content of key genes of interest in skeletal muscle samples.

Gene (Accession number)	Forward primer sequence (5'-3') Reverse primer sequence (5'-3')	Size (bp)	[Primer] reverse mix (nM)
DGAT1 (NM_010046)	GATCTGAGGTGCCATCGTCT GGATCAGCATCACACACAC	137	125
PDK4 (NM_013743)	CCATGAGAAGAGCCCAGAAG ATGCCTTGAGCCATTGTAGG	145	16.63
SCD1 (NM_009127)	CTATGGATATCGCCCCTACG TAGTCGAAGGGGAAGGTGTG	151	16.63
PPAR δ/β (NM_011145)	CGGGAAGAGGAGAAAGAGGA GAGGAAGGGGAGGAATTCTG	159	125
Slc27a4 (FATP4) (NM_011989)	CAGTGAGATGGCCTCAGCTA TCCAGAAGAGGGTCCAGATG	166	500
Slc27a1 (FATP1) (NM_011977)	GCAGGTACTACCGCATTGCT AACCCGTAGATGACGCACTG	173	500
INSIG1 (NM_153526)	GACGAGGTGATAGCCACCAT TGGCCATTCTCTCTTGAAC	179	500
ACC- β (NM_133904)	TGGAGTCCATCTTCCTGTCC GGACGCCATACAGACAACCT	186	125
UCP3 (NM_009464)	GATGTGGTGAAGGTCCGATT GGCATTCTTGATGTTGG	193	31.25
SIRT1 (NM_019812)	GACGCTGTGGCAGATTGTTA GTCAGGAATCCCACAGGAGA	200	1500
AMPK α 2 (NM_178143)	TGATCAGCACTCCGACAGAC TCAGGTCCCTATGGACAACC	214	500
POLR2C (NM_009090)	TGAGGTGCAATGAAGACCAG CTTGGCATAGGCTCGAAGTC	222	250
HK2 (NM_013820)	TCTCTGAAGCTGAGCCATGA CGGAAGTTTGTTCCTCCAAG	228	125
PFK-M (NM_021514)	TGGCACAGTGATTGGAAGTG TGATCTTCCCGTCTTTCTGG	234	16.63
SREBF1 (NM_011480)	GCAGTCTGCTTTGGAACCTC GAAGCAGCAAGATGTCCTCC	242	500
SOCS3 (NM_007707)	CAGCTCCAAAAGCGAGTACC GGATGCGTAGGTTCTTGGTC	249	500
FABPpm (NM_010325)	GCGGTTTTGACTTCTCTGGA CCAGGCATCCTTATCACCAT	255	62.5

Gene-specific forward and reverse primer sequences are flanked by a common universal primer sequence at the 5' end:

Forward universal = aggtgacactatagaata; Reverse universal = gtacgactcactataggga.

Table 4.1 (continued). The sequence, assigned product size and optimised concentration (in reverse multiplex mix) of primers used to determine the mRNA content of key genes of interest in skeletal muscle samples.

Gene (Accession number)	Forward primer sequence (5'-3') Reverse primer sequence (5'-3')	Size (bp)	[Primer] reverse mix (nM)
CPT1b (NM_009948)	GGTCGCTTCTTCAAGGTCTG AAGAAAGCAGCACGTTTCGAT	270	16.63
Lipe (HSL) (NM_001039507)	GGAACCTAAGTGGACGCAAGC TTGACATCAGAGGGGTGTGGA	277	500
FAT/CD36 (NM_007643)	GCTCTCCCTTGATTCTGCTG TGGGTTTTGCACATCAAAGA	286	125
UCP2 (NM_011671)	TGCTGAGCTGGTGACCTATG GAAGGCATGAACCCCTTGTA	292	1,500
TBP (NM_013684)	GGACCAGAACAACAGCCTTC GTGGGTTGCTGAGATGTTGA	298	500
RPLP0 (NM_007475)	GCATCACCACGAAAATCTCC TACCCGATCTGCAGACACAC	305	250
PI3Kr1 (NM_001024955)	TGACGAGAAGACGTGGAATG TTGAGGGAGTCATTGTGCTG	313	62.5
PGC1 α (NM_008904)	GTACAACAATGAGCCTGCGA AGTGCTAAGACCGCTGCATT	332	500
PPAR α (NM_001113418)	ACGATGCTGTCCTCCTTGAT TCATCTGGATGGTTGCTCTG	339	500
GYS1 (NM_030678)	GAATCCAGGAATTTGTGCGT TCGTAGAGCTTCCTCCCAA	347	500
AMPK α 1 (NM_00103367)	AGCCGACTTTGGTCTTTCAA ATCTTTTATTGCGGCCCTCT	356	1,500
Gene-specific forward and reverse primer sequences are flanked by a common universal primer sequence at the 5' end: Forward universal = agtgacactatagaata; Reverse universal = gtacgactcactataggga.			

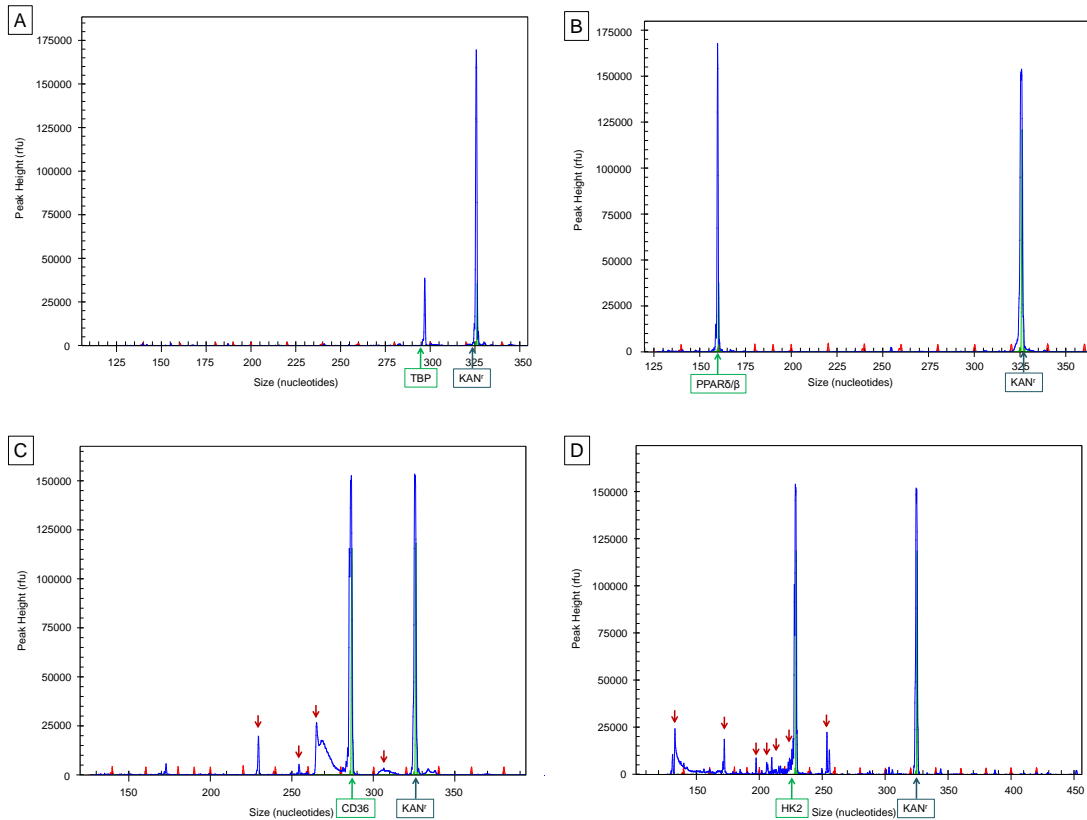


Figure 4.1 [A-D]. Resultant peaks of separated PCR products detected using the GenomeLab GeXP Genetic Analysis System during singlet primer testing. Singlet primer testing was successful if product was separated as a single well-defined peak at the assigned size [A, B], and unsuccessful if product was separated and unassigned peaks were generated [C, D].

Peaks shown in blue are product peaks, red peaks are size marker peaks, red arrows indicate unassigned peaks (requiring primer redesign). KAN^r is an internal control.

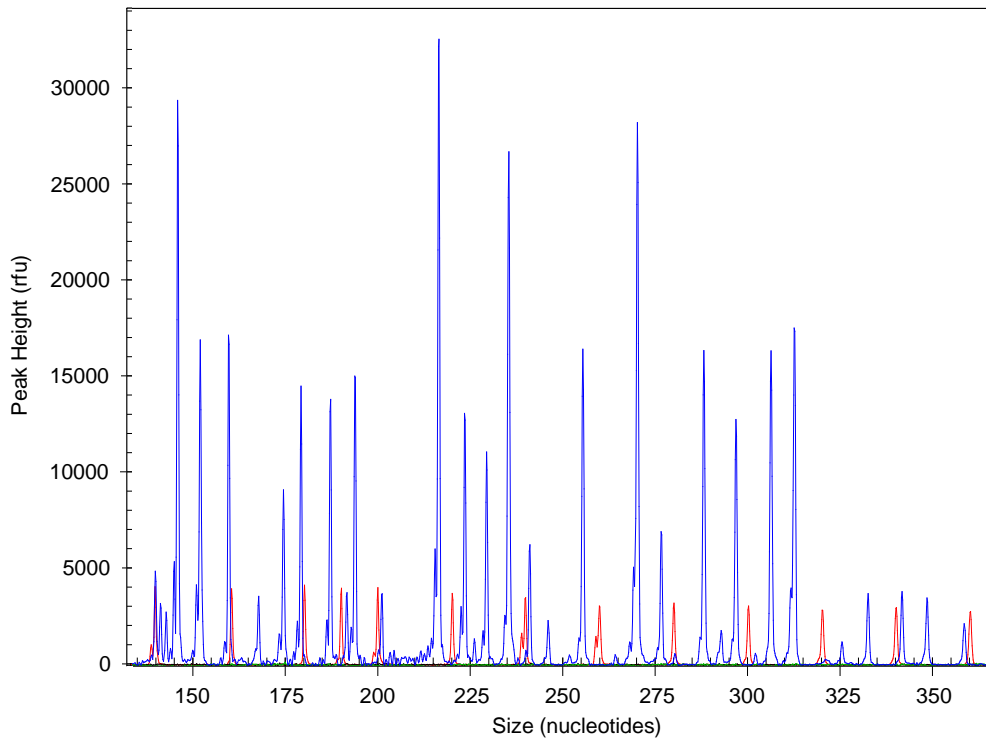


Figure 4.2. Resultant peaks of separated PCR products detected using the GenomeLab GeXP Genetic Analysis System during multiplex primer testing.

Peaks shown in blue are product peaks, red peaks are size marker peaks.

Multiplex primer testing was successful if products were separated as well-defined peaks at the assigned sizes. Primer concentrations were attenuated to ensure adequate signal detection of all separated products.

4.2.5 – Reverse Transcription of RNA Samples to Generate cDNA

Using RNA extracted from EDL and soleus muscles, cDNA was generated by reverse transcription. Reverse transcription, using the GenomeLab GeXP Genetic Analysis System, acts to generate cDNA of gene-specific sequences with a flanking universal sequence (**Figure 4.3**). In a total 20 µl reaction volume, 4 µl GenomeLab™ GeXP RT Buffer (5x)*, 5 µl GenomeLab™ GeXP KAN^r RNA with RI* as an internal control, 2 µl custom reverse chimeric primer “multiplex” mix, 5 µl template RNA sample, 1 µl GenomeLab™ GeXP Reverse Transcriptase* and 3 µl GenomeLab™ GeXP DNase/RNase Free water* were combined (*GenomeLab GeXP Start Kit, Beckman Coulter Inc, Fullerton, California, USA). The reverse transcription reaction was performed on the Eppendorf Mastercycler® Gradient (Eppendorf South Pacific Pty Ltd, North Ryde, New South Wales, Australia) incubated under the following program: 48°C for 1 minute, 42°C for 60 minutes and 95°C for 5 minutes, followed by a hold step at 4°C. Reverse transcription was performed in duplicate and resultant duplicate cDNA samples were combined.

4.2.6 – Polymerase Chain Reaction (PCR)

Using cDNA generated by reverse transcription of RNA from EDL and soleus muscles, PCR was performed to generate a double-stranded template. PCR, using the GenomeLab GeXP Genetic Analysis System is performed over 35 cycles, with cycle 1 and 2 being gene-specific primer driven, producing amplicons with universal tags at each end, and cycles 3 and onwards being universal primer driven, where templates are

amplified and labelled with dye for detection (**Figure 4.3**). In a total 20 μ l reaction volume, 4 μ l GenomeLab[™] GeXP PCR Buffer (5x) (GenomeLab GeXP Start Kit, Beckman Coulter Inc, Fullerton, California, USA), 4 μ l 25mM magnesium chloride (Thermo Fisher Scientific, Epsom, Surrey, UK), 2 μ l custom forward chimeric primer “multiplex” mix, 9.3 μ l cDNA sample, 0.7 μ l Thermo-Start Taq DNA Polymerase (Thermo Fisher Scientific, Epsom, Surrey, UK) were combined. The PCR reaction was performed on the Eppendorf Mastercycler[®] Gradient incubated under the following program: 1 cycle of 95°C for 10 minutes, followed by 35 cycles of 94°C for 30 seconds, 55°C for 30 seconds and 68°C for 1 minute, followed by 1 cycle of 72°C for 2 minutes and a hold step at 4°C. PCR was performed in duplicate and resultant duplicate PCR products were combined. To avoid possible contamination, RT and pre-PCR set up were prepared in a location physically separated from preparation using post-PCR products. Negative controls (no template control and no reverse transcriptase control) were also run to ensure reactions were contaminant free.

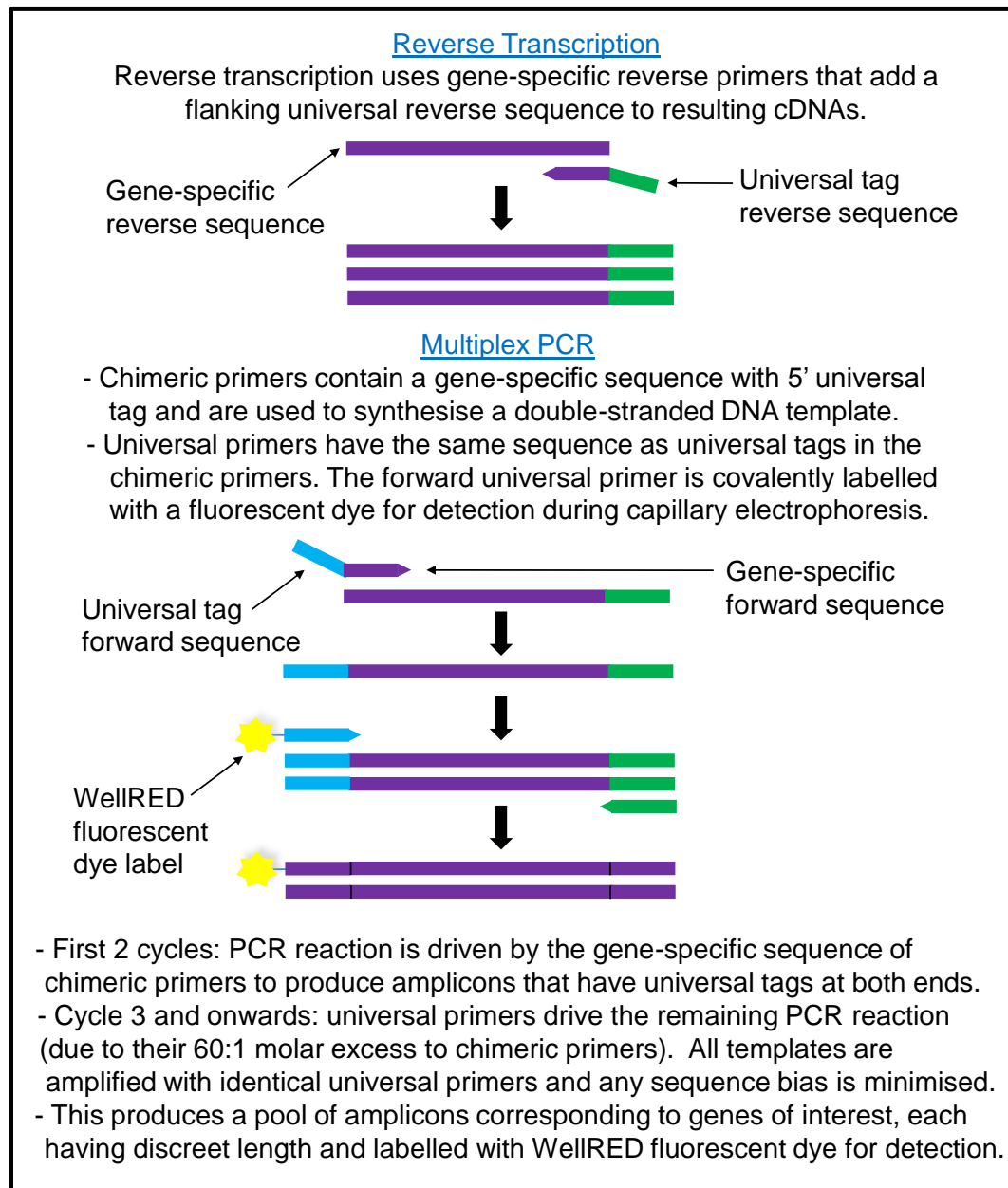


Figure 4.3. Description of multiplex reverse transcription and PCR reactions using the GenomeLab GeXP Genetic Analysis System.

4.2.7 – Separation of PCR Products by the GenomeLab GeXP Genetic Analysis System

Multiplex detection via capillary electrophoresis was then performed; fluorescently labelled PCR products were separated, detected and quantified using the GenomeLab GeXP Genetic Analysis System. In a total 40 µl reaction volume, 1 µl PCR product, 38.75 µl GenomeLab™ GeXP Sample Loading Solution and 0.25 µl GenomeLab™ GeXP DNA Size Standard-400 (GenomeLab GeXP Start Kit, Beckman Coulter Inc, Fullerton, California, USA) were added to wells of a 96-well plate. An overlaying drop of mineral oil was used to protect dyes and increase their stability. Reagents were then consolidated to the bottom of the 96-well plate by brief centrifugation at 1,500 rpm. Plates were loaded onto the GenomeLab GeXP Genetic Analysis System and PCR products were separated. Separated fragments were analysed using sensitive analysis parameters (slope threshold = 1, peak height threshold = 0) and GenomeLab eXpress Profiler software (ver.10.0 Beckman Coulter Inc, Fullerton, California, USA). Multiplex detection was performed in duplicate for every sample and data were combined to generate the mean of duplicate analyses. Output mRNA contents were then normalised to the average mRNA content of 3 housekeeping genes, TATA-binding protein (TBP), RNA Polymerase 2c (POLR2c) and large ribosomal protein P0 (RPLP0), to compensate for variation in reverse transcription efficiency. Housekeeping genes were validated to show absolute mRNA content remained unchanged between groups. Results are reported as mRNA content, the ratio of mean mRNA content of the target gene relative to the averaged mean mRNA content of three housekeeping genes (AU).

4.2.8 – *Statistical Analyses*

All data are presented as mean \pm standard error of the mean (SEM). Two-way Analysis of Variance (ANOVA), with pairwise comparisons (Bonferroni post-hoc analysis), was used to determine the effect of diet (C, HF-S, HF-n-3), muscle fibre type (EDL, soleus), gender (male, female) and their interaction on the mRNA content of key fatty acid metabolism genes. Simple linear regression analyses were used to determine the relationship of liver fat accumulation with the skeletal muscle mRNA content of pyruvate dehydrogenase kinase 4 (PDK4), fatty acid translocase (FAT/CD36) and peroxisome proliferative activated receptor γ coactivator 1 α (PGC1 α); plasma triglyceride concentration with skeletal muscle peroxisome proliferator activator receptor α (PPAR α) mRNA content; and plasma glucose concentration with skeletal muscle diacylglycerol acyltransferase 1 (DGAT1) and PPAR α mRNA content. Pearson correlation coefficients (r) were used to evaluate linear relationships.

All statistics were performed using the Statistical Package for Social Scientists (SPSS) (ver. 17.0.0, SPSS Inc, Chicago, Illinois, USA). A probability of less than 5% ($P < 0.05$) was considered statistically significant. Analyses are reported as percentage change; statistical effect: F(degrees of freedom: between subjects effect, degrees of freedom: within subjects effect) = F value, P value of effect; and subsequent P values of post-hoc or pairwise analyses.

4.3 – RESULTS

4.3.1 – Fatty Acid Transport (FAT/CD36, FABPpm, FATP1 and FATP4)

Fatty acid translocase (FAT/CD36) mRNA content was greater in HF-n-3 mice as compared to control and HF-S mice ($F(2, 114)=43.2, P\leq 0.001$; +44%, +23%, respectively; post-hoc tests: $P\leq 0.001$) and in HF-S mice as compared to control mice (+17%; post-hoc test: $P\leq 0.001$) (**Figure 4.4**). There was an effect of muscle fibre type on FAT/CD36 mRNA content, the soleus muscle exhibited greater FAT/CD36 mRNA as compared to the EDL muscle (+104%; $F(1, 114)=514.5, P\leq 0.001$). There was no significant effect of gender on FAT/CD36 mRNA content, although there was a trend towards increased FAT/CD36 mRNA in male mice as compared to female mice ($F(1, 114)=2.7, P=0.10$).

There was no effect of diet ($F(2, 114)=1.9, P=0.16$) on fatty acid binding protein (FABPpm) mRNA content. There was an effect of muscle fibre type on FABPpm mRNA content, the soleus muscle exhibited greater FABPpm mRNA as compared to the EDL muscle (+32%; $F(1, 114)=86.3, P\leq 0.001$) (**Figure 4.5**). There was no effect of gender on FABPpm mRNA content ($F(1, 114)=0.04, P=0.85$).

Fatty acid transport protein 1 (FATP1) mRNA content was greater in HF-S and HF-n-3 mice as compared to control mice ($F(2, 113)=13.6, P\leq 0.001$; +22%, +41%, respectively; post-hoc tests: $P\leq 0.005, P\leq 0.001$, respectively) (**Figure 4.6**). There was a gender*muscle interaction on FATP1 mRNA content ($F(1, 113)=4.8, P=0.031$), in both male and female mice, the soleus muscle exhibited greater FATP1 mRNA as compared

to the EDL muscle (+38%, +79%, respectively; pairwise comparisons: $P \leq 0.001$) and in the EDL muscle, male mice exhibited greater FATP1 mRNA as compared to female mice (+29%; pairwise comparison: $P \leq 0.001$).

Fatty acid transport protein 4 (FATP4) mRNA content was greater in HF-n-3 mice as compared to control mice ($F(2, 113)=4.9$, $P=0.009$; +21%; post-hoc test: $P \leq 0.02$) (**Figure 4.7**). There was also a trend towards greater FATP4 mRNA content in HF-n-3 mice as compared to HF-S mice (+13%; post-hoc test: $P=0.088$). There was an effect of muscle fibre type on FATP4 mRNA content, the soleus muscle exhibited greater FATP4 mRNA as compared to the EDL muscle (+22%; $F(1, 113)=13.0$, $P \leq 0.001$). There was no effect of gender on FATP4 mRNA content ($F(1, 113)=0.003$, $P=0.96$).

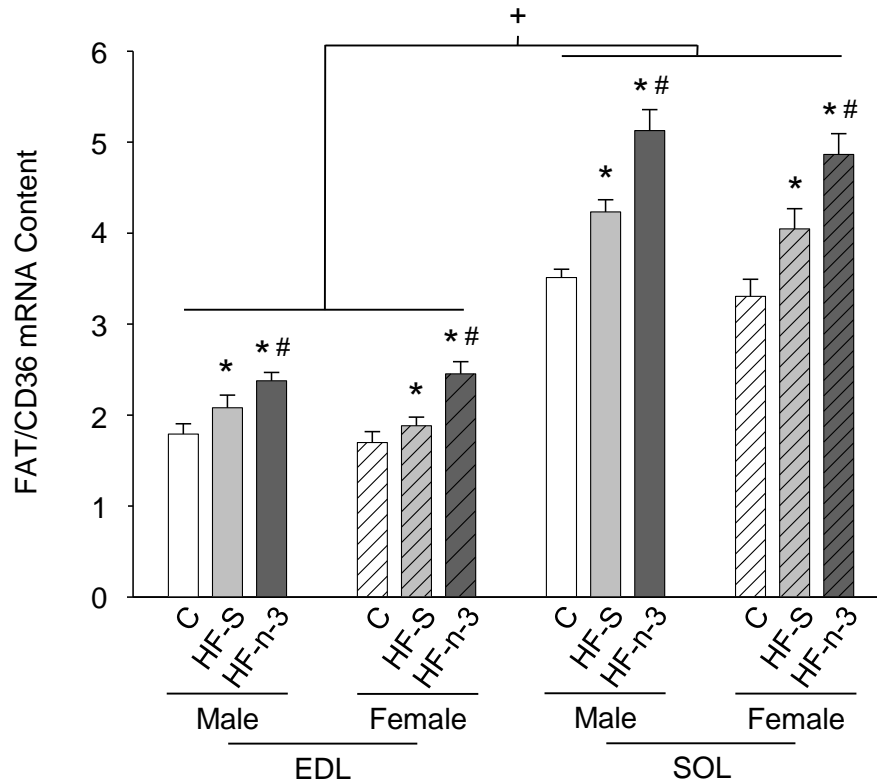


Figure 4.4. FAT/CD36 mRNA content in the white extensor digitorum longus and red soleus muscles of male and female mice fed control, high saturated fat or high fat n-3 PUFA enriched diets.

Data are expressed as mean (bars) \pm SEM (error bars), where solid bars indicate male (M) mice, lined bars indicate female (F) mice and colour represents diet: white, control (C); pale grey, high saturated fat (HF-S); dark grey, high fat n-3 polyunsaturated fatty acid enriched (HF-n-3). EDL, extensor digitorum longus muscle; SOL, soleus muscle; FAT/CD36, fatty acid translocase.

n: EDL - C(M/F) = 10/12, HF-S(M/F) = 11/11, HF-n-3(M/F) = 9/11;

n: SOL - C(M/F) = 10/12, HF-S(M/F) = 10/10, HF-n-3(M/F) = 9/11.

Statistics: Effect of diet: * $P \leq 0.001$, compared to C, # $P \leq 0.001$, compared to HF-S. Effect of muscle fibre type: + $P \leq 0.001$, SOL compared to EDL.

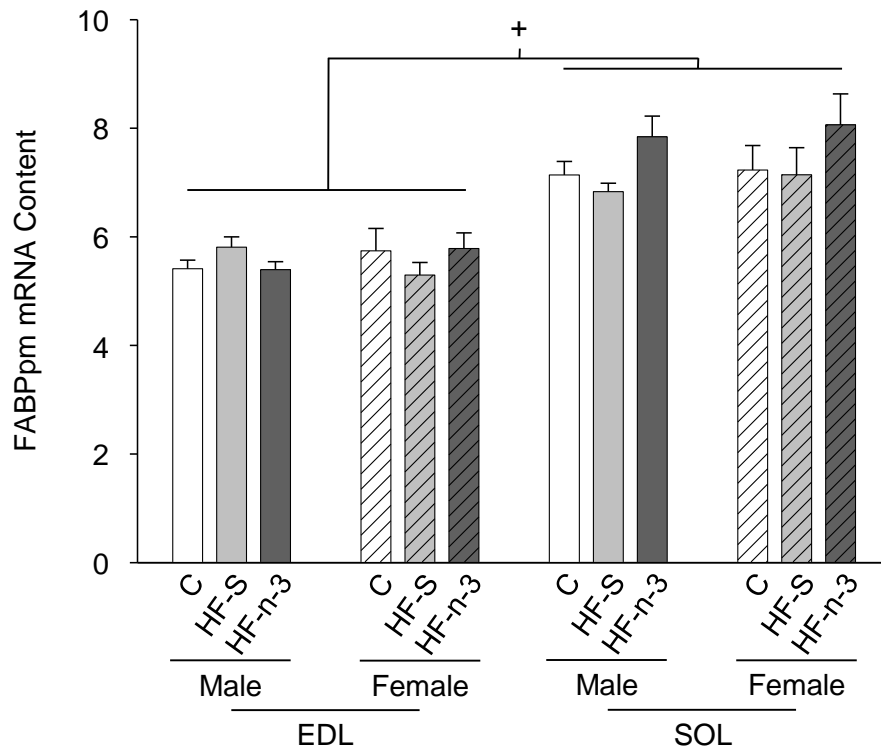


Figure 4.5. FABPpm mRNA content in the white extensor digitorum longus and red soleus muscles of male and female mice fed control, high saturated fat or high fat n-3 PUFA enriched diets.

Data are expressed as mean (bars) \pm SEM (error bars), where solid bars indicate male (M) mice, lined bars indicate female (F) mice and colour represents diet: white, control (C); pale grey, high saturated fat (HF-S); dark grey, high fat n-3 polyunsaturated fatty acid enriched (HF-n-3). EDL, extensor digitorum longus muscle; SOL, soleus muscle; FABPpm, fatty acid binding protein.

n: EDL - C(M/F) = 10/12, HF-S(M/F) = 11/11, HF-n-3(M/F) = 9/11;

n: SOL - C(M/F) = 10/12, HF-S(M/F) = 10/10, HF-n-3(M/F) = 9/11.

Statistics: Effect of muscle fibre type: $^+P \leq 0.001$, SOL compared to EDL.

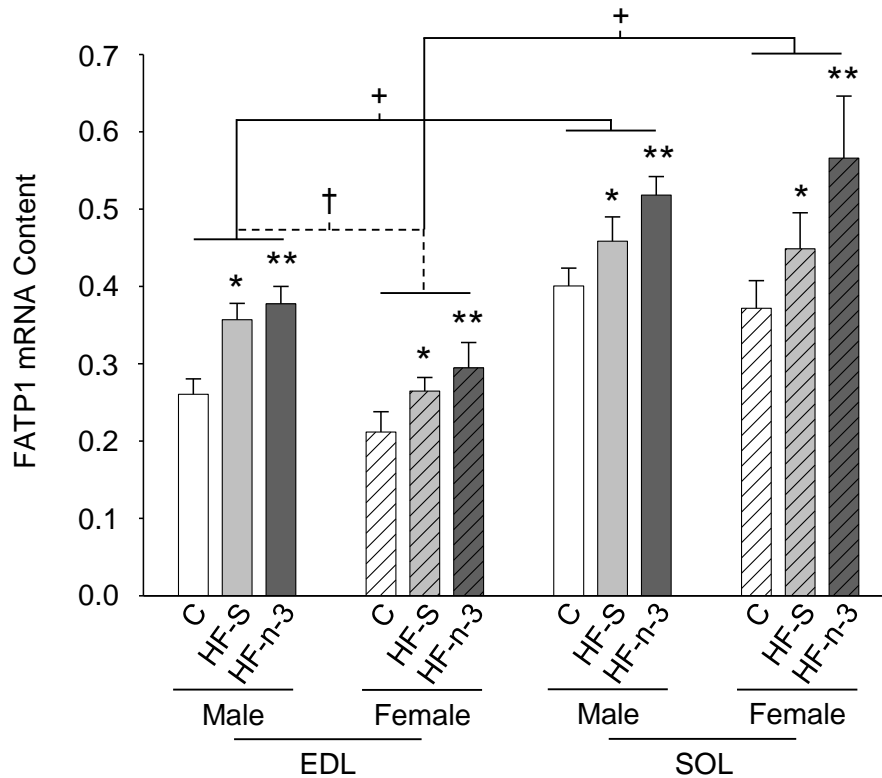


Figure 4.6. FATP1 mRNA content in the white extensor digitorum longus and red soleus muscles of male and female mice fed control, high saturated fat or high fat n-3 PUFA enriched diets.

Data are expressed as mean (bars) \pm SEM (error bars), where solid bars indicate male (M) mice, lined bars indicate female (F) mice and colour represents diet: white, control (C); pale grey, high saturated fat (HF-S); dark grey, high fat n-3 polyunsaturated fatty acid enriched (HF-n-3). EDL, extensor digitorum longus muscle; SOL, soleus muscle; FATP1, fatty acid transport protein 1.

n: EDL - C(M/F) = 10/11, HF-S(M/F) = 11/10, HF-n-3(M/F) = 9/11;

n: SOL - C(M/F) = 10/12, HF-S(M/F) = 10/10, HF-n-3(M/F) = 9/11.

Statistics: Effect of diet: * $P \leq 0.005$, ** $P \leq 0.001$ compared to C. Gender*muscle interaction: † $P \leq 0.001$, EDL compared to SOL (of same gender); †† $P \leq 0.001$, male compared to female (EDL).

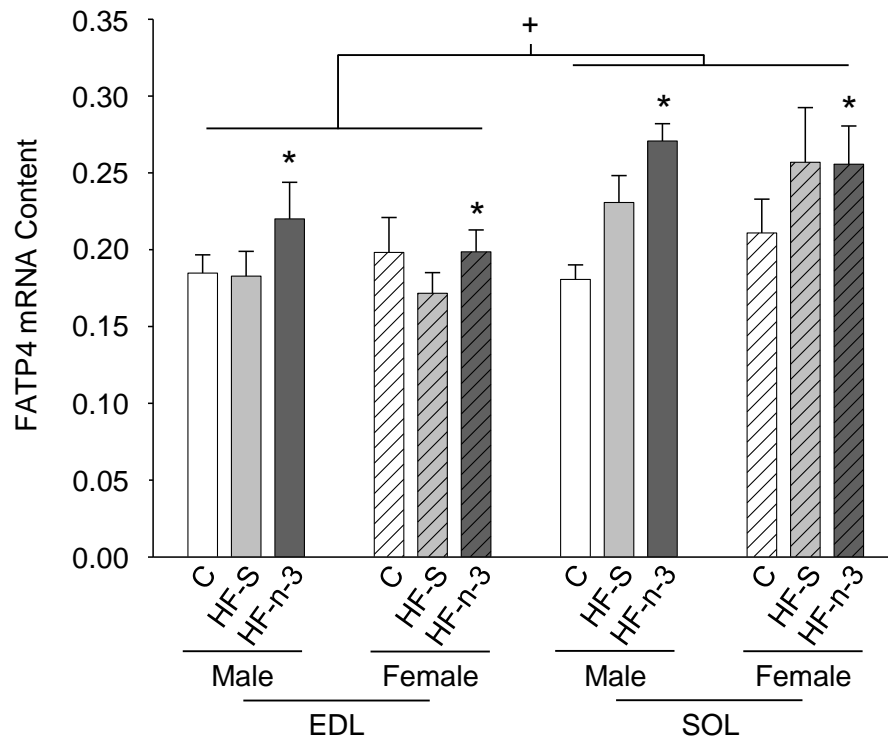


Figure 4.7. FATP4 mRNA content in the white extensor digitorum longus and red soleus muscles of male and female mice fed control, high saturated fat or high fat n-3 PUFA enriched diets.

Data are expressed as mean (bars) \pm SEM (error bars), where solid bars indicate male (M) mice, lined bars indicate female (F) mice and colour represents diet: white, control (C); pale grey, high saturated fat (HF-S); dark grey, high fat n-3 polyunsaturated fatty acid enriched (HF-n-3). EDL, extensor digitorum longus muscle; SOL, soleus muscle; FATP4, fatty acid transport protein 4.

n: EDL - C(M/F) = 10/11, HF-S(M/F) = 11/11, HF-n-3(M/F) = 9/11;

n: SOL - C(M/F) = 10/12, HF-S(M/F) = 10/10, HF-n-3(M/F) = 9/11.

Statistics: Effect of diet: $*P \leq 0.02$, compared to C. Effect of muscle fibre type: $^+P \leq 0.001$, SOL compared to EDL.

4.3.2 – Lipogenesis, Triglyceride Synthesis and Triglyceride Storage (*SREBF1*, *INSIG1*, *DGAT1*, *SCD1* and *HSL*)

Sterol regulatory element binding transcription factor 1 (*SREBF1*) mRNA content was greater in HF-S mice as compared to control mice ($F(2, 114)=3.7$, $P=0.027$; +27%; post-hoc test: $P\leq 0.02$) (**Figure 4.8**). There was a gender*muscle interaction on *SREBF1* mRNA content ($F(1, 114)=4.3$, $P=0.040$), in male mice, the soleus muscle exhibited lower *SREBF1* mRNA content as compared to the EDL muscle (-46%; pairwise comparison: $P\leq 0.001$) and in the EDL muscle, male mice exhibited greater *SREBF1* mRNA as compared to female mice (+24%; pairwise comparison: $P\leq 0.05$).

Insulin induced gene 1 (*INSIG1*) mRNA content was greater in HF-S mice as compared to control mice ($F(2, 114)=9.7$, $P\leq 0.001$; +21%; post-hoc test: $P\leq 0.02$) and was lower in HF-n-3 mice as compared to HF-S mice (-36%; post-hoc test: $P\leq 0.001$) (**Figure 4.9**). There was no effect of muscle fibre type ($F(1, 114)=1.0$, $P=0.33$) or gender ($F(1, 114)=0.3$, $P=0.59$) on *INSIG1* mRNA content.

There was a diet*muscle interaction on diacylglycerol acyltransferase 1 (*DGAT1*) mRNA content ($F(2, 113)=4.6$, $P=0.012$) (**Figure 4.10**), in the EDL muscle, HF-n-3 mice exhibited greater *DGAT1* mRNA as compared to control mice (+91%; pairwise comparison: $P\leq 0.02$) and in the soleus muscle, *DGAT1* mRNA was greater in HF-n-3 mice as compared to controls and HF-S mice (+143%, +49%, respectively; pairwise comparisons: $P\leq 0.001$) and in HF-S mice as compared to control mice (+64%; pairwise comparison: $P\leq 0.005$). In HF-S and HF-n-3 mice, the soleus muscle exhibited greater *DGAT1* mRNA as compared to the EDL muscle (+63%, +106%, respectively; pairwise

comparisons: $P \leq 0.005$, $P \leq 0.001$, respectively) and in control mice, there was also a strong trend towards greater DGAT1 mRNA content in the soleus muscle as compared to the EDL muscle (+61%; pairwise comparison: $P = 0.056$). There was an effect of gender on DGAT1 mRNA content, female mice exhibited greater DGAT1 mRNA than male mice (+19%; $F(1, 113) = 4.0$, $P = 0.048$).

There was a diet*muscle interaction on stearoyl-Coenzyme A desaturase 1 (SCD1) mRNA content ($F(2, 113) = 17.7$, $P \leq 0.001$) (**Figure 4.11**), in the EDL muscle, HF-n-3 mice exhibited lower SCD1 mRNA as compared to control and HF-S mice (-41%, -24%, respectively; pairwise comparisons: $P \leq 0.001$, $P \leq 0.02$, respectively) and in the soleus muscle, HF-n-3 mice exhibited lower SCD1 mRNA as compared to control and HF-S mice (-71%, -62%, respectively; pairwise comparisons: $P \leq 0.001$) and HF-S exhibited lower SCD1 mRNA as compared to controls (-23%; pairwise comparison: $P \leq 0.05$). There was also a trend in the EDL muscle towards lower SCD1 mRNA in HF-S mice as compared to controls (-22%; pairwise comparison: $P = 0.079$). In control and HF-S mice, the soleus exhibited greater SCD1 mRNA content as compared to the EDL muscle (+78%, +81%, respectively; pairwise comparisons: $P \leq 0.001$). There was also a gender*muscle interaction on SCD1 mRNA content ($F(1, 113) = 4.5$, $P = 0.036$), in male and female mice, the soleus muscle exhibited greater SCD1 mRNA content as compared to the EDL muscle (+6%, +13%, respectively; pairwise comparisons: $P \leq 0.02$, $P \leq 0.001$, respectively) and in the soleus muscle, female mice exhibited greater SCD1 mRNA content than male mice (+19%; pairwise comparison: $P \leq 0.005$).

Hormone sensitive lipase (HSL) mRNA content was greater in HF-n-3 mice as compared to control and HF-S mice ($F(2, 114)=11.8$, $P\leq 0.001$; +44%, +19%, respectively; post-hoc tests: $P\leq 0.001$, $P\leq 0.05$, respectively) (**Figure 4.12**). There was also a trend towards greater HSL mRNA content in HF-S mice as compared to controls (+20%; post-hoc test: $P=0.069$). There was an effect of muscle fibre type on HSL mRNA content, the soleus muscle exhibited greater HSL mRNA as compared to the EDL muscle (+64%; $F(1, 114)=72.9$, $P\leq 0.001$). There was no effect of gender on HSL mRNA content ($F(1, 114)=0.2$, $P=0.66$).

In HF-S-fed mice only, there was a significant negative correlation between plasma glucose concentrations and DGAT1 mRNA content in the EDL muscle ($r = -0.52$, $F(1, 20)=7.5$, $P=0.013$; male and female mice combined) and soleus muscle ($r = -0.51$, $F(1, 17)=6.0$, $P=0.026$; male and female mice combined) (**Figure 4.13**).

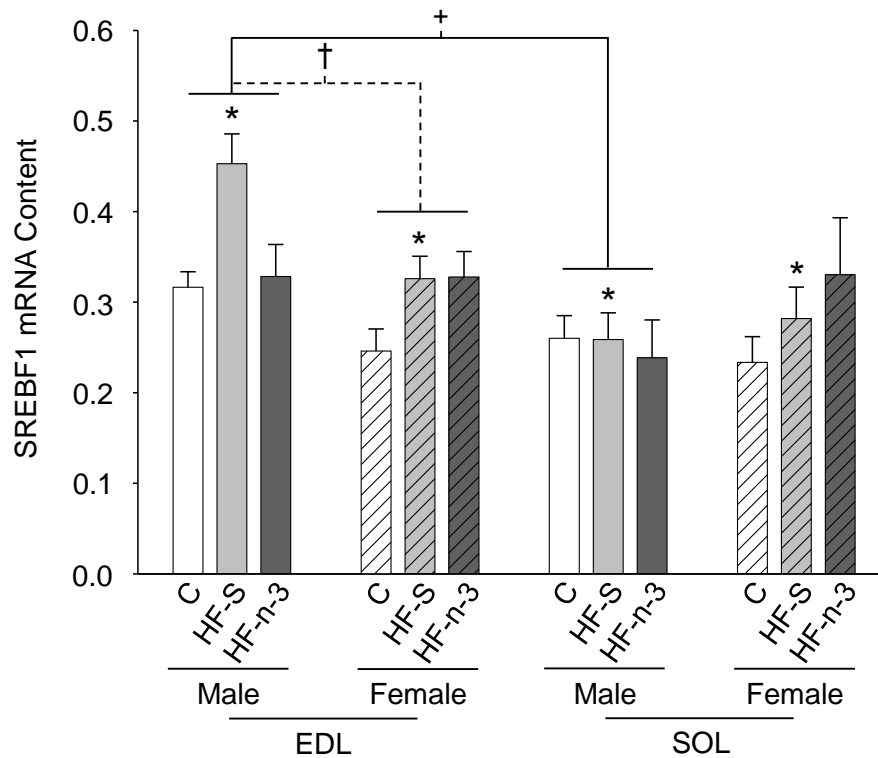


Figure 4.8. SREBF1 mRNA content in the white extensor digitorum longus and red soleus muscles of male and female mice fed control, high saturated fat or high fat n-3 PUFA enriched diets.

Data are expressed as mean (bars) \pm SEM (error bars), where solid bars indicate male (M) mice, lined bars indicate female (F) mice and colour represents diet: white, control (C); pale grey, high saturated fat (HF-S); dark grey, high fat n-3 polyunsaturated fatty acid enriched (HF-n-3). EDL, extensor digitorum longus muscle; SOL, soleus muscle; SREBF1, sterol regulatory element binding transcription factor 1.

n: EDL - C(M/F) = 10/12, HF-S(M/F) = 11/11, HF-n-3(M/F) = 9/11;

n: SOL - C(M/F) = 10/12, HF-S(M/F) = 10/10, HF-n-3(M/F) = 9/11.

Statistics: Effect of diet: * $P \leq 0.02$, compared to C. Gender*muscle interaction: † $P \leq 0.001$, male EDL compared to male SOL; † $P \leq 0.05$, male compared to female (EDL).

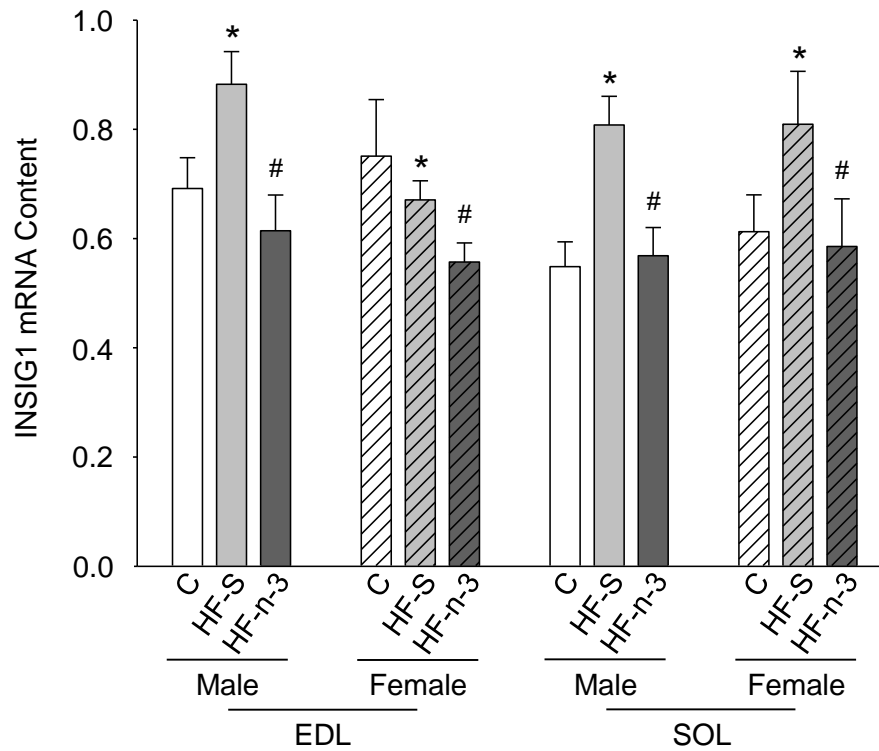


Figure 4.9. INSIG1 mRNA content in the white extensor digitorum longus and red soleus muscles of male and female mice fed control, high saturated fat or high fat n-3 PUFA enriched diets.

Data are expressed as mean (bars) \pm SEM (error bars), where solid bars indicate male (M) mice, lined bars indicate female (F) mice and colour represents diet: white, control (C); pale grey, high saturated fat (HF-S); dark grey, high fat n-3 polyunsaturated fatty acid enriched (HF-n-3). EDL, extensor digitorum longus muscle; SOL, soleus muscle; INSIG1, insulin induced gene 1.

n: EDL - C(M/F) = 10/12, HF-S(M/F) = 11/11, HF-n-3(M/F) = 9/11;

n: SOL - C(M/F) = 10/12, HF-S(M/F) = 10/10, HF-n-3(M/F) = 9/11.

Statistics: Effect of diet: * $P \leq 0.02$, compared to C; # $P \leq 0.001$, compared to HF-S.

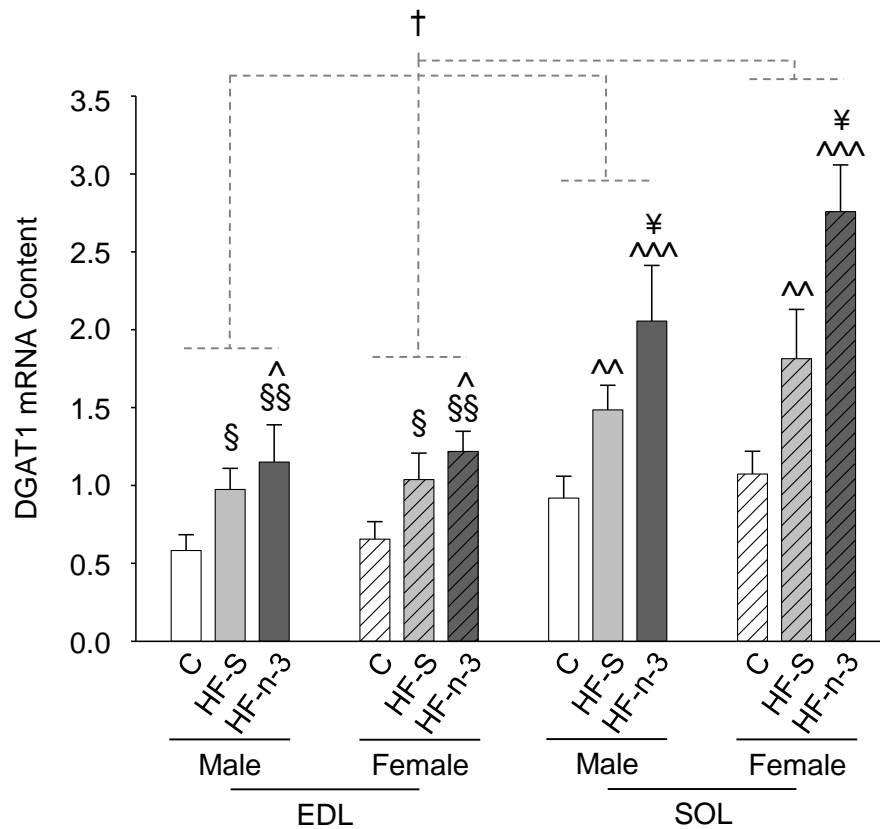


Figure 4.10. DGAT1 mRNA content in the white extensor digitorum longus and red soleus muscles of male and female mice fed control, high saturated fat or high fat n-3 PUFA enriched diets.

Data are expressed as mean (bars) \pm SEM (error bars), where solid bars indicate male (M) mice, lined bars indicate female (F) mice and colour represents diet: white, control (C); pale grey, high saturated fat (HF-S); dark grey, high fat n-3 polyunsaturated fatty acid enriched (HF-n-3). EDL, extensor digitorum longus muscle; SOL, soleus muscle; DGAT1, diacylglycerol acyltransferase 1.

n: EDL - C(M/F) = 10/12, HF-S(M/F) = 11/11, HF-n-3(M/F) = 9/11;

n: SOL - C(M/F) = 10/12, HF-S(M/F) = 10/9, HF-n-3(M/F) = 9/11.

Statistics: Diet*muscle interaction: $^{\wedge}P \leq 0.02$, $^{\wedge\wedge}P \leq 0.005$, $^{\wedge\wedge\wedge}P \leq 0.001$, compared to C (of same muscle); $^{\wedge}P \leq 0.001$, compared to HF-S (of same muscle); $^{\S}P \leq 0.005$, compared to HF-S (SOL); $^{\S\S}P \leq 0.001$, compared to HF-n-3 (SOL). Effect of gender: $^{\dagger}P \leq 0.05$, male compared to female.

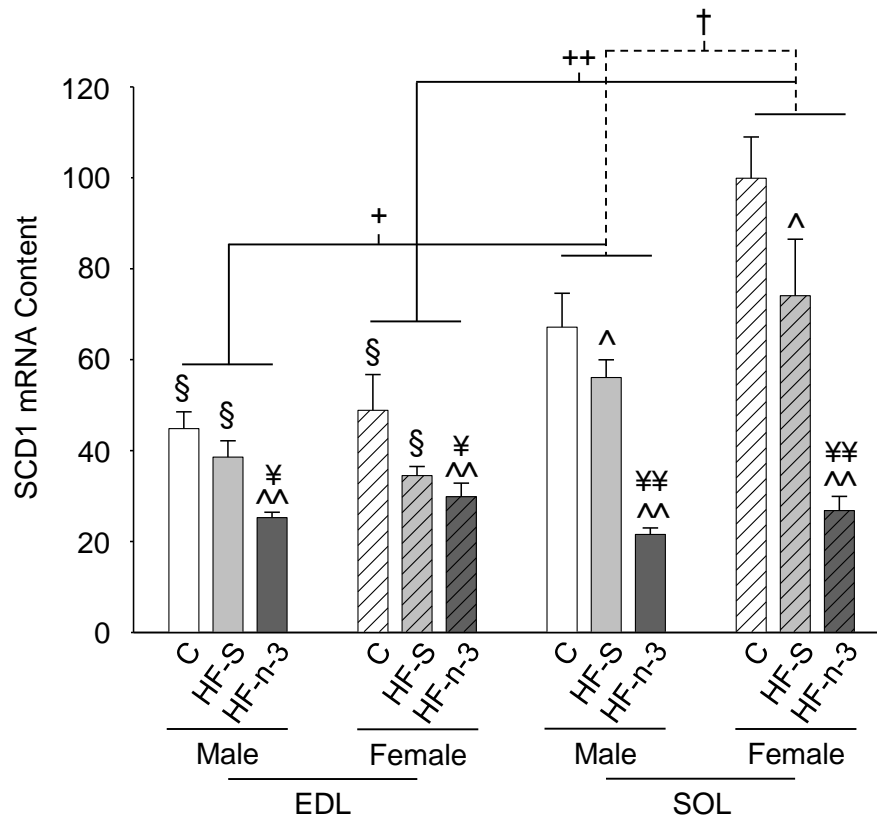


Figure 4.11. SCD1 mRNA content in the white extensor digitorum longus and red soleus muscles of male and female mice fed control, high saturated fat or high fat n-3 PUFA enriched diets.

Data are expressed as mean (bars) \pm SEM (error bars), where solid bars indicate male (M) mice, lined bars indicate female (F) mice and colour represents diet: white, control (C); pale grey, high saturated fat (HF-S); dark grey, high fat n-3 polyunsaturated fatty acid enriched (HF-n-3). EDL, extensor digitorum longus muscle; SOL, soleus muscle; SCD1, stearyl-CoA desaturase 1.

n: EDL - C(M/F) = 10/11, HF-S(M/F) = 11/11, HF-n-3(M/F) = 9/11;

n: SOL - C(M/F) = 10/12, HF-S(M/F) = 10/10, HF-n-3(M/F) = 9/11.

Statistics: Diet*muscle interaction: $^{\wedge}P < 0.05$, $^{\wedge}P < 0.001$, compared to C (of same muscle); $^{\text{¥}}P < 0.02$, $^{\text{¥¥}}P < 0.001$, compared to HF-S (of same muscle); $^{\text{§}}P < 0.001$, compared to SOL (of same dietary group). Gender*muscle interaction: $^{\text{†}}P < 0.02$, male EDL compared to male SOL; $^{\text{††}}P < 0.001$, female EDL compared to female SOL; $^{\text{†††}}P < 0.005$, male compared to female (SOL).

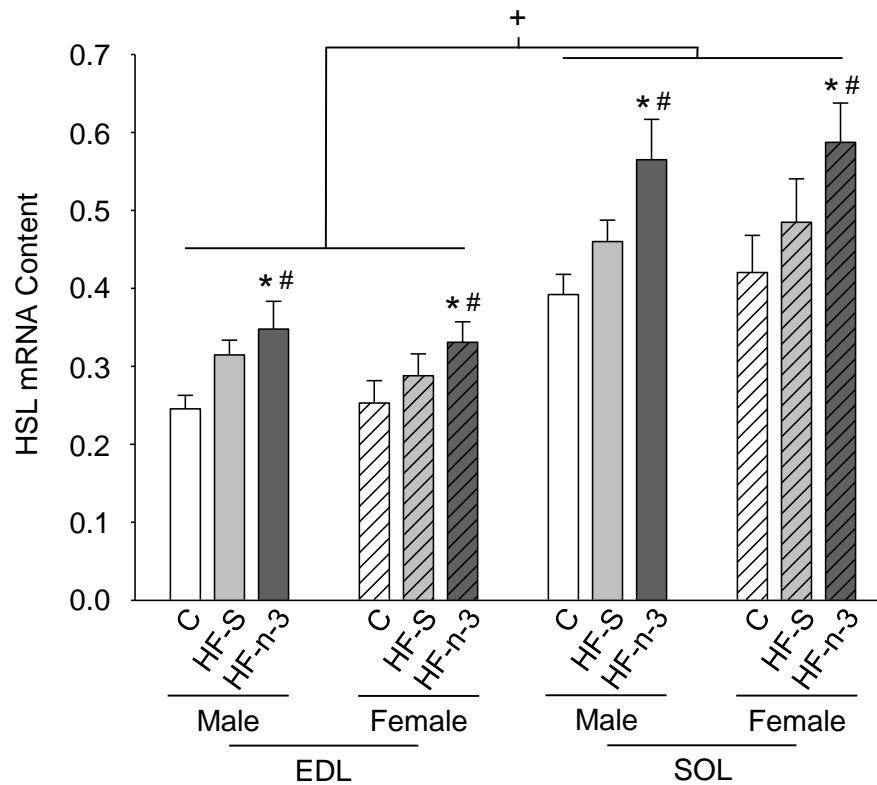


Figure 4.12. HSL mRNA content in the white extensor digitorum longus and red soleus muscles of male and female mice fed control, high saturated fat or high fat n-3 PUFA enriched diets.

Data are expressed as mean (bars) \pm SEM (error bars), where solid bars indicate male (M) mice, lined bars indicate female (F) mice and colour represents diet: white, control (C); pale grey, high saturated fat (HF-S); dark grey, high fat n-3 polyunsaturated fatty acid enriched (HF-n-3). EDL, extensor digitorum longus muscle; SOL, soleus muscle; HSL, hormone sensitive lipase.

n: EDL - C(M/F) = 10/12, HF-S(M/F) = 11/11, HF-n-3(M/F) = 9/11;

n: SOL - C(M/F) = 10/12, HF-S(M/F) = 10/10, HF-n-3(M/F) = 9/11.

Statistics: Effect of diet: * $P \leq 0.001$, compared to C, # $P \leq 0.05$, compared to HF-S.

Effect of muscle fibre type: + $P \leq 0.001$, SOL compared to EDL.

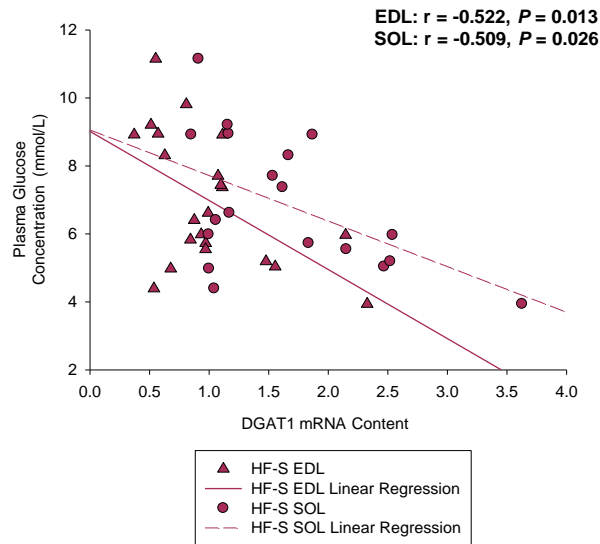


Figure 4.13. Correlations of plasma glucose concentrations with skeletal muscle DGAT1 mRNA content in mice exposed to a high saturated fat diet.

Symbol type represents dietary group and muscle type: see legend. HF-S, high saturated fat diet; EDL, extensor digitorum longus muscle; SOL, soleus muscle; DGAT1, diacylglycerol acyltransferase 1.

HF-S n(EDL/SOL) = 22/19.

There was a significant negative relationship between the plasma glucose concentration and the mRNA expression of DGAT1 in the EDL muscle of HF-S mice (male and female mice combined). There was also a significant negative relationship between the plasma glucose concentration and the mRNA expression of DGAT1 in the soleus muscle of HF-S mice (male and female mice combined).

4.3.3 – Fatty Acid Utilisation (*PDK4*, *AMPK α 1*, *AMPK α 2*, *ACC- β* , *CPT1b*, *UCP2*, *UCP3*, *SIRT1*, *PGC1 α* , *PPAR α* , *PPAR δ/β*)

Pyruvate dehydrogenase kinase 4 (PDK4) mRNA content was greater in HF-S and HF-n-3 mice as compared to control mice ($F(2, 114)=32.1$, $P\leq 0.001$; +58%, +99%, respectively; post-hoc tests: $P\leq 0.001$) (**Figure 4.14**). There was also a trend towards greater PDK4 mRNA content in HF-n-3 mice as compared to HF-S mice (+26%; post-hoc test: $P=0.09$). There was an effect of muscle fibre type on PDK4 mRNA content, the soleus muscle exhibited greater PDK4 mRNA as compared to the EDL muscle (+84%; $F(1, 114)=54.9$, $P\leq 0.001$). There was no effect of gender ($F(1, 114)=0.3$, $P=0.86$) on PDK4 mRNA content.

There was no effect of diet on AMP-activated protein kinase catalytic subunit $\alpha 1$ (AMPK $\alpha 1$) mRNA content ($F(2, 114)=1.3$, $P=0.28$). There was an effect of muscle fibre type on AMPK $\alpha 1$ mRNA content, the soleus muscle exhibited greater AMPK $\alpha 1$ mRNA as compared to the EDL muscle (+18%; $F(1, 114)=14.6$, $P\leq 0.001$) (**Figure 4.15**). There was no effect of gender on AMPK $\alpha 1$ mRNA content ($F(1, 114)=2.2$, $P=0.14$).

AMP-activated protein kinase catalytic subunit $\alpha 2$ (AMPK $\alpha 2$) mRNA content was greater in HF-S mice as compared to control and HF-n-3 mice ($F(2, 114)=5.5$, $P=0.005$; +9%, +15%, respectively; post-hoc tests: $P\leq 0.05$, $P\leq 0.001$, respectively) (**Figure 4.16**). There was a gender*muscle interaction on AMPK $\alpha 2$ mRNA content ($F(1, 114)=4.8$, $P=0.030$), in male and female mice, the EDL muscle exhibited greater

AMPK α 2 mRNA as compared to the soleus muscle (+53%, +37%, respectively; pairwise comparisons: $P \leq 0.001$) and in the EDL muscle, male mice exhibited greater AMPK α 2 mRNA than females (+13%; pairwise comparison: $P \leq 0.001$).

There was no effect of diet on acetyl-Coenzyme A carboxylase- β (ACC- β) mRNA content ($F(2, 113)=0.9, P=0.40$). There was an effect of muscle fibre type on ACC- β mRNA content, the soleus muscle exhibited greater ACC- β mRNA as compared to the EDL muscle (+64%; $F(1, 113)=43.2, P \leq 0.001$) (**Figure 4.17**). There was no effect of gender on ACC- β mRNA content ($F(1, 113)=0.08, P=0.77$).

There was a diet*muscle interaction on carnitine palmitoyl transferase 1b (CPT1b) mRNA content ($F(2, 113)=3.5, P=0.033$) (**Figure 4.18**), in the EDL muscle, HF-n-3 mice exhibited greater CPT1b mRNA as compared to control and HF-S mice (+34%, +20%, respectively; pairwise comparisons: $P \leq 0.001, P \leq 0.05$, respectively) and in the soleus muscle, HF-n-3 mice exhibited greater CPT1b mRNA as compared to control and HF-S mice (+42%, +30%, respectively; pairwise comparisons: $P \leq 0.001$). In all dietary groups, the soleus muscle exhibited greater CPT1b mRNA content as compared to the EDL muscle (+52% (C), +48% (HF-S), +61% (HF-n-3); pairwise comparisons: $P \leq 0.001$). There was an effect of gender on CPT1b mRNA content, male mice exhibited greater CPT1b mRNA than female mice (+22%; $F(1, 113)=31.3, P \leq 0.001$).

There was no effect of diet ($F(2, 114)=1.4, P=0.25$), muscle fibre type ($F(1, 114)=0.02, P=0.90$) or gender ($F(1, 114)=1.1, P=0.30$) on uncoupling protein 2 (UCP2) mRNA content (**Figure 4.19**).

There was a diet*muscle interaction on uncoupling protein 3 (UCP3) mRNA content ($F(2, 112)=4.7, P=0.011$) (**Figure 4.20**), in the EDL muscle, HF-n-3 mice exhibited greater UCP3 mRNA as compared to control mice (+68%; pairwise comparison: $P\leq 0.001$) and in the soleus muscle, HF-S and HF-n-3 mice exhibited greater UCP3 mRNA as compared to control mice (+109%, +153%, respectively; pairwise comparisons: $P\leq 0.001$). There was a trend in the EDL muscle towards greater UCP3 mRNA content in HF-S mice as compared to controls (+25%; pairwise comparison: $P=0.077$). In control mice, the EDL muscle exhibited greater UCP3 mRNA content as compared to the soleus muscle (+85%; pairwise comparison: $P\leq 0.001$). There was no effect of gender on UCP3 mRNA content ($F(1, 112)=1.5, P=0.22$).

There was no effect of diet ($F(2, 114)=0.4, P=0.64$), muscle fibre type ($F(1, 114)=0.6, P=0.44$) or gender ($F(1, 114)=0.2, P=0.68$) on skeletal muscle sirtuin 1 (SIRT1) mRNA content (**Figure 4.21**).

There was a diet*muscle interaction on peroxisome proliferative activated receptor γ coactivator 1 α (PGC1 α) mRNA content ($F(2, 113)=13.4, P\leq 0.001$) (**Figure 4.22**), in the soleus muscle, HF-S mice exhibited lower PGC1 α mRNA as compared to control mice (-67%; pairwise comparison: $P\leq 0.001$) and HF-n-3 mice exhibited greater PGC1 α mRNA as compared to control and HF-S mice (+76%, +193%, respectively; pairwise comparisons: $P\leq 0.001$). In control and HF-n-3 mice, the soleus muscle exhibited greater PGC1 α mRNA content as compared to EDL muscle (+97%, +219%, respectively; pairwise comparisons: $P\leq 0.001$). There was an effect of gender on PGC1 α mRNA content, male mice exhibited greater PGC1 α mRNA than female mice

(+23%; $F(1, 113)=9.6, P=0.002$).

Peroxisome proliferator activator receptor α (PPAR α) mRNA content was lower in HF-S mice as compared to control mice ($F(2, 114)=4.2, P=0.017$; -20%; post-hoc test: $P\leq 0.005$) and greater in HF-n-3 mice as compared to HF-S mice (+20%; post-hoc test: $P\leq 0.05$) (**Figure 4.23**). There was an effect of muscle fibre type on PPAR α mRNA content, the soleus muscle exhibited greater PPAR α mRNA as compared to the EDL muscle (+174%; $F(1, 114)=267.7, P\leq 0.001$). There was no effect of gender on PPAR α mRNA content ($F(1, 114)=0.7, P=0.41$).

There was no effect of diet ($F(2, 113)=1.1, P=0.33$), muscle fibre type ($F(1, 113)=0.3, P=0.61$) or gender ($F(1, 113)=0.003, P=0.96$) on peroxisome proliferator activator receptor δ/β (PPAR δ/β) mRNA content. There was a trend towards a diet*muscle interaction on PPAR δ/β mRNA content ($F(2, 113)=3.0, P=0.056$), in the EDL muscle, HF-S mice exhibited increased PPAR δ/β mRNA as compared to HF-n-3 mice (+49%; pairwise comparison: $P=0.044$) (**Figure 4.24**).

In mice consuming a HFD, liver fat content was negatively correlated with the mRNA expression of FAT/CD36 in the soleus muscle ($r = -0.59, F(1, 36)=19.5, P\leq 0.001$; all HF-S and HF-n-3 mice combined) (**Figure 4.25**). Furthermore, there was a negative correlation between liver fat content and the mRNA expression of PDK4 in the soleus muscle of mice fed a HFD ($r = -0.33, F(1, 36)=4.4, P=0.042$; all HF-S and HF-n-3 mice combined) (**Figure 4.25**). There was also a negative relationship between liver fat content and the mRNA expression of PGC1 α in the soleus muscle in high fat-fed mice

($r = -0.33$, $F(1, 35)=4.2$, $P=0.049$; all HF-S and HF-n-3 mice combined) (**Figure 4.25**).

In HF-n-3 fed mice only, there was a significant negative correlation between plasma triglyceride concentrations and PPAR α mRNA content in the EDL muscle ($r = -0.59$, $F(1, 17)=9.3$, $P=0.007$; male and female mice combined) and a trend towards a negative relationship between plasma triglyceride concentrations and PPAR α mRNA content in the soleus muscle ($r = -0.43$, $F(1, 17)=3.8$, $P=0.069$; male and female mice combined) (**Figure 4.26**). In HF-S fed mice only, plasma glucose concentrations were negatively correlated with PPAR α mRNA content in the EDL ($r = -0.51$, $F(1, 20)=7.0$, $P=0.016$; male and female mice combined) and soleus ($r = -0.51$, $F(1, 18)=6.3$, $P=0.022$; male and female mice combined) muscles (**Figure 4.26**).

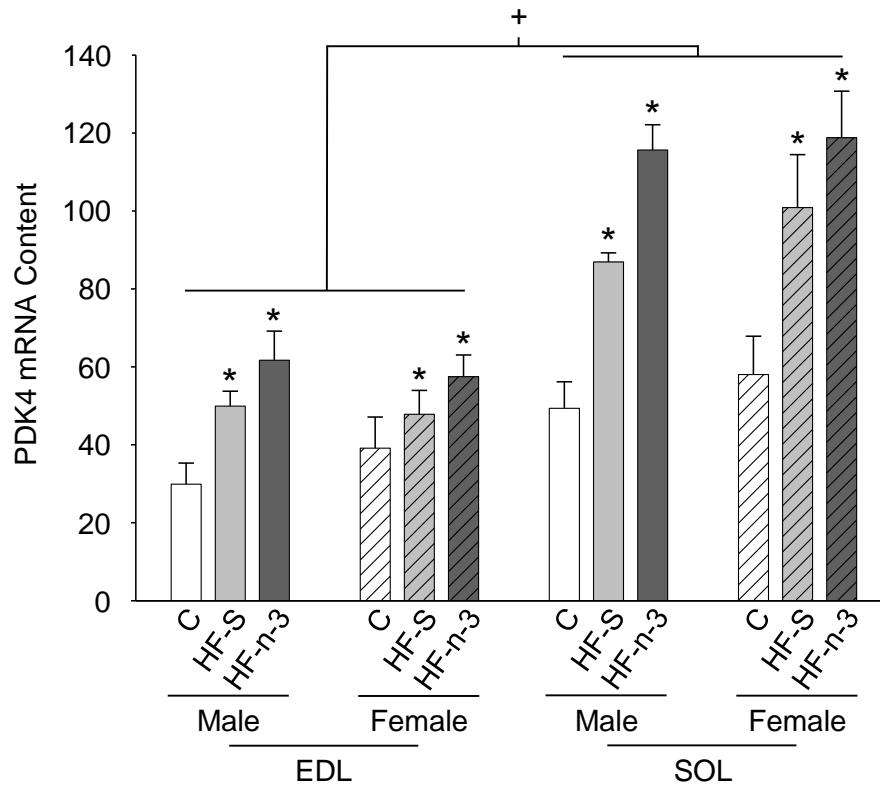


Figure 4.14. PDK4 mRNA content in the white extensor digitorum longus and red soleus muscles of male and female mice fed control, high saturated fat or high fat n-3 PUFA enriched diets.

Data are expressed as mean (bars) \pm SEM (error bars), where solid bars indicate male (M) mice, lined bars indicate female (F) mice and colour represents diet: white, control (C); pale grey, high saturated fat (HF-S); dark grey, high fat n-3 polyunsaturated fatty acid enriched (HF-n-3). EDL, extensor digitorum longus muscle; SOL, soleus muscle; PDK4, pyruvate dehydrogenase kinase 4.

n: EDL - C(M/F) = 10/11, HF-S(M/F) = 11/11, HF-n-3(M/F) = 9/11;

n: SOL - C(M/F) = 10/12, HF-S(M/F) = 10/10, HF-n-3(M/F) = 9/11.

Statistics: Effect of diet: * $P \leq 0.001$, compared to C. Effect of muscle fibre type: $^+P \leq 0.001$, SOL compared to EDL.

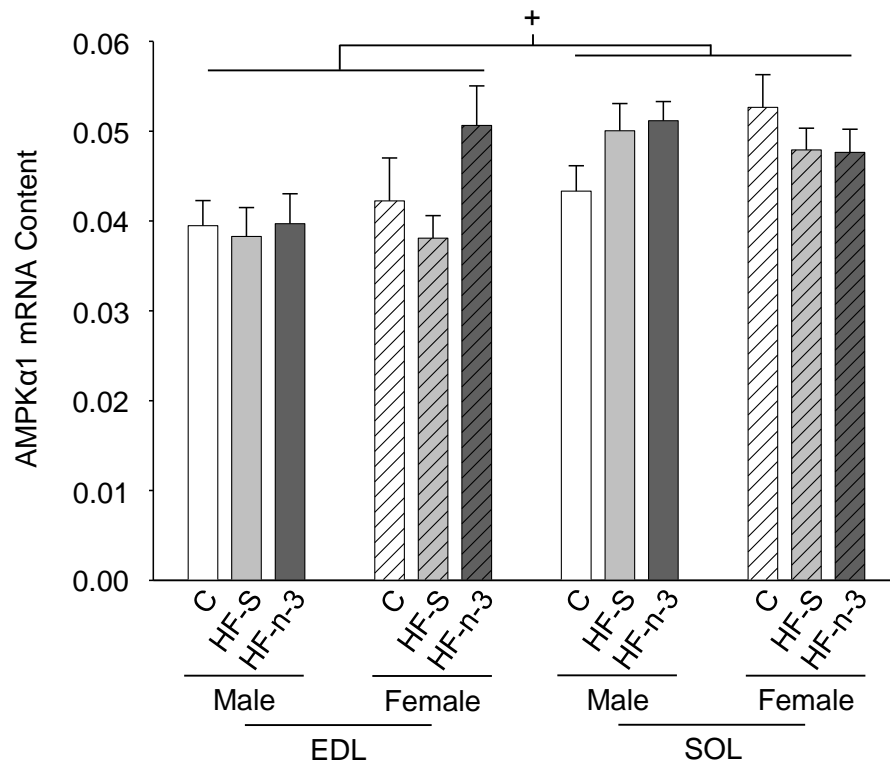


Figure 4.15. AMPKα1 mRNA content in the white extensor digitorum longus and red soleus muscles of male and female mice fed control, high saturated fat or high fat n-3 PUFA enriched diets.

Data are expressed as mean (bars) ± SEM (error bars), where solid bars indicate male (M) mice, lined bars indicate female (F) mice and colour represents diet: white, control (C); pale grey, high saturated fat (HF-S); dark grey, high fat n-3 polyunsaturated fatty acid enriched (HF-n-3). EDL, extensor digitorum longus muscle; SOL, soleus muscle; AMPKα1, AMP-activated protein kinase catalytic subunit α1.

n: EDL - C(M/F) = 10/12, HF-S(M/F) = 11/11, HF-n-3(M/F) = 9/11;

n: SOL - C(M/F) = 10/12, HF-S(M/F) = 10/10, HF-n-3(M/F) = 9/11.

Statistics: Effect of muscle fibre type: $^+P \leq 0.001$, SOL compared to EDL.

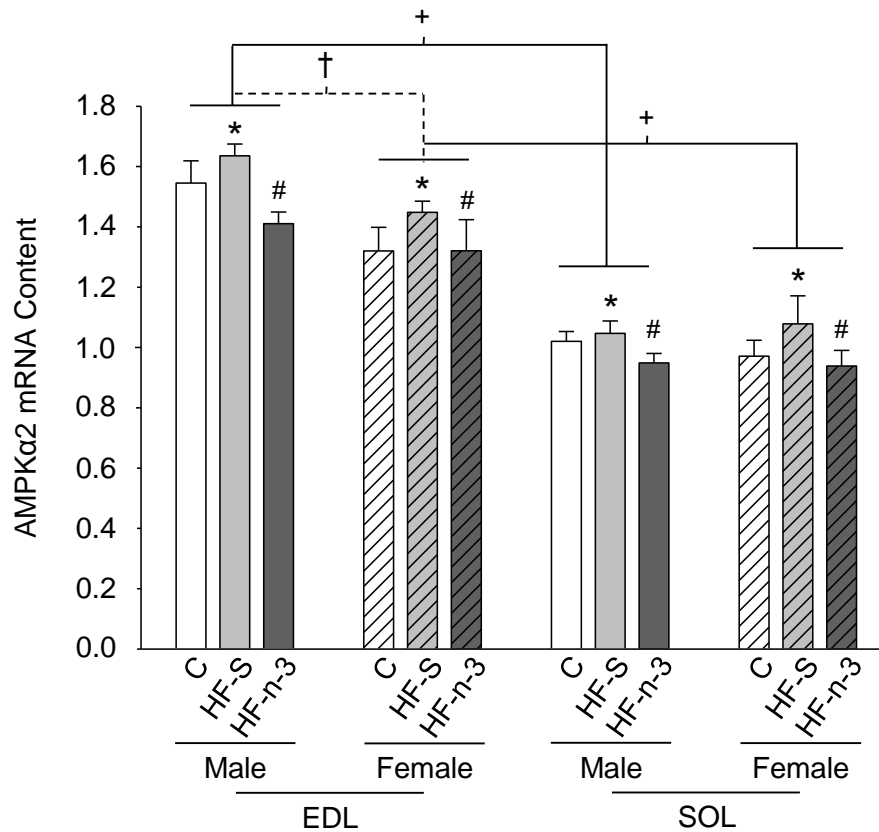


Figure 4.16. AMPKα2 mRNA content in the white extensor digitorum longus and red soleus muscles of male and female mice fed control, high saturated fat or high fat n-3 PUFA enriched diets.

Data are expressed as mean (bars) ± SEM (error bars), where solid bars indicate male (M) mice, lined bars indicate female (F) mice and colour represents diet: white, control (C); pale grey, high saturated fat (HF-S); dark grey, high fat n-3 polyunsaturated fatty acid enriched (HF-n-3). EDL, extensor digitorum longus muscle; SOL, soleus muscle; AMPKα2, AMP-activated protein kinase catalytic subunit α2.

n: EDL - C(M/F) = 10/12, HF-S(M/F) = 11/11, HF-n-3(M/F) = 9/11;

n: SOL - C(M/F) = 10/12, HF-S(M/F) = 10/10, HF-n-3(M/F) = 9/11.

Statistics: Effect of diet: * $P \leq 0.05$, compared to C; # $P \leq 0.001$, compared to HF-S. Gender*muscle interaction: † $P \leq 0.001$, EDL compared to SOL (of same gender); ‡ $P \leq 0.001$, male compared to female (EDL).

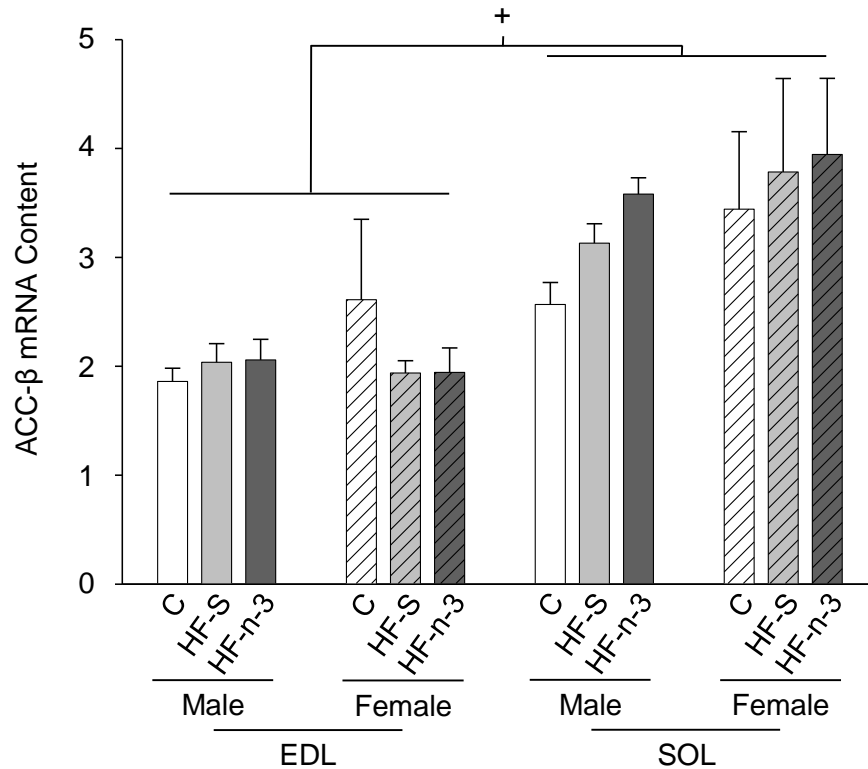


Figure 4.17. ACC- β mRNA content in the white extensor digitorum longus and red soleus muscles of male and female mice fed control, high saturated fat or high fat n-3 PUFA enriched diets.

Data are expressed as mean (bars) \pm SEM (error bars), where solid bars indicate male (M) mice, lined bars indicate female (F) mice and colour represents diet: white, control (C); pale grey, high saturated fat (HF-S); dark grey, high fat n-3 polyunsaturated fatty acid enriched (HF-n-3). EDL, extensor digitorum longus muscle; SOL, soleus muscle; ACC- β , acetyl-Coenzyme A carboxylase- β .

n: EDL - C(M/F) = 10/11, HF-S(M/F) = 11/11, HF-n-3(M/F) = 9/11;

n: SOL - C(M/F) = 10/12, HF-S(M/F) = 10/10, HF-n-3(M/F) = 9/11.

Statistics: Effect of muscle fibre type: $^+P \leq 0.001$, SOL compared to EDL.

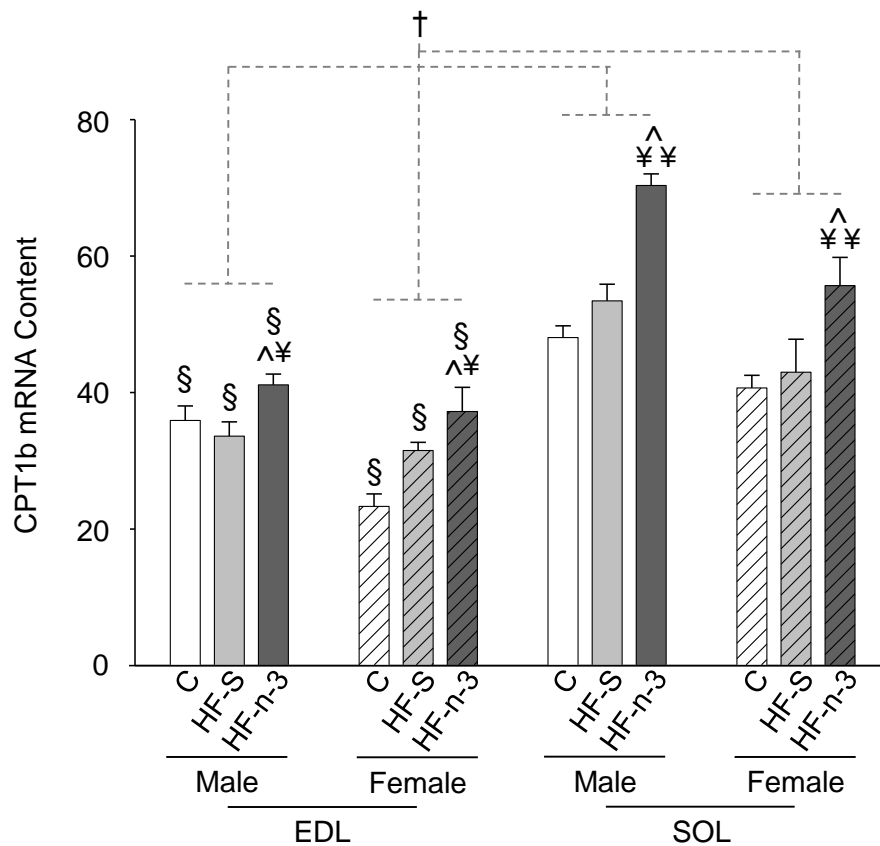


Figure 4.18. CPT1b mRNA content in the white extensor digitorum longus and red soleus muscles of male and female mice fed control, high saturated fat or high fat n-3 PUFA enriched diets.

Data are expressed as mean (bars) \pm SEM (error bars), where solid bars indicate male (M) mice, lined bars indicate female (F) mice and colour represents diet: white, control (C); pale grey, high saturated fat (HF-S); dark grey, high fat n-3 polyunsaturated fatty acid enriched (HF-n-3). EDL, extensor digitorum longus muscle; SOL, soleus muscle; CPT1b, carnitine palmitoyl transferase 1b.

n: EDL - C(M/F) = 10/12, HF-S(M/F) = 11/11, HF-n-3(M/F) = 9/11;

n: SOL - C(M/F) = 10/12, HF-S(M/F) = 10/10, HF-n-3(M/F) = 9/10.

Statistics: Diet*muscle interaction: $^{\wedge}P \leq 0.001$, compared to C (of same muscle); $^*P \leq 0.05$, $^{**}P \leq 0.001$, compared to HF-S (of same muscle); $^{\S}P \leq 0.001$, EDL compared to SOL (of same dietary group). Effect of gender: $^{\dagger}P \leq 0.001$, male compared to female.

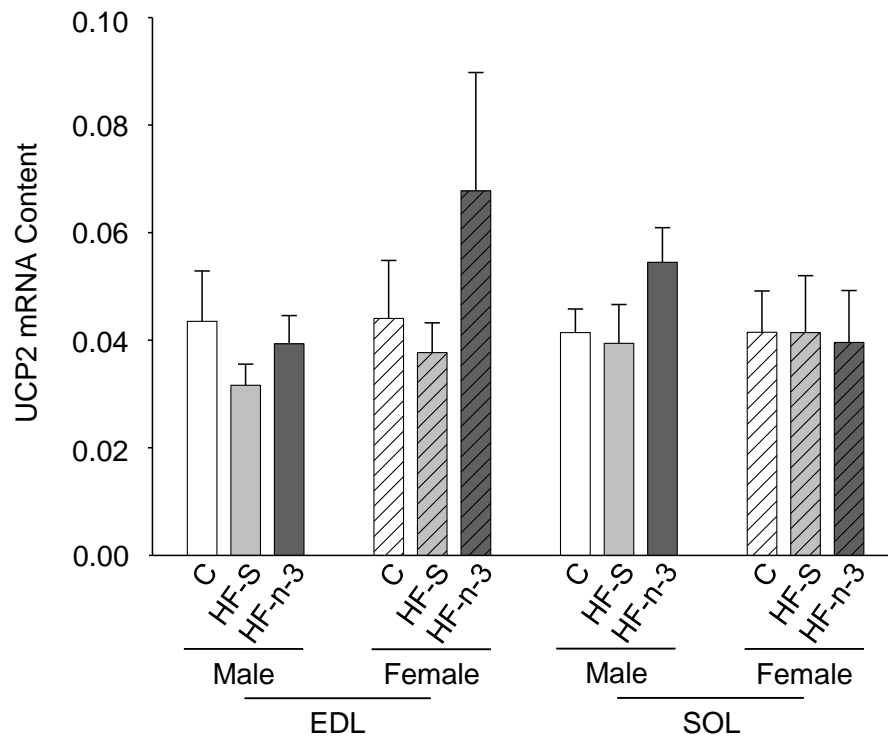


Figure 4.19. UCP2 mRNA content in the white extensor digitorum longus and red soleus muscles of male and female mice fed control, high saturated fat or high fat n-3 PUFA enriched diets.

Data are expressed as mean (bars) \pm SEM (error bars), where solid bars indicate male (M) mice, lined bars indicate female (F) mice and colour represents diet: white, control (C); pale grey, high saturated fat (HF-S); dark grey, high fat n-3 polyunsaturated fatty acid enriched (HF-n-3). EDL, extensor digitorum longus muscle; SOL, soleus muscle; UCP2, uncoupling protein 2.

n: EDL - C(M/F) = 10/12, HF-S(M/F) = 11/11, HF-n-3(M/F) = 9/11;

n: SOL - C(M/F) = 10/12, HF-S(M/F) = 10/10, HF-n-3(M/F) = 9/11.

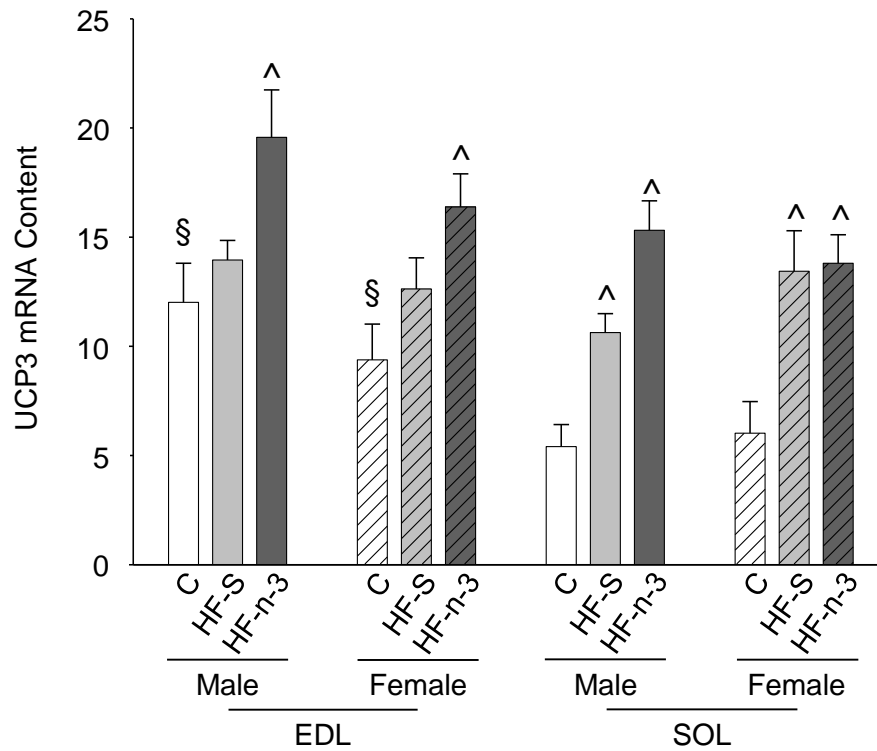


Figure 4.20. UCP3 mRNA content in the white extensor digitorum longus and red soleus muscles of male and female mice fed control, high saturated fat or high fat n-3 PUFA enriched diets.

Data are expressed as mean (bars) \pm SEM (error bars), where solid bars indicate male (M) mice, lined bars indicate female (F) mice and colour represents diet: white, control (C); pale grey, high saturated fat (HF-S); dark grey, high fat n-3 polyunsaturated fatty acid enriched (HF-n-3). EDL, extensor digitorum longus muscle; SOL, soleus muscle; UCP3, uncoupling protein 3.

n: EDL - C(M/F) = 10/11, HF-S(M/F) = 11/11, HF-n-3(M/F) = 9/11;

n: SOL - C(M/F) = 10/12, HF-S(M/F) = 10/10, HF-n-3(M/F) = 9/10.

Statistics: Diet*muscle interaction: $^{\wedge}P \leq 0.001$, compared to C (of same muscle type);

$^{\S}P \leq 0.001$, EDL compared to SOL (C).

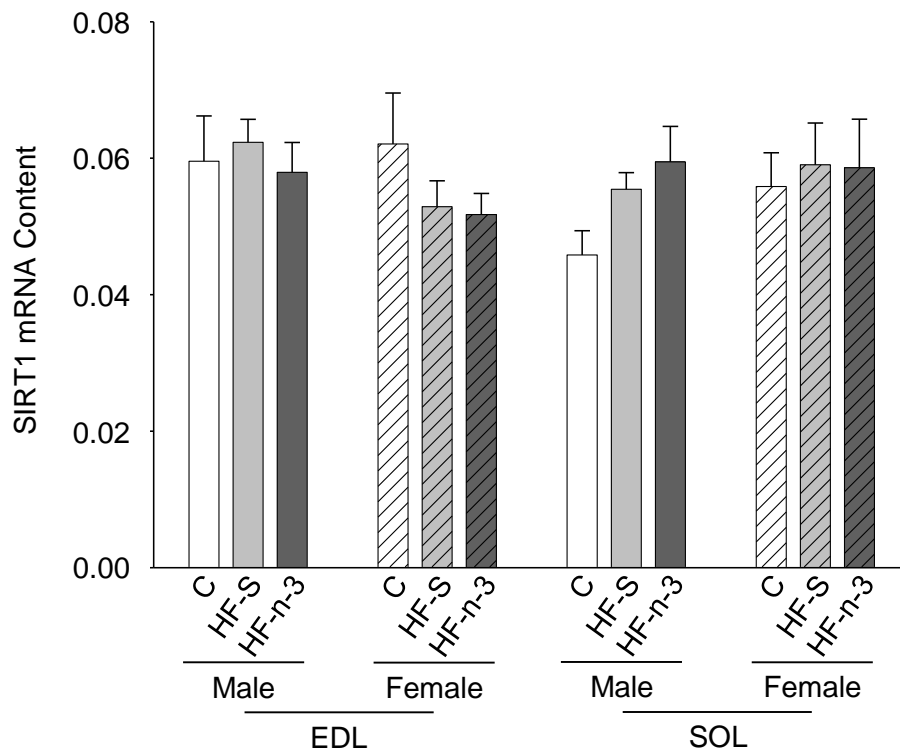


Figure 4.21. SIRT1 mRNA content in the white extensor digitorum longus and red soleus muscles of male and female mice fed control, high saturated fat or high fat n-3 PUFA enriched diets.

Data are expressed as mean (bars) \pm SEM (error bars), where solid bars indicate male (M) mice, lined bars indicate female (F) mice and colour represents diet: white, control (C); pale grey, high saturated fat (HF-S); dark grey, high fat n-3 polyunsaturated fatty acid enriched (HF-n-3). EDL, extensor digitorum longus muscle; SOL, soleus muscle; SIRT1, sirtuin 1.

n: EDL - C(M/F) = 10/12, HF-S(M/F) = 11/11, HF-n-3(M/F) = 9/11;

n: SOL - C(M/F) = 10/12, HF-S(M/F) = 10/10, HF-n-3(M/F) = 9/11.

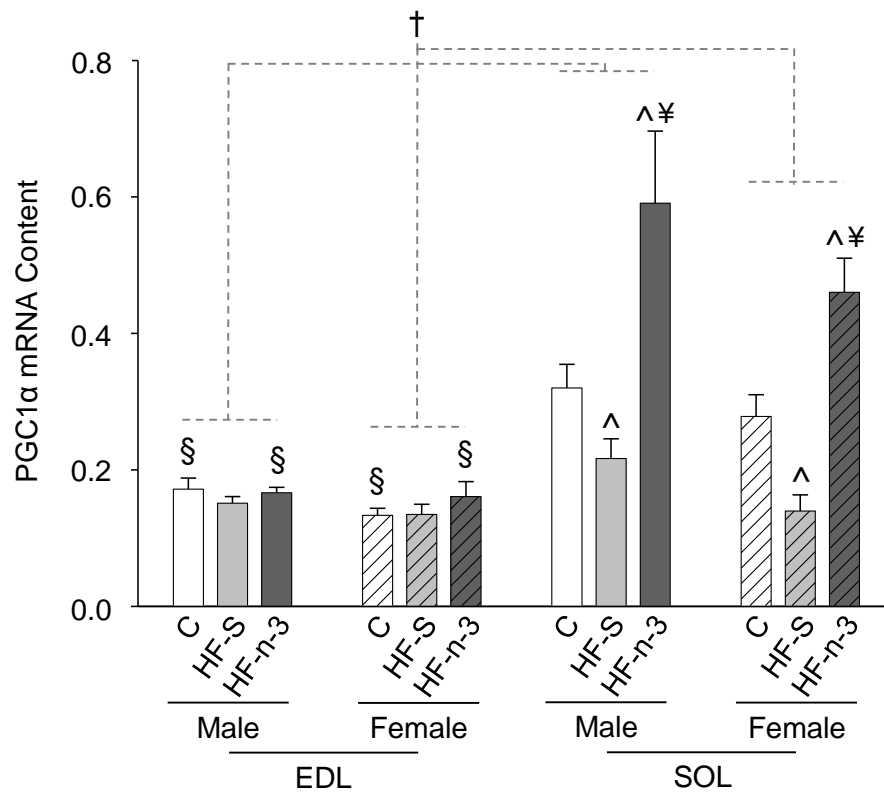


Figure 4.22. PGC1 α mRNA content in the white extensor digitorum longus and red soleus muscles of male and female mice fed control, high saturated fat or high fat n-3 PUFA enriched diets.

Data are expressed as mean (bars) \pm SEM (error bars), where solid bars indicate male (M) mice, lined bars indicate female (F) mice and colour represents diet: white, control (C); pale grey, high saturated fat (HF-S); dark grey, high fat n-3 polyunsaturated fatty acid enriched (HF-n-3). EDL, extensor digitorum longus muscle; SOL, soleus muscle; PGC1 α , peroxisome proliferator activated receptor γ coactivator 1 α .

n: EDL - C(M/F) = 10/12, HF-S(M/F) = 11/11, HF-n-3(M/F) = 9/11;

n: SOL - C(M/F) = 10/12, HF-S(M/F) = 10/10, HF-n-3(M/F) = 9/10.

Statistics: Diet*muscle interaction: $^{\wedge}P \leq 0.001$, compared to C (SOL); $^{\text{¥}}P \leq 0.001$, compared to HF-S (SOL); $^{\text{§}}P \leq 0.001$, EDL compared to SOL (of same dietary group).

Effect of gender: $^{\dagger}P \leq 0.005$, male compared to female.

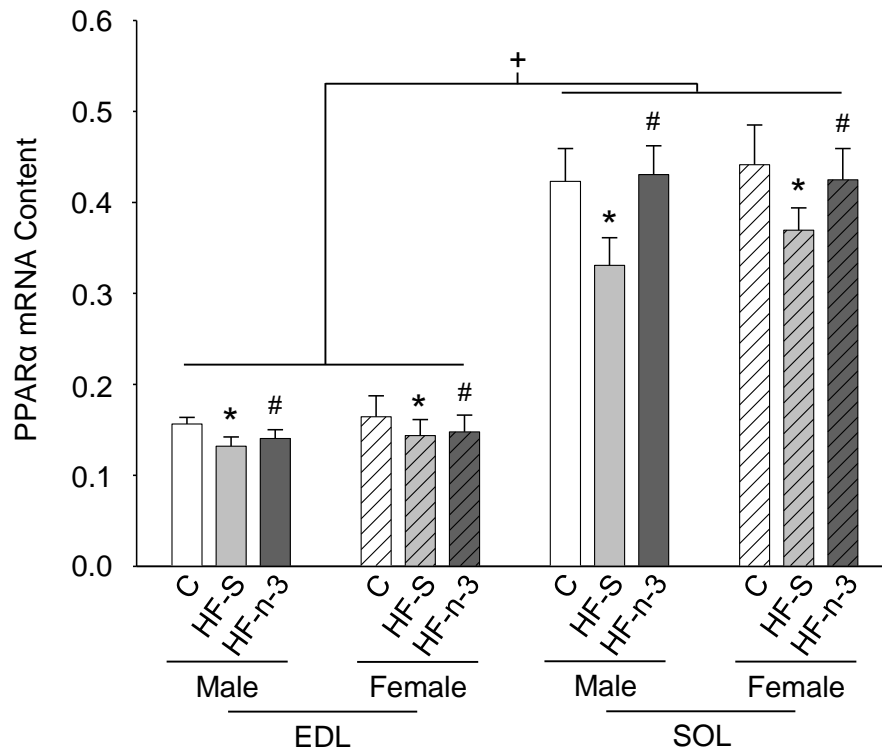


Figure 4.23. PPARα mRNA content in the white extensor digitorum longus and red soleus muscles of male and female mice fed control, high saturated fat or high fat n-3 PUFA enriched diets.

Data are expressed as mean (bars) ± SEM (error bars), where solid bars indicate male (M) mice, lined bars indicate female (F) mice and colour represents diet: white, control (C); pale grey, high saturated fat (HF-S); dark grey, high fat n-3 polyunsaturated fatty acid enriched (HF-n-3). EDL, extensor digitorum longus muscle; SOL, soleus muscle; PPARα, peroxisome proliferator activator receptor α.

n: EDL - C(M/F) = 10/12, HF-S(M/F) = 11/11, HF-n-3(M/F) = 9/11;

n: SOL - C(M/F) = 10/12, HF-S(M/F) = 10/10, HF-n-3(M/F) = 9/11.

Statistics: Effect of diet: * $P \leq 0.005$, compared to C; # $P \leq 0.05$, compared to HF-S. Effect of muscle fibre type: + $P \leq 0.001$, SOL compared to EDL.

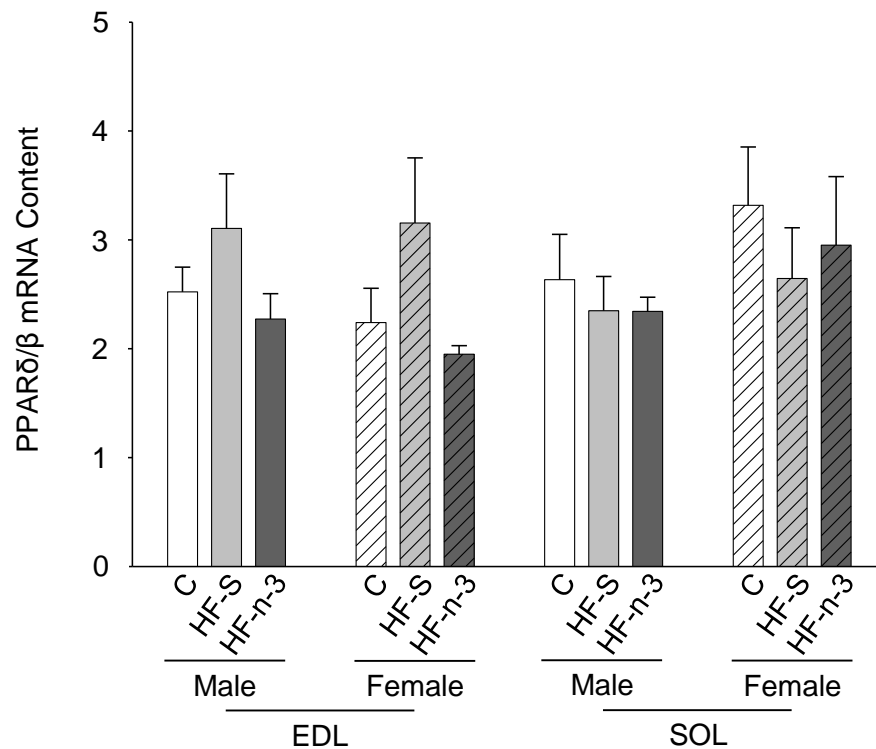


Figure 4.24. PPARδ/β mRNA content in the white extensor digitorum longus and red soleus muscles of male and female mice fed control, high saturated fat or high fat n-3 PUFA enriched diets.

Data are expressed as mean (bars) ± SEM (error bars), where solid bars indicate male (M) mice, lined bars indicate female (F) mice and colour represents diet: white, control (C); pale grey, high saturated fat (HF-S); dark grey, high fat n-3 polyunsaturated fatty acid enriched (HF-n-3). EDL, extensor digitorum longus muscle; SOL, soleus muscle; PPARδ/β, peroxisome proliferator activator receptor δ/β.

n: EDL - C(M/F) = 10/11, HF-S(M/F) = 11/11, HF-n-3(M/F) = 9/11;

n: SOL - C(M/F) = 10/12, HF-S(M/F) = 10/10, HF-n-3(M/F) = 9/11.

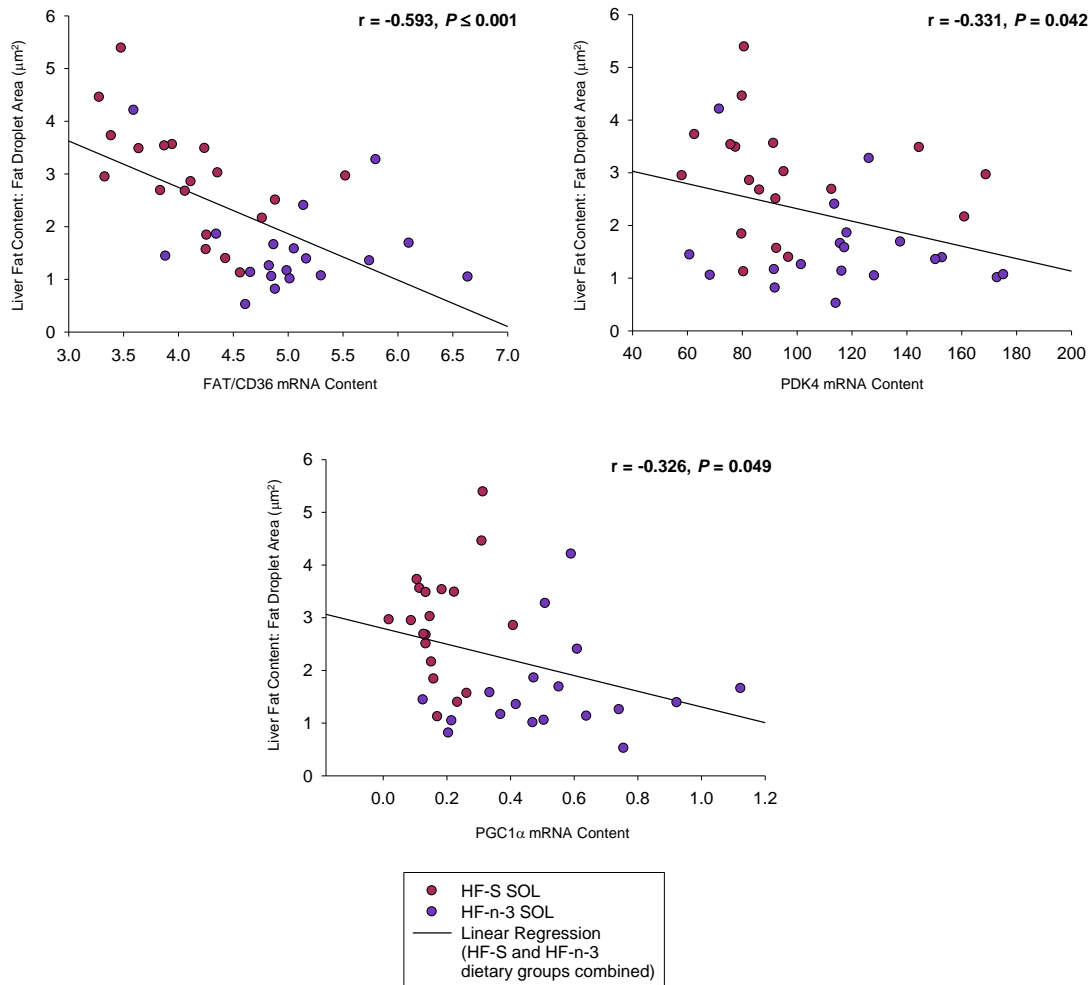


Figure 4.25. Relationships between liver fat content and the mRNA content of muscle oxidative genes in the soleus muscle of mice exposed to high fat overfeeding.

Symbol type represents dietary group: see legend. HF-S, high saturated fat diet; HF-n-3, high fat n-3 polyunsaturated fatty acid enriched diet; SOL, soleus muscle; FAT/CD36, fatty acid translocase; PDK4, pyruvate dehydrogenase kinase 4; PGC1 α , peroxisome proliferator activated receptor γ coactivator 1 α .

Correlation of liver weight with FAT/CD36, $n = 38$; with PDK4, $n = 38$; and with PGC1 α , $n = 37$.

There was a significant negative relationship between the liver fat content and the mRNA expression of FAT/CD36, PDK4 and PGC1 α in the soleus muscle (HF-S and HF-n-3 mice combined (including males and females)).

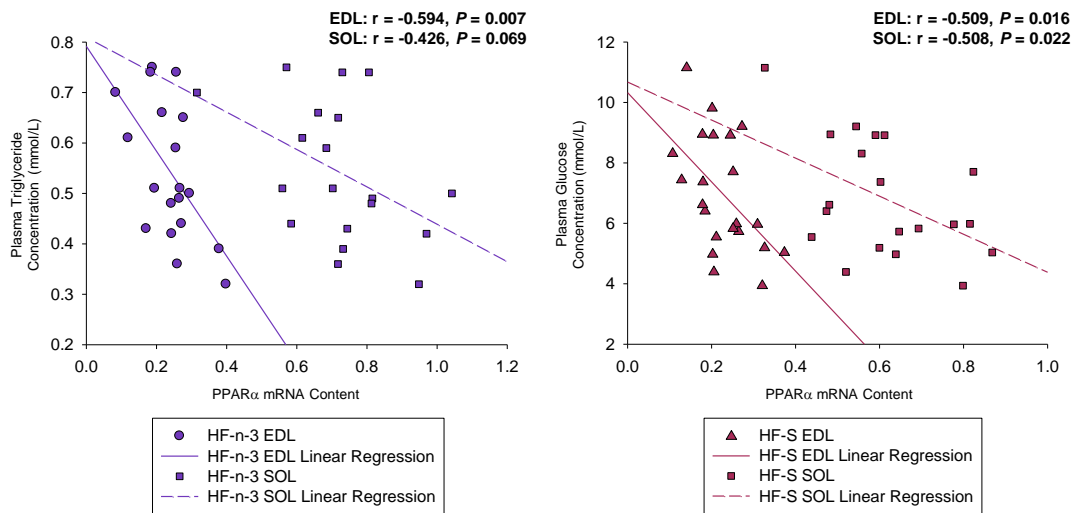


Figure 4.26. Correlations of plasma triglyceride and glucose concentrations with skeletal muscle PPAR α mRNA content in mice exposed to high fat overfeeding.

Symbol type represents dietary group and muscle type: see legend. HF-S, high saturated fat diet; HF-n-3, high fat n-3 polyunsaturated fatty acid enriched diet; EDL, extensor digitorum longus muscle; SOL, soleus muscle; PPAR α , peroxisome proliferator activator receptor α .

HF-n-3 n(EDL/SOL): = 19/19; HF-S n(EDL/SOL) = 22/20.

There was a significant negative relationship between the plasma triglyceride concentration and the mRNA expression of PPAR α in the EDL muscle of HF-n-3 mice, and trend towards this relationship in the soleus muscle of HF-n-3 mice (male and female mice combined). There was a significant negative relationship between the plasma glucose concentration and the mRNA expression of PPAR α in the EDL and soleus muscles of HF-S mice (male and female mice combined).

4.4 – DISCUSSION

This study is the first to comprehensively compare the effects of a high saturated fat and n-3 PUFA enriched HFDs on skeletal muscle fatty acid metabolism with respect to muscle fibre type and gender, and highlights the importance of muscle fibre type and gender to the overall characteristics, profile of gene expression and ultimate function of skeletal muscle.

4.4.1 – Skeletal Muscle Pattern of Gene Expression Reflects Muscle Fibre Type Properties

In the current study, it was demonstrated that the mRNA content of key genes involved in skeletal muscle fatty acid metabolism in the EDL and soleus muscles reflected the preferred substrate type of each muscle. The SO soleus muscle predominantly uses triglycerides for fuel (Samec *et al.*, 2002) and consistent with this notion, the current study showed that the soleus muscle exhibited greater mRNA content of genes involved in fatty acid transport (FAT/CD36, FABPpm, FATP1, FATP4), storage (DGAT1, SCD1, HSL) and utilisation (PDK4, CPT1b, PGC1 α , PPAR α), as compared to the EDL (FG-FOG) muscle. Conversely, it was demonstrated that the EDL muscle had greater mRNA content of AMPK α 2, a gene involved in mediating glucose uptake into muscle and both glucose and fatty acid oxidation (Towler and Hardie, 2007), reflecting the preference for glucose as a metabolic substrate in the EDL muscle (Samec *et al.*, 2002).

4.4.2 – Effect of Dietary Fatty Acid Composition on Skeletal Muscle Fatty Acid Uptake

In the current study it was demonstrated that the mRNA content of fatty acid transporters FAT/CD36 and FATP1 increased in response to both HFDs, but there was an even greater increase in FAT/CD36 mRNA content and a tendency for greater FATP4 mRNA content with HF-n-3 feeding. This is consistent with research in which differentiated myotubes exposed to eicosapentaenoic acid (EPA), an n-3 PUFA, exhibited increased FAT/CD36 mRNA content (Aas *et al.*, 2006). Aas and colleagues (Aas *et al.*, 2006) also showed that EPA treatment enhanced muscle fatty acid uptake. This suggests that n-3 PUFAs are more effective at enhancing the capacity for skeletal muscle fatty acid uptake *in vivo*.

Of the transporters measured in this study, FAT/CD36 has been shown to be the most effective transporter in increasing skeletal muscle fatty acid uptake (Schwenk *et al.*, 2010), and may therefore make a significant contribution to skeletal muscle fatty acid uptake and metabolism. Previous studies have highlighted the importance of FAT/CD36 cellular localisation at the sarcolemma in promoting skeletal muscle fatty acid uptake (Bonen *et al.*, 2004b) and in contributing to the increased fatty acid uptake in obesity (Han *et al.*, 2007; Chabowski *et al.*, 2006; Bonen *et al.*, 2004b). However, the abundance and localisation of fatty acid transport proteins have not been assessed in the current study.

The expression of fatty acid transporters in skeletal muscle has also been shown to influence the capacity for fatty acid uptake (Glatz *et al.*, 2010; Bonen *et al.*, 2004a; Coburn *et al.*, 2000; Febbraio *et al.*, 1999; Ibrahimi *et al.*, 1999). Increasing FAT/CD36 expression within the normal physiological range increases FAT/CD36 total protein (+60%) and sarcolemmal protein (+75%) content, and enhances fatty acid uptake (+62%) (Nickerson *et al.*, 2009). It is therefore possible that in the current study greater FAT/CD36 mRNA content may give rise to a greater intracellular pool of FAT/CD36 protein and increased sarcolemmal FAT/CD36, enhancing fatty acid uptake. In HF-n-3 mice, this process may occur through a PPAR α -mediated pathway, given that n-3 PUFAs are a PPAR α ligand (Hihi *et al.*, 2002; Desvergne and Wahli, 1999) and the FAT/CD36 sequence contains a PPAR response element to which activated PPAR α may bind, inducing FAT/CD36 expression (Mandard *et al.*, 2004). Furthermore, FAT/CD36 has also been shown to co-localise with mitochondrial fatty acid transporter, CPT1, at the mitochondrial membrane (Bezaire *et al.*, 2006; Campbell *et al.*, 2004) and overexpression of FAT/CD36 in skeletal muscle enhances the rate of fatty acid oxidation (Schwenk *et al.*, 2010). Therefore increased FAT/CD36 may promote fatty acid uptake into both the muscle and mitochondria. This is in keeping with a PPAR α regulated pathway, aiming to promote fatty acid oxidation in skeletal muscle (Desvergne and Wahli, 1999) (**Figure 4.27**).

In the current study it has been highlighted that FATP transporters are differentially regulated; high fat overfeeding, irrespective of the dietary fatty acid composition, increased FATP1 expression, whilst only HF-n-3 feeding upregulated FATP4 mRNA content. This finding is similar to the observations of Gimeno and colleagues

(Gimeno *et al.*, 2003), in which the transport capacity of the fatty acid transport protein in cardiac myocytes depended on the fatty acid used to assess fatty acid uptake (Glatz *et al.*, 2010; Gimeno *et al.*, 2003). The induction of FATP1, but not FATP4, mRNA expression by HF-S feeding is consistent with the observation that FATP1 exhibited greater transport capacity for saturated fat, palmitate, as compared to FATP4 (Glatz *et al.*, 2010; Gimeno *et al.*, 2003). Furthermore, Gimeno and colleagues (Gimeno *et al.*, 2003) also demonstrated that monounsaturated fatty acid, oleate, was more efficiently transported by FATP4 than FATP1 (Glatz *et al.*, 2010; Gimeno *et al.*, 2003) and as it was indicated that HF-n-3 feeding stimulated FATP4 expression in the present study, these data may suggest that FATP4 undertakes the preferential transport of unsaturated fats. Furthermore, previous research has shown that FATP4 is more effective, than FATP1, in increasing fatty acid uptake when both isoforms were overexpressed in muscle (Schwenk *et al.*, 2010; Nickerson *et al.*, 2009). In the current study, greater expression of FATP4 and FATP1 in HF-n-3 mice may indicate they have a greater capacity for skeletal muscle fatty acid uptake, as compared to HF-S mice, in which only the less effective transporter, FATP1, was upregulated.

In the current study, the observation that FABPpm was neither influenced by diet-induced obesity nor dietary fatty acid content is consistent with previous studies in which FABPpm protein in the whole muscle and at the plasma membrane was unchanged with obesity (Bonen *et al.*, 2003). However, FABPpm is identical in sequence and structure to mitochondrial aspartate aminotransferase (Stump *et al.*, 1993) and is also present in mitochondria and has consequently been proposed not only to function in fatty acid transport, but also in facilitating the transport of NADH across the

mitochondrial membrane (Glatz *et al.*, 2010; Clarke *et al.*, 2004). Given that it was shown that FABPpm was unchanged by greater fat availability in the present study and that in previous studies, FABPpm overexpression in skeletal muscle has been shown to increase the plasmalemmal FABPpm content by 173%, but enhance fatty acid transport only by 79% (Holloway *et al.*, 2007a), it is possible that FABPpm plays a minor role in fatty acid uptake.

Taken together, these data indicate that HF-S feeding promotes fatty acid transport, and this may contribute to muscle fat deposition. Enriching a HF-S diet with n-3 PUFAs produced an even greater increase in genes regulating fatty acid uptake. However, this occurred without increased fat accumulation in skeletal muscle, suggesting a role for increased fatty acid uptake in facilitating energy expenditure (**Figure 4.27**). The differential changes in skeletal muscle fatty acid transporter expression observed in response to high fat overfeeding diets of varying fatty acid composition highlights the need for further research to clarify the roles of each fatty acid transport protein in order to decipher the specific effects observed in this study.

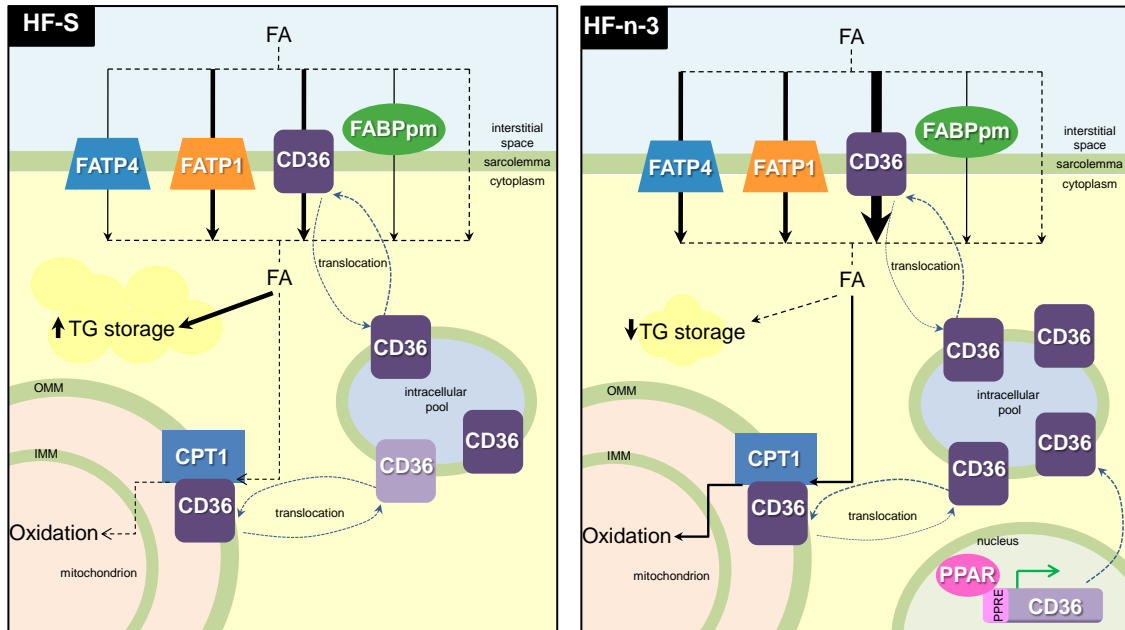


Figure 4.27. Schematic diagram depicting the differential effects that consuming a high saturated fat diet or n-3 PUFA enriched high fat diet exert on fatty acid transport into skeletal muscle.

In the skeletal muscle, HF-S feeding increased FAT/CD36 and FATP1 mRNA content. Therefore muscle fatty acid uptake may be enhanced and contribute to the observed increase in muscle fat accretion. HF-n-3 feeding increased skeletal muscle FAT/CD36 and FATP1 mRNA content and tended to increase FATP4 mRNA in comparison to control and HF-S diet feeding. Therefore increased fatty acid transporter expression may induce greater muscle fatty acid uptake in the HF-n-3 group. As intramyocellular fat accumulation was ameliorated by HF-n-3 feeding, fat may be channelled to pathways of expenditure. This may, in part, be facilitated by FAT/CD36 due to its localisation on the mitochondrial membrane, potentially enhancing mitochondrial fatty acid transport. Furthermore, the greater increase in FAT/CD36 expression observed with HF-n-3 feeding may be mediated through n-3 PUFA-induced PPAR α activation and consequently enhanced interaction of PPAR with the PPAR response element on FAT/CD36 gene would promote FAT/CD36 expression.

HF-S, high saturated fat diet; HF-n-3, high fat n-3 polyunsaturated fatty acid (PUFA) enriched diet; FA, fatty acid; CD36 (FAT/CD36), fatty acid translocase; FABPpm, fatty acid binding protein; FATP, fatty acid transport protein; TG, triglyceride; CPT1, carnitine palmitoyl transferase 1; OMM, outer mitochondrial membrane; IMM, inner mitochondrial membrane, PPAR, peroxisome proliferator activator receptor; PPRE, PPAR response element.

4.4.3 – Effect of Dietary Fatty Acid Composition on Skeletal Muscle Fatty Acid Storage and Lipogenesis

In the present study, DGAT1, the enzyme responsible for converting diacylglycerol (DAG) to triglyceride, was upregulated in the skeletal muscle of mice exposed to high fat overfeeding. The role of DGAT1 in mediating insulin sensitivity is controversial. Mice deficient in DGAT1 (DGAT1-knockout, DGAT1^{-/-}) are resistant to diet-induced obesity and exhibit reduced adiposity (Smith *et al.*, 2000). This appears to be a consequence of increased energy expenditure, greater locomotor activity (Smith *et al.*, 2000) and constitutively active thermogenesis (Chen *et al.*, 2003). Exposure to DGAT1 inhibitors *in vitro* similarly induces the mRNA expression of uncoupling proteins in adipocytes and myotubes (Yamamoto *et al.*, 2010). In contrast, DGAT1 overexpression *in vitro* (C2C12 myocytes) (Roorda *et al.*, 2005) and *in vivo* (MCK-DGAT1 mice) (Liu *et al.*, 2007) induces intramuscular triglyceride accretion, which *in vivo* is accompanied by reduced levels of DAG and ceramide. Thus, both models of DGAT1 inhibition (Chen *et al.*, 2004) and overexpression (Liu *et al.*, 2007), despite exhibiting disparate lipid metabolite levels, possess normal insulin sensitivity under conditions of standard chow feeding. However under conditions of high fat overfeeding, there are vast differences in insulin sensitivity (Liu *et al.*, 2007). HFD-fed DGAT1^{-/-} mice exhibit a greater reduction in insulin-stimulated glucose uptake concurrent with reduced triglycerides and increased DAG and ceramide in skeletal muscle when compared to HFD-fed wild type mice (Liu *et al.*, 2007). In contrast, HFD-fed MCK-DGAT1 mice are protected from insulin resistance through preferential storage of lipid as intramuscular triglyceride and lower DAG and ceramide levels and

are consequently more insulin sensitive than HFD-fed wild type mice (Liu *et al.*, 2007). This suggests that upregulation of DGAT1, but not DGAT1 inhibition, is beneficial under conditions of high fat feeding.

In the current study, mRNA expression analyses suggest that skeletal muscle fatty acid uptake was increased by both HFDs, although in the case of the HF-n-3 diet, fatty acid uptake was greater and the capacity for oxidation was increased. It is possible that the HFD-induced upregulation of DGAT1 in the present study acts to ensure non-oxidised fatty acids are disposed of through neutral triglyceride storage, rather than accumulating as harmful lipid intermediates. In HF-S mice, skeletal muscle fatty acid oxidation may have been limited, and although DGAT1 was upregulated this occurred to a far lesser extent than in response to HF-n-3 mice. Accordingly, the capacity to dispose of all fatty acids into either triglyceride or by oxidation may have been limited and as a consequence DAG and ceramide levels may have increased, as has previously been demonstrated in response to high fat feeding (Todd *et al.*, 2007; Lee *et al.*, 2006). This may have deleterious consequences as increased muscle DAG and ceramide levels are associated with reduced insulin sensitivity in humans (Strackowski *et al.*, 2007). In rats, after just 3 weeks HFD, muscle DAG and ceramide levels were significantly elevated with a parallel decrease in insulin-stimulated glucose uptake in skeletal muscle (Todd *et al.*, 2007). In the current study failure to appropriately upregulate DGAT1 was associated with an increase in plasma glucose concentrations in the HF-S group, but not HF-n-3 group. Therefore adequate upregulation of DGAT1 is an appropriate protective response against diet-induced insulin resistance. In the current scope of this thesis the concentrations of DAG and ceramide within the skeletal muscle have not

been measured; however, this would provide useful and interesting information in regards to differential DGAT1 expression and will therefore be measured in a future study extending from this thesis.

In the current study, the mRNA expression of HSL was unchanged by HF-S feeding. It is therefore possible that the capacity for intracellular triglyceride storage is increased as a consequence of reduced lipolysis and increased triglyceride synthesis, even though DGAT1 was not upregulated to the extent expected. In contrast, in HF-n-3 mice there was a parallel increase in DGAT1 and HSL mRNA contents. The simultaneous lipolysis of triglycerides, through increased HSL, and re-esterification of fatty acids to form triglycerides, through increased DGAT1, exhibited in the present study may promote the establishment of the triglyceride-fatty acid cycle (Wolfe *et al.*, 1990), a futile cycle in which opposing reactions, catalysed by different enzymes, expend energy without a net conversion of substrate to product (**Figure 4.28**). However evidence for triglyceride-fatty acid cycling in muscle is quite limited and has been demonstrated to be at a rate one-twentieth of that found in adipose tissue (Tagliaferro *et al.*, 1990).

In skeletal muscle, the flux of triglyceride entering storage in skeletal muscle is also dependent on lipogenic pathways (although to a lesser extent than that observed in other tissues, such as the liver which can display significant *de novo* fatty acid synthesis) regulated by transcription factor, SREBF1. As described in **Chapter 1**, activation of SREBF1 induces the expression of several target genes involved in lipogenesis. One such gene is SCD1, which encodes the enzyme responsible for

converting saturated fat to monounsaturated fatty acids, the preferred substrate for triglyceride synthesis (Sampath *et al.*, 2007). However, during times of fatty acid excess, lipid synthesis is prevented by a feedback control system, in which INSIG1 (see **Chapter 1**) acts to limit the induction of SREBF1 at both the mRNA and protein levels (Qin *et al.*, 2008; Engelking *et al.*, 2004; Takaishi *et al.*, 2004). In the present study, despite a marked increase in SREBF1 mRNA content in the EDL muscle of male HF-S mice, there was no apparent change in the mRNA content of SREBF1 in the soleus muscle with high fat overfeeding. It was also shown, in the present study, that the expression of INSIG1 in skeletal muscle was induced by consumption of a HF-S diet. In the liver, INSIG1 has been shown to be induced by PPAR δ/β (Qin *et al.*, 2008), though in the current study, despite altered INSIG1 expression, skeletal muscle PPAR δ/β mRNA content was unchanged. Given the increased fat accretion in the soleus muscle of HF-S fed mice (as described in **Chapter 3**), the INSIG1 feedback control mechanism may be activated in the soleus muscle upon HF-S feeding to inhibit the induction of SREBF1 expression, in turn preventing lipid synthesis in an already lipid-loaded muscle. Reduced expression of SREBF1 target gene SCD1 (Oh *et al.*, 2003; Horton *et al.*, 2002), provides evidence for the induction of the INSIG1 feedback control mechanism in response to HF-S feeding and may be a protective adaptation in response to increased fatty acid supply as previous studies have shown SCD1 deficiency reduces triglyceride synthesis (Dobrzyn *et al.*, 2005).

In the current study, it was also observed that SCD1 mRNA content was markedly reduced in the skeletal muscle of mice consuming a HFD enriched with n-3 PUFAs, despite unchanged SREBF1 and INSIG1 mRNA content. The present study's

observation of reduced SCD1 upon dietary supplementation with n-3 PUFAs is consistent with previous research in skeletal muscle and liver (Waters *et al.*, 2009; Kramer *et al.*, 2003; Engler *et al.*, 2000). SCD1 may play a lesser role in the skeletal muscle of HF-n-3 mice, as 7.5% of saturated fat replaced with n-3 PUFA, lowering the proportion of fat requiring desaturation by SCD1. Furthermore, research has shown that exposure to PUFAs may influence SREBF1 induced transcription of lipogenic genes by altering the interaction of SREBF1 with its target genes (Thewke *et al.*, 1998; Worgall *et al.*, 1998). Genes transcriptionally regulated by SREBF1 encode a sterol regulatory element within their promoter region, to which mature SREBF1 binds to promote expression of the target gene (Thewke *et al.*, 1998; Worgall *et al.*, 1998). Exposure to PUFAs suppresses the expression of promoters with sterol regulatory elements by reducing levels of mature SREBF1 (Worgall *et al.*, 1998), and this may play a causative role in the reduced expression of SCD1 upon HF-n-3 feeding (**Figure 4.28**).

Therefore, in the present study from mRNA expression analyses, it has been demonstrated that increased triglyceride synthesis in conjunction with unchanged lipolysis may contribute to HF-S-induced muscle fat accumulation. In contrast, the formation of the triglyceride-fatty acid cycle involving DGAT1 and HSL in HF-n-3 mice may expend energy, subsequently limiting triglyceride synthesis and preventing intramyocellular fat accumulation. In HF-n-3 mice, the PUFA component of the diet may also inhibit the maturation of SREBF1, preventing SREBF1-induced lipogenic expression, as seen in reduced SCD1, limiting pathways of lipogenesis (**Figure 4.28**).

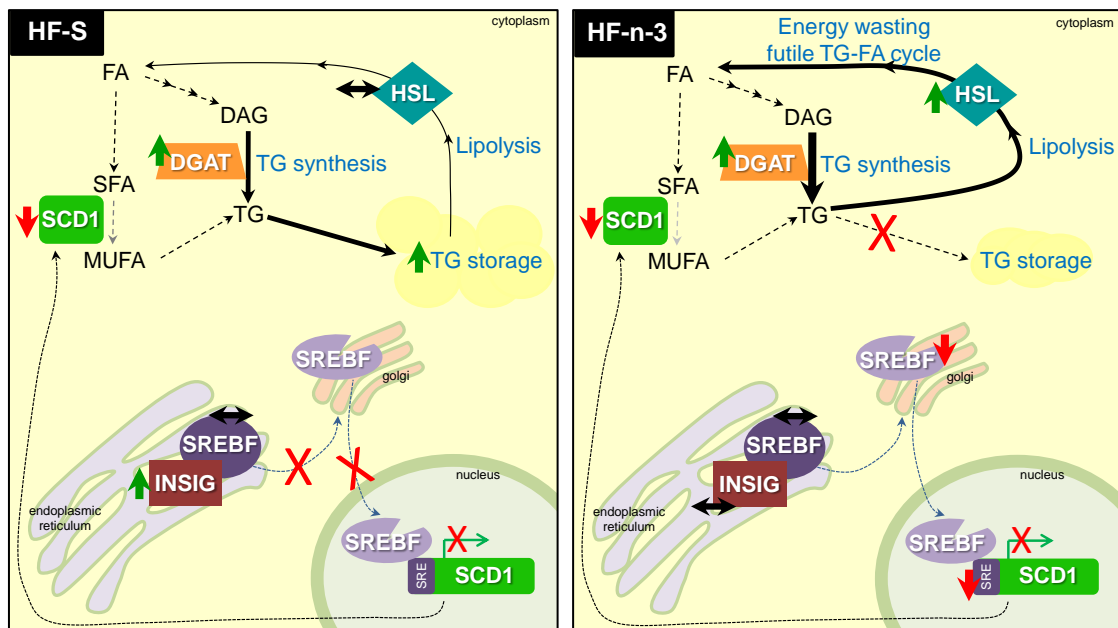


Figure 4.28. Schematic diagram depicting the differential effects that consuming a high saturated fat diet or n-3 PUFA enriched high fat diet exert on fatty acid storage and lipogenesis in skeletal muscle.

In the skeletal muscle, HF-S increased DGAT1 mRNA content, whilst HSL was unchanged; this may contribute to the increased muscle fat accumulation observed in HF-S mice. INSIG1 mRNA was increased in HF-S skeletal muscle. INSIG1 may bind SREBF1 in the endoplasmic reticulum, preventing SREBF1 maturation in the golgi body, which may subsequently reduce the transcription of SREBF1 target genes; this may explain reduced SCD1 mRNA content with HF-S feeding. In contrast, HF-n-3 feeding induced a greater increase in DGAT1 mRNA, whilst also increasing HSL mRNA. Simultaneous lipolysis of triglycerides and esterification of fatty acids, forms the triglyceride-fatty acid futile cycle, and may promote energy wasting, without fat deposition. HF-n-3 feeding may also reduce the expression of sterol regulatory elements on the promoter of SREBF1 target genes, such as SCD1, reducing mature SREBF1 protein and SCD1 mRNA content, preventing activation of lipogenic pathways.

HF-S, high saturated fat diet; HF-n-3, high fat n-3 polyunsaturated fatty acid (PUFA) enriched diet; FA, fatty acid; DAG, diacylglycerol; TG, triglyceride; SFA, saturated fatty acid; MUFA, monounsaturated fatty acid; SCD1, stearoyl-Coenzyme A desaturase 1; DGAT; diacylglycerol acyltransferase 1; HSL, hormone sensitive lipase; INSIG, insulin induced gene; SREBF, sterol regulatory element binding transcription factor; SRE, sterol regulatory element. Thickness of black arrows represents the relative contribution to the process being described. Thick green arrow, increased; thick red arrow, reduced; black double-ended arrow, unchanged; red cross, pathway reduced.

4.4.4 – Effect of Dietary Fatty Acid Composition on Skeletal Muscle Fatty Acid Utilisation

In the present study it was demonstrated that n-3 PUFA enrichment of a HFD increased the expression of genes involved in the transport of fatty acids into skeletal muscle. In turn these fatty acids within the muscle were prevented from entering intramyocellular storage as muscle fat content was lower in the HF-n-3 group. Consequently excess fatty acids may have been cleared by upregulation of skeletal muscle fatty acid oxidation, and therefore it was determined whether genes promoting fatty acid oxidation were upregulated by HF-n-3 feeding. Research has shown that increased dietary fatty acids act to stimulate PDK4 expression (Holness *et al.*, 2000), promoting a switch in muscle fuel metabolism to preferentially utilise fatty acids by suppressing the oxidative disposal of carbohydrate through the citric acid cycle (Jeoung and Harris, 2008); similarly it was shown that PDK4 mRNA content was increased by high fat feeding in the present study. Whilst no difference in PDK4 mRNA content was detected between the two high fat-fed groups in this study, previous studies have demonstrated that the type of dietary fatty acids influences PDK4 activity (Turvey *et al.*, 2005; Fryer *et al.*, 1995). These studies showed that enriching a HFD with n-3 PUFAs in rats, completely prevents (Fryer *et al.*, 1995), and in humans, partially ameliorates, the HFD-induced increase in PDK4 activity (Turvey *et al.*, 2005). Two isoenzymes of PDK, PDK2 and PDK4, are abundant in skeletal muscle (Bowker-Kinley *et al.*, 1998). PDK2 has also been shown to be induced by high fat overfeeding (Chokkalingam *et al.*, 2007; Holness *et al.*, 2000). In the current study only the mRNA content of PDK4 was measured, however, research has shown that PDK4 is the more

markedly increased isoenzyme under conditions of high fat feeding (Chokkalingam *et al.*, 2007; Holness *et al.*, 2000). Therefore a switch in the predominance of skeletal muscle PDK isoenzymes, to favour PDK2, is unlikely to account for the differential responses to n-3 PUFA enrichment of a HFD described in this and previous studies (Turvey *et al.*, 2005; Fryer *et al.*, 1995). Alternatively, the disparate effects of HF-n-3 feeding on PDK4 may be a consequence of the length of dietary intervention, rodents in Fryer and colleagues' (Fryer *et al.*, 1995) model were exposed to high fat feeding for 28 days, whilst Turvey *et al.* (Turvey *et al.*, 2005) provided participants with an acute 3 day HFD; therefore both studies provided a relatively short-term HFD. Research by Fryer *et al.* (Fryer *et al.*, 1995) highlighted that 28 days high fat feeding was insufficient to elicit one of the typical chronic effects of HFD consumption, altered skeletal muscle membrane fatty acid composition (Fryer *et al.*, 1995). Furthermore, it has been suggested that incorporation of n-3 PUFAs into metabolic tissues takes at least 4 months to reach steady state and exert their full metabolic effects (Arterburn *et al.*, 2006; Krebs *et al.*, 2006). In the present study, HFDs were provided for 3½ months duration; that is over 3 times the length of the intervention used by Fryer *et al.* (Fryer *et al.*, 1995), and therefore this study may represent the more chronic effects of enrichment of a HFD with n-3 PUFA on PDK4 mRNA content (**Figure 4.29**).

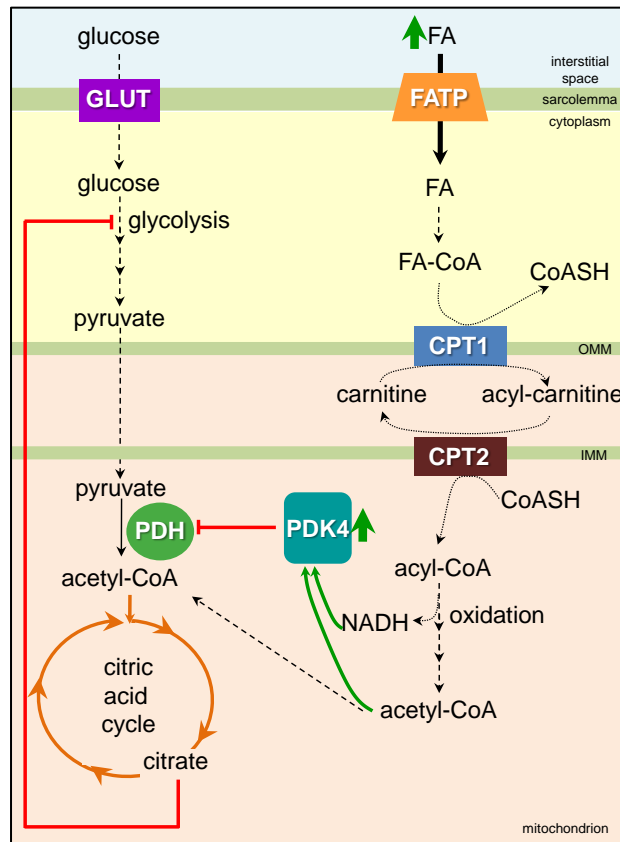


Figure 4.29. Schematic diagram depicting the mechanism by which high fat feeding induces a switch in fuel metabolism in skeletal muscle to reflect the increased availability of fatty acids.

High fat diet consumption results in fatty acid excess and consequentially, fatty acid uptake into the skeletal muscle is increased. With greater fatty acid availability in the muscle cell, more fatty acids undergo mitochondrial oxidation, giving rise to increased concentration of by-products, NADH and acetyl-CoA, which have been shown to induce PDK4 expression. Activated PDK4 inhibits the conversion of pyruvate to acetyl-CoA, which is catalysed by PDH and is the key reaction in driving products of glycolysis into the citric acid cycle. Furthermore, citric acid cycle metabolite, citrate, when increased inhibits glycolytic enzymes. Inhibition of glycolysis, allows the promotion of fatty acid oxidation in order to clear the predominant fuel in excess, fatty acids.

FA, fatty acid; FA-CoA, fatty acyl-Coenzyme A; CoASH, Coenzyme A (not attached to an acyl group); CPT, carnitine palmitoyl transferase; NADH, nicotinamide adenine dinucleotide; PDK4, pyruvate dehydrogenase kinase 4; PDH, pyruvate dehydrogenase; GLUT, glucose transporter; FATP, fatty acid transporter; IMM, inner mitochondrial membrane; OMM, outer mitochondrial membrane. Thick green arrow, increased; thin green arrow, activates, red line, inhibits.

The transfer of fatty acids into the mitochondria is the major rate limiting step for skeletal muscle fatty acid oxidation (Doh *et al.*, 2005). This study showed that the mRNA content of mitochondrial fatty acid transporter CPT1b and FAT/CD36, which can co-localize with CPT1 at the mitochondrial membrane (Bezair *et al.*, 2006; Campbell *et al.*, 2004), were increased by HF-n-3 feeding, potentially acting to increase fatty acid entry into the mitochondria. Increased expression of CPT1 protein in skeletal muscle has previously been shown to enhance fatty acid oxidation, whilst preventing the HFD-induced channelling of fatty acids into esterification and storage pathways, which in combination enhanced insulin sensitivity (Bruce *et al.*, 2009). Failure to upregulate skeletal muscle CPT1b in HF-S-fed mice may therefore result in greater flux of fatty acids driven towards pathways of storage, whilst increased CPT1b mRNA content in HF-n-3 mice may be implicated in the amelioration of HF-S induced intramyocellular fat accumulation, enhanced fatty acid oxidation and insulin sensitivity (**Figure 4.30**).

Furthermore, the cellular concentration of malonyl-CoA influences the shuttling of fatty acids across the mitochondrial membrane, through allosteric regulation of CPT1b (Winder, 2001; Ruderman *et al.*, 1999). In the skeletal muscle, ACC- β is actively involved in the conversion of acetyl-CoA to malonyl-CoA, whilst AMPK regulates ACC- β activation (Carling, 2005; Kahn *et al.*, 2005; Winder, 2001; Ruderman *et al.*, 1999) (see **Chapter 1**). In the current study, the mRNA content of ACC- β and the catalytic α 1 subunit of AMPK were not influenced by high fat overfeeding. However, AMPK is comprised of one of two α catalytic subunits, which previously (Philp *et al.*, 2008; Viollet *et al.*, 2003; Violett *et al.*, 2003) and in the present study, have been

shown to be differentially expressed in skeletal muscle; with AMPK α 1 less prevalent, and AMPK α 2 more predominantly expressed. The current study demonstrated that the more predominant catalytic subunit, AMPK α 2, was increased in the skeletal muscle of HF-S-, but not HF-n-3-fed mice. Enhanced AMPK α 2 may reflect a compensatory response to high fat feeding due to excess availability of fatty acids, with the intension of limiting ATP consuming pathways, such as fatty acid synthesis, and enhancing pathways that expend fuel and produce energy, such as fatty acid oxidation (Violett *et al.*, 2003; Winder, 2001). However, it was demonstrated that intramyocellular fat accumulation and pathways influencing fat storage were increased, whilst mitochondrial fatty acid transport was unchanged, with HF-S feeding. Similarly, Pimenta and colleagues (Pimenta *et al.*, 2008) showed that prolonged exposure of skeletal muscle cells to saturated fat, palmitate, increases muscle lipid accumulation and reduces palmitate oxidation, despite increased activation of AMPK. These studies therefore suggest that enhanced expression or activation of AMPK is inadequate to counteract the suppression of fatty acid oxidation induced by chronic exposure to saturated fat.

The entry of fatty acids into mitochondria is essential for ATP generation, as mitochondria are the chief site in which fatty acids are oxidised to yield energy (Sherwood, 2004; Veerkamp and van Moerkerk, 1986). Besides being channelled towards β -oxidation, fatty acids within the mitochondrion may also interact with uncoupling proteins. Some research has shown that conditions of fatty acid oversupply induce the skeletal muscle expression of UCPs (Turner *et al.*, 2007; Vettor *et al.*, 2002). Similarly, the present study demonstrated that the mRNA content of UCP3 was

increased with high fat feeding and this was irrespective of dietary fatty composition. The present study did not, however, detect alterations in UCP2 mRNA with high fat overfeeding, and this is consistent with research undertaken by Surwit and colleagues (Surwit *et al.*, 1998) and Sbraccia and associates (Sbraccia *et al.*, 2002). Greater expression of UCP3 may reflect an increased capacity for thermogenesis induced by fatty acid oversupply; however the original proposed role of UCP3 in acting to uncouple oxidative phosphorylation has been superseded with additional hypothesised functions (Bezaire *et al.*, 2007; Ricquier, 2005; Himms-Hagen and Harper, 2001). In an environment of fatty acid excess, increased UCP3 expression has been proposed to increase the mitochondrial export of fatty acid anions to allow continued rapid fatty acid oxidation in the mitochondria, averting the deleterious consequences of increased free fatty acid (Himms-Hagen and Harper, 2001). Furthermore, greater expression of UCP3 has been postulated to contribute to the regulation of reactive oxygen species production (Ricquier, 2005; Negre-Salvayre *et al.*, 1997) and in doing so may protect tissues from oxidative stress (Boss *et al.*, 2000).

It has been previously suggested that mitochondrial fatty acid transport, through CPT1, was increased with n-3 PUFA enrichment of a HFD, and the simultaneous increase in PDK4 expression, may reflect an enhanced capacity for fatty acid oxidation within the mitochondria, leading to the reduced intramyocellular fat accumulation apparent in HF-n-3-fed mice. Fatty acid oxidation is also enhanced by the interaction of transcription co-activator PGC1 α with transcription factor PPAR α (Liang and Ward, 2006). As previously mentioned, n-3 PUFAs are natural PPAR α agonists; long chain PUFAs are more proficient at activating PPAR α than short chain saturated fats (Hihi *et al.*, 2002).

Consistent with this notion, there was a marked increase in PGC1 α mRNA upon HF-n-3 feeding and a greater mRNA content of PGC1 α and PPAR α target gene CPT1b in this study. The HF-n-3-induced increase in PGC1 α mRNA content was not, however, observed in conjunction with altered expression of PGC1 α regulator, SIRT1. This may purely reflect that when facing excess fatty acid availability, SIRT1 is not a PGC1 α activator, as SIRT1 has been previously shown to influence PGC1 α 's regulation of glucose metabolism, but does not modulate the effects of PGC1 α on mitochondrial genes (Rodgers *et al.*, 2005). In contrast to HF-n-3 feeding, PGC1 α and PPAR α mRNA were reduced with HF-S feeding and this may confer reduced capacity for the activation of fatty acid oxidation in HF-S mice. Therefore the finding of increased PGC1 α and PPAR α mRNA content in HF-n-3 fed mice, as compared to those consuming a HF-S diet, is consistent with the belief that n-3 PUFAs are acting through PPAR α to direct fatty acid away from storage towards oxidation, preventing deleterious ectopic fat deposition (**Figure 4.30**).

Furthermore in **Chapter 2**, it was elucidated that diminished visceral adiposity and plasma triglyceride concentration, with increased insulin sensitivity in HF-n-3 mice may have been a response of n-3 PUFA mediated activation of PPAR α in peripheral tissues, as the phenotypic response to HF-n-3 feeding mimicked the characteristics seen as a result of PPAR α agonist treatment (Jeong and Yoon, 2009; Tsunoda *et al.*, 2008; Ye *et al.*, 2001). In the current study, greater skeletal muscle PPAR α mRNA content was associated with lower plasma triglyceride concentrations in HF-n-3-fed mice and therefore PPAR α activation may be implicated in the prevention of dyslipidemia

observed with HF-n-3 feeding, but not HF-S consumption. Moreover, it is possible that activated PPAR α may increase the skeletal muscle abundance of FAT/CD36, and this is also consistent with the notion that PPAR α plays a role in preventing hypertriglyceridemia, promoting an increased flux of fatty acids into skeletal muscle from the circulation. In the present study, it was also shown that skeletal muscle PPAR α expression was associated with insulin sensitivity, as in HF-S, but not HF-n-3, mice lower skeletal muscle PPAR α mRNA content correlated with increased plasma glucose concentrations, a marker of reduced insulin sensitivity.

Therefore in the present study, several mechanisms by which intramyocellular fat accumulation may be enhanced with HF-S feeding and prevented by consumption of a HF-n-3 diet (**Figure 4.30**) have been identified. Lower expression of PPAR α and PGC1 α combined with unchanged CPT1b mRNA content in skeletal muscle as a result of HF-S feeding may lead to reduced fatty acid flux into the mitochondria and consequently a decrease in fatty acid oxidation, which may contribute to intramyocellular fat accumulation. Conversely, greater expression of PPAR α and PGC1 α combined with higher CPT1b mRNA content in HF-n-3-fed muscle may result in greater channelling of fatty acids into the mitochondria and subsequent increase in fatty acid oxidation, which may contribute to the prevention of intramyocellular fat accumulation (**Figure 4.30**).

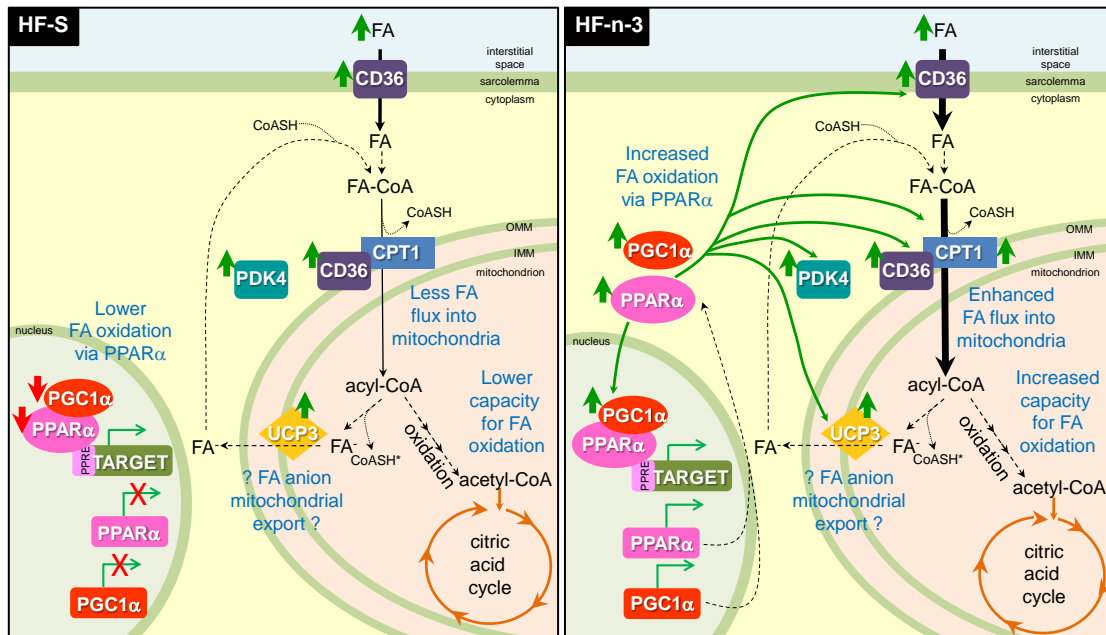


Figure 4.30. Schematic diagram depicting the mechanism behind the differential responses observed in pathways of skeletal muscle fatty acid utilisation with high saturated fat and high fat n-3 PUFA enriched diet feeding.

HFD consumption leads to fatty acid excess and increased skeletal muscle fatty acid uptake. CPT1b mRNA was increased with HF-n-3, but not HF-S, feeding, and there is therefore a greater flux of fatty acids into the mitochondria in the muscle of HF-n-3 mice. UCP3 mRNA was increased with both HFDs; this may promote the export of fatty acid anions from the mitochondria, liberating Coenzyme A (CoASH*) to ensure its availability in other steps of the fatty acid oxidation pathway and improving function. In HF-n-3 mice, skeletal muscle mRNA content of PPAR α and PGC1 α were greater than in HF-S mice. Activation of PPAR α may promote fatty acid oxidation pathways, with PPAR α and coactivator PGC1 α binding to the PPAR response elements of target genes, promoting their expression; target genes include CPT1b, UCP3, PDK4, FAT/CD36. In contrast, reduced PPAR α in HF-S mice may limit activation of PPAR α -mediated pathways and target genes, though CPT1 appeared to be the only PPAR target gene, of those mentioned above, affected.

FA, fatty acid; FA⁻, fatty acid anion; FA-CoA, fatty acyl-Coenzyme A; CPT, carnitine palmitoyl transferase; PDK4, pyruvate dehydrogenase kinase 4; CD36 (FAT/CD36), fatty acid translocase; UCP3, uncoupling protein 3; PPAR α , peroxisome proliferator activator receptor α ; PGC1 α , peroxisome proliferator activated receptor γ activator 1 α ; TARGET, PPAR α target gene; PPRE, PPAR response element; IMM, inner mitochondrial membrane; OMM, outer mitochondrial membrane. Thick green arrow, increased; thin green arrow, activates, red line, inhibits; red cross, pathway reduced.

4.4.5 – Mechanism behind Increased Oxidative Capacity Observed in HF-n-3 Skeletal Muscle despite Unchanged Muscle Fibre Type

In this chapter the mechanism by which n-3 PUFA enrichment of a HFD ameliorates HF-S-induced intramyocellular fat accretion was investigated and this study demonstrated that the response is mediated by the concurrent activation of pathways inducing fatty acid uptake and utilisation and suppression of pathways promoting fatty acid storage and lipogenesis. Whilst some studies have shown that a shift in muscle fibre type composition is implicated in altered skeletal muscle metabolic capacity and function (Oberbach *et al.*, 2006; Tanner *et al.*, 2002; Pette and Staron, 2000; Hickey *et al.*, 1995), in **Chapter 3** of this thesis, it was demonstrated that dietary fatty acid content had no effect on the distribution of muscle fibre type in the FG-FOG EDL and SO soleus muscles. Therefore the differential mRNA contents of key fatty acid metabolism genes reported in the current chapter are in response to altered dietary fatty acid content and not the result of a switch in muscle fibre type in this context.

Despite unchanged muscle fibre type, in **Chapter 3**, it was demonstrated that replacement of 7.5% of dietary saturated fat for n-3 PUFAs resulted in an increase in skeletal muscle oxidative capacity. This chapter has highlighted that n-3 PUFAs induce the expression of several genes implicated in fatty acid oxidation, including PPAR α and PGC1 α , which in comparison were suppressed by exposure to a HF-S diet. PGC1 α overexpression is believed to play a causative role in altered skeletal muscle fibre type composition, promoting the formation of SO muscle fibres (Mortensen *et al.*, 2006; Lin *et al.*, 2002). As the PGC1 α gene encodes a PPAR response element, PGC1 α

may be regulated at the transcriptional level by PPARs. Of the PPAR isoforms expressed in skeletal muscle, PPAR δ/β expression was higher than that of PPAR α , and this is consistent with previous research in which PPAR δ/β was shown to be ubiquitously expressed and the most abundant PPAR isoform expressed in tissues of high oxidative capacity (Escher *et al.*, 2001). PPAR δ/β has been proposed to influence PGC1 α -mediated metabolism as PPAR δ/β strongly associates with PGC1 α *in vivo* (Wang *et al.*, 2003). Schuler and colleagues (Schuler *et al.*, 2006) demonstrated that PPAR δ/β was responsible for regulating the muscle fibre type switch induced by PGC1 α , as in skeletal muscle myocytes, PPAR δ/β ablation produced a reduction in oxidative capacity, leading to a functional fibre type switch towards less oxidative fibres. Despite differential expression of PGC1 α with altered dietary fatty acid consumption, the current study showed that PPAR δ/β mRNA content was unchanged. In the present chapter and **Chapter 3**, it was demonstrated that saturated fat feeding resulted in unchanged/reduced oxidative capacity and a reduction in PPAR α expression, and in comparison n-3 PUFA enrichment of a HFD increased muscle oxidative capacity, and produced a PPAR α expression level greater than that observed with HF-S feeding. PPAR α and PPAR δ/β have been shown to be capable of acting at the same PPAR response elements in some genes (Abbot *et al.*, 2005; Solanes *et al.*, 2003; Mascaró *et al.*, 1998). It is therefore possible that PPAR α , but not PPAR δ/β , may stimulate PGC1 α transcription under conditions of HF-n-3 feeding, increasing the muscle oxidative capacity without the PPAR δ/β -mediated fibre type switch.

4.4.6 – Effect of Gender on Skeletal Muscle Fatty Acid Metabolism

A gender dimorphic response to high fat feeding has been previously demonstrated (Català-Niell *et al.*, 2008; Priego *et al.*, 2008). Females respond to a HFD by increasing adipose tissue storage and the oxidative capacity of skeletal muscle for fatty acids (Priego *et al.*, 2008). The current study has extended this observation by examining the expression of genes that may influence this gender-specific response. In particular, it was observed that the mRNA content of genes involved in fatty acid oxidation (CPT1b, PGC1 α , AMPK α 2) were reduced and those involved in fatty acid storage (DGAT1, SCD1) were preferentially increased in female mice. Receptors for the gonadal steroids, testosterone and estradiol-17 β , are expressed in skeletal muscle (Dahlberg, 1982; Michel and Baulieu, 1980). In sedentary female rats testosterone increases the activity of cytochrome c oxidase, a marker of mitochondrial oxidation, in the EDL muscle, and increases fatty acid binding protein content in the soleus muscle (van Breda *et al.*, 1992). Ovariectomised female mice, in contrast, have diminished expression of genes influencing lipogenesis and fatty acid synthesis (Kamei *et al.*, 2005). Therefore the direct action of gonadal steroids on skeletal muscle may be responsible for the differential expression of fatty acid metabolism genes demonstrated in this study, however this is speculative and further research is required. Furthermore, it may be speculated that a genetic profile favouring triglyceride storage and limiting fatty oxidation in skeletal muscle, may result in an increased propensity for fat storage in female mice, leading to an increased risk of obesity development.

4.4.7 – Limitations

In the current chapter, the findings reported are the outcome of mRNA content analyses, and whilst this provides useful information about the amount of gene transcribed, the mRNA content may not always totally align with the active protein product present in the cell. For instance, total amount of active protein product may be influenced by the stability of mRNA from which protein is translated; the translation of mRNA to protein; post-translational modifications and activation of protein. Two examples in the current chapter in which post-translational changes occur that would alter the functional capacity of that protein are:

SREBF1 – SREBF1 mRNA is translated to protein SREBP1. In the endoplasmic reticulum SREBP1 interacts with SREBP cleavage activating protein (SCAP), a lipid sensor activated when lipids are depleted. SCAP chaperones SREBP to the golgi body. In the golgi SREBP interacts with two proteases, resulting in the cleavage of the NH₂-terminal domain, which subsequently translocates to the nucleus, where it influences the transcription of target genes through binding to a sterol response element in their genetic sequence (Horton *et al.*, 2002).

AMPK – Activation of AMPK protein is dependent on the allosteric binding of AMP or on the phosphorylation of tyrosine residue 172 on AMPK by upstream kinase (Carling, 2005). Active AMPK then goes on to phosphorylate target genes, e.g. ACC- β (which when phosphorylated is deactivated).

Therefore the current study would have benefited from analysing the protein abundance and its activation/activity, hence future investigations may focus on the protein abundance

and activity of the key genes investigated. Furthermore in the current study, pathways of fatty acid uptake, storage and oxidation have been described as mRNA contents. It would also be advantageous to measure these pathways as a whole-process in order to determine their contribution to the overall fatty acid metabolism in skeletal muscle.

4.4.8 – Summary

In summary, this study highlights the influence of dietary fatty acid composition on skeletal muscle metabolism. In **Chapter 3** it was shown that consuming a HFD rich in saturated fat promotes accumulation of triglyceride in skeletal muscle, and conversely, enrichment of this high saturated fat diet with n-3 PUFAs prevented skeletal muscle fat accumulation, despite the super-physiological content of dietary fat present. In this chapter it was demonstrated that the amelioration of intramyocellular fat accretion may occur through an altered pattern of fatty acid metabolism gene expression in skeletal muscle, an effect seen particularly in the soleus muscle. This study was therefore the first, to the best of my knowledge, to identify the mechanisms by which n-3 PUFA enrichment of a HFD prevents intramyocellular fat accumulation, and this may specifically occur through the concurrent activation of pathways inducing fatty acid uptake and utilisation and suppression of pathways promoting fatty acid storage and lipogenesis (**Figure 4.31**). However, this study may have benefited from measuring the protein abundance of key proteins involved in the uptake, utilisation and storage of fatty acids. Furthermore this study highlights the importance of muscle fibre type and gender to the overall characteristics, profile of gene expression and ultimate function of skeletal muscle.

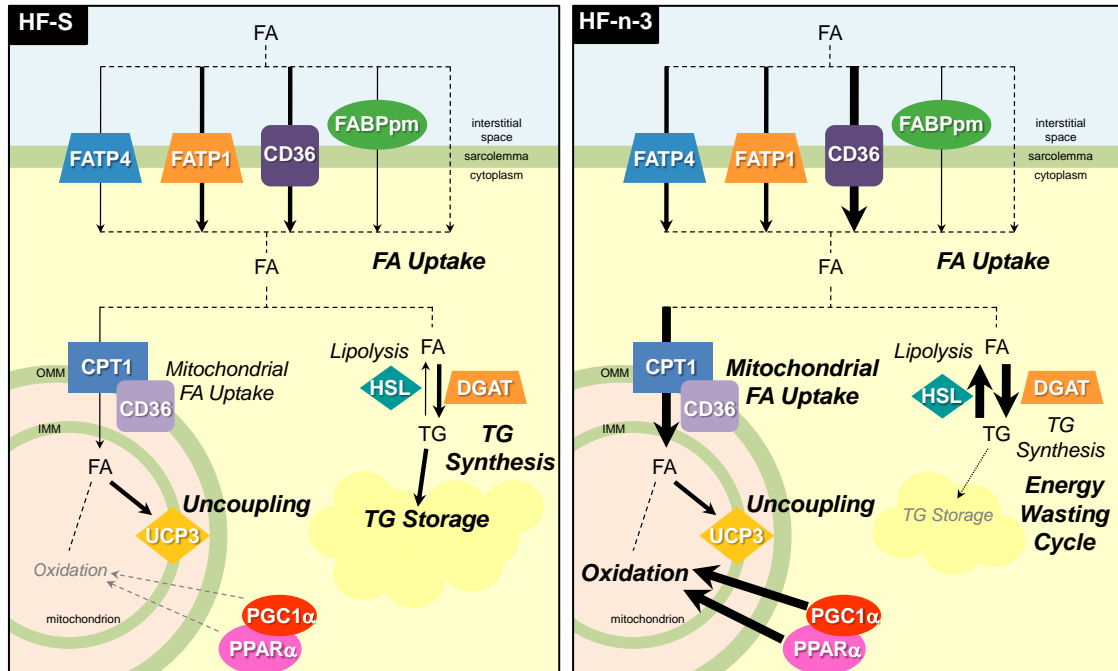


Figure 4.31. Schematic diagram depicting the mechanism behind the differential responses observed in pathways of skeletal muscle fatty acid uptake, storage and utilisation with high saturated fat and high fat n-3 PUFA enriched diet feeding.

The thickness of arrows and boldness of wording represents the relative contribution to the process being described. In skeletal muscle, HF-S feeding increased fatty acid uptake into the muscle, increased the storage capacity for triglycerides, impaired the oxidation of fatty acids in the mitochondria and increased the interaction with uncoupling proteins. In contrast to HF-S feeding, in skeletal muscle, HF-n-3 feeding, increased fatty acid uptake to a greater extent, prevented triglyceride from entering storage by generating an energy wasting cycle, stimulated fatty acid oxidation in the mitochondria, whilst also increasing the interaction with uncoupling proteins. HF-S, high saturated fat diet; high fat n-3 PUFA enriched diet, HF-n-3; FA, fatty acid; CD36 (FAT/CD36), fatty acid translocase; FATP1, fatty acid transport protein 1; FATP4, fatty acid transport protein 4; FABPpm, fatty acid binding protein; HSL, hormone sensitive lipase; DGAT, diacylglycerol acyltransferase; TG, triglyceride; CPT1, carnitine palmitoyl transferase 1; UCP3, uncoupling protein 3; PPAR α , peroxisome proliferator activator receptor α ; PGC1 α , peroxisome proliferative activated receptor γ coactivator 1 α .

CHAPTER 5

*The Effect of Dietary Fatty Acid Composition
and Gender on Hepatic Fatty Acid Metabolism
in Mice*

5.1 – INTRODUCTION

An increased intake of dietary fat poses a metabolic risk to energy homeostasis, as the body is limited in its ability to enhance fatty acid oxidation and subsequently surplus fatty acids are stored in adipose tissue and ectopic depots. In humans, increased saturated fat intake is associated with non-alcoholic fatty liver disease (NAFLD) (Centis, 2010; Musso *et al.*, 2003). In rodents, consuming a saturated fat-rich diet (HF-S) similarly results in increased triglyceride accumulation in hepatic stores, leading to fatty liver (Deng *et al.*, 2007; Buettner *et al.*, 2006; Svegliati-Baroni *et al.*, 2006; Ukropec *et al.*, 2003) (**Chapter 2**). Liver fat accretion is strongly associated with diminished insulin sensitivity (Qureshi *et al.*, 2010; Marchesini *et al.*, 2003; Chitturi *et al.*, 2002) and as the liver plays an essential role in maintaining whole-body energy homeostasis, in part through hepatic fatty acid metabolism, increased intrahepatic fat accumulation may be highly deleterious.

The dyslipidemia and fatty liver observed in response to HF-S feeding may stem from multiple dysfunctions in the hepatic fatty acid metabolism, including pathways of fatty acid uptake, synthesis, secretion and disposal. Increased fatty acid uptake via transporter proteins may contribute to fatty liver development (Bradbury, 2006), as HF-S feeding induces a parallel increase in fatty acid translocase (FAT/CD36) and liver triglyceride content (Koonen *et al.*, 2007), whilst silencing hepatic fatty acid transport protein 5 (FATP5), reversed HF-S-induced fatty liver (Doerge *et al.*, 2008). Increased endogenous fatty acid synthesis (Takaishi *et al.*, 2004; Browning and Horton, 2004) and reduced synthesis and secretion of very low density lipoproteins that act to export

fat from the liver (Reddy and Sambasiva Rao, 2006), may also play a causal role in hepatic fat accumulation. Furthermore, oxidative disposal of accumulated fat is impaired by saturated fat consumption (Reddy and Sambasiva Rao, 2006) due to reduced mitochondrial fatty acid transport via carnitine palmitoyl transferase 1a (CPT1a) (Buettner *et al.*, 2006) and diminished activation of oxidative pathways through peroxisome proliferator activator receptor α (PPAR α) (Svegliati-Baroni *et al.*, 2006). However, defective fatty acid metabolism and hepatic fat accretion can be ameliorated by partially replacing saturated fat for n-3 polyunsaturated fatty acids (PUFA) (Buettner *et al.*, 2006; Ruzickova *et al.*, 2004).

Dietary fish oils, rich in n-3 PUFA, have long been established to improve hypertriglyceridemia (Phillipson *et al.*, 1985), and reduce hepatic triglyceride accumulation in NAFLD (Masterton *et al.*, 2010; Ruzickova *et al.*, 2004; Buettner *et al.*, 2006). Whilst saturated fats exhibit a greater propensity to enter pathways of storage as opposed to being oxidised (Piers *et al.*, 2003; Pan *et al.*, 1994), n-3 PUFAs are less effective at promoting fat deposition and are believed to stimulate lipid oxidation (Pérez-Echarri *et al.*, 2009; Buettner *et al.*, 2006; Piers *et al.*, 2003; Ukropec *et al.*, 2003; Raclot *et al.*, 1997; Shillabeer and Lau, 1994). Whilst comparatively more studies have focused on the role of the liver, than that of skeletal muscle, in n-3 PUFA mediating the amelioration of HF-S-induced dyslipidemia, no study has directly compared the influence of HF-n-3 feeding on hepatic fatty acid metabolism in both genders.

Recently n-3 PUFAs have been considered as a potential clinical therapy against fatty liver (Masterton *et al.*, 2010). The metabolic response of both genders to n-3 PUFA dietary enrichment is an important consideration in treatment design, as epidemiological studies demonstrate that the prevalence of NAFLD is gender- and age-dependent (Hashimoto and Tokushige, 2010; Barshop *et al.*, 2008). Specifically, NAFLD is 2-3 times more common in young males, but after the age of 60, is more prevalent in females (Hashimoto and Tokushige, 2010). Ovariectomy has also been shown to increase liver lipid content in rodent models (Barsalani *et al.*, 2010; Leite *et al.*, 2009), indicating that gonadal hormones play a role in determining hepatic fat deposition. Furthermore, male and female rodents exposed to the same high fat diet (HFD) exhibit a gender-specific pattern of hepatic lipid metabolism (Priego *et al.*, 2008); males have been shown to exhibit greater liver triglyceride content, despite having increased expression of genes influencing fatty acid handling and oxidation. In contrast, female HFD-fed rodents better handle the surplus fat by channelling fatty acids into adipose tissue stores and upregulating fatty acid disposal via oxidation in skeletal muscle (Priego *et al.*, 2008). Given that the vast majority of studies investigating the partial replacement of saturated fat with n-3 PUFAs were conducted in male rodents, the differing vulnerability of males and females to hepatic fat accretion may therefore require important consideration when contemplating perspective treatments or interventions for NAFLD.

In the current study, I therefore aimed to determine:

- I. the effect of replacing 7.5% of saturated fat with n-3 PUFAs (derived from fish oil) in a high saturated fat diet on the hepatic mRNA content of key genes involved in:
 - i) fatty acid uptake
 - ii) lipogenesis and triglyceride storage
 - iii) fatty acid utilisation
- II. the influence of gender on the mRNA content of key genes involved in hepatic fatty acid metabolism in mice

In relation to aim (I) I hypothesised that replacement of 7.5% of saturated fat with n-3 PUFAs prevents the ectopic deposition of fat in the liver (as described in **Chapter 2**) by:

- i) promoting the mRNA expression of genes influencing the uptake of fatty acids into the liver
- ii) preventing the mRNA expression of genes controlling lipogenesis and
- iii) upregulating the mRNA expression of genes that would lead to enhanced oxidation.

And finally, in relation to aim (II) I hypothesised that the increased liver fat content in female mice reported in **Chapter 2**, despite previous studies showing greater liver fat accretion in males (Priego *et al.*, 2008), would be the result of female mice having greater mRNA content of genes influencing fatty acid uptake and storage, as compared to male mice.

5.2 – MATERIALS AND METHODOLOGY

5.2.1 – *Animals, Nutrition Regime and Tissue Collection*

As described in **Chapter 2 Section 2.1**, male and female C57BL/6J mice in cohort 1 were provided either a standard chow (control, C), high saturated fat (HF-S) or high fat n-3 PUFA enriched (HF-n-3) diet for 14 weeks (\pm 4 days). All procedures were approved by the University of Adelaide Animal Ethics Committee and the Institute of Medical and Veterinary Science Animal Ethics Committee. As described in **Chapter 2 Section 2.2**, following the experimental dietary period, mice underwent surgery whilst in the fed-state and the liver was rapidly collected post-mortem, divided and a portion was snap frozen and stored under liquid nitrogen vapour phase storage until subsequent mRNA content analyses.

5.2.2 - *Extraction of RNA from Liver Samples*

Total RNA from a sample of the liver (~10-17 mg) was isolated using TRIzol[®] reagent (Invitrogen Australia Pty Ltd, Mount Waverley, Victoria, Australia) at a volume of 1,000 μ l. Liver samples were homogenised using 5 mm stainless steel beads (Qiagen GmbH, Hilden, Germany, Europe) and Qiagen TissueLyser (Qiagen GmbH, Hilden, Germany, Europe) set at 30 Hz for 2 minutes. The resultant homogenate was centrifuged at 13,200 rpm for 15 minutes at 4°C to pellet cell debris. The supernatant was collected and 400 μ l chloroform was added, samples were inverted several times and placed on ice for 5 minutes. Samples were then centrifuged at 13,000 rpm for 15 minutes at 4°C to separate RNA (upper-phase) from DNA and protein. The upper-

phase was collected and 500 µl 2-propanol was added, and samples were then incubated at -20°C for 2 hours to precipitate RNA. Samples were then centrifuged at 13,200 rpm for 20 minutes at 4°C to pellet RNA and subsequently, RNA pellets were washed with ethanol. RNA was re-suspended in nuclease free water and incubated at 60°C for 10 minutes. RNA quality and concentration were evaluated by measuring absorbance at 260 nm and 280 nm (NanoDrop 1000 Spectrophotometer (ThermoScientific Inc, Wilmington, Delaware, USA)). The ratio of OD260 to OD280 provided a score of RNA quality and all calculated ratios scored >1.8. RNA concentration was determined using the modified Beer-Lambert equation, where concentration (ng/µl) is equal to the absorbance at 260 nm (AU) * extinction coefficient constant of RNA (40 ng-cm/µl) divided by the pathlength (cm). RNA was subsequently treated to eliminate genomic DNA contamination using deoxyribonuclease I (amplification grade; Invitrogen Australia Pty Ltd, Mount Waverley, Victoria, Australia). RNA was stored at -80°C, until incorporation into mRNA content analyses on the GenomeLab GeXP Genetic Analysis System (Beckman Coulter Inc, Fullerton, California, USA).

5.2.3 - Multiplex Primer Design

Forward and reverse primers were designed using the accession numbers of genes of interest (*mus musculus* mRNA transcripts). Accession numbers were imported into GenomeLab GeXP eXpress Profiler software (ver.10.0 Beckman Coulter Inc, Fullerton, California, USA). Primers were designed to generate amplified products with similar guanine (G)/cytosine (C) content (50%) and melting temperature (60°C). Primers utilised to amplify genes of interest in liver samples were designed to generate an

amplified product with a gene fragment length between 145-356 nucleotides and separation size of least 5 nucleotides between products. Under additional constraints, primers were targeted to amplify a section of the protein coding sequence as determined by Entrez Nucleotide (National Center for Biotechnology Information, Bethesda, Maryland, USA). To ensure amplification of cDNA without unwanted amplification of contaminating DNA, where possible, forward and reverse primers were designed to be positioned in different exons, as determined by Ensembl (European Bioinformatics Institute/Wellcome Trust Sanger Institute, Cambridge, United Kingdom, Europe). Finally primer sequences were submitted to BLAST (Basic Local Alignment Search Tool, National Center for Biotechnology Information, Bethesda, Maryland, USA) to ensure primer sequences aligned specifically with the gene of interest. When aligned, if any mRNA sequence was found to have a high similarity defined by a probability (E value) of ≤ 0.05 , the primer was redesigned. The design software then added a universal primer sequence to both forward and reverse designed primer sequences, generating chimeric primers. Resultant forward and reverse primers (GeneWorks Pty Ltd, Hindmarsh, South Australia, Australia) utilised to amplify genes of interest in liver samples are listed in **Table 5.1**.

5.2.4 - Optimisation of Liver Multiplex

Similar to that described in **Chapter 4 Section 2.4**, a reference liver RNA sample was generated by combining equal parts of RNA from all liver samples and this reference liver RNA was used to test multiplex primers, with the aim of ensuring polymerase chain reaction (PCR) products separated into well-defined peaks at the designed size. Due to substrate competition between high and low expressing primer products, the

liver multiplex primers were subsequently separated into separate multiplexes to ensure adequate signal of low expressing products when separated on the GenomeLab GeXP Genetic Analysis System. The concentrations of reverse primers, in multiplex, were then optimised to ensure adequate detection of assigned product peaks (**Table 5.1**).

5.2.5 - Reverse Transcription of RNA and Subsequent PCR

Using RNA extracted from liver samples, cDNA was generated by reverse transcription using the GenomeLab GeXP Genetic Analysis System, using methodology described in **Chapter 4 Section 2.5**. Using cDNA generated by reverse transcription of RNA from liver samples, PCR was performed to generate a double-stranded template using the GenomeLab GeXP Genetic Analysis System, using methodology described in **Chapter 4 Section 2.6**.

Table 5.1. The sequence, assigned product size and optimised concentration (in reverse multiplex mix) of primers used to determine the mRNA content of key genes of interest in liver samples.

Gene (Accession number)	Forward primer sequence (5'-3') Reverse primer sequence (5'-3')	Size (bp)	[Primer] reverse mix (nM)
PDK4 (NM_013743)*	CCATGAGAAGAGCCCAGAAG ATGCCTTGAGCCATTGTAGG	145	500
SCD1 (NM_009127)*	CTATGGATATCGCCCCTACG TAGTCGAAGGGGAAGGTGTG	151	5.00
PPAR δ/β (NM_011145) [#]	CGGGAAGAGGAGAAAGAGGA GAGGAAGGGGAGGAATTCTG	159	500
Slc27a5 (FATP5) (NM_009512)*	GCAGAGCTGATGATGTGGTC AATCGGGAGGCAGAGAACTT	167	250
Slc27a2 (FATP2) (NM_011978)*	CAGGCCTTGCTATGTGCGAGT TTGCTCCGCAAAGCTAAAGT	173	500
INSIG1 (NM_153526)*	GACGAGGTGATAGCCACCAT TGGCCATTCTCTCTTGAAC	179	250
ACC- β (NM_133904)*	TGGAGTCCATCTTCCTGTCC GGACGCCATACAGACAACCT	186	500
ACC- α (NM_133904)*	CAGGCATATGGAGACAAGCA TGATGAGTGACTGCCGAAAC	194	500
SIRT1 (NM_019812) [#]	GACGCTGTGGCAGATTGTTA GTCAGGAATCCCACAGGAGA	200	500
PEPCK (NM_011044)*	GGAGTCACCATCACCTCCTG ACGCCACCAAAGATGATAC	208	500
AMPK α 2 (NM_178143) [#]	TGATCAGCACTCCGACAGAC TCAGGTCCTATGGACAACC	214	500
POLR2C (NM_009090)* [#]	TGAGGTGCAATGAAGACCAG CTTGGCATAGGCTCGAAGTC	222	500
GCK (NM_010292)*	TGGAGGAGATGCAGAATGTG CATGTACTTCCGCCAATGA	228	125
PFK-L (NM_008826)*	CCAGAGGACCTTTGTTTTGG CCTCTGCGATGATGATGATG	234	500
SREBF1 (NM_011480)*	GTACCTGCGGGACAGCTTAG TCAGGTCATGTTGGAAACCA	243	500
SOCS3 (NM_007707) [#]	CTTTTCGCTGCAGAGTGACC CGCCCCAGAATAGATGTAG	249	500
FABPpm (NM_010325)*	GCGGTTTTGACTTCTCTGGA CCAGGCATCCTTATCACCAT	255	500

Primers in: multiplex 1*, multiplex 2[#]. Gene-specific forward and reverse primer sequences are flanked by a common universal primer sequence at the 5' end:
Forward universal = aggtgacactatagaata; Reverse universal = gtacgactcactataggga.

Table 5.1 (continued). The sequence, assigned product size and optimised concentration (in reverse multiplex mix) of primers used to determine the mRNA content of key genes of interest in liver samples.

Gene (Accession number)	Forward primer sequence (5'-3') Reverse primer sequence (5'-3')	Size (bp)	[Primer] reverse mix (nM)
PPAR γ (NM_001127330) [#]	AAGAGCTGACCCAATGGTTG GCATCCTTCACAAGCATGAA	263	500
CPT1a (NM_013495)*	CCAGGCTACAGTGGGACATT CATGGAAGCCTCATACTGTA	270	500
Lipe (HSL) (NM_001039507) [#]	GGAACCTAAGTGGACGCAAGC TTGACATCAGAGGGTGTGGA	277	500
FAT/CD36 (NM_007643)*	GCTCTCCCTTGATTCTGCTG TGGGTTTTGCACATCAAAGA	286	500
UCP2 (NM_011671) [#]	GTCCACGCAGCCTCTACAAT GCTCTGGTATCTCCGACCAC	291	500
TBP (NM_013684)* [#]	GGACCAGAACAACAGCCTTC GTGGGTTGCTGAGATGTTGA	298	500
RPLP0 (NM_007475)* [#]	GCATCACCACGAAAATCTCC TACCCGATCTGCAGACACAC	305	500
FAS (NM_007988)*	ACATGGTAGCTGCCCTCAAG TGGAAGCTGGTATCCTCCAC	311	500
DGAT2 (NM_026384)*	ACTGCTGGCTGATAGCTGTG ATAGGGCCTTATGCCAGGAA	318	500
PGC1 α (NM_008904) [#]	GTACAACAATGAGCCTGCGA AGTGCTAAGACCGCTGCATT	332	500
PPAR α (NM_001113418)*	ACGATGCTGTCCTCCTTGAT TCATCTGGATGGTTGCTCTG	339	500
GYS2 (NM_145572)*	GGCATCCCCAGTGTGACTAC TGGGCTCTAGGTGGAATTTG	347	500
AMPK α 1 (NM_00103367) [#]	AGCCGACTTTGGTCTTTCAA ATCTTTTATTGCGGCCCTCT	356	500

Primers in: multiplex 1*, multiplex 2[#]. Gene-specific forward and reverse primer sequences are flanked by a common universal primer sequence at the 5' end:
Forward universal = aggtgacactatagaata; Reverse universal = gtacgactcactatagga

5.2.6 - Separation of PCR Products by the GenomeLab GeXP Genetic Analysis System

Multiplex detection via capillary electrophoresis was then performed; fluorescently labelled PCR products were separated, detected and quantified using the GenomeLab GeXP Genetic Analysis system, as described in **Chapter 4, Section 2.7**. Separated fragments were analysed using sensitive analysis parameters (slope threshold = 1, peak height threshold = 0) and GenomeLab eXpress Profiler software (ver.10.0 Beckman Coulter Inc, Fullerton, California, USA). Multiplex detection was performed in duplicate for every sample and data were combined to generate the mean of duplicate analyses. Output mRNA contents were then normalised to the average mRNA content of 3 housekeeping genes, TATA-binding protein (TBP), RNA Polymerase 2c (POLR2c) and large ribosomal protein P0 (RPLP0), to compensate for variation in reverse transcription efficiency. Housekeeping genes were validated to show absolute mRNA content remained unchanged between groups. Results are reported as mRNA content, the ratio of mean mRNA content of the target gene relative to the averaged mean mRNA content of three housekeeping genes (AU).

5.2.7 – Statistical Analyses

All data are presented as mean \pm standard error of the mean (SEM). Two-way Analysis of Variance (ANOVA), with pairwise comparisons (Bonferroni post-hoc analysis), was used to determine the effect of diet (C, HF-S, HF-n-3), gender (male, female) and their interaction on the mRNA content of key fatty acid metabolism genes. Simple linear regression analyses were used to determine the relationship of fatty acid translocase

(FAT/CD36) mRNA content with measures of liver fat accumulation; fatty acid transport protein 2 (FATP2) mRNA content with measures of liver fat accumulation, diacylglycerol acyltransferase 2 (DGAT2) mRNA content with plasma triglyceride concentrations, pyruvate dehydrogenase kinase 4 (PDK4) mRNA content with plasma glucose concentrations, and uncoupling protein 2 (UCP2) mRNA content with final body weight. Pearson correlation coefficients (r) were used to evaluate linear relationships.

All statistics were performed using the Statistical Package for Social Scientists (SPSS) (ver. 17.0.0, SPSS Inc, Chicago, Illinois, USA). A probability of less than 5% ($P < 0.05$) was considered statistically significant. Analyses are reported as percentage change; statistical effect: $F(\text{degrees of freedom: between subjects effect, degrees of freedom: within subjects effect}) = F$ value, P value of effect; and subsequent P values of post-hoc or pairwise analyses.

5.3 – RESULTS

5.3.1 - Fatty Acid Transport (*FAT/CD36*, *FABPpm*, *FATP2* and *FATP5*)

Fatty acid translocase (*FAT/CD36*) mRNA content was greater in HF-n-3 mice as compared to control and HF-S mice ($F(2, 57)=181.2$, $P\leq 0.001$; +1.7 fold, +1.5 fold, respectively; post-hoc tests: $P\leq 0.001$) (**Figure 5.1A**). There was an effect of gender on *FAT/CD36* mRNA content, female mice exhibited greater *FAT/CD36* mRNA than male mice (+40%; $F(1, 57)=31.9$, $P\leq 0.001$).

There was no effect of diet ($F(2, 57)=0.8$, $P=0.46$) or gender ($F(1, 57)=0.1$, $P=0.75$) on fatty acid binding protein (*FABPpm*) mRNA content (**Figure 5.1B**).

Fatty acid transport protein 2 (*FATP2*) mRNA content was in greater in HF-n-3 mice as compared to HF-S mice ($F(2, 57)=3.8$, $P=0.028$; +12%; post-hoc test: $P\leq 0.05$) (**Figure 5.2A**). There was no effect of gender on *FATP2* mRNA content ($F(1, 57)=1.9$, $P=0.17$).

Fatty acid transport protein 5 (*FATP5*) mRNA content was lower in HF-S and HF-n-3 mice as compared to control mice ($F(2, 57)=9.3$, $P\leq 0.001$; -16%, -27%, respectively; post-hoc tests: $P\leq 0.05$, $P\leq 0.001$) (**Figure 5.2B**). There was no effect of gender on *FATP5* mRNA content ($F(1, 57)=0.3$, $P=0.58$).

FAT/CD36 mRNA was positively correlated with liver fat content (fat droplet area) in HF-S, but not HF-n-3, mice (HF-S, $r = +0.49$, $F(1, 18)=5.5$, $P=0.030$; HF-n-3, $r = -0.28$, $F(1, 17)=1.5$, $P=0.24$) (**Figure 5.3**). In the HF-n-3 group only, there was a trend towards a negative correlation between FATP2 mRNA and liver fat content (percentage area stained positively for fat) (HF-n-3, $r = -0.44$, $F(1, 17)=4.0$, $P=0.062$; HF-S, $r = +0.068$, $F(1, 18)=0.8$, $P=0.78$) (**Figure 5.3**).

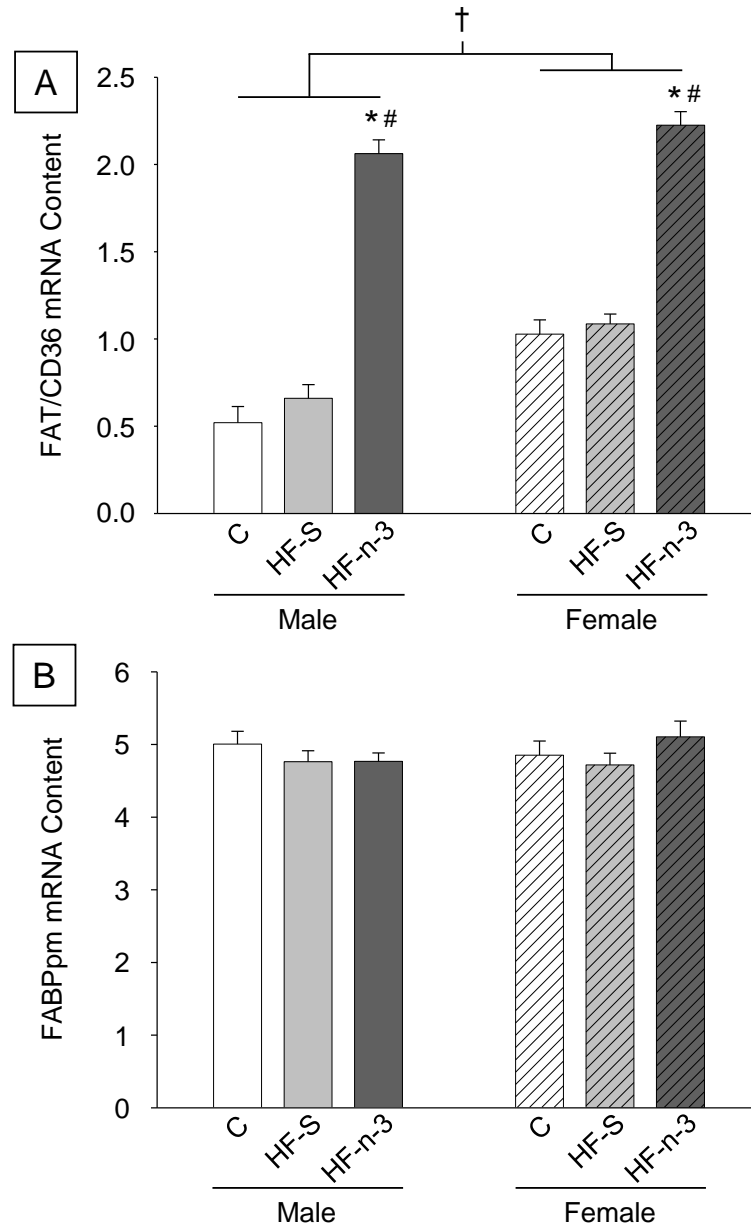


Figure 5.1 [A-B]. FAT/CD36 [A] and FABPpm [B] mRNA content in the liver of male and female mice fed control, high saturated fat or high fat n-3 PUFA enriched diets.

Data are expressed as mean (bars) \pm SEM (error bars), where solid bars indicate male (M) mice, lined bars indicate female (F) mice and colour represents diet: white, control (C); pale grey, high saturated fat (HF-S); dark grey, high fat n-3 polyunsaturated fatty acid enriched (HF-n-3). FAT/CD36, fatty acid translocase; FABPpm, fatty acid binding protein. [A-B]: n: C(M/F) = 10/12, HF-S(M/F) = 11/10, HF-n-3(M/F) = 9/11. Statistics: Effect of diet: * $P \leq 0.001$, compared to C, # $P \leq 0.001$, compared to HF-S. Effect of gender: † $P \leq 0.001$, male compared to female.

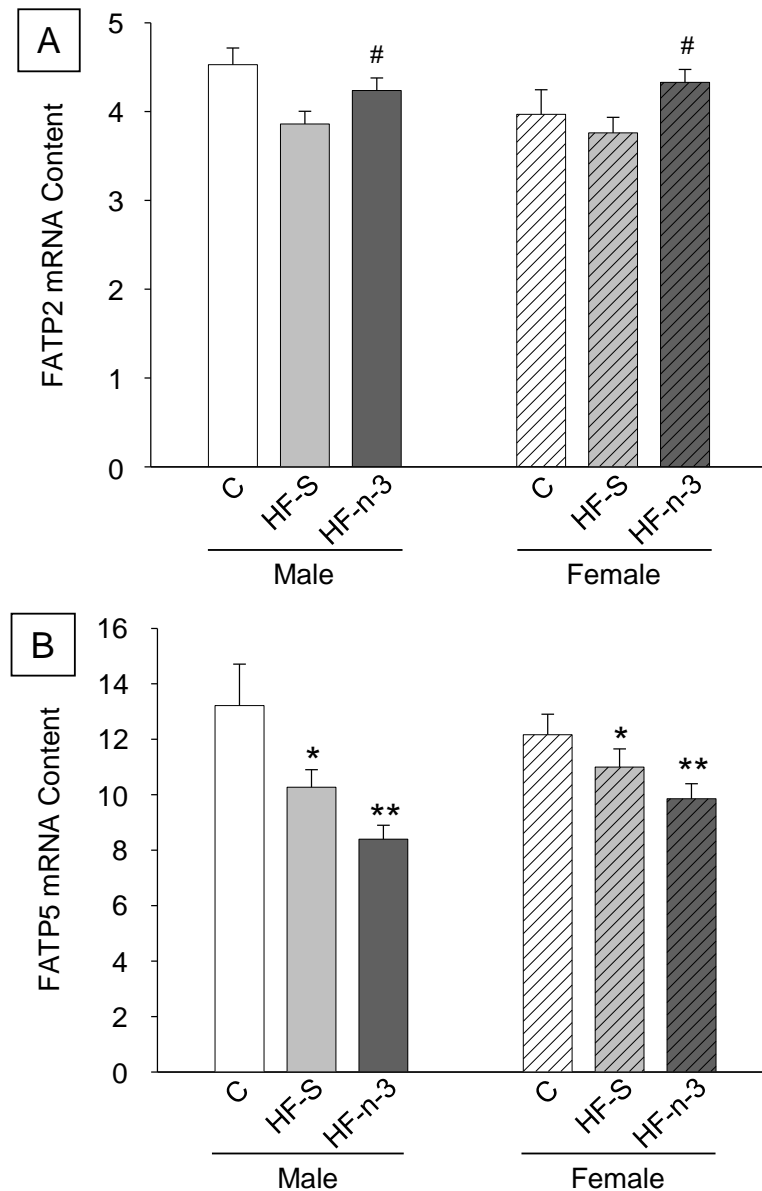


Figure 5.2 [A-B]. FATP2 [A] and FATP5 [B] mRNA content in the liver of male and female mice fed control, high saturated fat or high fat n-3 PUFA enriched diets.

Data are expressed as mean (bars) \pm SEM (error bars), where solid bars indicate male (M) mice, lined bars indicate female (F) mice and colour represents diet: white, control (C); pale grey, high saturated fat (HF-S); dark grey, high fat n-3 polyunsaturated fatty acid enriched (HF-n-3). FATP, fatty acid transport protein.

[A-B]: n: C(M/F) = 10/12, HF-S(M/F) = 11/10, HF-n-3(M/F) = 9/11.

Statistics: Effect of diet: * $P \leq 0.05$, ** $P \leq 0.001$, compared to C; # $P \leq 0.05$, compared to HF-S.

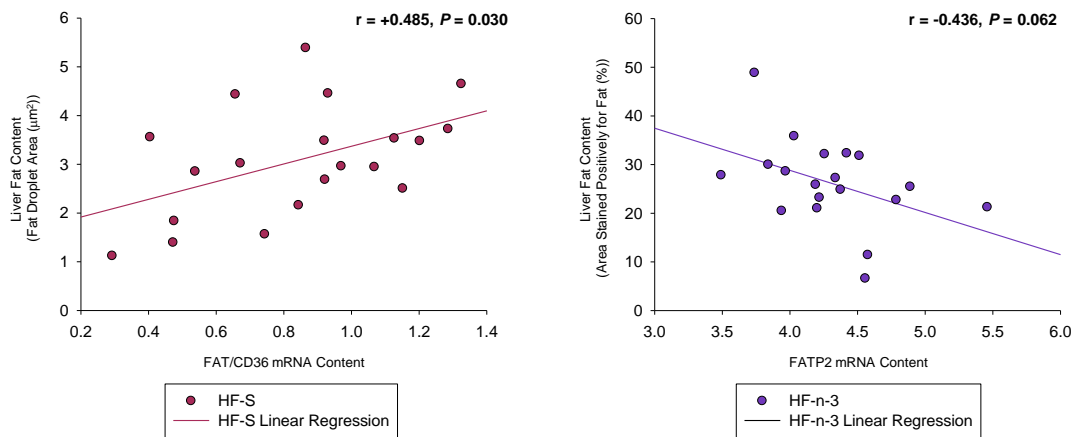


Figure 5.3. The relationships between liver fat content and the hepatic mRNA content of fatty acid transporters FAT/CD36 and FATP2.

Symbol type represents dietary group: see legend. FAT/CD36, fatty acid translocase; FATP2, fatty acid transport protein 2; HF-S, high saturated fat diet; HF-n-3, high fat n-3 polyunsaturated fatty acid enriched diet.

n: HF-S = 20, n: HF-n-3 = 19.

There was a significant positive relationship between liver fat content (fat droplet area) and hepatic FAT/CD36 mRNA expression in HF-S mice only (males and females combined). There was a tendency for a negative relationship between liver fat content (percentage area stained positively for fat) and hepatic FATP2 mRNA expression in HF-n-3 mice only (males and females combined).

5.3.2 - Lipogenesis, Triglyceride Synthesis and Storage (*SREBF1*, *INSIG1*, *FAS*, *ACC- α* , *DGAT2*, *SCD1* and *HSL*)

Sterol regulatory element binding transcription factor 1 (*SREBF1*) mRNA content was lower in HF-n-3 mice as compared to control and HF-S mice ($F(2, 58)=12.1$, $P\leq 0.001$; -47%, -36%, respectively; post-hoc tests: $P\leq 0.001$, $P\leq 0.01$, respectively) (**Figure 5.4A**). There was no effect of gender on *SREBF1* mRNA content ($F(1, 58)=1.7$, $P=0.20$).

Insulin induced gene 1 (*INSIG1*) mRNA content was lower in HF-n-3 mice as compared to control and HF-S mice ($F(2, 57)=53.1$, $P\leq 0.001$; -1.6 fold, -1.4 fold, respectively; post-hoc tests: $P\leq 0.001$) (**Figure 5.4B**). There was no effect of gender on *INSIG1* mRNA content ($F(1, 57)=0.7$, $P=0.40$).

Fatty acid synthase (*FAS*) mRNA content was lower in HF-n-3 mice as compared to control and HF-S mice ($F(2, 56)=90.3$, $P\leq 0.001$; -6.7 fold, -6.0 fold, respectively; post-hoc tests: $P\leq 0.001$) (**Figure 5.5A**). There was no significant effect of gender on *FAS* mRNA content, although there was a trend towards greater *FAS* mRNA content in male mice as compared to female mice (+37%; $F(1, 56)=3.0$, $P=0.09$).

Acetyl-Coenzyme A carboxylase- α (*ACC- α*) mRNA content was lower in HF-n-3 mice as compared to control and HF-S mice ($F(2, 58)=87.0$, $P\leq 0.001$; -125%, -104%, respectively; post-hoc tests: $P\leq 0.001$) (**Figure 5.5B**). There was an effect of gender on *ACC- α* mRNA content, male mice exhibited greater *ACC- α* mRNA than female mice (+15%; $F(1, 58)=6.3$, $P=0.015$).

Diacylglycerol acyltransferase 2 (DGAT2) mRNA content was lower in HF-S and HF-n-3 mice as compared to control mice ($F(2, 57)=10.0$, $P\leq 0.001$; -18%, -32%, respectively; post-hoc tests: $P\leq 0.02$, $P\leq 0.001$, respectively) (**Figure 5.6A**). There was no significant effect of gender on DGAT2 mRNA content, although there was strong trend towards greater DGAT2 mRNA content in female mice as compared to male mice (+11%; $F(1, 57)=4.0$, $P=0.051$).

Stearoyl-Coenzyme A desaturase 1 (SCD1) mRNA content was lower in HF-n-3 mice as compared to control and HF-S mice ($F(2, 57)=193.3$, $P\leq 0.001$; -11.3 fold, -10.2 fold, respectively; post-hoc tests: $P\leq 0.001$) (**Figure 5.6B**). There was no effect of gender on SCD1 mRNA content ($F(1, 57)=0.07$, $P=0.79$).

Hormone sensitive lipase (HSL) mRNA content was greater in HF-n-3 mice as compared to control and HF-S mice ($F(2, 58)=7.7$, $P\leq 0.001$; +14%, +11%, respectively; post-hoc tests: $P\leq 0.001$, $P\leq 0.02$, respectively) (**Figure 5.7**). There was no effect of gender on HSL mRNA content ($F(1, 58)=1.0$, $P=0.32$).

DGAT2 mRNA content was positively correlated with plasma triglyceride concentrations (when the entire cohort were combined) ($r = +0.33$, $F(1, 58)=7.2$, $P=0.009$) (**Figure 5.8**).

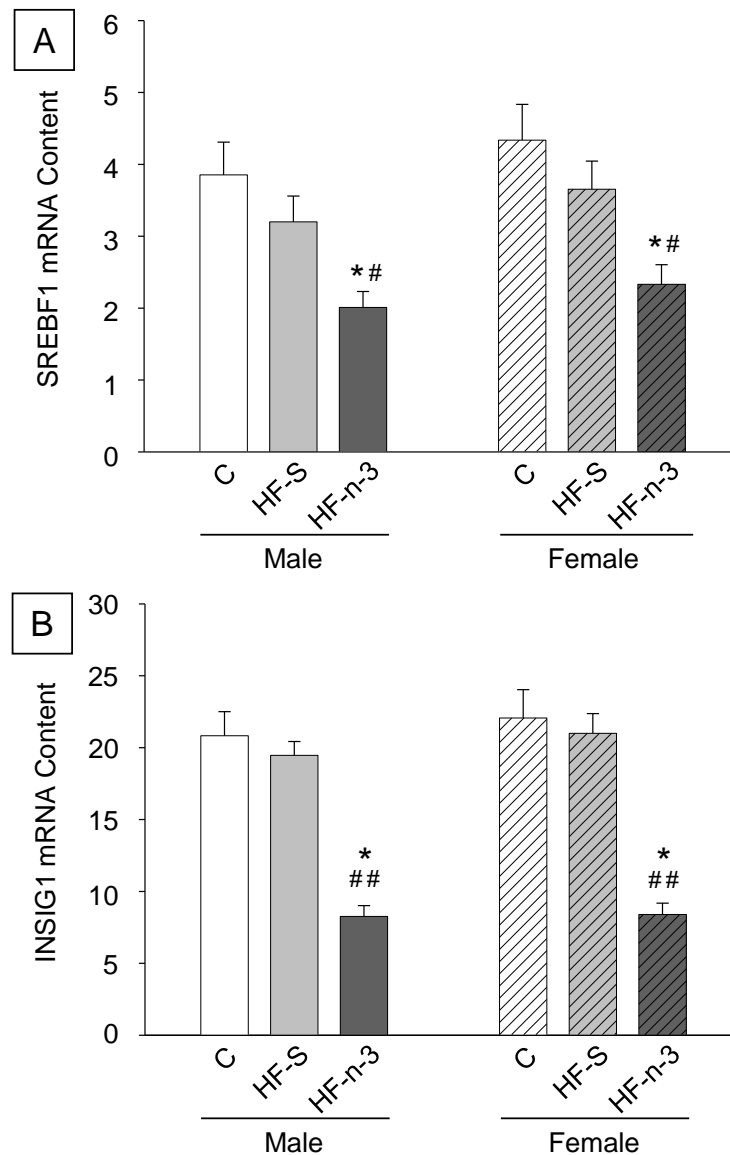


Figure 5.4 [A-B]. SREBF1 [A] and INSIG1 [B] mRNA content in the liver of male and female mice fed control, high saturated fat or high fat n-3 PUFA enriched diets.

Data are expressed as mean (bars) ± SEM (error bars), where solid bars indicate male (M) mice, lined bars indicate female (F) mice and colour represents diet: white, control (C); pale grey, high saturated fat (HF-S); dark grey, high fat n-3 polyunsaturated fatty acid enriched (HF-n-3). SREBF1, sterol regulatory element binding transcription factor 1; INSIG1, insulin induced gene 1.

[A]: n: C(M/F) = 10/12, HF-S(M/F) = 11/11, HF-n-3(M/F) = 9/11.

[B]: n: C(M/F) = 10/12, HF-S(M/F) = 11/10, HF-n-3(M/F) = 9/11.

Statistics: Effect of diet: * $P \leq 0.001$, compared to C; # $P \leq 0.01$, ## $P \leq 0.001$, compared to HF-S.

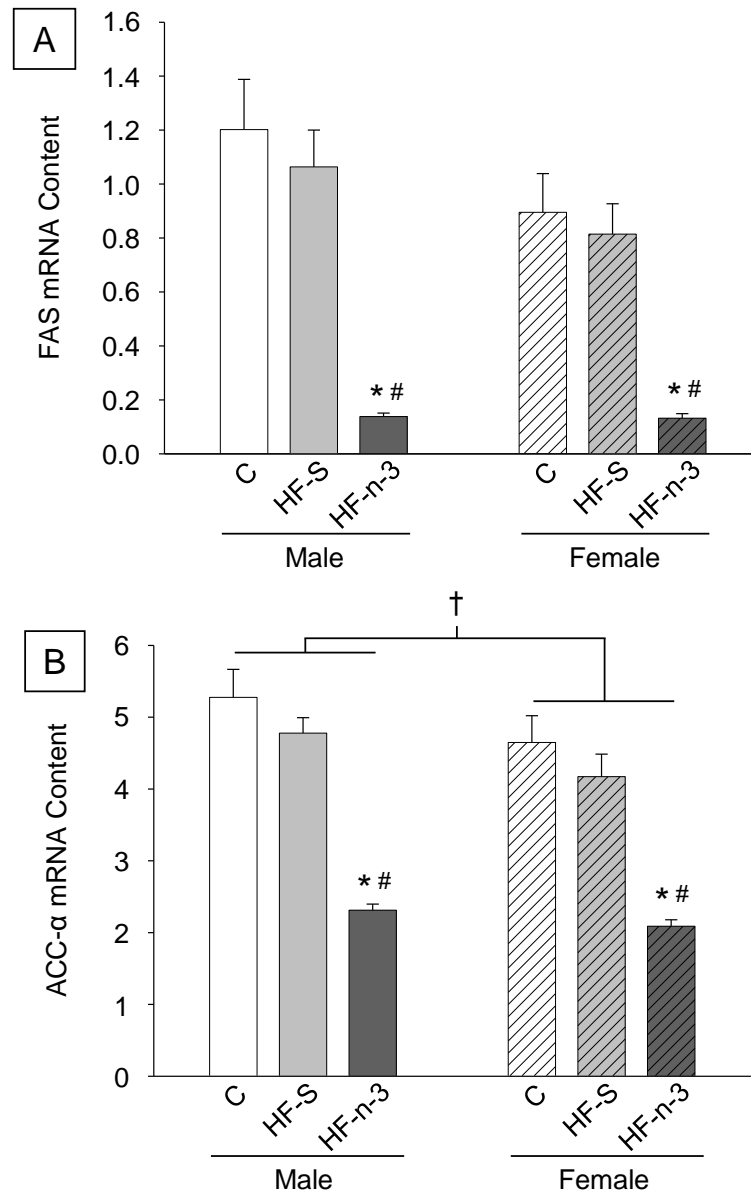


Figure 5.5 [A-B]. FAS [A] and ACC- α [B] mRNA content in the liver of male and female mice fed control, high saturated fat or high fat n-3 PUFA enriched diets.

Data are expressed as mean (bars) \pm SEM (error bars), where solid bars indicate male (M) mice, lined bars indicate female (F) mice and colour represents diet: white, control (C); pale grey, high saturated fat (HF-S); dark grey, high fat n-3 polyunsaturated fatty acid enriched (HF-n-3). FAS, fatty acid synthase; ACC- α , acetyl-Coenzyme A carboxylase- α .

[A]: n: C(M/F) = 10/11, HF-S(M/F) = 11/10, HF-n-3(M/F) = 9/11.

[B]: n: C(M/F) = 10/12, HF-S(M/F) = 11/11, HF-n-3(M/F) = 9/11.

Statistics: Effect of diet: * $P \leq 0.001$, compared to C; # $P \leq 0.001$, compared to HF-S. Effect of gender: † $P \leq 0.02$, male compared to female.

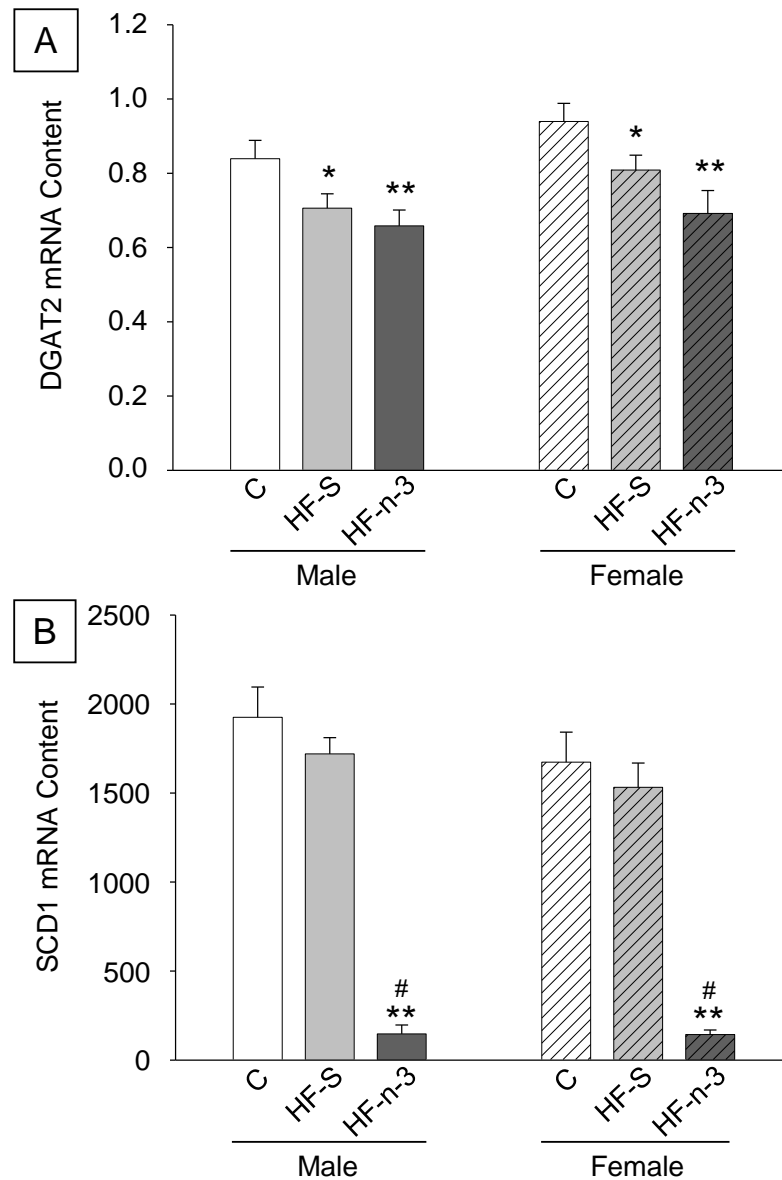


Figure 5.6 [A-B]. DGAT2 [A] and SCD1 [B] mRNA content in the liver of male and female mice fed control, high saturated fat or high fat n-3 PUFA enriched diets.

Data are expressed as mean (bars) ± SEM (error bars), where solid bars indicate male (M) mice, lined bars indicate female (F) mice and colour represents diet: white, control (C); pale grey, high saturated fat (HF-S); dark grey, high fat n-3 polyunsaturated fatty acid enriched (HF-n-3). DGAT2, diacylglycerol acyltransferase 2; SCD1, stearoyl-Coenzyme A desaturase 1.

[A-B]: n: C(M/F) = 10/12, HF-S(M/F) = 11/10, HF-n-3(M/F) = 9/11;

Statistics: Effect of diet: * $P \leq 0.02$, ** $P \leq 0.001$, compared to C; # $P \leq 0.001$, compared to HF-S.

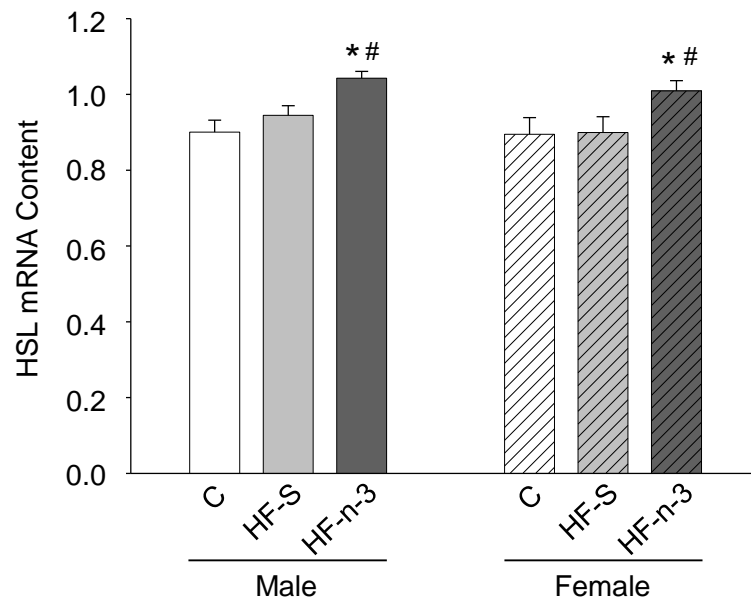


Figure 5.7. HSL mRNA content in the liver of male and female mice fed control, high saturated fat or high fat n-3 PUFA enriched diets.

Data are expressed as mean (bars) \pm SEM (error bars), where solid bars indicate male (M) mice, lined bars indicate female (F) mice and colour represents diet: white, control (C); pale grey, high saturated fat (HF-S); dark grey, high fat n-3 polyunsaturated fatty acid enriched (HF-n-3). HSL, hormone sensitive lipase.

n: C(M/F) = 10/12, HF-S(M/F) = 11/11, HF-n-3(M/F) = 9/11;

Statistics: Effect of diet: * $P \leq 0.001$, compared to C; # $P \leq 0.02$, compared to HF-S.

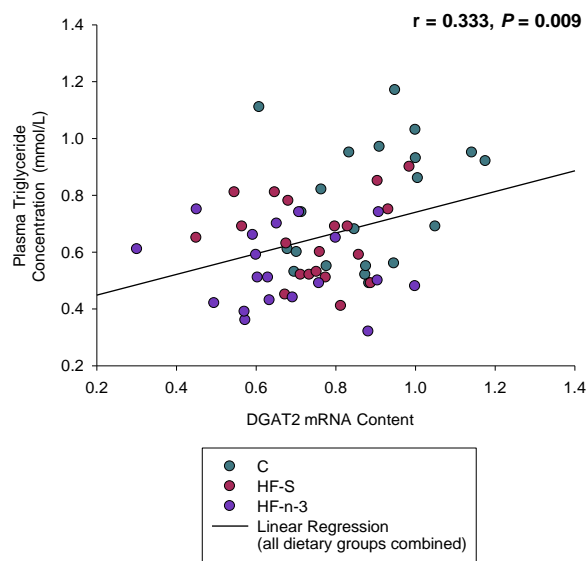


Figure 5.8. The relationship between plasma triglyceride concentrations and the hepatic mRNA content of DGAT2.

Symbol type represents dietary group: see legend. DGAT2, diacylglycerol acyltransferase 2; C, control diet; HF-S, high saturated fat diet; HF-n-3, high fat n-3 polyunsaturated fatty acid enriched diet.

n: = 60, C = 21, HF-S = 20, HF-n-3 = 19.

There was a significant positive relationship between plasma triglyceride content and hepatic DGAT2 mRNA expression in all mice (cohorts combined to include C, HF-S and HF-n-3 diets).

5.3.3- Fatty Acid Utilisation (*PDK4*, *AMPK α 1*, *AMPK α 2*, *ACC- β* , *CPT1 α* , *UCP2*, *SIRT1*, *PGC1 α* , *PPAR α* , *PPAR δ / β* , *PPAR γ*)

Pyruvate dehydrogenase kinase 4 (PDK4) mRNA content was greater in HF-n-3 mice as compared to control and HF-S mice ($F(2, 57)=11.7$, $P\leq 0.001$; +93%, +111%, respectively; post-hoc tests: $P\leq 0.001$) (**Figure 5.9**). There was an effect of gender on PDK4 mRNA content, female mice exhibited greater PDK4 mRNA than male mice (+34%; $F(1, 57)=8.4$, $P=0.005$).

There was no effect of diet ($F(2, 58)=1.4$, $P=0.24$) or gender ($F(1, 58)=0.2$, $P=0.63$) on AMP-activated protein kinase catalytic subunit $\alpha 1$ (AMPK $\alpha 1$) mRNA content (**Figure 5.10A**).

There was no effect of diet on AMP-activated protein kinase catalytic subunit $\alpha 2$ (AMPK $\alpha 2$) mRNA content ($F(2, 58)=1.4$, $P=0.25$). There was an effect of gender on AMPK $\alpha 2$ mRNA content, male mice exhibited greater AMPK $\alpha 2$ mRNA than female mice (+16%; $F(1, 58)=23.6$, $P\leq 0.001$) (**Figure 5.10B**).

Acetyl-Coenzyme A carboxylase- β (ACC- β) mRNA content was lower in HF-n-3 mice as compared to control and HF-S mice ($F(2, 58)=300.8$, $P\leq 0.001$; -81%, -86%, respectively; post-hoc tests: $P\leq 0.001$) and greater in HF-S mice as compared to control mice (+32%; post-hoc test: $P\leq 0.001$) (**Figure 5.11A**). There was an effect of gender on ACC- β mRNA content, male mice exhibited greater ACC- β mRNA than female mice (+23%; $F(1, 58)=6.0$, $P=0.017$).

There was no effect of diet ($F(2, 58)=2.3, P=0.11$) or gender ($F(1, 58)=0.05, P=0.83$) on carnitine palmitoyl transferase 1a (CPT1a) mRNA content (**Figure 5.11B**).

Uncoupling protein 2 (UCP2) mRNA content was greater in HF-n-3 mice as compared to control and HF-S mice ($F(2, 58)=11.3, P\leq 0.001$; +15%, +10%, respectively; post-hoc tests: $P\leq 0.001, P\leq 0.01$, respectively) (**Figure 5.12A**). There was an effect of gender on UCP2 mRNA content, female mice exhibited greater UCP2 mRNA than male mice (+6%; $F(1, 58)=6.5, P=0.014$).

There was no effect of diet ($F(2, 58)=0.5, P=0.60$) or gender ($F(1, 58)=1.2, P=0.28$) on sirtuin 1 (SIRT1) mRNA content (**Figure 5.12B**).

There was no effect of diet ($F(2, 58)=2.8, P=0.069$) or gender ($F(1, 58)=0.2, P=0.64$) on peroxisome proliferative activated receptor γ coactivator 1 α (PGC1 α) mRNA content. There was however a trend towards greater PGC1 α mRNA content in HF-n-3 mice as compared to control mice (+17%; post-hoc test: $P=0.058$) (**Figure 5.13A**).

There was no effect of diet ($F(2, 58)=0.9, P=0.43$) or gender ($F(1, 58)=0.2, P=0.65$) on peroxisome proliferator activator receptor α (PPAR α) mRNA content (**Figure 5.13B**).

Peroxisome proliferator activator receptor δ/β (PPAR δ/β) mRNA content was lower in HF-n-3 mice as compared to HF-S mice ($F(2, 58)=5.9, P=0.005$; -32%; post-hoc test: $P\leq 0.005$) (**Figure 5.14A**). There was also a tendency for increased PPAR δ/β mRNA in HF-S mice as compared to controls (+24%; post-hoc test: $P=0.11$). There was an effect of gender on PPAR δ/β mRNA content, female mice exhibited greater PPAR δ/β

mRNA than male mice (+18%; $F(1, 58)=4.3$, $P=0.043$).

There was a diet*gender interaction on peroxisome proliferator activator receptor γ (PPAR γ) mRNA content ($F(2, 58)=5.8$, $P=0.005$) (**Figure 5.14B**), in male mice PPAR γ mRNA was greater in HF-S and HF-n-3 mice as compared to control mice (+45%, +52%, respectively; pairwise comparisons: $P\leq 0.001$). In control mice, females exhibited greater PPAR γ mRNA as compared to males (+17%, pairwise comparison: $P\leq 0.05$) and in HF-S mice, males exhibited greater PPAR γ mRNA as compared to females (+18%, pairwise comparison: $P\leq 0.05$). In HF-n-3 mice, there was also a strong trend towards increased PPAR γ mRNA in male mice as compared to female mice (+16%, pairwise comparison: $P=0.051$).

PDK4 mRNA content was negatively correlated with plasma glucose concentrations in HF-S, but not HF-n-3, mice (HF-S, $r = -0.48$, $F(1, 20)=5.9$, $P=0.024$; HF-n-3, $r = -0.26$, $F(1, 16)=1.1$, $P=0.30$) (**Figure 5.15**). UCP2 mRNA content was negatively correlated with final body weight in HF-n-3, but not HF-S, mice (HF-n-3, $r = -0.45$, $F(1, 18)=4.6$, $P=0.046$; HF-S, $r = +0.09$, $F(1, 20)=0.1$, $P=0.71$) (**Figure 5.15**).

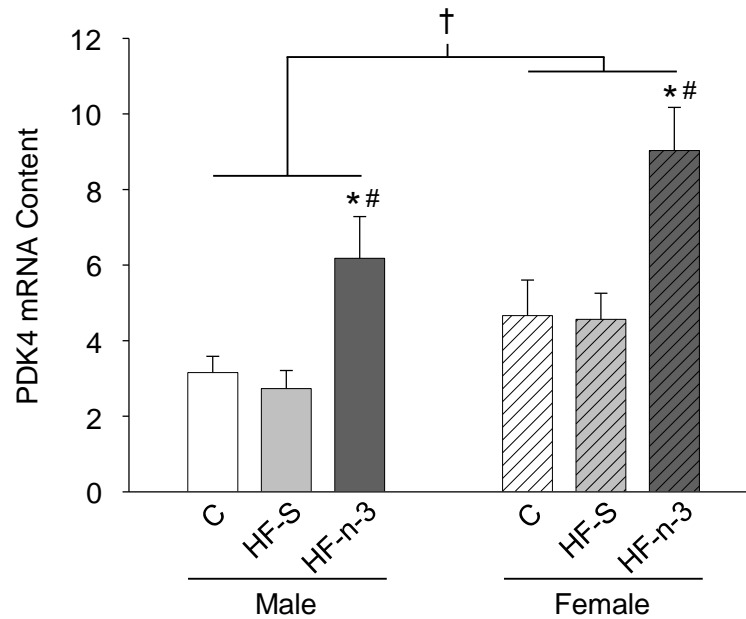


Figure 5.9. PDK4 mRNA content in the liver of male and female mice fed control, high saturated fat or high fat n-3 PUFA enriched diets.

Data are expressed as mean (bars) \pm SEM (error bars), where solid bars indicate male (M) mice, lined bars indicate female (F) mice and colour represents diet: white, control (C); pale grey, high saturated fat (HF-S); dark grey, high fat n-3 polyunsaturated fatty acid enriched (HF-n-3). PDK4, pyruvate dehydrogenase kinase 4.

n: C(M/F) = 10/12, HF-S(M/F) = 11/11, HF-n-3(M/F) = 9/10.

Statistics: Effect of diet: $*P \leq 0.001$, compared to C, $\#P \leq 0.001$, compared to HF-S.

Effect of gender: $\dagger P \leq 0.005$, male compared to female.

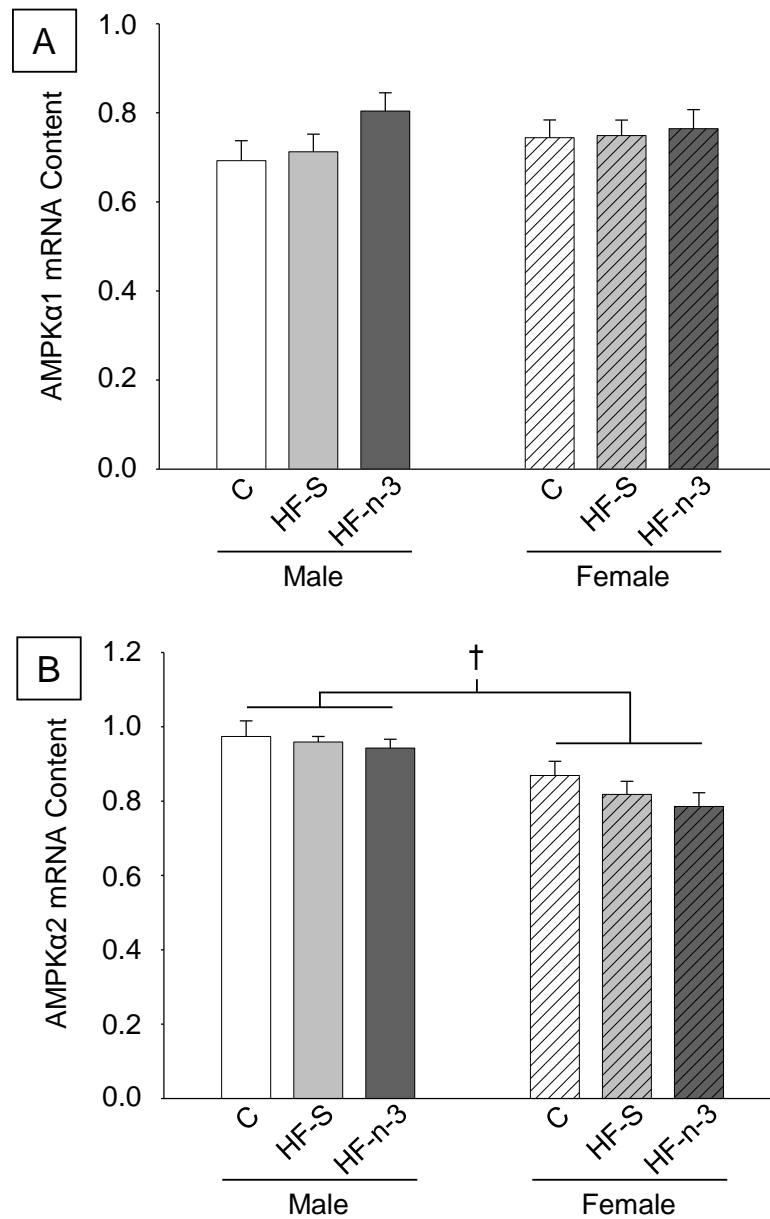


Figure 5.10 [A-B]. AMPKα1 [A] and AMPKα2 [B] mRNA content in the liver of male and female mice fed control, high saturated fat or high fat n-3 PUFA enriched diets.

Data are expressed as mean (bars) ± SEM (error bars), where solid bars indicate male (M) mice, lined bars indicate female (F) mice and colour represents diet: white, control (C); pale grey, high saturated fat (HF-S); dark grey, high fat n-3 polyunsaturated fatty acid enriched (HF-n-3). AMPK, AMP-activated protein kinase catalytic subunit α.

[A-B]: n: C(M/F) = 10/12, HF-S(M/F) = 11/11, HF-n-3(M/F) = 9/11.

Statistics: Effect of gender: † $P \leq 0.001$, male compared to female.

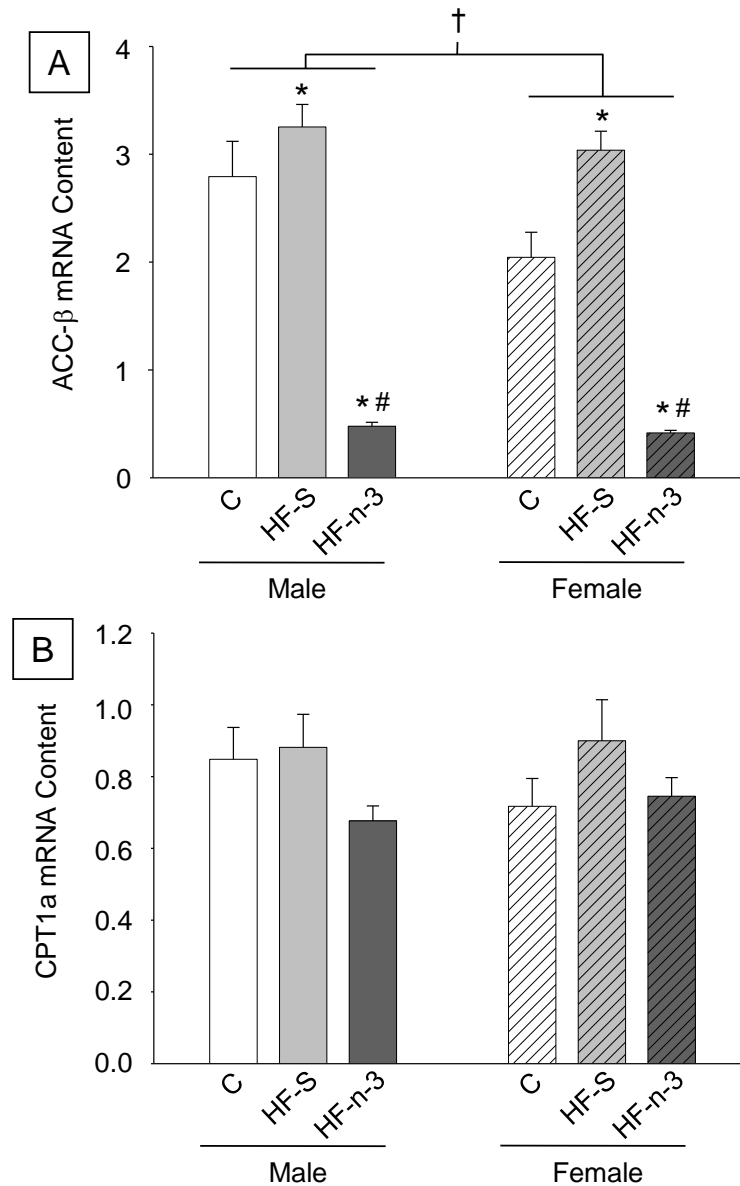


Figure 5.11 [A-B]. ACC-β [A] and CPT1a [B] mRNA content in the liver of male and female mice fed control, high saturated fat or high fat n-3 PUFA enriched diets.

Data are expressed as mean (bars) \pm SEM (error bars), where solid bars indicate male (M) mice, lined bars indicate female (F) mice and colour represents diet: white, control (C); pale grey, high saturated fat (HF-S); dark grey, high fat n-3 polyunsaturated fatty acid enriched (HF-n-3). ACC- β , acetyl-Coenzyme A carboxylase- β ; CPT1a, carnitine palmitoyl transferase 1a.

[A-B]: n: C(M/F) = 10/12, HF-S(M/F) = 11/11, HF-n-3(M/F) = 9/11.

Statistics: Effect of diet: * $P \leq 0.001$, compared to C, # $P \leq 0.001$, compared to HF-S. Effect of gender: † $P \leq 0.02$, male compared to female.

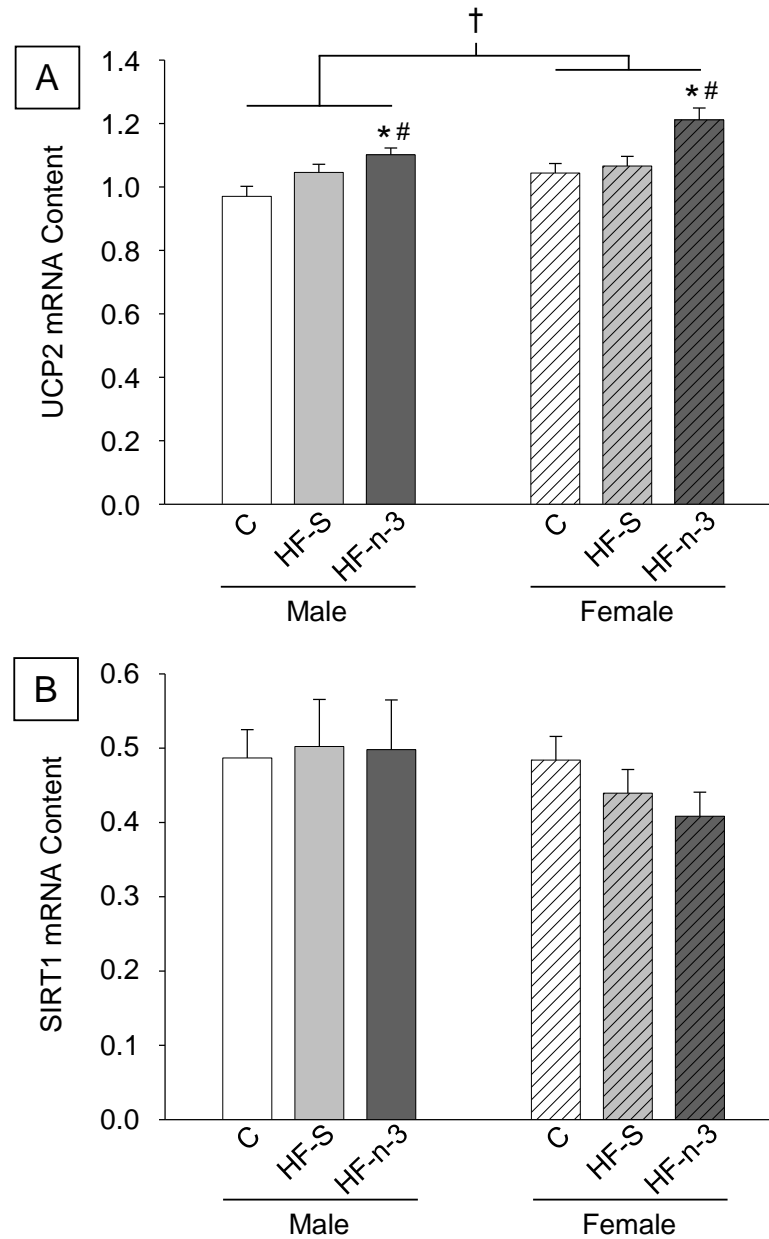


Figure 5.12 [A-B]. UCP2 [A] and SIRT1 [B] mRNA content in the liver of male and female mice fed control, high saturated fat or high fat n-3 PUFA enriched diets.

Data are expressed as mean (bars) ± SEM (error bars), where solid bars indicate male (M) mice, lined bars indicate female (F) mice and colour represents diet: white, control (C); pale grey, high saturated fat (HF-S); dark grey, high fat n-3 polyunsaturated fatty acid enriched (HF-n-3). UCP2, uncoupling protein 2; SIRT1, sirtuin 1.

[A-B]: n: C(M/F) = 10/12, HF-S(M/F) = 11/11, HF-n-3(M/F) = 9/11.

Statistics: Effect of diet: * $P \leq 0.001$, compared to C; # $P \leq 0.01$, compared to HF-S. Effect of gender: † $P \leq 0.02$, male compared to female.

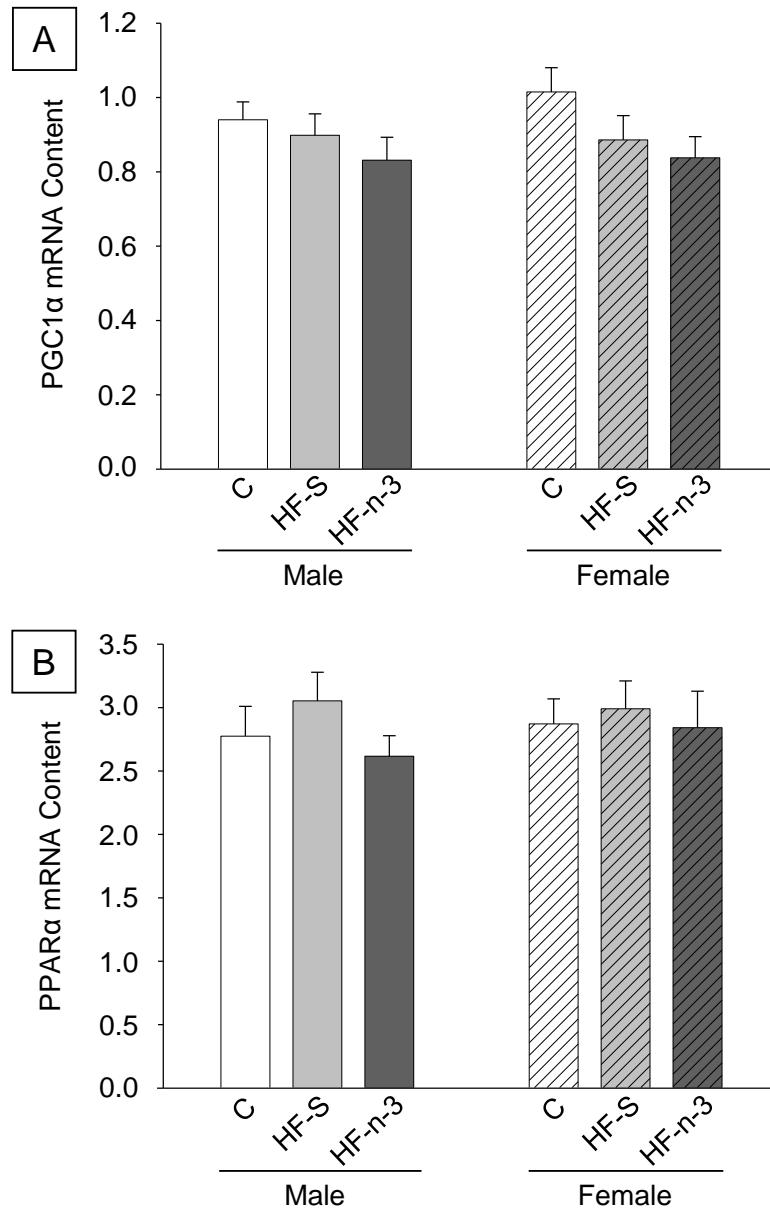


Figure 5.13 [A-B]. PGC1 α [A] and PPAR α [B] mRNA content in the liver of male and female mice fed control, high saturated fat or high fat n-3 PUFA enriched diets.

Data are expressed as mean (bars) \pm SEM (error bars), where solid bars indicate male (M) mice, lined bars indicate female (F) mice and colour represents diet: white, control (C); pale grey, high saturated fat (HF-S); dark grey, high fat n-3 polyunsaturated fatty acid enriched (HF-n-3). PGC1 α , peroxisome proliferative activated receptor γ coactivator 1 α ; PPAR α , peroxisome proliferator activator receptor α .

[A-B]: n: C(M/F) = 10/12, HF-S(M/F) = 11/11, HF-n-3(M/F) = 9/11.

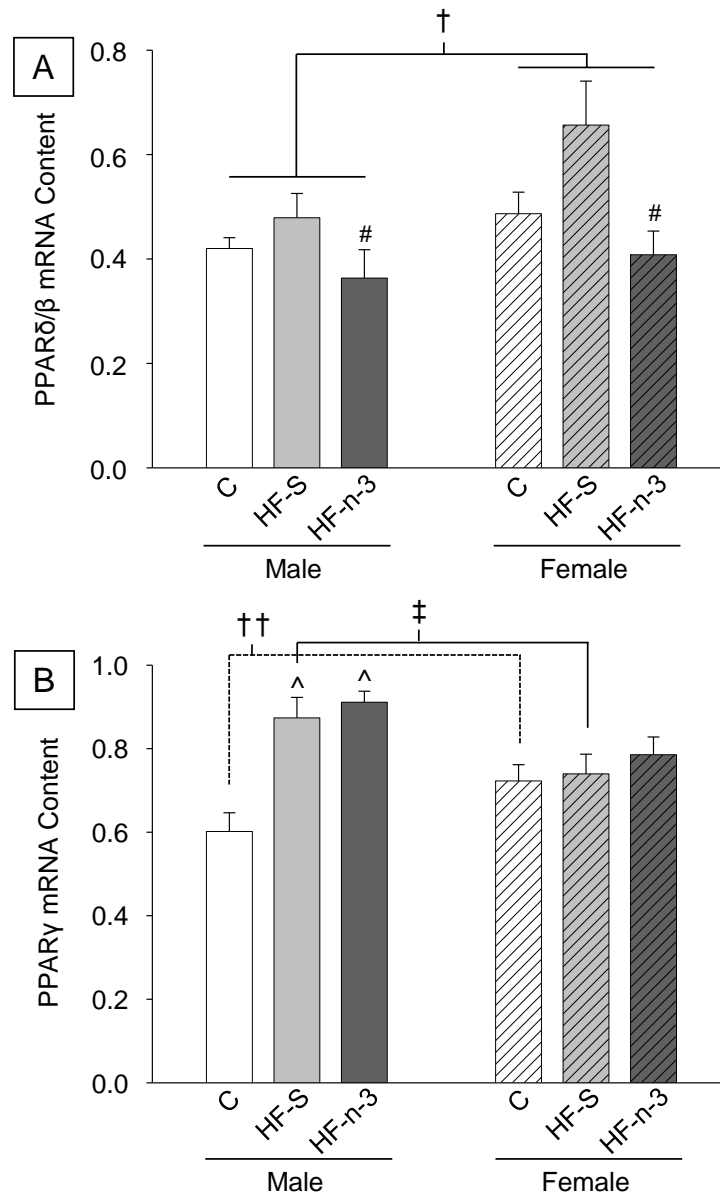


Figure 5.14 [A-B]. PPAR δ/β [A] and PPAR γ [B] mRNA content in the liver of male and female mice fed control, high saturated fat or high fat n-3 PUFA enriched diets.

Data are expressed as mean (bars) \pm SEM (error bars), where solid bars indicate male (M) mice, lined bars indicate female (F) mice and colour represents diet: white, control (C); pale grey, high saturated fat (HF-S); dark grey, high fat n-3 polyunsaturated fatty acid enriched (HF-n-3). PPAR, peroxisome proliferator activator receptor.

[A-B]: n: C(M/F) = 10/12, HF-S(M/F) = 11/11, HF-n-3(M/F) = 9/11.

Statistics: Effect of diet: # $P \leq 0.005$, compared to HF-S. Effect of gender: † $P \leq 0.05$, male compared to female. Diet*gender interaction: ^ $P \leq 0.001$, compared to C male; †† $P \leq 0.05$, male compared to female (C); ‡ $P \leq 0.05$, male compared to female (HF-S).

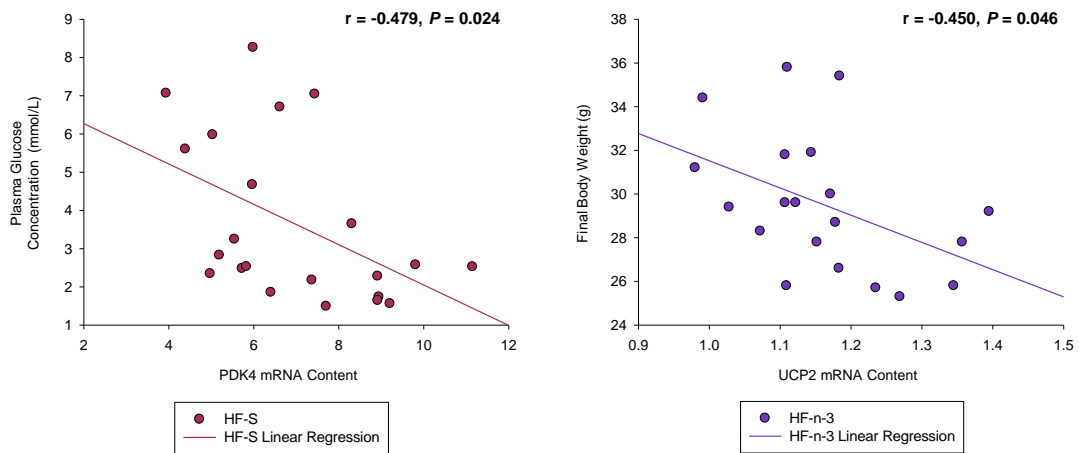


Figure 5.15. The relationships between plasma glucose concentrations and the hepatic mRNA content of PDK4 in high saturated fat-fed mice and between body weight and the hepatic mRNA content of UCP2 in mice fed a high fat n-3 PUFA enriched diet.

Symbol type represents dietary group: see legend. PDK4, pyruvate dehydrogenase kinase 4; UCP2, uncoupling protein 2; HF-S, high saturated fat diet; HF-n-3, high fat n-3 polyunsaturated fatty acid enriched diet.

n: HF-S = 20, HF-n-3 = 20.

There was a significant negative relationship between plasma glucose content and hepatic PDK4 mRNA expression in the HF-S group only (males and females combined). There was a significant negative relationship between final body weight and hepatic UCP2 mRNA expression in the HF-n-3 group only (males and females combined).

5.4 – DISCUSSION

This study is the first to comprehensively compare the effects of a high saturated fat and n-3 PUFA enriched HFDs on liver fatty acid metabolism with respect to gender. These data suggest that consumption of a HF-S diet induces hepatic fat accumulation through an impaired capacity to oxidise fatty acids, without significant changes in fatty acid uptake or synthesis. In contrast, replacing 7.5% of saturated fat in the HF-S diet with n-3 PUFAs prevented intracellular fat accretion in the liver by inducing genes involved in fatty acid utilisation and suppressing pathways promoting fatty acid storage and lipogenesis even though there was a potential for increased fatty acid uptake. These are the first data reporting gender-dimorphic effects on genes involved in hepatic fatty acid metabolism in response to dietary enrichment with n-3 PUFAs.

5.4.1 – Effect of Dietary Fatty Acid Composition on Hepatic Fatty Acid Uptake

The reduction in FATP5 mRNA content observed in the current study may be an adaptive response to prevent liver fat uptake and hence hepatic fat accumulation. Although this is inconsistent with previous studies that have identified FATP5 to play a role in the development of hepatosteatosis (Auinger *et al.*, 2010; Doege *et al.*, 2006), research in FATP5 knockout mice has supported the notion of this adaptive response. FATP5 null mice exhibit reduced hepatic fatty acid uptake and liver triglyceride accumulation and there is some evidence that this leads to the redistribution of lipid from the liver to other peripheral tissues (Doege *et al.*, 2006). Given that FATP5 is preferentially localised at the space of Disse and its expression tracks closely with the hepatic microvasculature (Doege *et al.*, 2006), it has been suggested to play a role at

the hepatocyte/sinusoidal interface mediating the uptake of fatty acids from the circulation. It is therefore possible that the suppression of FATP5 prevents fatty acid uptake through this transporter, leading to greater circulating fatty acids and consequently uptake by other peripheral tissues. Consistent with this notion, it was demonstrated in **Chapter 4** that lower liver fat content was associated with the increased expression of genes regulating fatty acid oxidation in skeletal muscle, and this may indicate that liver fat may be redistributed to skeletal muscle for oxidative disposal.

The observation that FATP2 was increased by HF-n-3, but not HF-S, feeding is consistent with its role in promoting the activation of long and very long chain fatty acids at the peroxisome (Falcon *et al.*, 2010). Research conducted by Falcon and colleagues (Falcon *et al.*, 2010) supports a role for FATP2 in channelling fatty acids to oxidation, given that FATP2 has been identified at the plasma membrane and modestly at the peroxisome (~10%), and that knockdown of FATP2 suppresses the long chain fatty acid uptake and peroxisomal long chain (-51%) and very long chain (-59%) acyl-CoA synthetase activity. The correlation between increased FATP2 mRNA content and lower liver fat content in HF-n-3, but not HF-S mice, in the current study further supports a role for FATP2 in preferentially channelling fatty acids into pathways of disposal. Consistent with this notion, FATP2 expression is upregulated by PPAR α -specific agonists in the small intestine of mice (Hirai *et al.*, 2007), whilst hepatic FATP is also induced by PPAR α activators, although in the latter study the isoform of the FATP gene measured was not specified given the early date of the study (Motojima *et al.*, 1998). PPAR α plays a role in promoting peroxisomal fatty acid oxidation

(Smith, 2002) and as previously described, n-3 PUFAs are ligands to PPAR α (Hihi *et al.*, 2002). When combined these data suggest that PPAR α activation may mediate the HF-n-3-induced increase in hepatic FATP2 expression, increasing the flux of fatty acid into the liver and the activation of fatty acid at the peroxisome.

The absence of an effect of HF-S on hepatic FAT/CD36 mRNA is consistent with studies of similar diet duration (10-19 weeks) (Ito *et al.*, 2007; Buettner *et al.*, 2006). However, when the animal was exposed to the HFD for a longer duration (34-50 weeks), a significant increase in FAT/CD36 mRNA was observed and this was associated with well-developed steatohepatitis (at 50 weeks) (Ito *et al.*, 2007). On the other hand, a study by Koonen and colleagues (Koonen *et al.*, 2007), despite using mice of identical strain and gender and similar age, fed diets providing identical energy from fat as those used by Ito and associates (Ito *et al.*, 2007), both FAT/CD36 mRNA and protein content increased following just 5 weeks diet. The reason for this discrepancy is unknown. Although FAT/CD36 mRNA was not increased in response to HF-S feeding in the current study, greater FAT/CD36 mRNA content was associated with increased hepatic fat accumulation in HF-S, but not HF-n-3, mice. These data suggest that there may be underlying metabolic changes in FAT/CD36 protein, resulting in greater fatty acid uptake and accretion and given the capacity of FAT/CD36 to relocate to the plasma membrane is also present in liver cells (Luiken *et al.*, 2002), it is possible that the HF-S diet stimulates translocation of FAT/CD36 protein.

The observation that HF-n-3 feeding induced FAT/CD36 mRNA expression is consistent with previous reports (Buettner *et al.*, 2006). As was described previously,

the FAT/CD36 gene possesses a PPAR response element (Mandard *et al.*, 2004) and n-3 PUFAs naturally activate PPAR α (Hihi *et al.*, 2002; Desvergne and Wahli, 1999), therefore FAT/CD36 expression may increase in response to PPAR α activation in the liver also. Consistent with this notion, Buettner and colleagues (Buettner *et al.*, 2006) demonstrated a tendency (although not statistically significant) for higher PPAR α mRNA expression in addition to greater expression of PPAR target gene, FAT/CD36, in their high fat fish oil-fed rodent model. Furthermore, Motojima and associates (Motojima *et al.*, 1998) have shown that hepatic FAT/CD36 expression was induced by 4 different PPAR α agonists in mice. Although FAT/CD36 mRNA expression was significantly upregulated in response to HF-n-3 feeding, there was no direct relationship between FAT/CD36 mRNA and the liver fat content in the HF-n-3 group and this is presumably due to mechanisms of fatty acid disposal.

Despite the hepatic mRNA expression of FAT/CD36 and the FATPs being altered in response to high fat overfeeding, FABPpm was unchanged in the liver of HFD-fed mice. This is consistent with the response seen in skeletal muscle (**Chapter 4**). Unlike FAT/CD36 and FATPs, FABPpm does not respond to PPAR α activation (Motojima *et al.*, 1998), and may account for this response, suggesting that FABPpm plays a minor role in responding to HFD-induced fatty acid oversupply.

Although we have investigated the effect of HF-S feeding on fatty acid transport purely at the level of mRNA expression, together this data indicates that hepatic fatty acid transporters do not play a major role in contributing to HF-S-induced fatty liver (**Figure 5.16**). However, partial replacement of saturated fat for n-3 PUFAs induced

the expression of fatty acid transporters FAT/CD36 and FATP2 in parallel with the amelioration of HF-S-induced fatty liver. These findings suggest that n-3 PUFA-induced fatty acid transporters may play a role in increasing fatty acid uptake and facilitating energy expenditure (**Figure 5.16**). The differential expression of hepatic fatty acid transporters observed in response to high fat overfeeding highlights the need for further investigation to clarify the roles of each fatty acid transport protein in order to decipher the specific effects observed in this study.

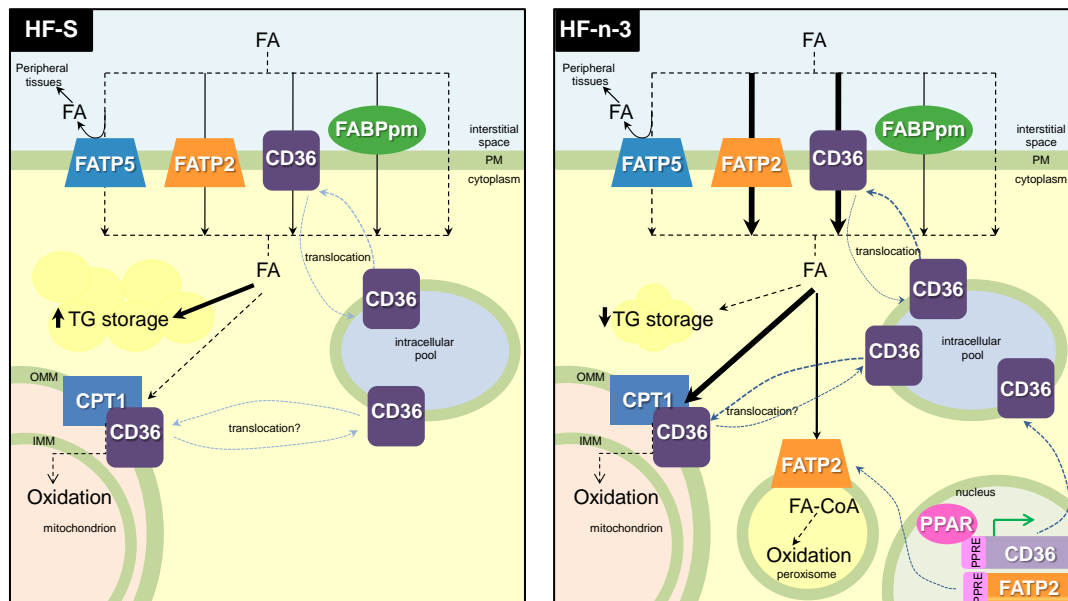


Figure 5.16. Schematic diagram depicting the differential effects that consuming a high saturated fat diet or n-3 PUFA enriched HFD exert on fatty acid transport into the hepatocyte.

In the liver, HF-S decreased FATP5 mRNA content, with no influence on FATP2, FAT/CD36 or FABPpm mRNA content. Reduced FATP5 expression may consequently act as a compensatory response to redirect fat away from a lipid-laden liver to peripheral tissues. Liver fat accretion was increased with HF-S feeding and therefore altered fatty acid uptake does not appear to play a major role in this response. In contrast to HF-S feeding, HF-n-3 increased FAT/CD36 and FATP2 mRNA content and this may lead to greater mitochondrial or peroxisomal oxidation, respectively. Increased PPAR α may contribute to increased FAT/CD36 and FATP2 expression, binding to the PPAR response element on the target genes and enhancing expression. As hepatic fat accumulation was ameliorated by HF-n-3, FAT/CD36 and FATP2 may therefore be implicated in channelling fat into pathways of oxidation. FATP5 was also reduced with HF-n-3 feeding, and may possibly also play a role in redirecting fat to peripheral tissues.

FA, fatty acid; FA-CoA, fatty acyl CoA; CD36 (FAT/CD36), fatty acid translocase; FABPpm, fatty acid binding protein; FATP, fatty acid transport protein; TG, triglyceride; CPT1, carnitine palmitoyl transferase 1; PM, plasma membrane; OMM, outer mitochondrial membrane; IMM, inner mitochondrial membrane, PPAR, peroxisome proliferator activator receptor; PPRE, PPAR response element; translocation?, assumed pathway from characterisation of skeletal muscle CD36.

5.4.2 – Effect of Dietary Fatty Acid Composition on Hepatic Lipogenesis and Triglyceride Storage

The data in this chapter highlight that exposure to HFDs of differing fatty acid composition influences the pattern of expression of key genes involved in fatty acid synthesis and triglyceride hydrolysis, which may contribute to altered hepatic fat storage (as reported in **Chapter 2**).

The observation that SREBF1 was unchanged in response to HF-S feeding in the current study is similar to research by Field and colleagues (Field *et al.*, 2002) in which the mRNA expression of SREBF1a and SREBF1c were unchanged in CaCo-2 cells exposed to saturated fat, stearic acid (18:0). However, other studies in rodents have demonstrated a tendency for enhanced SREBF1 mRNA expression when exposed to a high fat cafeteria diet (Quesada *et al.*, 2009) or a significant increase in SREBF1 mRNA when exposed to a HF-S diet of predominantly coconut oil or lard (Buettner *et al.*, 2006). The inconsistencies in SREBF1 expression in the aforementioned studies may reflect changes in the daily rhythm of SREBF1 expression, as SREBF1 has been recently shown to have “Clock-sensitive” circadian rhythmicity (Matsumoto *et al.*, 2010). Genetically obese rodents lack the normal daily rhythmic pattern of SREBF1 mRNA expression, with constitutively upregulated SREBF1 expression (Matsumoto *et al.*, 2010). Therefore the slight and marked increases in SREBF1 expression in the aforementioned studies (Quesada *et al.*, 2009; Buettner *et al.*, 2006) may reflect the gradual progress towards a defect in SREBF1 rhythmicity in response to obesity development. In contrast, unchanged SREBF1 mRNA in the current study may reflect that SREBF1 rhythmicity is not yet defective in our model of diet-induced obesity.

Despite both high fat groups consuming similar total amounts of dietary fat, HF-n-3 feeding induced a reduction in SREBF1 mRNA, which is consistent with past reports (Nakatani *et al.*, 2003; Kim *et al.*, 1999; Mater *et al.*, 1999; Xu *et al.*, 1999b). But given that post-transcriptional modifications to SREBF1 determine its level of activity, factors other than the altered mRNA content may be at play. The mechanism by which this may occur is through PUFAs inhibiting the maturation of SREBF1 protein by preventing SREBF1 precursor protein release from the endoplasmic reticulum (Xu *et al.*, 1999b; Worgall *et al.*, 1998) and by accelerating SREBF1 transcript decay, reducing SREBF1 mRNA and precursor protein (Xu *et al.*, 2001). In contrast to n-3 PUFAs, saturated fat has no effect on the maturation of hepatic SREBF1 protein (Yahagi *et al.*, 1999) and therefore SREBF1 activity is likely to be normal in HF-S mice. The expression of upstream regulators of SREBF1, INSIG1 and PPAR δ/β , also provide evidence that hepatic SREBF1 activity is altered by HF-n-3, but not HF-S, feeding. Despite a tendency for greater PPAR δ/β expression in HF-S-fed mice, INSIG1 and SREBF1 mRNA content were unchanged by HF-S feeding, suggesting SREBF1 activity is normal and may contribute to the development of fatty liver (**Chapter 2**). In contrast, a consistent reduction in PPAR δ/β and INSIG1 were observed in addition to SREBF1 suppression in HF-n-3 mice and it is therefore possible that the need for feedback control is lowered by HF-n-3 feeding.

A limitation of the current study is that the protein abundance of SREBF1 (in the precursor or active state) or of its regulators INSIG1 or PPAR δ/β have not been measured. However, downstream SREBF1 target genes were also determined and may provide an overview of the output of SREBF1 activity. In accordance with lower

SREBF1 expression, in the present study SREBF1 target genes, SCD1, ACC- α and FAS, were suppressed in response to HF-n-3 feeding. This response is consistent with several previous studies in which dietary supplementation with n-3 PUFAs inhibited SCD1, ACC and FAS mRNA expression (Mori *et al.*, 2007; Nakatani *et al.*, 2003; Field *et al.*, 2002; Kim *et al.*, 1999; Mater *et al.*, 1999). Therefore, the reduced expression of key genes involved in the fatty acid synthesis pathway in response to HF-n-3 feeding may in part contribute to the reduced fat accumulation observed in HF-n-3 livers. However, in the present study, HF-S feeding did not induce the mRNA expression of SCD1, ACC- α and FAS, as previous studies have reported (Li *et al.*, 2009; Buettner *et al.*, 2006; Biddinger *et al.*, 2005; Hu *et al.*, 2004). This is consistent however, with the observation that hepatic SREBF1 mRNA was unchanged with HF-S feeding in the present study. Although genes influencing fatty acid synthesis were not affected at the level of transcription, HF-S mice exhibited a marked increase in hepatic fat accumulation (**Chapter 2**). This possibly indicates that the protein abundance or activity of fatty acid synthesis genes may be altered or perhaps the increased hepatic fat accumulation results from a reduction in the disposal of fatty acids through impaired oxidation, lipolysis and/or triglyceride secretion to peripheral tissues.

The lipolytic action of triglyceride lipases may contribute to liver triglyceride accumulation, as liberated fatty acids are directed to pathways of re-esterification for secretion or oxidation for disposal (Turpin *et al.*, 2010; Nagle *et al.*, 2009; Gibbons *et al.*, 2004). In the current study, the n-3 PUFA-induced increase in hepatic HSL expression is consistent with previous research (Sun *et al.*, 2010) and may be indicative of increased breakdown of intrahepatic triglyceride, potentially increasing fatty acid

disposal. In contrast, the lack of an effect of HF-S feeding on HSL mRNA expression, may ultimately contribute to greater intrahepatic fat storage as less triglyceride is broken down. However, the contribution of HSL to overall hepatic triglyceride lipolysis has been questioned by some studies, with the suggestion that HSL only contributes modestly to hepatic triglyceride lipase activity (~10%) (Reid *et al.*, 2008). Additional enzymes with triglyceride lipase activity, triglyceride hydrolase (TGH) (Sun *et al.*, 2010) and adipose triglyceride lipase (ATGL) (Ong *et al.*, 2010; Reid *et al.*, 2008) have been shown to contribute to hepatic triglyceride hydrolysis, and the latter, ATGL, accounts for 30-40% of triglyceride hydrolase activity (Ong *et al.*, 2010; Reid *et al.*, 2008). Although, it appears no study has investigated the impact of HF-n-3 feeding on ATGL expression or activity, mice exposed to n-3 PUFA, docosahexaenoic acid (DHA), exhibit unchanged hepatic TGH expression but enhanced hepatic HSL expression (Sun *et al.*, 2010). These data suggest that HSL plays a role in mobilising triglyceride, potentially limiting triglyceride storage, but further research is required to understand the full contribution of triglyceride hydrolase activity to reduced hepatic triglyceride storage in HF-n-3 mice.

In the liver, triglyceride storage is also dependent on the flux of triglyceride entering lipoproteins for secretion, mediated in part by DGAT2. The observed reduction in hepatic DGAT2 mRNA content with high fat overfeeding, irrespective of the dietary fatty acid composition, may indicate that less triglycerides are synthesised and packaged into lipoproteins, which could ultimately reduce hepatic triglyceride secretion. Consistent with this notion, lower hepatic DGAT2 mRNA content was associated with lower plasma triglyceride levels. It is also possible that this contributes

to the hypotriglyceridemic effect observed with HF-n-3 feeding and as liver fat content was not enhanced by HF-n-3 feeding (**Chapter 2**) nor was the triglyceride synthesis and secretion through DGAT2, excess triglycerides may have been channelled into pathways of oxidation in the livers of HF-n-3 mice. The reduced expression of DGAT2 observed with HF-S feeding may have contributed to the increased hepatic fat accumulation in these animals (**Chapter 2**). DGAT2 knockout (DGAT2^{-/-}) mice have been reported to be severely triglyceride deficient and lack vital substrates for oxidative metabolism (Stone *et al.*, 2004), DGAT2^{-/+} mice with mixed genetic background (~50% DGAT2) are more comparable to the HF-S mice in this study (~20%). A modest reduction in DGAT2 expression is not sufficient to limit triglyceride synthesis in DGAT2^{-/+} mice (Chen and Farese, 2005) and does not protect them from developing diet-induced obesity. These data therefore suggest that lower triglyceride secretion due to reduced hepatic DGAT2 expression may contribute to HF-S-induced fatty liver.

In combination these data suggest that although several genes influencing fatty acid synthesis were unchanged by HF-S feeding, increased liver fat deposition (**Chapter 2**) reflects defective lipid metabolism. It is possible that suppression of triglyceride secretion from the liver may contribute to liver fat accumulation and lower DGAT2 expression is consistent with this notion. This may also be compounded by impaired fatty acid oxidation, a notion that is to be discussed in the following section. In contrast, HF-n-3 feeding reduced the expression of key genes involved in fatty acid synthesis via SREBF1 inhibition; this may contribute to the reduced hepatic fat accumulation in HF-n-3 mice. Hepatic triglyceride secretion via DGAT2 was also suppressed in the livers of HF-n-3-fed mice and this may contribute to the systemic

triglyceride lowering effect observed with HF-n-3 feeding. In addition to reduced fatty acid synthesis and secretion, it may also be speculated that enhanced oxidation may contribute to the reduced liver fat content of HF-n-3–fed mice (**Figure 5.17**) and this too is discussed in the following section.

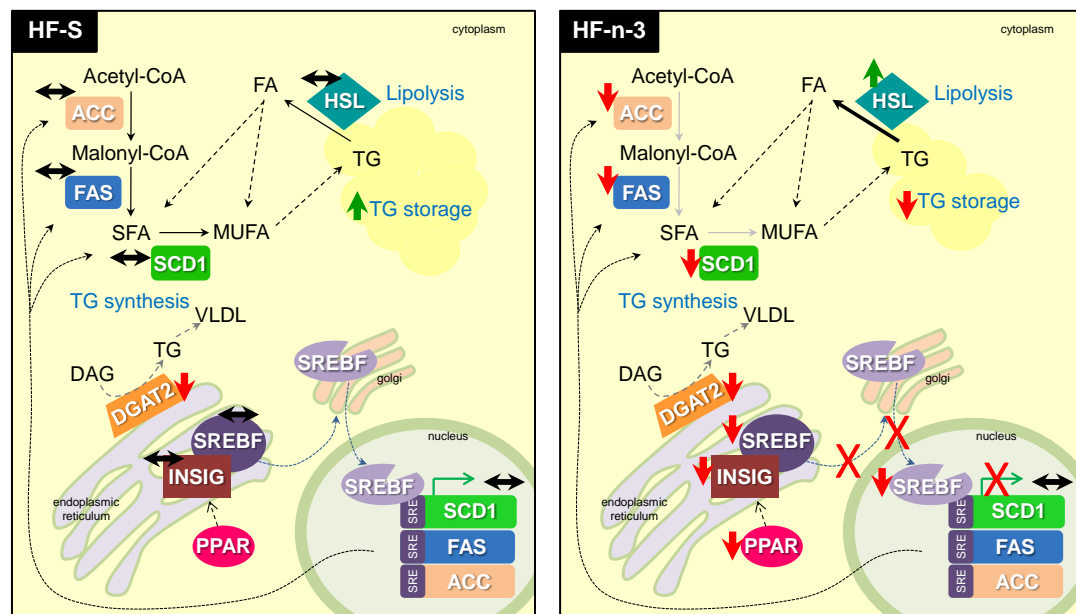


Figure 5.17. Schematic diagram depicting the differential effects that consuming a high saturated fat diet or n-3 PUFA enriched high fat diet exert on fatty acid storage and lipogenesis in the liver.

In the liver, SREBF1, INSIG1, PPAR δ/β , SCD1, FAS, ACC- α and HSL were unchanged and we speculate that lipogenesis does not by itself make a major contribution to the development of fatty liver observed in HF-S mice. However, DGAT2 mRNA content was reduced by HF-S feeding, and given its role in packaging triglycerides for secretion, may contribute to fat accumulation in the liver. In contrast to HF-S mice, the lipogenic pathways were markedly downregulated when consuming a HF-n-3 diet. In HF-n-3 mice, SREBF1 mRNA was reduced and consequently target genes SCD1, FAS and ACC- α were also downregulated. Reduced lipogenesis may therefore be implicated in the lower liver fat content in HF-n-3 mice. Given the marked downregulation of SREBF1, INSIG1 and PPAR δ/β were also reduced and this may reflect a lesser need for feedback inhibition. HSL was increased in the liver by HF-n-3 feeding, and given its role in triglyceride breakdown, may also contribute to reduced intracellular fat accumulation. DGAT2 was reduced by HF-n-3 feeding and given its role in packaging triglycerides for secretion, may contribute to the hypotriglyceridemic effect of n-3 PUFAs.

HF-S, high saturated fat diet; HF-n-3, high fat n-3 polyunsaturated fatty acid (PUFA) enriched diet; FA, fatty acid; DAG, diacylglycerol; -CoA, coenzyme A; VLDL, very low density lipoprotein; SFA, saturated fatty acid; MUFA, monounsaturated fatty acid; SCD1, stearoyl-Coenzyme A desaturase 1; DGAT2; diacylglycerol acyltransferase 2; HSL, hormone sensitive lipase; INSIG, insulin induced gene; SREBF, sterol regulatory element binding transcription factor; PPAR δ/β , peroxisome proliferator activator receptor δ/β ; FAS, fatty acid synthase; ACC- α , acetyl CoA carboxylase α ; SRE, sterol regulatory element. Thickness of black arrows represents the relative contribution to the process being described. Thick green arrow, increased; thick red arrow, reduced; black double-ended arrow, unchanged; red cross, pathway reduced.

5.4.3 – Effect of Dietary Fatty Acid Composition on Hepatic Fatty Acid Utilisation

In the preceding sections it has been demonstrated that n-3 PUFA enrichment of a HFD may increase the transport of fatty acids into the liver. However, since liver fat content was reduced, these fatty acids may be prevented from entering intracellular storage, despite an apparent reduction in triglyceride synthesis and potentially secretion; suggesting fatty acids may be cleared by upregulation of hepatic fatty acid oxidation.

In the current study, both HFD groups, despite the marked differences in the level of hepatic fat stored in these groups exhibited similar mRNA content of the rate-limiting enzyme controlling mitochondrial fatty acid transport (McGarry and Brown, 1997), CPT1a. This is consistent with research in which NAFLD patients have been shown to exhibit similar CPT1a mRNA expression to healthy individuals with normal liver fat content (Westerbacka *et al.*, 2007). In some rodent studies however, HF-S feeding has been shown to suppress CPT1 mRNA expression (Buettner *et al.*, 2006) and activity (Yun *et al.*, 2008), whilst in other rodent and bovine studies exposure to n-3 PUFAs had no effect on CPT1a expression (Litherland *et al.*, 2010; Rokling-Andersen *et al.*, 2009; Buettner *et al.*, 2006; Deng *et al.*, 2004). Although at the level of transcription CPT1a was unchanged, there is some evidence that the activity of CPT1a may be influenced by the two HFDs, as ACC- β , an enzyme that catalyses the formation of CPT1 inhibitor malonyl-CoA, was differentially expressed in the livers of HF-S and HF-n-3 mice. HF-S feeding upregulated ACC- β mRNA content and this may give rise to increased hepatic malonyl-CoA levels. Although CPT1a is less sensitive to malonyl-CoA inhibition compared to muscle-dominant CPT1b isoform (Bird and Saggerson, 1984; Mills *et al.*, 1983), malonyl-CoA may act to suppress CPT1a activity, impairing

mitochondrial fatty acid oxidation. In contrast, suppression of ACC- β by the HF-n-3 diet may reduce malonyl-CoA levels, relieving the inhibition of CPT1a, leading to enhanced oxidation. Consistent with this notion, ACC- β knockout mice (ACC- $\beta^{-/-}$) exhibit greater hepatic fat oxidation as a result of lower malonyl-CoA levels relieving CPT1a inhibition, allowing for greater CPT1a activity (Choi *et al.*, 2007; Abu-Elheiga *et al.*, 2003; Abu-Elheiga *et al.*, 2001). Consequently, hepatic DAG content was reduced and insulin sensitivity improved (Choi *et al.*, 2007). Therefore in the current study reduced ACC- β and consequently enhanced fat oxidation in HF-n-3 mice may contribute to the reduced liver fat content and improved insulin sensitivity in these animals.

Furthermore, ACC- β is regulated at the gene (Woods *et al.*, 2000) and protein level by active AMPK (Winder, 2001), which phosphorylates and deactivates ACC- β protein, lowering malonyl-CoA production (Winder, 2001). Therefore in the current study, suppressed ACC- β mRNA expression in response to HF-n-3 feeding may reflect enhanced activity of AMPK in the liver of HF-n-3 mice. Although the mRNA content of catalytic AMPK α 1 and α 2 subunits were unchanged by diet in the current study, n-3 PUFAs have been previously shown to stimulate hepatic AMPK α 2 expression (Rokling-Andersen *et al.*, 2009) and can even enhance hepatic AMPK activity in the fed-state without altering the content of the AMPK α 1 or AMPK α 2 subunits at the level of expression (Suchankova *et al.*, 2005). Activation of AMPK by 5-aminoimidazole-4-carboxamide-riboside (AICAR) also inhibits the expression of SREBF1 mRNA (Zhou *et al.*, 2001). Deletion of the SREBF1a isoform in mice leads to reduced hepatic ACC- β

expression (Im *et al.*, 2009), whilst SREBF1c also controls ACC- β expression through a sterol regulatory element in the promoter region of the ACC- β genetic sequence (Oh *et al.*, 2003). Consequently the lower expression of ACC- β in HF-n-3 mice may reflect the suppression of SREBF1 mRNA and activity through increased activation of AMPK. Although the mechanism requires further investigation, the consequence of differential ACC- β expression in HF-S and HF-n-3 mice is clear; greater ACC- β contributes to fat accumulation in HF-S mice and reduced ACC- β expression in HF-n-3 mice aids in channelling fatty acids into the mitochondria for oxidation, reflected in reduced fat accumulation in HF-n-3 livers.

UCP2 has been suggested to play a role in protecting against excessive fat accumulation in the liver during conditions of fat oversupply by inducing mitochondrial uncoupling (Serviddio *et al.*, 2008). Consistent with this notion, HF-n-3 feeding induced UCP2 mRNA expression whilst reducing hepatic fat accumulation, but HF-S-fed mice with fatty livers failed to induce UCP2 mRNA. UCP2 may therefore be involved in the amelioration of HF-S-induced hepatic fat accretion by HF-n-3 feeding. Although hepatic UCP2 expression has been shown to be upregulated in genetically obese rodents (Carmiel-Haggai *et al.*, 2005; Chavin *et al.*, 1999), dietary studies in which obesity was induced in Wistar rats by a saturated fat-rich diet of lard or coconut oil (Buettner *et al.*, 2006) or in lean and obese Zucker rats by HF-S feeding (Carmiel-Haggai *et al.*, 2005) have also demonstrated that UCP2 expression remained stable in the HF-S liver. Studies examining the influence of dietary fish oil consumption on UCP2 expression have also shown divergent results, with some demonstrating that UCP2

is unchanged by exposure to n-3 PUFAs (Buettner *et al.*, 2006; Deng *et al.*, 2004) and others showing a marked increase in hepatic UCP2 expression in response to fish oil feeding (Mori *et al.*, 2007; Tsuboyama-Kasaoka *et al.*, 1999). Those studies demonstrating unchanged hepatic UCP2 mRNA in response to HF-n-3 were conducted in rats with a shorter diet duration (2-12 weeks), whilst those showing enhanced UCP2 when exposed to fish oil were conducted in mice over a much longer dietary period (5 months). It is possible that species differences may impact the expression of UCP2, as UCP2 has shown differential expression in different strains of mice (obesity-prone, obesity-resistant and diabetes-resistant strains) (Surwit *et al.*, 1998) and this may compound with the longer diet duration, leading to a significant enhancement of UCP2.

Furthermore, Tsuboyama-Kasaoka and colleagues (Tsuboyama-Kasaoka *et al.*, 2008) showed that fish oil-fed mice did not develop obesity, unlike lard-fed mice and they suggested that UCP2 may be implicated in the prevention of diet-induced obesity in the fish oil-fed group. Although body weight was similar in HF-n-3 and HF-S mice in the current study, increased hepatic UCP2 was associated with reduced final body weight in the HF-n-3, but not HF-S group, suggesting UCP2 may play a role in enhancing energy expenditure in the HF-n-3 group. Whilst upregulation of UCP2 has been suggested to protect against excessive liver fat accumulation it has also been associated with chronic ATP depletion (Serviddio *et al.*, 2008; Carmiel-Haggai *et al.*, 2005). AMP is generally increased when cellular ATP is diminished, leading to an elevated cellular AMP:ATP ratio, which has been shown to trigger AMPK activation (Corton *et al.*, 1994). These data further support a role for AMPK activation by n-3 PUFA enrichment of a HFD and as AMPK activation inhibits lipogenesis and promotes fatty

acid oxidation in the liver (Towler and Hardie, 2007; Winder and Hardie, 1999), AMPK may also be implicated in the amelioration of HF-S-induced hepatic fat accretion with HF-n-3 feeding.

Although PPAR γ exhibits only low expression in the liver (Matsusue *et al.*, 2003; Fajas *et al.*, 1997), exposure to natural ligands, fatty acids, enhances PPAR γ activity (Yamamoto *et al.*, 2005; Kliewer *et al.*, 1997), ultimately leading to lipid storage (Patsouris *et al.*, 2006). Consistent with this notion, hepatic PPAR γ expression was induced by high fat overfeeding in male mice in the present study and this is in accordance with previous research (Rokling-Andersen *et al.*, 2009; Rahimian *et al.*, 2001; Memon *et al.*, 2000). PPAR γ agonists are also insulin sensitising agents, influencing the expression of several genes which lead to improved insulin sensitivity in the liver (Coletta *et al.*, 2009; LeBrasseur *et al.*, 2006), such as AMPK (LeBrasseur *et al.*, 2006). FAT/CD36 is also a PPAR γ target gene that promotes lipid partitioning and in doing so may enhance insulin sensitivity (Sato *et al.*, 2002). Therefore PPAR γ may be involved in stimulating hepatic FAT/CD36 expression in the current study. However, FAT/CD36 was induced only by HF-n-3, and not by HF-S feeding, despite similarly enhanced expression of PPAR γ in HF-n-3 and HF-S mice.

In addition to PPAR γ , FAT/CD36 expression is also influenced by PPAR α (Fu *et al.*, 2005; Mandard *et al.*, 2004; Sato *et al.*, 2002), the most abundant PPAR isoform in the current study. Whilst PPAR γ expression was influenced by high fat feeding, irrespective of the dietary fatty acid composition, PPAR α has also been shown to be

stimulated by fatty acids, but preferentially binds n-3 PUFAs (Hihi *et al.*, 2002; Xu *et al.*, 1999a). Although we reported that the mRNA content of PPAR α , its co-activator, PGC1 α , and their regulator, SIRT1, were unchanged by high fat overfeeding, PPAR α activity may be altered with HF-n-3 feeding. Buettner and colleagues (Buettner *et al.*, 2006) showed that PPAR α mRNA did not have to be significantly increased for the significant upregulation of several PPAR α target genes to occur. Increased FAT/CD36 and FATP2 expressions in HF-n-3, but not HF-S mice, are consistent with increased PPAR α activity, and may act to partition fatty acids to fates of mitochondrial (Bezaire *et al.*, 2006; Campbell *et al.*, 2004) and peroxisomal (Falcon *et al.*, 2010) oxidation, respectively. Furthermore, in **Chapter 2** it was reported that livers were markedly enlarged in mice exposed to the HF-n-3 diet and it was speculated this may be due to peroxisomal proliferation. Given that PPAR α agonist WY-14,643 also induces hepatomegaly by increasing the size and number of peroxisomes (Sinal *et al.*, 2001), it is possible that PPAR α activation is involved in the increased liver size in the current study. This study may therefore have benefited from measuring key genes involved in peroxisomal metabolism, and this may be addressed in future studies.

Whilst it has been demonstrated that fatty acid oxidation may be enhanced by HF-n-3 feeding, but impaired in the HF-S group, PDK4 mRNA was subsequently measured to determine if there had been a fuel shift. Previous research has demonstrated that an increased presence of free fatty acid, palmitate, stimulates hepatic PDK4 expression *in vitro* (Huang *et al.*, 2002). *In vivo*, PDK4 expression is also induced in a rodent model with elevated free fatty acids (Bajotto *et al.*, 2006), although this is inconsistent with the current study. The lack of an increase in PDK4 mRNA content with high fat

feeding may be a diluted response due to differences in the time of tissue collection as hepatic PDK4 has recently been shown to display strong circadian rhythmicity (Hsieh *et al.*, 2010). On the other hand, the lack of a response is consistent, with research by Buettner and associates (Buettner *et al.*, 2006) that showed both hepatic PDK2 and PDK4 expressions were unchanged with HF-S feeding and by Holness and colleagues (Holness *et al.*, 2003) in which the hepatic PDK2, but not PDK4, isoform was increased by consuming a HFD. Of the two PDK isoforms expressed in the liver, PDK2 is the more dominant (Bowker-Kinley *et al.*, 1998) and it is therefore possible that PDK2 plays a greater role in promoting a switch in hepatic fuel metabolism to preferentially utilise fatty acids by suppressing the oxidative disposal of carbohydrate through the citric acid cycle (Jeoung and Harris, 2008). However, PDK activation in response to high fat feeding may contribute to the development of hyperglycaemia and ultimately type 2 diabetes (Sugden *et al.*, 1995). Therefore the fatty acid-induced increase in PDK expression may be inhibited in HF-S mice in this study as an adaptive response to prevent further metabolic dysfunction. Consistent with this notion, insulin has been shown to suppress hepatic PDK mRNA and protein expression *in vitro* (Huang *et al.*, 2002). It was also demonstrated in the current study that greater plasma glucose concentrations were associated with lower levels of PDK4 mRNA in the HF-S group only, further supporting the proposed adaptive response to HF-S feeding. Furthermore, the lack of PDK4 upregulation in HF-S livers suggests that the complete oxidation of fatty acids is impaired these mice, leading to lower production of acetyl-CoA and NADH, which are known to activate PDK4 (**Figure 5.18**).

In contrast, HF-n-3 produced a striking increase in hepatic PDK4 expression, indicative of enhanced fatty acid oxidation (**Figure 5.18**). An early study by Sugden and colleagues (Sugden *et al.*, 1998) demonstrated that feeding rats for 28 days with a HF-S diet enriched with n-3 PUFA inhibited total PDK activity in the liver. Buettner and associates (Buettner *et al.*, 2006) similarly examined hepatic PDK expression in high fat fish oil-fed rats, but demonstrated PDK2 and PDK4 expressions were unchanged. Although few studies have investigated the effect of n-3 PUFA consumption on PDK4 expression, each study provides a different standpoint. However, in the current study the observed stimulation of PDK4 expression by n-3 PUFAs is consistent with the response seen upon PPAR α activation. Exposing hepatoma cells to PPAR α agonists, WY-14,643 and clofibrate, induces PDK4 mRNA expression and protein abundance (Huang *et al.*, 2002). In rats, treatment with WY-14,643 for 3 days similarly induced PDK4 mRNA and protein (Huang *et al.*, 2002). Furthermore, just 24 hours after a dose of WY-14,643, hepatic PDK4 protein is increased in rats fed a standard chow diet or HFD (Holness *et al.*, 2003). Therefore the increased PDK4 expression in the current study is consistent with that observed following PPAR α agonist treatment, and given n-3 PUFAs are natural PPAR α agonists (Hihi *et al.*, 2002), PPAR α may be implicated in the HF-n-3-induced increase in PDK4. This is in keeping with PPAR α 's role of promoting pathways of fatty acid use.

In combination these data suggest that n-3 PUFAs may stimulate fatty acid oxidation through mitochondrial and peroxisomal pathways, this is consistent with the increase in hepatic PDK4 expression and may be causal in the reduced hepatic fat deposition in HF-n-3 mice (**Figure 5.19**). In contrast, the lack of an increase in PDK4 in the HF-S

group may suggest oxidative disposal of fatty acids is blunted, leading to hepatic fat accretion. However, this study would benefit from measuring the aforementioned genes at the level of protein abundance or activity, which would provide some further insight to the mechanisms behind the differential fat deposition in the HF-S and HF-n-3 dietary groups.

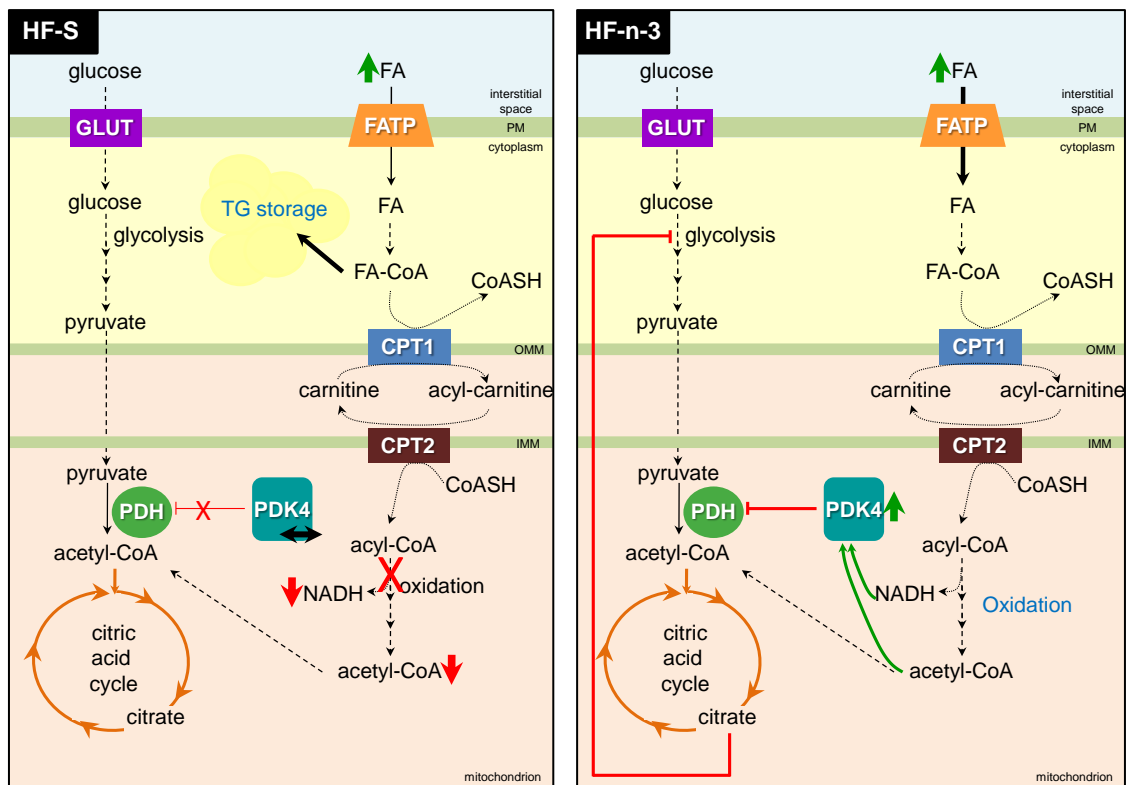


Figure 5.18. Schematic diagram depicting the mechanism by which feeding a high fat diet enriched with n-3 PUFAs may induce a switch in fuel metabolism in the liver to reflect the increased availability of fatty acids and by which exposure to saturated fats fails to increase pyruvate dehydrogenase kinase activity.

HF-n-3 diet consumption results in fatty acid excess and increased hepatic fatty acid uptake. With greater fatty acid availability in the liver cell, more fatty acids may undergo mitochondrial oxidation, giving rise to increased concentration of byproducts, NADH and acetyl-CoA, which induces PDK4 expression. Activated PDK4 inhibits the conversion of pyruvate to acetyl-CoA, which is catalysed by PDH and is the key reaction in driving products of glycolysis into the citric acid cycle. Furthermore, citric acid cycle metabolite, citrate, when increased inhibits glycolytic enzymes. Inhibition of glycolysis, allows the promotion of fatty acid oxidation in order to clear the predominant fuel in excess, fatty acids. In contrast, HF-S feeding does not promote PDK4 expression, this may be due to impaired fatty acid oxidation, resulting in less NADH and acetyl-CoA to enhance PDK4 activation. However, this may also be a compensatory response aiming to prevent HF-S-induced hyperglycemia, by relieving the inhibition of the glycolytic pathway, promoting glucose oxidation. HF-S, high saturated fat diet; HF-n-3, high fat n-3 polyunsaturated fatty acid enriched diet; FA, fatty acid; TG, triglyceride; FA-CoA, fatty acyl-Coenzyme A; CoASH, Coenzyme A (not attached to an acyl group); CPT, carnitine palmitoyl transferase; NADH, nicotinamide adenine dinucleotide; PDK4, pyruvate dehydrogenase kinase 4; PDH, pyruvate dehydrogenase; GLUT, glucose transporter; FATP, fatty acid transporter; PM, plasma membrane; IMM, inner mitochondrial membrane; OMM, outer mitochondrial membrane. Thick green arrow, increased; thin green arrow, activates, red line, inhibits.

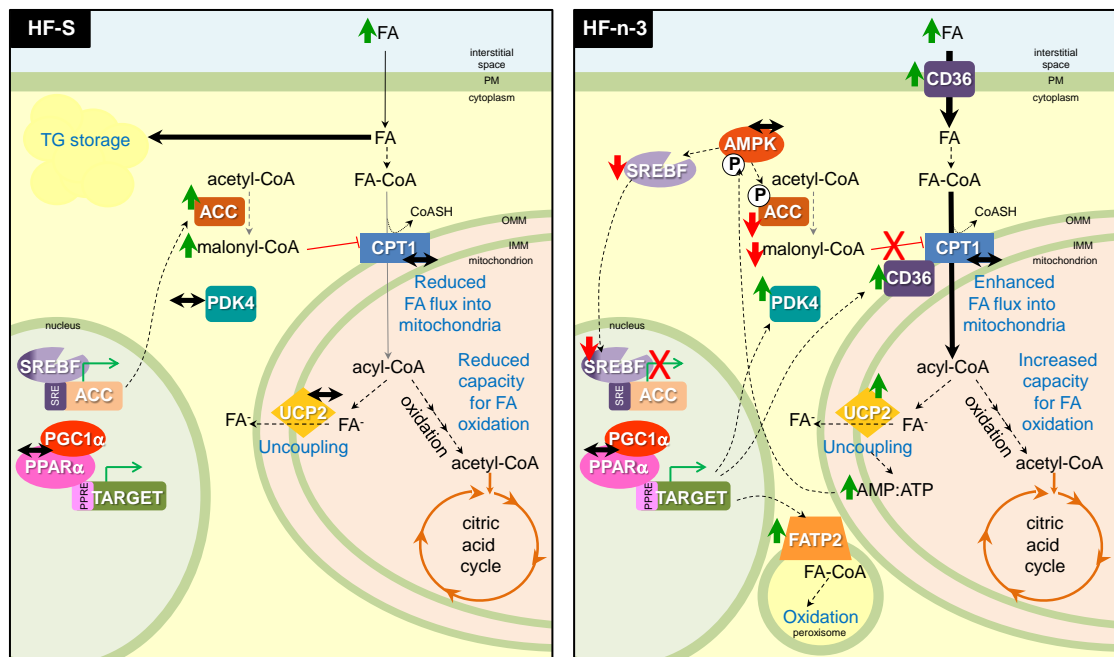


Figure 5.19. Schematic diagram depicting the mechanism behind the differential responses observed in pathways of hepatic fatty acid utilisation with high saturated fat and high fat n-3 PUFA enriched diet feeding.

Hepatic fatty acid uptake was increased by HF-n-3. In HF-n-3 mice, although CPT1a mRNA expression was unchanged, ACC- β mRNA content was lower, potentially through reduced SREBF1 as a result of AMPK activation. Reduced ACC- β may prevent malonyl-CoA production, relieving its inhibition on CPT1a, enhancing fatty acid flux into the mitochondria, possibly through the cooperation of CPT1a and CD36. Once within the mitochondria, fatty acids may be oxidised and as UCP3 was enhanced by HF-n-3 feeding, may undergo uncoupling, leading to energy expenditure. Increased UCP3 may reduce ATP production, leading to AMPK activation and ATP generating pathways. Although PPAR α mRNA was unchanged by HF-n-3 feeding, it may be activated by PUFAs, leading to greater expression of its target genes PDK4 and CD36, enhancing mitochondrial oxidation, and FATP2, enhancing peroxisomal oxidation. These pathways may be implicated in the reduced fat storage in HF-n-3 livers. In contrast, HF-S feeding enhanced ACC- β mRNA content, which may promote malonyl-CoA production, leading to CPT1a inhibition. Consequently mitochondrial fatty acid entry and oxidation may be reduced by HF-S, and failure to enhance PDK4 reflects this. Hence, excess fat is driven into storage, leading to fatty liver.

FA, fatty acid; TG, triglyceride; FA⁻, fatty acid anion; FA-CoA, fatty acyl-Coenzyme A; CPT1, carnitine palmitoyl transferase; PDK4, pyruvate dehydrogenase kinase 4; FATP2, fatty acid transport protein 2; CD36, fatty acid translocase; UCP2, uncoupling protein 2; SREBF1, sterol regulatory element binding transcription factor 1; SRE, sterol regulatory element; PPAR α , peroxisome proliferator activator receptor α ; PGC1 α , peroxisome proliferator activated receptor γ activator 1 α ; TARGET, PPAR α target gene; PPRE, PPAR response element; PM, plasma membrane; IMM, inner mitochondrial membrane; OMM, outer mitochondrial membrane; P, phosphorylated. Red line, inhibits; red cross, pathway reduced; green arrow, increased; red arrow, reduced; black double-headed arrow, unchanged.

5.4.4 – Effect of Gender on Hepatic Fatty Acid Metabolism

A gender dimorphic response to high fat feeding has been previously demonstrated (Català-Niell *et al.*, 2008; Priego *et al.*, 2008). In these studies HFD-fed males exhibited greater hepatic triglyceride content, despite a concurrent increase in the expression of genes regulating fatty acid oxidation (Priego *et al.*, 2008). However, in the current study we demonstrated that female mice exhibited greater hepatic fat accretion (**Chapter 2**). In **Chapter 2** it was speculated that this may be the result of a greater affinity of fatty acids for hepatic fatty acid transport system in female mice, as previous research has shown that FAT/CD36 is more abundant in female rats and humans (Stahlberg *et al.*, 2004), and ovariectomy elicits a marked reduction on hepatic FAT/CD36 expression (Kano and Doi, 2006). In this study, it too was shown that FAT/CD36 expression was greatest in the liver of female mice, and may therefore contribute to enhanced fatty acid uptake and consequently fat deposition. In addition to FAT/CD36, nine other genes were differentially expressed between male and female mice. There was greater expression of genes involved in promoting triglyceride synthesis and secretion (DGAT2) and utilisation (PDK4, UCP2) and those inhibiting pathways of lipogenesis (PPAR δ/β) in female mice. Furthermore, the current study detected greater expression of genes involved in fatty acid synthesis and storage (FAS, ACC- α , PPAR γ), and in promoting fatty acid utilisation (AMPK α 2, ACC- β) in male mice. From these data there appears to be no single process, other than fatty acid uptake, that is upregulated solely in a specific gender, as both fatty acid oxidation and synthesis genes are represented as being gender-dimorphic, but show representative genes regulating these processes to be greater in either sex. It is unknown whether the

increase in FAT/CD36, in addition to the different vulnerabilities of both genders, is sufficient to account for greater triglyceride content in the liver of female mice. However, it has been suggested that gender differences in the utilisation of monounsaturated fatty acid, oleate, by mature hepatocytes reveal gender differences in the total fatty acid uptake and not merely in the channelling of fatty acids into pathways of fatty acid metabolism (Ockner *et al.*, 1980).

Although further research is required to elucidate the differential deposition of fat in the livers of male and female mice, there is some evidence from a recent study that PUFA metabolism and docosahexaenoic acid (DHA) bioconversion, a process that mainly occurs in the liver (Rapoport *et al.*, 2007), is gender-dimorphic (Extier *et al.*, 2010). When exposed to an a dose of α -linoleic acid (ALA), differential bioconversion of this fatty acid is reflected in the blood metabolites, as from ALA males produced eicosapentaenoic acid (EPA) and docosapentaenoic acid (DPA) (Burdge *et al.*, 2002), and females in addition to these two fatty acid metabolites produced a third, DHA (Burdge and Wootton, 2002). In the liver, female rodents exhibit greater DHA content as compared to males (Burdge *et al.*, 2008) and this gender-dimorphic response may be influenced by gonadal steroid, oestrogen, as estradiol replacement in ovariectomised rats enhanced the hepatic concentration of PUFAs (Noh *et al.*, 1999). Due to their lipid lowering and insulin sensitising effects, n-3 PUFAs have been considered as a potential therapy against fatty liver (Masterton *et al.*, 2010). As we demonstrated that liver fat deposition is greater in females, and given that previous research has provided evidence for gonadal steroids influencing the metabolism of PUFAs, gender and hormonal status

should be considered when contemplating PUFAs as a potential therapeutic in the treatment of NAFLD.

5.4.5 – Limitations

In the current chapter the findings reported are the outcome of mRNA content analyses, and whilst this provides useful information about the amount of gene transcribed, the mRNA content may not always totally align with the active protein product present in the cell. For instance, total amount of active protein product may be influenced by the stability of mRNA from which protein is translated; the translation of mRNA to protein; post-translational modifications and activation of protein. Examples of genes that undergo post-translational changes leading to altered functional capacity of that protein are described in **Chapter 4 Section 4.7**. Therefore the current study would have benefited from analysing the protein abundance and its activation/activity, hence future investigations may focus on the protein abundance and activity of the key genes investigated. Furthermore in the current study, we describe pathways of fatty acid uptake, storage and oxidation, which would also be advantageous to measure as a whole-process in order to determine their contribution to the overall fatty acid metabolism in the liver.

5.4.6 – Summary

In summary, this study highlights the influence of dietary fatty acid composition on hepatic fatty acid metabolism. In **Chapter 2** it was shown that consuming a HFD rich in saturated fat promotes intracellular accumulation of triglyceride in the liver, and in contrast, enrichment of this high saturated fat diet with n-3 PUFAs ameliorated hepatic

fat accretion, despite the super-physiological content of dietary fat present. In this chapter it was shown that the amelioration of intrahepatic fat accretion occurred through an altered pattern of fatty acid metabolism gene expression in the liver, specifically through the concurrent activation of pathways inducing fatty acid uptake and utilisation and suppression of pathways promoting fatty acid storage and lipogenesis (**Figure 5.20**). Furthermore this work highlights the gender differences in hepatic fatty acid metabolism, but also reflects that further research is required to elucidate the increase in hepatic fat deposition in the female cohort of this study.

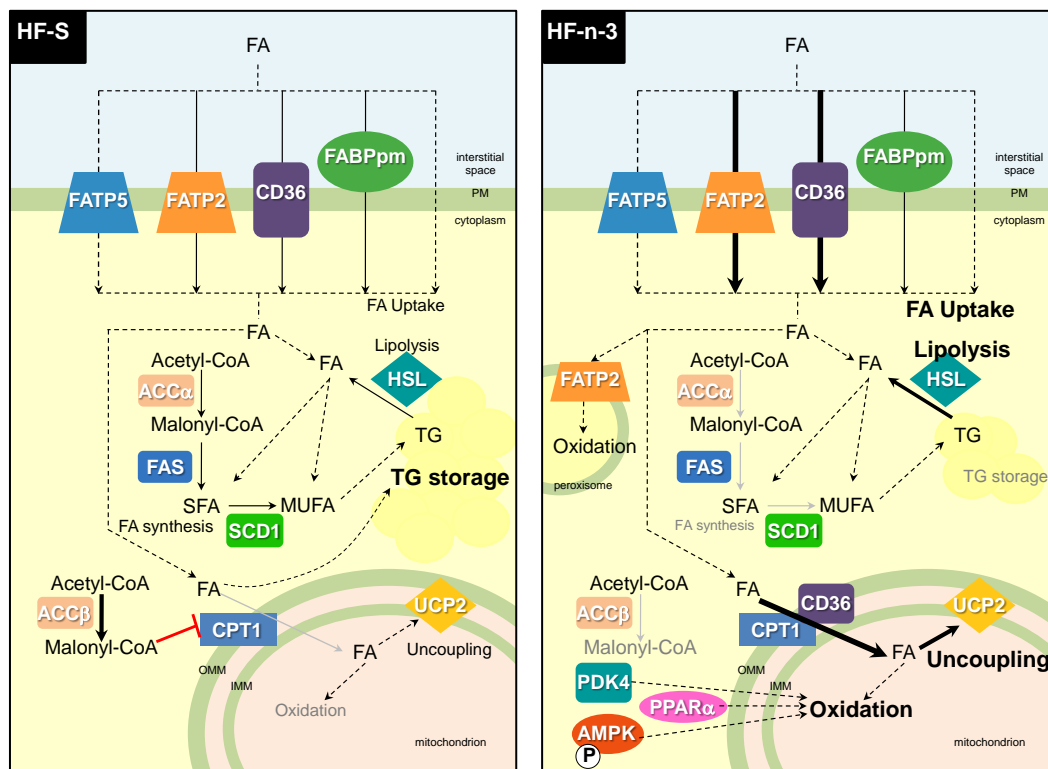


Figure 5.20. Schematic diagram depicting the mechanism behind the differential responses observed in pathways of hepatic fatty acid uptake, storage and utilisation with high saturated fat and high fat n-3 PUFA enriched diet feeding.

The thickness of arrows and boldness of wording represents the relative contribution to the process being described. In the liver, HF-n-3, but not HF-S, feeding increased fatty acid uptake. HF-S feeding did not significantly alter the expression of genes in the lipogenic pathway, but HF-n-3 feeding lead to the downregulation of several lipogenic genes. HF-S feeding inhibited fatty acid oxidation, and in direct contrast, HF-n-3 feeding enhanced the capacity for fatty acid oxidation and uncoupling. Reduced oxidative capacity with normal lipogenic capacity may lead to increased storage capacity for triglycerides, explaining the fatty liver observed in HF-S mice. In contrast to HF-S feeding, the increased fatty acid uptake, impaired lipogenesis and enhanced oxidation of fatty acids in the mitochondria and peroxisomes, may be implicated in the amelioration of HF-S-induced fatty liver with HF-n-3 feeding. HF-S, high saturated fat diet; high fat n-3 PUFA enriched diet, HF-n-3; FA, fatty acid; CD36, fatty acid translocase (FAT/CD36); FATP2, fatty acid transport protein 2; FATP5, fatty acid transport protein 5; FABPpm, fatty acid binding protein; HSL, hormone sensitive lipase; TG, triglyceride; CPT1, carnitine palmitoyl transferase 1; UCP2, uncoupling protein 2; PPARα, peroxisome proliferator activator receptor α; PGC1α, Peroxisome proliferative activated receptor γ coactivator 1α; ACC, acetyl-CoA carboxylase; SCD1, stearoyl-Coenzyme A desaturase 1; FAS, fatty acid synthase; PDK4, pyruvate dehydrogenase 4; AMPK, AMP-activated protein kinase; SFA, saturated fatty acid; MUFA, monounsaturated fatty acid; CoA, coenzyme A; PM, plasma membrane; IMM, inner mitochondrial membrane; OMM, outer mitochondrial membrane; P, phosphorylated.

CHAPTER 6

*The Effect of Dietary Fatty Acid Composition
and Gender on Glucose Metabolism in the
Skeletal Muscle and Liver of Mice*

6.1 – INTRODUCTION

In humans, an increased consumption of saturated fat is associated with reduced insulin sensitivity and impaired glucose tolerance (Risérus *et al.*, 2007; Rivellesse *et al.*, 2002; Hu *et al.*, 2001; Vessby *et al.*, 2001; Marshall *et al.*, 1997). In contrast, consuming a diet rich in n-3 polyunsaturated fatty acids (PUFA) improves both insulin sensitivity and glucose tolerance in humans (Tsitouras *et al.*, 2008; Ebbesson *et al.*, 2005; Ebbesson *et al.*, 1999; Lardinois, 1987). In rats, enriching a safflower oil-rich diet, known to impair insulin sensitivity, with n-3 PUFAs ameliorates high fat diet (HFD)-induced insulin resistance at the whole-body level (Storlien *et al.*, 1987). Consuming a high saturated fat (HF-S) diet leads to the development of peripheral insulin resistance and glucose-stimulated insulin secretion in rats after just 4 weeks (Holness *et al.*, 2004). However, the saturated fat-induced insulin hypersecretion by perfused islets is prevented by replacing a small portion of saturated fat in the HF-S diet with n-3 PUFAs for just 24 hours (Holness *et al.*, 2004). Moreover, chronic consumption of a HFD rich in n-3 PUFAs, provided through fish or perilla oil, results in a less diabetic glucose tolerance curve compared to saturated fat feeding in mice (Ikemoto *et al.*, 1996).

Peripheral insulin sensitivity contributes to whole-body insulin resistance. Given that the skeletal muscle is the predominant site of insulin-stimulated glucose uptake and disposal and that the liver is the chief site of endogenous glucose production, both organs contribute to maintaining whole-body insulin sensitivity. Within just a couple of days of high fat overfeeding the disposal of glucose through glycolysis is impaired in skeletal muscle (Kim *et al.*, 1996); this precedes the development of insulin resistance

which is evident with longer-term high fat overfeeding and manifests in impaired insulin-stimulated glucose transport and glucose metabolism, including glycogen synthesis (Kim *et al.*, 1996; Storlien *et al.*, 1987; Grundleger and Thenen, 1982). High fat feeding (lard (Holness *et al.*, 2003) or safflower oil (Samuel *et al.*, 2004)) also impairs hepatic insulin sensitivity as demonstrated by impaired suppression of hepatic glucose production by insulin and this therefore influences whole-body glucose homeostasis. The impaired peripheral insulin sensitivity associated with high fat overfeeding (safflower oil) can be improved by enriching the HFD with n-3 PUFAs, and this contributes to the improvement in whole-body insulin sensitivity (Storlien *et al.*, 1987). Whilst studies have investigated the effect of n-3 PUFA enrichment of a HFD on insulin sensitivity in either male (safflower oil (Storlien *et al.*, 1987)) or female (lard (Holness *et al.*, 2004; Holness *et al.*, 2003; Ikemoto *et al.*, 1996) or palm oil (Ikemoto *et al.*, 1996)) rodents, to the best of my knowledge, no study has directly compared the effects in the two genders. Given that female mice are less likely to exhibit an impaired insulin sensitivity profile in response to increased fatty acid supply (when exposed to a cafeteria diet (Gómez-Pérez *et al.*, 2008) or intravenous lipid infusion (Hevener *et al.*, 2002)), the effect of n-3 PUFA enrichment of a HFD should be investigated. This is an important matter given that n-3 PUFAs have been considered as a potential therapeutic against insulin resistance (Fedor and Kelley, 2009).

In the current study, I therefore aimed to determine:

- I. the effect of replacing 7.5% of saturated fat in a high saturated fat diet with n-3 PUFAs (derived from fish oil) on glucose metabolism in the skeletal muscle and liver
- II. the influences of muscle fibre type on glucose metabolism in the skeletal muscle
- III. the influences of gender on glucose metabolism in the skeletal muscle and liver

In relation to aim (I) I hypothesised that replacement of 7.5% of saturated fat with n-3 PUFAs would exert beneficial effects on insulin sensitivity by maintaining the phosphorylation and subsequent disposal of glucose in skeletal muscle and liver (assessed by mRNA expression analyses).

In relation to aim (II) I hypothesised that the expression of genes influencing glycolysis would be greater in the fast-twitch glycolytic (FG)-fast-twitch oxidative-glycolytic (FOG) extensor digitorum longus (EDL) muscle, and those influencing insulin sensitivity would be greater in the slow-twitch oxidative (SO) soleus muscle.

And finally, in relation to aim (III) I hypothesised that the male mice would exhibit a greater impairment in skeletal muscle and liver glucose metabolism with HF-S feeding than female mice.

6.2 – MATERIALS AND METHODOLOGY

6.2.1 – Animals, Nutrition Regime and Tissue Collection

As described in **Chapter 2 Section 2.1**, male and female C57BL/6J mice in cohort 1 were provided either a standard chow (control, C), high saturated fat (HF-S) or high fat n-3 polyunsaturated fatty acid (PUFA) enriched (HF-n-3) diet for 14 weeks (\pm 4 days). All procedures were approved by the University of Adelaide Animal Ethics Committee and the Institute of Medical and Veterinary Science Animal Ethics Committee. As described in **Chapter 2 Section 2.2**, following the experimental dietary period, surgery was performed, whilst in the fed-state, to collect skeletal muscles, which were subsequently snap frozen and stored under liquid nitrogen vapour phase storage until subsequent mRNA content analyses. The liver was rapidly collected post-mortem, divided and a portion was snap frozen and stored under liquid nitrogen vapour phase storage until subsequent mRNA content analyses.

6.2.2 – mRNA Content Analyses using the GenomeLab GeXP Genetic Analysis System

As described previously, the mRNA contents of key metabolic genes in skeletal muscle (**Chapter 4 Sections 2.2 - 2.7**) and liver (**Chapter 5 Sections 2.2 - 2.6**) were determined using the GenomeLab GeXP Genetic Analysis System (Beckman Coulter Inc, Fullerton, California, USA). Total RNA was extracted from the whole extensor digitorum longus (EDL) and soleus muscles (see **Chapter 4 Section 2.2**) and a sample of liver (see **Chapter 5 Section 2.2**). Chimeric multiplex primers were designed to

amplify genes of interest in skeletal muscle (**Table 4.1**) and liver (**Table 5.1**) samples; included in these skeletal muscle and liver multiplexes were key genes controlling glucose metabolism. Reverse transcription and polymerase chain reaction (PCR) were performed (see **Chapter 4 Sections 2.5 - 2.6** (muscle) and **Chapter 5 Section 2.5** (liver)). Resultant PCR products were separated, detected and analysed using the GenomeLab GeXP Genetic Analysis System and GenomeLab eXpress Profiler software (ver.10.0 Beckman Coulter Inc, Fullerton, California, USA) and normalised to the average mRNA content of three housekeeping genes (see **Chapter 4 Section 2.7** (muscle) and **Chapter 5 Section 2.6** (liver)). Results are reported as mRNA content, the ratio of mean mRNA content of the target gene relative to the averaged mean mRNA content of three housekeeping genes (AU).

6.2.3 – Statistical Analyses

6.2.3.1 – Skeletal Muscle mRNA Contents of Key Glucose Metabolism Genes

All data are presented as mean \pm standard error of the mean (SEM). Two-way Analysis of Variance (ANOVA), with pairwise comparisons (Bonferroni post-hoc analysis), was used to determine the effect of diet (C, HF-S, HF-n-3), muscle fibre type (EDL, soleus), gender (male, female) and their interaction on the mRNA content of key glucose metabolism genes. Simple linear regression analyses were used to determine the relationship of the mRNA content of hexokinase 2 (HK2) in the EDL muscle with the liver content of glycogen and fat (mean fat droplet area); plasma glucose concentration with the mRNA content of phosphatidylinositol 3-kinase, regulatory subunit, polypeptide 1 (PI3Kr1) in the soleus muscle; and the plasma insulin concentration with

the mRNA content of suppressor of cytokine signalling 3 (SOCS3) in the soleus muscle. Pearson correlation coefficients (r) were used to evaluate linear relationships.

All statistics were performed using the Statistical Package for Social Scientists (SPSS) (ver. 17.0.0, SPSS Inc, Chicago, Illinois, USA). A probability of less than 5% ($P < 0.05$) was considered statistically significant. Analyses are reported as percentage change; statistical effect: F(degrees of freedom: between subjects effect, degrees of freedom: within subjects effect) = F value, P value of effect; and subsequent P values of post-hoc or pairwise analyses.

6.2.3.2 – Liver mRNA Contents of Key Glucose Metabolism Genes

All data are presented as mean \pm SEM. Two-way ANOVA, with pairwise comparisons (Bonferroni post-hoc analysis), was used to determine the effect of diet (C, HF-S, HF-n-3), gender (male, female) and their interaction on the mRNA content of key glucose metabolism genes. Simple linear regression analyses were used to determine the relationship of plasma glucose concentration with the liver mRNA contents of SOCS3 and phosphofructokinase (PFK-L). Pearson correlation coefficients (r) were used to evaluate linear relationships.

All statistics were performed using SPSS (ver. 17.0.0, SPSS Inc, Chicago, Illinois, USA). A probability of less than 5% ($P < 0.05$) was considered statistically significant. Analyses are reported as percentage change; statistical effect: F(degrees of freedom: between subjects effect, degrees of freedom: within subjects effect) = F value, P value of effect; and subsequent P values of post-hoc or pairwise analyses.

6.3 – RESULTS

6.3.1 – Glucose Phosphorylation - Committing to Glucose Metabolism

6.3.1.1 – Skeletal Muscle Hexokinase 2

There was a diet*muscle interaction on skeletal muscle hexokinase 2 (HK2) mRNA content ($F(2, 114)=3.1$, $P=0.049$) (**Figure 6.1**), in the EDL muscle, HF-S mice exhibited lower HK2 mRNA as compared to control mice (-15%; pairwise comparison: $P\leq 0.02$). In HF-S mice, the soleus muscle exhibited greater HK2 mRNA as compared to the EDL muscle (+29%; pairwise comparison: $P\leq 0.001$) and in HF-n-3 mice, there was also a trend towards greater HK2 mRNA content in the soleus muscle as compared to the EDL muscle (+13%; pairwise comparison: $P=0.073$). There was also a gender*muscle interaction on skeletal muscle HK2 mRNA content ($F(1, 114)=7.2$, $P=0.008$), in female mice, the soleus muscle exhibited greater HK2 mRNA content as compared to the EDL muscle (+25%; pairwise comparisons: $P\leq 0.001$) and in the soleus muscle, female mice exhibited greater HK2 mRNA content than male mice (+11%; pairwise comparison: $P\leq 0.05$). In the EDL muscle, there was also a trend towards greater HK2 mRNA content in male mice as compared to female mice (+7%; pairwise comparison: $P=0.081$).

In the HF-S, but not HF-n-3, group, there was a significant negative correlation between the mRNA content of HK2 in the EDL muscle and the amount of glycogen stored in the liver (HF-S, $r = -0.52$, $F(1, 20)=7.4$, $P=0.013$, male and female mice combined; HF-n-3, $r = +0.12$, $F(1, 16)=0.2$, $P=0.65$) (**Figure 6.2**). Also in the HF-S group only, the mRNA content of HK2 in the EDL muscle was negatively correlated with

the amount of fat stored in the liver (HF-S, $r = -0.46$, $F(1, 19)=5.2$, $P=0.035$, male and female mice combined; HF-n-3, $r = +0.35$, $F(1, 17)=2.4$, $P=0.14$) (**Figure 6.2**).

6.3.1.2 – Liver Glucokinase

Hepatic glucokinase (GCK) mRNA content was lower in HF-n-3 mice as compared to control and HF-S mice ($F(2, 57)=19.5$, $P\leq 0.001$; -80%, -40%, respectively; post-hoc tests: $P\leq 0.001$) (**Figure 6.3**). There was no effect of gender on hepatic GCK mRNA content ($F(1, 57)=0.3$, $P=0.56$).

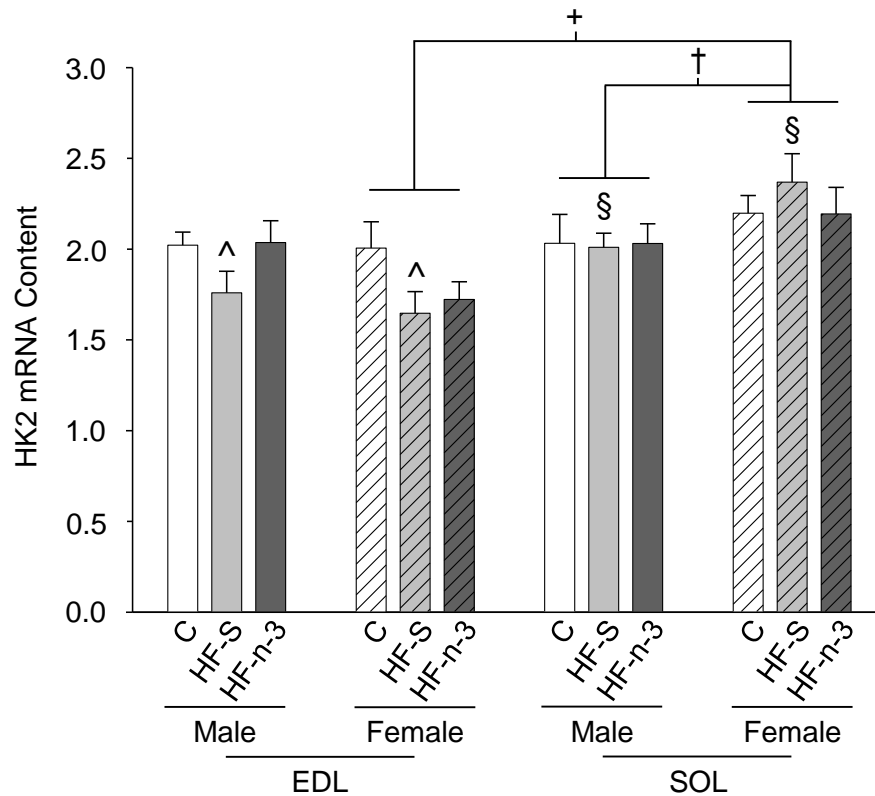


Figure 6.1. HK2 mRNA content in the white extensor digitorum longus and red soleus muscles of male and female mice fed control, high saturated fat or high fat n-3 PUFA enriched diets.

Data are expressed as mean (bars) \pm SEM (error bars), where solid bars indicate male (M) mice, lined bars indicate female (F) mice and colour represents diet: white, control (C); pale grey, high saturated fat (HF-S); dark grey, high fat n-3 polyunsaturated fatty acid enriched (HF-n-3). EDL, extensor digitorum longus muscle; SOL, soleus muscle; HK2, hexokinase 2.

n: EDL - C(M/F) = 10/12, HF-S(M/F) = 11/11, HF-n-3(M/F) = 9/11;

n: SOL - C(M/F) = 10/12, HF-S(M/F) = 10/10, HF-n-3(M/F) = 9/11.

Statistics: Diet*muscle interaction: [^] $P \leq 0.02$, compared to C (EDL); [§] $P \leq 0.001$, SOL compared to EDL (HF-S). Gender*muscle interaction: ⁺ $P \leq 0.001$, female EDL compared to female SOL; [†] $P \leq 0.05$, male compared to female (SOL).

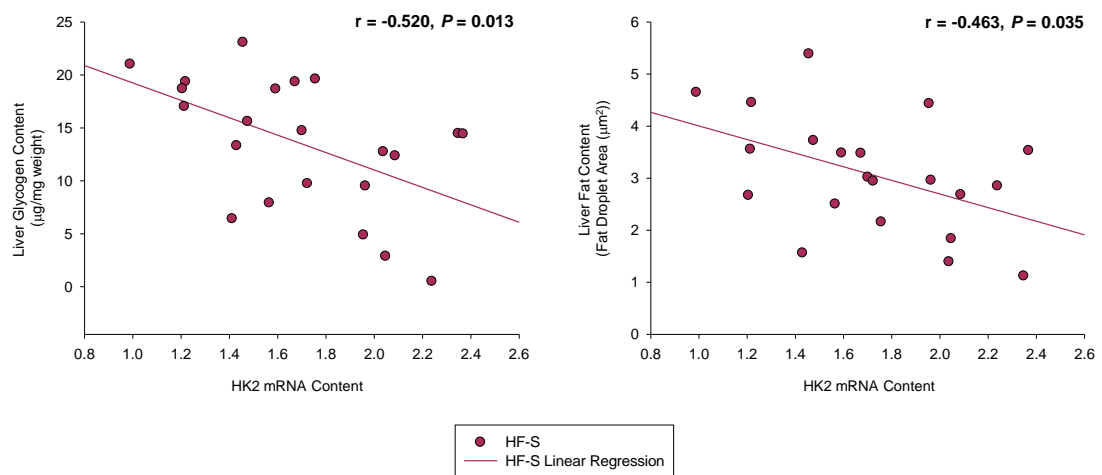


Figure 6.2. Correlations between HK2 mRNA content in the EDL muscle with the amount of liver glycogen and fat in mice exposed to a high saturated fat diet.

Symbol type represents dietary group and muscle type: see legend. HF-S, high saturated fat diet; EDL, extensor digitorum longus muscle; HK2, hexokinase 2.

Liver glycogen, HF-S (EDL) $n = 22$; liver fat, HF-S (EDL) $n = 21$.

There was a significant negative relationship between HK2 mRNA content in the EDL muscle and the amount of liver glycogen in HF-S mice (male and female mice combined). There was also a significant negative relationship between HK2 mRNA content in the EDL muscle and liver fat accumulation in the HF-S group (male and female mice combined).

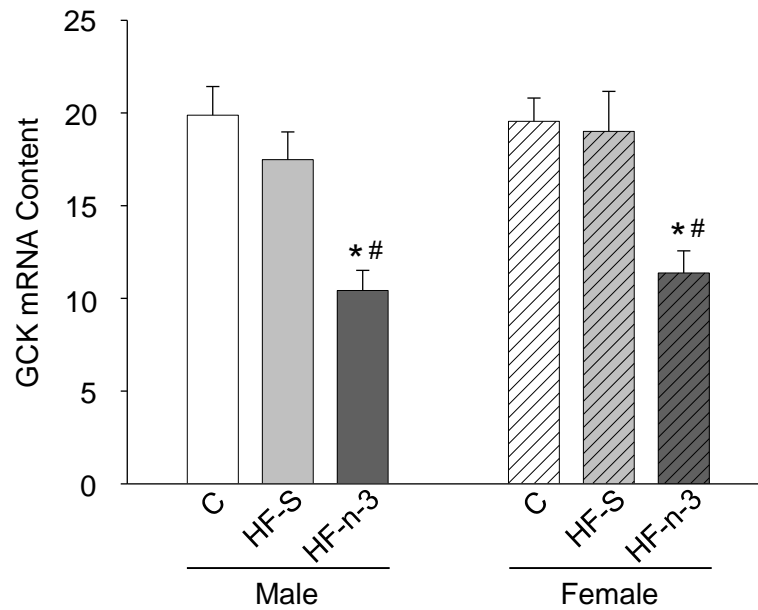


Figure 6.3. GCK mRNA content in the liver of male and female mice fed control, high saturated fat or high fat n-3 PUFA enriched diets.

Data are expressed as mean (bars) \pm SEM (error bars), where solid bars indicate male (M) mice, lined bars indicate female (F) mice and colour represents diet: white, control (C); pale grey, high saturated fat (HF-S); dark grey, high fat n-3 polyunsaturated fatty acid enriched (HF-n-3). GCK, glucokinase.

n: C(M/F) = 10/12, HF-S(M/F) = 11/10, HF-n-3(M/F) = 9/11.

Statistics: Effect of diet: * $P \leq 0.001$, compared to C; # $P \leq 0.001$, compared to HF-S.

6.3.2 – Glycolysis

6.3.2.1 – Skeletal Muscle Phosphofructokinase

There was no effect of diet on skeletal muscle phosphofructokinase (PFK-M) mRNA content ($F(2, 114)=0.6, P=0.53$) (**Figure 6.4**). There was an effect of muscle fibre type on PFK-M mRNA content, the EDL muscle exhibited greater PFK-M mRNA as compared to the soleus muscle (+1.6-fold; $F(1, 114)=329.3, P\leq 0.001$). There was an effect of gender on PFK-M mRNA content, male mice exhibited greater PFK-M mRNA than female mice (+24%; $F(1, 114)=14.9, P\leq 0.001$).

6.3.2.2 – Liver Phosphofructokinase

There was a diet*gender interaction on liver phosphofructokinase (PFK-L) mRNA content ($F(2, 57)=5.4, P=0.007$) (**Figure 6.5**), in female mice, PFK-L mRNA was greater in HF-n-3 mice as compared to control mice (+15%; pairwise comparisons: $P\leq 0.05$). In control mice, males exhibited greater PFK-L mRNA as compared to females (+14%, pairwise comparison: $P\leq 0.05$) and in HF-n-3 mice, females exhibited greater PFK-L mRNA as compared to males (+16%, pairwise comparison: $P\leq 0.02$).

In HF-n-3 mice, there was a tendency for the plasma glucose concentrations to be negatively correlated with the mRNA content of PFK-L in the liver (HF-n-3, $r = -0.34, F(1, 17)=2.2, P=0.15$, male and female mice combined; HF-S, $r = +0.30, F(1, 19)=1.9, P=0.18$) (data not shown).

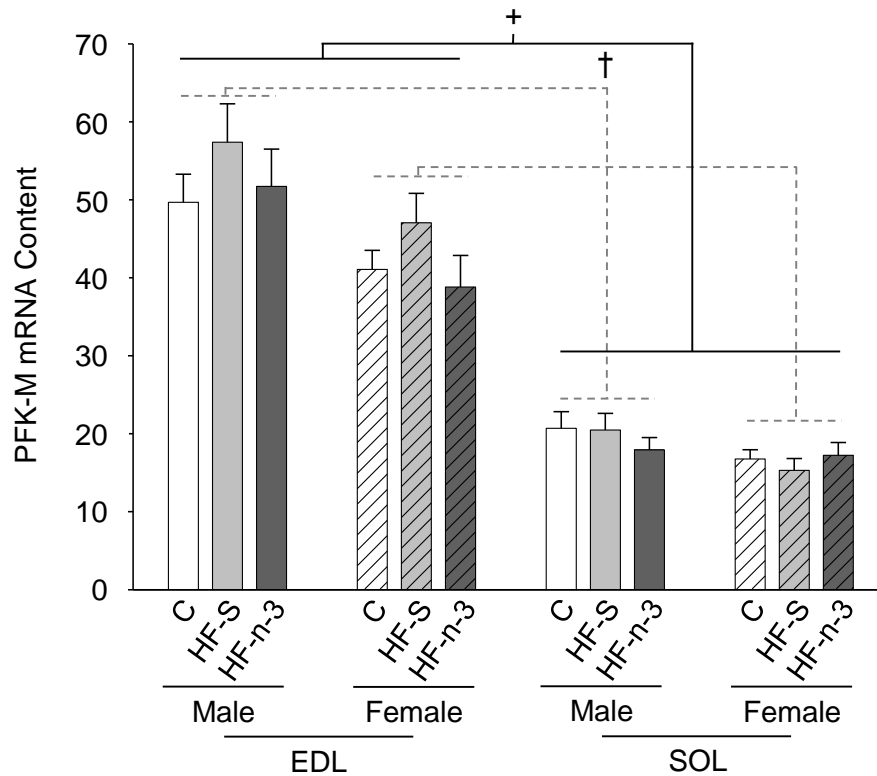


Figure 6.4. PFK-M mRNA content in the white extensor digitorum longus and red soleus muscles of male and female mice fed control, high saturated fat or high fat n-3 PUFA enriched diets.

Data are expressed as mean (bars) \pm SEM (error bars), where solid bars indicate male (M) mice, lined bars indicate female (F) mice and colour represents diet: white, control (C); pale grey, high saturated fat (HF-S); dark grey, high fat n-3 polyunsaturated fatty acid enriched (HF-n-3). EDL, extensor digitorum longus muscle; SOL, soleus muscle; PFK-M, phosphofructokinase.

n: EDL - C(M/F) = 10/12, HF-S(M/F) = 11/11, HF-n-3(M/F) = 9/11;

n: SOL - C(M/F) = 10/12, HF-S(M/F) = 10/10, HF-n-3(M/F) = 9/11.

Statistics: Effect of muscle fibre type: $^+P \leq 0.001$, SOL compared to EDL. Effect of gender: $^\dagger P \leq 0.001$, male compared to female.

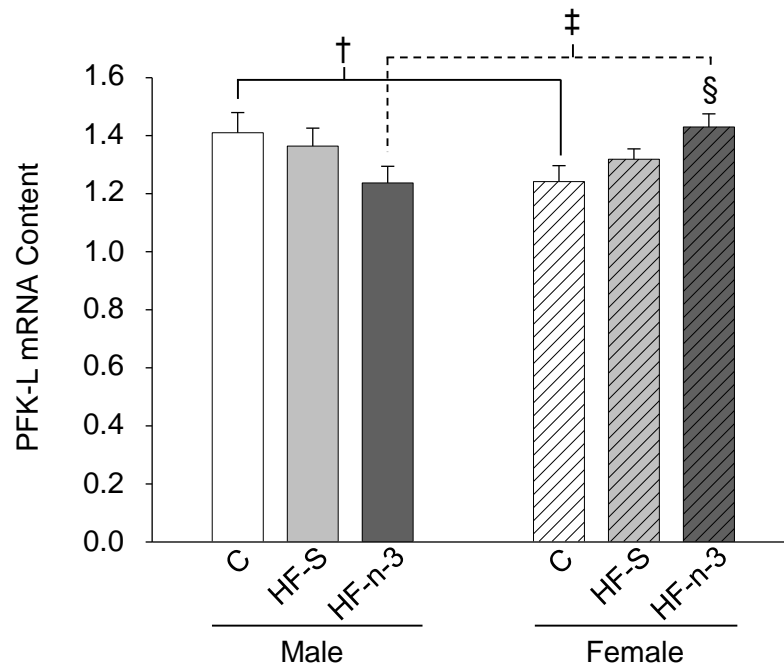


Figure 6.5. PFK-L mRNA content in the liver of male and female mice fed control, high saturated fat or high fat n-3 PUFA enriched diets.

Data are expressed as mean (bars) \pm SEM (error bars), where solid bars indicate male (M) mice, lined bars indicate female (F) mice and colour represents diet: white, control (C); pale grey, high saturated fat (HF-S); dark grey, high fat n-3 polyunsaturated fatty acid enriched (HF-n-3). PFK-L, phosphofructokinase.

n: C(M/F) = 10/12, HF-S(M/F) = 11/10, HF-n-3(M/F) = 9/11.

Statistics: Diet*gender interaction: $^{\S}P \leq 0.05$, compared to C (Female); $^{\dagger}P \leq 0.05$, C male compared to C female; $^{\ddagger}P \leq 0.02$, HF-n-3 male compared to HF-n-3 female.

6.3.3 – Glycogenesis

6.3.3.1 – Skeletal Muscle Glycogen Synthase

There was no effect of diet ($F(2, 114)=0.3, P=0.74$) on skeletal muscle glycogen synthase 1 (GYS1) mRNA content. There was an effect of muscle fibre type on GYS1 mRNA content, the soleus muscle exhibited greater GYS1 mRNA as compared to the EDL muscle (+43%; $F(1, 114)=74.8, P\leq 0.001$) (**Figure 6.6**). There was no effect of gender on GYS1 mRNA content ($F(1, 114)=0.2, P=0.62$).

6.3.3.2 – Liver Glycogen Synthase

There was no effect of diet ($F(2, 58)=2.9, P=0.064$) on liver glycogen synthase 2 (GYS2) mRNA content, although there was a trend towards reduced GYS2 mRNA content in HF-n-3 mice as compared to control mice (-17%; post-hoc test: $P=0.060$) (**Figure 6.7**). There was an effect of gender on GYS2 mRNA content, male mice exhibited greater GYS2 mRNA than female mice (+27%; $F(1, 58)=16.2, P\leq 0.001$).

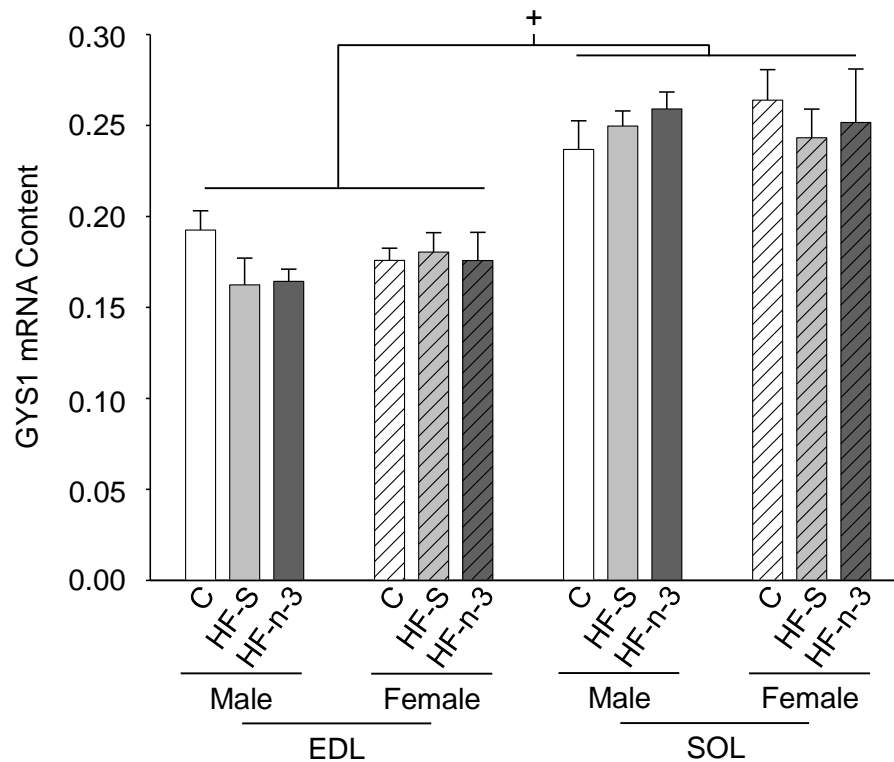


Figure 6.6. GYS1 mRNA content in the white extensor digitorum longus and red soleus muscles of male and female mice fed control, high saturated fat or high fat n-3 PUFA enriched diets.

Data are expressed as mean (bars) \pm SEM (error bars), where solid bars indicate male (M) mice, lined bars indicate female (F) mice and colour represents diet: white, control (C); pale grey, high saturated fat (HF-S); dark grey, high fat n-3 polyunsaturated fatty acid enriched (HF-n-3). EDL, extensor digitorum longus muscle; SOL, soleus muscle; GYS1, glycogen synthase 1.

n: EDL - C(M/F) = 10/12, HF-S(M/F) = 11/11, HF-n-3(M/F) = 9/11;

n: SOL - C(M/F) = 10/12, HF-S(M/F) = 10/10, HF-n-3(M/F) = 9/11.

Statistics: Effect of muscle fibre type: $^+P \leq 0.001$, SOL compared to EDL.

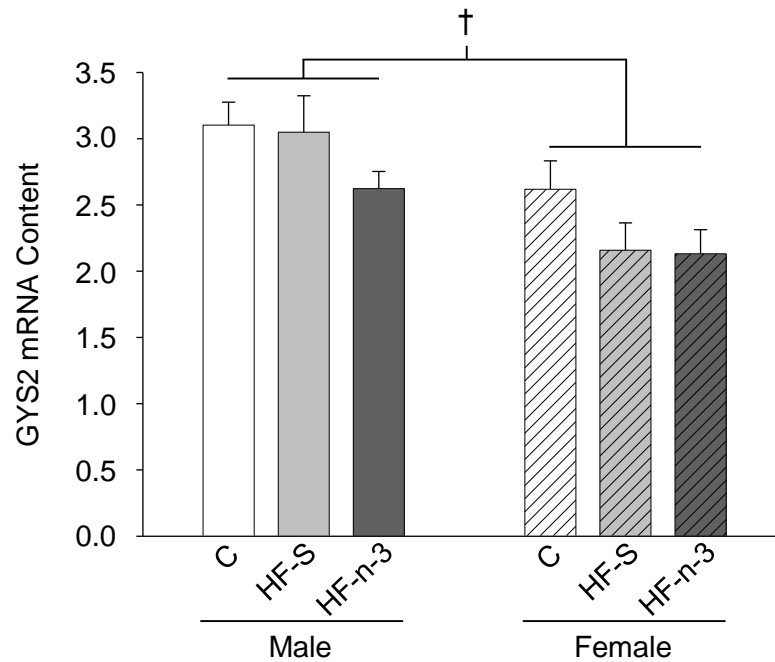


Figure 6.7. GYS2 mRNA content in the liver of male and female mice fed control, high saturated fat or high fat n-3 PUFA enriched diets.

Data are expressed as mean (bars) \pm SEM (error bars), where solid bars indicate male (M) mice, lined bars indicate female (F) mice and colour represents diet: white, control (C); pale grey, high saturated fat (HF-S); dark grey, high fat n-3 polyunsaturated fatty acid enriched (HF-n-3). GYS2, glycogen synthase 2.

n: C(M/F) = 10/12, HF-S(M/F) = 11/11, HF-n-3(M/F) = 9/11.

Statistics: Effect of gender: $^{\dagger}P \leq 0.001$, male compared to female.

6.3.4 – Hepatic Gluconeogenesis

Liver phosphoenolpyruvate carboxykinase (PEPCK) mRNA content was lower in HF-n-3 mice as compared to control mice ($F(2, 58)=4.1$, $P=0.021$; -15%; post-hoc test: $P\leq 0.05$) (**Figure 6.8**). There also was a strong trend towards reduced PEPCK mRNA in HF-n-3 mice as compared to HF-S mice (-14%; $P=0.052$). There was no effect of gender on PEPCK mRNA content ($F(1, 58)=0.3$, $P=0.61$).

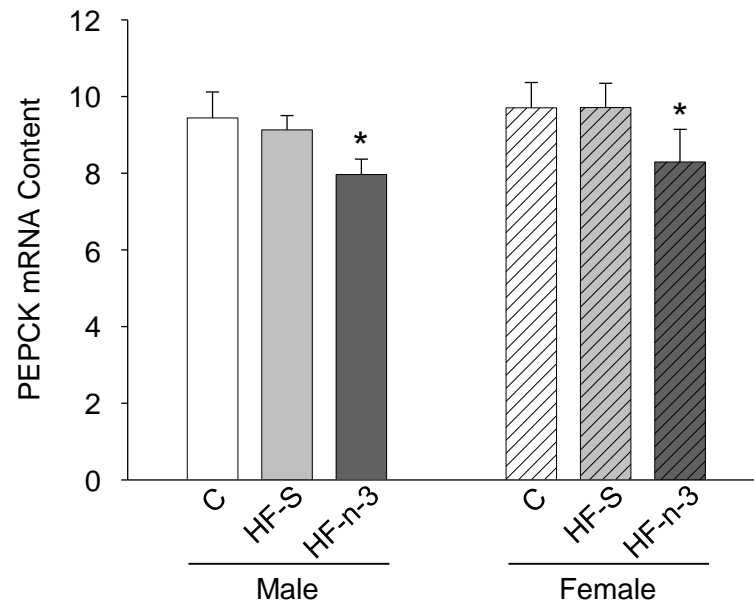


Figure 6.8. PEPCK mRNA content in the liver of male and female mice fed control, high saturated fat or high fat n-3 PUFA enriched diets.

Data are expressed as mean (bars) \pm SEM (error bars), where solid bars indicate male (M) mice, lined bars indicate female (F) mice and colour represents diet: white, control (C); pale grey, high saturated fat (HF-S); dark grey, high fat n-3 polyunsaturated fatty acid enriched (HF-n-3). PEPCK, phosphoenolpyruvate carboxykinase 1.

n: C(M/F) = 10/12, HF-S(M/F) = 11/11, HF-n-3(M/F) = 9/11.

Statistics: Effect of diet: * $P \leq 0.05$, compared to C.

6.3.5 – Influencing Insulin Signalling

6.3.5.1 – Skeletal Muscle Phosphatidylinositol 3-kinase

There was no effect of diet ($F(2, 114)=0.1, P=0.90$) on skeletal muscle phosphatidylinositol 3-kinase, regulatory subunit, polypeptide 1 (PI3Kr1) mRNA content. There was an effect of muscle fibre type on PI3Kr1 mRNA content, the soleus muscle exhibited greater PI3Kr1 mRNA as compared to the EDL muscle (+14%; $F(1, 114)= 4.8, P=0.031$) (**Figure 6.9**). There was no effect of gender on PI3Kr1 mRNA content ($F(1, 114)=0.06, P=0.81$).

In the HF-S, but not HF-n-3, group, there tended to be a negative correlation between the mRNA content of PI3Kr1 in the soleus muscle and the plasma glucose concentration, although this did not reach statistical significance (HF-S, $r = -0.35, F(1, 18)=2.6, P=0.13$, male and female mice combined; HF-n-3, $r = -0.21, F(1, 17)=0.8, P=0.39$) (**Figure 6.10**).

6.3.5.2 – Skeletal Muscle Suppressor of Cytokine Signalling

There was no effect of diet ($F(2, 113)=1.2, P=0.30$), muscle fibre type ($F(1, 113)=0.4, P=0.53$) or gender ($F(1, 113)=0.8, P=0.36$) on suppressor of cytokine signalling 3 (SOCS3) mRNA content in skeletal muscle (**Figure 6.11**).

In the HF-n-3, but not HF-S, group, there tended to be a negative correlation between the mRNA content of SOCS3 in the soleus muscle and plasma insulin concentrations, although this did not reach statistical significance (HF-n-3, $r = -0.34, F(1, 17)=2.2,$

$P=0.16$, male and female mice combined; HF-S, $r = -0.23$, $F(1, 18)=1.0$, $P=0.32$) (data not shown).

6.3.5.3 – *Hepatic Suppressor of Cytokine Signalling*

There was no effect of diet ($F(2, 58)=1.1$, $P=0.35$) on liver SOCS3 mRNA content (**Figure 6.12**). There was an effect of gender on hepatic SOCS3 mRNA content, male mice exhibited greater SOCS3 mRNA than female mice (+24%; $F(1, 58)=4.6$, $P=0.036$).

In the HF-S, but not HF-n-3, group, there was a significant positive correlation between the mRNA content of SOCS3 in the liver and the plasma concentration of glucose (HF-S, $r = +0.58$, $F(1, 20)=10.2$, $P=0.005$, male and female mice combined; HF-n-3, $r = -0.34$, $F(1, 17)=2.1$, $P=0.16$) (**Figure 6.13**).

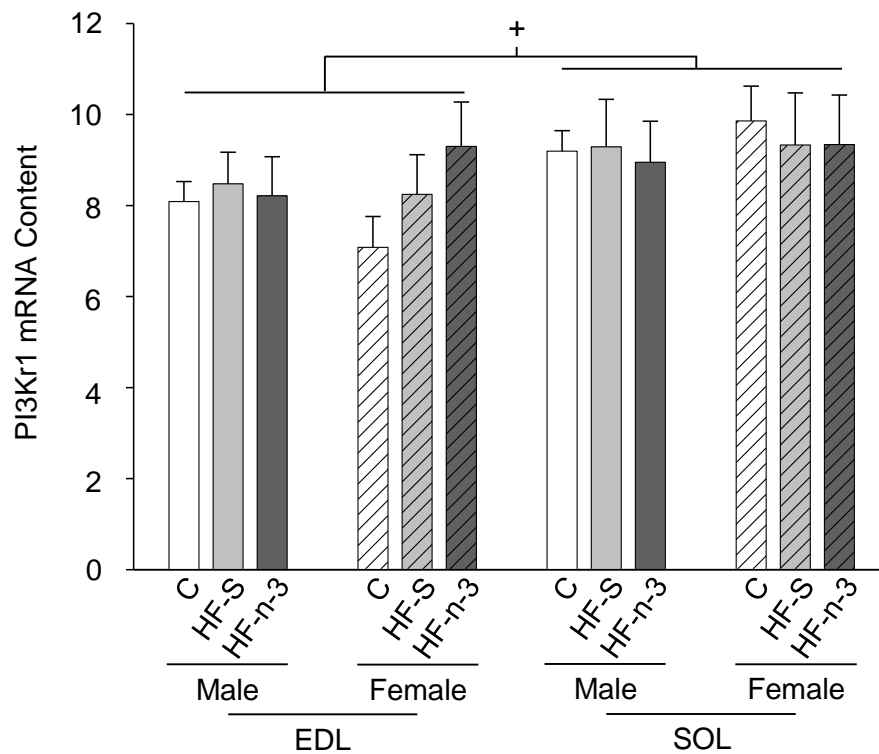


Figure 6.9. PI3Kr1 mRNA content in the white extensor digitorum longus and red soleus muscles of male and female mice fed control, high saturated fat or high fat n-3 PUFA enriched diets.

Data are expressed as mean (bars) \pm SEM (error bars), where solid bars indicate male (M) mice, lined bars indicate female (F) mice and colour represents diet: white, control (C); pale grey, high saturated fat (HF-S); dark grey, high fat n-3 polyunsaturated fatty acid enriched (HF-n-3). EDL, extensor digitorum longus muscle; SOL, soleus muscle; PI3Kr1, phosphatidylinositol 3-kinase, regulatory subunit, polypeptide 1.

n: EDL - C(M/F) = 10/12, HF-S(M/F) = 11/11, HF-n-3(M/F) = 9/11;

n: SOL - C(M/F) = 10/12, HF-S(M/F) = 10/10, HF-n-3(M/F) = 9/11.

Statistics: Effect of muscle fibre type: $^+P \leq 0.05$, SOL compared to EDL.

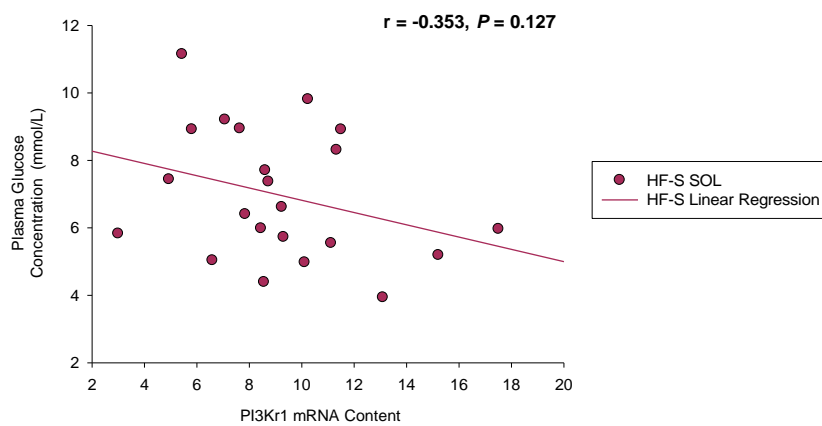


Figure 6.10. Relationship between the plasma glucose concentration and mRNA content of PI3Kr1 in the soleus muscle of mice exposed to a high saturated fat diet.

Symbol type represents dietary group and muscle type: see legend. HF-S, high saturated fat diet; SOL, soleus muscle; PI3Kr1, phosphatidylinositol 3-kinase, regulatory subunit, polypeptide 1. HF-S $n = 22$.

There was a negative relationship between the PI3Kr1 mRNA content in the soleus muscle and plasma concentration of glucose in the HF-S group (male and female mice combined).

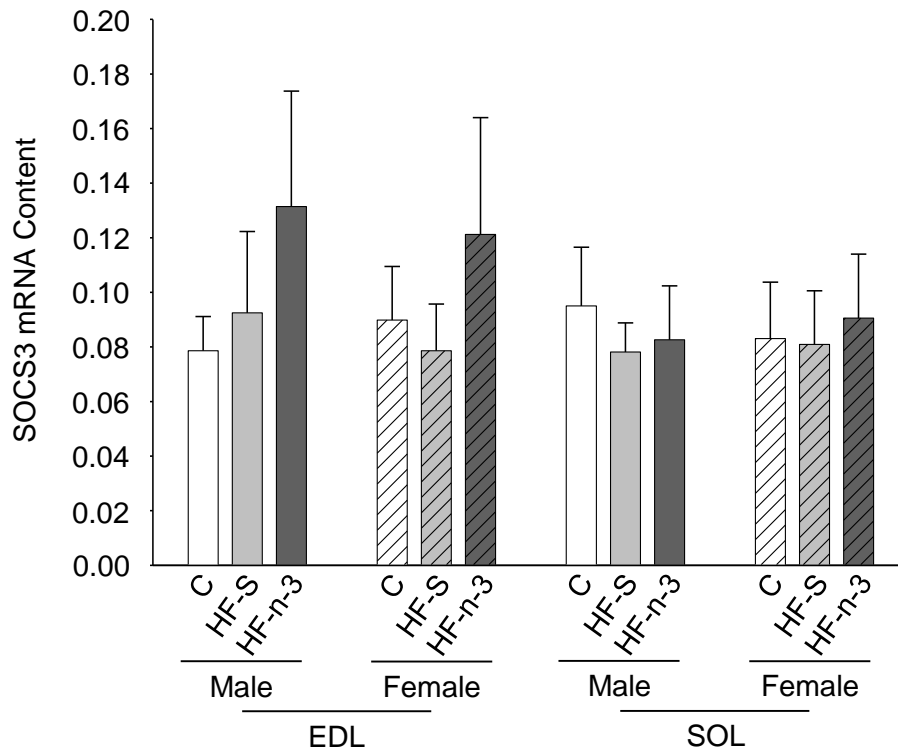


Figure 6.11. SOCS3 mRNA content in the white extensor digitorum longus and red soleus muscles of male and female mice fed control, high saturated fat or high fat n-3 PUFA enriched diets.

Data are expressed as mean (bars) \pm SEM (error bars), where solid bars indicate male (M) mice, lined bars indicate female (F) mice and colour represents diet: white, control (C); pale grey, high saturated fat (HF-S); dark grey, high fat n-3 polyunsaturated fatty acid enriched (HF-n-3). EDL, extensor digitorum longus muscle; SOL, soleus muscle; SOCS3, suppressor of cytokine signalling 3.

n: EDL - C(M/F) = 10/12, HF-S(M/F) = 11/11, HF-n-3(M/F) = 9/10;

n: SOL - C(M/F) = 10/12, HF-S(M/F) = 10/10, HF-n-3(M/F) = 9/11.

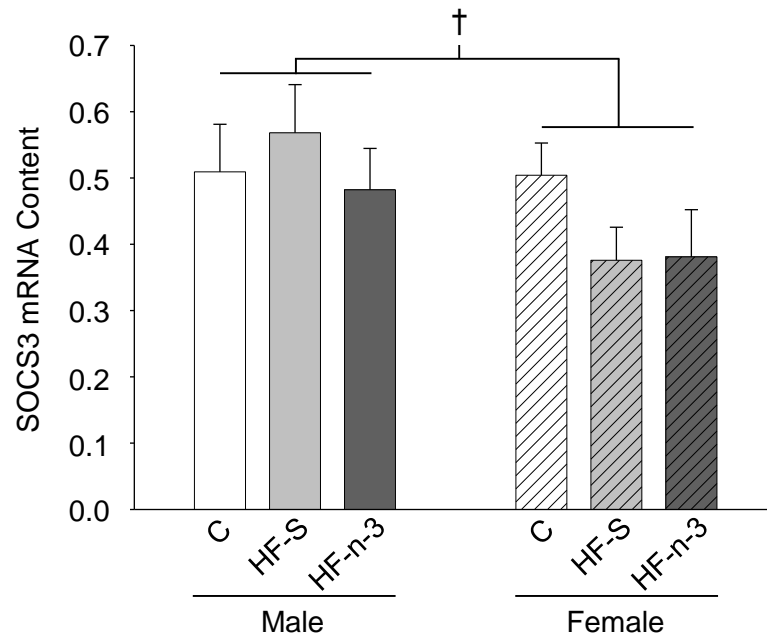


Figure 6.12. SOCS3 mRNA content in the liver of male and female mice fed control, high saturated fat or high fat n-3 PUFA enriched diets.

Data are expressed as mean (bars) \pm SEM (error bars), where solid bars indicate male (M) mice, lined bars indicate female (F) mice and colour represents diet: white, control (C); pale grey, high saturated fat (HF-S); dark grey, high fat n-3 polyunsaturated fatty acid enriched (HF-n-3). SOCS3, suppressor of cytokine signalling 3.

n: C(M/F) = 10/12, HF-S(M/F) = 11/11, HF-n-3(M/F) = 9/11.

Statistics: Effect of gender: $^{\dagger}P \leq 0.05$, male compared to female.

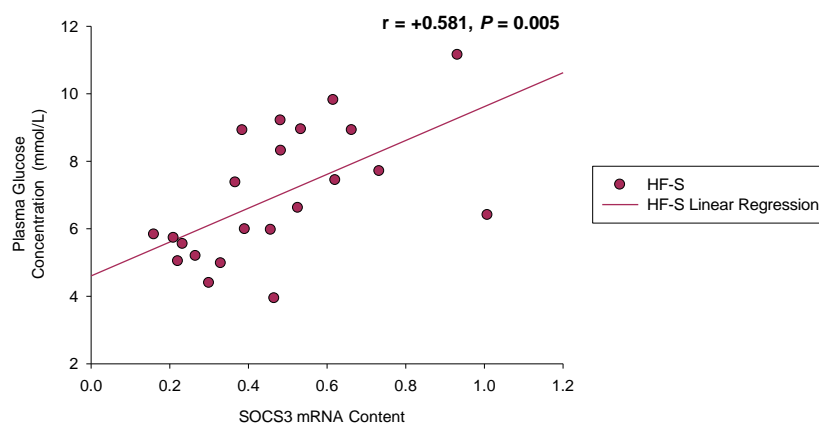


Figure 6.13. Correlation between hepatic SOCS3 mRNA content and the plasma concentration of glucose in mice exposed to a high saturated fat diet.

Symbol type represents dietary group: see legend. HF-S, high saturated fat diet; SOCS3, suppressor of cytokine signalling 3. HF-S $n = 22$.

There was a significant positive relationship between the SOCS3 mRNA content in the liver and the plasma glucose concentration in HF-S mice (male and female mice combined).

6.4 – DISCUSSION

Enrichment of a HFD with n-3 PUFAs has been shown to prevent the HFD-induced decline in whole-body and peripheral insulin sensitivity (Storlien *et al.*, 1987). The current study illustrates, through mRNA content analyses of key pathways of glucose metabolism, that n-3 PUFA enrichment of a HF-S diet prevents the HF-S-induced reduction in glycogen phosphorylation in skeletal muscle and this may result in enhanced oxidative disposal of glucose. Whilst n-3 PUFA enrichment of a HF-S diet may inhibit glucose phosphorylation in the liver and may prevent the hepatic synthesis of endogenous glucose and although less glucose is phosphorylated, the predominant metabolic pathway for the phosphorylated fraction is most likely glycolysis.

6.4.1 – Effect of Dietary Fatty Acid Composition on Skeletal Muscle Glucose Metabolism

6.4.1.1 – Glucose Phosphorylation – Committing to Glucose Metabolism

Following the uptake of glucose into the muscle cell, HK2 catalyses the rapid and irreversible phosphorylation of glucose, forming glucose-6-phosphate (Elliott and Elliott, 2001) which is the substrate for subsequent non-oxidative glucose metabolism, glycogen synthesis, or oxidative glycolysis (Pehleman *et al.*, 2005). Previous studies have reported that the skeletal muscle expression and activity of HK2 are unchanged by obesity (Ducluzeau *et al.*, 2001; Kim *et al.*, 2000; Kruszynska *et al.*, 1998). The current study demonstrates that HF-S feeding suppresses the mRNA content of HK2 in the EDL muscle; to my knowledge this has not previously been described.

Research by Ivy and colleagues (Ivy *et al.*, 1986), also conducted in rodents, showed that HF-S feeding induced a reduction in HK activity in the gastrocnemius muscles, although this failed to reach statistical significance in their study. Insulin treatment is known to induce HK2 mRNA transcription *in vitro* in adipose tissue (3T3-F442A, BFC-1B) and skeletal muscle (C2C12, L6) cell lines (Printz *et al.*, 1993). Furthermore, Printz and colleagues (Printz *et al.*, 1993) demonstrated that HK2 mRNA content was reduced in the adipose tissue from diabetic rats, but was restored to normal levels upon insulin supplementation. Similarly, Da Silva and colleagues (Da Silva *et al.*, 2010) showed HK2 activity is significantly decreased in the skeletal muscle, liver and adipose tissue of streptozotocin-treated diabetic mice. The observation that HK2 is suppressed in conditions of pronounced insulin resistance (Da Silva *et al.*, 2010; Ducluzeau *et al.*, 2001; Kruszynska *et al.*, 1998) may indicate that HF-S mice in the current study exhibit reduced insulin sensitivity, and the elevated plasma insulin levels of HF-S mice support this notion.

In accordance with the theory of the Randle cycle (Randle *et al.*, 1963), reduced oxidative disposal of glucose, as a result of pyruvate dehydrogenase kinase 4 (PDK4) activation, may lead to inhibition of HK2 due to inadequate disposal of glucose-6-phosphate (Roden, 2004). The suppression of HK2 expression by HF-S feeding is therefore consistent with the increased PDK4 mRNA content observed in the HF-S group (**Chapter 4**). The suppression of the oxidative disposal of glucose in skeletal muscle may therefore contribute to the development of hyperglycaemia in HF-S mice. The positive correlation between HK2 mRNA content in the EDL muscle and liver

glycogen and fat content in the HF-S group suggests that greater glucose uptake into the liver may compensate for reduced glucose phosphorylation in skeletal muscle. Consistent with this notion that the liver compensates for a lack of glucose phosphorylation in the skeletal muscle, insulin resistant obese subjects exposed to a 5 day “Western” HFD exhibit a marked increase in hepatic *de novo* lipogenesis (Schwarz *et al.*, 2003). Although in the current study the carbohydrate content of the HFDs was low (~21.2% of energy), the failure to oxidise glucose in skeletal muscle and the limited capacity for glycogen storage in the liver, may lead to surplus glucose being converted to fat for storage in an attempt to clear elevated circulating glucose. The observation that plasma glucose levels were not elevated in HF-S-fed mice together with a marked increase in liver fat content may therefore support a role for hepatic *de novo* lipogenesis in the current study. Interestingly, in female HF-S mice, the plasma glucose level appeared to be even lower than control levels, and the significantly higher hepatic fat content is consistent with the aforementioned notion.

In contrast to HF-S feeding, few studies have investigated the effect of HF-n-3 feeding on the expression or activity of HK2. In a rodent model, high sucrose feeding for 6 months followed by consumption of the sucrose diet supplemented with fish oil for 2 months ameliorated the high sucrose-induced reduction in HK2 activity in cardiac muscle (D'Alessandro *et al.*, 2008). Despite the very obvious dietary differences between the current study and that of D'Alessandro and colleagues (D'Alessandro *et al.*, 2008), both HF-S and high sucrose rodent models exhibit dyslipidaemia and reduced insulin sensitivity, that was ameliorated by fish oil supplementation. Both studies also consistently demonstrate that replacement of ~7% of dietary fat with fish

oil prevents suppression of HK2 (D'Alessandro *et al.*, 2008). Research has demonstrated that activation of AMP-activated protein kinase (AMPK) by 5-aminoimidazole-4-carboxamide-1- β -D-ribofuranoside (AICAR) stimulates an increase in HK2 mRNA in skeletal muscle (Leick *et al.*, 2010). However, AMPK activated by AICAR also synergistically acts with fatty acids to enhance PDK4 expression (Houten *et al.*, 2009). Therefore AMPK allows the simultaneous oxidation of fatty acids and uptake of glucose in skeletal muscle (Winder and Hardie, 1999) and may be involved in the upregulation of PDK4 (**Chapter 4**) and prevention of HFD-induced HK2 suppression with HF-n-3 feeding.

6.4.1.2 – Glycolysis

PFK is one of the key rate-limiting enzymes involved in controlling glycolysis (Ristow *et al.*, 1997; Dunaway *et al.*, 1988), catalysing the first committing reaction in the glycolytic pathway (Elliott and Elliott, 2001). In the current study, the absence of an effect of HF-S feeding on PFK-M mRNA expression is in accordance with previous reports that demonstrated PFK activity was unchanged by high fat consumption in rodent and equine skeletal muscle (Dourmashkin *et al.*, 2005; Geelen *et al.*, 2001; Kern *et al.*, 1990). In contrast, acute exposure to a HFD has been shown to suppress PFK activity in the skeletal muscle of rodents (Kim *et al.*, 1996; Nemeth *et al.*, 1992). However, this acute response was diminished following 3 weeks HFD, by which time there was no significant decrease in PFK-M in rodent skeletal muscle (Nemeth *et al.*, 1992). Despite unchanged muscle PFK-M expression or activity, research has shown that the whole-body rate of glycolysis is reduced by high fat feeding shortening in rats

(Kim *et al.*, 2000). In the current study, given that HK2 was suppressed by HF-S feeding, it is possible that there is lower phosphorylation of glucose. Furthermore, given that PDK4 was induced by HFD consumption in the present study, citrate may accumulate as a result of inactivation of pyruvate dehydrogenase by increased PDK4 (**Chapter 4**). In combination this may lead to the inhibition of PFK-M activity and hence impaired glycolysis in HF-S-fed mice.

Enriching the HFD with n-3 PUFAs had no effect on skeletal muscle PFK-M mRNA content in the current study. Although few studies have determined the direct effect of HF-n-3 feeding on PFK, Higuchi and colleagues (Higuchi *et al.*, 2008) showed that fish oil supplemented into a low fat lard diet did not significantly alter PFK activity in skeletal muscle. Sato and associates (Sato *et al.*, 2010) demonstrated that eicosapentaenoic acid (EPA) enrichment of a high fat-high sucrose diet had no influence on PFK-M mRNA expression in skeletal muscle. Rustan and colleagues (Rustan *et al.*, 1993) showed that the substrate utilisation of glucose was significantly increased in HF-n-3-fed rats compared to rats fed a HFD of lard. The reduction in muscle glycogen (**Chapter 3**) and unchanged plasma glucose levels (**Chapter 2**) observed in HF-n-3 mice are consistent with the notion of greater glucose use in skeletal muscle with HF-n-3 feeding. However, PDK4 mRNA expression was also induced by HF-n-3 feeding (**Chapter 4**), and as a result of increased citrate, produced from fatty acid oxidation, it may feedback to inhibit PFK activity (Randle, 1998; Ramadoss *et al.*, 1976). However, AMPK activation has been shown to produce a modest increase in PFK-M activity in skeletal muscle (Putman *et al.*, 2003) and as

previously described AMPK activation also enhances PDK4 expression (Houten *et al.*, 2009). Although in the current study the activity of AMPK was not measured, PDK4 mRNA expression was increased. Therefore it is possible that through this mechanism, glycolysis may occur alongside fatty acid oxidation in HF-n-3 mice.

6.4.1.3 – Glycogenesis

Several studies have demonstrated differential effects of high fat feeding on skeletal muscle glycogen content and glycogen synthesis. Some studies have provided evidence for a reduced rate of glycogen synthesis (Yaspelkis *et al.*, 2004; Kim *et al.*, 2000) whereas most other studies have found that HF-S feeding has no influence on glycogen storage (Kuda *et al.*, 2009; Rokling-Andersen *et al.*, 2009; Tanaka *et al.*, 2007; Yaspelkis *et al.*, 2004; Helge *et al.*, 1998) or GYS activity (Yaspelkis *et al.*, 2004; Huang *et al.*, 2003; Kim *et al.*, 2000; Helge *et al.*, 1998) in skeletal muscle. Furthermore, Huang and colleagues (Huang *et al.*, 2003), following exposure to a HFD, demonstrated neither GYS activity nor GYS mRNA expression is changed in the skeletal muscle of C57BL/6 mice. The findings of this study, that HF-S feeding had no effect on skeletal muscle glycogen content (**Chapter 3**), nor did it alter the mRNA content of GYS1 in skeletal muscle, are consistent with the aforementioned studies.

Previous studies have reported that muscle glycogen content is reduced (Rustan *et al.*, 1993) or tends to be reduced (Rokling-Andersen *et al.*, 2009) with HF-n-3 feeding in rodents. In accordance with these reports, there was, in the current study, a tendency for reduced glycogen storage with HF-n-3 feeding (**Chapter 3**), despite having no effect

on the muscle mRNA content of GYS1. In contrast, Kuda and colleagues (Kuda *et al.*, 2009) demonstrated that muscle glycogen content was unchanged in the skeletal muscle of mice fed a HFD supplemented with EPA and docosahexaenoic acid (DHA) concentrate, despite also showing that GYS1 mRNA tended to be lower in these mice. Taken together, these data suggest that n-3 PUFAs may alter non-oxidative glucose metabolism, and it is possible that this is a consequence of reduced glycogen synthesis activity, as EPA suppresses both basal and insulin-stimulated glycogen synthesis in differentiated myotubes *in vitro* (Aas *et al.*, 2006). AMPK phosphorylates and deactivates the GYS enzyme (Jørgensen *et al.*, 2004; Carling and Hardie, 1989) and reduced skeletal muscle glycogen content has been observed to occur in association with increased AMPK activation (Sibut *et al.*, 2008). Therefore activation of AMPK may be implicated in the reduced glycogen content observed in the current study, without directly affecting GYS1 at the mRNA level, but by influencing GYS1 protein deactivation, although this remains to be tested.

6.4.1.4 – Influencing Insulin Signalling

The abundance of the PI3K regulatory subunit has been reported to be reduced in skeletal muscle of obese insulin resistant humans (Goodyear *et al.*, 1995), although the mRNA expression of the PI3K regulatory subunit is unaffected by obesity or type 2 diabetes mellitus (Andreelli *et al.*, 1999). Similarly, in the present study, all dietary groups exhibited similar PI3Kr1 mRNA expression, despite their apparent differences in insulin sensitivity. These data are also consistent with research that has demonstrated the protein abundance of the PI3K regulatory subunit is unchanged with

HF-S feeding (Cresser *et al.*, 2010) and the activity of PI3K to be similar with HF-n-3 feeding (Taouis *et al.*, 2002), in rat skeletal muscle when compared to high carbohydrate-fed animals. It has also been shown that in the liver the PI3K and the PI3K regulatory subunit exhibit comparable mRNA expression in lard-fed, fish oil-fed or high carbohydrate-fed rats (Buettner *et al.*, 2006). Despite the absence of a dietary effect on PI3K α mRNA content, reduced PI3K α mRNA in the soleus muscle tended to be associated with increased plasma glucose concentrations in HF-S, but not HF-n-3, mice, which suggests that PI3K α may be implicated in the apparent reduction in insulin sensitivity in the HF-S group.

The transcription factor, SOCS3, is induced by proinflammatory cytokines and in turn controls cytokine signalling through the Janus kinase/signal transducer and activation of transcription (JAK/STAT) pathway (Sachithanandan *et al.*, 2010). The skeletal muscle mRNA expression of SOCS3 is affected by insulin sensitivity; in non-diabetic obese humans SOCS3 mRNA is reduced, but in type 2 diabetics SOCS3 mRNA is markedly upregulated and is inversely related to insulin-stimulated glucose uptake (Rieusset *et al.*, 2004). However, in the current study, SOCS3 mRNA content was highly variable in the skeletal muscle and was not significantly different between the dietary groups or between muscle fibre types. This is in contrast to the findings of Steinberg and colleagues (Steinberg *et al.*, 2004) and Yaspelkis III and associates (Yaspelkis *et al.*, 2009) which showed that SOCS3 mRNA and protein (respectively) were increased by HFD consumption in rats. However, the aforementioned studies were conducted in rodents fed HFDs of safflower oil (PUFA-rich) (Steinberg *et al.*, 2004) and coconut oil (medium chain saturated fat-rich) (Yaspelkis *et al.*, 2009), and

they differ to studies conducted in rodents fed a HF-S diet of lard (Mullen *et al.*, 2010; Kleemann *et al.*, 2010). As in the current study, Mullen *et al.* (Mullen *et al.*, 2010) showed that HF-S feeding rats had no influence on SOCS3 protein abundance, and they also demonstrated that PUFA-rich safflower oil did not affect SOCS3 protein abundance, contrasting with Steinberg and associates' (Steinberg *et al.*, 2004) work. The disparities indicated in studies using safflower oil-rich diets may be the consequence of dietary time course (3 days (Mullen *et al.*, 2010) vs. 4 weeks (Steinberg *et al.*, 2004)). In contrast, lard feeding consistently had no effect on SOCS3 irrespective of dietary time course (Kleemann *et al.*, 2010; Mullen *et al.*, 2010), as Kleemann and associates (Kleemann *et al.*, 2010) followed animals for a duration comparable to the current study, and they similarly demonstrated no change in skeletal muscle SOCS3 protein with HF-S feeding.

As far as can be determined, no study has investigated the effect of n-3 PUFAs on SOCS3 mRNA expression in skeletal muscle, although a study in adipocytes revealed a dose-responsive increase in SOCS3 mRNA following exposure to DHA, but not palmitate (Bradley *et al.*, 2008). In the current study SOCS3 mRNA exhibited great variability, rendering what appeared to be an increase in SOCS3 mRNA in the EDL of HF-n-3 mice statistically insignificant. Despite this variability, there tended to be an inverse relationship between SOCS3 expression and plasma insulin levels in the HF-n-3 group. There are, however, some discrepancies in the literature surrounding the induction of SOCS3 and insulin sensitivity, as exercise training, known to induce insulin sensitivity in skeletal muscle, leads to enhanced SOCS3 mRNA in rodent muscle (Spangenburg *et al.*, 2006) and in obesity the upregulation of SOCS3 expression

in insulin sensitive tissues is associated with insulin resistance (Yaspelkis *et al.*, 2009; Steinberg *et al.*, 2004; Ueki *et al.*, 2004). Therefore further research is required to determine if HF-n-3 truly increases SOCS3 expression in skeletal muscle and the effect this has on insulin sensitivity.

6.4.2 – Effect of Dietary Fatty Acid Composition on Hepatic Glucose Metabolism

6.4.2.1 – Glucose Phosphorylation – Committing to Glucose Metabolism

In the current study, the HF-S diet was without affect on hepatic GCK mRNA content. In contrast a number of studies in rodents demonstrated an increase in hepatic GCK mRNA expression with HF-S feeding (Pérez-Echarri *et al.*, 2009a; Pérez-Echarri *et al.*, 2009b; Gorman *et al.*, 2008; Buettner *et al.*, 2006). A diet with a modest increase in tallow induced a small, but insignificant increase in hepatic GCK activity (Toussant *et al.*, 1981). Other studies, for example, Kim and associates (Kim *et al.*, 2010) demonstrated that hepatic GCK activity was similar in high carbohydrate-fed and HFD-fed mice. Furthermore Commerford and colleagues (Commerford *et al.*, 2002) reported unchanged GCK activity in the isolated hepatocytes of high fat-fed rats under both low and high glucose conditions. Commerford and colleagues (Commerford *et al.*, 2002) did, however, demonstrate that when exposed to high concentrations of insulin and glucose, insulin failed to stimulate the translocation of hepatic GCK *in vitro*. In the context of the current study, it is therefore possible that elevated insulin levels in the HF-S group may prevent the induction of GCK expression and may lead to less effective GCK activation. However, plasma glucose levels were not significantly elevated, suggesting that hepatic GCK activity may remain intact, although not measured

in the current study, and may possibly act to increase hepatic glucose uptake in lieu of reduced skeletal muscle glucose phosphorylation (**Chapter 6 Section 4.1.1**).

The n-3 PUFA-induced suppression of hepatic GCK mRNA expression in the present study has similarly been demonstrated previously (Pérez-Echarri *et al.*, 2009a; Pérez-Echarri *et al.*, 2009b; Toussant *et al.*, 1981; Jump *et al.*, 1994). Rats fed a high carbohydrate diet enriched with n-3 PUFA-rich menhaden oil exhibit lower liver GCK mRNA content than those rats supplemented with monounsaturated fatty acids (Jump *et al.*, 1994). Furthermore, exposure to EPA ethyl ester significantly reduced GCK activity in the liver of high carbohydrate-fed rats (Pérez-Echarri *et al.*, 2009a) but failed to produce a significant reduction, despite a small decrease, in hepatic GCK activity in HFD-fed overweight rats (Pérez-Echarri *et al.*, 2009a; Pérez-Echarri *et al.*, 2009b). As previously described, n-3 PUFAs are a natural ligand for peroxisome proliferator activator receptor α (PPAR α), and given that 3 weeks exposure to PPAR α agonist, clofibrate, suppresses GCK activity in both high carbohydrate- and HFD-fed rats (Gustafson *et al.*, 2002), PPAR α activation may be involved in the n-3 PUFA-mediated suppression of GCK mRNA in the current study. In **Chapter 5** it was speculated that AMPK may be activated by n-3 PUFAs in the livers of HF-n-3 mice, and this may therefore be involved in the suppression of GCK, as AMPK activation prevents glucose-stimulated translocation of GCK (Mukhtar *et al.*, 2008). However, the activity of AMPK was not investigated in the current study.

Although the mechanism behind HF-n-3-induced suppression of GCK requires further investigation, reduced GCK expression may prevent glucose from entering the liver, as

demonstrated in the reduced liver glucose concentrations in HF-n-3-fed mice (**Chapter 2**). This may prevent glucose acting as a substrate for fat synthesis through hepatic *de novo* lipogenesis and therefore the reduction in GCK mRNA may ultimately contribute, in part, to the amelioration of HF-S-induced fatty liver in HF-n-3 mice.

6.4.2.2 – Glycolysis

The observation that PFK-L was unchanged in the liver of HF-S mice is consistent with research conducted by Buettner and colleagues (Buettner *et al.*, 2006) in rats fed a HF-S diet of lard or coconut oil. Unlike GCK that may function defectively as a consequence of insulin resistance, PFK-L mRNA is neither influenced by the insulin resistant diabetic phenotype nor by insulin administration (Hotta *et al.*, 1991). The contribution that PFK-L makes to glycolysis in the current study is therefore unknown. However, HF-S feeding produced a marked increase in liver glycogen content, compared to control mice that had a much higher carbohydrate intake (**Chapter 2**), which may suggest glycogen synthesis, but not glycolysis, is the major pathway of glucose metabolism favoured in HF-S mice.

This study, in contrast to other studies which showed that dietary fish oil supplementation had no influence on PFK-L mRNA expression or activity in the liver (Higuchi *et al.*, 2008; Buettner *et al.*, 2006), demonstrated that replacing 7.5% of saturated fat in the HF-S diet with n-3 PUFAs significantly increased hepatic PFK-L mRNA content, this was associated with a tendency for reduced plasma glucose concentrations. Rustan and colleagues (Rustan *et al.*, 1993) demonstrated that replacing 6.5% lard with EPA and DHA ethyl ester concentrate in a HFD induced the

utilisation of carbohydrate as a substrate. This may suggest that despite a reduction in glucose phosphorylation with HF-n-3 feeding, the circulating glucose that does enter the liver enters pathways of oxidative glucose metabolism, and this may be partly reflected in the reduced liver glucose content in HF-n-3 mice (**Chapter 2**). Furthermore, the increase in PFK-L in the current study is therefore consistent with this notion.

6.4.2.3 – Glycogenesis

In the current study, hepatic GYS2 mRNA content was unchanged and glycogen content increased (**Chapter 2**) with HF-S feeding. In contrast, rats fed a saturated fat-rich lard or coconut oil HFD displayed lower hepatic GYS mRNA expression as compared to high carbohydrate-fed controls (Buettner *et al.*, 2006) and in another study, HF-S feeding reduced liver glycogen content (Helge *et al.*, 1998). In type 2 diabetics, liver glycogen levels decrease prior to a meal (during fasting) but are significantly increased in the postprandial-state as compared to healthy controls (Krssak *et al.*, 2004). Therefore the discrepancies observed in the aforementioned studies may reflect the differences in fasting and feeding on measures of glycogen metabolism. The current study was conducted in the fed-state, whereas in previously reported studies, livers were collected following a 5-6 hour (Helge *et al.*, 1998) or 16 hour fast (Buettner *et al.*, 2006).

The HF-n-3-induced reduction in liver glycogen content, compared to HF-S-fed mice, as reported in **Chapter 2**, is consistent with previous studies in rodents (Holness *et al.*, 2003; Rustan *et al.*, 1993), and most likely is a consequence of phosphorylation and

deactivation of GYS2 (Villar-Palasi and Guinovart, 1997); although GYS2 mRNA did not change. In the liver, glucose-6-phosphate acts to potently activate GYS2 (Villar-Palasi and Guinovart, 1997; Gilboe and Nuttall, 1982) and hepatic GCK has been demonstrated to produce a pool of glucose-6-phosphate that specifically activates GYS2 (Gomis *et al.*, 2002). Therefore the reduction in GCK mRNA in the livers of HF-n-3 mice may lead to lower concentrations of glucose-6-phosphate and hence less activation of GYS2.

6.4.2.4 – Gluconeogenesis

The observation that PEPCK mRNA content was unchanged by HF-S feeding, given that PEPCK is regulated at the level of gene transcription (Murakami *et al.*, 2010; Shao *et al.*, 2005), suggests that HF-S mice exhibit a similar level of gluconeogenesis to mice fed a high carbohydrate diet. In another study, HF-S feeding lard also had no influence on PEPCK mRNA in the rat liver and their model similarly developed signs of insulin resistance with elevated plasma insulin concentrations, elevated HOMA-index and less efficient insulin-stimulated glucose disposal (Buettner *et al.*, 2006). This is also consistent with another study performed in HFD-fed streptozotocin-treated diabetic rats, in which PEPCK mRNA and protein were unchanged despite increased rates of endogenous glucose production (Samuel *et al.*, 2009). In contrast, the HF-n-3-induced suppression of PEPCK mRNA in the current study is inconsistent with previous work (Buettner *et al.*, 2006) in which hepatic PEPCK expression was unchanged by HF-n-3 feeding. However, research has demonstrated that dietary supplementation with n-3 PUFA-rich menhaden oil leads to a slight, but insignificant, reduction in hepatic PEPCK

gene transcription activity, compared to dietary enrichment with saturated fat-rich tripalmitin (Blake and Clarke, 1990). Also consistent with the present study, dietary supplementation with EPA, DHA, a mix of EPA and DHA or fish oil significantly suppresses PEPCCK in the retroperitoneal fat pad, but not subcutaneous adipose depot (Raclot *et al.*, 1997). The reason for these discrepancies is unknown, although, in the liver, peroxisome proliferative activated receptor γ coactivator 1 (PGC1) co-activates the transcription of PEPCCK mRNA expression and this transcription is inhibited by AMPK activation (Viollet *et al.*, 2006; Foretz *et al.*, 2005). Therefore AMPK may be implicated in the reduction in PEPCCK mRNA in the current study and although dietary enrichment with n-3 PUFAs did not influence the hepatic expression of AMPK α 1 or AMPK α 2 mRNA (**Chapter 5**), research has demonstrated that n-3 PUFAs were able to enhance hepatic AMPK activity in the fed-state without altering the content of the AMPK α 1 or AMPK α 2 subunits at the level of expression (Suchankova *et al.*, 2005). Given that recent research supports a role for AMPK α 2 in mediating the prevention of hepatic insulin resistance by n-3 PUFAs (Jelenik *et al.*, 2010), the suppression of gluconeogenesis may contribute to improved insulin sensitivity elicited by dietary n-3 PUFA enrichment.

6.4.2.5 – *Insulin Signalling*

As in the skeletal muscle, SOCS3 mRNA also showed considerable variability in the liver. There is some evidence from previous research that the mRNA and protein contents of SOCS3 are upregulated in the liver of rodents by high fat overfeeding (Sachithanandan *et al.*, 2010; Barbuio *et al.*, 2007), although in response to lard feeding

rodents for a duration similar to the current study, hepatic SOCS3 protein was unchanged (Kleemann *et al.*, 2010). Moreover there is no effect of variation in insulin sensitivity in mice on hepatic SOCS3 mRNA; C57BL/6J mice with HFD-induced obesity and insulin resistant db/db mice exhibited similar SOCS3 mRNA expression as compared to lean mice (Kanatani *et al.*, 2007).

Liver-specific deletion of SOCS3, however, results in fasting hyperglycaemia and hyperinsulinemia when mice are exposed to high fat feeding (Sachithanandan *et al.*, 2010). In the current study there was a positive relationship between hepatic SOCS3 mRNA and plasma glucose levels in the HF-S group. It is possible that the key difference in these models may be related to the ceramide levels present in the liver, as research conducted by Yang and colleagues (Yang *et al.*, 2009) showed higher ceramide levels were associated with greater SOCS3 mRNA in the adipocytes of HFD-fed rodents and blocking *de novo* ceramide synthesis resulted in a striking reduction in adipose tissue SOCS3 mRNA expression. Sachithanandan and colleagues (Sachithanandan *et al.*, 2010) liver-specific SOCS3 knockout model developed fatty liver without increased ceramide concentrations. In contrast, enhanced ceramide concentrations in the liver have been identified in both genetically- (Turinsky *et al.*, 1990) and diet-induced (Chocian *et al.*, 2010) obese rodents. Therefore increased ceramide content may accompany fatty liver in the current study, which given ceramides proposed role in defective insulin sensitivity, may account for the relationship between higher plasma glucose and hepatic SOCS3 mRNA content.

As far as I can determine, no study has investigated the influence of n-3 PUFAs on hepatic SOCS3 mRNA. In the adipocyte, acute DHA exposure induces a dose-responsive increase in SOCS3 mRNA (Bradley *et al.*, 2008), but this was not true for SOCS3 mRNA content in the livers of mice fed a longer-term HF-n-3 diet in the current study. Given that HF-n-3 fed rodents exhibit reduced liver fat content in the current study (**Chapter 2**) and hepatic ceramide concentrations have in other HF-n-3 models been shown to be similar to lean control animals (Neschen *et al.*, 2002), SOCS3 is less likely to contribute to altered insulin sensitivity in HF-n-3- than HF-S-fed rodents.

6.4.3 – Effect of Muscle Fibre Type on Glucose Metabolism

It is well-understood that the profile of gene expression in skeletal muscle reflects the metabolic characteristics of its muscle fibre type composition. The observation that the FG-FOG EDL muscle exhibited greater mRNA content of glycolytic enzyme, PFK-M, is consistent with previous studies that have reported PFK-M to be greater in white muscle (Lawler *et al.*, 1993; Essén *et al.*, 1975) and in individual type II fibres, especially type IIB fibres, than type I fibres (Essén *et al.*, 1975). Furthermore, the observations that genes involved in glucose phosphorylation (HK2), glycogen synthesis (GYS1) and insulin signalling (PI3Kr1) were greater in the SO soleus muscle also agrees with previous reports (Azpiazu *et al.*, 2000; Song *et al.*, 1999; Lawrence and Trayer, 1985; Green *et al.*, 1983; Hintz *et al.*, 1980; Bocek and Beatty, 1966; Stubbs and Blanchaer, 1965). In combination these data reflect the greater intrinsic capacity of SO muscle for enhanced insulin sensitivity and responsiveness and glycogen synthesis

(James *et al.*, 1986) and the FG-FOG muscle for greater glycolytic flux.

6.4.4 – Effect of Gender on Glucose Metabolism

Female mice are less prone to developing a profile of impaired insulin sensitivity in response to greater fatty acid supply (Gómez-Pérez *et al.*, 2008; Hevener *et al.*, 2002). In **Chapter 2** it was suggested that the greater plasma glucose levels in male mice may predispose them to the development of HFD-induced impaired insulin sensitivity. It was also postulated that lower plasma glucose levels in females may arise from a greater capacity for glucose uptake in the peripheral tissues, and the increase in hepatic storage of glycogen observed in female mice was consistent with this notion (**Chapter 2**). However, it has been demonstrated in this chapter that males exhibited greater expression of genes influencing glucose phosphorylation (HK2) and glycolysis (PFK-M) in the skeletal muscle, and, in the liver, displayed greater expression of genes mediating glycogen synthesis (GYS2) and insulin signalling (SOCS3). Of all the genes observed to have gender-dimorphic expression, males demonstrated predominantly greater expression in contrast to females. The observations that male mice exhibit greater hepatic GCK and muscle HK2 are consistent with early studies that demonstrated hepatic GCK activity was increased in male rats (Teutsch and Lowry, 1982) and muscle HK activity was greater in male humans (Simoneau and Bouchard, 1989; Green *et al.*, 1984), when compared to females. An increased capacity for glycolysis has also been consistently demonstrated in the skeletal muscle of males (Jaworowski *et al.*, 2002; Simoneau and Bouchard, 1989; Green *et al.*, 1984). Given that the skeletal muscle is the chief mediator of insulin-stimulated glucose disposal, a

greater inherent capacity for glucose phosphorylation and its subsequent glycolysis, may reflect a greater requirement for these functions to maintain insulin sensitivity in healthy males. It is therefore possible that male mice may be more affected by the dysfunctional glucose phosphorylation and subsequent reduction in glucose metabolism that result from HF-S feeding, leading to reduced insulin sensitivity.

6.4.5 – Limitations

In the current chapter, the findings reported are the outcome of mRNA content analyses (due to time constraints), and whilst this provides useful information about the amount of gene transcribed, the study would have benefited from measuring the enzyme activity or protein abundance of the target genes also. Given the focus on fatty acid metabolism, this study provides a limited view on glucose metabolism, having chosen just one gene representing the major pathways of glucose metabolism in skeletal muscle and liver. Therefore expanding this study to investigate the effect of n-3 PUFA enrichment of a HF-S diet on more glucose metabolism genes may provide further evidence for altered glucose metabolism and insulin signalling, especially if genes influencing glucose uptake and insulin signalling were investigated. Furthermore for a more definitive investigation of the effect of dietary fat content on insulin resistance, this study would have benefited from using the hyperinsulinaemic euglycemic clamp technique, the gold-standard approach in measuring insulin sensitivity (DeFronzo *et al.*, 1979). However, the principle aim was to determine the mRNA content of a few key genes involved in the main regulatory pathways of glucose metabolism in skeletal muscle and liver. Therefore performing the hyperinsulinaemic euglycemic clamp

technique on this cohort of animals may have influenced the mRNA expression of key genes.

6.4.6 – Summary

In summary, this study provides some insight into the effect of dietary fatty acid composition on glucose metabolism in the skeletal muscle and liver. In this chapter it was demonstrated that n-3 PUFA enrichment of a HFD prevented the HF-S-induced suppression of HK2 in skeletal muscle; subsequently phosphorylated glucose may enter oxidative disposal, but is less likely to undergo non-oxidative disposal (**Figure 6.14**) and reduced muscle glycogen levels (**Chapter 3**) are consistent with this notion. It was also demonstrated that n-3 PUFA enrichment of a HFD reduced the phosphorylation of glucose in the liver and this was speculated to prevent *de novo* lipogenesis. Of the phosphorylated glucose entering glucose metabolism in the liver, the majority was most likely to undergo oxidative disposal, not glycogenesis (**Figure 6.15**). Furthermore, HF-n-3 feeding prevented *de novo* glucose synthesis in the liver. This study therefore provides evidence that n-3 PUFA enrichment of a HFD prevents the dysfunctional glucose metabolism and possibly insulin signalling observed with HF-S feeding, primarily by promoting glucose clearance.

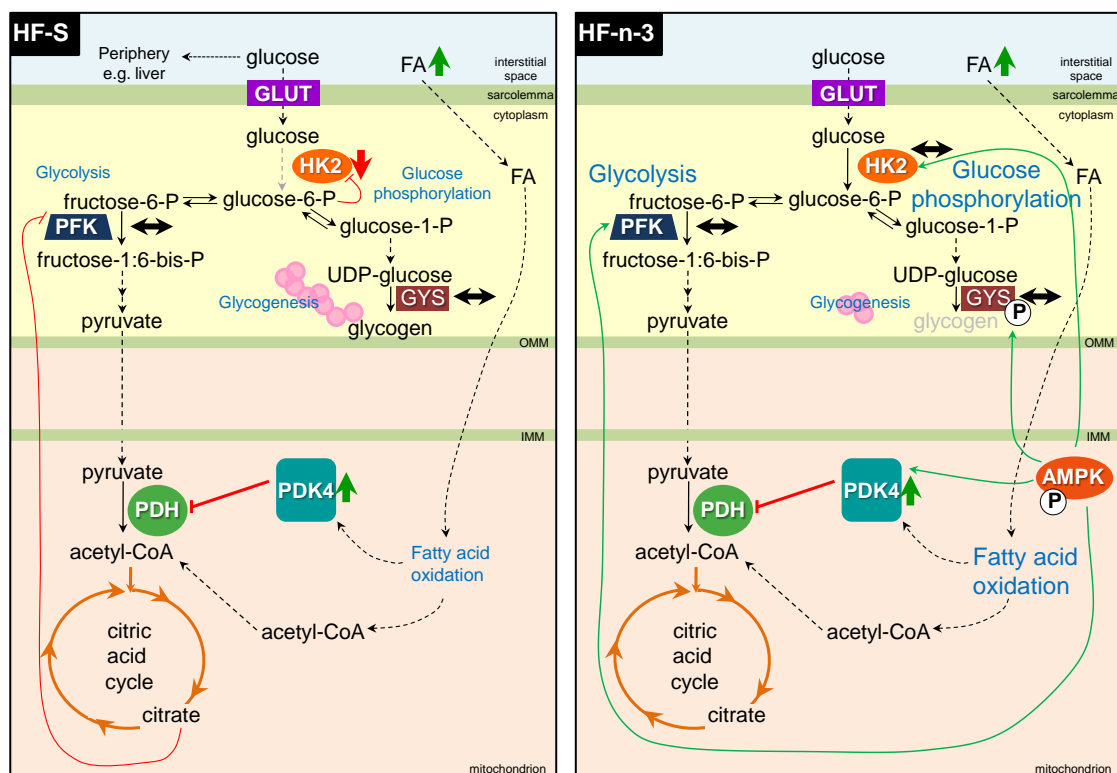


Figure 6.14. Schematic diagram depicting the mechanism behind the differential responses observed in pathways of skeletal muscle glucose metabolism with high saturated fat and high fat n-3 PUFA enriched diet feeding.

HF-S feeding leads to a reduction in HK2 mRNA, which reduces the amount of glucose that is phosphorylated and enters glucose metabolism. Muscle glycogen content in HF-S mice is similar to controls, suggesting this pathway is not altered. However, glycolysis may be inhibited by citrate due to PDH inactivation through increased PDK4. In combination, activated glucose-6-phosphate if not entering pathways of glucose metabolism may build up and through a feedback loop inhibit HK2 to reduce glucose phosphorylation. Lower HK2 was associated with increased liver glycogen and fat, suggesting glucose may be redirected to the liver for glycogen storage or to enter *de novo* lipogenesis. In contrast, HF-n-3 mice exhibit normal HK2, suggesting more glucose enters glucose metabolism in this group. Glycogen content was reduced, without altered GYS mRNA, but this may be a consequence of increased AMPK activity initiating the phosphorylation and deactivation of GYS protein. AMPK may also act to promote HK2 and PFK-M, preventing the PDK4-induced inhibition of glycolytic pathways; as a result glycolysis may be increased in HF-n-3 mice.

FA, fatty acid; PDH, pyruvate dehydrogenase; PDK4, pyruvate dehydrogenase kinase 4; GLUT, glucose transporter; PFK, phosphofructokinase; GYS, glycogen synthase; HK2, hexokinase 2; P, phosphate; AMPK, AMP activated protein kinase; IMM, inner mitochondrial membrane; OMM, outer mitochondrial membrane. Thick green arrow, increased; thin green arrow, activates, red line, inhibits; red cross, pathway reduced; thick black double-ended arrow, unchanged.

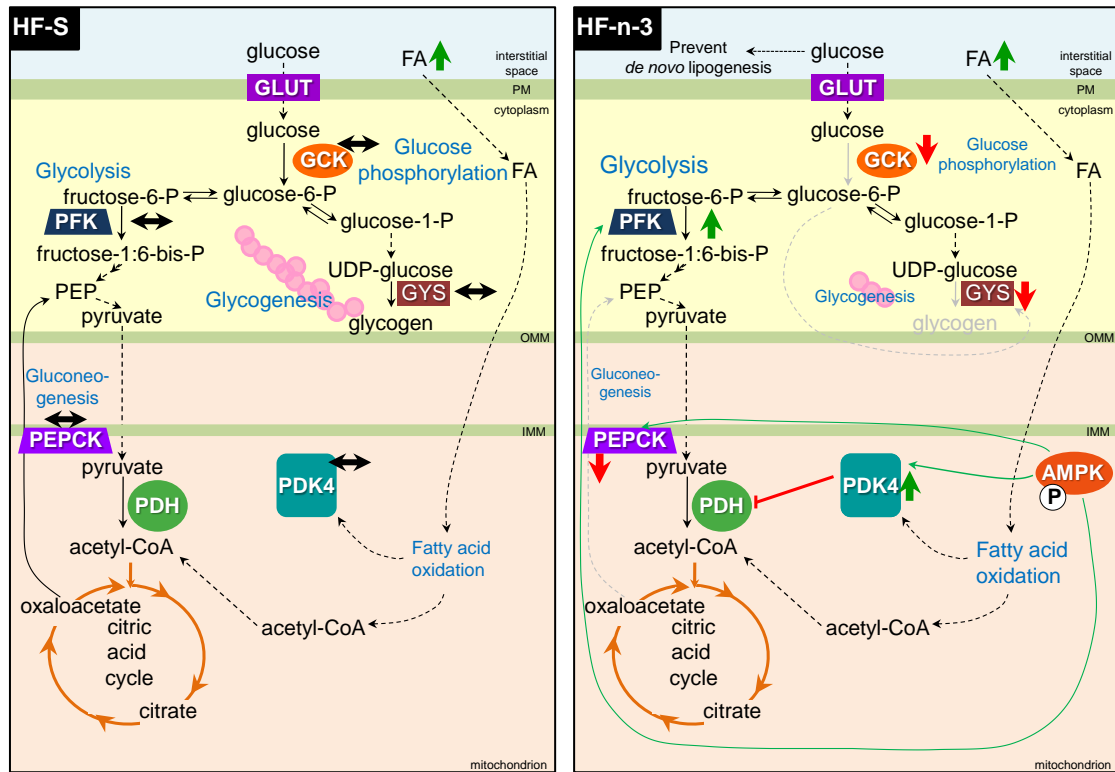


Figure 6.15. Schematic diagram depicting the mechanism behind the differential responses observed in pathways of hepatic glucose metabolism with high saturated fat and high fat n-3 PUFA enriched diet feeding.

HF-S feeding has no influence on the mRNA content of GCK, PFK, PEPCK or PDK4 mRNA, therefore glucose metabolism may not play a major role in the HF-S liver. Despite unchanged GYS, glycogen content was increased, suggesting the major pathway of hepatic glucose metabolism in HF-S mice is non-oxidative. In contrast, GCK mRNA was reduced in HF-n-3 mice; this may play a protective role in preventing glucose being converted to fatty acid through *de novo* lipogenesis. The glucose that is phosphorylated appears not to enter glycogen storage, as GYS mRNA and glycogen content were reduced. Glycolysis, however, appears to play a greater role in HF-n-3 fed mice, with increased PFK mRNA, possibly the result of AMPK activation. PEPCK mRNA was reduced, suggesting a lower role for gluconeogenesis in HF-n-3 livers.

FA, fatty acid; CoA, Coenzyme A; PDH, pyruvate dehydrogenase; PDK4, pyruvate dehydrogenase kinase 4; GLUT, glucose transporter; PFK, phosphofructokinase; GYS, glycogen synthase; GCK, glucokinase; P, phosphate; AMPK, AMP activated protein kinase; PEPCK, phosphoenolpyruvate carboxykinase; IMM, inner mitochondrial membrane; PM, plasma membrane; OMM, outer mitochondrial membrane. Thick green arrow, increased; thin green arrow, activates, red line, inhibits; red cross, pathway reduced; thick black double-ended arrow, unchanged.

CHAPTER 7

*Summary of Findings, Implications and
Future Studies*

7.1 – SUMMARY OF FINDINGS AND IMPLICATIONS

7.1.1 – Effect of Diet

This thesis examined, in male and female mice, the impact of replacing 7.5% of saturated fat with n-3 polyunsaturated fatty acids (PUFA) in a high saturated fat diet on the metabolic profile, adipose tissue distribution, muscle fibre type composition, and key genes regulating the pathways of fatty acid and glucose metabolism. Prior to the findings presented in this thesis, enriching a high fat diet (HFD) with n-3 PUFAs (HF-n-3) had been demonstrated to ameliorate the weight gain, adipose tissue hypertrophy, hyperlipidemia, ectopic fat deposition and insulin resistance associated with high fat overfeeding in rodents. The aim of **Chapter 2** of this thesis was to define the phenotype of mice fed a n-3 PUFA enriched high saturated fat diet (HF-n-3) compared to a high saturated fat diet (HF-S) alone. Although body weight and total fat mass were increased similarly with both HF-S and HF-n-3 feeding, as hypothesised n-3 PUFA enrichment of a HF-S diet reduced visceral adiposity, prevented ectopic fat deposition in the liver and tended to ameliorate insulin resistance. In addition brown fat mass was increased. Although several studies had focused on the mechanisms behind the improved blood lipid profile and insulin sensitivity associated with enriching a HFD with n-3 PUFAs, few studies had determined the reasons for the amelioration of ectopic fat deposition in organs influencing energy balance, the skeletal muscle and liver and consequently the subsequent studies in this thesis aimed to determine the cause.

Although previous studies have described a muscle fibre type switch as a result of obesity (enhanced glycolytic capacity) and in response to greater skeletal muscle n-3

PUFA content (enhanced oxidative capacity), the studies described in **Chapter 3** of this thesis showed that neither obesity nor dietary fatty acid content influenced the muscle fibre type composition of the extensor digitorum longus (EDL; fast-twitch glycolytic-fast-twitch oxidative glycolytic (FG-FOG)) and soleus (slow-twitch oxidative (SO)) muscles. Nevertheless, the HF-S and HF-n-3 diets induced metabolic differences in the muscles, as most obviously seen in the reduced lipid content (as hypothesised) and glycogen content in the SO soleus muscle with HF-n-3 feeding. These findings suggest that muscle oxidative capacity increased with HF-n-3 consumption, despite failing to induce the hypothesised muscle fibre type switch. This was confirmed by staining for enzymes that reflect oxidative capacity in the muscle fibres of HF-n-3-fed mice.

Subsequently, **Chapter 4** of this thesis provides evidence that the HF-n-3-induced amelioration of intramyocellular fat accretion may have occurred through an altered pattern of fatty acid metabolism gene expression in skeletal muscle. This study is the first, as far as can be determined, to identify the mechanisms by which n-3 PUFA enrichment of a HFD prevents intramyocellular fat accumulation; specifically this, as hypothesised, may occur through the concurrent activation of genes involved in pathways inducing fatty acid uptake and utilisation and suppression of genes regulating pathways of fatty acid storage and lipogenesis. This study therefore supported a role for n-3 PUFAs enhancing muscle oxidative capacity, as described in **Chapter 3**, and showed that this occurs at the level of mRNA content.

Furthermore, the current study (**Chapter 2**) and previous research have provided evidence that n-3 PUFAs play a role in ameliorating HF-S-induced fatty liver. The

work comprised in **Chapter 5** of this thesis provides evidence that n-3 PUFA enrichment of a HF-S diet ameliorated HF-S-induced fatty liver through an altered pattern of fatty acid metabolism gene expression in the liver. The mechanisms by which n-3 PUFA enrichment of a HFD prevents intrahepatic fat accretion may be (**Chapter 5**) specifically through the concurrent activation of genes involved in pathways inducing fatty acid uptake and utilisation and suppression of genes regulating pathways of fatty acid storage and lipogenesis, as hypothesised.

Finally, the work comprised in **Chapter 6** of this thesis provided some insight into the effect of dietary fatty acid composition on glucose metabolism in the skeletal muscle and liver. Replacement of 7.5% of saturated fat with n-3 PUFAs prevented the HF-S-induced suppression of the gene involved in glucose phosphorylation in skeletal muscle; subsequently phosphorylated glucose may enter oxidative disposal, but is less likely to undergo non-oxidative disposal and reduced muscle glycogen levels (**Chapter 3**) are consistent with this notion. It was also demonstrated that replacement of 7.5% of saturated fat with n-3 PUFAs reduced the expression of the gene involved in the hepatic phosphorylation of glucose and this was speculated to prevent *de novo* lipogenesis. Of the phosphorylated glucose entering glucose metabolism in the liver, the majority was most likely to undergo oxidative disposal, not glycogenesis. Furthermore, HF-n-3 feeding prevented *de novo* glucose synthesis in the liver. This study therefore provides evidence that n-3 PUFA enrichment of a HFD has beneficial effects for hepatic glucose as well as lipid metabolism through coordinated changes in the regulation of intermediary metabolism. These changes, accompanied by lower plasma insulin levels, are consistent with direct and/or secondary benefits for insulin signalling.

7.1.2 – Effect of Gender

Although several previous studies have described gender differences in the development of the obese phenotype and in response to high fat overfeeding, it was unknown if there was a gender-specific effect in response to n-3 PUFA enrichment of a HFD. Male mice were shown to have greater plasma glucose levels in comparison to females (**Chapter 2**). Previous studies have shown that female mice are less likely to exhibit an impaired insulin sensitivity profile in response to the increased fatty acid supply of a HFD. The increase in hepatic storage of glycogen observed in female mice is also consistent with greater insulin sensitivity (**Chapter 2**). Male mice, however, had increased mRNA content of genes influencing glucose phosphorylation (hexokinase 2 (HK2)) and glycolysis (phosphofructokinase (PFK)) in skeletal muscle, and those mediating glycogen synthesis (glycogen synthase (GYS2)) and insulin signalling (suppressor of cytokine signalling (SOCS3)) in the liver (**Chapter 6**). Given that the skeletal muscle is the chief mediator of insulin-stimulated glucose disposal, a greater inherent capacity for glucose phosphorylation and its subsequent glycolysis, may reflect a greater requirement for these functions to maintain insulin sensitivity in healthy males. It is therefore possible that male mice may be more affected by the dysfunctional glucose phosphorylation and subsequent reduction in glucose metabolism that results from HF-S feeding, leading to reduced insulin sensitivity.

Female mice also exhibited greater hepatic storage of fat (**Chapter 2**). Gonadal steroids have been shown to mediate the expression of hepatic fatty acid transporter, fatty acid translocase (FAT/CD36), and FAT/CD36 was more abundant in female mice (**Chapter 5**). Therefore increased liver fat in female mice may be a consequence of

increased fatty acid uptake via FAT/CD36 (Sorrentino *et al.*, 1992). In addition to an increase in hepatic fat, high fat feeding has been shown previously to increase adipose tissue mass to a greater extent in female than male mice, concurrent with an increase in the oxidative capacity of skeletal muscle. This observation was extended by examining the skeletal muscle mRNA content of genes that may influence this gender-specific response (**Chapter 4**). In particular, it was observed that the mRNA content of genes involved in fatty acid oxidation (carnitine palmitoyl transferase 1 (CPT1b), peroxisome proliferative activated receptor γ coactivator 1 α (PGC1 α), AMP-activated protein kinase catalytic subunit α 2 (AMPK α 2)) were reduced and those involved in fatty acid storage (diacylglycerol acyltransferase 1 (DGAT1), stearoyl-Coenzyme A desaturase 1 (SCD1)) were preferentially increased in female mice. The direct action of gonadal steroids on skeletal muscle may be responsible for the differential expression of fatty acid metabolism genes demonstrated in this study; however this is speculative and further research is required. Furthermore, it may be speculated that a genetic profile favouring triglyceride storage and limiting fatty oxidation in skeletal muscle, may result in an increased propensity for fat storage in female mice, leading to an increased risk of obesity development. The roles of gonadal steroids and their mechanism of effect in this regard requires further investigation. In female mice there was greater expression of genes involved in promoting triglyceride synthesis and secretion (diacylglycerol acyltransferase 2 (DGAT2)) and utilisation (pyruvate dehydrogenase kinase 4 (PDK4), uncoupling protein 2 (UCP2)) and those inhibiting pathways of lipogenesis (peroxisome proliferator activator receptor δ/β (PPAR δ/β)) (**Chapter 5**).

Whilst in male mice, greater expression of genes involved in fatty acid synthesis and storage (fatty acid synthase (FAS), acetyl-Coenzyme A carboxylase- α (ACC- α), peroxisome proliferator activator receptor γ (PPAR γ)), and in promoting fatty acid utilisation (AMPK α 2, acetyl-Coenzyme A carboxylase- β (ACC- β)) were detected (**Chapter 5**). These data suggest that intricate differences in fatty acid metabolism may contribute to the greater fat deposition in the livers of female mice and therefore gender should be considered when contemplating PUFAs as a potential therapeutic in the treatment of fatty liver.

7.1.3 – Effect of Muscle Fibre Type

HF-n-3 feeding ameliorated the HF-S-induced intramyocellular fat accumulation, an effect seen particularly in the SO soleus muscle (**Chapter 3**) and the mRNA content of key genes involved in skeletal muscle fatty acid metabolism in the FG-FOG EDL and SO soleus muscles reflected the preferred substrate type of each muscle (**Chapter 4**). The SO soleus muscle predominantly uses triglycerides for fuel (Samec *et al.*, 2002) and consistent with this notion, the current study showed that the soleus muscle exhibited greater mRNA content of genes involved in fatty acid transport (FAT/CD36, fatty acid binding protein (FABPpm), fatty acid transport protein 1 (FATP1), fatty acid transport protein 4 (FATP4)), storage (DGAT1, SCD1, hormone sensitive lipase (HSL)) and utilisation (PDK4, CPT1b, PGC1 α , peroxisome proliferator activator receptor α (PPAR α)), as compared to the EDL (FG-FOG) muscle. Conversely, it was demonstrated that the EDL muscle had greater mRNA content of AMPK α 2, a gene involved in mediating glucose uptake into muscle and both glucose and fatty acid

oxidation, reflecting the preference for glucose as a metabolic substrate in the EDL muscle. Furthermore, the mRNA content of glycolytic enzyme, PFK-M, was greater in the FG-FOG EDL muscle, whilst genes involved in glucose phosphorylation (HK2), glycogen synthesis (glycogen synthase 1 (GYS1)) and insulin signalling (phosphatidylinositol 3-kinase, regulatory subunit, polypeptide 1 (PI3Kr1)) were greater in the SO soleus muscle (**Chapter 6**). In combination these data reflect the greater intrinsic capacity of SO muscle for enhanced insulin sensitivity and responsiveness and glycogen synthesis and the FG-FOG muscle for greater glycolytic flux. It is therefore possible that exposure to certain fatty acids, such as saturated fats, may impact a certain muscle type to a greater extent given their inherent function, leading to metabolic vulnerability.

7.1.4 – Implications

The studies comprising this thesis have demonstrated that the dietary fatty acid composition may influence overall metabolic profile. The average Australian adult consumes approximately 6% above the recommended intake of saturated fat and less than half the recommended daily amount of long chain n-3 polyunsaturated fatty acids (PUFA) (Food Standards Australia New Zealand, 2009). Saturated fatty acids promote weight gain in addition to dyslipidemia, ectopic fat accumulation and reduced insulin sensitivity. The current studies demonstrate that, at least in mice, replacing 7.5% of dietary saturated fat with n-3 PUFAs ameliorates these negative health effects (but has no effect on body weight gain). The effects of a reduction in saturated fat and increase in n-3 PUFAs in an otherwise controlled dietary pattern remains to be determined in humans, although it is clear that n-3 supplementation in humans decreases triglyceride

levels, gender differences and relationships to gonadal steroids have not been, to my knowledge, explored. The findings of this thesis further our understanding of the molecular mechanisms behind the positive health effects of n-3 PUFAs at the whole-body level, as well as in organs controlling energy balance, the skeletal muscle and liver. Furthermore, the findings of the studies comprising this thesis were gender dimorphic and muscle fibre type-specific in nature and therefore highlight the importance of exploring both gender and muscle fibre type in future studies considering n-3 PUFAs as a therapeutic agent. Care must be taken however, when extrapolating data from the current studies, conducted in mice, to clinical studies, as replacing 7.5% of saturated fat with n-3 PUFAs is the equivalent of a relatively high intake of n-3 PUFAs in humans.

7.2 – FUTURE STUDIES

7.2.1 – Measuring Thermogenesis

As discussed in **Chapter 2**, enlargement of the brown adipose tissue depot, an important site of energy expenditure in rodents (Vidal-Puig *et al.*, 1997), may indicate an increased capacity for thermogenesis, given that PUFAs have been shown to stimulate thermogenesis in brown fat (Mercer and Trayhurn, 1987). Therefore increased thermogenic capacity, and hence energy expenditure, may over time attenuate body weight gain, which may explain the discrepancies in body weight observed in HF-n-3 feeding studies (Dorfmeister *et al.*, 2006; Wang *et al.*, 2002; Ikemoto *et al.*, 1996; Rustan *et al.*, 1993). Therefore measuring whole-body thermogenesis in a future study may provide useful information.

7.2.2 – Quantifying Muscle Fibre Type with Respect to Gender

As discussed in **Chapter 3**, although muscle fibre type composition is not gender-dependent, studies in untrained male and female humans have shown that the area occupied by slow-twitch fibres is greater in women, and the area occupied by fast-twitch fibres is greater in men (Staron *et al.*, 2000). Given that the sample size used to determine muscle fibre type (in **Chapter 3**) was only small (n=5-6 per group, including only 2-3 males and females), a greater sample size of male and female mice in future studies would allow exploration and comparison of the effects of diet on muscle fibre type with respect to gender.

7.2.3 – Assaying Diacylglycerol (DAG) and Ceramide

As discussed in **Chapter 4**, DAG and ceramide levels may have increased in response to high fat feeding (Todd *et al.*, 2007; Lee *et al.*, 2006) and this may be deleterious, given that increased muscle DAG and ceramide levels are associated with reduced insulin sensitivity (Strackowski *et al.*, 2007). In **Chapter 4** failure to appropriately upregulate DGAT1, the enzyme responsible for converting DAG to triglyceride, was associated with an increase in plasma glucose concentrations in the HF-S group, but not HF-n-3 group. Therefore future studies may investigate the effect of n-3 PUFA enrichment of a HFD on tissue DAG and ceramide levels.

7.2.4 – Quantifying Protein Abundance or Activity of Key Metabolic Genes or Whole Processes of Metabolic Pathways

As discussed in **Chapters 4, 5 and 6**, the findings reported are the outcome of mRNA content analyses, and whilst this provides useful information about the amount of gene transcribed, the mRNA content may not always totally align with the active protein product present in the cell. For instance, the total amount of active protein product may be influenced by the stability of mRNA from which protein is translated; the translation of mRNA to protein; post-translational modifications and activation of protein. Therefore as a primary aim for future studies beyond the scope of this thesis, further analyses will focus on the protein abundance, phosphorylation or activity of key genes measured, further validating their distinct role in pathways.

Furthermore, pathways of fatty acid uptake, storage and oxidation and glucose metabolism have been described as mRNA contents. It would also be advantageous to measure these pathways as a whole-process in order to determine their contribution to the overall fatty acid/glucose metabolism in the skeletal muscle and liver.

7.2.5 – Focusing on the Effect of Gender – Gonadectomy Studies

Given that gender differences were seen in response to high fat overfeeding, it may be beneficial to explore the factors influencing the gender-specific responses. This is important as studies have demonstrated gender differences in the development of the obese phenotype (Haugaard *et al.*, 2009; Moro *et al.*, 2009; Català-Niell *et al.*, 2008; Gómez-Pérez *et al.*, 2008; Priego *et al.*, 2008). This may potentially involve ovariectomy

and gonadectomy studies with or without gonadal steroid supplementation (oestrogen in females, testosterone in males). Using such gonadectomy models may provide further understanding of the gender-specific response to high fat overfeeding, and may provide useful information that could be extrapolated to human studies, allowing gender-specific interventions when considering n-3 PUFA supplementation.

7.2.6 – Focusing on the Effect of n-3 PUFAs – Which Fatty Acid is having the Greatest Effect?

In the studies comprised in this thesis, fish oil was used in the replacement of 7.5% of saturated fat with n-3 PUFAs. This fish oil was provided as HiDHA[®] 25N tuna oil which has a fatty acid profile of 26% docosahexaenoic acid (DHA) and 6% eicosapentaenoic acid (EPA) (35% total n-3 PUFA content). Given the differential responses observed when feeding diets of different fatty acid content (HF-S, HF-n-3); it may be beneficial to identify which of the individual n-3 PUFAs plays a greater role in altering fatty acid metabolism. Few studies have focused on which n-3 PUFA is most beneficial in a high fat diet setting. By using *in vitro* cell culture systems, it would be possible to test the direct affects of incubation with certain fatty acid types on the expression and abundance of key genes in skeletal muscle or liver cells. For example, it would be possible to further dissect the fatty acid component, within the fish oil, causing this effect, e.g. by applying either DHA, EPA or both, to see which is having the greater effect on the genes of interest.

BIBLIOGRAPHY

- Aas, V., Rokling-Andersen, M.H., Kase, E.T., Thoresen, G.H. & Rustan, A.C. (2006). Eicosapentaenoic acid (20:5 n-3) increases fatty acid and glucose uptake in cultured human skeletal muscle cells. *J Lipid Res* **47**(2): 366-374.
- Abbot, E.L., McCormack, J.G., Reynet, C., Hassall, D.G., Buchan, K.W. & Yeaman, S.J. (2005). Diverging regulation of pyruvate dehydrogenase kinase isoform gene expression in cultured human muscle cells. *FEBS J* **272**(12): 3004-3014.
- Abu-Elheiga, L., Almarza-Ortega, D.B., Baldini, A. & Wakil, S.J. (1997). Human acetyl-CoA carboxylase 2. Molecular cloning, characterization, chromosomal mapping, and evidence for two isoforms. *J Biol Chem* **272**(16): 10669-10677.
- Abu-Elheiga, L., Brinkley, W.R., Zhong, L., Chirala, S.S., Woldegiorgis, G. & Wakil, S.J. (2000). The subcellular localization of acetyl-CoA carboxylase 2. *Proc Natl Acad Sci U S A* **97**(4): 1444-1449.
- Abu-Elheiga, L., Matzuk, M.M., Abo-Hashema, K.A. & Wakil, S.J. (2001). Continuous fatty acid oxidation and reduced fat storage in mice lacking acetyl-CoA carboxylase 2. *Science* **291**(5513): 2613-2616.
- Abu-Elheiga, L., Oh, W., Kordari, P. & Wakil, S.J. (2003). Acetyl-CoA carboxylase 2 mutant mice are protected against obesity and diabetes induced by high-fat/high-carbohydrate diets. *Proc Natl Acad Sci USA* **100**(18): 10207-10212.
- Adachi, T., Kikuchi, N., Yasuda, K., Anahara, R., Gu, N., Matsunaga, T., et al. (2007). Muscle fibre type distribution and gene expression levels of both succinate dehydrogenase and peroxisome proliferator-activated receptor-gamma coactivator-1alpha of fibres in the soleus muscle of Zucker diabetic fatty rats. *Exp Physiol* **92**(2): 449-455.
- Agius, L. (1998). The physiological role of glucokinase binding and translocation in hepatocytes. *Adv Enzyme Regul* **38**: 303-331.
- Agius, L. (2008). Glucokinase and molecular aspects of liver glycogen metabolism. *Biochem J* **414**(1): 1-18.
- Alam, N. & Saggerson, E.D. (1998). Malonyl-CoA and the regulation of fatty acid oxidation in soleus muscle. *Biochem J* **334**(Pt 1): 233-241.
- Alonso, M.D., Lomako, J., Lomako, W.M. & Whelan, W.J. (1995). A new look at the biogenesis of glycogen. *FASEB J* **9**(12): 1126-1137.

-
- Andreelli, F., Laville, M., Ducluzeau, P.H., Vega, N., Vallier, P., Khalfallah, Y., et al. (1999). Defective regulation of phosphatidylinositol-3-kinase gene expression in skeletal muscle and adipose tissue of non-insulin-dependent diabetes mellitus patients. *Diabetologia* **42**(3): 358-364.
- Ardehali, H., Printz, R.L., Whitesell, R.R., May, J.M. & Granner, D.K. (1999). Functional interaction between the N- and C-terminal halves of human hexokinase II. *J Biol Chem* **274**(23): 15986-15989.
- Arterburn, L.M., Hall, E.B. & Oken, H. (2006). Distribution, interconversion, and dose response of n-3 fatty acids in humans. *Am J Clin Nutr* **83**(6): S1467-1476.
- Astrup, A., Hill, J.O. & Rossner, S. (2004). The cause of obesity: are we barking up the wrong tree? *Obes Rev* **5**(3): 125-127.
- Auinger, A., Valenti, L., Pfeuffer, M., Helwig, U., Herrmann, J., Fracanzani, A.L., et al. (2010). A promoter polymorphism in the liver-specific fatty acid transport protein 5 is associated with features of the metabolic syndrome and steatosis. *Horm Metab Res* **42**(12): 854-859.
- Azpiazu, I., Manchester, J., Skurat, A.V., Roach, P.J. & Lawrence, J.C.J. (2000). Control of glycogen synthesis is shared between glucose transport and glycogen synthase in skeletal muscle fibers. *Am J Physiol Endocrinol Metab* **278**(2): E234-243.
- Bajotto, G., Murakami, T., Nagasaki, M., Qin, B., Matsuo, Y., Maeda, K., et al. (2006). Increased expression of hepatic pyruvate dehydrogenase kinases 2 and 4 in young and middle-aged Otsuka Long-Evans Tokushima Fatty rats: induction by elevated levels of free fatty acids. *Metabolism* **55**(3): 317-323.
- Bär, A. & Pette, D. (1988). Three fast myosin heavy chains in adult rat skeletal muscle. *FEBS Lett* **235**(1-2): 153-155.
- Barbuio, R., Milanski, M., Bertolo, M.B., Saad, M.J. & Velloso, L.A. (2007). Infliximab reverses steatosis and improves insulin signal transduction in liver of rats fed a high-fat diet. *J Endocrinol* **194**(3): 539-550.
- Barsalani, R., Chapados, N.A. & Lavoie, J.M. (2010). Hepatic VLDL-TG production and MTP gene expression are decreased in ovariectomized rats: effects of exercise training. *Horm Metab Res* **42**(12): 860-867.
- Barshop, N.J., Sirlin, C.B., Schwimmer, J.B. & Lavine, J.E. (2008). Review article: epidemiology, pathogenesis and potential treatments of paediatric non-alcoholic fatty liver disease. *Aliment Pharmacol Ther* **28**(1): 13-24.

-
- Barthel, A. & Schmoll, D. (2003). Novel concepts in insulin regulation of hepatic gluconeogenesis. *Am J Physiol Endocrinol Metab* **285**(4): E685-692.
- Batch, J.A. & Baur, L.A. (2005). Management and prevention of obesity and its complications in children and adolescents. *Med J Aust* **182**(3): 130-135.
- Belzung, F., Raclot, T. & Groscolas, R. (1993). Fish oil n-3 fatty acids selectively limit the hypertrophy of abdominal fat depots in growing rats fed high-fat diets. *Am J Physiol Regul Integr Comp Physiol* **264**(6): R1111-1118.
- Berger, J., Truppe, C., Neumann, H. & Forss-Petter, S. (1998). A novel relative of the very-long-chain acyl-CoA synthetase and fatty acid transporter protein genes with a distinct expression pattern. *Biochem Biophys Res Commun* **247**(2): 255-260.
- Berk, P.D., Zhou, S.-L., Kiang, C.-L., Stump, D., Bradbury, M. & Isola, L.M. (1997). Uptake of long chain free fatty acids is selectively up-regulated in adipocytes of Zucker rats with genetic obesity and non-insulin-dependent diabetes mellitus. *J Biol Chem* **272**(13): 8830-8835.
- Bertoni-Freddari, C., Fattoretti, P., Casoli, T., Di Stefano, G., Solazzi, M., Gracciotti, N., et al. (2001). Mapping of mitochondrial metabolic competence by cytochrome oxidase and succinic dehydrogenase cytochemistry. *J Histochem Cytochem* **49**(9): 1191-1192.
- Bezaire, V., Bruce, C.R., Heigenhauser, G.J.F., Tandon, N.N., Glatz, J.F.C., Luiken, J.J.J.F., et al. (2006). Identification of fatty acid translocase on human skeletal muscle mitochondrial membranes: essential role in fatty acid oxidation. *Am J Physiol Endocrinol Metab* **290**(3): E509-515.
- Bezaire, V., Seifert, E.L. & Harper, M.-E. (2007). Uncoupling protein-3: clues in an ongoing mitochondrial mystery. *FASEB J* **21**(2): 312-324.
- Biddinger, S.B., Almind, K., Miyazaki, M., Kokkotou, E., Ntambi, J.M. & Kahn, C.R. (2005). Effects of diet and genetic background on sterol regulatory element-binding protein-1c, stearoyl-CoA desaturase 1, and the development of the metabolic syndrome. *Diabetes* **54**(5): 1314-1323.
- Binas, B., Han, X.-X., Erol, E., Luiken, J.J.F.P., Glatz, J.F.C., Dyck, D.J., et al. (2003). A null mutation in H-FABP only partially inhibits skeletal muscle fatty acid metabolism. *Am J Physiol Endocrinol Metab* **285**(3): E481-489.
- Bird, M.I. & Saggerson, E.D. (1984). Binding of malonyl-CoA to isolated mitochondria. Evidence for high- and low-affinity sites in liver and heart and relationship to inhibition of carnitine palmitoyltransferase activity. *Biochem J* **222**(3): 639-647.
-

-
- Biscione, F., Pignalberi, C., Totteri, A., Messina, F. & Altamura, G. (2007). Cardiovascular effects of omega-3 free fatty acids. *Curr Vasc Pharmacol* **5**(2): 163-172.
- Bizeau, M.E., Short, C., Thresher, J.S., Commerford, S.R., Willis, W.T. & Pagliassotti, M.J. (2001). Increased pyruvate flux capacities account for diet-induced increases in gluconeogenesis in vitro. *Am J Physiol Regul Integr Comp Physiol* **281**(2): R427-433.
- Blaak, E.E., Hul, G., Verdich, C., Stich, V., Martinez, A., Petersen, M., et al. (2006). Fat oxidation before and after a high fat load in the obese insulin-resistant state. *J Clin Endocrinol Metab* **91**(4): 1462-1469.
- Blake, W.L. & Clarke, S.D. (1990). Suppression of rat hepatic fatty acid synthase and S14 gene transcription by dietary polyunsaturated fat. *J Nutr* **120**(12): 1727-1729.
- Bobinac, D., Malnar-Dragojević, D., Bajek, S., Soić-Vranić, T. & Jerković, R. (2000). Muscle fiber type composition and morphometric properties of denervated rat extensor digitorum longus muscle. *Croat Med J* **41**(3): 294-297.
- Bocek, R.M. & Beatty, C.H. (1966). Glycogen synthetase and phosphorylase in red and white muscle of rat and rhesus monkey. *J Histochem Cytochem* **14**(7): 549-559.
- Bocher, V., Pineda-Torra, I., Fruchart, J.-C. & Staels, B. (2002). PPARs: transcription factors controlling lipid and lipoprotein metabolism. *Ann NY Acad Sci* **967**(1): 7-18.
- Bonen, A., Benton, C.R., Campbell, S.E., Chabowski, A., Clarke, D.C., Han, X.X., et al. (2003). Plasmalemmal fatty acid transport is regulated in heart and skeletal muscle by contraction, insulin and leptin, and in obesity and diabetes. *Acta Physiol Scand* **178**(4): 347-356.
- Bonen, A., Campbell, S.E., Benton, C.R., Chabowski, A., Coort, S.L.M., Han, X.-X., et al. (2004a). Regulation of fatty acid transport by fatty acid translocase/CD36. *Proc Nutr Soc* **63**(2): 245-249.
- Bonen, A., Han, X.-X., Habets, D.D.J., Febbraio, M., Glatz, J.F.C. & Luiken, J.J.F.P. (2007). A null mutation in skeletal muscle FAT/CD36 reveals its essential role in insulin-, and AICAR-stimulated fatty acid metabolism. *Am J Physiol Endocrinol Metab* **292**(6): E1740-1749.
- Bonen, A., Luiken, J.J.F.P. & Glatz, J.F.C. (2002). Regulation of fatty acid transport and membrane transporters in health and disease. *Mol Cell Biochem* **239**(1): 181-192.
-

-
- Bonen, A., Parolin, M.L., Steinberg, G.R., Calles-Escandon, J., Tandon, N.N., Glatz, J.F.C., et al. (2004b). Triacylglycerol accumulation in human obesity and type 2 diabetes is associated with increased rates of skeletal muscle fatty acid transport and increased sarcolemmal FAT/CD36. *FASEB J* **18**(10): 1144-1146.
- Bonora, E. (2000). Relationship between regional fat distribution and insulin resistance. *Int J Obes Relat Metab Disord* **24**(Suppl 2): S32-S35.
- Borkman, M., Storlien, L.H., Pan, D.A., Jenkins, A.B., Chisholm, D.J. & Campbell, L.V. (1993). The relation between insulin sensitivity and the fatty-acid composition of skeletal-muscle phospholipids. *N Engl J Med* **328**(4): 238-244.
- Boss, O., Hagen, T. & Lowell, B.B. (2000). Uncoupling proteins 2 and 3: potential regulators of mitochondrial energy metabolism. *Diabetes* **49**(2): 143-156.
- Bowker-Kinley, M.M., Davis, W.I., Wu, P., Harris, R.A. & Popov, K.M. (1998). Evidence for existence of tissue-specific regulation of the mammalian pyruvate dehydrogenase complex. *Biochem J* **329**(Pt 1): 191-196.
- Bradbury, M.W. (2006). Lipid metabolism and liver inflammation. I. Hepatic fatty acid uptake: possible role in steatosis. *Am J Physiol Gastrointest Liver Physiol* **290**(2): G194-198.
- Bradley, R.L., Fisher, F.F. & Maratos-Flier, E. (2008). Dietary fatty acids differentially regulate production of TNF-alpha and IL-10 by murine 3T3-L1 adipocytes. *Obesity (Silver Spring)* **16**(5): 938-944.
- Bray, G.A. & Popkin, B.M. (1998). Dietary fat intake does affect obesity! *Am J Clin Nutr* **68**(6): 1157-1173.
- Brown, M.S. & Goldstein, J.L. (1999). A proteolytic pathway that controls the cholesterol content of membranes, cells, and blood. *Proc Natl Acad Sci U S A* **96**(20): 11041-11048.
- Brown, N.F., Hill, J.K., Esser, V., Kirkland, J.L., Corkey, B.E., Foster, D.W., et al. (1997). Mouse white adipocytes and 3T3-L1 cells display an anomalous pattern of carnitine palmitoyltransferase (CPT) I isoform expression during differentiation. Inter-tissue and inter-species expression of CPT I and CPT II enzymes. *Biochem J* **327**(Pt 1): 225-231.
- Browning, J.D. & Horton, J.D. (2004). Molecular mediators of hepatic steatosis and liver injury. *J Clin Invest* **114**(2): 147-152.
- Brownlow, B.S., Petro, A., Feinglos, M.N. & Surwit, R.S. (1996). The role of motor activity in diet-induced obesity in C57BL/6J mice. *Physiol Behav* **60**(1): 37-41.

- Bruce, C.R., Hoy, A.J., Turner, N., Watt, M.J., Allen, T.L., Carpenter, K., et al. (2009). Overexpression of carnitine palmitoyltransferase-1 in skeletal muscle is sufficient to enhance fatty acid oxidation and improve high-fat diet-induced insulin resistance. *Diabetes* **58**(3): 550-558.
- Bruce, C.R., Mertz, V.A., Heigenhauser, G.J.F. & Dyck, D.J. (2005). The stimulatory effect of globular adiponectin on insulin-stimulated glucose uptake and fatty acid oxidation is impaired in skeletal muscle from obese subjects. *Diabetes* **54**(11): 3154-3160.
- Buettner, R., Parhofer, K.G., Woenckhaus, M., Wrede, C.E., Kunz-Schughart, L.A., Scholmerich, J., et al. (2006). Defining high-fat-diet rat models: metabolic and molecular effects of different fat types. *J Mol Endocrinol* **36**(3): 485-501.
- Burdge, G.C., Jones, A.E. & Wootton, S.A. (2002). Eicosapentaenoic and docosapentaenoic acids are the principal products of alpha-linolenic acid metabolism in young men. *Br J Nutr* **88**(4): 355-363.
- Burdge, G.C., Slater-Jefferies, J.L., Grant, R.A., Chung, W.S., West, A.L., Lillycrop, K.A., et al. (2008). Sex, but not maternal protein or folic acid intake, determines the fatty acid composition of hepatic phospholipids, but not of triacylglycerol, in adult rats. *Prostaglandins Leukot Essent Fatty Acids* **78**(1): 73-9.
- Burdge, G.C. & Wootton, S.A. (2002). Conversion of alpha-linolenic acid to eicosapentaenoic, docosapentaenoic and docosahexaenoic acids in young women. *Br J Nutr* **88**(4): 411-420.
- Cameron-Smith, D., Burke, L.M., Angus, D.J., Tunstall, R.J., Cox, G.R., Bonen, A., et al. (2003). A short-term, high-fat diet up-regulates lipid metabolism and gene expression in human skeletal muscle. *Am J Clin Nutr* **77**(2): 313-318.
- Campbell, S.E., Tandon, N.N., Woldegiorgis, G., Luiken, J.J.F.P., Glatz, J.F.C. & Bonen, A. (2004). A novel function for fatty acid translocase (FAT)/CD36: involvement in long chain fatty acid transfer into the mitochondria. *J Biol Chem* **279**(35): 36235-36241.
- Campbell, W.G., Gordon, S.E., Carlson, C.J., Pattison, J.S., Hamilton, M.T. & Booth, F.W. (2001). Differential global gene expression in red and white skeletal muscle. *Am J Physiol Cell Physiol* **280**(4): C763-768.
- Canbay, A., Bechmann, L. & Gerken, G. (2007). Lipid metabolism in the liver. *Z Gastroenterol* **45**(1): 35-41.
- Carling, D. (2005). AMP-activated protein kinase: balancing the scales. *Biochimie* **87**(1): 87-91.

-
- Carling, D. & Hardie, D.G. (1989). The substrate and sequence specificity of the AMP-activated protein kinase. Phosphorylation of glycogen synthase and phosphorylase kinase. *Biochim Biophys Acta* **1012**(1): 81-86.
- Carmiel-Haggai, M., Cederbaum, A.I. & Nieto, N. (2005). A high-fat diet leads to the progression of non-alcoholic fatty liver disease in obese rats. *FASEB J* **19**(1): 136-138.
- Cases, S., Smith, S.J., Zheng, Y.-W., Myers, H.M., Lear, S.R., Sande, E., et al. (1998). Identification of a gene encoding an acyl CoA:diacylglycerol acyltransferase, a key enzyme in triacylglycerol synthesis. *Proc Natl Acad Sci U S A* **95**(22): 13018-13023.
- Cases, S., Stone, S.J., Zhou, P., Yen, E., Tow, B., Lardizabal, K.D., et al. (2001). Cloning of DGAT2, a second mammalian diacylglycerol acyltransferase, and related family members. *J Biol Chem* **276**(42): 38870-38876.
- Castle, J.C., Hara, Y., Raymond, C.K., Garrett-Engle, P., Ohwaki, K., Kan, Z., et al. (2009). ACC2 is expressed at high levels human white adipose and has an isoform with a novel N-terminus. *PLoS ONE* **4**(2): e4369.
- Català-Niell, A., Estrany, M.E., Proenza, A.M., Gianotti, M. & Llado, I. (2008). Skeletal muscle and liver oxidative metabolism in response to a voluntary isocaloric intake of a high fat diet in male and female rats. *Cell Physiol Biochem* **22**(1-4): 327-336.
- Centis, E., Marzocchi R, Di Domizio S, Ciaravella MF, Marchesini G. (2010). The effect of lifestyle changes in non-alcoholic fatty liver disease. *Dig Dis* **28**(1): 267-273.
- Chabowski, A., Chatham, J.C., Tandon, N.N., Calles-Escandon, J., Glatz, J.F.C., Luiken, J.J.F.P., et al. (2006). Fatty acid transport and FAT/CD36 are increased in red but not in white skeletal muscle of ZDF rats. *Am J Physiol Endocrinol Metab* **291**(3): E675-682.
- Chabowski, A., Coort, S.L.M., Calles-Escandon, J., Tandon, N.N., Glatz, J.F.C., Luiken, J.J.F.P., et al. (2004). Insulin stimulates fatty acid transport by regulating expression of FAT/CD36 but not FABPpm. *Am J Physiol Endocrinol Metab* **287**(4): E781-789.
- Chakravarthy, M.V., Pan, Z., Zhu, Y., Tordjman, K., Schneider, J.G., Coleman, T., et al. (2005). "New" hepatic fat activates PPAR α to maintain glucose, lipid, and cholesterol homeostasis. *Cell Metab* **1**(5): 309-322.

-
- Chalon, S., Delion-Vancassel, S., Belzung, C., Guilloteau, D., Leguisquet, A.-M., Besnard, J.-C., et al. (1998). Dietary fish oil affects monoaminergic neurotransmission and behavior in rats. *J Nutr* **128**(12): 2512-2519.
- Chang, P.Y., Jensen, J., Printz, R.L., Granner, D.K., Ivy, J.L. & Moller, D.E. (1996). Overexpression of hexokinase II in transgenic mice. Evidence that increased phosphorylation augments muscle glucose uptake. *J Biol Chem* **271**(25): 14834-14839.
- Chavin, K.D., Yang, S., Lin, H.Z., Chatham, J., Chacko, V.P., Hoek, J.B., et al. (1999). Obesity induces expression of uncoupling protein-2 in hepatocytes and promotes liver ATP depletion. *J Biol Chem* **274**(9): 5692-5700.
- Chen, H.C. & Farese, R.V., Jr. (2005). Inhibition of triglyceride synthesis as a treatment strategy for obesity: lessons from DGAT1-deficient mice. *Arterioscler Thromb Vasc Biol* **25**(3): 482-486.
- Chen, H.C., Jensen, D.R., Myers, H.M., Eckel, R.H. & Farese, R.V. (2003a). Obesity resistance and enhanced glucose metabolism in mice transplanted with white adipose tissue lacking acyl CoA: diacylglycerol acyltransferase 1. *J Clin Invest* **111**(11): 1715.
- Chen, H.C., Ladha, Z., Smith, S.J. & Farese, R.V., Jr. (2003b). Analysis of energy expenditure at different ambient temperatures in mice lacking DGAT1. *Am J Physiol Endocrinol Metab* **284**(1): E213-218.
- Chen, H.C., Rao, M., Sajan, M.P., Standaert, M., Kanoh, Y., Miura, A., et al. (2004). Role of adipocyte-derived factors in enhancing insulin signaling in skeletal muscle and white adipose tissue of mice lacking acyl CoA:diacylglycerol acyltransferase 1.(Signal Transduction). *Diabetes* **53**(6): 1445(7).
- Chen, H.C., Stone, S.J., Zhou, P., Buhman, K.K. & Farese, R.V., Jr. (2002). Dissociation of obesity and impaired glucose disposal in mice overexpressing acyl coenzyme A:diacylglycerol acyltransferase 1 in white adipose tissue. *Diabetes* **51**(11): 3189-3195.
- Chen, M.B., McAinch, A.J., Macaulay, S.L., Castelli, L.A., O'Brien, P.E., Dixon, J.B., et al. (2005). Impaired activation of AMP-kinase and fatty acid oxidation by globular adiponectin in cultured human skeletal muscle of obese type 2 diabetics. *J Clin Endocrinol Metab* **90**(6): 3665-3672.
- Chirala, S.S., Chang, H., Matzuk, M., Abu-Elheiga, L., Mao, J., Mahon, K., et al. (2003). Fatty acid synthesis is essential in embryonic development: fatty acid synthase null mutants and most of the heterozygotes die in utero. *Proc Natl Acad Sci U S A* **100**(11): 6358-6363.
-

-
- Chisholm, K.W. & O'Dea, K. (1987). Effect of short-term consumption of a high fat diet on glucose tolerance and insulin sensitivity in the rat. *J Nutr Sci Vitaminol (Tokyo)* **33**(5): 377-390.
- Chitturi, S., Abeygunasekera, S., Farrell, G.C., Holmes-Walker, J., Hui, J.M., Fung, C., et al. (2002). NASH and insulin resistance: Insulin hypersecretion and specific association with the insulin resistance syndrome. *Hepatology* **35**(2): 373-379.
- Chocian, G., Chabowski, A., Zendzian-Piotrowska, M., Harasim, E., Łukaszuk, B. & Górski, J. (2010). High fat diet induces ceramide and sphingomyelin formation in rat's liver nuclei. *Mol Cell Biochem* **340**(1-2): 125-131.
- Choi, C.S., Savage, D.B., Abu-Elheiga, L., Liu, Z.X., Kim, S., Kulkarni, A., et al. (2007). Continuous fat oxidation in acetyl-CoA carboxylase 2 knockout mice increases total energy expenditure, reduces fat mass, and improves insulin sensitivity. *Proc Natl Acad Sci U S A* **104**(42): 16480-16485.
- Chokkalingam, K., Jewell, K., Norton, L., Littlewood, J., van Loon, L.J.C., Mansell, P., et al. (2007). High-fat/low-carbohydrate diet reduces insulin-stimulated carbohydrate oxidation but stimulates nonoxidative glucose disposal in humans: An important role for skeletal muscle pyruvate dehydrogenase kinase 4. *J Clin Endocrinol Metab* **92**(1): 284-292.
- Chomentowski, P., Coen, P.M., Radiková, Z., Goodpaster, B.H. & Toledo, F.G. (2011). Skeletal muscle mitochondria in insulin resistance: differences in intermyofibrillar versus subsarcolemmal subpopulations and relationship to metabolic flexibility. *J Clin Endocrinol Metab* **96**(2): 494-503.
- Chong, E.W.T., Sinclair, A.J. & Guymer, R.H. (2006). Facts on fats. *Clin Experiment Ophthalmol* **34**(5): 464-471.
- Cinti, S. (2005). The adipose organ. *Prostaglandins Leukot Essent Fatty Acids* **73**(1): 9-15.
- Clarke, D.C., Miskovic, D., Han, X.X., Calles-Escandon, J., Glatz, J.F., Luiken, J.J., et al. (2004). Overexpression of membrane-associated fatty acid binding protein (FABPpm) in vivo increases fatty acid sarcolemmal transport and metabolism. *Physiol Genomics* **17**(1): 31-37.
- Coburn, C.T., Knapp, F.F.J., Febbraio, M., Beets, A.L., Silverstein, R.L. & Abumrad, N.A. (2000). Defective uptake and utilization of long chain fatty acids in muscle and adipose tissue of CD36 knockout mice. *J Biol Chem* **275**(42): 32523-32529.
- Coe, N.R., Smith, A.J., Frohnert, B.I., Watkins, P.A. & Bernlohr, D.A. (1999). The fatty acid transport protein (FATP1) is a very long chain acyl-CoA synthetase. *J Biol Chem* **274**(51): 36300-36304.
-

- Coletta, D.K., Sriwijitkamol, A., Wajcberg, E., Tantiwong, P., Li, M., Prentki, M., et al. (2009). Pioglitazone stimulates AMP-activated protein kinase signalling and increases the expression of genes involved in adiponectin signalling, mitochondrial function and fat oxidation in human skeletal muscle in vivo: a randomised trial. *Diabetologia* **52**(4): 723-732.
- Commerford, S.R., Ferniza, J.B., Bizeau, M.E., Thresher, J.S., Willis, W.T. & Pagliassotti, M.J. (2002). Diets enriched in sucrose or fat increase gluconeogenesis and G-6-Pase but not basal glucose production in rats. *Am J Physiol Endocrinol Metab* **283**(3): E545-555.
- Corton, J.M., Gillespie, J.G. & Hardie, D.G. (1994). Role of the AMP-activated protein kinase in the cellular stress response. *Curr Biol* **4**(4): 315-324.
- Cresser, J., Bonen, A., Chabowski, A., Stefanyk, L.E., Gulli, R., Ritchie, I., et al. (2010). Oral administration of a PPAR-delta agonist to rodents worsens, not improves, maximal insulin-stimulated glucose transport in skeletal muscle of different fibers. *Am J Physiol Regul Integr Comp Physiol* **299**(2): R470-479.
- D'Alessandro, M.E., Chicco, A. & Lombardo, Y.B. (2008). Dietary fish oil reverses lipotoxicity, altered glucose metabolism, and nPKCepsilon translocation in the heart of dyslipemic insulin-resistant rats. *Metabolism* **57**(7): 911-919.
- Da Silva, D., Zancan, P., Coelho, W.S., Gomez, L.S. & Sola-Penna, M. (2010). Metformin reverses hexokinase and 6-phosphofructo-1-kinase inhibition in skeletal muscle, liver and adipose tissues from streptozotocin-induced diabetic mouse. *Arch Biochem Biophys* **496**(1): 53-60.
- Dahlberg, E. (1982). Characterization of the cytosolic estrogen receptor in rat skeletal muscle. *Biochim Biophys Acta* **717**(1): 65-75.
- Dauncey, M.J. (1986). Activity-induced thermogenesis in lean and genetically obese (ob/ob) mice. *Cell Mol Life Sci* **42**(5): 547-549.
- Davidson, M.H. (2006). Mechanisms for the hypotriglyceridemic effect of marine omega-3 fatty acids. *Am J Cardiol* **98**(4, Suppl 1): 27-33.
- De Craemer, D., Vamecq, J., Roels, F., Vallée, L., Pauwels, M. & Van den Branden, C. (1994). Peroxisomes in liver, heart, and kidney of mice fed a commercial fish oil preparation: original data and review on peroxisomal changes induced by high-fat diets. *J Lipid Res* **35**(7): 1241-1250.
- de Meijer, V.E., Le, H.D., Meisel, J.A., Sharif, M.R., Pan, A., Nosé, V., et al. (2010). Dietary fat intake promotes the development of hepatic steatosis independently from excess caloric consumption in a murine model. *Metabolism* **59**(8): 1092-1105.

- De Paepe, B., Smet, J., Lammens, M., Seneca, S., Martin, J.-J., De Bleecker, J., et al. (2009). Immunohistochemical analysis of the oxidative phosphorylation complexes in skeletal muscle from patients with mitochondrial DNA encoded tRNA gene defects. *J Clin Pathol* **62**(2): 172-176.
- de Wilde, J., Mohren, R., van den Berg, S., Boekschoten, M., Dijk, K.W.-V., de Groot, P., et al. (2008). Short-term high fat-feeding results in morphological and metabolic adaptations in the skeletal muscle of C57BL/6J mice. *Physiol Genomics* **32**(3): 360-369.
- DeFronzo, R.A., Tobin, J.D. & Andres, R. (1979). Glucose clamp technique: a method for quantifying insulin secretion and resistance. *Am J Physiol Endocrinol Metab* **237**(3): E214-223.
- DeLany, J.P., Windhauser, M.M., Champagne, C.M. & Bray, G.A. (2000). Differential oxidation of individual dietary fatty acids in humans. *Am J Clin Nutr* **72**(4): 905-911.
- Delp, M.D. & Duan, C. (1996). Composition and size of type I, IIA, IID/X and IIB fibers and citrate synthase activity of rat muscle. *J Appl Physiol* **80**(1): 261-270.
- Demaugre, F., Bonnefont, J.P., Mitchell, G., Nguyen-Hoang, N., Pelet, A., Rimoldi, M., et al. (1988). Hepatic and muscular presentations of carnitine palmitoyl transferase deficiency: two distinct entities. *Pediatr Res* **24**(3): 308-311.
- den Hoed, M., Hesselink, M.K.C., van Kranenburg, G.P.J. & Westerterp, K.R. (2008). Habitual physical activity in daily life correlates positively with markers for mitochondrial capacity. *J Appl Physiol* **105**(2): 561-568.
- Deng, X.-Q., Chen, L.-L. & Li, N.-X. (2007). The expression of SIRT1 in nonalcoholic fatty liver disease induced by high-fat diet in rats. *Liver Int* **27**(5): 708-715.
- Deng, X., Elam, M.B., Wilcox, H.G., Cagen, L.M., Park, E.A., Raghov, R., et al. (2004). Dietary olive oil and menhaden oil mitigate induction of lipogenesis in hyperinsulinemic corpulent JCR:LA-cp rats: microarray analysis of lipid-related gene expression. *Endocrinology* **145**(12): 5847-5861.
- Desvergne, B. & Wahli, W. (1999). Peroxisome proliferator-activated receptors: nuclear control of metabolism. *Endocr Rev* **20**(5): 649-688.
- Dickerson, L.M. & Carek, P.J. (2000). Drug therapy for obesity. *Am Fam Physician* **61**(7): 2131-2138.
- DiRusso, C.C., Li, H., Darwis, D., Watkins, P.A., Berger, J. & Black, P.N. (2005). Comparative biochemical studies of the murine fatty acid transport proteins (FATP) expressed in yeast. *J Biol Chem* **280**(17): 16829-16837.

- Dobrzyn, A., Dobrzyn, P., Lee, S.-H., Miyazaki, M., Cohen, P., Asilmaz, E., et al. (2005). Stearoyl-CoA desaturase-1 deficiency reduces ceramide synthesis by downregulating serine palmitoyltransferase and increasing beta-oxidation in skeletal muscle. *Am J Physiol Endocrinol Metab* **288**(3): E599-607.
- Dobrzyn, P., Dobrzyn, A., Miyazaki, M., Cohen, P., Asilmaz, E., Hardie, D.G., et al. (2004). Stearoyl-CoA desaturase 1 deficiency increases fatty acid oxidation by activating AMP-activated protein kinase in liver. *Proc Natl Acad Sci U S A* **101**(17): 6409-14.
- Doerge, H., Baillie, R.A., Ortegon, A.M., Tsang, B., Wu, Q., Punreddy, S., et al. (2006). Targeted deletion of FATP5 reveals multiple functions in liver metabolism: Alterations in hepatic lipid homeostasis. *Gastroenterology* **130**(4): 1245-1258.
- Doerge, H., Grimm, D., Falcon, A., Tsang, B., Storm, T.A., Xu, H., et al. (2008). Silencing of hepatic fatty acid transporter protein 5 in vivo reverses diet-induced non-alcoholic fatty liver disease and improves hyperglycemia. *J Biol Chem* **283**(32): 22186-22192.
- Doh, K.-O., Kim, Y.-W., Park, S.-Y., Lee, S.-K., Park, J.S. & Kim, J.-Y. (2005). Interrelation between long-chain fatty acid oxidation rate and carnitine palmitoyltransferase 1 activity with different isoforms in rat tissues. *Life Sci* **77**(4): 435-443.
- Dorfmeister, B., Brandlhofer, S., Schaap, F., Hermann, M., Fürnsinn, C., Hagerty, B., et al. (2006). Apolipoprotein AV does not contribute to hypertriglyceridaemia or triglyceride lowering by dietary fish oil and rosiglitazone in obese Zucker rats. *Diabetologia* **49**(6): 1324-1332.
- Dourmashkin, J.T., Chang, G.Q., Gayles, E.C., Hill, J.O., Fried, S.K., Julien, C., et al. (2005). Different forms of obesity as a function of diet composition. *Int J Obes (Lond)* **29**(11): 1368-1378.
- Drewnowski, A. (2004). Obesity and the food environment: dietary energy density and diet costs. *Am J Prev Med* **27**(3 Suppl): 154-162.
- Drewnowski, A. (2007). The real contribution of added sugars and fats to obesity. *Epidemiol Rev* **29**(1): 160-171.
- Ducluzeau, P.H., Perretti, N., Laville, M., Andreelli, F., Vega, N., Riou, J.P., et al. (2001). Regulation by insulin of gene expression in human skeletal muscle and adipose tissue. Evidence for specific defects in type 2 diabetes. *Diabetes* **50**(5): 1134-1142.

-
- Dulloo, A.G., Gubler, M., Montani, J.P., Seydoux, J. & Solinas, G. (2004). Substrate cycling between de novo lipogenesis and lipid oxidation: a thermogenic mechanism against skeletal muscle lipotoxicity and glucolipotoxicity. *Int J Obes* **28**S29-37.
- Dunaway, G.A. & Kasten, T.P. (1987). Nature of the subunits of the 6-phosphofructo-1-kinase isoenzymes from rat tissues. *Biochem J* **242**(3): 667-671.
- Dunaway, G.A., Kasten, T.P., Sebo, T. & Trapp, R. (1988). Analysis of the phosphofructokinase subunits and isoenzymes in human tissues. *Biochem J* **251**(3): 677-683.
- Ebbesson, S.O., Kennish, J., Ebbesson, L., Go, O. & Yeh, J. (1999). Diabetes is related to fatty acid imbalance in Eskimos. *Int J Circumpolar Health* **58**(2): 108-119.
- Ebbesson, S.O., Risica, P.M., Ebbesson, L.O., Kennish, J.M. & Tejero, M.E. (2005). Omega-3 fatty acids improve glucose tolerance and components of the metabolic syndrome in Alaskan Eskimos: the Alaska Siberia project. *Int J Circumpolar Health* **64**(4): 396-408.
- Elliott, W.H. & Elliott, D.C. 2001. *Biochemistry and molecular biology*, 2nd Edition, Oxford; Melbourne, Oxford University Press 67-207.
- Engelking, L.J., Kuriyama, H., Hammer, R.E., Horton, J.D., Brown, M.S., Goldstein, J.L., et al. (2004). Overexpression of Insig-1 in the livers of transgenic mice inhibits SREBP processing and reduces insulin-stimulated lipogenesis. *J Clin Invest* **113**(8): 1168-1175.
- Engler, M., Bellenger-Germain, S., Engler, M., Narce, M. & Poisson, J.-P. (2000). Dietary docosahexaenoic acid affects stearic acid desaturation in spontaneously hypertensive rats. *Lipids* **35**(9): 1011-1015.
- Escher, P., Braissant, O., Basu-Modak, S., Michalik, L., Wahli, W. & Desvergne, B. (2001). Rat PPARs: Quantitative analysis in adult rat tissues and regulation in fasting and refeeding. *Endocrinology* **142**(10): 4195-4202.
- Essén, B., Jansson, E., Henriksson, J., Taylor, A.W. & Saltin, B. (1975). Metabolic characteristics of fibre types in human skeletal muscle. *Acta Physiol Scand* **95**(2): 153-165.
- Extier, A., Langelier, B., Perruchot, M.H., Guesnet, P., Van Veldhoven, P.P., Lavialle, M., et al. (2010). Gender affects liver desaturase expression in a rat model of n-3 fatty acid repletion. *J Nutr Biochem* **21**(3): 180-187.
-

-
- Fajas, L., Auboeuf, D., Raspé, E., Schoonjans, K., Lefebvre, A.M., Saladin, R., et al. (1997). The organization, promoter analysis, and expression of the human PPARgamma gene. *J Biol Chem* **272**(30): 18779-18789.
- Falcon, A., Doege, H., Fluitt, A., Tsang, B., Watson, N., Kay, M.A., et al. (2010). FATP2 is a hepatic fatty acid transporter and peroxisomal very long-chain acyl-CoA synthetase. *Am J Physiol Endocrinol Metab* **299**(3): E384-393.
- Febbraio, M., Abumrad, N.A., Hajjar, D.P., Sharma, K., Cheng, W., Pearce, S.F.A., et al. (1999). A null mutation in murine CD36 reveals an important role in fatty acid and lipoprotein metabolism. *J Biol Chem* **274**(27): 19055-19062.
- Febbraio, M., Hajjar, D.P. & Silverstein, R.L. (2001). CD36: a class B scavenger receptor involved in angiogenesis, atherosclerosis, inflammation, and lipid metabolism. *J Clin Invest* **108**(6): 785-791.
- Fedor, D. & Kelley, D.S. (2009). Prevention of insulin resistance by n-3 polyunsaturated fatty acids. *Curr Opin Clin Nutr Metab Care* **12**(2): 138-146.
- Ferrannini, E., Bjorkman, O., Reichard, G.A.J., Pilo, A., Olsson, M., Wahren, J., et al. (1985). The disposal of an oral glucose load in healthy subjects. A quantitative study. *Diabetes* **34**(6): 580-588.
- Ferre, T., Riu, E., Bosch, F. & Valera, A. (1996). Evidence from transgenic mice that glucokinase is rate limiting for glucose utilization in the liver. *FASEB J* **10**(10): 1213-1218.
- Ferre, T., Riu, E., Franckhauser, S., Agudo, J. & Bosch, F. (2003). Long-term overexpression of glucokinase in the liver of transgenic mice leads to insulin resistance. *Diabetologia* **46**(12): 1662-1668.
- Field, F.J., Born, E., Murthy, S. & Mathur, S.N. (2002). Polyunsaturated fatty acids decrease the expression of sterol regulatory element-binding protein-1 in CaCo-2 cells: effect on fatty acid synthesis and triacylglycerol transport. *Biochem J* **368**(Pt 3): 855-864.
- Flachs, P., Mohamed-Ali, V., Horakova, O., Rossmeisl, M., Hosseinzadeh-Attar, M., Hensler, M., et al. (2006). Polyunsaturated fatty acids of marine origin induce adiponectin in mice fed a high-fat diet. *Diabetologia* **49**(2): 394-397.
- Foretz, M., Ancellin, N., Andreelli, F., Saintillan, Y., Grondin, P., Kahn, A., et al. (2005). Short-term overexpression of a constitutively active form of AMP-activated protein kinase in the liver leads to mild hypoglycemia and fatty liver. *Diabetes* **54**(5): 1331-1339.
-

-
- Fredrikson, G. & Belfrage, P. (1983). Positional specificity of hormone-sensitive lipase from rat adipose tissue. *J Biol Chem* **258**:14253-14256.
- Fredrikson, G., Stralfors, P., Nilsson, N.O. & Belfrage, P. (1981). Hormone-sensitive lipase of rat adipose tissue: purification and some properties. *J Biol Chem* **256**:6311-6320.
- Freitas, E.M.S., Dal Pai Silva, M. & da Cruz-Höfling, M.A. (2002). Histochemical differences in the responses of predominantly fast-twitch glycolytic muscle and slow-twitch oxidative muscle to veratrine. *Toxicon* **40**(10): 1471-1481.
- Fryer, L.G.D., Orfali, K.A., Holness, M.J., Saggerson, E.D. & Sugden, M.C. (1995). The long-term regulation of skeletal muscle pyruvate dehydrogenase kinase by dietary lipid is dependent on fatty acid composition. *Eur J Biochem* **229**(3): 741-748.
- FSANZ (2009a). Food Standards Australia New Zealand: Intakes of trans fatty acids in New Zealand and Australia. <http://www.foodstandards.gov.au/>. Website viewed 21 September 2010.
- FSANZ (2009b). Food Standards Australia New Zealand: Trans fatty acids in the New Zealand and Australian food supply. <http://www.foodstandards.gov.au/>. Website viewed 21 September 2010.
- Fu, J., Oveisi, F., Gaetani, S., Lin, E. & Piomelli, D. (2005). Oleoylethanolamide, an endogenous PPAR- α agonist, lowers body weight and hyperlipidemia in obese rats. *Neuropharmacology* **48**(8): 1147-1153.
- Fu, M.H., Maher, A.C., Hamadeh, M.J., Ye, C. & Tarnopolsky, M.A. (2009). Exercise, sex, menstrual cycle phase, and 17 β -estradiol influence metabolism-related genes in human skeletal muscle. *Physiol Genomics* **40**(1): 34-47.
- Gaíva, M.H., Couto, R.C., Oyama, L.M., Couto, G.E.C., Silveira, V.L.F., Ribeiro, E.B., et al. (2003). Diets rich in polyunsaturated fatty acids: Effect on hepatic metabolism in rats. *Nutrition* **19**(2): 144-149.
- Gao, X.F., Chen, W., Kong, X.P., Xu, A.M., Wang, Z.G., Sweeney, G., et al. (2009). Enhanced susceptibility of Cpt1c knockout mice to glucose intolerance induced by a high-fat diet involves elevated hepatic gluconeogenesis and decreased skeletal muscle glucose uptake. *Diabetologia* **52**(5): 912-920.
- García-Martínez, C., Marotta, M., Moore-Carrasco, R., Guitart, M., Camps, M., Busquets, S., et al. (2005). Impact on fatty acid metabolism and differential localization of FATP1 and FAT/CD36 proteins delivered in cultured human muscle cells. *Am J Physiol Cell Physiol* **288**(6): C1264-1272.
-

-
- García, M., Pujol, A., Ruzo, A., Riu, E., Ruberte, J., Arbós, A., et al. (2009). Phosphofructo-1-kinase deficiency leads to a severe cardiac and hematological disorder in addition to skeletal muscle glycogenosis. *PLoS Genet* **5**(8): e1000615.
- Geelen, S.N., Blázquez, C., Geelen, M.J., Sloet van Oldruitenborgh-Oosterbaan, M.M. & Beynen, A.C. (2001). High fat intake lowers hepatic fatty acid synthesis and raises fatty acid oxidation in aerobic muscle in Shetland ponies. *Br J Nutr* **86**(1): 31-36.
- Geer, E.B. & Shen, W. (2009). Gender differences in insulin resistance, body composition, and energy balance. *Gend Med* **6**(Suppl 1): 60-75.
- Gehrich, S.C., Gekakis, N. & Sul, H.S. (1988). Liver (B-type) phosphofructokinase mRNA. Cloning, structure and expression. *J Biol Chem* **263**(24): 11755-11759.
- Getty-Kaushik, L., Viereck, J.C., Goodman, J.M., Guo, Z., LeBrasseur, N.K., Richard, A.M., et al. (2010). Mice deficient in phosphofructokinase-M have greatly decreased fat stores. *Obesity (Silver Spring)* **18**(3): 434-440.
- Gibbons, G.F., Wiggins, D., Brown, A.M. & Hebbachi, A.M. (2004). Synthesis and function of hepatic very-low-density lipoprotein. *Biochem Soc Trans* **32**(Pt 1): 59-64.
- Gilboe, D.P. & Nuttall, F.Q. (1982). Stimulation of liver glycogen particle synthase D phosphatase activity by caffeine, AMP, and glucose 6-phosphate. *Arch Biochem Biophys* **219**(1): 179-185.
- Gimeno, R.E., Hirsch, D.J., Punreddy, S., Sun, Y., Ortegon, A.M., Wu, H., et al. (2003a). Targeted deletion of fatty acid transport protein-4 results in early embryonic lethality. *J Biol Chem* **278**(49): 49512-49516.
- Gimeno, R.E., Ortegon, A.M., Patel, S., Punreddy, S., Ge, P., Sun, Y., et al. (2003b). Characterization of a heart-specific fatty acid transport protein. *J Biol Chem* **278**(18): 16039-16044.
- Glatz, J.F., Luiken, J.J. & Bonen, A. (2010). Membrane fatty acid transporters as regulators of lipid metabolism: implications for metabolic disease. *Physiol Rev* **90**(1): 367-417.
- Glatz, J.F.C., Luiken, J.J.F.P., van Bilsen, M. & van der Vusse, G.J. (2002). Cellular lipid binding proteins as facilitators and regulators of lipid metabolism. *Mol Cell Biochem* **239**(1): 3-7.
-

- Gómez-Pérez, Y., Amengual-Cladera, E., Català-Niell, A., Thomàs-Moyà, E., Gianotti, M., Proenza, A.M., et al. (2008). Gender dimorphism in high-fat-diet-induced insulin resistance in skeletal muscle of aged rats. *Cell Physiol Biochem* **22**(5-6): 539-548.
- Gomis, R.R., Cid, E., García-Rocha, M., Ferrer, J.C. & Guinovart, J.J. (2002). Liver glycogen synthase but not the muscle isoform differentiates between glucose 6-phosphate produced by glucokinase or hexokinase. *J Biol Chem* **277**(26): 23246-23252.
- Goodpaster, B.H., He, J., Watkins, S. & Kelley, D.E. (2001). Skeletal muscle lipid content and insulin resistance: evidence for a paradox in endurance-trained athletes. *J Clin Endocrinol Metab* **86**(12): 5755-5761.
- Goodpaster, B.H., Thaete, F.L., Simoneau, J.A. & Kelley, D.E. (1997). Subcutaneous abdominal fat and thigh muscle composition predict insulin sensitivity independently of visceral fat. *Diabetes* **46**(10): 1579-1585.
- Goodyear, L.J., Giorgino, F., Sherman, L.A., Carey, J., Smith, R.J. & Dohm, G.L. (1995). Insulin receptor phosphorylation, insulin receptor substrate-1 phosphorylation, and phosphatidylinositol 3-kinase activity are decreased in intact skeletal muscle strips from obese subjects. *J Clin Invest* **95**(5): 2195-2204.
- Gorman, T., Hope, D.C.D., Brownlie, R., Yu, A., Gill, D., Löfvenmark, J., et al. (2008). Effect of high-fat diet on glucose homeostasis and gene expression in glucokinase knockout mice. *Diabetes Obes Metab* **10**(10): 885-897.
- Goudriaan, J.R., Dahlmans, V.E.H., Teusink, B., Ouwens, D.M., Febbraio, M., Maassen, J.A., et al. (2003). CD36 deficiency increases insulin sensitivity in muscle, but induces insulin resistance in the liver in mice. *J Lipid Res* **44**(12): 2270-2277.
- Green, H.J., Fraser, I.G. & Ranney, D.A. (1984). Male and female differences in enzyme activities of energy metabolism in vastus lateralis muscle. *J Neurol Sci* **65**(3): 323-331.
- Green, H.J., Reichmann, H. & Pette, D. (1982). A comparison of two ATPase based schemes for histochemical muscle fibre typing in various mammals. *Histochemistry* **76**(1): 21-31.
- Green, H.J., Reichmann, H. & Pette, D. (1983). Fibre type specific transformations in the enzyme activity pattern of rat vastus lateralis muscle by prolonged endurance training. *Pflugers Arch* **399**(3): 216-222.

- Greenberg, A.S. & Obin, M.S. (2006). Obesity and the role of adipose tissue in inflammation and metabolism. *Am J Clin Nutr* **83**(2): 461S-465.
- Greene, E.C. 1955. *Anatomy of the rat*, New York, Hafner Publishing Co. 82 (Figure 100).
- Griffin, M.E., Marcucci, M.J., Cline, G.W., Bell, K., Barucci, N., Lee, D., et al. (1999). Free fatty acid-induced insulin resistance is associated with activation of protein kinase C theta and alterations in the insulin signaling cascade. *Diabetes* **48**(6): 1270-1274.
- Grundleger, M.L. & Thenen, S.W. (1982). Decreased insulin binding, glucose transport, and glucose metabolism in soleus muscle of rats fed a high fat diet. *Diabetes* **31**(3): 232-237.
- Guilherme, A., Virbasius, J.V., Puri, V. & Czech, M.P. (2008). Adipocyte dysfunctions linking obesity to insulin resistance and type 2 diabetes. *Nat Rev Mol Cell Biol* **9**(5): 367-377.
- Guillerm-Regost, C., Louveau, I., Sebert, S.P., Damon, M., Champ, M.M. & Gondret, F. (2006). Cellular and biochemical features of skeletal muscle in obese yucatan minipigs. *Obesity* **14**(10): 1700-1707.
- Gustafson, L.A., Kuipers, F., Wiegman, C., Sauerwein, H.P., Romijn, J.A. & Meijer, A.J. (2002). Clofibrate improves glucose tolerance in fat-fed rats but decreases hepatic glucose consumption capacity. *J Hepatol* **37**(4): 425-431.
- Guth, L. & Samaha, F.J. (1969). Qualitative differences between actomyosin ATPase of slow and fast mammalian muscle. *Exp Neurol* **25**(1): 138-152.
- Guth, L. & Samaha, F.J. (1970). Procedure for the histochemical demonstration of actomyosin ATPase. *Exp Neurol* **28**(2): 365-367.
- Gutiérrez-Juárez, R., Pocai, A., Mulas, C., Ono, H., Bhanot, S., Monia, B.P., et al. (2006). Critical role of stearoyl-CoA desaturase-1 (SCD1) in the onset of diet-induced hepatic insulin resistance. *J Clin Invest* **116**(6): 1686-95.
- Haemmerle, G., Zimmerman, R., Hayn, M., Theussl, C., Waeg, G. & Wagner, E. (2002). Hormone-sensitive lipase deficiency in mice causes diglyceride accumulation in adipose tissue, muscle and testis. *J Biol Chem* **277**(7): 4806-4815.
- Hageman, R.S., Wagener, A., Hantschel, C., Svenson, K.L., Churchill, G.A. & Brockmann, G.A. (2010). High-fat diet leads to tissue-specific changes reflecting risk factors for diseases in DBA/2J mice. *Physiol Genomics* **42**(1): 55-66.

- Hall, A.M., Smith, A.J. & Bernlohr, D.A. (2003). Characterization of the Acyl-CoA synthetase activity of purified murine fatty acid transport protein 1. *J Biol Chem* **278**(44): 43008-43013.
- Hallauer, P.L. & Hastings, K.E.M. (2000). Human cytomegalovirus IE1 promoter/enhancer drives variable gene expression in all fiber types in transgenic mouse skeletal muscle. *BMC Genetics* **1**(1): 1 - 1.
- Hamalainen, N. & Pette, D. (1993). The histochemical profiles of fast fiber types IIB, IID, and IIA in skeletal muscles of mouse, rat, and rabbit. *J Histochem Cytochem* **41**(5): 733-743.
- Han, X.-X., Chabowski, A., Tandon, N.N., Calles-Escandon, J., Glatz, J.F.C., Luiken, J.J.F.P., et al. (2007). Metabolic challenges reveal impaired fatty acid metabolism and translocation of FAT/CD36 but not FABPpm in obese Zucker rat muscle. *Am J Physiol Endocrinol Metab* **293**(2): E566-575.
- Handschin, C., Chin, S., Li, P., Liu, F., Maratos-Flier, E., Lebrasseur, N.K., et al. (2007). Skeletal muscle fiber-type switching, exercise intolerance, and myopathy in PGC-1alpha muscle-specific knock-out animals. *J Biol Chem* **282**(41): 30014-30021.
- Harada, K., Shen, W.J., Patel, S., Natu, V., Wang, J., Osuga, J., et al. (2003). Resistance to high-fat diet-induced obesity and altered expression of adipose-specific genes in HSL-deficient mice. *Am J Physiol Endocrinol Metab* **285**(6): W1182-1195.
- Harada, N., Oda, Z., Hara, Y., Fujinami, K., Okawa, M., Ohbuchi, K., et al. (2007). Hepatic de novo lipogenesis is present in liver-specific ACC1-deficient mice. *Mol Cell Biol* **27**(5): 1881-1888.
- Hardie, D.G., Hawley, S.A. & Scott, J.W. (2006). AMP-activated protein kinase - development of the energy sensor concept. *J Physiol* **574**(1): 7-15.
- Hashimoto, E. & Tokushige, K. (2011). Prevalence, gender, ethnic variations, and prognosis of NASH. *J Gastroenterol* **46**(Suppl 1): 63-69.
- Haugaard, S.B., Mu, H., Vaag, A. & Madsbad, S. (2009). Intramyocellular triglyceride content in man, influence of sex, obesity and glycaemic control. *Eur J Endocrinol* **161**(1): 57-64.
- Hawes, M.L., Kennedy, W., O'Callaghan, M.W. & Thurberg, B.L. (2007). Differential muscular glycogen clearance after enzyme replacement therapy in a mouse model of Pompe disease. *Mol Genet Metab* **91**(4): 343-351.

-
- Heal, J.W. (1975). An animal activity monitor using a microwave Doppler system. *Med Biol Eng* **13**(2): 317.
- Heikkinen, S., Pietilä, M., Halmekytö, M., Suppola, S., Pirinen, E., Deeb, S.S., et al. (1999). Hexokinase II-deficient mice. Prenatal death of homozygotes without disturbances in glucose tolerance in heterozygotes. *J Biol Chem* **274**(32): 22517-22523.
- Helge, J.W., Ayre, K., Chaunchaiyakul, S., Hulbert, A.J., Kiens, B. & Storlien, L.H. (1998). Endurance in high-fat-fed rats: effects of carbohydrate content and fatty acid profile. *J Appl Physiol* **85**(4): 1342-1348.
- Herrmann, T., Buchkremer, F., Gosch, I., Hall, A.M., Bernlohr, D.A. & Stremmel, W. (2001). Mouse fatty acid transport protein 4 (FATP4): Characterization of the gene and functional assessment as a very long chain acyl-CoA synthetase. *Gene* **270**(1-2): 31-40.
- Herrmann, T., van der Hoeven, F., Grone, H.J., Stewart, A.F., Langbein, L., Kaiser, I., et al. (2003). Mice with targeted disruption of the fatty acid transport protein 4 (Fatp 4, Slc27a4) gene show features of lethal restrictive dermopathy. *J Cell Biol* **161**(6): 1105-1115.
- Hevener, A., Reichart, D., Janez, A. & Olefsky, J. (2002). Female rats do not exhibit free fatty acid-induced insulin resistance. *Diabetes* **51**(6): 1907-1912.
- Hickey, M.S., Carey, J.O., Azevedo, J.L., Houmard, J.A., Pories, W.J., Israel, R.G., et al. (1995). Skeletal muscle fiber composition is related to adiposity and in vitro glucose transport rate in humans. *Am J Physiol Endocrinol Metab* **268**(3): E453-457.
- Higuchi, T., Shirai, N., Saito, M., Suzuki, H. & Kagawa, Y. (2008). Levels of plasma insulin, leptin and adiponectin, and activities of key enzymes in carbohydrate metabolism in skeletal muscle and liver in fasted ICR mice fed dietary n-3 polyunsaturated fatty acids. *J Nutr Biochem* **19**(9): 577-586.
- Hihi, A.K., Michalik, L. & Wahli, W. (2002). PPARs: transcriptional effectors of fatty acids and their derivatives. *Cell Mol Life Sci* **59**(5): 790-798.
- Himms-Hagen, J. & Harper, M.-E. (2001). Physiological role of UCP3 may be export of fatty acids from mitochondria when fatty acid oxidation predominates: An hypothesis. *Exp Biol Med* **226**(2): 78-84.
- Hintz, C.S., Lowry, C.V., Kaiser, K.K., McKee, D. & Lowry, O.H. (1980). Enzyme levels in individual rat muscle fibers. *Am J Physiol Cell Physiol* **239**(3): C58-65.

- Hirai, T., Fukui, Y. & Motojima, K. (2007). PPARalpha agonists positively and negatively regulate the expression of several nutrient/drug transporters in mouse small intestine. *Biol Pharm Bull* **30**(11): 2185-2190.
- Hirsch, D., Stahl, A. & Lodish, H.F. (1998). A family of fatty acid transporters conserved from mycobacterium to man. *Proc Natl Acad Sci USA* **95**(15): 8625-8629.
- Holloway, G.P., Bezaire, V., Heigenhauser, G.J.F., Tandon, N.N., Glatz, J.F.C., Luiken, J.J.F.P., et al. (2006). Mitochondrial long chain fatty acid oxidation, fatty acid translocase/CD36 content and carnitine palmitoyltransferase I activity in human skeletal muscle during aerobic exercise. *J Physiol* **571**(1): 201-210.
- Holloway, G.P., Lally, J., Nickerson, J.G., Alkhateeb, H., Snook, L.A., Heigenhauser, G.J., et al. (2007a). Fatty acid binding protein facilitates sarcolemmal fatty acid transport but not mitochondrial oxidation in rat and human skeletal muscle. *J Physiol* **582**(Pt 1): 393-405.
- Holloway, G.P., Thrush, A.B., Heigenhauser, G.J.F., Tandon, N.N., Dyck, D.J., Bonen, A., et al. (2007b). Skeletal muscle mitochondrial FAT/CD36 and palmitate oxidation are not decreased in obese women. *Am J Physiol Endocrinol Metab* **292**(6): E1782-1789.
- Holmes, B.F., Kurth-Kraczek, E.J. & Winder, W.W. (1999). Chronic activation of 5'-AMP-activated protein kinase increases GLUT-4, hexokinase, and glycogen in muscle. *J Appl Physiol* **87**(5): 1990-1995.
- Holness, M.J., Bulmer, K., Smith, N.D. & Sugden, M.C. (2003a). Investigation of potential mechanisms regulating protein expression of hepatic pyruvate dehydrogenase kinase isoforms 2 and 4 by fatty acids and thyroid hormone. *Biochem J* **369**(Pt 3): 687-695.
- Holness, M.J., Greenwood, G.K., Smith, N.D. & Sugden, M.C. (2003b). Diabetogenic impact of long-chain ω -3 fatty acids on pancreatic β -cell function and the regulation of endogenous glucose production. *Endocrinology* **144**(9): 3958-3968.
- Holness, M.J., Kraus, A., Harris, R.A. & Sugden, M.C. (2000). Targeted upregulation of pyruvate dehydrogenase kinase (PDK)-4 in slow-twitch skeletal muscle underlies the stable modification of the regulatory characteristics of PDK induced by high-fat feeding. *Diabetes* **49**(5): 775-781.

-
- Holness, M.J., Smith, N.D., Greenwood, G.K. & Sugden, M.C. (2004). Acute omega-3 fatty acid enrichment selectively reverses high-saturated fat feeding-induced insulin hypersecretion but does not improve peripheral insulin resistance. *Diabetes* **53**(Suppl 1): S166-171.
- Horton, J.D., Goldstein, J.L. & Brown, M.S. (2002). SREBPs: activators of the complete program of cholesterol and fatty acid synthesis in the liver. *J Clin Invest* **109**(9): 1125.
- Hotta, K., Nakajima, H., Yamasaki, T., Hamaguchi, T., Kuwajima, M., Noguchi, T., et al. (1991). Rat-liver-type phosphofructokinase mRNA. Structure, tissue distribution and regulation. *Eur J Biochem* **202**(2): 293-298.
- Hou, X.G., Moser, S., Sarr, M.G., Thompson, G.B., Que, F.G. & Jensen, M.D. (2009). Visceral and subcutaneous adipose tissue diacylglycerol acyltransferase activity in humans. *Obesity (Silver Spring)* **17**(6): 1129-1134.
- Houten, S.M., Chegary, M., Te Brinke, H., Wijnen, W.J., Glatz, J.F., Luiken, J.J., et al. (2009). Pyruvate dehydrogenase kinase 4 expression is synergistically induced by AMP-activated protein kinase and fatty acids. *Cell Mol Life Sci* **66**(7): 1283-1294.
- Howe, P., Meyer, B., Record, S. & Baghurst, K. (2006a). Dietary intake of long-chain omega-3 polyunsaturated fatty acids: contribution of meat sources. *Nutrition* **22**(1): 47-53.
- Howe, P., Mori, T. & Buckley, J. (2006b). The relationship between omega-3 fatty acid intake and risk of cardiovascular disease. A review of diet-disease relationship prepared for Food Standards Australia and New Zealand. <http://www.foodstandards.gov.au/>. Website viewed 21 September 2010.
- Hsieh, M.C., Yang, S.C., Tseng, H.L., Hwang, L.L., Chen, C.T. & Shieh, K.R. (2010). Abnormal expressions of circadian-clock and circadian clock-controlled genes in the livers and kidneys of long-term, high-fat-diet-treated mice. *Int J Obes (Lond)* **34**(2): 227-239.
- Hu, C.C., Qing, K. & Chen, Y. (2004). Diet-induced changes in stearoyl-CoA desaturase 1 expression in obesity-prone and -resistant mice. *Obes Res* **12**(8): 1264-1270.
- Hu, F.B., van Dam, R.M. & Liu, S. (2001). Diet and risk of Type II diabetes: the role of types of fat and carbohydrate. *Diabetologia* **44**(7): 805-817.
- Hu, T., Foxworthy, P., Siesky, A., Ficorilli, J.V., Gao, H., Li, S., et al. (2005). Hepatic peroxisomal fatty acid beta-oxidation is regulated by liver X receptor alpha. *Endocrinology* **146**(12): 5380-5387.
-

-
- Huang, B., Wu, P., Bowker-Kinley, M.M. & Harris, R.A. (2002). Regulation of pyruvate dehydrogenase kinase expression by peroxisome proliferator-activated receptor-alpha ligands, glucocorticoids, and insulin. *Diabetes* **51**(2): 276-283.
- Huang, X., Hansson, M., Laurila, E., Ahrén, B. & Groop, L. (2003). Fat feeding impairs glycogen synthase activity in mice without effects on its gene expression. *Metabolism* **52**(5): 535-539.
- Hue, L. & Taegtmeyer, H. (2009). The Randle cycle revisited: a new head for an old hat. *Am J Physiol Endocrinol Metab* **297**(3): E578-591.
- Hwang, J.-H., Pan, J.W., Heydari, S., Hetherington, H.P. & Stein, D.T. (2001). Regional differences in intramyocellular lipids in humans observed by in vivo ¹H-MR spectroscopic imaging. *J Appl Physiol* **90**(4): 1267-1274.
- Ibrahimi, A., Bonen, A., Blinn, W.D., Hajri, T., Li, X., Zhong, K., et al. (1999). Muscle-specific overexpression of FAT/CD36 enhances fatty acid oxidation by contracting muscle, reduces plasma triglycerides and fatty acids, and increases plasma glucose and insulin. *J Biol Chem* **274**(38): 26761-26766.
- Ibrahimi, A., Sfeir, Z., Magharaie, H., Amri, E.Z., Grimaldi, P. & Abumrad, N.A. (1996). Expression of the CD36 homolog (FAT) in fibroblast cells: effects on fatty acid transport. *Proc Natl Acad Sci U S A* **93**(7): 2646-2651.
- Ikemoto, S., Takahashi, M., Tsunoda, N., Maruyama, K., Itakura, H. & Ezaki, O. (1996). High-fat diet-induced hyperglycemia and obesity in mice: differential effects of dietary oils. *Metabolism* **45**(12): 1539-1546.
- Im, S.S., Hammond, L.E., Yousef, L., Nugas-Selby, C., Shin, D.J., Seo, Y.K., et al. (2009). Sterol regulatory element binding protein 1a regulates hepatic fatty acid partitioning by activating acetyl coenzyme A carboxylase 2. *Mol Cell Biol* **29**(17): 4864-4872.
- Ito, M., Suzuki, J., Tsujioka, S., Sasaki, M., Gomori, A., Shirakura, T., et al. (2007). Longitudinal analysis of murine steatohepatitis model induced by chronic exposure to high-fat diet. *Hepatol Res* **37**(1): 50-57.
- Ivy, J.L. & Kuo, C.-H. (1998). Regulation of GLUT4 protein and glycogen synthase during muscle glycogen synthesis after exercise. *Acta Physiol Scand* **162**(3):295-304.
- Ivy, J.L., Sherman, W.M., Cutler, C.L. & Katz, A.L. (1986). Exercise and diet reduce muscle insulin resistance in obese Zucker rat. *Am J Physiol* **251**(3 Pt 1): E299-E305.
-

-
- Iynedjian, P.B., Pilot, P.R., Nospikel, T., Milburn, J.L., Quaade, C., Hughes, S., et al. (1989). Differential expression and regulation of the glucokinase gene in liver and islets of Langerhans. *Proc Natl Acad Sci U S A* **86**(20): 7838-7842.
- Jain, S.S., Chabowski, A., Snook, L.A., Schwenk, R.W., Glatz, J.F., Luiken, J.J., et al. (2009). Additive effects of insulin and muscle contraction on fatty acid transport and fatty acid transporters, FAT/CD36, FABPpm, FATP1, 4 and 6. *FEBS Lett* **583**(13): 2294-2300.
- James, D.E., Zorzano, A., Böni-Schnetzler, M., Nemenoff, R.A., Powers, A., Pilch, P.F., et al. (1986). Intrinsic differences of insulin receptor kinase activity in red and white muscle. *J Biol Chem* **261**(32): 14939-14944.
- Janovská, A., Hatzinikolas, G., Mano, M. & Wittert, G.A. (2010). The effect of dietary fat content on phospholipid fatty acid profile is muscle fiber type dependent. *Am J Physiol Endocrinol Metab* **298**(4):E779-786.
- Jaworowski, A., Porter, M.M., Holmbäck, A.M., Downham, D. & Lexell, J. (2002). Enzyme activities in the tibialis anterior muscle of young moderately active men and women: relationship with body composition, muscle cross-sectional area and fibre type composition. *Acta Physiol Scand* **176**(3): 215-225.
- Jelenik, T., Rossmeisl, M., Kuda, O., Jilkova, Z.M., Medrikova, D., Kus, V., et al. (2010). AMP-activated protein kinase $\alpha 2$ subunit is required for the preservation of hepatic insulin sensitivity by n-3 polyunsaturated fatty acids. *Diabetes* **59**(11): 2737-2746.
- Jeong, S. & Yoon, M. (2009). Fenofibrate inhibits adipocyte hypertrophy and insulin resistance by activating adipose PPARalpha in high fat diet-induced obese mice. *Exp Mol Med* **41**(6): 397-405.
- Jeoung, N.H. & Harris, R.A. (2008). Pyruvate dehydrogenase kinase-4 deficiency lowers blood glucose and improves glucose tolerance in diet-induced obese mice. *Am J Physiol Endocrinol Metab* **295**(1): E46-54.
- Jetton, T.L., Liang, Y., Pettepher, C.C., Zimmerman, E.C., Cox, F.G., Horvath, K., et al. (1994). Analysis of upstream glucokinase promoter activity in transgenic mice and identification of glucokinase in rare neuroendocrine cells in the brain and gut. *J Biol Chem* **269**(5): 3641-3654.
- Jeukendrup, A.E. (2002). Regulation of fat metabolism in skeletal muscle. *Ann NY Acad Sci* **967**(1): 217-235.
- Ji, S., You, Y., Kerner, J., Hoppel, C.L., Schoeb, T.R., Chick, W.S., et al. (2008). Homozygous carnitine palmitoyltransferase 1b (muscle isoform) deficiency is lethal in the mouse. *Mol Genet Metab* **93**(3): 314-322.

-
- Johnston, S.L., Souter, D.M., Tolkamp, B.J., Gordon, I.J., Illius, A.W., Kyriazakis, I., et al. (2007). Intake compensates for resting metabolic rate variation in female C57BL/6J mice fed high-fat diets. *Obesity (Silver Spring)* **15**(3): 600-606.
- Jørgensen, S.B., Nielsen, J.N., Birk, J.B., Olsen, G.S., Viollet, B., Andreelli, F., et al. (2004). The alpha2-5'AMP-activated protein kinase is a site 2 glycogen synthase kinase in skeletal muscle and is responsive to glucose loading. *Diabetes* **53**(12): 3074-3081.
- Jue, T., Rothman, D.L., Shulman, G.I., Tavitian, B.A., DeFronzo, R.A. & Shulman, R.G. (1989). Direct observation of glycogen synthesis in human muscle with ¹³C NMR. *Proc Natl Acad Sci U S A* **86**(12): 4489-4491.
- Jump, D.B., Clarke, S.D., Thelen, A. & Liimatta, M. (1994). Coordinate regulation of glycolytic and lipogenic gene expression by polyunsaturated fatty acids. *J Lipid Res* **35**(6): 1076-1084.
- Kahn, B.B., Alquier, T., Carling, D. & Hardie, D.G. (2005). AMP-activated protein kinase: Ancient energy gauge provides clues to modern understanding of metabolism. *Cell Metab* **1**(1): 15-25.
- Kamei, Y., Suzuki, M., Miyazaki, H., Tsuboyama-Kasaoka, N., Wu, J., Ishimi, Y., et al. (2005). Ovariectomy in mice decreases lipid metabolism-related gene expression in adipose tissue and skeletal muscle with increased body fat. *J Nutr Sci Vitaminol (Tokyo)* **51**(2): 110-117.
- Kanatani, Y., Usui, I., Ishizuka, K., Bukhari, A., Fujisaka, S., Urakaze, M., et al. (2007). Effects of pioglitazone on suppressor of cytokine signaling 3 expression: potential mechanisms for its effects on insulin sensitivity and adiponectin expression. *Diabetes* **56**(3): 795-803.
- Kano, S. & Doi, M. (2006). NO-1886 (Ibrolipim), a lipoprotein lipase-promoting agent, accelerates the expression of UCP3 messenger RNA and ameliorates obesity in ovariectomized rats. *Metabolism* **55**(2): 151-158.
- Karunaratne, J.F., Ashton, C.J. & Stickland, N.C. (2005). Fetal programming of fat and collagen in porcine skeletal muscles. *J Anat* **207**(6): 763-768.
- Katzen, H.M. (1967). The multiple forms of mammalian hexokinase and their significance to the action of insulin. *Adv Enzyme Regul* **5**: 335-356.
- Kelley, D., Mitrakou, A., Marsh, H., Schwenk, F., Benn, J., Sonnenberg, G., et al. (1988). Skeletal muscle glycolysis, oxidation, and storage of an oral glucose load. *J Clin Invest* **81**(5): 1563-1571.

-
- Kelley, D.E. & Storlien, L. 2004. Skeletal Muscle and Obesity. In: BRAY, G.A. & BOUCHARD, C. (Eds.) Handbook of obesity: etiology and pathophysiology. Second edition. New York, Marcel Dekker Inc.
- Keppler, D. & Decker, K. 1984. Glycogen. . In: BERGMAYER, H.U., BERGMAYER, J. & GRASSL, M. (Eds.) Methods of enzymatic analysis. Third edition. Weinheim, Verlag Chemie.
- Kern, M., Tapscott, E.B., Downes, D.L., Frisell, W.R. & Dohm, G.L. (1990). Insulin resistance induced by high-fat feeding is only partially reversed by exercise training. *Pflugers Arch* **417**(1): 79-83.
- Khan, A.H. & Pessin, J.E. (2002). Insulin regulation of glucose uptake: interplay of intracellular signalling pathways. *Diabetologia* **45**(11): 1475-1483.
- Kiens, B. (2006). Skeletal muscle lipid metabolism in exercise and insulin resistance. *Physiol Rev* **86**(1): 205-243.
- Kim, C.H., Kim, M.S., Youn, J.Y., Park, H.S., Song, H.S., Song, K.H., et al. (2003). Lipolysis in skeletal muscle is decreased in high-fat-fed rats. *Metabolism* **52**(12): 1586-1592.
- Kim, C.H., Youn, J.H., Park, J.Y., Hong, S.K., Park, K.S., Park, S.W., et al. (2000a). Effects of high-fat diet and exercise training on intracellular glucose metabolism in rats. *Am J Physiol Endocrinol Metab* **278**(6): E977-984.
- Kim, H.J., Takahashi, M. & Ezaki, O. (1999). Fish oil feeding decreases mature sterol regulatory element-binding protein 1 (SREBP-1) by down-regulation of SREBP-1c mRNA in mouse liver. A possible mechanism for down-regulation of lipogenic enzyme mRNAs. *J Biol Chem* **274**(36): 25892-25898.
- Kim, J.-J.P. & Battaile, K.P. (2002). Burning fat: the structural basis of fatty acid β -oxidation. *Curr Opin Struct Biol* **12**(6): 721-728.
- Kim, J.-Y., Hickner, R.C., Cortright, R.L., Dohm, G.L. & Houmard, J.A. (2000b). Lipid oxidation is reduced in obese human skeletal muscle. *Am J Physiol Endocrinol Metab* **279**(5): E1039-1044.
- Kim, J.-Y., Nolte, L.A., Hansen, P.A., Han, D.-H., Ferguson, K., Thompson, P.A., et al. (2000c). High-fat diet-induced muscle insulin resistance: relationship to visceral fat mass. *Am J Physiol Regul Integr Comp Physiol* **279**(6): R2057-2065.
- Kim, J.K., Wi, J.K. & Youn, J.H. (1996). Metabolic impairment precedes insulin resistance in skeletal muscle during high-fat feeding in rats. *Diabetes* **45**(5): 651-658.
-

-
- Kim, S.M., Rico, C.W., Lee, S.C. & Kang, M.Y. (2010). Modulatory effect of rice bran and phytic acid on glucose metabolism in high fat-fed C57BL/6N mice. *J Clin Biochem Nutr* **47**(1): 12-17.
- Kleemann, R., van Erk, M., Verschuren, L., van den Hoek, A.M., Koek, M., Wielinga, P.Y., et al. (2010). Time-resolved and tissue-specific systems analysis of the pathogenesis of insulin resistance. *PLoS One* **5**(1): e8817.
- Kliwer, S.A., Sundseth, S.S., Jones, S.A., Brown, P.J., Wisely, G.B., Koble, C.S., et al. (1997). Fatty acids and eicosanoids regulate gene expression through direct interactions with peroxisome proliferator-activated receptors alpha and gamma. *Proc Natl Acad Sci U S A* **94**(9): 4318-4323.
- Koonen, D.P., Jacobs, R.L., Febbraio, M., Young, M.E., Soltys, C.L., Ong, H., et al. (2007). Increased hepatic CD36 expression contributes to dyslipidemia associated with diet-induced obesity. *Diabetes* **56**(12): 2863-2871.
- Koonen, D.P.Y., Glatz, J.F.C., Bonen, A. & Luiken, J.J.F.P. (2005). Long-chain fatty acid uptake and FAT/CD36 translocation in heart and skeletal muscle. *Biochim Biophys Acta* **1736**(3): 163-180.
- Koval, J.A., DeFronzo, R.A., O'Doherty, R.M., Printz, R., Ardehali, H., Granner, D.K., et al. (1998). Regulation of hexokinase II activity and expression in human muscle by moderate exercise. *Am J Physiol* **274**(2 Pt 1): E304-308.
- Krachler, B., Eliasson, M., Stenlund, H., Johansson, I., Hallmans, G. & Lindahl, B. (2009). Population-wide changes in reported lifestyle are associated with redistribution of adipose tissue. *Scand J Public Health* **37**(5): 545-553.
- Kraemer, W.J., Staron, R.S., Gordon, S.E., Volek, J.S., Koziris, L.P., Duncan, N.D., et al. (2000). The effects of 10 days of spaceflight on the shuttle Endeavor on predominantly fast-twitch muscles in the rat. *Histochem Cell Biol* **114**(5): 349-355.
- Kramer, J.A., LeDeaux, J., Butteiger, D., Young, T., Crankshaw, C., Harlow, H., et al. (2003). Transcription profiling in rat liver in response to dietary docosahexaenoic acid implicates stearyl-Coenzyme A desaturase as a nutritional target for lipid lowering. *J Nutr* **133**(1): 57-66.
- Krebs, J.D., Browning, L.M., McLean, N.K., Rothwell, J.L., Mishra, G.D., Moore, C.S., et al. (2006). Additive benefits of long-chain n-3 polyunsaturated fatty acids and weight-loss in the management of cardiovascular disease risk in overweight hyperinsulinaemic women. *Int J Obes (Lond)* **30**(10): 1535-1544.
-

-
- Kreitzman, S.N., Coxon, A.Y. & Szaz, K.F. (1992). Glycogen storage: illusions of easy weight loss, excessive weight regain, and distortions in estimates of body composition. *Am J Clin Nutr* **56**(1): 292S-293.
- Kriketos, A.D., Pan, D.A., Lillioja, S., Cooney, G.J., Baur, L.A., Milner, M.R., et al. (1996). Interrelationships between muscle morphology, insulin action, and adiposity. *Am J Physiol Regul Integr Comp Physiol* **270**(6): R1332-1339.
- Krssak, M., Brehm, A., Bernroider, E., Anderwald, C., Nowotny, P., Dalla Man, C., et al. (2004). Alterations in postprandial hepatic glycogen metabolism in type 2 diabetes. *Diabetes* **53**(12): 3048-3056.
- Kruszynska, Y.T., Mulford, M.I., Baloga, J., Yu, J.G. & Olefsky, J.M. (1998). Regulation of skeletal muscle hexokinase II by insulin in nondiabetic and NIDDM subjects. *Diabetes* **47**(7): 1107-1113.
- Kuda, O., Jelenik, T., Jilkova, Z., Flachs, P., Rossmeisl, M., Hensler, M., et al. (2009). n-3 Fatty acids and rosiglitazone improve insulin sensitivity through additive stimulatory effects on muscle glycogen synthesis in mice fed a high-fat diet. *Diabetologia* **52**(5): 941-951.
- Lage, R., Diéguez, C., Vidal-Puig, A. & López, M. (2008). AMPK: a metabolic gauge regulating whole-body energy homeostasis. *Trends Mol Med* **14**(12): 539-549.
- Lara-Castro, C. & Garvey, W.T. (2008). Intracellular lipid accumulation in liver and muscle and the insulin resistance syndrome. *Endocrinol Metab Clin North Am* **37**(4): 841-856.
- Lardinois, C.K. (1987). The role of omega 3 fatty acids on insulin secretion and insulin sensitivity. *Med Hypotheses* **24**(3): 243-248.
- Latasa, M.J., Moon, Y.S., Kim, K.H. & Sul, H.S. (2000). Nutritional regulation of the fatty acid synthase promoter in vivo: sterol regulatory element binding protein functions through an upstream region containing a sterol regulatory element. *Proc Natl Acad Sci U S A* **97**(19): 10619-10624.
- Lavoie, J.M. & Gauthier, M.S. (2006). Regulation of fat metabolism in the liver: link to non-alcoholic hepatic steatosis and impact of physical exercise. *Cell Mol Life Sci* **63**(12): 1393-1409.
- Lawler, J.M., Powers, S.K., Visser, T., Van Dijk, H., Kordus, M.J. & Ji, L.L. (1993). Acute exercise and skeletal muscle antioxidant and metabolic enzymes: effects of fiber type and age. *Am J Physiol* **265**(6 Pt 2): R1344-1350.
- Lawrence, G.M. & Trayer, I.P. (1985). The localization of hexokinase isoenzymes in red and white skeletal muscles of the rat. *Histochem J* **17**(3): 353-371.
-

- LeBrasseur, N.K., Kelly, M., Tsao, T.S., Farmer, S.R., Saha, A.K., Ruderman, N.B., et al. (2006). Thiazolidinediones can rapidly activate AMP-activated protein kinase in mammalian tissues. *Am J Physiol Endocrinol Metab* **291**(1): E175-181.
- Lee, J.S., Pinnamaneni, S.K., Eo, S.J., Cho, I.H., Pyo, J.H., Kim, C.K., et al. (2006a). Saturated, but not n-6 polyunsaturated, fatty acids induce insulin resistance: role of intramuscular accumulation of lipid metabolites. *J Appl Physiol* **100**(5): 1467-1474.
- Lee, S.-H., Dobrzyn, A., Dobrzyn, P., Rahman, S.M., Miyazaki, M. & Ntambi, J.M. (2004). Lack of stearoyl-CoA desaturase 1 upregulates basal thermogenesis but causes hypothermia in a cold environment. *J Lipid Res* **45**(9): 1674-1682.
- Lee, W.J., Kim, M., Park, H.-S., Kim, H.S., Jeon, M.J., Oh, K.S., et al. (2006b). AMPK activation increases fatty acid oxidation in skeletal muscle by activating PPAR α and PGC-1. *Biochem Biophys Res Commun* **340**(1): 291-295.
- Leick, L., Fentz, J., Biensø, R.S., Knudsen, J.G., Jeppesen, J., Kiens, B., et al. (2010). PGC-1 alpha is required for AICAR-induced expression of GLUT4 and mitochondrial proteins in mouse skeletal muscle. *Am J Physiol Endocrinol Metab* **299**(3): E456-465.
- Leite, R.D., Prestes, J., Bernardes, C.F., Shiguemoto, G.E., Pereira, G.B., Duarte, J.O., et al. (2009). Effects of ovariectomy and resistance training on lipid content in skeletal muscle, liver, and heart; fat depots; and lipid profile. *Appl Physiol Nutr Metab* **34**(6): 1079-1086.
- Leonard, A.E., Pereira, S.L., Sprecher, H. & Huang, Y.S. (2004). Elongation of long-chain fatty acids. *Prog Lipid Res* **43**(1): 36-54.
- Li, Z.-f., Shelton, G.D. & Engvall, E. (2005). Elimination of myostatin does not combat muscular dystrophy in dy mice but increases postnatal lethality. *Am J Pathol* **166**(2): 491-497.
- Li, Z.Z., Berk, M., McIntyre, T.M. & Feldstein, A.E. (2009). Hepatic lipid partitioning and liver damage in nonalcoholic fatty liver disease: role of stearoyl-CoA desaturase. *J Biol Chem* **284**(9): 5637-5644.
- Liang, G., Yang, J., Horton, J.D., Hammer, R.E., Goldstein, J.L. & Brown, M.S. (2002). Diminished hepatic response to fasting/refeeding and liver X receptor agonists in mice with selective deficiency of sterol regulatory element-binding protein-1c. *J Biol Chem* **277**(11): 9520-9528.

- Liang, H. & Ward, W.F. (2006). PGC-1 α : a key regulator of energy metabolism. *Advan Physiol Edu* **30**(4): 145-151.
- Liberopoulos, E.N., Mikhailidis, D.P. & Elisaf, M.S. (2005). Diagnosis and management of the metabolic syndrome in obesity. *Obes Rev* **6**(4): 283-296.
- Lillie, R.D. 1965. Histopathologic technique and practical histochemistry, Third edition, New York, McGraw-Hill Book Co. 170-176.
- Lillioja, S., Young, A.A., Culter, C.L., Ivy, J.L., Abbott, W.G., Zawadzki, J.K., et al. (1987). Skeletal muscle capillary density and fiber type are possible determinants of in vivo insulin resistance in man. *J Clin Invest* **80**(2): 415-424.
- Lin, J., Wu, H., Tarr, P.T., Zhang, C.Y., Wu, Z., Boss, O., et al. (2002). Transcriptional co-activator PGC-1 alpha drives the formation of slow-twitch muscle fibres. *Nature* **418**(6899): 797-801.
- Litherland, N.B., Bionaz, M., Wallace, R.L., Loo, J.J. & Drackley, J.K. (2010). Effects of the peroxisome proliferator-activated receptor-alpha agonists clofibrate and fish oil on hepatic fatty acid metabolism in weaned dairy calves. *J Dairy Sci* **93**(6): 2404-2418.
- Little, T.J., Horowitz, M. & Feinle-Bisset, C. (2007). Modulation by high-fat diets of gastrointestinal function and hormones associated with the regulation of energy intake: implications for the pathophysiology of obesity. *Am J Clin Nutr* **86**(3): 531-541.
- Liu, L., Shi, X., Choi, C.S., Shulman, G.I., Klaus, K., Nair, K.S., et al. (2009). Paradoxical coupling of triglyceride synthesis and fatty acid oxidation in skeletal muscle overexpressing DGAT1. *Diabetes* **58**(11): 2516-2524.
- Liu, L., Zhang, Y., Chen, N., Shi, X., Tsang, B. & Yu, Y.-H. (2007). Upregulation of myocellular DGAT1 augments triglyceride synthesis in skeletal muscle and protects against fat-induced insulin resistance. *J Clin Invest* **117**(6): 1679-1689.
- Liu, Y., Shen, T., Randall, W. & Schneider, M. (2005). Signaling pathways in activity-dependent fiber type plasticity in adult skeletal muscle. *J Muscle Res Cell Motil* **26**(1): 13-21.
- Lloyd, A.C., Carpenter, C.A. & Saggerson, E.D. (1986). Intertissue differences in the hysteric behaviour of carnitine palmitoyltransferase in the presence of malonyl-CoA. *Biochem J* **237**(1): 289-291.

-
- Loizzo, A., Loizzo, S., Galietta, G., Caiola, S., Spampinato, S., Campana, G., et al. (2006). Overweight and metabolic and hormonal parameter disruption are induced in adult male mice by manipulations during lactation period. *Pediatr Res* **59**(1): 111-115.
- Lombardo, Y.B. & Chicco, A.G. (2006). Effects of dietary polyunsaturated n-3 fatty acids on dyslipidemia and insulin resistance in rodents and humans. A review. *J Nutr Biochem* **17**(1): 1-13.
- Long, Y.C. & Zierath, J.R. (2006). AMP-activated protein kinase signaling in metabolic regulation. *J Clin Invest* **116**(7): 1776-1783.
- Lopaschuk, G.D., Folmes, C.D.L. & Stanley, W.C. (2007). Cardiac energy metabolism in obesity. *Circ Res* **101**(4): 335-347.
- Lovejoy, J.C., Bray, G.A., Bourgeois, M.O., Macchiavelli, R., Rood, J.C., Greeson, C., et al. (1996). Exogenous androgens influence body composition and regional body fat distribution in obese postmenopausal women - a clinical research center study. *J Clin Endocrinol Metab* **81**(6): 2198-2203.
- Lovejoy, J.C., Sainsbury, A. & Group, S.C.W. (2009). Sex differences in obesity and the regulation of energy homeostasis. *Obesity Reviews* **10**: 154-167.
- Lovejoy, J.C., Windhauser, M.M., Rood, J.C. & de la Bretonne, J.A. (1998). Effect of a controlled high-fat versus low-fat diet on insulin sensitivity and leptin levels in African-American and Caucasian women. *Metabolism* **47**(12): 1520-1524.
- Luiken, J.J., Arumugam, Y., Bell, R.C., Calles-Escandon, J., Tandon, N.N., Glatz, J.F., et al. (2002). Changes in fatty acid transport and transporters are related to the severity of insulin deficiency. *Am J Physiol Endocrinol Metab* **283**(3): E612-E621.
- Luiken, J.J.F.P., Arumugam, Y., Dyck, D.J., Bell, R.C., Pelsers, M.M.L., Turcotte, L.P., et al. (2001). Increased rates of fatty acid uptake and plasmalemmal fatty acid transporters in obese Zucker rats. *J Biol Chem* **276**(44): 40567-40573.
- Luo, J., Sobkiw, C.L., Hirshman, M.F., Logsdon, M.N., Li, T.Q., Goodyear, L.J., et al. (2006). Loss of class IA PI3K signaling in muscle leads to impaired muscle growth, insulin response, and hyperlipidemia. *Cell Metab* **3**(5): 355-366.
- Manco, M., Mingrone, G., Greco, A.V., Capristo, E., Gniuli, D., De Gaetano, A., et al. (2000). Insulin resistance directly correlates with increased saturated fatty acids in skeletal muscle triglycerides. *Metabolism* **49**(2): 220-224.
- Mandard, S., Müller, M. & Kersten, S. (2004). Peroxisome proliferator-activated receptor alpha target genes. *Cell Mol Life Sci* **61**(4): 393-416.
-

- Mao, J., DeMayo, F.J., Li, H., Abu-Elheiga, L., Gu, Z., Shaikenov, T.E., et al. (2006). Liver-specific deletion of acetyl-CoA carboxylase 1 reduces hepatic triglyceride accumulation without affecting glucose homeostasis. *Proc Natl Acad Sci U S A* **103**(22): 8552-8557.
- Marchesini, G., Bugianesi, E., Forlani, G., Cerrelli, F., Lenzi, M., Manini, R., et al. (2003). Nonalcoholic fatty liver, steatohepatitis, and the metabolic syndrome. *Hepatology* **37**(4): 917-923.
- Mårin, P., Andersson, B., Krotkiewski, M. & Björntorp, P. (1994). Muscle fiber composition and capillary density in women and men with NIDDM. *Diabetes Care* **17**(5): 382-386.
- Marotta, M., Ferrer-Martinez, A., Parnau, J., Turini, M., Mace, K. & Gomez Foix, A.M. (2004). Fiber type- and fatty acid composition-dependent effects of high-fat diets on rat muscle triacylglyceride and fatty acid transporter protein-1 content. *Metabolism* **53**(8): 1032-1036.
- Marshall, J.A., Bessesen, D.H. & Hamman, R.F. (1997). High saturated fat and low starch and fibre are associated with hyperinsulinaemia in a non-diabetic population: the San Luis Valley Diabetes Study. *Diabetologia* **40**(4): 430-438.
- Mascaró, C., Acosta, E., Ortiz, J.A., Marrero, P.F., Hegardt, F.G. & Haro, D. (1998). Control of human muscle-type carnitine palmitoyltransferase I gene transcription by peroxisome proliferator-activated receptor. *J Biol Chem* **273**(15): 8560-3.
- Masterton, G.S., Plevris, J.N. & Hayes, P.C. (2010). Review article: omega-3 fatty acids - a promising novel therapy for non-alcoholic fatty liver disease. *Aliment Pharmacol Ther* **31**(7): 679-692.
- Mater, M.K., Thelen, A.P., Pan, D.A. & Jump, D.B. (1999). Sterol response element-binding protein 1c (SREBP1c) is involved in the polyunsaturated fatty acid suppression of hepatic S14 gene transcription. *J Biol Chem* **274**(46): 32725-32732.
- Matsumoto, E., Ishihara, A., Tamai, S., Nemoto, A., Iwase, K., Hiwasa, T., et al. (2010). Time of day and nutrients in feeding govern daily expression rhythms of the gene for sterol regulatory element-binding protein (SREBP)-1 in the mouse liver. *J Biol Chem* **285**(43): 33028-33036.
- Matsusue, K., Haluzik, M., Lambert, G., Yim, S.H., Gavrilova, O., Ward, J.M., et al. (2003). Liver-specific disruption of PPARgamma in leptin-deficient mice improves fatty liver but aggravates diabetic phenotypes. *J Clin Invest* **111**(5): 737-747.

-
- Maughan, R.J. & Williams, C. (1982). Muscle citrate content and the regulation of metabolism in fed and fasted human skeletal muscle. *Clin Physiol* **2**(1): 21-27.
- Mayer-Davis, E.J., Monaco, J.H., Hoen, H.M., Carmichael, S., Vitolins, M.Z., Rewers, M.J., et al. (1997). Dietary fat and insulin sensitivity in a triethnic population: the role of obesity. The Insulin Resistance Atherosclerosis Study (IRAS). *Am J Clin Nutr* **65**(1): 79-87.
- McAinch, A.J., Lee, J.-S., Bruce, C.R., Tunstall, R.J., Hawley, J.A. & Cameron-Smith, D. (2003). Dietary regulation of fat oxidative gene expression in different skeletal muscle fiber types. *Obes Res* **11**(12): 1471-1479.
- McGarry, J.D. & Brown, N.F. (1997). The mitochondrial carnitine palmitoyltransferase system. From concept to molecular analysis. *Eur J Biochem* **244**(1): 1-14.
- McGarry, J.D. & Foster, D.W. (1980). Regulation of hepatic fatty acid oxidation and ketone body production. *Annu Rev Biochem* **49**: 395-420.
- McGee, S.L., Howlett, K.F., Starkie, R.L., Cameron-Smith, D., Kemp, B.E. & Hargreaves, M. (2003). Exercise increases nuclear AMPK alpha2 in human skeletal muscle. *Diabetes* **52**(4): 926-928.
- McManus, B.M., Horley, K.J., Wilson, J.E., Malcom, G.T., Kendall, T.J., Miles, R.R., et al. (1995). Prominence of coronary arterial wall lipids in human heart allografts. Implications for pathogenesis of allograft arteriopathy. *Am J Pathol* **147**(2): 293-308.
- Memon, R.A., Tecott, L.H., Nonogaki, K., Beigneux, A., Moser, A.H., Grunfeld, C., et al. (2000). Up-regulation of peroxisome proliferator-activated receptors (PPAR- α) and PPAR- γ messenger ribonucleic acid expression in the liver in murine obesity: troglitazone induces expression of PPAR- γ -responsive adipose tissue-specific genes in the liver of obese diabetic mice. *Endocrinology* **141**(11): 4021-4031.
- Menendez, J.A., Vazquez-Martin, A., Ortega, F.J. & Fernandez-Real, J.M. (2009). Fatty acid synthase: association with insulin resistance, type 2 diabetes, and cancer. *Clin Chem* **55**(3): 425-438.
- Mercer, S.W. & Trayhurn, P. (1987). Effect of high fat diets on energy balance and thermogenesis in brown adipose tissue of lean and genetically obese ob/ob mice. *J Nutr* **117**(12): 2147-2153.
- Meyer, B., Mann, N., Lewis, J., Milligan, G., Sinclair, A. & Howe, P. (2003). Dietary intakes and food sources of omega-6 and omega-3 polyunsaturated fatty acids. *Lipids* **38**(4): 391-398.
-

-
- Michel, G. & Baulieu, E.-E. (1980). Androgen receptor in rat skeletal muscle: characterization and physiological variations. *Endocrinology* **107**(6): 2088-2098.
- Mills, S.E., Foster, D.W. & McGarry, J.D. (1983). Interaction of malonyl-CoA and related compounds with mitochondria from different rat tissues. Relationship between ligand binding and inhibition of carnitine palmitoyltransferase I. *Biochem J* **214**(1): 83-91.
- Mokdad, A.H., Ford, E.S., Bowman, B.A., Dietz, W.H., Vinicor, F., Bales, V.S., et al. (2003). Prevalence of obesity, diabetes, and obesity-related health risk factors, 2001. *JAMA* **289**(1): 76-79.
- Mooradian, A.D., Haas, M.J., Wehmeier, K.R. & Wong, N.C.W. (2008). Obesity-related changes in high-density lipoprotein metabolism. *Obesity* **16**(6): 1152-1160.
- Moore, M.C., Cherrington, A.D., Cline, G., Pagliassotti, M.J., Jones, E.M., Neal, D.W., et al. (1991). Sources of carbon for hepatic glycogen synthesis in the conscious dog. *J Clin Invest* **88**(2): 578-587.
- Mori, T., Kondo, H., Hase, T., Tokimitsu, I. & Murase, T. (2007). Dietary fish oil upregulates intestinal lipid metabolism and reduces body weight gain in C57BL/6J mice. *J Nutr* **137**(12): 2629-2634.
- Moro, C., Galgani, J.E., Luu, L., Pasarica, M., Mairal, A., Bajpeyi, S., et al. (2009). Influence of gender, obesity, and muscle lipase activity on intramyocellular lipids in sedentary individuals. *J Clin Endocrinol Metab* **94**(9): 3440-3447.
- Mortensen, O.H., Frandsen, L., Schjerling, P., Nishimura, E. & Grunnet, N. (2006). PGC-1alpha and PGC-1beta have both similar and distinct effects on myofiber switching toward an oxidative phenotype. *Am J Physiol Endocrinol Metab* **291**(4): E807-816.
- Motojima, K., Passilly, P., Peters, J.M., Gonzalez, F.J. & Latruffe, N. (1998). Expression of putative fatty acid transporter genes are regulated by peroxisome proliferator-activated receptor alpha and gamma activators in a tissue- and inducer-specific manner. *J Biol Chem* **273**(27): 16710-16714.
- Moulson, C.L., Martin, D.R., Lugas, J.J., Schaffer, J.E., Lind, A.C. & Miner, J.H. (2003). Cloning of wrinkle-free, a previously uncharacterized mouse mutation, reveals crucial roles for fatty acid transport protein 4 in skin and hair development. *Proc Natl Acad Sci U S A* **100**(9): 5274-5279.
- Moussavi, N., Gavino, V. & Receveur, O. (2008). Could the quality of dietary fat, not just its quantity, be related to risk of obesity? *Obesity (Silver Spring)* **16**(1): 7-15.

- Mukhtar, M.H., Payne, V.A., Arden, C., Harbottle, A., Khan, S., Lange, A.J., et al. (2008). Inhibition of glucokinase translocation by AMP-activated protein kinase is associated with phosphorylation of both GKRP and 6-phosphofructo-2-kinase/fructose-2,6-bisphosphatase. *Am J Physiol Regul Integr Comp Physiol* **294**(3): R766-774.
- Mullen, K.L., Smith, A.C., Junkin, K.A. & Dyck, D.J. (2007). Globular adiponectin resistance develops independently of impaired insulin-stimulated glucose transport in soleus muscle from high-fat-fed rats. *Am J Physiol Endocrinol Metab* **293**(1): E83-90.
- Mullen, K.L., Tishinsky, J.M., Robinson, L.E. & Dyck, D.J. (2010). Skeletal muscle inflammation is not responsible for the rapid impairment in adiponectin response with high-fat feeding in rats. *Am J Physiol Regul Integr Comp Physiol* **299**(2): R500-508.
- Murakami, R., Murakami, H., Kataoka, H., Cheng, X.W., Takahashi, R., Numaguchi, Y., et al. (2010). Unmetabolized fenofibrate, but not fenofibric acid, activates AMPK and inhibits the expression of phosphoenolpyruvate carboxykinase in hepatocytes. *Life Sci* **87**(15-16): 496-500.
- Musso, G., Gambino, R., De Michieli, F., Cassader, M., Rizzetto, M., Durazzo, M., et al. (2003). Dietary habits and their relations to insulin resistance and postprandial lipemia in nonalcoholic steatohepatitis. *Hepatology* **37**(4): 909-916.
- Nagle, C.A., Klett, E.L. & Coleman, R.A. (2009). Hepatic triacylglycerol accumulation and insulin resistance. *J Lipid Res* **50**(Suppl): S74-79.
- Nakajima, H., Raben, N., Hamaguchi, T. & Yamasaki, T. (2002). Phosphofructokinase deficiency; past, present and future. *Curr Mol Med* **2**(2): 197-212.
- Nakatani, T., Kim, H.J., Kaburagi, Y., Yasuda, K. & Ezaki, O. (2003). A low fish oil inhibits SREBP-1 proteolytic cascade, while a high-fish-oil feeding decreases SREBP-1 mRNA in mice liver: relationship to anti-obesity. *J Lipid Res* **44**(2): 369-379.
- Nakatani, T., Nakashima, T., Kita, T., Hirofuji, C., Itoh, K., Itoh, M., et al. (1999). Succinate dehydrogenase activities of fibers in the rat extensor digitorum longus, soleus, and cardiac muscles. *Arch Histol Cytol* **62**(4): 393-399.
- Negre-Salvayre, A., Hirtz, C., Carrera, G., Cazenave, R., Trolly, M., Salvayre, R., et al. (1997). A role for uncoupling protein-2 as a regulator of mitochondrial hydrogen peroxide generation. *FASEB J* **11**(10): 809-815.

-
- Nemeth, P.M., Rosser, B.W., Choksi, R.M., Norris, B.J. & Baker, K.M. (1992). Metabolic response to a high-fat diet in neonatal and adult rat muscle. *Am J Physiol* **262**(2 Pt 1): C282-286.
- Neschen, S., Moore, I., Regittnig, W., Yu, C.L., Wang, Y., Pypaert, M., et al. (2002). Contrasting effects of fish oil and safflower oil on hepatic peroxisomal and tissue lipid content. *Am J Physiol Endocrinol Metab* **282**(2): E395-401.
- Nettleton, J.A. (1995). Omega-3 fatty acids and health. USA: Chapman & Hall: A Thomson Publishing Company: New York, London. 1-359.
- Nettleton, J.A. & Katz, R. (2005). n-3 long-chain polyunsaturated fatty acids in type 2 diabetes: A review. *J Am Diet Assoc* **105**(3): 428-440.
- NHMRC (2006). National Health and Medical Research Council, Australia: Nutrient reference values for Australia and New Zealand. Including recommended dietary intakes.
http://www.nhmrc.gov.au/_files_nhmrc/file/publications/synopses/n35.pdf.
Website viewed 21 September 2010.
- Nickerson, J.G., Alkhateeb, H., Benton, C.R., Lally, J., Nickerson, J., Han, X.X., et al. (2009). Greater transport efficiencies of the membrane fatty acid transporters FAT/CD36 and FATP4 compared with FABPpm and FATP1 and differential effects on fatty acid esterification and oxidation in rat skeletal muscle. *J Biol Chem* **284**(24): 16522-30.
- Noh, S.K., Koo, S.I. & Jeon, I.J. (1999). Estradiol replacement in ovariectomized rats increases the hepatic concentration and biliary secretion of alpha-tocopherol and polyunsaturated fatty acids. *J Nutr Biochem* **10**(2): 110-117.
- Ntambi, J.M., Miyazaki, M., Stoehr, J.P., Lan, H., Kendzioriski, C.M., Yandell, B.S., et al. (2002). Loss of stearyl-CoA desaturase-1 function protects mice against adiposity. *Proc Natl Acad Sci U S A* **99**(17): 11482-11486.
- Nunnari, J.J., Zand, T., Joris, I. & Majno, G. (1989). Quantitation of oil red O staining of the aorta in hypercholesterolemic rats. *Exp Mol Pathol* **51**(1): 1-8.
- Nyman, L.R., Cox, K.B., Hoppel, C.L., Kerner, J., Barnoski, B.L., Hamm, D.A., et al. (2005). Homozygous carnitine palmitoyltransferase 1a (liver isoform) deficiency is lethal in the mouse. *Mol Genet Metab* **86**(1-2): 179-187.
- O'Doherty, R.M., Lehman, D.L., Télémaque-Potts, S. & Newgard, C.B. (1999). Metabolic impact of glucokinase overexpression in liver: lowering of blood glucose in fed rats is accompanied by hyperlipidemia. *Diabetes* **48**(10): 2022-2027.
-

-
- Oberbach, A., Bossenz, Y., Lehmann, S., Niebauer, J., Adams, V., Paschke, R., et al. (2006). Altered fiber distribution and fiber-specific glycolytic and oxidative enzyme activity in skeletal muscle of patients with type 2 diabetes. *Diabetes Care* **29**(4): 895-900.
- Ockner, R.K., Lysenko, N., Manning, J.A., Monroe, S.E. & Burnett, D.A. (1980). Sex steroid modulation of fatty acid utilization and fatty acid binding protein concentration in rat liver. *J Clin Invest* **65**(5): 1013-1023.
- Oh, S.-Y., Park, S.-K., Kim, J.-W., Ahn, Y.-H., Park, S.-W. & Kim, K.-S. (2003). Acetyl-CoA carboxylase β gene is regulated by sterol regulatory element-binding protein-1 in liver. *J Biol Chem* **278**(31): 28410-28417.
- Ong, K.T., Mashek, M.T., Bu, S.Y., Greenberg, A.S. & Mashek, D.G. (2011). Adipose triglyceride lipase is a major hepatic lipase that regulates triacylglycerol turnover and fatty acid signaling and partitioning. *Hepatology* **53**(1): 116-126.
- Ono, T., Guthold, R. & Strong, K. (2010). World Health Organisation global comparable estimates. <http://infobase.who.int>. Website viewed 03 November 2010.
- Osler, M.E. & Zierath, J.R. (2008). Minireview: Adenosine 5'-monophosphate-activated protein kinase regulation of fatty acid oxidation in skeletal muscle. *Endocrinology* **149**(3): 935-941.
- Otto, D.A., Tsai, C.E., Baltzell, J.K. & Wooten, J.T. (1991). Apparent inhibition of hepatic triacylglycerol secretion, independent of synthesis, in high-fat fish oil-fed rats: role for insulin. *Biochim Biophys Acta - Lipids and Lipid Metabolism* **1082**(1): 37-48.
- Pan, D.A., Hulbert, A.J. & Storlien, L.H. (1994). Dietary fats, membrane phospholipids and obesity. *J Nutr* **124**(9): 1555-1565.
- Papamandjaris, A.A., Macdougall, D.E. & Jones, P.J.H. (1998). Medium chain fatty acid metabolism and energy expenditure: Obesity treatment implications. *Life Sci* **62**(14): 1203-1215.
- Parrish, C.C., Pathy, D.A. & Angel, A. (1990). Dietary fish oils limit adipose tissue hypertrophy in rats. *Metabolism* **39**(3): 217-219.
- Patsouris, D., Reddy, J.K., Müller, M. & Kersten, S. (2006). Peroxisome proliferator-activated receptor alpha mediates the effects of high-fat diet on hepatic gene expression. *Endocrinology* **147**(3): 1508-1516.
-

-
- Pehleman, T.L., Peters, S.J., Heigenhauser, G.J. & Spriet, L.L. (2005). Enzymatic regulation of glucose disposal in human skeletal muscle after a high-fat, low-carbohydrate diet. *J Appl Physiol* **98**(1): 100-107.
- Pelsers, M.M.A.L., Tsintzas, K., Boon, H., Jewell, K., Norton, L., Luiken, J.J.F.P., et al. (2007). Skeletal muscle fatty acid transporter protein expression in type 2 diabetes patients compared with overweight, sedentary men and age-matched, endurance-trained cyclists. *Acta Physiol (Oxf)* **190**(3): 209-219.
- Pérez-Echarri, N., Pérez-Matute, P., Marcos-Gómez, B., Marti, A., Martínez, J.A. & Moreno-Aliaga, M.J. (2009a). Down-regulation in muscle and liver lipogenic genes: EPA ethyl ester treatment in lean and overweight (high-fat-fed) rats. *J Nutr Biochem* **20**(9): 705-714.
- Pérez-Echarri, N., Pérez-Matute, P., Marcos-Gómez, B., Martínez, J.A. & Moreno-Aliaga, M.J. (2009b). Effects of eicosapentaenoic acid ethyl ester on visfatin and apelin in lean and overweight (cafeteria diet-fed) rats. *Br J Nutr* **101**(7): 1059-1067.
- Perrone, G., Liu, Y., Capri, O., Critelli, C., Barillaro, F., Galoppi, P., et al. (1999). Evaluation of the body composition and fat distribution in long-term users of hormone replacement therapy. *Gynecol Obstet Invest* **48**(1): 52-55.
- Peter, J.B., Barnard, R.J., Edgerton, V.R., Gillespie, C.A. & Stempel, K.E. (1972). Metabolic profiles of three fiber types of skeletal muscle in guinea pigs and rabbits. *Biochemistry* **11**(14): 2627-2633.
- Pette, D. & Staron, R.S. (2000). Myosin isoforms, muscle fiber types, and transitions. *Microsc Res Tech* **50**(6): 500-509.
- Phillips, D.I.W., Caddy, S., Ilic, V., Fielding, B.A., Frayn, K.N., Borthwick, A.C., et al. (1996). Intramuscular triglyceride and muscle insulin sensitivity: Evidence for a relationship in nondiabetic subjects. *Metabolism* **45**(8): 947-950.
- Phillipson, B.E., Rothrock, D.W., Connor, W.E., Harris, W.S. & Illingworth, D.R. (1985). Reduction of plasma lipids, lipoproteins, and apoproteins by dietary fish oils in patients with hypertriglyceridemia. *N Engl J Med* **312**(19): 1210-1216.
- Philp, L.K., Muhlhausler, B.S., Janovska, A., Wittert, G.A., Duffield, J.A. & McMillen, I.C. (2008). Maternal overnutrition suppresses the phosphorylation of 5'-AMP-activated protein kinase in liver, but not skeletal muscle, in the fetal and neonatal sheep. *Am J Physiol Regul Integr Comp Physiol* **295**(6): R1982-1990.
- Piers, L.S., Walker, K.Z., Stoney, R.M., Soares, M.J. & O'Dea, K. (2003a). Substitution of saturated with monounsaturated fat in a 4-week diet affects body weight and composition of overweight and obese men. *Br J Nutr* **90**(3): 717-727.

-
- Piers, L.S., Walker, K.Z., Stoney, R.M., Soares, M.J. & O'Dea, K. (2003b). Substitution of saturated with monounsaturated fat in a 4-week diet affects body weight and composition of overweight and obese men. *Br J Nutr* **90**(3): 717-727
- Pimenta, A.S., Gaidhu, M.P., Habib, S., So, M., Fediuc, S., Mirpourian, M., et al. (2008). Prolonged exposure to palmitate impairs fatty acid oxidation despite activation of AMP-activated protein kinase in skeletal muscle cells. *J Cell Physiol* **217**(2): 478-485.
- Pool, C., Diegenbach, P. & Scholten, G. (1979). Quantitative succinate-dehydrogenase histochemistry. *Histochemistry* **64**(3): 251-262.
- Postic, C. & Girard, J. (2008). Contribution of de novo fatty acid synthesis to hepatic steatosis and insulin resistance: lessons from genetically engineered mice. *J Clin Invest* **118**(3): 829-838.
- Poulos, A. (1995). Very long chain fatty acids in higher animals--a review. *Lipids* **30**(1): 1-14.
- Priego, T., Sánchez, J., Picó, C. & Palou, A. (2008). Sex-differential expression of metabolism-related genes in response to a high-fat diet. *Obesity* **16**(4): 819-826.
- Printz, R.L., Koch, S., Potter, L.R., O'Doherty, R.M., Tiesinga, J.J., Moritz, S., et al. (1993). Hexokinase II mRNA and gene structure, regulation by insulin, and evolution. *J Biol Chem* **268**(7): 5209-5219.
- Putman, C.T., Kiricsi, M., Pearcey, J., MacLean, I.M., Bamford, J.A., Murdoch, G.K., et al. (2003). AMPK activation increases uncoupling protein-3 expression and mitochondrial enzyme activities in rat muscle without fibre type transitions. *J Physiol* **551**(Pt 1): 169-178.
- Puustjärvi, K., Tammi, M., Reinikainen, M., Helminen, H. & Paljärvi, L. (1994). Running training alters fiber type composition in spinal muscles. *Eur Spine J* **3**(1): 17-21.
- Qin, X., Xie, X., Fan, Y., Tian, J., Guan, Y., Wang, X., et al. (2008). Peroxisome proliferator-activated receptor- δ induces insulin-induced gene-1 and suppresses hepatic lipogenesis in obese diabetic mice. *Hepatology* **48**(2): 432-441.
- Quesada, H., del Bas, J.M., Pajuelo, D., Díaz, S., Fernandez-Larrea, J., Pinent, M., et al. (2009). Grape seed proanthocyanidins correct dyslipidemia associated with a high-fat diet in rats and repress genes controlling lipogenesis and VLDL assembling in liver. *Int J Obes (Lond)* **33**(9): 1007-1012.
-

-
- Qureshi, K., Clements, R.H., Saeed, F. & Abrams, G.A. (2010). Comparative evaluation of whole body and hepatic insulin resistance using indices from oral glucose tolerance test in morbidly obese subjects with nonalcoholic fatty liver disease. *J Obes* **2010**(pii): 741521.
- Rabbani, P.I., Alam, H.Z., Chirtel, S.J., Duvall, R.E., Jackson, R.C. & Ruffin, G. (2001). Subchronic toxicity of fish oil concentrates in male and female rats. *J Nutr Sci Vitaminol (Tokyo)* **47**(3): 201-212.
- Raclot, T., Groscolas, R., Langin, D. & Ferré, P. (1997). Site-specific regulation of gene expression by n-3 polyunsaturated fatty acids in rat white adipose tissues. *J Lipid Res* **38**(10): 1963-1972.
- Rahimian, R., Masih-Khan, E., Lo, M., van Breemen, C., McManus, B.M. & Dubé, G.P. (2001). Hepatic over-expression of peroxisome proliferator activated receptor gamma2 in the ob/ob mouse model of non-insulin dependent diabetes mellitus. *Mol Cell Biochem* **224**(1-2): 29-37.
- Ramadoss, C.S., Uyeda, K. & Johnston, J.M. (1976). Studies on the fatty acid inactivation of phosphofructokinase. *J Biol Chem* **251**(1): 98-107.
- Randle, P.J. (1998). Regulatory interactions between lipids and carbohydrates: the glucose fatty acid cycle after 35 years. *Diabetes Metab Rev* **14**(4): 263-283.
- Randle, P.J., Garland, P.B., Hales, C.N. & Newsholme, E.A. (1963). The glucose fatty-acid cycle. Its role in insulin sensitivity and the metabolic disturbances of diabetes mellitus. *Lancet* **1**(7285): 785-789.
- Rapoport, S.I., Rao, J.S. & Igarashi, M. (2007). Brain metabolism of nutritionally essential polyunsaturated fatty acids depends on both the diet and the liver. *Prostaglandins Leukot Essent Fatty Acids* **77**(5-6): 251-261.
- Reddy, J.K. & Hashimoto, T. (2001). Peroxisomal beta-oxidation and peroxisome proliferator-activated receptor alpha: an adaptive metabolic system. *Annu Rev Nutr* **21**(1): 193-230.
- Reddy, J.K. & Sambasiva Rao, M. (2006). Lipid metabolism and liver Inflammation. II. Fatty liver disease and fatty acid oxidation. *Am J Physiol Gastrointest Liver Physiol* **290**(5): G852-858.
- Reid, B.N., Ables, G.P., Otlivanchik, O.A., Schoiswohl, G., Zechner, R., Blaner, W.S., et al. (2008). Hepatic overexpression of hormone-sensitive lipase and adipose triglyceride lipase promotes fatty acid oxidation, stimulates direct release of free fatty acids, and ameliorates steatosis. *J Biol Chem* **283**(19): 13087-13099.
-

-
- Reyes, A. & Cárdenas, M.L. (1984). All hexokinase isoenzymes coexist in rat hepatocytes. *Biochem J* **221**(2): 303-309.
- Richard, A.M., Webb, D.L., Goodman, J.M., Schultz, V., Flanagan, J.N., Getty-Kaushik, L., et al. (2007). Tissue-dependent loss of phosphofructokinase-M in mice with interrupted activity of the distal promoter: impairment in insulin secretion. *Am J Physiol Endocrinol Metab* **293**(3): E794-E801.
- Ricquier, D. (2005). Respiration uncoupling and metabolism in the control of energy expenditure. *Proc Nutr Soc* **64**(1): 47-52.
- Rieusset, J., Bouzakri, K., Chevillotte, E., Ricard, N., Jacquet, D., Bastard, J.P., et al. (2004). Suppressor of cytokine signaling 3 expression and insulin resistance in skeletal muscle of obese and type 2 diabetic patients. *Diabetes* **53**(9): 2232-2241.
- Risérus, U., Arnlöv, J. & Berglund, L. (2007). Long-term predictors of insulin resistance: role of lifestyle and metabolic factors in middle-aged men. *Diabetes Care* **30**(11): 2928-2933.
- Ristow, M., Vorgerd, M., Möhlig, M., Schatz, H. & Pfeiffer, A. (1997). Deficiency of phosphofructo-1-kinase/muscle subtype in humans impairs insulin secretion and causes insulin resistance. *J Clin Invest* **100**(11): 2833-2841.
- Rivellese, A.A., De Natale, C. & Lilli, S. (2002). Type of dietary fat and insulin resistance. *Ann N Y Acad Sci* **967**: 329-335.
- Roden, M. (2004). How free fatty acids inhibit glucose utilization in human skeletal muscle. *News Physiol Sci* **19**: 92-96.
- Rodgers, J.T., Lerin, C., Haas, W., Gygi, S.P., Spiegelman, B.M. & Puigserver, P. (2005). Nutrient control of glucose homeostasis through a complex of PGC-1(alpha) and SIRT1. *Nature* **434**(7029): 113-118.
- Roepstorff, C., Helge, J.W., Vistisen, B. & Kiens, B. (2004). Studies of plasma membrane fatty acid-binding protein and other lipid-binding proteins in human skeletal muscle. *Proc Nutr Soc* **63**(2): 239-244.
- Rokling-Andersen, M.H., Rustan, A.C., Wensaas, A.J., Kaalhus, O., Wergedahl, H., Rost, T.H., et al. (2009a). Marine n-3 fatty acids promote size reduction of visceral adipose depots, without altering body weight and composition, in male Wistar rats fed a high-fat diet. *Br J Nutr* **102**(7): 995-1006.
-

-
- Roorda, B.D., Hesselink, M.K.C., Schaart, G., Moonen-Kornips, E., Martinez-Martinez, P., Losen, M., et al. (2005). DGAT1 overexpression in muscle by in vivo DNA electroporation increases intramyocellular lipid content. *J Lipid Res* **46**(2): 230-236.
- Rossmeisl, M., Jelenik, T., Jilkova, Z., Slamova, K., Kus, V., Hensler, M., et al. (2009). Prevention and reversal of obesity and glucose intolerance in mice by DHA derivatives. *Obesity* **17**(5): 1023-1031.
- Ruderman, N.B., Saha, A.K., Vavvas, D. & Witters, L.A. (1999). Malonyl-CoA, fuel sensing, and insulin resistance. *Am J Physiol Endocrinol Metab* **276**(1): E1-18.
- Rustan, A.C., Hustvedt, B.E. & Drevon, C.A. (1993). Dietary supplementation of very long-chain n-3 fatty acids decreases whole body lipid utilization in the rat. *J Lipid Res* **34**(8): 1299-1309.
- Ruzickova, J., Rossmeisl, M., Prazak, T., Flachs, P., Sponarova, J., Veck, M., et al. (2004). Omega-3 PUFA of marine origin limit diet-induced obesity in mice by reducing cellularity of adipose tissue. *Lipids* **39**(12): 1177-1185.
- Sachithanandan, N., Fam, B.C., Fynch, S., Dzamko, N., Watt, M.J., Wormald, S., et al. (2010). Liver-specific suppressor of cytokine signaling-3 deletion in mice enhances hepatic insulin sensitivity and lipogenesis resulting in fatty liver and obesity. *Hepatology* **52**(5): 1632-1642.
- Saha, A.K., Schwarsin, A.J., Roduit, R., Masse, F., Kaushik, V., Tornheim, K., et al. (2000). Activation of malonyl-CoA decarboxylase in rat skeletal muscle by contraction and the AMP-activated protein kinase activator 5-aminoimidazole-4-carboxamide-1-beta-D-ribofuranoside. *J Biol Chem* **275**(32): 24279-24283.
- Samec, S., Seydoux, J., Russell, A.P., Montani, J.P. & Dulloo, A.G. (2002). Skeletal muscle heterogeneity in fasting-induced upregulation of genes encoding UCP2, UCP3, PPARgamma and key enzymes of lipid oxidation. *Pflugers Arch* **445**(1): 80-6.
- Sampath, H., Miyazaki, M., Dobrzyn, A. & Ntambi, J.M. (2007). Stearoyl-CoA desaturase-1 mediates the pro-lipogenic effects of dietary saturated fat. *J Biol Chem* **282**(4): 2483-2493.
- Samuel, V.T., Beddow, S.A., Iwasaki, T., Zhang, X.M., Chu, X., Still, C.D., et al. (2009). Fasting hyperglycemia is not associated with increased expression of PEPCCK or G6Pc in patients with Type 2 Diabetes. *Proc Natl Acad Sci U S A* **106**(29): 12121-12126.
-

-
- Samuel, V.T., Liu, Z.X., Qu, X., Elder, B.D., Bilz, S., Befroy, D., et al. (2004). Mechanism of hepatic insulin resistance in non-alcoholic fatty liver disease. *J Biol Chem* **279**(31): 32345-32353.
- Sato, A., Kawano, H., Notsu, T., Ohta, M., Nakakuki, M., Mizuguchi, K., et al. (2010). Antiobesity effect of eicosapentaenoic acid in high-fat/high-sucrose diet-induced obesity: importance of hepatic lipogenesis. *Diabetes* **59**(10): 2495-2504.
- Sato, O., Kuriki, C., Fukui, Y. & Motojima, K. (2002). Dual promoter structure of mouse and human fatty acid translocase/CD36 genes and unique transcriptional activation by peroxisome proliferator-activated receptor alpha and gamma ligands. *J Biol Chem* **277**(18): 15703-15711.
- Sbraccia, P., D'Adamo, M., Leonetti, F., Buongiorno, A., Silecchia, G., Basso, M.S., et al. (2002). Relationship between plasma free fatty acids and uncoupling protein-3 gene expression in skeletal muscle of obese subjects: in vitro evidence of a causal link. *Clin Endocrinol (Oxf)* **57**(2): 199-207.
- Schaffer, J.E. & Lodish, H.F. (1994). Expression cloning and characterization of a novel adipocyte long chain fatty acid transport protein *Cell* **79**(3): 427-436.
- Scheffler, I.E. (1998). Molecular genetics of succinate:quinone oxidoreductase in eukaryotes. *Prog Nucleic Acid Res Mol Biol* **60**: 267-315.
- Schenk, S. & Horowitz, J.F. (2006). Coimmunoprecipitation of FAT/CD36 and CPT I in skeletal muscle increases proportionally with fat oxidation after endurance exercise training. *Am J Physiol Endocrinol Metab* **291**(2): E254-260.
- Schrauwen, P., van Marken Lichtenbelt, W.D., Saris, W.H. & Westerterp, K.R. (1997). Changes in fat oxidation in response to a high-fat diet. *Am J Clin Nutr* **66**(2): 276-282.
- Schuler, M., Ali, F., Chambon, C., Duteil, D., Bornert, J.-M., Tardivel, A., et al. (2006). PGC1 alpha expression is controlled in skeletal muscles by PPAR beta, whose ablation results in fiber-type switching, obesity, and type 2 diabetes. *Cell Metab* **4**(5): 407-414.
- Schwarz, J.M., Linfoot, P., Dare, D. & Aghajanian, K. (2003). Hepatic de novo lipogenesis in normoinsulinemic and hyperinsulinemic subjects consuming high-fat, low-carbohydrate and low-fat, high-carbohydrate isoenergetic diets. *Am J Clin Nutr* **77**(1): 43-50.
- Schwenk, R.W., Holloway, G.P., Luiken, J.J.F.P., Bonen, A. & Glatz, J.F.C. (2010). Fatty acid transport across the cell membrane: Regulation by fatty acid transporters. *Prostaglandins Leukot Essent Fatty Acids* **82**(4-6): 149-154.
-

-
- Seedorf, U. & Aberle, J. (2007). Emerging roles of PPAR delta in metabolism. *Biochim Biophys Acta* **1771**(9): 1125-1131.
- Semenkovich, C.F., Coleman, T. & Fiedorek, F.T.J. (1995). Human fatty acid synthase mRNA: tissue distribution, genetic mapping, and kinetics of decay after glucose deprivation. *J Lipid Res* **36**(7): 1507-1521.
- Seoane, J., Barberà, A., Télémaque-Potts, S., Newgard, C.B. & Guinovart, J.J. (1999). Glucokinase overexpression restores glucose utilization and storage in cultured hepatocytes from male Zucker diabetic fatty rats. *J Biol Chem* **274**(45): 31833-31838.
- Seoane, J., Gómez-Foix, A.M., O'Doherty, R.M., Gómez-Ara, C., Newgard, C.B. & Guinovart, J.J. (1996). Glucose 6-phosphate produced by glucokinase, but not hexokinase I, promotes the activation of hepatic glycogen synthase. *J Biol Chem* **271**(39): 23756-23760.
- Serviddio, G., Bellanti, F., Tamborra, R., Rollo, T., Capitanio, N., Romano, A.D., et al. (2008). Uncoupling protein-2 (UCP2) induces mitochondrial proton leak and increases susceptibility of non-alcoholic steatohepatitis (NASH) liver to ischaemia-reperfusion injury. *Gut* **57**(7): 957-965.
- Shao, J., Qiao, L., Janssen, R.C., Pagliassotti, M. & Friedman, J.E. (2005). Chronic hyperglycemia enhances PEPCCK gene expression and hepatocellular glucose production via elevated liver activating protein/liver inhibitory protein ratio. *Diabetes* **54**(4): 976-984.
- Sherwood, L. (2004). Human physiology. From cells to systems. 5th Edition. Brookes/Cole; California : Thomson Learning Inc, 2004 (Ch 2): 34.
- Shillabeer, G. & Lau, D.C. (1994). Regulation of new fat cell formation in rats: the role of dietary fats. *J Lipid Res* **35**(4): 592-600.
- Shimano, H. (2001). Sterol regulatory element-binding proteins (SREBPs): transcriptional regulators of lipid synthetic genes. *Prog Lipid Res* **40**(6): 439-452.
- Shimano, H., Shimomura, I., Hammer, R.E., Herz, J., Goldstein, J.L., Brown, M.S., et al. (1997). Elevated levels of SREBP-2 and cholesterol synthesis in livers of mice homozygous for a targeted disruption of the SREBP-1 gene. *J Clin Invest* **100**(8): 2115-2124.
- Shimomura, I., Shimano, H., Horton, J.D., Goldstein, J.L. & Brown, M.S. (1997). Differential expression of exons 1a and 1c in mRNAs for sterol regulatory element binding protein-1 in human and mouse organs and cultured cells. *J Clin Invest* **99**(5): 838-845.
-

- Sibut, V., Le Bihan-Duval, E., Tesseraud, S., Godet, E., Bordeau, T., Cailleau-Audouin, E., et al. (2008). Adenosine monophosphate-activated protein kinase involved in variations of muscle glycogen and breast meat quality between lean and fat chickens. *J Anim Sci* **86**(11): 2888-2896.
- Simončíkova, P., Wein, S., Gasperikova, D., Ukropec, J., Certik, M., Klimes, I., et al. (2002). Comparison of the extrapancreatic action of gamma-linolenic acid and n-3 PUFAs in the high fat diet-induced insulin resistance. *Endocr Regul* **36**(4): 143-149.
- Simoneau, J.A. & Bouchard, C. (1989). Human variation in skeletal muscle fiber-type proportion and enzyme activities. *Am J Physiol* **257**(4 Pt 1): E567-572.
- Sinal, C.J., Yoon, M. & Gonzalez, F.J. (2001). Antagonism of the actions of peroxisome proliferator-activated receptor-alpha by bile acids. *J Biol Chem* **276**(50): 47154-47162.
- Smith, A.C., Mullen, K.L., Junkin, K.A., Nickerson, J., Chabowski, A., Bonen, A., et al. (2007). Metformin and exercise reduce muscle FAT/CD36 and lipid accumulation and blunt the progression of high-fat diet induced hyperglycemia. *Am J Physiol Endocrinol Metab* **293**(1): E172-181.
- Smith, S.A. (2002). Peroxisome proliferator-activated receptors and the regulation of mammalian lipid metabolism. *Biochem Soc Trans* **30**(Pt 6): 1086-1090.
- Smith, S.J., Cases, S., Jensen, D.R., Chen, H.C., Sande, E., Tow, B., et al. (2000). Obesity resistance and multiple mechanisms of triglyceride synthesis in mice lacking Dgat. *Nat Genet* **25**(1): 87.
- Sohal, P.S., Baracos, V.E. & Clandinin, M.T. (1992). Dietary omega 3 fatty acid alters prostaglandin synthesis, glucose transport and protein turnover in skeletal muscle of healthy and diabetic rats. *Biochem J* **286**(Pt 2): 405-411.
- Solanes, G., Pedraza, N., Iglesias, R., Giralt, M. & Villarroya, F. (2003). Functional relationship between MyoD and peroxisome proliferator-activated receptor-dependent regulatory pathways in the control of the human uncoupling protein-3 gene transcription. *Mol Endocrinol* **17**(10): 1944-1958.
- Song, X.M., Ryder, J.W., Kawano, Y., Chibalin, A.V., Krook, A. & Zierath, J.R. (1999). Muscle fiber type specificity in insulin signal transduction. *Am J Physiol* **277**(6 Pt 2): R1690-1696.
- Sorrentino, D., Zhou, S.L., Kokkotou, E. & Berk, P.D. (1992). Sex differences in hepatic fatty acid uptake reflect a greater affinity of the transport system in females. *Am J Physiol Gastrointest Liver Physiol* **263**(3): G380-385.

-
- Soukup, T., Vydra, J. & Černý, M. (1979). Changes in ATPase and SDH reactions of the rat extrafusal and intrafusal muscle fibres after preincubations at different pH. *Histochemistry* **60**(1): 71-84.
- Spangenburg, E.E., Brown, D.A., Johnson, M.S. & Moore, R.L. (2006). Exercise increases SOCS-3 expression in rat skeletal muscle: potential relationship to IL-6 expression. *J Physiol* **572**(Pt 3): 839-848.
- Stahl, A. (2004). A current review of fatty acid transport proteins (SLC27). *Pflugers Arch* **447**(5): 722-727.
- Stahlberg, N., Rico-Bautista, E., Fisher, R.M., Wu, X., Cheung, L., Flores-Morales, A., et al. (2004). Female-predominant expression of fatty acid translocase/CD36 in rat and human liver. *Endocrinology* **145**(4): 1972-1979.
- Staron, R.S., Hagerman, F.C., Hikida, R.S., Murray, T.F., Hostler, D.P., Crill, M.T., et al. (2000). Fiber type composition of the vastus lateralis muscle of young men and women. *J Histochem Cytochem* **48**(5): 623-630.
- Staron, R.S., Kraemer, W.J., Hikida, R.S., Fry, A.C., Murray, J.D. & Campos, G.E.R. (1999). Fiber type composition of four hindlimb muscles of adult Fisher 344 rats. *Histochem Cell Biol* **111**(2): 117-123.
- Staron, R.S. & Pette, D. (1986). Correlation between myofibrillar ATPase activity and myosin heavy chain composition in rabbit muscle fibers. *Histochemistry* **86**(1): 19-23.
- Steenenbergh, P.A., Beekhof, P.K., Feskens, E.J., Lips, C.J., Höppener, J.W. & Beems, R.B. (2002). Long-term effect of fish oil diet on basal and stimulated plasma glucose and insulin levels in ob/ob mice. *Diabetes Nutr Metab* **15**(4): 205-214.
- Stefan, N., Peter, A., Cegan, A., Staiger, H., Machann, J., Schick, F., et al. (2008). Low hepatic stearyl-CoA desaturase 1 activity is associated with fatty liver and insulin resistance in obese humans. *Diabetologia* **51**(4): 648-656.
- Steinberg, G.R., Smith, A.C., van Denderen, B.J.W., Chen, Z., Murthy, S., Campbell, D.J., et al. (2004a). AMP-activated protein kinase is not down-regulated in human skeletal muscle of obese females. *J Clin Endocrinol Metab* **89**(9): 4575-4580.
- Steinberg, G.R., Smith, A.C., Wormald, S., Malenfant, P., Collier, C. & Dyck, D.J. (2004b). Endurance training partially reverses dietary-induced leptin resistance in rodent skeletal muscle. *Am J Physiol Endocrinol Metab* **286**(1): E57-63.
-

- Steinberg, S.J., Mihalik, S.J., Kim, D.G., Cuebas, D.A. & Watkins, P.A. (2000). The human liver-specific homolog of very long-chain acyl-CoA synthetase is cholate:CoA ligase. *J Biol Chem* **275**(21): 15605-15608.
- Steinberg, S.J., Wang, S.J., McGuinness, M.C. & Watkins, P.A. (1999). Human liver-specific very-long-chain acyl-coenzyme A synthetase: cDNA cloning and characterization of a second enzymatically active protein. *Mol Genet Metab* **68**(1): 32-42.
- Stellingwerff, T., Boon, H., Gijzen, A., Stegen, J., Kuipers, H. & van Loon, L. (2007). Carbohydrate supplementation during prolonged cycling exercise spares muscle glycogen but does not affect intramyocellular lipid use. *Pflügers Arch* **454**(4): 635-647.
- Stone, S.J., Myers, H.M., Watkins, S.M., Brown, B.E., Feingold, K.R., Elias, P.M., et al. (2004). Lipopenia and skin barrier abnormalities in DGAT2-deficient mice. *J Biol Chem* **279**(12): 11767-11776.
- Storlien, L., Oakes, N.D. & Kelley, D.E. (2004). Metabolic flexibility. *Proc Nutr Soc* **63**(2): 363-8.
- Storlien, L.H., Jenkins, A.B., Chisholm, D.J., Pascoe, W.S., Khouri, S. & Kraegen, E.W. (1991). Influence of dietary fat composition on development of insulin resistance in rats. Relationship to muscle triglyceride and omega-3 fatty acids in muscle phospholipid. *Diabetes* **40**(2): 280-289.
- Storlien, L.H., Kraegen, E.W., Chisholm, D.J., Ford, G.L., Bruce, D.G. & Pascoe, W.S. (1987). Fish oil prevents insulin resistance induced by high-fat feeding in rats. *Science* **237**(4817): 885-888.
- Storlien, L.H., Kriketos, A.D., Calvert, G.D., Baur, L.A. & Jenkins, A.B. (1997). Fatty acids, triglycerides and syndromes of insulin resistance. *Prostaglandins Leukot Essent Fatty Acids* **57**(4-5): 379-385.
- Straczkowski, M., Kowalska, I., Baranowski, M., Nikolajuk, A., Otziomek, E., Zabielski, P., et al. (2007). Increased skeletal muscle ceramide level in men at risk of developing type 2 diabetes. *Diabetologia* **50**(11): 2366-2373.
- Stremmel, W., Strohmeyer, G. & Berk, P.D. (1986). Hepatocellular uptake of oleate is energy dependent, sodium linked, and inhibited by an antibody to a hepatocyte plasma membrane fatty acid binding protein. *Proc Natl Acad Sci U S A* **83**(11): 3584-3588.
- Stremmel, W., Strohmeyer, G., Borchard, F., Kochwa, S. & Berk, P.D. (1985). Isolation and partial characterization of a fatty acid binding protein in rat liver plasma membranes. *Proc Natl Acad Sci U S A* **82**(1): 4-8.

-
- Stubbs, S.S. & Blanchaer, M.C. (1965). Glycogen phosphorylase and glycogen synthetase activity in red and white skeletal muscle in the guinea pig. *Can J Biochem Physiol* **43**: 463-468.
- Stump, D.D., Zhou, S.L. & Berk, P.D. (1993). Comparison of plasma membrane FABP and mitochondrial isoform of aspartate aminotransferase from rat liver. *Am J Physiol Gastrointest Liver Physiol* **265**(5): G894-902.
- Suchankova, G., Tekle, M., Saha, A.K., Ruderman, N.B., Clarke, S.D. & Gettys, T.W. (2005). Dietary polyunsaturated fatty acids enhance hepatic AMP-activated protein kinase activity in rats. *Biochem Biophys Res Commun* **326**(4): 851-858.
- Sugden, M.C., Fryer, L.G., Orfali, K.A., Priestman, D.A., Donald, E. & Holness, M.J. (1998). Studies of the long-term regulation of hepatic pyruvate dehydrogenase kinase. *Biochem J* **329**(Pt 1): 89-94.
- Sugden, M.C., Orfali, K.A. & Holness, M.J. (1995). The pyruvate dehydrogenase complex: nutrient control and the pathogenesis of insulin resistance. *J Nutr* **125**(6 Suppl): 1746S-1752S.
- Sun, C., Wei, Z.-w. & Li, Y. (2011). DHA regulates lipogenesis and lipolysis genes in mice adipose and liver. *Mol Biol Rep* **38**(2): 731-737.
- Sun, L., Shukair, S., Naik, T.J., Moazed, F. & Ardehali, H. (2008). Glucose phosphorylation and mitochondrial binding are required for the protective effects of hexokinases I and II. *Mol Cell Biol* **28**(3): 1007-1017.
- Surovtseva, Z.F. (1974). Glycogen content in skeletal muscles and liver of rabbits in the antenatal and neonatal periods. *Bull Exp Biol Med* **77**(6): 599-600.
- Surwit, R.S., Wang, S., Petro, A.E., Sanchis, D., Raimbault, S., Ricquier, D., et al. (1998). Diet-induced changes in uncoupling proteins in obesity-prone and obesity-resistant strains of mice. *Proc Natl Acad Sci USA* **95**(7): 4061-4065.
- Svegliati-Baroni, G., Candelaresi, C., Saccomanno, S., Ferretti, G., Bachetti, T., Marzioni, M., et al. (2006). A model of insulin resistance and nonalcoholic steatohepatitis in rats: role of peroxisome proliferator-activated receptor- α and n-3 polyunsaturated fatty acid treatment on liver injury. *Am J Pathol* **169**(3): 846-860.
- Swinburn, B., Sacks, G. & Ravussin, E. (2009). Increased food energy supply is more than sufficient to explain the US epidemic of obesity. *Am J Clin Nutr* **90**(6): 1453-1456.
-

-
- Tagliaferro, A.R., Dobbin, S., Curi, R., Leighton, B., Meeker, L.D. & Newsholme, E.A. (1990). Effects of diet and exercise on the in vivo rates of the triglyceride-fatty acid cycle in adipose tissue and muscle of the rat. *Int J Obes* **14**(11): 957-971.
- Takaishi, K., Duplomb, L., Wang, M.-Y., Li, J. & Unger, R.H. (2004). Hepatic insig-1 or -2 overexpression reduces lipogenesis in obese Zucker diabetic fatty rats and in fasted/refed normal rats. *Proc Natl Acad Sci U S A* **101**(18): 7106-7111.
- Takeuchi, H., Inoue, Y., Ishihara, H. & Oka, Y. (1996). Overexpression of either liver type or pancreatic beta cell type glucokinase via recombinant adenovirus enhances glucose oxidation in isolated rat hepatocytes. *FEBS Lett* **393**(1): 60-64.
- Tanaka, S., Hayashi, T., Toyoda, T., Hamada, T., Shimizu, Y., Hirata, M., et al. (2007). High-fat diet impairs the effects of a single bout of endurance exercise on glucose transport and insulin sensitivity in rat skeletal muscle. *Metabolism* **56**(12): 1719-1728.
- Tanner, C.J., Barakat, H.A., Dohm, G.L., Pories, W.J., MacDonald, K.G., Cunningham, P.R.G., et al. (2002). Muscle fiber type is associated with obesity and weight loss. *Am J Physiol Endocrinol Metab* **282**(6): E1191-1196.
- Taouis, M., Dagou, C., Ster, C., Durand, G., Pinault, M. & Delarue, J. (2002). N-3 Polyunsaturated fatty acids prevent the defect of insulin receptor signaling in muscle. *Am J Physiol Endocrinol Metab* **282**(3): E664-671.
- Tengan, C.H., Kiyomoto, B.H., Godinho, R.O., Gamba, J., Neves, A.C., Schmidt, B., et al. (2007). The role of nitric oxide in muscle fibers with oxidative phosphorylation defects. *Biochem Biophys Res Commun* **359**(3): 771-777.
- Termin, A., Staron, R.S. & Pette, D. (1989a). Myosin heavy chain isoforms in histochemically defined fiber types of rat muscle. *Histochemistry* **92**(6): 453-457.
- Teutsch, H.F. & Lowry, O.H. (1982). Sex specific regional differences in hepatic glucokinase activity. *Biochem Biophys Res Commun* **106**(2): 533-538.
- Thewke, D.P., Panini, S.R. & Sinensky, M. (1998). Oleate potentiates oxysterol inhibition of transcription from sterol regulatory element-1-regulated promoters and maturation of sterol regulatory element-binding proteins. *J Biol Chem* **273**(33): 21402-21407.
- Thomas, B., Bishop, J. & Association, B.D. 2007. Manual of dietetic practice, 4th Edition, Oxford, Blackwell Publishing Ltd 150-156.

- Thomas, C.D., Peters, J.C., Reed, G.W., Abumrad, N.N., Sun, M. & Hill, J.O. (1992). Nutrient balance and energy expenditure during ad libitum feeding of high-fat and high-carbohydrate diets in humans. *Am J Clin Nutr* **55**(5): 934-942.
- Thorburn, A.W. (2005). Prevalence of obesity in Australia. *Obes Rev* **6**(3): 187-189.
- Thyfault, J.P., Kraus, R.M., Hickner, R.C., Howell, A.W., Wolfe, R.R. & Dohm, G.L. (2004). Impaired plasma fatty acid oxidation in extremely obese women. *Am J Physiol Endocrinol Metab* **287**(6): E1076-1081.
- Todd, M.K., Watt, M.J., Le, J., Hevener, A.L. & Turcotte, L.P. (2007). Thiazolidinediones enhance skeletal muscle triacylglycerol synthesis while protecting against fatty acid-induced inflammation and insulin resistance. *Am J Physiol Endocrinol Metab* **292**(2): E485-E493.
- Tomé, D., Dubarry, M. & Fromentin, G. (2004). Nutritional value of milk and meat products derived from cloning. *Cloning Stem Cells* **6**(2): 172-177.
- Toussant, M.J., Wilson, M.D. & Clarke, S.D. (1981). Coordinate suppression of liver acetyl-CoA carboxylase and fatty acid synthetase by polyunsaturated fat. *J Nutr* **111**(1): 146-153.
- Towler, M.C. & Hardie, D.G. (2007). AMP-activated protein kinase in metabolic control and insulin signaling. *Circ Res* **100**(3): 328-341.
- Troyer, D.L., Oyster, R.O. & Hunt, M.C. (1991). A combination histochemical stain for equine muscle. *Anat Histol Embryol* **20**(1): 44-47.
- Trumble, G.E., Smith, M.A. & Winder, W.W. (1995). Purification and characterization of rat skeletal muscle acetyl-CoA carboxylase. *Eur J Biochem* **231**(1): 192-198.
- Tsitouras, P.D., Gucciardo, F., Salbe, A.D., Heward, C. & Harman, S.M. (2008). High omega-3 fat intake improves insulin sensitivity and reduces CRP and IL6, but does not affect other endocrine axes in healthy older adults. *Horm Metab Res* **40**(3): 199-205.
- Tsuboyama-Kasaoka, N., Sano, K., Shozawa, C., Osaka, T. & Ezaki, O. (2008). Studies of UCP2 transgenic and knockout mice reveal that liver UCP2 is not essential for the antiobesity effects of fish oil. *Am J Physiol Endocrinol Metab* **294**(3): E600-606.
- Tsuboyama-Kasaoka, N., Takahashi, M., Kim, H. & Ezaki, O. (1999). Up-regulation of liver uncoupling protein-2 mRNA by either fish oil feeding or fibrate administration in mice. *Biochem Biophys Res Commun* **257**(3): 879-885.

-
- Tsunoda, M., Kobayashi, N., Ide, T., Utsumi, M., Nagasawa, M. & Murakami, K. (2008). A novel PPARalpha agonist ameliorates insulin resistance in dogs fed a high-fat diet. *Am J Physiol Endocrinol Metab* **294**(5): E833-840.
- Turcotte, L.P., Swenberger, J.R., Tucker, M.Z., Yee, A.J., Trump, G., Luiken, J.J., et al. (2000). Muscle palmitate uptake and binding are saturable and inhibited by antibodies to FABP(PM). *Mol Cell Biochem* **210**(1-2): 53-63.
- Turinsky, J., O'Sullivan, D.M. & Bayly, B.P. (1990). 1,2-Diacylglycerol and ceramide levels in insulin-resistant tissues of the rat in vivo. *J Biol Chem* **265**(28): 16880-16885.
- Turner, N., Bruce, C.R., Beale, S.M., Hoehn, K.L., So, T., Rolph, M.S., et al. (2007). Excess lipid availability increases mitochondrial fatty acid oxidative capacity in muscle: Evidence against a role for reduced fatty acid oxidation in lipid-induced insulin resistance in rodents. *Diabetes* **56**(8): 2085-2092.
- Turpin, S.M., Hoy, A.J., Brown, R.D., Garcia Rudaz, C., Honeyman, J., Matzaris, M., et al. (2010). Adipose triacylglycerol lipase is a major regulator of hepatic lipid metabolism but not insulin sensitivity in mice. *Diabetologia* **54**(1): 146-156.
- Turvey, E.A., Heigenhauser, G.J.F., Parolin, M. & Peters, S.J. (2005). Elevated n-3 fatty acids in a high-fat diet attenuate the increase in PDH kinase activity but not PDH activity in human skeletal muscle. *J Appl Physiol* **98**(1): 350-355.
- Ueki, K., Kondo, T. & Kahn, C.R. (2004). Suppressor of cytokine signaling 1 (SOCS-1) and SOCS-3 cause insulin resistance through inhibition of tyrosine phosphorylation of insulin receptor substrate proteins by discrete mechanisms. *Mol Cell Biol* **24**(12): 5434-5446.
- Ukropec, J., Reseland, J.E., Gasperikova, D., Demcakova, E., Madsen, L., Berge, R.K., et al. (2003). The hypotriglyceridemic effect of dietary n-3 FA is associated with increased beta-oxidation and reduced leptin expression. *Lipids* **38**(10): 1023-1029.
- van Breda, E., Keizer, H.A., Vork, M.M., Surtel, D.A.M., de Jong, Y.F., van der Vusse, G.J., et al. (1992). Modulation of fatty-acid-binding protein content of rat heart and skeletal muscle by endurance training and testosterone treatment. *Pflügers Archiv* **421**(2): 274-279.
- Veerkamp, J.H. & van Moerkerk, H.T.B. (1986). Peroxisomal fatty acid oxidation in rat and human tissues. Effect of nutritional state, clofibrate treatment and postnatal development in the rat. *Biochim Biophys Acta - Lipids and Lipid Metabolism* **875**(2): 301-310.
-

-
- Vessby, B., Gustafsson, I.B., Tengblad, S., Boberg, M. & Andersson, A. (2002). Desaturation and elongation of fatty acids and insulin action. *Ann NY Acad Sci* **967**(1): 183-195.
- Vessby, B., Uusitupa, M., Hermansen, K., Riccardi, G., Rivellesse, A.A., Tapsell, L.C., et al. (2001). Substituting dietary saturated for monounsaturated fat impairs insulin sensitivity in healthy men and women: The KANWU Study. *Diabetologia* **44**(3): 312-319.
- Vettor, R., Fabris, R., Serra, R., Lombardi, A.M., Tonello, C., Granzotto, M., et al. (2002). Changes in FAT/CD36, UCP2, UCP3 and GLUT4 gene expression during lipid infusion in rat skeletal and heart muscle. *Int J Obes Relat Metab Disord* **26**(6): 838-847.
- Vidal-Puig, A., Jimenez-Linan, M., Lowell, B.B., Hamann, A., Hu, E., Spiegelman, B., et al. (1996). Regulation of PPAR gamma gene expression by nutrition and obesity in rodents. *J Clin Invest* **97**(11): 2553-2561.
- Vidal-Puig, A., Solanes, G., Grujic, D., Flier, J.S. & Lowell, B.B. (1997). UCP3: An uncoupling protein homologue expressed preferentially and abundantly in skeletal muscle and brown adipose tissue. *Biochem Biophys Res Commun* **235**(1): 79-82.
- Villar-Palasi, C. & Guinovart, J.J. (1997). The role of glucose 6-phosphate in the control of glycogen synthase. *FASEB J* **11**(7): 544-558.
- Violett, B., Andreelli, F., Jorgensen, S.B., Perrin, C., Geloan, A., Flamez, D., et al. (2003). The AMP-activated protein kinase $\alpha 2$ catalytic subunit controls whole-body insulin sensitivity. *J Clin Invest* **111**(1): 91.
- Viollet, B., Andreelli, F., Jorgensen, S.B., Perrin, C., Flamez, D., Mu, J., et al. (2003). Physiological role of AMP-activated protein kinase (AMPK): insights from knockout mouse models. *Biochem Soc Trans* **31**(Pt 1): 216-219.
- Viollet, B., Foretz, M., Guigas, B., Horman, S., Dentin, R., Bertrand, L., et al. (2006). Activation of AMP-activated protein kinase in the liver: a new strategy for the management of metabolic hepatic disorders. *J Physiol* **574**(1): 41-53.
- Wahlefeld, A.W. 1974. Triglycerides. Determination after enzymatic hydrolysis. In: BERGMAYER, H. (Ed.) *Methods of enzymatic analysis*. New York, Academic Press.
- Wakil, S.J. (1989). Fatty acid synthase, a proficient multifunctional enzyme. *Biochemistry* **28**(11): 4523-4530.
-

-
- Wakil, S.J. & Abu-Elheiga, L.A. (2009). Fatty acid metabolism: target for metabolic syndrome. *J Lipid Res* **50**(Suppl): S138-143.
- Wang, H., Storlien, L.H. & Huang, X.-F. (2002). Effects of dietary fat types on body fatness, leptin, and ARC leptin receptor, NPY, and AgRP mRNA expression. *Am J Physiol Endocrinol Metab* **282**(6): E1352-1359.
- Wang, S.P., Laurin, N., Himms-Hagen, J., Rudnicki, M.A., Levy, E., Robert, M.F., et al. (2001). The adipose tissue phenotype of hormone-sensitive lipase deficiency in mice. *Obes Res* **9**(2): 119-128.
- Wang, Y.-X., Lee, C.-H., Tjep, S., Yu, R.T., Ham, J., Kang, H., et al. (2003). Peroxisome-proliferator-activated receptor delta activates fat metabolism to prevent obesity. *Cell* **113**(2): 159-170.
- Waters, S.M., Kelly, J.P., O'Boyle, P., Moloney, A.P. & Kenny, D.A. (2009). Effect of level and duration of dietary n-3 polyunsaturated fatty acid supplementation on the transcriptional regulation of Delta-9-desaturase in muscle of beef cattle. *J Anim Sci* **87**(1): 244-252.
- Watson, R.T. & Pessin, J.E. (2001). Intracellular organisation of insulin signalling and GLUT4 translocation. *Recent Prog Horm Res* **56**: 175-93.
- Watt, M.J. (2009). Triglyceride lipases alter fuel metabolism and mitochondrial gene expression. *Appl Physiol Nutr Metab* **34**(3): 340-347.
- Watt, M.J. & Steinberg, G.R. (2008). Regulation and function of triacylglycerol lipases in cellular metabolism. *Biochem J* **414**(3): 313-325.
- Westerbacka, J., Kolak, M., Kiviluoto, T., Arkkila, P., Sirén, J., Hamsten, A., et al. (2007). Genes involved in fatty acid partitioning and binding, lipolysis, monocyte/macrophage recruitment, and inflammation are overexpressed in the human fatty liver of insulin-resistant subjects. *Diabetes* **56**(11): 2759-2765.
- WHO (2010). World Health Organisation fact sheet: Obesity and overweight. <http://www.who.int/mediacentre/factsheets/fs311/en/index.html>. Website viewed 03 November 2010.
- Winder, W.W. (2001). Energy-sensing and signaling by AMP-activated protein kinase in skeletal muscle. *J Appl Physiol* **91**(3): 1017-1028.
- Winder, W.W. & Hardie, D.G. (1999). AMP-activated protein kinase, a metabolic master switch: possible roles in type 2 diabetes. *Am J Physiol Endocrinol Metab* **277**(1): E1-10.
-

- Winder, W.W., Wilson, H.A., Hardie, D.G., Rasmussen, B.B., Hutber, C.A., Call, G.B., et al. (1997). Phosphorylation of rat muscle acetyl-CoA carboxylase by AMP-activated protein kinase and protein kinase A. *J Appl Physiol* **82**(1): 219-225.
- Wojtaszewski, J.F., Jørgensen, S.B., Hellsten, Y., Hardie, D.G. & Richter, E.A. (2002). Glycogen-dependent effects of 5-aminoimidazole-4-carboxamide (AICA)-riboside on AMP-activated protein kinase and glycogen synthase activities in rat skeletal muscle. *Diabetes* **51**(2): 284-292.
- Wolfe, R.R., Klein, S., Carraro, F. & Weber, J.M. (1990). Role of triglyceride-fatty acid cycle in controlling fat metabolism in humans during and after exercise. *Am J Physiol Endocrinol Metab* **258**(2): E382-389.
- Woods, A., Azzout-Marniche, D., Foretz, M., Stein, S.C., Lemarchand, P., Ferré, P., et al. (2000). Characterization of the role of AMP-activated protein kinase in the regulation of glucose-activated gene expression using constitutively active and dominant negative forms of the kinase. *Mol Cell Biol* **20**(18): 6704-6711.
- Worgall, T.S., Sturley, S.L., Seo, T., Osborne, T.F. & Deckelbaum, R.J. (1998). Polyunsaturated fatty acids decrease expression of promoters with sterol regulatory elements by decreasing levels of mature sterol regulatory element-binding protein. *J Biol Chem* **273**(40): 25537-25540.
- Wu, C., Kang, J.E., Peng, L.J., Li, H., Khan, S.A., Hillard, C.J., et al. (2005). Enhancing hepatic glycolysis reduces obesity: differential effects on lipogenesis depend on site of glycolytic modulation. *Cell Metab* **2**(2): 131-140.
- Wu, Q., Ortegon, A.M., Tsang, B., Doege, H., Feingold, K.R. & Stahl, A. (2006). FATP1 is an insulin-sensitive fatty acid transporter involved in diet-induced obesity. *Mol Cell Biol* **26**(9): 3455-3467.
- Xu, H.E., Lambert, M.H., Montana, V.G., Parks, D.J., Blanchard, S.G., Brown, P.J., et al. (1999a). Molecular recognition of fatty acids by peroxisome proliferator-activated receptors. *Mol Cell* **3**(3): 397-403.
- Xu, J., Nakamura, M.T., Cho, H.P. & Clarke, S.D. (1999b). Sterol regulatory element binding protein-1 expression is suppressed by dietary polyunsaturated fatty acids. A mechanism for the coordinate suppression of lipogenic genes by polyunsaturated fats. *J Biol Chem* **273**(33): 23577-23583.
- Xu, J., Teran-Garcia, M., Park, J.H., Nakamura, M.T. & Clarke, S.D. (2001). Polyunsaturated fatty acids suppress hepatic sterol regulatory element-binding protein-1 expression by accelerating transcript decay. *J Biol Chem* **276**(13): 9800-9807.

-
- Yahagi, N., Shimano, H., Hasty, A.H., Amemiya-Kudo, M., Okazaki, H., Tamura, Y., et al. (1999). A crucial role of sterol regulatory element-binding protein-1 in the regulation of lipogenic gene expression by polyunsaturated fatty acids. *J Biol Chem* **274**(50): 35840-35844.
- Yamamoto, K., Itoh, T., Abe, D., Shimizu, M., Kanda, T., Koyama, T., et al. (2005). Identification of putative metabolites of docosahexaenoic acid as potent PPARgamma agonists and antidiabetic agents. *Bioorg Med Chem Lett* **15**(3): 517-522.
- Yamamoto, T., Yamaguchi, H., Miki, H., Kitamura, S., Nakada, Y., Aicher, T.D., et al. (2010). A novel coenzyme A:diacylglycerol acyltransferase 1 inhibitor stimulates lipid metabolism in muscle and lowers weight in animal models of obesity. *Eur J Pharmacol* **650**(2-3): 663-672.
- Yamori, Y. (2004). Worldwide epidemic of obesity: hope for Japanese diets. *Clin Exp Pharmacol Physiol* **31**(Suppl 2): S2-4.
- Yang, G., Badeanlou, L., Bielawski, J., Roberts, A.J., Hannun, Y.A. & Samad, F. (2009). Central role of ceramide biosynthesis in body weight regulation, energy metabolism, and the metabolic syndrome. *Am J Physiol Endocrinol Metab* **297**(1): E211-224.
- Yaspelkis, B.B.r., Kvasha, I.A. & Figueroa, T.Y. (2009). High-fat feeding increases insulin receptor and IRS-1 coimmunoprecipitation with SOCS-3, IKKalpha/beta phosphorylation and decreases PI-3 kinase activity in muscle. *Am J Physiol Regul Integr Comp Physiol* **296**(6): R1909-1715.
- Yaspelkis, B.B.r., Singh, M.K., Krisan, A.D., Collins, D.E., Kwong, C.C., Bernard, J.R., et al. (2004). Chronic leptin treatment enhances insulin-stimulated glucose disposal in skeletal muscle of high-fat fed rodents. *Life Sci* **74**(14): 1801-1816.
- Ye, J.-M., Doyle, P.J., Iglesias, M.A., Watson, D.G., Cooney, G.J. & Kraegen, E.W. (2001). Peroxisome proliferator-activated receptor (PPAR)-alpha activation lowers muscle lipids and improves insulin sensitivity in high fat-fed rats: comparison with PPAR-gamma activation. *Diabetes* **50**(2): 411-417.
- Yu, C., Chen, Y., Cline, G.W., Zhang, D., Zong, H., Wang, Y., et al. (2002). Mechanism by which fatty acids inhibit insulin activation of insulin receptor substrate-1 (IRS-1) associated phosphatidylinositol 3-kinase activity in muscle. *J Biol Chem* **277**(52): 50230-50236.
- Yun, J.W., Shin, E.S., Cho, S.Y., Kim, S.H., Kim, C.W., Lee, T.R., et al. (2008). The effects of BADGE and caffeine on the time-course response of adiponectin and lipid oxidative enzymes in high fat diet-fed C57BL/6J mice: correlation with reduced adiposity and steatosis. *Exp Anim* **57**(5): 461-469.
-

- Zhang, X., Fitzsimmons, R.L., Cleland, L.G., Ey, P.L., Zannettino, A.C., Farmer, E.A., et al. (2003). CD36/fatty acid translocase in rats: distribution, isolation from hepatocytes, and comparison with the scavenger receptor SR-B1. *Lab Invest* **83**(3): 317-332.
- Zheng, D., MacLean, P.S., Pohnert, S.C., Knight, J.B., Olson, A.L., Winder, W.W., et al. (2001). Regulation of muscle GLUT-4 transcription by AMP-activated protein kinase. *J Appl Physiol* **91**(3): 1073-1083.
- Zhou, G., Myers, R., Li, Y., Chen, Y., Shen, X., Fenyk-Melody, J., et al. (2001). Role of AMP-activated protein kinase in mechanism of metformin action. *J Clin Invest* **108**(8): 1167-1174.
- Zierath, J.R. & Hawley, J.A. (2004). Skeletal muscle fiber type: influence on contractile and metabolic properties. *PLoS Biol* **2**(10): 1523-1527.
- Zurlo, F., Lillioja, S., Esposito-Del Puente, A., Nyomba, B.L., Raz, I., Saad, M.F., et al. (1990). Low ratio of fat to carbohydrate oxidation as predictor of weight gain: study of 24-h RQ. *Am J Physiol Endocrinol Metab* **259**(5): E650-657.